The Dissertation Committee for Hamid Reza Lashgari
Certifies that this is the approved version of the following dissertation:

Development of a Four-Phase Thermal-Chemical Reservoir Simulator for Heavy Oil

Approved by Committee:

Kamy Sepehrnoori, Supervisor

Gary A. Pope

Mojdeh Delshad

Kishore Mohanty

Eric DeRouffignac

Development of a Four-Phase Thermal-Chemical Reservoir Simulator for Heavy Oil

by

Hamid Reza Lashgari, B.S. ; M.Sc.

Dissertation

Presented to the Faculty of the Graduate School of

The University of Texas at Austin

in Partial Fulfillment

of the Requirements

for the Degree of

Doctor of Philosophy

The University of Texas at Austin

December 2014

Dedication

To
My wife

Maryam

and

To
My parents

for their unconditional support

Acknowledgements

This dissertation would not have been possible without the support of many people. It is really a great honor for me to thank some of those many, to whom I owe my deepest gratitude. I would like to express my sincere gratitude to my supervisor Dr. Kamy Sepehrnoori, for his continuous guidance, support, and encouragement. I have learned a lot from his profound insight, keen observations, and vast knowledge. I am privileged to have had an opportunity to work with him. I personally believe that his constant encouragement, invaluable support, and endless patience were the principal keys to my success. He has been everything that one could want in an advisor.

I would also like to express my sincere gratitude to my committee members, Dr. Gary A. Pope, Dr. Mojdeh Delshad, Dr. Kishore Mohanty, and Dr. Eric DeRouffignac. I really appreciate the time, valuable comments, and feedback of my committee.

Dr. Mojdeh Delshad and Dr. Eric DeRouffignac must be acknowledged for their invaluable technical supports and contributions in this research project. I would also thank to Dr. Chowdhury Mamun for grammatical and technical review and helpful comments on my dissertation. I would like to extend my appreciation to Dr. Larry Lake for long discussion and sound suggestions on the four-phase compressible and real mixture flow formulation.

I would like to acknowledge the staff of the Petroleum and Geosystems Engineering Department at The University of Texas at Austin, Dr. Roger Terzian, Jouhn, John Cassibry, Joanna Castillo, Cheryl Kruzie, Frankie Hart, and Mary Pettengill for their technical and administrative support.

I am indebted to many of my friends and colleagues who through their sincere suggestions and fruitful discussions shaped this dissertation in so many ways. Without

their support, this important research would not be possible. In particular, I would like to thank Dr. Jean-Philippe Nicot for giving some ideas on compositional model and phase behavior of gas, Dr. Abdoljalil Varavei for description of UTCHEM and technical discussion, Mohammad Lotfollahi in helping on the four-phase relative permeability model, Aboulghasem Kazemi Nia for technical discussion, Mojtaba Ghasemi for helping in use of the solvers, Ali Goudarzi for related technical discussion, Walter Fair for discussion on blackoil model, Wei Yu for related technical discussion, Masoud Behzadei Nasab for implementation of steam table, and Elif Ozdingis for running and reporting the bugs of code. I am also very grateful to my friends Mohammad Reza Beigi, Reza Tavakoli, Seyyed Abolfazel Hosseini, Mahdy Shirdel, Ehsan Saadatpoor, Amir Reza Rahmani, Reza Ganjedanesh, Sergio Jose Cavalcante Filho, Shayan Tavassoli, Emad Al-Shalabi, Mahmood Shakiba, Ali Abouie, Yifei Xu, and many other friends that I have not mentioned their names for all their support and making my life so pleasant during these years.

The work presented in this dissertation was funded by the sponsors of the Reservoir Simulation Joint Industry Project (RSJIP) at the Center for Petroleum and Geosystems Engineering at The University of Texas at Austin.

Finally, I would like to extend my appreciation to my wife, Maryam Shafiekhani, and my parents for their love, patience, understanding, and encouragement towards my achievements.

December 2014

Abstract

Development of a Four-Phase Thermal-Chemical Reservoir Simulator for Heavy Oil

Hamid Reza Lashgari, Ph.D
The University of Texas at Austin, 2014

Supervisor: Kamy Sepehrnoori

Thermal and chemical recovery processes are important EOR methods used often by the oil and gas industry to improve recovery of heavy oil and high viscous oil reservoirs. Knowledge of underlying mechanisms and their modeling in numerical simulation are crucial for a comprehensive study as well as for an evaluation of field treatment. EOS-compositional, thermal, and blackoil reservoir simulators can handle gas (or steam)/oil/water equilibrium for a compressible multiphase flow. Also, a few three-phase chemical flooding reservoir simulators that have been recently developed can model the oil/water/microemulsion equilibrium state. However, an accurate phase behavior and fluid flow formulations are absent in the literature for the thermal chemical processes to capture four-phase equilibrium. On the other hand, numerical simulation of such four-phase model with complex phase behavior in the equilibrium condition between coexisting phases (oil/water/microemulsion/gas or steam) is challenging. Inter-

phase mass transfer between coexisting phases and adsorption of components on rock should properly be modeled at the different pressure and temperature to conserve volume balance (e.g. vaporization), mass balance (e.g. condensation), and energy balance (e.g. latent heat).

Therefore, efforts to study and understand the performance of these EOR processes using numerical simulation treatments are quite necessary and of utmost importance in the petroleum industry. This research focuses on the development of a robust four-phase reservoir simulator with coupled phase behaviors and modeling of different mechanisms pertaining to thermal and chemical recovery methods. Development and implementation of a four-phase thermal-chemical reservoir simulator is quite important in the study as well as the evaluation of an individual or hybrid EOR methods.

In this dissertation, a mathematical formulation of multi (pseudo) component, four-phase fluid flow in porous media is developed for mass conservation equation. Subsequently, a new volume balance equation is obtained for pressure of compressible real mixtures. Hence, the pressure equation is derived by extending a black oil model to a pseudo-compositional model for a wide range of components (water, oil, surfactant, polymer, anion, cation, alcohol, and gas). Mass balance equations are then solved for each component in order to compute volumetric concentrations. In this formulation, we consider interphase mass transfer between oil and gas (steam and water) as well as microemulsion and gas (microemulsion and steam). These formulations are derived at reservoir conditions. These new formulations are a set of coupled, nonlinear partial differential equations. The equations are approximated by finite difference methods implemented in a chemical flooding reservoir simulator (UTCHEM), which was a three-

phase slightly compressible simulator, using an implicit pressure and an explicit concentration method.

In our flow model, a comprehensive phase behavior is required for considering interphase mass transfer and phase tracking. Therefore, a four-phase behavior model is developed for gas (or steam)/ oil/water /microemulsion coexisting at equilibrium. This model represents coupling of the solution gas or steam table methods with Hand's rule. Hand's rule is used to capture the equilibrium between surfactant, oil, and water components as a function of salinity and concentrations for oil/water/microemulsion phases. Therefore, interphase mass transfer between gas/oil or steam/water in the presence of the microemulsion phase and the equilibrium between phases are calculated accurately.

In this research, the conservation of energy equation is derived from the first law of thermodynamics based on a few assumptions and simplifications for a four-phase fluid flow model. This energy balance equation considers latent heat effect in solving for temperature due to phase change between water and steam. Accordingly, this equation is linearized and then a sequential implicit scheme is used for calculation of temperature.

We also implemented the electrical Joule-heating process, where a heavy oil reservoir is heated in-situ by dissipation of electrical energy to reduce the viscosity of oil. In order to model the electrical Joule-heating in the presence of a four-phase fluid flow, Maxwell classical electromagnetism equations are used in this development. The equations are simplified and assumed for low frequency electric field to obtain the conservation of electrical current equation and the Ohm's law. The conservation of electrical current and the Ohm's law are implemented using a finite difference method in a four-phase chemical flooding reservoir simulator (UTCHEM). The Joule heating rate

due to dissipation of electrical energy is calculated and added to the energy equation as a source term.

Finally, we applied the developed model for solving different case studies. Our simulation results reveal that our models can accurately and successfully model the hybrid thermal chemical processes in comparison to existing models and simulators.

Table of Contents

List of Tables

List of Figures

Chapter 1: Introduction

In this chapter, we explain the problem statement and then describe the scope of this dissertation and the main objectives pursued and achieved in this research. In addition, we describe the structure and the different chapters of the dissertation.

1.1 PROBLEM DESCRIPTION

Heavy oil reservoirs are considered future alternative resources for fuel energies. In October 2009, United States Geological Survey (USGS) reported that the heavy oil resources around the world are more than twice the conventional light oil. However, recovery rates from heavy oil reservoirs are often limited to 5 to 30 percent of the original oil in place (Dusseault, 2001).The reason behind such a low oil recovery is mainly due to the high viscosity, and high density (API gravity less than 20) which make the production of that oil a challenge. On the other hand, the relatively shallow depth of heavy oil fields can contribute to lower production costs. Several enhanced oil recovery methods (EOR) are used to improve oil production from heavy oil reservoirs. These include thermal methods such as steam flooding, cyclic steam stimulation, Steam Assisted Gravity Drainage (SAGD), and electrical heating; as well as non-thermal methods such as cold production with sand, solvent flooding, and chemical flooding. Thermal and chemical methods are the more efficient methods boosting the recovery from such these reservoirs.

Chemical enhanced oil recovery processes (e.g. surfactant) are important EOR methods often used by the oil and gas industry to improve recovery of a wide range of conventional light to heavy oil reservoirs. The knowledge of underlying mechanisms and their modeling in numerical simulation are crucial for a comprehensive study as well as for an evaluation of field treatment. New computing techniques including fluid flow models, phase-behavior calculations, linear solvers, and numerical approximations enable

numerical reservoir simulators to perform accurately the modeling of multiphase flow model in pours media.

EOS compositional and black oil reservoir simulators can handle gas/oil/water equilibrium for a compressible multiphase flow. In addition, only few three-phase chemical flooding reservoir simulators that have been recently developed can model oil/water/microemulsion equilibrium state as well (Nelson and Pope, 1978; Delshad et.al., 1996). However, an accurate phase behavior and fluid flow formulations are absent in the literature for the chemical processes to capture a four-phase equilibrium. The existing simulators can handle gas/oil/water equilibrium for a compressible multiphase flow (Odeh, 1981; Acs *et al.,* 1985; Watts, 1986; Coats *et al.,* 1998; Cao and Aziz, 2002; Rezaveisi *et al.,* 2013).

Chemical flooding phase behavior ought to be thoroughly modeled at reservoir conditions to evaluate the performance of surfactant flooding in the presence of live oil (i.e. solution gas) in oil at reservoir temperature and pressure. Most laboratory studies have been reported the effect of solution gas on the microemulsion phase behavior for different oils (Nelson, 1983 and Bourrel *et al.,* 1987). Several experimental studies report a decrease in the optimum salinity when gas (methane) is added to crude oil (Puerto and Reed, 1983; Roshanfekr *et al.,* 2009; Southwick *et al.,* 2012, Sagi *et al.,* 2013). But, Cottin *et al.* (2012), Jang *et al.* (2014) reported a slight increase in optimum salinity for the live oil compared to dead oil. However, the main challenge in the modeling of such process in the presence of solution gas and free gas is absence of a comprehensive flow and mass-transport formulation for flow of compressible and real mixture. In addition, an accurate phase behavior is the absent in the literature for the chemical processes to capture four-phase equilibrium. On the other hand, numerical simulation of such four-phase model with complex phase behavior in the equilibrium condition between

coexisting phases (oil/water/microemulsion/gas) is challenging. Inter-phase mass transfer between coexisting phases and adsorption of components on rock should properly be modeled at different pressure and temperature to conserve volume balance (e.g. vaporization), mass balance (*e.g.* condensation), and energy balance (*e.g.* latent heat).

UTCHEM (University of Texas Chemical flooding Simulator) is a multicomponent and multiphase model of chemical flooding processes; it accounts for complex phase behavior, chemical and physical transformations properties. The solution scheme is analogous to IMPES, where pressure is solved implicitly, but concentrations rather than saturations are then solved explicitly (IMPEC). The complex phase behavior of micellar fluids as a function of surfactant, alcohol, oil, and aqueous components was developed earlier and has been extensively verified against enhanced oil recovery experiments. Generalizations by Saad(1989), Bhuyan *et al.* (1990), Kim(1995), Delshad *et al.*(1998) have extended the model to include other chemical and physical processes. The flow and mass-transport equations are solved for any number of components (water, oil, surfactant, polymer, anion, divalent cation, alcohol, etc.) in this simulator. These components can form up to four fluid phases (air, water, oil, and microemulsion) and any number of solid minerals depending on the overall composition. Microemulsion phase forms only above the critical micelle concentration of the surfactant. This phase is a thermodynamically stable mixture of water, surfactant, and oil components. This simulator has been successfully tested and validated against laboratory measurements and history-matching purposes of observed field data (Goudarzi *et al.,* 2012; Goudarzi *e*t *al*., 2013; Korrani,2013; Taghavifar *et al*., 2014; Lashgari *et al.,* 2014a; Tavassoli *et al.,* 2014).

Fluid flow and mass-transport formulations are valid only for slightly compressible flow as well as ideal mixture flow and the reason UTCHEM cannot model

the presence of gas phase. Meanwhile, the mass-transfer between oil and gas cannot be considered in original formulation of UTCHEM (2011) as shown in Table 1-1. Although, this simulator has four-phase (air/water/oil/microemulsion) flow capability, equilibrium condition of this simulator is calculated only for three phases (oil/water/microemulsion) using Hand's rule.

Patacchini *et al.* (2013) presented a four phase fully implicit simulation in the presence of surfactant using EOS base and hand's rule. Lashgari *et al.* (2014b) presented a steam-surfactant-foam model by considering four-phase flow (steam/oil/water /microemulsion) in equilibrium to reveal the efficiency of hybrid thermal-chemical method in improvement of recovery from heavy oil reservoirs (Lashgari *et al.,* 2014a; Lashgari *et al.,* 2014b).

In this paper, a mathematical formulation of multi (pseudo) component, four-phase fluid flow in porous media is developed for mass conservation equation. A new volume balance equation is subsequently obtained for pressure of compressible and real mixture flow. Hence, the pressure equation is derived by extending a black oil model to a compositional model for a wide range of components (water, oil, surfactant, polymer, anion, cation, alcohol, and gas). Mass transport equations are then solved for each component in order to compute volumetric concentrations. In this formulation, we consider interphase mass transfer between oil and gas as well as microemulsion and gas at reservoir conditions. These new formulations are a set of coupled, nonlinear partial differential equations. The equations are approximated by finite difference methods and then implemented.

In the developed flow and mass transport model, a comprehensive phase behavior is required for considering interphase mass transfer and phase tracking. Therefore, a four-phase behavior model is developed for gas/oil/water/microemulsion coexisting at

equilibrium as shown in Table 1-2. This model represents coupling of the solution gas method with Hand's rule used to capture the equilibrium of surfactant, oil, and water components as a function of salinity and concentrations for oil/water/microemulsion phases. Therefore, both interphase mass transfer between gas/oil or steam/water in the presence of the microemulsion phase and the equilibrium between phases are calculated accurately. Finally, we applied the developed model for solving different case studies.

Table 1-1-The mass transfer of components among phases in original UTCHEM.

Comp. / **Phase**	**Water** (c_1)	**Oil** (c_2)	**Surfactant** (c_3)	**Polymer** (c_4)	**Anions** (c_5)	**Cation** (c_6)	**Alcohol** (c_7)	**Air** (c_8)
Water *(l*=1*)*	1	0	1	1	1	1	1	0
Oil (*l*=2)	0	1	0	0	0	0	0	0
ME (*l*=3)	1	1	1	1	1	1	1	0
Air (*l*=4)	0	0	0	0	0	0	0	1

Table 1-2-The mass transfer of components among phases in the developed four-phase UTCHEM (The goal of this research).

Comp. / **Phase**	**Water** (c_1)	**Oil** (c_2)	**Surfactant** (c_3)	**Polymer** (c_4)	**Anions** (c_5)	**Cation** (c_6)	**Alcohol** (c_7)	**Gas** (c_8)
Water *(l*=1*)*	1	0	1	1	1	1	1	0
Oil (*l*=2)	0	1	0	0	0	0	0	1
ME (*l*=3)	1	1	1	1	1	1	1	1
Gas (*l*=4)	0	0	0	0	0	0	0	1

A better understanding of the complex displacement mechanisms and the physics are required to improve recovery from heavy oil reservoirs. In the literature the incomplete understanding of these mechanisms is considered as the main gap and to be a major importance. This lack of understanding causes devaluing the heavy oil reservoirs as a producible source of oil reserves.

Thermal and chemical recovery processes are the most important EOR methods used widely by the oil and gas industry to improve recovery of heavy oil and unconventional oil reservoirs. Knowledge of involving mechanisms and their modeling in numerical simulation are crucial for comprehensive study as well as evaluation of field treatment. EOS-compositional, thermal, and blackoil reservoir simulators can handle gas (or steam)/oil/water equilibrium for a compressible multiphase flow. Also, a few three-phase chemical flooding reservoir simulators that have been recently developed by the University of Texas at Austin can only model oil/water/microemulsion equilibrium state. Since this simulator can only model slightly compressible fluid flow with considering ideal mixture (no mass transfer between phases), in the cases of gas or steam injection the results of this simulator is not acceptable. As shown in Figure 1-1, original UTCHEM functions with gas injection as slightly compressible without solution gas effect. Therefore pressure wrongly increases in this model and results are not accurate for compressible flow and real mixtures.

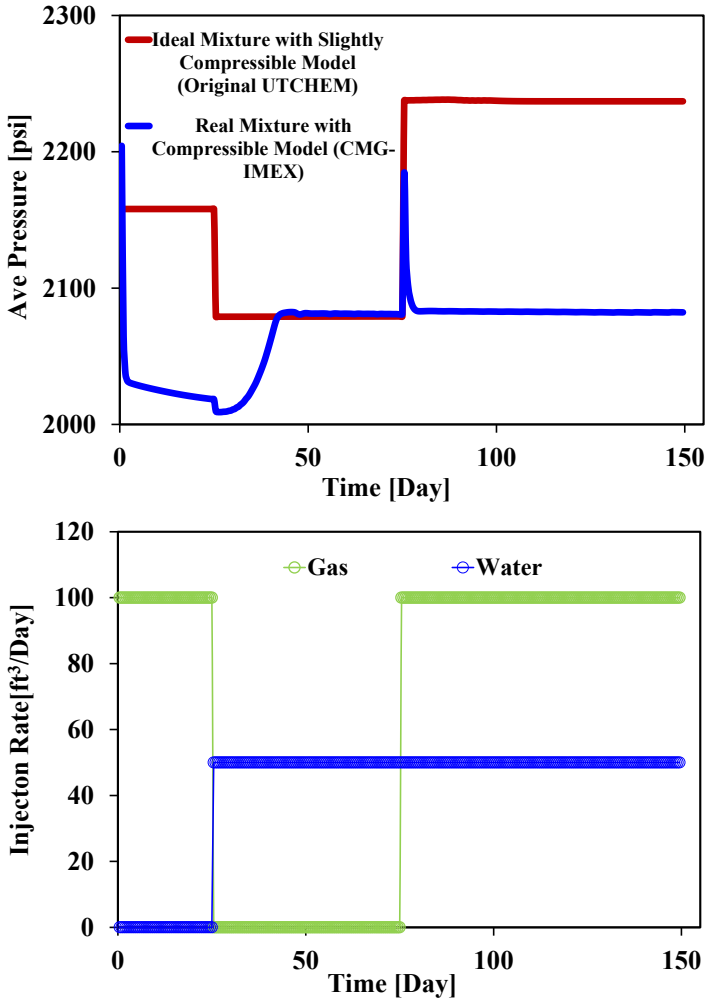

Figure 1-1-Comparison of average pressure of a case with gas and water injection in original UTCHEM (slightly compressible without solution gas effect) and CMG-IMEX.

However, an accurate phase behavior and fluid flow formulations are absent in the literature for the thermal chemical processes to capture four-phase equilibrium. On the other hand, numerical simulation of a nonlinear four-phase thermal-chemical simulator equations in the presence of complex phase behavior to model the equilibrium condition between coexisting phases (oil/water/microemulsion/gas or steam) are really challenging. Interphase mass transfer between coexisting phases and adsorption of

components on rock should be properly model at the different pressure and temperature to conserve volume (e.g. vaporization), mass (e.g. condensation), and energy (e.g. latent heat).

Therefore, efforts to study in understanding of the performance of such these EOR processes using numerical simulation treatments are very necessary and importance to the petroleum industry.

Comprehensive numerical simulation study for heavy oil reservoirs can be a major factor in understanding production rates and reducing production costs. Existing numerical simulators only can model three-phase flow models with limited involving mechanisms, which are mostly presented in the literature and they do not emphasize the importance of comprehensive study of a thermal-chemical EOR method thoroughly. Capturing mechanisms properly and determining the optimal production rates, energy injection rates, well spacing, well configuration, and the other related parameters can make the recovery process feasible or unfeasible from a technical and an economic point of view by using a comprehensive four-phase reservoir simulator.

1.2 RESEARCH OBJECTIVE

This research focuses on development of a robust four-phase reservoir simulator with coupled phase behaviors and modeling of different mechanisms existing in thermal and chemical recovery methods.

Development and implementation of a four-phase thermal chemical reservoir simulator is presented in this study to enable UTCHEM simulator, or any such simulator, for evaluation of an individual or hybrid EOR methods. The goals of this dissertation are mostly development, implementation, and probing a few applications of related processes in thermal and chemical methods listed as follows:

- Development of a four-phase flow mathematical model
- Implementation of the four-phase flow.
- Coupling of solution gas phase behavior with surfactant phase behavior (Hand's rule).
- Development and implementation of an implicit thermal model.
- Development and implementation of low frequency electrical Joule heating model
- Simulation of a steam-surfactant-foam case.

1.3 REVIEW OF CHAPTERS

This dissertation describes the development and the application of a coupled thermal chemical model.

Chapter 2 reviews existing recovery methods in the literature being applied to heavy oil reservoirs. Then this chapter discusses modeling and simulation of those, as well as advantage and disadvantages of these methods and undelaying mechanisms.

In Chapter 3, a mathematical formulation of multi (pseudo) component, four-phase fluid compressible flow in porous media is developed for the mass conservation equation. Subsequently, a new volume balance equation is obtained for pressure of compressible real mixtures.

In Chapter 4, we discusses the discretization and the implementation of numerical solution of the flow equations into a chemical flooding reservoir simulator (UTCHEM), which was initially a three-phase slightly compressible simulator, using an implicit pressure and an explicit concentration method.

In Chapter 5, a comprehensive coupled phase behavior model is presented for considering interphase mass transfer and phase tracking for a four-phase flow model with gas (or steam)/ oil/water /microemulsion coexisting at equilibrium.

In Case 6, several test cases are run by the four-phase developed model. Results are validated and compared against the existing three-phase models (original UTCHEM and CMG-IMEX). A case with four phases is then simulated and investigated to show the performance of the developed model. Chapter 7 describes the derivation of the conservation of energy equation from the first law of thermodynamics based on a few assumptions and simplifications for a four-phase fluid flow model. This equation is linearized; a sequential implicit scheme is subsequently used for calculation of temperature. In addition, a few test cases are simulated in our code and then results are validated against CMG-STARS.

Chapter 8 describes the electrical Joule-heating process developed and implemented into the UTCHEM simulator in order to improve recovery of heavy oil reservoirs. In Chapter 9, an application of a thermal-chemical process, which is steam-surfactant-foam, is modeled to compare the different mechanisms, including oil solubilization in microemulsion phase, mobility control, and oil viscosity reduction. In Chapter 10, we present the summary of the dissertation and the concluding remarks. Finally, we recommend the tasks that can be accomplished for further developments.

Chapter 2: Background and Literature Review

In this chapter, we briefly present the overview and summary of the main related papers in the recovery methods using for heavy oil reservoirs. These methods are cold production, water flooding, thermal flooding, and chemical flooding. The first order and major mechanisms are discussed in different methods. A detail literature study has been done on this subject.

2.1 LITERATURE REVIEW

Heavy oil reservoirs are one of the promising resources of energy around the world providing an interesting situation for economic development. Heavy oils are often in high permeability and porosity geologically. But these types of oil reservoirs have high viscosity and density that make production more difficult. These unconventional reservoirs are laid at relatively shallow depth and this advantage could contribute to lower production costs (Mai and Kantzas, 2009). Heavy oils have been defined with less than 20 °API gravity and with viscosity more than 1000 cp (Dusseault, 2001; Memon *et al*., 2010). Essentially, molecular compositions of crude oils make the difference between viscosity and specific gravity or density of heavy and light oils. The most heavy oil reservoirs consist of unconsolidated sand formations. This issue makes it difficult to characterize fluid and rock properties (Dusseault, 2001; Memon *et al.,* 2010). Fluid and rock characterization and evaluation of heavy oils are necessary to understand optimization of production, recovery processes, and mechanisms (Memon *et al.,* 2010). Mobility and behavior of crude oil mobility during the production process are the main parameters of heavy oil (Memon *et al.,* 2010).

This part of the dissertation provides an overview of common recovery methods in the industry along with the advantages and the disadvantages of these recovery processes and their mechanisms.

2.2 COLD PRODUCTION

The production process of cold depletion (Bernard *et al.,* 1997) is a well-known primary production process for heavy oil reservoirs, whereby sand and oil are produced under primary conditions. Main drive mechanism is dissolved solution gas drive (Smith, 1988; Bernard *et al.,* 1997; Tang and Firoozabadi, 1999). This process is an isothermal process based on expansion of oil due to solution gas. In the other words, compressibility and viscosity control the oil production associated with sand. This primary cold production can be used when the viscosity of heavy oil at reservoir conditions is sufficiently low to allow high viscous oil hardly flows to the surface. However, recovery reported in some fields is between 5 to 10 percent depending on the amount of solution gas in heavy oils (Tang and Firoozabadi, 1999). Smith 1988 presented the physics behind cold production from solution gas drive in heavy oil reservoirs. He considered a pseudo-single phase model. Then, he claimed that the reasons for high recovery of solution gas drive in heavy oils are due to improvement of permeability around the well because of sand production, oil viscosity reduction during gas bubble formation and continuous oil phase flow as well as discontinuous gas phase in the form of tiny bubbles, and compressibility because of high gas bubble presence. Since compressibility with and without the presence of gas in oil is significantly different (Firoozabadi, 2001), a simple expression assumption as $c = \chi/p$ may not describe the compressibility that Smith made in 1988. He suggested that the apparent viscosity of a heavy oil with dispersed gas bubbles decreases drastically. He showed that the apparent viscosities calculated from the buildup

analysis were of the order of 1-5 poise, whereas for the same oils in single phase, the viscosities were in the 17-35 poise range.

Among other parameters, Smith (1988) used the compressibility from c =χ/p to calculate the apparent viscosity. Pooladi-Darvish and Firoozabadi (1999), Tang and Firoozabadi (1999) and Firoozabadi (2001) showed that the pressure drop across a core increases when gas bubbles form in the oil. They considered two phase model, such as the conventional two phase model, for cold production. They described two parameters (one was gas saturation and second was oil and gas relative permeabilities) to investigate the effect of compressibility and viscosity as recovery mechanisms during cold production. They assigned gas viscosity to the viscosity of the disconnected gas phase and oil viscosity to the viscosity of the continuous oil phase. In spite of the single phase assumption, an apparent viscosity is not necessary for two-phase model. They recognized that in heavy oil, viscosity is a function of rate or velocity dependent due to the viscoelastic behavior.

2.3 WATER FLOODING

The second recovery process of heavy oils is water flooding, which is an isothermal oil recovery method to produce heavy oil with relatively low viscosity (Dusseault, 2001; Mai and Kantzas, 2009). Water flood recoveries are known to be low for high viscosity oil due to the adverse mobility ratio between oil and injected water. Despite the presumed inefficiency of this process, water flooding is still commonly applied in many heavy oil fields, since it is relatively inexpensive. Also, field operators have years of experience designing and controlling water flooding in this type of reservoir.

Based on literature review (Moore and Slobod, 1955; Harley Y., 1966; Mai and Kantzas, 2009; Scott *et al.,* 1965; Harley, 1966) the mechanism of water flooding over viscous oil or heavy oil recovery in general has not been well understood. Water flooding of conventional oil reservoirs is well known as secondary recovery. Water flooding in conventional oil reservoirs deals with same order of magnitude between water and oil viscosities, but in heavy oil the story is completely different. During water flooding of light oils, capillarity controls recovery mechanism and efficiency of recovery and trapped oils are due to capillary trapping or heterogeneity of reservoir, but the residual oil in the light oil reservoir is left in place due to reservoir heterogeneities or capillary trapping. Therefore, capillary bypassing is the main mechanism responsible for trapping oil. This recovery process could not have been successful for very high viscosity heavy oil. Reasons are because of heterogeneity channelizing and hydrodynamic viscous fingering due to highly unfavorable mobility ratio that may result in very poor sweep efficiency. However, the high oil viscosity is the main cause of oil bypassing and residual oil at the end. Therefore, in general, water flooding is not expected to be successful due to poor sweep efficiency. The main benefit of this recovery method is its low expense. Consequently, this method is often employed even in some high viscosity heavy oil reservoirs, but the recoveries reported have been less than ten percent (Mai and Kantzas, 2009).

Mai and Kantzas in 2009 showed that for viscous oils, capillary forces are not negligible compared to viscous forces for low rate water injection, when viscous fingering is controlled in oil recovery. The reason behind this is that at low injection rates, water imbibition can be used to stabilize the water flood and improve oil recovery.

2.4 SOLVENT INJECTION

Solvent injection is another recovery process applied for heavy oil reservoirs. Butler and Mokrys (1989); Das and Butler (1996); Butler and Jiang (2000); Boustani and Maini (2001); Nghiem *et al.* (2001), Cuthiell *et al.* (2003); Jha (1986) have investigated the injection of solvents into heavy oils experimentally and then have modeled and simulated the behavior of solvents in the presence of heavy oil in order to improve recovery. Solvents injection recovery is controlled by different mechanisms, such as reduction of oil viscosity through molecular diffusion (Das and Butler, 1996a; Boustani and Maini, 2001; Nghiem *et al.,* 2001; Cuthiell *et al.,* 2003; Jha, 1986), swelling of the heavy oil phase (Yang and Gu, 2006) to mobilize oil (Campbell 1983). Also swelling increases oil saturation and consequently the relative permeability of the oil is increased (Yang and Gu, 2006). Reduction of interfacial tension and miscibility is another recovery mechanism during solvent injection into heavy oils.

Molecular diffusion process during solvent injection leads to a decrease oil viscosity and an increase in gas/oil interfacial area as well as interfacial instabilities (Kapadia *et al.,* 2006). The injection of solvent such as carbon dioxide (CO_2) into heavy oil reservoirs is a very common recovery method. CO_2 could be miscible or immiscible during injection to reservoir. The miscibility or immiscibility depends to reservoir condition (pressure and temperature). At a constant reservoir temperature, the pressure will define the degree of miscibility reached. The minimum pressure at which miscibility is achieved is defined as the minimum miscibility pressure (MMP). CO_2 and oil are not initially miscible at first contact. However, upon repeated contact through a kind of evaporation condensation process (Jarrel *et al.,* 2002), miscibility is achieved. The sweep efficiency depends strongly on the miscibility condition. Main mechanisms that

contribute to improved recovery when CO_2 is dissolved in oil are summarized as the following (Qamar and Islam, 2000; Jha, 1986):

- Oil viscosity reduction,
- Oil swelling, interfacial tension reduction,
- Water-oil emulsification (formation of emulsions that control the water mobility).

Qamar and Islam (2000) and Jha (1986) have reported that miscible rather than immiscible CO_2 displacement results in high recovery. Accordingly, in order to achieve above MMP to get miscible displacement, the deep reservoirs with high pressure are good target for solvent injection, where pressures are above MMP (Qamar and Islam, 2000). CO_2 injection below MMP results in an unfavorable CO_2-oil mobility ratio, which contributes to very poor heavy oil recovery because it implies poor sweep efficiency due to the viscous fingering phenomena (Sahimi, 1993). The CO_2 flooding above MMP results in the formation of a single phase that is less viscous than the initial oil phase viscosity, which improves oil mobility.

2.5 THERMAL OIL RECOVERY

Thermal recovery methods are important recovery processes in heavy oil reservoirs. Different common thermal recovery processes, such as hot water injection, steam flooding, insitu combustion, and electrical heating, have been successfully applied in some heavy oil reservoirs around the world. The effect of temperature on water viscosity is well known, and similar data are available and have been measured for heavy and light oils. Empirical formulas for the heat capacities of water, light and heavy oil are also available.

Thermal conductivities of reservoir rock and fluids, heat capacities of reservoir rocks, and the thermal conductivity of porous systems have been measured and studied. Changes in rock permeability, due to heating by steam injection, have also been measured, and some data are available in the literature on the effect of temperature on relative permeability that will be discussed in the section on wettability alteration.

The principal mechanisms of thermal processes have been identified as viscosity reduction and thermal expansion or swelling of the heavy oils. This is because most heavy oils at a relatively high temperature of around 200 ^{o}C (400 ^{o}F) have the viscosity about 1 cp (Farough Ali, 2003). Hot water injection, electrical heating, and steam injection can achieve these mechanisms. In this study, the focus area will be on steam injection and electrical heating methods. Recovery by steam is greater for lighter oils or conventional reservoir, because they contain a greater fraction of steam distillable components (Willman *et al.,* 1961). The viscosity of heavy oil reservoirs at the original pressure and temperature is significantly high. Therefore, the oil is difficult to move in the reservoir under the initial condition. Upon heating, the viscosity of the oil drops by a large amount and propels oil to move more easily (Nasr and Ayodele, 2005). Steam injection is among the thermal processes proposed successfully for heavy oil recovery because it significantly reduces the viscosity compared with hot water flooding and steam distillation. Steam distillation is defined as vaporization of a portion of the heavy oil left by hot condensate water, while it moves ahead of the steam zone. The distillable portions of the oil are the light, as opposed to the heavy, components. The mixture of steam and oil vapor resulting from the distillation is pushed ahead until a cooler portion of the rock is encountered. Then both the oil and the water vapor are condensed.

Most recently, steam injection methods and processes have been successfully applied to some heavy oil reservoirs around the world. Various existing recovery

methods have been combined with steam and then applied other process to improve the recovery and efficiency, such as cyclic steam stimulation (CSS), steam assisted gravity drainage (SAGD), expanding solvent-SAGD (ES-SAGD), solvent vapor extraction (VAPEX), electrical heating with solvent, steam-foam, steam-surfactant, and steam alkaline. These methods have significantly improved sweep efficiencies, increased oil rates, and reduced production costs (Nasr and Ayodele, 2005; Butler *et al.,* 1981; Das and Butler, 1998; Butler and Jiang, 2000). Some of major processes are discussed in the following.

2.5.1 Cyclic Steam Stimulation (CSS)

In cyclic steam stimulation (CSS) recovery process, steam at high temperatures is injected under high pressure into heavy oil reservoirs for a while and then the well is shut. After soaking time, the same well is placed on production. The injected steam is exposed to the reservoir and the heat reduces the viscosity of the oil, and the heated oil is then produced from the same well.

Soak time is usually short, less than one week. During this process, the injected steam period depends on the injectivity of well and cold oil viscosity. But the oil production rate in any cycle depends on heterogeneity, geological connectivity, solution gas and gas cap, bottom water zone or aquifer, initial water saturation and residual oil saturation at end of each cycle, heat lost rate, steam injectivity and oil productivity, injected steam rate, and thermal properties of fluids and rock. The main advantage of this process, compared to steam flooding, is less heat loss, applicable for poor connectivity of reservoir and quick oil production (Farouq Ali S.M. and Meldau, 1979; Beattie *et al.,* 1991).

2.5.2 Steam Flooding

Steam flooding as a process of in-situ thermal recovery has been used for some heavy oil fields successfully. This process involves injecting steam from a vertical injection well to sweep oil towards a vertical producer similar to the conventional water flooding process. It is a pattern driven operation. The process sweeps more area as compared to the cyclic steam stimulation (CSS). It also recovers more oil than the CSS process.

The efficiency of this process also depends on heterogeneity, geological connectivity, solution gas and gas cap, bottom water zone or aquifer, initial water saturation and residual oil saturation during steam injection, heat lost rate, steam injectivity and oil productivity, injected steam rate, and thermal properties of fluids and rock. Heated oil could flow toward the production well as a result of gravity and viscous forces (Farouq Ali S.M. and Meldau, 1979). The advantage of this process is much larger area is swept by the steam than in the CSS. On the other hand, the heat loss is greater because the steam is exposed to a larger area compared to the CSS.

2.5.3 Steam Assisted Gravity Drainage (SAGD)

Another steam injection recovery method that was developed by Butler *et al.*, 1981, is steam assisted gravity drainage (SAGD). The process consists of steam injection into a horizontal injection well and a parallel horizontal producer in the same vertical plane. Steam is injected continuously into the upper horizontal well, while the oil flows down by gravity into the bottom production well. The basis of the process is that the injected steam forms a steam chamber growing vertically and laterally in the reservoir formation.

The steam heat reduces the viscosity of the heavy oil which allows it to flow down into the production well. The steam and distillated gases from heavy oils rise

because of gravity segregation to guarantee that steam is not produced at the production well. The distillated gases released, which include methane, carbon dioxide, and usually some hydrogen sulfide, tend to rise in the steam chamber. This causes filling of the void space left by the oil and formation of an insulating heat blanket above the steam. Heated oil and condensed water flows are by a countercurrent, viscous, and gravity-driven drainage into the production well. This process requires a relatively high thickness and less heterogeneity with good local connectivity around the producer and the injector.

2.5.4 Electrical Resistance Low Frequency (Joule) Heating

Steam injection is sometimes not a reliable process for heavy oil production. This might be true for a shallow reservoir due to heat lost across reservoir or deep reservoirs due to high heat lost along wellbore (Bogdanov *et al.,* 2011). A thermal method, electrical low frequency heating of the reservoir was presented by Amba *et al.* (1964) to overcome these above disadvantages. Electrical heating is a thermal recovery process that passes electrical current through fluids of reservoir. The flow of electrical current through reservoir leads to heating the reservoir and thereby reduces oil viscosity. In this process, the reservoir rock and fluid are used as electrical resistance elements (Hiebert *et al.,* 1986).

The amount of electrical heating depends on the frequency of the electrical current, since polar molecules tend to align and relax with the alternating electric field. The molecular movement may result in significant heating (Rangel-German *et al.,* 2004). Essentially, rock does not have enough electrical conductivity. Therefore, for electrical current to be able to pass through porous media to generate heat, one of liquid phases should be continuous and conductible. The conducting path for electrical current is normally through the continuous brine phase. Electrical energy is converted to heat along

these pathways in the brine and the heat is transferred to the oil by thermal conduction. Due to the large surface area between the water films, oil, rock particles, the heat transfer occurs rapidly. This process has been applied in heavy oil reservoirs and has been reported in most cases to be successful in near well area. Applications of electric heating can mainly be valuable in cases where steam injection cannot be functional due to a deep reservoir, low injectivity and productivity, high heat loss rate, existence of thief zones, and high water saturation (McGee and Vermeulen, 2007).

In fact, the water saturation and electrical conductivity of this phase have an important effect on the heating process. The reason is that the electrical conductivity of water phase is relatively high compared to rock, oil, and gas phases. The electrical conductivity of water phase can also be easily increased by injecting high saline water into the reservoir to increase heating substantially. This is incredibly beneficial and the main advantage of electrical heating mechanism is to obtain high recovery in comparison to steam flooding. Since steam is roughly a non-conductible electrically phases, operation of this process can be designed to keep temperature below the boiling point to avoid evaporation.

The efficiency of this process depends on heterogeneity, geological connectivity, solution gas and gas cap, bottom water zone or aquifer, initial water saturation and residual oil saturation during operation. It also depends on the amount of heat-loss in overburden and upper burden as well as inside of the reservoir productivity and the thermal and electrical properties of fluids and rock.

2.5.5 Thermal Effect on Geomechanics

Steam flooding might lead to a change in permeability for low temperature of shallow heavy oil reservoirs, as reported by Benzagouta and Amro (2009). However,

typically temperature that induced stress changes are near-wellbore phenomena as permeability is less sensitive at high reservoir temperature (> 60 ºC) (Sanyal *et al.,* 1974; Muralidharan *et al.,* 2005; Ferno *et al.,* 2010). Cyclic Steam Stimulation (CSS) and SAGD are the current leading thermal process for heavy oil unconsolidated sand reservoirs. SAGD increases reservoir pressures and temperatures sufficiently to cause shear failure within and beyond the growing steam chamber in oil sands. This shear failure results increase in bulk volume, a phenomenon called "dilation" that it causes aincrease in permeability. This increase in permeability of oil sands can reach up to ten-fold of the original vertical permeability (Collins, 2007; Yale *et al.,* 2010). The direction of steam chamber propagation is dictated by the stresses acting on the rock matrix that is a function of the reservoir depth and the tectonic loading. According to a study by Collins (2007), SAGD would be more efficient if steam is injected at higher rates resulting in shear failure and improved permeability. Hence, detailed geomechanical study could help in determining an optimal steam injection rate to improve recovery by increasing permeability.

2.6 CHEMICAL FLOODING

Chemical flooding is a promising recovery method for heavy oil reservoirs. Heavy oils have low mobility because of high viscosity and very low relative permeability. As a result, the mobility ratio would be unfavorable in a water displacement process. Chemical flooding can improve recovery in two ways: first, the oil-water interfacial tension would be lowered, resulting in lower residual oil saturation despite an inefficient displacement; and second, the low IFT would support the formation of an emulsion phase, and this makes the effective mobility ratio less unfavorable. Many heavy oil reservoirs would lose significant thermal energy due to thin formation thickness and

due to shallow depth injected gas would be below MMP; thus, miscible processes would not be applicable. Under these conditions, solvent flooding and cold production may be useful to increase recovery properly. Polymer, alkaline, and surfactant flooding methods are more important methods to improve the mobility of heavy oils and reduce the oil viscosity. Other chemical flooding methods rely on combinations of the above methods as hybrid processes.

Chemical injection methods might overcome most of the above mentioned disadvantages. This is because of no heat loss, applicability for low initial pressure, and gas solution. Polymer, Surfactant- Polymer (SP), Alkali-Polymer (AP) and Alkali-Surfactant-Polymer (ASP) are different methods that can be selected based on the rock and fluid reservoir characteristics. Mineralogy, permeability contrast, heterogeneity, initial and residual oil saturation, oil viscosity, pH, temperature, salinity, hardness, reservoir pressure, oil composition, solution gas, and total acid number (TAN) are the major factors in chemical flooding (Pope and Nelson, 1978; Pope *et al.,* 1978; Delshad *et al.,* 1996; Kazemi Nia *et al.,* 2014; Tavassoli 2014; Taghavifar *et al.,* 2014). The main mechanisms for recovery are due to lower oil-water interfacial tension, the same as conventional oil reservoirs. Alternatively, the formations of water-in-oil (W-O) emulsion phase and oil-in-water (O-W) emulsion phase have been reported as possible recovery mechanisms. The W-O emulsion phase often has almost the same viscosity as oil. Consequently, the mobility ratio should be enhanced to obtain a more favorable displacement and improve the sweep efficiency of the flood.

The formation of W-O emulsion also can increase the resistance to water phase flow in water channels or viscous fingers. It diverts the injected water to un-swept regions and improves oil recovery. Therefore, W-O emulsions could provide a significant reduction in water phase relative permeability. By considering the emulsion phase as a

separated phase, this phase can be assigned a small exponent and an endpoint of relative permeability. In the O-W emulsion phase(where oil is emulsified into water) the oil droplets either plug rock pores to improve sweep efficiency, or entrained along with the flowing aqueous phase (Bryan and Kantzas, 2007; Liu *et al.,* 2007; Dong *et al.,* 2009).

In heavy oil reservoirs, a trapping mechanism during water flooding and the resulting immobility of oil are due to high viscosity and instability or hydrodynamic or viscous fingerings. This is because of a high unfavorable or adverse mobility ratio between displaced and displacing fluids. Consequently, chemical flooding improves the mobility ratio and then makes a more stable displacement of oil since the emulsion phase forms under conditions of shear and low interfacial (Wang and Dong, 2009).

2.6.1 Alkaline-Surfactant Steam-Foam Flooding

One of the combination of thermal and chemical (hybrid) recovery methods is the steam- surfactant-foam process that was proposed by Needham (1968). He described a process to plug a high permeability zone to divert steam into a low permeability zone and control gravity override due to gravity segregation. Therefore, the application of steam foam was developed to control the mobility in order to improve the sweep efficiency (Hiraski 1989a; Patzek 1996; Lashgari *et al.,* 2014a). Steam injection that is unstable by gravity can have a poor vertical sweep efficiency due to gravity overlay in a thick high permeability layer and poor areal sweep efficiency in high permeability channels with high conductivity. The pressure gradient in the steam swept region is increased due to reduction of mobility of steam foam. This leads to displacing the heated oil better and to divert the steam to cold places (Hiraski 1989b; Patzek and Myhill 1989).

Alkaline and Surfactants lower the steam mobility by stabilizing the liquid lamellae that cause some or all of the steam to exist as a discontinuous phase. The

propagation of the surfactant is retarded by adsorption. In the case of ion exchange of divalent ions from the clays, the surfactant is also retarded by precipitation and/or partitioning into the oil. The rate of propagation of foam is also determined by mechanisms that generate and destroy foam. The generation mechanisms include leave-behind, snap-off, and division. The destruction mechanisms include condensation and evaporation, coalescence by a limiting capillary pressure, and coalescence resulting from the presence of oil. The foam texture can be predicted from a population balance that includes these mechanisms.

2.6.2 Modeling of Emulsion Viscosity

Numerical modeling the chemical flooding for heavy oil recovery is far from satisfactory in the literature. Unlike the case of conventional oil, ultra-low oil and water interfacial tension is not always the dominant mechanism during alkaline and /or surfactant flooding for heavy oils. The dominant mechanism is emulsification, which have not been thoroughly investigated in the literature. Since high viscosity and small relative permeability of heavy oil make it to be low mobility but chemical flooding, as mentioned in the previous section, leads to form emulsion. Emulsification has low viscosity compared to oil and high viscosity compared to water. Therefore, emulsification makes the effective mobility ratio less unfavorable. Based on implementation of emulsion viscosity in the first task, we have to observe that the emulsion lowers the mobility of the displacing fluid through drop entrainment and entrapment processes.

In the literature, there are three theories describing the viscosity of emulsion in porous media:

- The homogenous model
- The droplet retardation model

- The filtration model

The simple viscosity model was proposed by Alvarado and Marsden (1979) in which emulsion was considered as a homogeneous, single-phase fluid. This model was suitable for the description of the flow of emulsions with smaller drop-size to pore-size ratio, where the flow could reach steady state quickly. Abou-Kassem and Farouq Ali (1995) modified the viscosity model to describe both Newtonian and non-Newtonian fluids. The modified model quantitatively describes the effect of pore size distribution and tortuosity of porous media on flow.

McAuliffe (1973) proposed a droplet retardation model for describing the flow of stable O-W emulsions in porous media. In this model, the dispersed drops flow slower than the continuous phase, because a capillary retarding force is encountered when the drops are flowing through pore throats smaller than drops themselves. The retardation model can arrive at larger permeability reduction with lower flow rate and higher drop size-to-pore size ratio; however, it cannot predict the permanent permeability reduction observed in laboratory.

Schmidt *et al.* (1984) proposed a model for emulsion entrapment process and they assumed that the flow should be stable. In this model, dispersed drops can be captured in pores by both straining and interception, resulting in permeability reduction.

Chapter 3: Four-Phase Fluid Flow Model

In this Chapter, a mathematical formulation of multi (pseudo) component, four phase fluid flow in porous media is developed. A new volume balance equation is subsequently obtained for pressure of compressible real mixtures. Hence, the pressure equation is derived by extending a blackoil model to a pseudo-compositional model for a wide range of components (water, oil, surfactant, polymer, anion, cation, alcohol, and gas). Mass balance equations are then solved for each component in order to compute volumetric concentrations.

3.1 BASIC ASSUMPTION

The following assumptions have been made in developing the mathematical model in this research:

- Permeability tensor is orthogonal and aligned with the coordinate system
- Fluid flow is characterized by Darcy's law for multiphase flow.
- Physical dispersion follows a generalization of Fick's law for four phase flow in porous media.
- Slightly compressible for rock formation is considered.
- The model permits a maximum of four phases to coexist as microemulsion/oil /water/gas or steam.
- Local equilibrium exists between surfactant/oil/water and oil/gas (water/steam) except for specified chemical reactions.
- Only gas component (either hydrocarbon or steam) can exist in the gas phase.
- Geomechanical effect on fluid dynamics is neglected.

3.2 MASS CONSERVATION EQUATION

In this section, a new mathematical formulation for multi (pseudo)component, four phase fluid flow in porous media is presented for simulation of thermal and chemical flooding processes. The multi (pseudo) component, four-phase flow in porous media occurs during transport of chemical species in multiple homogenous phases under the influence of viscous, gravity, and capillary forces. The mass conservation equations and the pressure equation are derived for four compressible phases with several components. These four phase fluids including water (***l=1***), oil (***l=2***), microemulsion (***l=3***) and gas or steam ***(l=4***) as compressible fluids with pseudo-components including water (***h=1***), oil (***h=2***), surfactant (***h=3***), polymer (***h=4***), total anion (***h=5***), total divalent cations (***h=6***), alcohol (***h=7***), and gas (***h=8***). The general mass conservation equation for component ***h*** can be written as

$$\frac{\partial w_h}{\partial t} + \vec{\nabla} \bullet \vec{F}_h - R_h = 0 \qquad\qquad h = 1,..,n_c \tag{3-1}$$

In the accumulation term, w_h is the overall mass concentration of component ***h***, including both the total mass of component ***h*** in the flowing and stationary phases (adsorbed on the rock surface):

$$w_h = \phi(1 - \sum_{h=1}^{n_c} \hat{c}_h) \sum_{l=1}^{n_p} \rho_l S_l w_{hl} + (1-\phi)\rho_G \hat{w}_h \tag{3-2}$$

where $\phi(1 - \sum_{k=1}^{n_c} \hat{c}_h)$ represents reduction in pore volume due to adsorption, $\hat{c}_h$ is the volume concentration of concentration ***h*** adsorbed per unit pore volume and, $\hat{w}_h$ is the mass of component ***h*** on the rock surface per unit mass of rock, ρ_l is the density of

phase l, S_l is the saturation of phase l, and w_{hl} is the mass fraction of species h in phase l. We can easily define a relationship for $\hat{c}_h$ and $\hat{w}_h$ as

$$(1-\phi)\rho_G \hat{w}_h = \phi \rho_h \hat{c}_h \tag{3-3}$$

where ρ_h is the density of component h. Also, the concentration of component h in phase l denoted by c_{hl}, in the unit of volume fraction, can be defined as

$$c_{hl} = \frac{w_{hl}\rho_l}{\rho_h} \tag{3-4}$$

We substitute Equations (3-3) and (3-4) in Equation (3-2), the following expression is obtained

$$w_h = \phi(1-\sum_{h=1}^{n_c}\hat{c}_h)\sum_{l=1}^{n_p}\rho_h S_l c_{hl} + \phi\rho_h\hat{c}_h \tag{3-5}$$

We assume that the density of component h is the same in all the phases except the gas component, which only exist in the gas phase. Therefore, the above equation can be written as

$$w_h = \phi\rho_h\left[(1-\sum_{h=1}^{n_c}\hat{c}_h)\sum_{l=1}^{n_p}S_l c_{hl} + \hat{c}_h\right] \tag{3-6}$$

This expression is valid for the gas component as well. The reason is that the only component that can exist in the gas phase is the gas component; therefore, the density of gas component can be same as the gas phase. As known and defined, c_h is the total volume of component h per unit fluid volume as the total concentration and $\tilde{c}_h$, is overall volume of component h per unit pore volume is defined as

$$\tilde{c}_h = \left[(1 - \sum_{h=1}^{n_c} \hat{c}_h) c_h + \hat{c}_h \right] \tag{3-7}$$

Therefore, overall mass concentration w_h can be written as

$$w_h = \phi \rho_h \tilde{c}_h \tag{3-8}$$

The flux term $\vec{F}_h$ in Equation (3-1) is the sum of mass flux of component h in all the flowing phases. This flux consists of a convection term determined by the supercritical phase velocity, $\vec{u}_l$ and a dispersion term demined by this dispersion tensor $\overline{\overline{D}}_{hl}$. Therefore, the flux term is expressed as

$$\vec{F}_h = \sum_{l=1}^{n_p} \vec{F}_{hl} = \sum_{l=1}^{n_p} (\rho_l w_{hl} \vec{u}_l - \phi \rho_l S_l \overline{\overline{D}}_{hl} \bullet \vec{\nabla} w_{hl}) \tag{3-9}$$

By substituting the same definitions in accumulation term, the flux term is obtained as follow:

$$\vec{F}_h = \sum_{l=1}^{n_p} \left[\rho_h c_{hl} \vec{u}_l - \phi \rho_l S_l \overline{\overline{D}}_{hl} \bullet \vec{\nabla} (\frac{c_{hl} \rho_h}{\rho_l}) \right], \qquad h = 1, ..., n_c \tag{3-10}$$

We consider and extend the dispersion part of the above equation in X, Y, and Z directions of the Cartesian coordinate system and by using the ideal mixture definition of components it can be written for the liquid phases as

$$\rho_l \nabla (\frac{c_{hl} \rho_h}{\rho_l}) = \rho_h \nabla c_{hl} \tag{3-11}$$

This equation is valid for compressible fluid, such as gas or steam, when only gas component exists in the gas phase ($\rho_{l=4} = \rho_{h=8}$). Meanwhile, in the case of high

convection, as opposed to dispersion and molecular diffusion or high Peclet number, we can assume

$$\left|\rho_l \nabla (c_{hl}\rho_h)\right| >> \frac{c_{hl}\rho_h}{\rho_l}\left|\nabla \rho_l\right| \tag{3-12}$$

or

$$\left|c_{hl}\nabla \rho_h\right| << \left|\rho_h \nabla c_{hl}\right| \tag{3-13}$$

Finally, by substituting above assumptions with equations in Equation (3-10), the flux term is defined as

$$\vec{F}_h = \sum_{l=1}^{n_p}\left[\rho_h c_{hl}\vec{u}_l - \phi\rho_h S_l \overline{\overline{D}}_{hl}\bullet\vec{\nabla}c_{hl}\right] \qquad h = 1,...,n_c \tag{3-14}$$

On the other hand, the dispersion tensor for component h in phase l can be expanded as

$$\overline{\overline{D}}_{hl} = \begin{bmatrix} D_{xxhl} & D_{xyhl} & D_{xzhl} \\ D_{yxhl} & D_{yyhl} & D_{yzhl} \\ D_{zxhl} & D_{zyhl} & D_{zzhl} \end{bmatrix} \tag{3-15}$$

The elements of $\overline{\overline{D}}_{hl}$ for multiphase, multicomponent flow in permeable media along with molecular diffusion in Cartesian coordinates on the main diagonal are given by the following expression

$$D_{xxkl} = \frac{D'_{kl}}{\tau} + \frac{\alpha_{Ll}}{\phi S_l}\frac{u_{xl}^2}{|u_l|} + \frac{\alpha_{Tl}}{\phi S_l}\left(\frac{u_{yl}^2}{|u_l|} + \frac{u_{zl}^2}{|u_l|}\right) \tag{3-16}$$

$$D_{yykl} = \frac{D'_{kl}}{\tau} + \frac{\alpha_{Ll}}{\phi S_l}\frac{u_{yl}^2}{|u_l|} + \frac{\alpha_{Tl}}{\phi S_l}\left(\frac{u_{xl}^2}{|u_l|} + \frac{u_{zl}^2}{|u_l|}\right) \tag{3-17}$$

$$D_{zzkl} = \frac{D'_{kl}}{\tau} + \frac{\alpha_{Ll}}{\phi S_l}\frac{u_{zl}^2}{|u_l|} + \frac{\alpha_{Tl}}{\phi S_l}\left(\frac{u_{xl}^2}{|u_l|} + \frac{u_{yl}^2}{|u_l|}\right) \tag{3-18}$$

where D'_{hl} is molecular diffusivity of component h in the phase l and τ is the tortuosity of reservoir formation. α_{Ll} is longitudinal dispersion coefficient of phase l. Upper and lower diagonals are given by

$$D_{xyhl} = D_{yxhl} = \frac{\alpha_{Ll} - \alpha_{Tl}}{\phi S_l} \frac{u_{xl} u_{yl}}{|u_l|} \tag{3-19}$$

$$D_{xzhl} = D_{zxhl} = \frac{\alpha_{Ll} - \alpha_{Tl}}{\phi S_l} \frac{u_{xl} u_{zl}}{|u_l|} \tag{3-20}$$

$$D_{yzhl} = D_{zyhl} = \frac{\alpha_{Ll} - \alpha_{Tl}}{\phi S_l} \frac{u_{yl} u_{zl}}{|u_l|} \tag{3-21}$$

Finally, the following mass equation can describe the mass transport of compressible pseudo-component in the porous media.

$$\frac{\partial}{\partial t}\left(\phi \rho_h (1 - \sum_{h=1}^{n_c} \hat{c}_h) c_h + \phi \rho_h \hat{c}_h \right) + \nabla \bullet \sum_{l=1}^{n_p} \left(\rho_h c_{hl} \vec{u}_l \right) - \nabla \bullet \left(\sum_{l=1}^{n_p} \phi \rho_h S_l \overline{\overline{D}}_{hl} \bullet \vec{\nabla} c_{hl} \right) = \rho_h q_h \tag{3-22}$$
$$h = 1, \ldots, n_c$$

This form of mass equation can be used for compressible pseudo-components such as gas, steam, oil, water, and surfactant occupying the portion of pore volume under any pressure. Other pseudo-components, such as anions (c_5), polymer (c_4), and cations (c_6), are not functions of pressure. These components are dissolved in the volume base component. These types of components are considered as part of mass within the volume base component. These components do not occupy volume in the porous media.

Since in this formulation, Equation of State (EOS) is not applicable, we use the solution gas approach to take care of the mass transfer between gas and oil phases. For phase behavior treatment, we need to modify transport equations or mass equation for the gas component to satisfy its mass balance. We add the solution gas part to the mass

balance equation of the gas component by adding the solution gas part to this equation. The goal is to model vaporization and condensation phenomena between oil and gas/steam on account of mass transfer in the face of change in reservoir pressure.

3.3 PRESSURE EQUATION

The four phase flow equations for the water (***l=1***), oil (***l=2***), microemulsion (***l=3***), and gas (***l=4***) system are determined by specifying the fluxes and the concentrations in the mass conservation equations. As discussed earlier, in the original formulation, the pressure equation can be obtained by summing the mass equations of components that occupy the pore volume. We use the procedure in four-phase flow formulation to solve the flow equations which required simplifying n_c equations by multiplying the component density functions in mass equations. Then, we combine all equations together with appropriate terms to have pressure as the only unknown. In this approach, the terms involving time derivatives of c_1 through c_{n_c} vanish identically and the pressure stays only unknown.

We use the mass equation of components that occupy the volume to modify for gas component for solution gas. This equation can be written as

$$\frac{\partial}{\partial t}\left(\phi\rho_h\left(1-\sum_{h=1}^{n_c}\hat{c}_h\right)c_h+\phi\rho_h\hat{c}_h\right)+\nabla\bullet\sum_{l=1}^{n_p}\left(\rho_h c_{hl}\vec{u}_l\right)=\frac{\rho_h q_h}{V_b},\qquad h=1,...,n_c \text{ and } h\neq 8 \tag{3-23}$$

This equation conserves mass for component gas under compressible flow, but only for the free gas component in each phase. Since solution gas should be conserved as well, we need to consider solution gas in Equation (3-23).

We assume that only gas can be dissolved in oil component. By assuming no gas adsorption, for gas component $\hat{c}_h = 0$ then, the total gas as free and in solution are written as

$$\frac{\partial}{\partial t}\left(\phi\rho_8 c_8 + \phi\rho_{82} c_2\right) + \nabla\bullet\left(\sum_{l=1}^{n_p}\left(\rho_8 c_{8l}\vec{u}_l + \rho_{8l} c_{2l}\vec{u}_l\right)\right) = \frac{\rho_8 q_8}{V_b} + \frac{\rho_{82} q_2}{V_b} \tag{3-24}$$

Where ρ_8 is gas component density, but ρ_{8l} is the partial mass density of gas component in phase l. In fact, partial mass density represents the amount of mass of a component per unit volume that dissolved in a phase. The more detail of partial mass density is elaborate in Chapter 5. For instance, we only consider in this implementation that gas component can be dissolved in oil phase and also it can exist as free component in gas phase. Therefore ρ_{82} is defined as the partial mass density of gas component in oil phase. This equation can address solution gas of oil component at each phase, such as microemulsion or the oleic phases. Equation (3-24) for gas component, Equation (3-23) for components that occupy the pore volume are used in the UTCHEM simulator for pressure and concentrations.

3.3.1 Accumulation Term

A glance at conservation of mass equation shows part of the complexity of the basic three-dimensional, four-phase equations. An equivalent but a much simpler in appearance form of equations that impact volume balance between fluid volumes and pore volume are convection, accumulation, and source terms as

$$\frac{\partial}{\partial t}\left(\phi\rho_h c_h\right) = -\vec{\nabla}\bullet\sum_{l=1}^{n_p}\left(\rho_h c_{hl}\vec{u}_l\right) + \frac{\rho_h q_h}{V_b} \qquad h = 1,...,n_c \text{ and } h \neq 8 \tag{3-25}$$

where V_b is the bulk volume. By using the Darcy velocity definition for phase l

$$\vec{u}_l = -\bar{\bar{K}}\lambda_{rl}\left(\vec{\nabla}p_1 + \vec{\nabla}p_{cl} - \gamma_l\vec{\nabla}h\right) \tag{3-26}$$

The phase mobility λ_{lr} is defined as the ratio of the relative permeability of a phase to its viscosity, thus

$$\lambda_{lr} = \frac{k_{rl}}{\mu_l} \tag{3-27}$$

By substituting the velocity in mass equation, conservation of mass equation can be written as

$$\frac{\partial}{\partial t}\left(\phi \rho_h c_h\right) = \vec{\nabla} \bullet \sum_{l=1}^{n_p}\left(\rho_h c_{hl} \bar{\bar{K}} \lambda_{rl} (\vec{\nabla} p_1 + \vec{\nabla} p_{cl} - \gamma_l \vec{\nabla} h)\right) + \frac{\rho_h q_h}{V_b}, \quad h = 1, ..., n_c, h \neq 8 \tag{3-28}$$

But for the gas component, mass balance is written for free gas and solution gas as follows

$$\frac{\partial}{\partial t}\left[\phi\left(\rho_8 c_8 + \rho_{82} c_2\right)\right] =$$
$$\vec{\nabla} \bullet \sum_{l=1}^{n_p}\left((\rho_8 c_{8l} + \rho_{82} c_{2l})\vec{u}_l\right) + \tag{3-29}$$
$$\frac{\rho_8 q_8}{V_b} + \frac{\rho_{82} q_2}{V_b}$$

In this equation, we assume that gas component can exist in the oil phase and the amount of solution gas in the microemulsion phase due to solubilization of oil component in this phase is also to be considered. Therefore, Equation (3-28) can be written as

$$\frac{\partial}{\partial t}\left[\phi\left(\rho_8 c_8 + \rho_{82} c_2\right)\right] =$$
$$\vec{\nabla} \bullet \sum_{l=1}^{n_p}\left((\rho_8 c_{82} + \rho_{82} c_{2l})\vec{u}_l\right) \tag{3-30}$$
$$\frac{\rho_8 q_8}{V_b} + \frac{\rho_{82} q_2}{V_b}$$

In the UTCHEM simulator, we simplify the amount of solution gas mass produced from oil component in the microemulsion and oil phase in the reservoir condition.

The procedure we use in UTCHEM to solve the flow equations requires that to combine all mass equations for components that occupy the volume such that we have only an equation remaining for the unknown pressure. We proceed by using the following right hand side for all components except gas component:

$$L_h = \frac{\partial}{\partial t}\left(\phi \rho_h c_h\right), \qquad h = 1,...,n_c, h \neq 8 \tag{3-31}$$

For gas component, the left hand side consists of dissolved gas and free gas and is obtained as

$$L_8 = \frac{\partial}{\partial t}\left[\phi\left(\rho_8 c_8 + \rho_{82} c_2\right)\right] \tag{3-32}$$

Recognizing that the component densities and the porosity are functions of pressure, we use the chain rule to expand the accumulation terms (time derivatives) of Equations (3-31) through (3-32). For all components except gas, the left hand side, the accumulation term of mass conservation can be written as

$$L_h = \phi \rho_h \frac{\partial c_h}{\partial t} + c_h \left[\phi \frac{\partial \rho_h}{\partial p} + \rho_h \frac{\partial \phi}{\partial p}\right] \frac{\partial p}{\partial t} \qquad h = 1,...,n_c, h \neq 8 \tag{3-33}$$

But for the gas component, solution gas effect should be considered. Therefore, the left hand side, the accumulation term is expanded as

$$\begin{aligned} L_8 &= \phi \rho_4 \frac{\partial c_8}{\partial t} + c_8 \left[\phi \frac{\partial \rho_4}{\partial p} + \rho_4 \frac{\partial \phi}{\partial p}\right] \frac{\partial p}{\partial t} \\ &+ \phi \rho_{82} \frac{\partial c_2}{\partial t} + c_2 \left[\phi \frac{\partial \rho_{82}}{\partial p} + \rho_{82} \frac{\partial \phi}{\partial p}\right] \frac{\partial p}{\partial t} \end{aligned} \tag{3-34}$$

Using the summation of component concentrations

$$\sum_{h=1}^{n_c} c_h = 1 \tag{3-35}$$

This equation is used to remove $\partial c_8 / \partial t$ from Equation (3-34). Differentiation of Equation (3-35) respect to time and rearranging gives

$$\frac{\partial c_8}{\partial t} = -\sum_{h=1}^{n_c} \frac{\partial c_h}{\partial t} \tag{3-36}$$

Substituting Equation (3-36) into Equation (3-34) and simplifying yields

$$\begin{aligned} L_8 = &-\phi\rho_8 \left[\sum_{h=1, h\neq 8}^{n_c} \frac{\partial c_h}{\partial t} \right] + c_8 \left[\phi \frac{\partial \rho_8}{\partial p} + \rho_8 \frac{\partial \phi}{\partial p} \right] \frac{\partial p}{\partial t} \\ &+ \phi\rho_{82} \frac{\partial c_2}{\partial t} + c_2 \left[\phi \frac{\partial \rho_{82}}{\partial p} + \rho_{82} \frac{\partial \phi}{\partial p} \right] \frac{\partial p}{\partial t} \end{aligned} \tag{3-37}$$

Equations (3-33) and (3-37) include n_c equations with n_c unknowns $p, c_1, ..., c_{n_c}$, $8 \notin n_c$. Multiplying the term $\frac{1}{\rho_2}\left(1 - \frac{\rho_{82}}{\rho_8}\right)$ with mass equation of oil component and the rest of mass component equations are multiplied by their density inverses, $\frac{1}{\rho_h}$. All equations are added together resulting in the following

$$\left(\frac{1}{\rho_{22}} - \frac{\rho_{82}}{\rho_{22}\rho_8} \right) L_2 + \sum_{h=1, h\neq 2}^{n_c} \frac{1}{\rho_h} L_h = R_{tot} \tag{3-38}$$

We expand Equation (3-38) as

$$
\begin{aligned}
&\phi\rho_{22}\left(\frac{1}{\rho_{22}}-\frac{\rho_{82}}{\rho_{22}\rho_8}\right)\frac{\partial c_2}{\partial t}+c_2\left(\frac{1}{\rho_{22}}-\frac{\rho_{82}}{\rho_{22}\rho_8}\right)\left(\phi\frac{\partial\rho_{22}}{\partial p}+\rho_{22}\frac{\partial\phi}{\partial p}\right)\frac{\partial p}{\partial t}\\
&+\phi\sum_{h=1,h\neq2,8}^{n_c}\left(\rho_h\frac{1}{\rho_h}\frac{\partial c_h}{\partial t}\right)+\sum_{h=1,h\neq2,8}^{n_c}\left(c_h\frac{1}{\rho_h}\left(\phi\frac{\partial\rho_h}{\partial p}+\rho_h\frac{\partial\phi}{\partial p}\right)\right)\frac{\partial p}{\partial t}\\
&-\phi\rho_8\frac{1}{\rho_8}\left(\sum_{h=1,h\neq8}^{n_c}\frac{\partial c_h}{\partial t}\right)+c_8\frac{1}{\rho_8}\left(\phi\frac{\partial\rho_8}{\partial p}+\rho_8\frac{\partial\phi}{\partial p}\right)\frac{\partial p}{\partial t}\\
&+\phi\rho_{82}\frac{1}{\rho_8}\frac{\partial c_2}{\partial t}+c_2\frac{1}{\rho_8}\left(\phi\frac{\partial\rho_{82}}{\partial p}+\rho_{82}\frac{\partial\phi}{\partial p}\right)\frac{\partial p}{\partial t}\\
&=R_{tot}
\end{aligned}
\tag{3-39}
$$

After few simplifications and rearrangements

$$
\begin{aligned}
&\phi\frac{\partial c_2}{\partial t}-\frac{\rho_{82}}{\rho_8}\frac{\partial c_2}{\partial t}+c_2\left(\frac{1}{\rho_{22}}-\frac{\rho_{82}}{\rho_{22}\rho_2}\right)\left(\phi\frac{\partial\rho_{22}}{\partial p}+\rho_{22}\frac{\partial\phi}{\partial p}\right)\frac{\partial p}{\partial t}\\
&+\phi\sum_{h=1,h\neq2,8}^{n_c}\frac{\partial c_h}{\partial t}+\sum_{h=1,h\neq2,8}^{n_c}c_h\frac{1}{\rho_h}\left(\phi\frac{\partial\rho_h}{\partial p}+\rho_k\frac{\partial\phi}{\partial p}\right)\frac{\partial p}{\partial t}\\
&-\phi\frac{\partial c_2}{\partial t}-\phi\sum_{h=1,h\neq2,8}^{n_c}\frac{\partial c_h}{\partial t}+c_8\frac{1}{\rho_8}\left(\phi\frac{\partial\rho_8}{\partial p}+\rho_8\frac{\partial\phi}{\partial p}\right)\frac{\partial p}{\partial t}\\
&+\phi\frac{\rho_{82}}{\rho_8}\frac{\partial c_2}{\partial t}+c_2\frac{1}{\rho_8}\left(\phi\frac{\partial\rho_{82}}{\partial p}+\rho_{82}\frac{\partial\phi}{\partial p}\right)\frac{\partial p}{\partial t}\\
&=R_{tot}
\end{aligned}
\tag{3-40}
$$

3.3.2 Fluid Compressibility

Equation (3-40) can be greatly simplified by multiplying the bracketed terms and then combining with appropriate terms in the brackets. We also notice that the terms involving time derivatives of c_1 through c_{n_c} vanish identically. The remaining terms in the equation are the time derivative of porosity and density of fluids. We use chain rule for time derivative of porosity and fluid density terms to time derivative of pressure as

$$\left(\frac{1}{\rho_{22}}-\frac{\rho_{82}}{\rho_{82}\rho_8}\right)L_2+\sum_{h=1,h\neq 2,8}^{n_c}\frac{1}{\rho_h}L_h+\frac{1}{\rho_8}L_8=-\frac{c_{22}\rho_{82}}{\rho_{22}\rho_8}\left(\phi\frac{\partial\rho_{22}}{\partial p}+\rho_{22}\frac{\partial\phi}{\partial p}\right)\frac{\partial p}{\partial t}$$
$$\frac{c_2}{\rho_{22}}\left(\phi\frac{\partial\rho_{22}}{\partial p}+\rho_{22}\frac{\partial\phi}{\partial p}\right)\frac{\partial p}{\partial t}$$
$$+\sum_{h=1,h\neq 2,8}^{n_c}\frac{c_h}{\rho_h}\left(\phi\frac{\partial\rho_h}{\partial p}+\rho_h\frac{\partial\phi}{\partial p}\right)\frac{\partial p}{\partial t} \qquad (3\text{-}41)$$
$$+\frac{c_8}{\rho_8}\left(\phi\frac{\partial\rho_8}{\partial p}+\rho_8\frac{\partial\phi}{\partial p}\right)\frac{\partial p}{\partial t}$$
$$+\frac{c_2}{\rho_8}\left(\phi\frac{\partial\rho_{82}}{\partial p}+\rho_{82}\frac{\partial\phi}{\partial p}\right)\frac{\partial p}{\partial t}$$

Then after rearrangement, the above equation becomes

$$\left(\frac{1}{\rho_{22}}-\frac{\rho_{82}}{\rho_{82}\rho_8}\right)L_2+\sum_{h=1,h\neq 2,8}^{n_c}\frac{1}{\rho_h}L_h+\frac{1}{\rho_8}L_8=(-\phi\frac{c_2\rho_{82}}{\rho_{22}\rho_8}\frac{\partial\rho_{22}}{\partial p}-\frac{c_2\rho_{82}}{\rho_8}\frac{\partial\phi}{\partial p}$$
$$+\phi\frac{c_2}{\rho_{22}}\frac{\partial\rho_{22}}{\partial p}+c_2\frac{\partial\phi}{\partial p}$$
$$+\phi\sum_{h=1,h\neq 2,8}^{n_c}\frac{c_h}{\rho_h}\frac{\partial\rho_h}{\partial p}+\frac{\partial\phi}{\partial p}\sum_{h=1,h\neq 2,8}^{n_c}c_h \qquad (3\text{-}42)$$
$$+\phi\frac{c_8}{\rho_8}\frac{\partial\rho_8}{\partial p}+c_8\frac{\partial\phi}{\partial p}$$
$$+\phi\frac{c_2}{\rho_8}\frac{\partial\rho_{82}}{\partial p}+\frac{c_2\rho_{82}}{\rho_8}\frac{\partial\phi}{\partial p})\frac{\partial p}{\partial t}$$

Compressibility of the components and rock are identified as

$$\varsigma_2=\frac{1}{\rho_{22}}\left(1-\frac{\rho_{82}}{\rho_8}\right)\frac{\partial\rho_{22}}{\partial p}+\frac{1}{\rho_8}\frac{\partial\rho_{82}}{\partial p}=-\frac{1}{B_{l=2}}\frac{\partial B_{l=2}}{\partial p}+\frac{B_{l=4}}{B_{l=2}}\frac{\partial R_{so}}{\partial p} \qquad (3\text{-}43)$$

$$\varsigma_k=\frac{1}{\rho_h}\frac{\partial\rho_h}{\partial p} \qquad h=1,..n_c \text{ and } h\neq 2,8 \qquad (3\text{-}44)$$

$$\varsigma_8=\frac{1}{\rho_{h=8}}\frac{\partial\rho_{h=8}}{\partial p}=-\frac{1}{B_{l=4}}\frac{\partial B_{l=4}}{\partial p} \qquad (3\text{-}45)$$

$$\varsigma_r = -\frac{1}{\phi}\frac{\partial \phi}{\partial p} \tag{3-46}$$

Since gas component (***h=8***) can only exist in the gas phase ***(l=4),*** we can consider that the formation volume factor of gas is same as its phase. Accordingly, total compressibility is defined as

$$\varsigma_{tot} = \varsigma_r + \sum_{h=1}^{n_c} \varsigma_h c_h \tag{3-47}$$

Similarly employing this definition, Equation (3-42) gives

$$\left(\frac{1}{\rho_{22}} - \frac{\rho_{82}}{\rho_{82}\rho_8}\right) L_2 + \sum_{h=1,h\neq 2,8}^{n_c} \frac{1}{\rho_h} L_h + \frac{1}{\rho_8} L_8 = \phi \varsigma_{tot} \frac{\partial p}{\partial t} \tag{3-48}$$

3.3.3 Diffusion and Source/Sink terms

By applying multipliers to diffusion and source/sink terms to Equation (3-22), it can be written as

$$\begin{aligned}
&\left(\frac{1}{\rho_{22}} - \frac{\rho_{82}}{\rho_{22}\rho_8}\right)\left[\vec{\nabla}\bullet\sum_{l=1}^{n_p}\left(\rho_{22} c_{2l} \bar{\bar{K}} \lambda_{r2}(\vec{\nabla}p_1 + \vec{\nabla}p_{c2} - \gamma_2 \vec{\nabla}h)\right)\right] \\
&+ \sum_{h=1,h\neq 2,8}^{n_c} \frac{1}{\rho_h}\left[\vec{\nabla}\bullet\sum_{l=1}^{n_p}\left(\rho_h c_{hl} \bar{\bar{K}} \lambda_{rl}(\vec{\nabla}p_1 + \vec{\nabla}p_{cl} - \gamma_l \vec{\nabla}h)\right)\right] \\
&\frac{1}{\rho_8}\left[\vec{\nabla}\bullet\sum_{l=1}^{n_p}\left((\rho_8 c_{8l} + \rho_{82} c_{2l}) \bar{\bar{K}} \lambda_{rl}(\vec{\nabla}p_1 + \vec{\nabla}p_{cl} - \gamma_l \vec{\nabla}h)\right)\right] \\
&+ \frac{\sum_{h=1}^{nc} q_h}{V_b} = \sum_{h=1,h\neq 2,8}^{nc} \frac{1}{\rho_h} L_h + \left(\frac{1}{\rho_{22}} - \frac{\rho_{82}}{\rho_{22}\rho_8}\right) L_2 + \frac{1}{\rho_8} L_8
\end{aligned} \tag{3-49}$$

As observed from this equation, solution gas effect has been disappeared from source and sinks terms. Hence, the formulation that has been derived is at reservoir

conditions. Similar justification is possible for the accumulation term. This means solution gas cannot impact high pressure change or pressure transience.

Accordingly, the pressure equation that is used to solve for volume balance in the UTCHEM simulator is written as

$$\left(\frac{1}{\rho_{22}}-\frac{\rho_{82}}{\rho_{22}\rho_{8}}\right)\left[\vec{\nabla}\bullet\sum_{l=1}^{n_p}\left(\rho_{22}c_{2l}\bar{\bar{K}}\lambda_{r2}(\vec{\nabla}p_1+\vec{\nabla}p_{c2}-\gamma_2\vec{\nabla}h)\right)\right]$$
$$+\sum_{h=1,h\neq 2,8}^{n_c}\frac{1}{\rho_h}\left[\vec{\nabla}\bullet\sum_{l=1}^{n_p}\left(\rho_h c_{hl}\bar{\bar{K}}\lambda_{rl}(\vec{\nabla}p_1+\vec{\nabla}p_{cl}-\gamma_l\vec{\nabla}h)\right)\right] \qquad (3\text{-}50)$$
$$+\frac{1}{\rho_8}\left[\vec{\nabla}\bullet\sum_{l=1}^{n_p}(\rho_8 c_{8l}+\rho_{82}c_{2l})\bar{\bar{K}}\lambda_{rl}(\vec{\nabla}p_1+\vec{\nabla}p_{cl}-\gamma_l\vec{\nabla}h)\right]$$
$$+\frac{\sum_{h=1}^{n_c}q_h}{V_b}=\phi\varsigma_{tot}\frac{\partial p}{\partial t}$$

Equation (3-50) is called the pressure equation because no explicit time derivatives of concentrations are present.

Our approach is to solve the three-dimensional, four phase flow equations with multi (pseudo)components by first numerically solving the pressure equation for water pressure implicitly; then using the results in mass component equations to compute total concentration explicitly. Afterward, the energy equation is solved implicitly for temperature; subsequently, phase saturations in the presence of complex surfactant phase behavior and oil/gas phase behavior are addressed. The solution procedure will be discussed and elaborated in subsequent chapters.

Chapter 4: Numerical Formulation

The pressure equation and the conservation of mass equations in Chapter 3 are a set of coupled, nonlinear partial differential equations. These equations are approximated by finite difference methods in UTCHEM. An implicit pressure and an explicit composition method are used to solve for $n_c + 1$ unknowns ($p, c_1, .. c_{n_c}$).

4.1 Discretization of Pressure Equation

We need to determine a suitable average fluid mobility $k_{rl} / \mu_l \rho_k$. Industry experience (e.g. Crichlow in 1977) has shown that use of a phase mobility in the block which has the larger phase potential of the two neighboring blocks yields more reliable results. The calculation in UTCHEM uses the value of the phase saturation and the concentration of the upstream block at time level n to determine an upstream phase relative permeability and concentration. But midpoint weighting for density and viscosity is applied to calculate phase mobility at the gridblock boundaries. Therefore, upstream relative permeability and concentration of component h in phase l are combined with the arithmetic mean value of the phase viscosity and component density, giving as

$$\lambda_{rl} \rho_h c_{hl} = \frac{k_{rl}}{\mu_l} \rho_h c_{hl} = \frac{k_{rl\,(upstream)}}{\mu_{l\,(midpoint)}} \rho_{h\,(midpoint)} c_{rl\,(upstream)} \tag{4-1}$$

For instance, in order to evaluate the above mentioned parameters between gridblocks i and $i+1$ we use

$$\left(\frac{k_{rl}}{\mu_l} \rho_h c_{hl} \right)_{i+1/2} = \frac{2k_{rl,i}}{\mu_{l,i} + \mu_{l,i+1}} \left(\frac{\rho_{h,i} + \rho_{h,i+1}}{2} \right) c_{rl,i} \quad , \; if \quad p_i + \bar{\gamma}_i h_i > p_{i+1} + \bar{\gamma}_{i+1} h_{i+1} \tag{4-2}$$

For evaluation of the specific phase density at the boundary of a gridblock, UTCHEM uses the midpoint weighing as

$$\gamma_l = \gamma_{l,(midpoint)} \tag{4-3}$$

For instance, the specific phase density between gridblocks ***i*** and ***i+1*** is evaluated as

$$\gamma_{l,i+1/2} = \frac{\gamma_{i+1} + \gamma_i}{2} \tag{4-4}$$

We consider the movement of fluids between two blocks and assume that the conditions needed for assuming Darcy flow are satisfied and ignoring the instant changes in phase mobility, phase density, and concentration of components in phase. In order to discretize the pressure equation, we first define the transmissibility of phase at the six boundaries between a main gridblock (ijk) and its six neighbor gridblocks.

The transmissibility of each phase at boundary $i-1/2jk$ is discretized as

$$T_{l,i-1/2jk} = \left(1 - \frac{\rho_{82,ijk}}{\rho_{8,ijk}}\right) \frac{\rho_{22,i-1/2jk} c_{2l,i-1/2jk} \lambda_{l,i-1/2jk}}{\rho_{22,ijk}} \left(\frac{2\Delta y_{ijk} \Delta z_{ijk}}{\frac{\Delta x_{i-1jk}}{K_{x,i-1jk}} + \frac{\Delta x_{ijk}}{K_{x,ijk}}} \right) +$$

$$\sum_{h=1,h\neq 2,8}^{n_c} \frac{\rho_{h,i-1/2,j,k} c_{hl,i-1/2,j,k} \lambda_{l,i-1/2,j,k}}{\rho_{h,ijk}} \left(\frac{2\Delta y_{ijk} \Delta z_{ijk}}{\frac{\Delta x_{i-1jk}}{K_{x,i-1jk}} + \frac{\Delta x_{ijk}}{K_{x,ijk}}} \right) + \tag{4-5}$$

$$\frac{\left(\rho_{8,i-1/2jk} c_{8l,i-1/2jk} + \rho_{82,i-1/2jk} c_{2l,i-1/2jk}\right) \lambda_{l,i-1/2jk}}{\rho_{8,ijk}} \left(\frac{2\Delta y_{ijk} \Delta z_{ijk}}{\frac{\Delta x_{i-1jk}}{K_{x,i-1jk}} + \frac{\Delta x_{ijk}}{K_{x,ijk}}} \right)$$

For the boundary $(i+1/2jk)$ discretization of the fluid transmissibility is as follows

$$T_{l,i+1/2\,jk}=\left(1-\frac{\rho_{82,ijk}}{\rho_{8,ijk}}\right)\frac{\rho_{22,i+1/2\,jk}c_{2l,i+1/2\,jk}\lambda_{l,i+1/2\,jk}}{\rho_{22,ijk}}\left(\frac{2\Delta y_{ijk}\Delta z_{ijk}}{\frac{\Delta x_{i+1\,jk}}{K_{x,i+1\,jk}}+\frac{\Delta x_{ijk}}{K_{x,ijk}}}\right)+$$

$$\sum_{h=1,h\neq 2,8}^{nc}\frac{\rho_{h,i+1/2\,jk}c_{hl,i+1/2\,jk}\lambda_{l,i+1/2\,jk}}{\rho_{h,ijk}}\left(\frac{2\Delta y_{ijk}\Delta z_{ijk}}{\frac{\Delta x_{i+1\,jk}}{K_{x,i+1\,jk}}+\frac{\Delta x_{ijk}}{K_{x,ijk}}}\right)+ \tag{4-6}$$

$$\frac{\left(\rho_{8,i+1/2\,jk}c_{8l,i+1/2\,jk}+\rho_{82,i+1/2\,jk}c_{2l,i+1/2\,jk}\right)\lambda_{l,i+1/2\,jk}}{\rho_{8,ijk}}\left(\frac{2\Delta y_{ijk}\Delta z_{ijk}}{\frac{\Delta x_{i+1\,jk}}{K_{x,i+1\,jk}}+\frac{\Delta x_{ijk}}{K_{x,ijk}}}\right)$$

In similar manner, for boundary $(ij-1/2k)$, the transmissibility of phase is discretized as follows

$$T_{l,ij-1/2k}=\left(1-\frac{\rho_{82,ijk}}{\rho_{8,ijk}}\right)\frac{\rho_{22,ij-1/2k}c_{2l,ij-1/2k}\lambda_{l,ij-1/2k}}{\rho_{22,ijk}}\left(\frac{2\Delta x_{ijk}\Delta z_{ijk}}{\frac{\Delta y_{ij-1k}}{K_{y,ij-1k}}+\frac{\Delta y_{ijk}}{K_{y,ijk}}}\right)+$$

$$\sum_{h=1,h\neq 2,8}^{nc}\frac{\rho_{h,ij-1/2k}c_{hl,ij-1/2k}\lambda_{l,ij-1/2k}}{\rho_{h,ijk}}\left(\frac{2\Delta x_{ijk}\Delta z_{ijk}}{\frac{\Delta y_{ij-1k}}{K_{y,ij-1k}}+\frac{\Delta y_{ijk}}{K_{y,ijk}}}\right)+ \tag{4-7}$$

$$\frac{\left(\rho_{8,ij-1/2k}c_{8l,ij-1/2k}+\rho_{82,ij-1/2k}c_{2l,ij-1/2k}\right)\lambda_{l,ij-1/2k}}{\rho_{8,ijk}}\left(\frac{2\Delta x_{ijk}\Delta z_{ijk}}{\frac{\Delta y_{ij-1k}}{K_{y,ij-1k}}+\frac{\Delta y_{ijk}}{K_{y,ijk}}}\right)$$

and the phase transmissibility at the boundary $(ij+1/2k)$ becomes

$$T_{l,ij+1/2k}=\left(1-\frac{\rho_{82,i,j,k}}{\rho_{8,ijk}}\right)\frac{\rho_{22,ij+1/2k}c_{2l,ij+1/2k}\lambda_{l,ij+1/2k}}{\rho_{22,ijk}}\left(\frac{2\Delta x_{ijk}\Delta z_{ijk}}{\frac{\Delta y_{ij+1k}}{K_{y,ij+1k}}+\frac{\Delta y_{ijk}}{K_{y,ijk}}}\right)+$$

$$\sum_{h=1,h\neq 2,8}^{nc}\frac{\rho_{h,ij+1/2k}c_{hl,ij+1/2k}\lambda_{l,ij+1/2k}}{\rho_{h,ijk}}\left(\frac{2\Delta x_{ijk}\Delta z_{ijk}}{\frac{\Delta y_{ij+1k}}{K_{y,ij+1k}}+\frac{\Delta y_{ijk}}{K_{y,ijk}}}\right)+ \tag{4-8}$$

$$\frac{\left(\rho_{8,ij+1/2k}c_{8l,i,j+1/2,k}+\rho_{82,ij+1/2k}c_{2l,ij+1/2k}\right)\lambda_{l,ij+1/2k}}{\rho_{8,ijk}}\left(\frac{2\Delta x_{ijk}\Delta z_{ijk}}{\frac{\Delta y_{ij+1k}}{K_{y,ij+1k}}+\frac{\Delta y_{ijk}}{K_{y,ijk}}}\right)$$

For boundary $(ijk-1/2)$, transmissibility is discretized as

$$T_{l,ijk-1/2}=\left(1-\frac{\rho_{82,ijk}}{\rho_{8,ijk}}\right)\frac{\rho_{22,ijk-1/2}c_{2l,ijk-1/2}\lambda_{l,ijk-1/2}}{\rho_{22,i,j,k}}\left(\frac{2\Delta x_{ijk}\Delta y_{ijk}}{\frac{\Delta z_{ijk-1}}{K_{z,ijk-1}}+\frac{\Delta z_{ijk}}{K_{z,ijk}}}\right)+$$

$$\sum_{h=1,h\neq 2,8}^{nc}\frac{\rho_{h,ijk-1/2}c_{hl,ijk-1/2}\lambda_{l,ijk-1/2}}{\rho_{h,ijk}}\left(\frac{2\Delta x_{ijk}\Delta y_{ijk}}{\frac{\Delta z_{ijk-1}}{K_{z,ijk-1}}+\frac{\Delta z_{ijk}}{K_{z,ijk}}}\right)+ \tag{4-9}$$

$$\frac{\left(\rho_{8,ijk-1/2}c_{8l,i,j,k-1/2}+\rho_{82,ijk-1/2}c_{2l,ijk-1/2}\right)\lambda_{l,ijk-1/2}}{\rho_{8,ijk}}\left(\frac{2\Delta x_{ijk}\Delta y_{ijk}}{\frac{\Delta z_{ijk-1}}{K_{z,ijk-1}}+\frac{\Delta z_{ijk}}{K_{z,ijk}}}\right)$$

Similarly for boundary $(ijk+1/2)$ transmissibility is obtained

$$T_{l,ijk+1/2}=\left(1-\frac{\rho_{82,ijk}}{\rho_{8,ijk}}\right)\frac{\rho_{22,ijk+1/2}c_{2l,ijk+1/2}\lambda_{l,ijk+1/2}}{\rho_{22,ijk}}\left(\frac{2\Delta x_{ijk}\Delta y_{ijk}}{\frac{\Delta z_{ijk+1}}{K_{z,ijk+1}}+\frac{\Delta z_{ijk}}{K_{z,ijk}}}\right)+$$

$$\sum_{h=1,h\neq 2,8}^{nc}\frac{\rho_{h,ijk+1/2}c_{hl,ijk+1/2}\lambda_{l,ijk+1/2}}{\rho_{h,ijk}}\left(\frac{2\Delta x_{ijk}\Delta y_{ijk}}{\frac{\Delta z_{ijk+1}}{K_{z,ijk+1}}+\frac{\Delta z_{ijk}}{K_{z,ijk}}}\right)+ \tag{4-10}$$

$$\frac{\left(\rho_{8,ijk+1/2}c_{8l,ijk+1/2}+\rho_{82,ijk+1/2}c_{2l,ijk+1/2}\right)\lambda_{l,ijk+1/2}}{\rho_{8,ijk}}\left(\frac{2\Delta x_{ijk}\Delta y_{ijk}}{\frac{\Delta z_{ijk+1}}{K_{z,ijk+1}}+\frac{\Delta z_{ijk}}{K_{z,ijk}}}\right)$$

We use finite difference approximations after converting the partial differential equations into the numerical form to solve for pressure. This equation is multiplied by the bulk volume element V_{ijk} of that gridblock. First, a linear difference operator is defined as follows:

$$\Delta\left(T\Delta p\right)=\Delta_x\left(T_x\Delta p_x\right)+\Delta_y\left(T_y\Delta p_y\right)+\Delta_z\left(T_z\Delta p_z\right) \tag{4-11}$$

where

$$\begin{aligned}\Delta_x\left(T_x\Delta p_x\right)&=T_{i-1/2jk}\left(p_{i-1jk}-p_{ijk}\right)+T_{i+1/2jk}\left(p_{i+1jk}-p_{ijk}\right)\\ \Delta_y\left(T_y\Delta p_y\right)&=T_{ij-1/2k}\left(p_{ij-1,k}-p_{ijk}\right)+T_{ij+1/2k}\left(p_{ij+1k}-p_{ijk}\right)\\ \Delta_x\left(T_x\Delta p_x\right)&=T_{ijk-1/2}\left(p_{ijk-1}-p_{ijk}\right)+T_{ijk+1/2}\left(p_{ijk+1}-p_{ijk}\right)\end{aligned} \tag{4-12}$$

Using the above notation, the resulting difference equations become

$$\sum_{l=1}^{n_p}\left(\Delta_x T_{lx}^n \Delta p^{n+1} + \Delta_x T_{lx}^n \Delta p_{cl}^n - \Delta_x T_{lx}^n \gamma_{lx} \Delta h\right)_{ijk} +$$
$$\sum_{l=1}^{n_p}\left(\Delta_y T_{ly}^n \Delta p^{n+1} + \Delta_y T_{ly}^n \Delta p_{cl}^n - \Delta_y T_{ly}^n \gamma_{ly} \Delta h\right)_{ijk} + \qquad (4\text{-}13)$$
$$\sum_{l=1}^{n_p}\left(\Delta_z T_{lz}^n \Delta p^{n+1} + \Delta_z T_{lz}^n \Delta p_{cl}^n - \Delta T_{lz}^n \gamma_{lz} \Delta_z h\right)_{ijk} +$$
$$+\sum_{h=1}^{nc} q_{h,ijk} = \left(V_{b,ijk} \frac{\phi_{ijk}^n \varsigma_{tot}^n}{\Delta t}\right)\left(p_{ijk}^{n+1} - p_{ijk}^n\right)$$

In this pressure equation, we need to understand the diffusion and source and sinks terms to treat them for having volume balance equation.

$$
\begin{aligned}
&\sum_{l=1}^{n_p}\left(T_{l,i-1/2jk}^{n}\left(p_{i-1jk}^{n+1}-p_{ijk}^{n+1}\right)+T_{l,i+1/2jk}^{n}\left(p_{i+1jk}^{n+1}-p_{ijk}^{n+1}\right)\right)+\\
&\sum_{l=1}^{n_p}\left(T_{i-1/2jk}^{n}\left(p_{cl,i-1jk}^{n}-p_{cl,ijk}^{n}-\gamma_{l,i-1/2jk}^{n}\left(h_{ij-1k}-h_{ijk}\right)\right)\right)+\\
&\sum_{l=1}^{n_p}\left(T_{i+1/2jk}^{n}\left(p_{cl,i+1jk}^{n}-p_{cl,ijk}^{n}-\gamma_{l,i+1/2jk}^{n}\left(h_{i+1jk}-h_{ijk}\right)\right)\right)+\\
&\sum_{l=1}^{n_p}\left(T_{l,ij-1/2k}^{n}\left(p_{ij-1k}^{n+1}-p_{ijk}^{n+1}\right)+T_{l,ij+1/2k}^{n}\left(p_{ij+1k}^{n+1}-p_{ijk}^{n+1}\right)\right)+\\
&\sum_{l=1}^{n_p}\left(T_{ij-1/2k}^{n}\left(p_{cl,ij-1k}^{n}-p_{cl,i1jk}^{n}-\gamma_{l,ij-1/2k}^{n}\left(h_{ij-1k}-h_{ijk}\right)\right)\right)+\\
&\sum_{l=1}^{n_p}\left(T_{ij+1/2k}^{n}\left(p_{cl,ij+1k}^{n}-p_{cl,ijk}^{n}-\gamma_{l,ij+1/2k}^{n}\left(h_{ij+1k}-h_{ijk}\right)\right)\right)+\\
&\sum_{l=1}^{n_p}\left(T_{l,ijk-1/2}^{n}\left(p_{ijk-1}^{n+1}-p_{ijk}^{n+1}\right)+T_{l,ijk+1/2}^{n}\left(p_{ijk+1}^{n+1}-p_{ijk}^{n+1}\right)\right)+\\
&\sum_{l=1}^{n_p}\left(T_{ijk-1/2}^{n}\left(p_{cl,ijk-1}^{n}-p_{cl,i1jk}^{n}-\gamma_{l,ijk-1/2}^{n}\left(h_{ijk-1}-h_{ijk}\right)\right)\right)+\\
&\sum_{l=1}^{n_p}\left(T_{ijk+1/2}^{n}\left(p_{cl,ijk+1}^{n}-p_{cl,ijk}^{n}-\gamma_{l,ijk+1/2}^{n}\left(h_{ijk+1}-h_{ijk}\right)\right)\right)+\\
&\sum_{h=1}^{nc}q_{h,ijk}=\left(V_{b,ijk}\frac{\phi_{ijk}^{n}\varsigma_{tot}^{n}}{\Delta t}\right)\left(p_{ijk}^{n+1}-p_{ijk}^{n}\right)
\end{aligned}
\tag{4-14}
$$

Solution gas in source and sink terms cannot affect the pressure equation. It can be seen that in the equations the terms, which include it, are cancelled out.

It is observed that a forward difference approximation has been used for representing time derivatives. The superscripts ***n*** and ***n+1*** denote the old and the new time levels, respectively. Quantities with superscript ***n*** can be computed using existing data, whereas quantities with superscript ***n+1*** are the unknown variables in pressure equation and are required to solve.

We now have all of the basic elements necessary for writing the system of algebraic equations corresponding to the nonlinear, partial differential flow equations of

our four-phase model. Once again it is useful to define new variables to simplify the notation. In particular, the pressure equation is cast in a relatively simple form by making the following definitions:

$$AE_i = \sum_{l=1}^{n_p} T_{l,i+1/2\,jk} \tag{4-15}$$

$$AW_i = \sum_{l=1}^{n_p} T_{l,i-1/2\,jk} \tag{4-16}$$

$$AS_j = \sum_{l=1}^{n_p} T_{l,ij+1/2k} \tag{4-17}$$

$$AN_j = \sum_{l}^{n_p} T_{l,ij-1/2k} \tag{4-18}$$

$$AB_k = \sum_{l=1}^{n_p} T_{l,ijk+1/2} \tag{4-19}$$

$$AT_k = \sum_{l}^{n_p} T_{l,ijk-1/2} \tag{4-20}$$

For main diagonal coefficient this is represented AC_{ijk} defined as

$$AC_{ijk} = -\left(\sum_{l}^{n_p}\left(T_{l,i-1/2\,jk} + T_{l,i-1/2\,jk} + T_{l,ij-1/2k} + T_{l,ij-1/2k} + T_{l,ijk-1/2} + T_{l,ijk+1/2}\right)\right) + \left(V_{b,ijk}\frac{\phi_{ijk}^n \varsigma_{tot}^n}{\Delta t}\right) + \frac{\psi_{ijk}\delta_{ijk}}{\Delta t} \tag{4-21}$$

where δ_{ijk} can be either 0 or 1 and it depends on the well constraint definition. If the well constraint is constant rate, $\delta_{ijk} = 0$. Otherwise, for constant bottom-hole pressure this function will be $\delta_{ijk} = 1$ and ψ_{ijk} is calculated as explained in the well model section. All of the quantities in transmissibilities are evaluated at the old time level. Eventually, the pressure equation becomes

$$AT_k\ p_{ijk-1}^{n+1} + AN_j\ p_{ij-1k}^{n+1} + AW_i\ p_{i-1jk}^{n+1} + AB_k\ p_{ijk+1}^{n+1} + AS_j\ p_{ij+1k}^{n+1} + AE_i\ p_{i+1jk}^{n+1} + AC_{ijk}\, p_{ijk}^{n+1} = BV_{ijk} \tag{4-22}$$

All other terms that are coefficients of pressure at old time level, along with gravity and capillary terms, are considered in right hand side, $BV_{i,j,k}$ as

$$\begin{aligned}
BV_{ijk} = &-\sum_{l=1}^{n_p}\left(T_{i-1/2jk}^{n}\left(p_{cl,i-1jk}^{n} - p_{cl,ijk}^{n} - \gamma_{l,i-1/2\,jk}^{n}\left(h_{ij-1k} - h_{ijk}\right)\right)\right) + \\
&-\sum_{l=1}^{n_p}\left(T_{i+1/2jk}^{n}\left(p_{cl,i+1jk}^{n} - p_{cl,ijk}^{n} - \gamma_{l,i+1/2\,jk}^{n}\left(h_{i+1\,jk} - h_{ijk}\right)\right)\right) + \\
&-\sum_{l=1}^{n_p}\left(T_{ij-1/2k}^{n}\left(p_{cl,ij-1k}^{n} - p_{cl,i1jk}^{n} - \gamma_{l,ij-1/2k}^{n}\left(h_{ij-1k} - h_{ijk}\right)\right)\right) + \\
&-\sum_{l=1}^{n_p}\left(T_{ij+1/2k}^{n}\left(p_{cl,ij+1k}^{n} - p_{cl,ijk}^{n} - \gamma_{l,ij+1/2k}^{n}\left(h_{ij+1k} - h_{ijk}\right)\right)\right) + \\
&-\sum_{l=1}^{n_p}\left(T_{ijk-1/2}^{n}\left(p_{cl,ijk-1}^{n} - p_{cl,i1jk}^{n} - \gamma_{l,ijk-1/2}^{n}\left(h_{ijk-1} - h_{ijk}\right)\right)\right) + \\
&-\sum_{l=1}^{n_p}\left(T_{ijk+1/2}^{n}\left(p_{cl,ijk+1}^{n} - p_{cl,ijk}^{n} - \gamma_{l,ijk+1/2}^{n}\left(h_{ijk+1} - h_{ijk}\right)\right)\right) + \\
&-\left(V_{b,ijk}\,\frac{\phi_{ijk}^{n}\varsigma_{tot}^{n}}{\Delta t}\,p_{ijk}^{n}\right)_{ijk} + \frac{\omega_{ijk}}{\Delta t}
\end{aligned} \tag{4-23}$$

In principle and in practice, the coefficients of the ***n+1*** pressure in Equation (4-22) are all known at the present or the old time level and an equation like Equation (4-22) exists for each gridblock. The total system of algebraic equations is solved for the pressures at the new ***n+1*** time level. This system of linear equations is expressed in a form using matrix and vector notation as follows:

$$\bar{\bar{A}}^{n}\,\bar{p}^{n+1} = \bar{b}^{n} \tag{4-24}$$

where $\bar{\bar{A}}$ is the coefficient matrix with seven diagonals, $\bar{p}$ is the unknown vector and $\bar{b}$ is the right hand side vector. Solution methods using different solvers with different algorithms are not discussed in this research.

4.2 DISCRETIZATION OF MASS CONCENTRATION EQUATION

Once the new pressures have been solved, phase velocities should be calculated by using Equation (3-38). After updating the new phase velocities, concentrations are solved explicitly $c_1^{n+1}, ..., c_{n_c}^{n+1}$. In this section, we discretize Equation (4-25) in the present or the new time level. Although this research focuses on accumulation, convection, and source and sink terms, discretization of dispersion and molecular terms are considered here as well. Conservation of mass equations discretized in this section has been derived in Chapter 4 as the follows:

$$\frac{\partial}{\partial t}\left(\phi\rho_h(1-\sum_{k=1}^{n_c}\hat{c}_h)c_h+\phi\rho_h\hat{c}_h\right)+\nabla\bullet\sum_{l=1}^{n_p}\left(\rho_h c_{hl}\vec{u}_l\right)-\nabla\bullet\left(\sum_{l=1}^{n_p}\phi\rho_h S_l\bar{\bar{D}}_{hl}\bullet\vec{\nabla}c_{hl}\right)=\frac{\rho_h q_h}{V_b} \tag{4-25}$$

4.2.1 Accumulation Term

For time-dependent problems, the finite difference approximation of the first order derivative term in time is considered. We consider $\partial\left(\phi\rho_h c_h\right)/\partial t$ for a gridblock (***ijk***) and finite difference method to approximate it as

$$\frac{\partial}{\partial t}\left(\phi\rho_h c_h\right)\cong\frac{1}{\Delta t}\Delta_t\left(\phi\rho_h c_h\right)_{ijk} \tag{4-26}$$

This equation can be expanded in new and old time levels as follows

$$\frac{1}{\Delta t}\Delta_t\left(\phi\rho_h c_h\right)_{ijk}=\frac{1}{\Delta t}\left(\left(\phi\rho_h\right)_{ijk}^{n+1}\left(c_{h,ijk}^{n+1}-c_{h,ijk}^{n}\right)+c_{h,ijk}^{n}\left(\left(\phi\rho_h\right)_{ijk}^{n+1}-\left(\phi\rho_h\right)_{ijk}^{n}\right)\right) \tag{4-27}$$

The only unknown variable in this term is $c_{h,ijk}^{n+1}$. Other quantities in ***n+1*** have been updated after solving for pressure at the new time step.

4.2.2 Convection Term

After updating the phase velocities, convection term should be calculated at the boundaries of a gridblock ***(ijk)*** and then by using upstream weighting and midpoint weighting, the discretized form of convection term can be written as

$$\sum_{l=1}^{n_p} \frac{\partial\left(\rho_h c_{hl} \vec{u}_l\right)}{\partial x} \cong \sum_{l=1}^{n_p} \frac{\left(\left(\rho_h c_{hl} u_l\right)_{i+1/2\,jk}^{n} - \left(\rho_h c_{hl} u_l\right)_{i-1/2\,jk}^{n}\right)}{\Delta x_{ijk}} \tag{4-28}$$

All quantities of convection terms are evaluated at the old time level and the only new time step unknown is in the accumulation term which is expanded in Equation (4-27). Convection part is calculated for concentration at old time step, but the velocities and the densities of components are considered at the new time step.

4.2.3 Dispersion and Molecular Diffusion Term

Dispersion and molecular diffusion terms are discretized in space as

$$\nabla\bullet\left(\phi\rho_h S_l \overline{\overline{D}}_{hl}\bullet\vec{\nabla}c_{hl}\right) \cong \frac{1}{\Delta x_{ijk}}\left(N_{hl,ijk}^{n} - N_{i-1\,jk}^{n}\right) + \frac{1}{\Delta y_{ijk}}\left(N_{hl,ijk}^{n} - N_{ij-1k}^{n}\right) + \frac{1}{\Delta z_{ijk}}\left(N_{hl,ijk}^{n} - N_{ijk-1}^{n}\right) \tag{4-29}$$

We consider dispersion tensor as mentioned in Equation (3-15) that it is

$$\overline{\overline{D}}_{hl} = \begin{bmatrix} D_{xxhl} & D_{xyhl} & D_{xzhl} \\ D_{yxhl} & D_{yyhl} & D_{yzhl} \\ D_{zxhl} & D_{zyhl} & D_{zzhl} \end{bmatrix} \tag{4-30}$$

Expanding dispersion and molecular diffusion terms in X direction on boundaries of a gridblock (***ijk***) as

$$
\begin{aligned}
&N_{hl,i+1/2\,jk} = \\
&\left(\phi_{i+1/2\,jk}\rho_{h,i+1/2\,jk}S_{l,i+1/2\,jk}D_{xxhl,i+1/2\,jk}\right)\left(c_{hl,i+1\,jk}-c_{hl,ijk}\right)\frac{2}{\Delta x_{ijk}+\Delta x_{i+1\,jk}}+ \\
&\left(\phi_{i+1/2\,jk}\rho_{h,i+1/2\,jk}S_{l,i+1/2\,jk}D_{xyhl,i+1/2\,jk}\right)\left(c_{hl,ij+1k}-c_{hl,ij-1k}\right)\frac{2}{\Delta y_{ij-1k}+\Delta y_{ij+1k}+2\Delta y_{ijk}}+ \\
&\left(\phi_{i+1/2\,jk}\rho_{h,i+1/2\,jk}S_{l,i+1/2\,jk}D_{xzhl,i+1/2\,jk}\right)\left(c_{hl,ijk+1}-c_{hl,ijk-1}\right)\frac{2}{\Delta z_{ijk-1}+\Delta z_{ijk+1}+2\Delta z_{ijk}}+ \\
&N_{hl,i-1/2\,jk} = \\
&\left(\phi_{i-1/2\,jk}\rho_{h,i-1/2\,jk}S_{l,i-1/2\,jk}D_{xxhl,i-1/2\,jk}\right)\left(c_{hl,ijk}-c_{hl,i-1\,jk}\right)\frac{2}{\Delta x_{i-1\,jk}+\Delta x_{ijk}}+ \\
&\left(\phi_{i-1/2\,jk}\rho_{h,i-1/2\,jk}S_{l,i-1/2\,jk}D_{xyhl,i-1/2\,jk}\right)\left(c_{hl,i-1\,j+1k}-c_{hl,i-1\,j-1k}\right)\frac{2}{\Delta y_{i-1\,j-1k}+\Delta y_{i-1\,j+1k}+2\Delta y_{i-1\,jk}}+ \\
&\left(\phi_{i-1/2\,jk}\rho_{h,i-1/2\,jk}S_{l,i-1/2\,jk}D_{xyhl,i-1/2\,jk}\right)\left(c_{hl,i-1\,jk+1}-c_{hl,i-1\,jk-1}\right)\frac{2}{\Delta z_{i-1\,jk-1}+\Delta z_{i-1\,jk+1}+2\Delta z_{i-1\,jk}}+
\end{aligned}
\tag{4-31}
$$

Similar to X direction, we discretize in Y direction on boundaries of a gridblock (***ijk***) as

$$N_{hl,ij+1/2k} =$$

$$\left(\phi_{ij+1/2k}\rho_{h,ij+1/2k}S_{l,ij+1/2k}D_{yxhl,ij+1/2k}\right)\left(c_{hl,i+1jk}-c_{hl,i-1jk}\right)\frac{2}{\Delta x_{i-1jk}+\Delta x_{i+1jk}+2\Delta x_{ijk}}+$$

$$\left(\phi_{ij+1/2k}\rho_{h,ij+1/2k}S_{l,ij+1/2k}D_{yyhl,ij+1/2k}\right)\left(c_{hl,ij+1k}-c_{hl,ijk}\right)\frac{2}{\Delta y_{ijk}+\Delta y_{ij+1k}+}+$$

$$\left(\phi_{ij+1/2k}\rho_{h,ij+1/2k}S_{l,ij+1/2k}D_{yzhl,ij+1/2k}\right)\left(c_{hl,ijk+1}-c_{hl,ijk-1}\right)\frac{2}{\Delta z_{ijk-1}+\Delta z_{ijk+1}+2\Delta z_{ijk}}+$$

$$N_{hl,ij-1/2k} = \qquad (4\text{-}32)$$

$$\left(\phi_{ij-1/2k}\rho_{h,ij-1/2k}S_{l,ij+1/2k}D_{yxhl,ij-1/2k}\right)\left(c_{hl,i+1j-1k}-c_{hl,i-1j-1k}\right)\frac{2}{\Delta x_{i-1j-1k}+\Delta x_{i+1j-1k}+2\Delta x_{ij-1k}}+$$

$$\left(\phi_{ij-1/2k}\rho_{h,ij-1/2k}S_{l,ij-1/2k}D_{yyhl,ij-1/2k}\right)\left(c_{hl,ijk}-c_{hl,ij-1k}\right)\frac{2}{\Delta y_{ij-1k}+\Delta y_{ijk}+}+$$

$$\left(\phi_{ij-1/2k}\rho_{h,ij-1/2k}S_{l,ij-1/2k}D_{yzhl,ij-1/2k}\right)\left(c_{hl,ij-1k+1}-c_{hl,ij-1k-1}\right)\frac{2}{\Delta z_{ij-1k-1}+\Delta z_{ij-1k+1}+2\Delta z_{ij-1k}}+$$

Also, the discretization on $\boldsymbol{Z}$ direction on boundaries of a gridblock ($\boldsymbol{ijk}$) is given by

$$N_{hl,ijk+1/2} =$$

$$\left(\phi_{ijk+1/2}\rho_{h,ijk+1/2}S_{l,ijk+1/2}D_{zxhl,ijk+1/2}\right)\left(c_{hl,i+1jk}-c_{hl,i-1jk}\right)\frac{2}{\Delta x_{i-1jk}+\Delta x_{i+1jk}+2\Delta x_{ijk}}+$$

$$\left(\phi_{ijk+1/2}\rho_{h,ijk+1/2}S_{l,ijk+1/2}D_{zyhl,ijk+1/2}\right)\left(c_{hl,ij+1k}-c_{hl,ij-1k}\right)\frac{2}{\Delta y_{ij-1k}+\Delta y_{ij+1k}+2\Delta y_{ijk}}$$

$$\left(\phi_{ijk+1/2}\rho_{h,ijk+1/2}S_{l,ijk+1/2}D_{zzhl,ijk+1/2}\right)\left(c_{hl,ijk+1}-c_{hl,ijk}\right)\frac{2}{\Delta z_{ijk}+\Delta z_{ijk+1}}$$

$$N_{hl,ijk-11/2} = \qquad (4\text{-}33)$$

$$\left(\phi_{ijk-1/2}\rho_{h,ijk-1/2}S_{l,ijk-1/2}D_{zxhl,ijk-1/2}\right)\left(c_{hl,i+1jk-1}-c_{hl,i-1jk-1}\right)\frac{2}{\Delta x_{i-1jk-1}+\Delta x_{i+1jk-1}+2\Delta x_{ijk-1}}+$$

$$\left(\phi_{ijk-1/2}\rho_{h,ijk-1/2}S_{l,ijk-1/2}D_{zyhl,ijk-1/2}\right)\left(c_{hl,ij+1k-1}-c_{hl,ij-1k-1}\right)\frac{2}{\Delta y_{ij-1k-1}+\Delta y_{ij+1k-1}+2\Delta y_{ijk-1}}$$

$$\left(\phi_{ijk-1/2}\rho_{h,ijk-1/2}S_{l,ijk-1/2}D_{zzhl,ijk-1/2}\right)\left(c_{hl,ijk}-c_{hl,ijk-1}\right)\frac{2}{\Delta z_{ijk-1}+\Delta z_{ijk}}$$

Upstream weighting is used for all parameters, such as porosity, liquid saturations, dispersion values, and concentration of component ***h*** in phase ***l***. But the density of components is considered as midpoint weighted, mentioned in pressure equation section in Chapter 3. Therefore, the finite difference approximation of dispersion and molecular diffusion can be written as

$$V_{ijk}\nabla\bullet\sum_{l=1}^{n_p}\left(\phi\rho_h S_l \overline{\overline{D}}_{hl}\bullet\vec{\nabla}c_{hl}\right)\cong\frac{V_{ijk}}{\Delta x_{ijk}}\sum_{l=1}^{n_p}\left(N_{hl,ijk}-N_{hl,i-1jk}\right)+$$
$$\frac{V_{ijk}}{\Delta y_{ijk}}\sum_{l=1}^{n_p}\left(N_{hl,ijk}-N_{hl,ij-1k}\right)+ \qquad (4\text{-}34)$$
$$\frac{V_{ijk}}{\Delta z_{ijk}}\sum_{l=1}^{n_p}\left(N_{hl,ijk}-N_{hl,ijk-1}\right)$$

Dispersion tensor arrays ***(D_{xxhl}, D_{xyhl}, D_{xzhl}, D_{yxhl}, D_{yyhl}, D_{yzhl}, D_{zxhl}, D_{zyhl}, D_{zzhl})*** are defined in Equation (3-16) through (3-21). By using upstream weighting for velocities and concentration of components in phases and also applying midpoint weighting for component densities, the finite difference approximation of conservation of mass is solved explicitly in UTCHEM that it is presented as

$$
\begin{aligned}
c_{h,ijk}^{n+1} &= c_{h,ijk}^{n} + \\
&\frac{\Delta t}{\left(\phi\rho_h\right)_{ijk}^{n+1}}\left(\frac{\rho_{h,ijk}^{n+1} q_{h,ijk}^{n+1}}{V_{ijk}}\right) - \\
&\frac{\Delta t}{\left(\phi\rho_h\right)_{ijk}^{n+1}}\left(\frac{1}{\Delta x_{ijk}}\sum_{l=1}^{n_p}\left(\left(\rho_h^{n+1} c_{hl}^{n} u_l^{n+1}\right)_{ijk} - \left(\rho_h^{n+1} c_{hl}^{n} u_l^{n+1}\right)_{i-1\,jk}\right)\right) - \\
&\frac{\Delta t}{\left(\phi\rho_h\right)_{ijk}^{n+1}}\left(\frac{1}{\Delta y_{ijk}}\sum_{l=1}^{n_p}\left(\left(\rho_h^{n+1} c_{hl}^{n} u_l^{n+1}\right)_{ijk} - \left(\rho_h^{n+1} c_{hl}^{n} u_l^{n+1}\right)_{ij-1k}\right)\right) - \\
&\frac{\Delta t}{\left(\phi\rho_h\right)_{ijk}^{n+1}}\left(\frac{1}{\Delta z_{ijk}}\sum_{l=1}^{n_p}\left(\left(\rho_h^{n+1} c_{hl}^{n} u_l^{n+1}\right)_{ijk} - \left(\rho_h^{n+1} c_{hl}^{n} u_l^{n+1}\right)_{ijk-1}\right)\right) + \\
&\frac{\Delta t}{\left(\phi\rho_h\right)_{ijk}^{n+1}}\left(\frac{1}{\Delta x_{ijk}}\sum_{l=1}^{n_p}\left(N_{hl,ijk}^{n} - N_{hl,i-1\,jk}^{n}\right)\right) + \\
&\frac{\Delta t}{\left(\phi\rho_h\right)_{ijk}^{n+1}}\left(\frac{1}{\Delta y_{ijk}}\sum_{l=1}^{n_p}\left(N_{hl,ijk}^{n} - N_{hl,ij-1k}^{n}\right)\right) + \\
&\frac{\Delta t}{\left(\phi\rho_h\right)_{ijk}^{n+1}}\left(\frac{1}{\Delta z_{ijk}}\sum_{l=1}^{n_p}\left(N_{hl,ijk}^{n} - N_{hl,ijk-1}^{n}\right)\right) - \\
&\frac{c_{h,ijk}^{n}}{\left(\phi\rho_h\right)_{ijk}^{n+1}}\left(\left(\phi\rho_h\right)_{ijk}^{n+1} - \left(\phi\rho_h\right)_{ijk}^{n}\right)
\end{aligned}
\tag{4-35}
$$

After solving concentration of components, Hand's phase behavior rule in the presence of surfactant at different salinities is used to calculate the concentrations of components in the different phases, $c_{1l}^{n+1}, ..., c_{n_c l}^{n+1}$; then phase saturations are calculated.. The new pressures and concentrations are deemed as old values and the calculation is repeated. Figure 5-11 shows the flow chart for numerical solution of all flow equations in UTCHEM.

4.3 DISCRETIZATION OF WELL MODEL

This section describes the numerical form of well models implemented in the UTCHEM simulator. As discussed in Chapter 3, flow formulations are considered at reservoir condition. Hence, well model calculations in the four-phase model are also considered at reservoir condition similar in the original formulation. Therefore, the amount of gas injected and/or produced represents production or injection of free gas at reservoir condition.

4.3.1 Vertical Wells

Two basic well conditions of constant flow rate or constant flowing bottomhole pressure are implemented. Application of Darcy's law to a wellblock ***(ijk)*** results in

$$q_{ijk}^{n+1} = \sum_{l=1}^{n_p} q_{l,ijk}^{n+1} = \sum_{l=1}^{n_p} PI_{ijkl}^{n} \left(p_{wf,ijk}^{n} - p_{l,ijk}^{n+1} \right) \tag{4-36}$$

where $p_l = p_1 - p_{cl}$ and PI is productivity index of phase l. For two dimensional areal ***(X-Y)*** and three-dimensional simulation, the PI is given by

$$PI_{l,ijk}^{n} = \frac{2\pi\sqrt{k_{x,ijk}k_{y,ijk}}\,\Delta z_{ijk}}{0.15802\left(\ln\dfrac{r_o}{r_w} + S\right)}\lambda_{rl,ijk}^{n} \tag{4-37}$$

and for one-dimensional and cross-sectional(***Y-Z***) simulation it is given by

$$PI_{l,ijk}^{n} = \frac{k_{x,ijk}\Delta y_{ijk}\Delta z_{ijk}}{0.15802\left(\dfrac{\Delta x}{2}\right)}\lambda_{rl,ijk}^{n} \tag{4-38}$$

where the constant in the above equations is a unit conversion factor with permeability in Darcy and gridblock size in ***ft*** and mobility in ***cp^{-1}*** to result in ***psi.*** The equivalent radius, r_o is calculated using Peacman's model (Peacman, 1983).

$$r_o = 0.28 \left(\frac{\left(\frac{k_{x,ijk}}{k_{y,ijk}}\right)^{1/2} \Delta y_{ijk}^2 + \left(\frac{k_{y,ijk}}{k_{x,ijk}}\right)^{1/2} \Delta x_{ijk}^2}{\left(\frac{k_{x,ijk}}{k_{y,ijk}}\right)^{1/4} + \left(\frac{k_{y,ijk}}{k_{x,ijk}}\right)^{1/4}} \right)^{1/2} \tag{4-39}$$

The well bottom hole flowing pressure in any layer k, $p_{wf,ijk}$ is given by

$$p_{wf,ijk}^n = p_{wf,ijk-1}^n + \bar{\gamma}_{ijk-1}^n, \; k = 2, \ldots, n_{bz} \tag{4-40}$$

where n_{bz} is the number of perforated layers and $\bar{\gamma}_{ijk}^n = \gamma_{ijk}^n \frac{\Delta z_{ijk}}{2} + \gamma_{ijk-1}^n \frac{\Delta z_{ijk-1}}{2}$. But γ_{ijk}^n is calculated from

$$\gamma_{ijk}^n = \frac{\sum_{l=1}^{np} \gamma_{l,ijk}^n PI_{l,ijk}^n}{\sum_{l=1}^{n_p} PI_{l,ijk}^n} \tag{4-41}$$

For the producer wellblock, specific weights of the produced fluids, $\gamma_{l,ijk}^n$, are used in the above calculations, while for the injection wells, the specific weights of the injected phases are calculated using

$$\gamma_{l,ijk}^n = \sum_{h=1}^{n_c} \left(c_{Inj,hl,ijk}^n \right) \gamma_h \tag{4-42}$$

4.3.1.1 Rate Constraint for Injection Wells

When the phase injection rates, $q_{inj,l}$ are specified, the positive injection rates are allocated to the individual layer k that is perforated according to

$$q^n_{l,ijk} = q^n_{nj,l} \frac{\sum_{l=1}^{n_p} PI^n_{l,ijk}}{\sum_{k=1}^{n_{bz}} \sum_{l=1}^{n_p} PI^n_{l,ijk}} \tag{4-43}$$

and the total injection phase rate for the ijk block is given by

$$q^n_{ijk} = \sum_{l=1}^{n_p} q^n_{l,ijk} \tag{4-44}$$

But the component rate h is calculated from

$$q^n_{h,ijk} = \sum_{l=1}^{n_p} c^n_{hl,ijk}\ q^n_{l,ijk} \tag{4-45}$$

The above term is then added to the right hand side vector BV_{ijk} of the pressure equation at the ijk block. In Equation (4-44) , it is assumed that the potential gradient between the wellbore and the gridblock pressure is the same for all the layers in the reservoir model. Nolen and Berry (1972) have shown that including the potential differences in Equation (4-45) may result in stability problems. Equation (4-45) may give erroneous results in the case of large vertical heterogeneity and especially when non-communicating layers exist. However, in the absence of a very low permeability zone or small cross flow, the above formulation does not produce a significant error.

4.3.1.2 Pressure Constraint for Injection Wells

When bottomhole injection pressure for the first perforated layer, $p_{wf,ijk=1}$, is specified, Equation (4-44) is used. The term $\omega^n_{ijk} = \sum_{l=1}^{n_p} PI^n_{l,ijk} \left(p^n_{wf,ijk} - p^n_{cl,ijk} \right)$ is added to

the constant vector of the pressure equation BV_{ijk} for gridblock ***(ijk)*** and term $\psi_{ijk} = \sum_{l=1}^{n_p} PI_{l,ijk}^{n}$ is added to main diagonal of matrix, AC_{ijk} .

After the pressure equation is solved, Equation (4-44) is used to obtain the total injection rate at the end of the time step, q_{ijk}^{n+1}. The injected phase cuts for each layer are the same as the total injected cuts:

$$q_{l,ijk}^{n+1} = q_{ijk}^{n+1} \frac{q_{Inj,l,ijk}^{n+1}}{\sum_{k=1}^{n_p} q_{Inj,l,ijk}^{n+1}} \tag{4-46}$$

The phase injection rates, $q_{Inj,l}$ specified as input values, are treated as phase cuts and the component rate is calculated as

$$q_{h,ijk}^{n+1} = \sum_{l=1}^{n_p} c_{hl,ijk}^{n} q_{l,ijk}^{n+1} \tag{4-47}$$

4.3.1.3 Rate Constraint for Productions Wells

When the total production rate, input as a negative value (q_{total}) is specified, the withdrawal rate for each layer ***k*** is calculated using

$$q_{ijk}^{n+1} = q_{total} \frac{\sum_{l=1}^{n_p} PI_{l,ijk}^{n}}{\sum_{k=1}^{n_{bz}} \sum_{l=1}^{n_p} PI_{l,ijk}^{n}} \tag{4-48}$$

and the produced phase cuts are then calculated using

$$q_{l,ijk}^{n+1} = q_{ijk}^{n+1} \frac{\lambda_{rl,ijk}^{n}}{\sum_{l=1}^{n_p} \lambda_{rl,ijk}^{n}} \tag{4-49}$$

Then component rate h is calculated

$$q^n_{h,ijk} = \sum_{l=1}^{n_p} c^n_{hl,ijk}\ q^n_{l,ijk} \tag{4-50}$$

The above term, similar to injection well, is added to the right hand side vector BV_{ijk} of the pressure equation at the gridblock ***(ijk).***

4.3.1.4 Pressure Constraint for Productions Wells

When bottomhole pressure for a producer is specified, Equation (4-48) is used to calculate the total production rate (q^{n+1}_{total}) in the same manner as was described above for the injection well on pressure constraint. The produced phase cuts are then obtained similar to injection well from

$$q^{n+1}_{l,ijk} = q^{n+1}_{total} \frac{PI^n_{l,ijk}}{\sum_{l=1}^{n_p} PI^n_{l,ijk}} \tag{4-51}$$

4.3.2 Horizontal Well with Cartesian Gridblocks

Horizontal wells use the same well model equations as vertical wells. Only parameters related to the direction of the wellbore were modified. When the wellbore is parallel to the Z direction, the calculation of the productivity index uses the gridblock height, Δz, the permeability in the X direction, k_x, and the permeability in the y direction, ky. The productivity index calculations were generalized for horizontal wells parallel to either the x direction or the y direction by taking into account the pertinent directional properties. When the wellbore is parallel to the x direction the productivity index calculation uses Δx as the wellblock dimension parallel to the wellbore. Since the

wellbore is perpendicular to the y and z directions, the productivity index calculation uses the permeability in the y direction and the permeability in the ***Z*** direction:

$$PI^{n}_{l,ijk} = \frac{2\pi\sqrt{k_{z,ijk}k_{y,ijk}}\,\Delta x_{ijk}}{0.15802\left(\ln\frac{r_o}{r_w}+S\right)}\lambda^{n}_{rl,ijk} \tag{4-52}$$

The calculations of the equivalent wellblock radius were also generalized for horizontal wells by taking into account reservoir properties perpendicular to the direction of the wellbore. In case the wellbore is parallel to the x direction, the equivalent wellblock radius, based on Peaceman (1983), uses wellblock properties in the y and z directions such as the dimensions Δy and Δz and the permeability values and k_z:

$$r_o = 0.28\left(\frac{\left(\frac{k_{y,ijk}}{k_{z,ijk}}\right)^{1/2}\Delta z^2_{ijk}+\left(\frac{k_{z,ijk}}{k_{y,ijk}}\right)^{1/2}\Delta y^2_{ijk}}{\left(\frac{k_{y,ijk}}{k_{z,ijk}}\right)^{1/4}+\left(\frac{k_{z,ijk}}{k_{y,ijk}}\right)^{1/4}}\right)^{1/2} \tag{4-53}$$

When the wellbore is parallel to the ***Y*** direction the productivity index calculation uses Δy as the wellblock dimension parallel to the wellbore. Since the wellbore is perpendicular to the ***X*** and ***Z*** directions, the productivity index calculation uses the permeability in the x direction and the permeability in the ***Z*** direction:

$$PI^{n}_{l,ijk} = \frac{2\pi\sqrt{k_{z,ijk}k_{x,ijk}}\,\Delta y_{ijk}}{0.15802\left(\ln\frac{r_o}{r_w}+S\right)}\lambda^{n}_{rl,ijk} \tag{4-54}$$

In case the wellbore is parallel to the y direction, the equivalent wellblock radius uses wellblock properties in the x and z directions such as the dimensions Δx and Δz and the permeability values k_x and k_z

$$r_o = 0.28 \left(\frac{\left(\frac{k_{x,ijk}}{k_{z,ijk}}\right)^{1/2} \Delta z_{ijk}^2 + \left(\frac{k_{z,ijk}}{k_{x,ijk}}\right)^{1/2} \Delta x_{ijk}^2}{\left(\frac{k_{x,ijk}}{k_{z,ijk}}\right)^{1/4} + \left(\frac{k_{z,ijk}}{k_{x,ijk}}\right)^{1/4}} \right)^{1/2} \quad (4\text{-}55)$$

Chapter 5: Four-Phase Behavior Equilibrium Formulation

EOS-compositional, thermal, and black oil reservoir simulators can handle gas (or steam)/oil/water equilibrium for a compressible multiphase flow. Also, a few three-phase chemical flooding reservoir simulators that have been recently developed can model oil/water/microemulsion equilibrium state. However, an accurate phase behavior and fluid flow formulations are absent in the literature for the thermal chemical processes to capture four-phase equilibrium.

In this chapter, we present a four-phase model that is developed for gas (or steam)/oil/water/microemulsion, co-existing at equilibrium. This model represents coupling of the solution gas or steam table methods with Hand's rule. Hand's rule is used to capture the equilibrium between surfactant, oil, and water component as a function of salinity and concentrations for oil/water/microemulsion phases.

Therefore, interphase mass transfer between gas/oil or steam/water in the presence of the microemulsion phase and the equilibrium between phases are calculated accurately.

5.1 PHASE DENSITY

Phase densities are modeled in two different ways in the case of existence of steam or gas which may occur during the simulation. When UTCHEM simulates steam injection process or any other process that causes vaporization of water phase, steam and water phase densities are calculated from steam table as shown in Figure 5-3. But, oil phase density is computed from slightly compressible model. Microemulation phase density is calculated as a function of concentration of each component as follows

$$\rho_3 = c_{13}\rho_1 + c_{13}\rho_1 + c_{33}\rho_3 + 0.02533c_{53} + 0.001299c_{63} \tag{5-1}$$

In the case of gas existence, the oil and gas phase densities are related to gas and oil formation volume factors and amount of gas solubility in oil. Since, UTCHEM is a non-EOS simulator, phase behavior is given as table in order to calculate the densities in the saturated and undersaturated conditions. Afterward, compressibility of oil and gas are obtained from Equations (3-43) through (3-47).

In order to make the phase behavior table consistent with commercial simulators, we use the same table within CMG-IMEX and ECLIPS100 containing parameters such as solution gas ratio (R_{so}), bubble point pressure (p_{sat}), formation volume factor of gas and oil (B_g and B_o) and oil and gas viscosities (μ_g and μ_o) as shown in Figure 5-1.

P_{sat} [psi]	R_{so} [scf/stb]	B_o [rb/stb]	B_g [rb/scf]	μ_g [cp]	μ_o [cp]
⋮	⋮	⋮	⋮	⋮	⋮

Figure 5-1-Format of phase behavior or PVT table for oil/gas mass transfer calculations and properties.

Similar to oil viscosity, oil and gas formation volume factors are calculated directly through PVT table by a linear interpolation method. When undersaturated condition arises; oil formation volume factor is calculated from the following equations

$$B_2 = B_{2sat}\left(p_{sat}\right)\left(1-\left(p-p_{sat}\right)\left.\frac{\partial B_2}{\partial p}\right|_{unsat}\right) \tag{5-2}$$

In this study, we assume that solution gas ratio does not change in saturated and undersaturated conditions at a fixed bubble point pressure ($\left.\frac{\partial R_{so}}{\partial p}\right|_{unsat} = 0$). But for an increase in pressure, the undersaturated condition leads to a drop in oil formation volume

factor. In UTCHEM, the change of oil formation volume factor with respect to pressure is considered a constant negative value $\left.\frac{\partial B_2}{\partial p}\right|_{unsat} = -constant$. This value must be provided as input in the UTCHEM simulator.

As Figure 5-2 depicts, undersaturated curves are shown as blue lines and saturated curves are depicted by red lines for a bubble point p_{sat}. As the reservoir is depleted, the value of each oil property moves along the appropriate curve in the direction of decreasing pressure Figure 5-2 illustrates the behavior of solution gas ratio and the formation volume factors with respect to pressure and bubble point pressure. In order to use these parameters directly into the flow formulation, we need to solve the pressure equation and mass equations at standard condition.

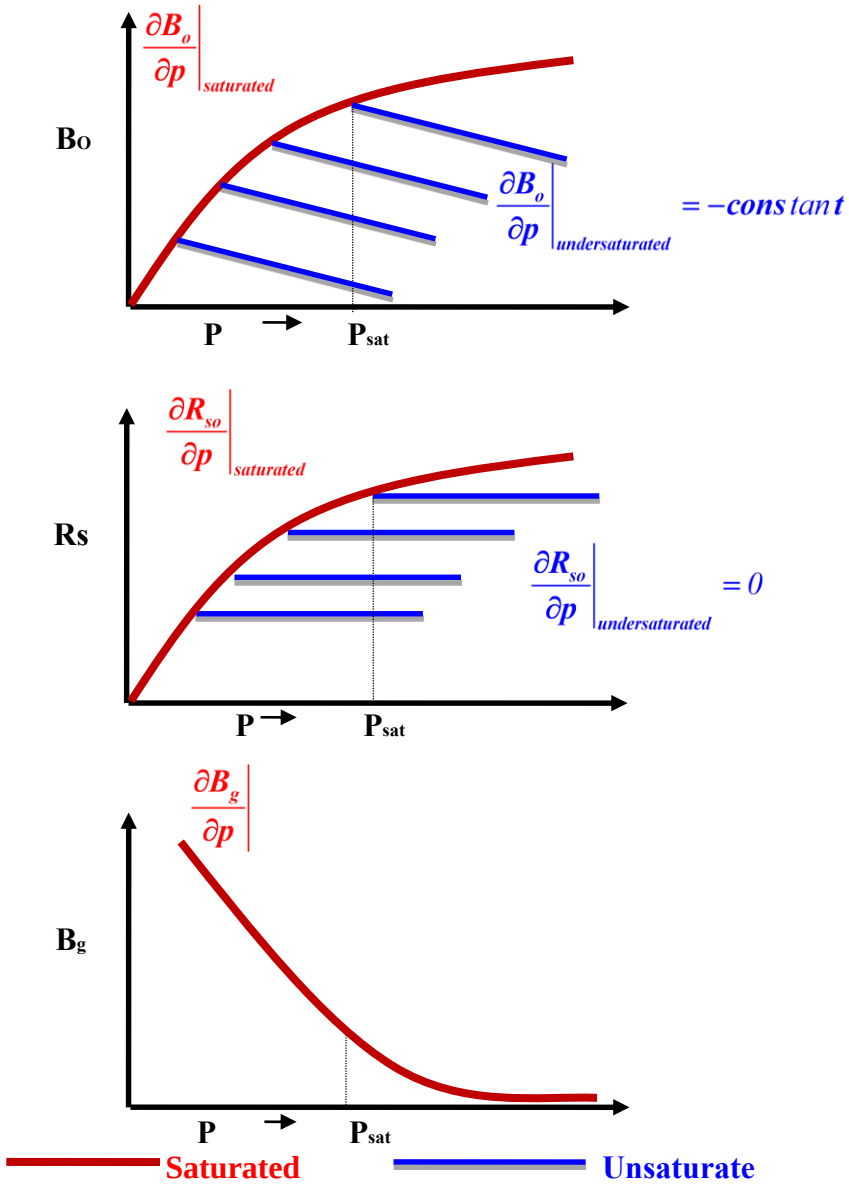

Figure 5-2-Schematic of solution gas ratio, oil, and gas formation volume factors used in UTCHEM to calculate partial mass density of gas in oil phase and mass density of oil and gas components.

Since the flow formulations that have been already developed in the original UTCHEM are at reservoir condition, we need to develop the four-phase model at reservoir condition and convert all phase behavior parameters from standard to reservoir

condition. As mentioned earlier, partial mass density is defined to convey the solution gas ratio from standard condition to reservoir condition as in the following expression:

$$\rho_{82} = \frac{R_{so}\,\rho_{8sc}}{B_2} \tag{5-3}$$

where ρ_{82} is the partial mass density of gas in the oil phase and it represents solution gas ratio at reservoir condition properly. R_{so} is the solution gas ratio at standard condition. ρ_{8sc} is the gas density phase at standard condition and B_2 is the formation volume factor of oil. Similar, we define the partial mass density of oil component in the oil phase in the same manner as in the oil phase

$$\rho_{22} = \frac{\rho_{2sc}}{B_2} \tag{5-4}$$

where ρ_{2sc} is oil phase density at standard condition. This phase density is calculated at the reservoir condition as in the following expression:

$$\rho_2 = \rho_{22} + \rho_{82} \tag{5-5}$$

Gas phase density, which is crucial and sensitive to pressure, is computed from the formation volume factor of gas and density of gas at standard condition as in the following expression:

$$\rho_4 = \frac{\rho_{4sc}}{B_4} \tag{5-6}$$

B_4 is the formation volume factor of gas and, as explained, it is obtained from PVT table. Water phase density is calculated based on the slightly compressible fluid definition as

$$\rho_l = \rho_{1ref}\,(1-\xi_1(\,p-p_{ref}\,)) \tag{5-7}$$

But microemulsion phase density is considered a function of the concentration of each component as follows:

$$\rho_l = c_{1l}\rho_{h=1} + c_{2l}\rho_{h=2} + c_{3l}\rho_{h=3} + 0.02533c_{5l} + 0.001299c_{6l} + 0.00433c_{4l} \quad l = 1 \text{ or } 3. \tag{5-8}$$

In the case of steam injection or thermal flooding, density of steam and water are calculated from steam table for saturated condition. Figure 5-3 shows density of water and steam at saturated condition (pressure and temperature). These values have been tableted in the UTCHEM code to be directly calculated.

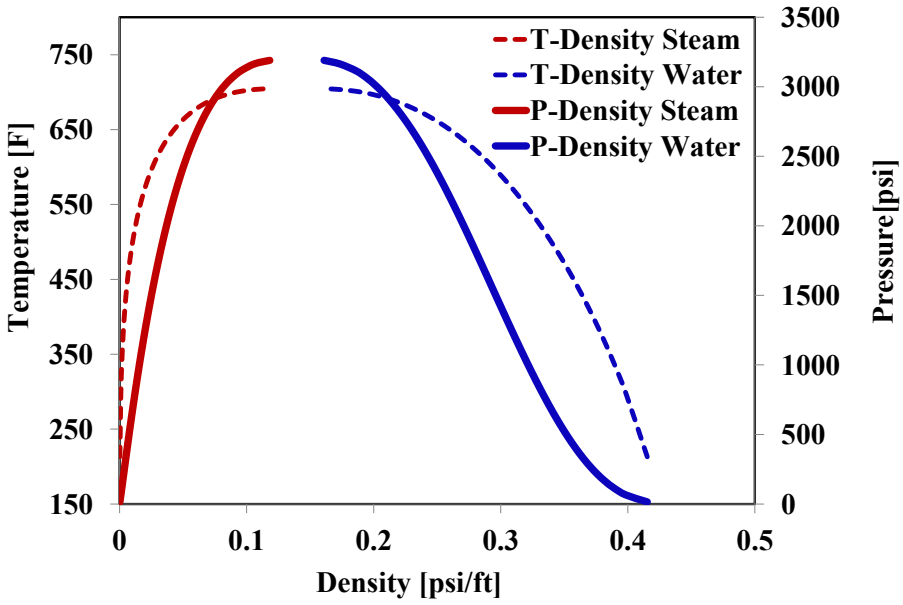

Figure 5-3- Density of water and steam at different saturated points in new four-phase model (Lashgari *et at.,* 2014)

5.2 PHASE VISCOSITY

Gas or steam viscosities are calculated from phase behavior table or steam table, respectively. In the case of gas flooding or in the presence of gas as solution gas or free gas, oil viscosity is obtained from phase behavior table for saturated conditions. For unsaturated condition the viscosity is calculated from the following equations

$$\mu_2 = \mu_{sat}\left(p_{sat}\right)\left(1+\left(p-p_{sat}\right)\frac{\partial\mu_2}{\partial p}\bigg|_{unsat}\right) \tag{5-9}$$

Figure 5-4 shows a schematic of oil viscosity at saturated condition, marked by red line, and in undersaturated condition by blue lines with constant slope. Also, Figure 5-5 depicts gas viscosity with respect to pressure. In the case of steam flooding, water viscosity is also calculated from steam table as shown in Figure 5-6.

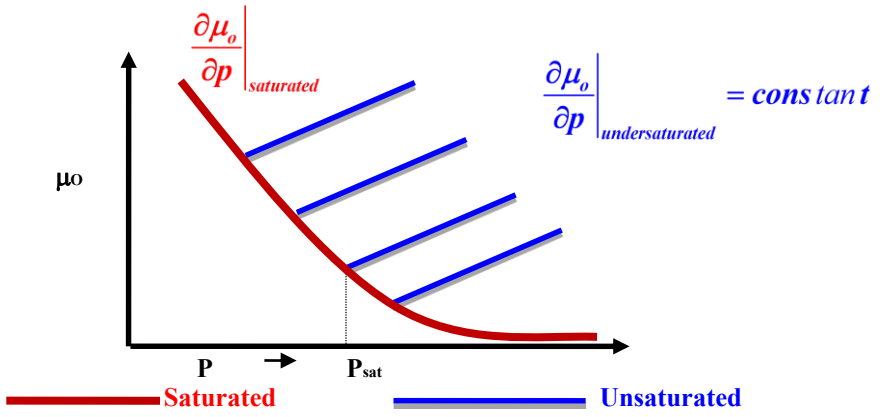

Figure 5-4- Schematic of oil viscosity calculation in the four-phase model for saturated and unsaturated condition

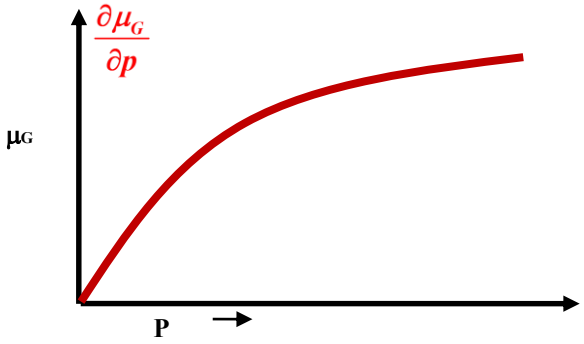

Figure 5-5- Schematic of gas viscosity calculation in four-phase model

Phase viscosity is modeled in terms of pure viscosities and the concentrations of water, oil, surfactant in each phase:

$$\mu_l = c_{1l}\mu_w e^{\alpha_1(c_{2l}+c_{3l})} + c_{2l}\mu_o e^{\alpha_2(c_{2l}+c_{3l})} + c_{3l}\alpha_3 e^{(\alpha_4 c_{1l}+\alpha_5 c_{2l})}, \qquad l = 1,2,3 \tag{5-10}$$

where α parameters are coefficients determined from laboratory data by matching of measured viscosities. This model shows that in the absence of surfactant and polymer, water or oil phase viscosities reduce to its water or oil viscosities that are read from phase behavior table, steam table, or pure component water and oil viscosities.

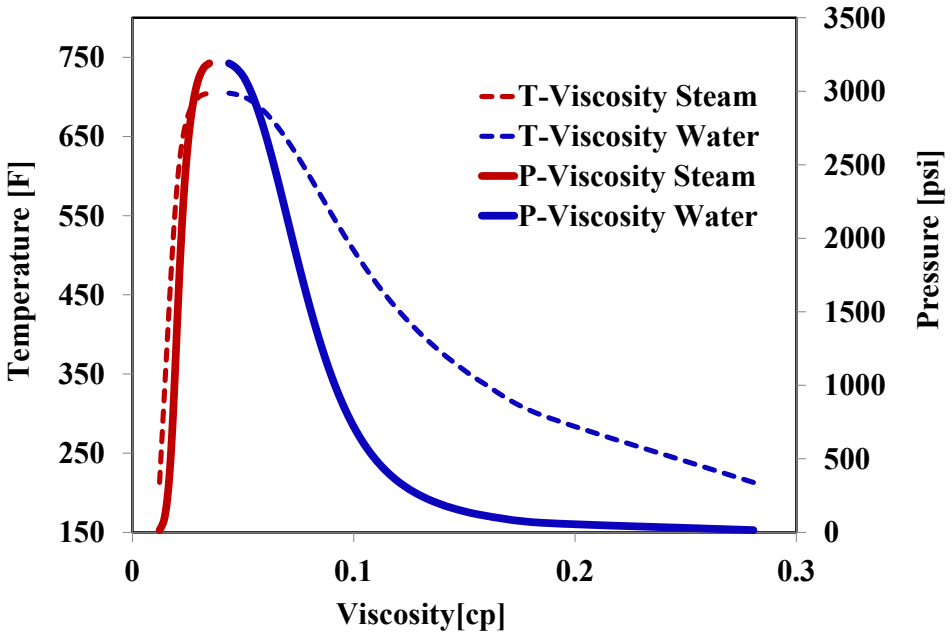

Figure 5-6- Viscosity of water and steam at different saturated points in four-phase model (Lashgari *et at.,* 2014a).

In order to model the effect of temperature on oil viscosity, the four-phase model in UTCHEM uses the following exponential function to compute oil viscosity as a function of temperature (T):

$$\mu_{oil} = \mu_{oil,ref}\, exp\left[b_{oil}\left(\frac{1}{T} - \frac{1}{T_{ref}} \right) \right] \tag{5-11}$$

where $\mu_{oil,ref}$ is the viscosity at a reference temperature T_{ref} and b_{oil} is a constant reduction factor. For instance, in Chapter 8, there are some examples that show viscosity reduction with respect to temperature variations in heavy oil reservoirs by using b_{oil} of 5000 ^{o}F and a reference of viscosity 5000 cp at temperature 65 ^{o}F.

5.3 SURFACTANT PHASE BEHAVIOR

The surfactant/oil/water phase behavior has been formed based on Winsor (1954), Reed and Healy (1977), Nelson and Pope (1978), Prouvost *et al.* (1985), and Camilleri *et al.*, (1987). The volumetric total concentrations of the three components (c_1, c_2, c_3) are used as the coordinates on a ternary diagram. Although the presence of salinity, divalent cations, and alcohol (c_5, c_6, c_7) impact the surfactant phase behavior significantly, we model, in this study, the surfactant phase behavior as being affected by salinity alone and assume the absence of divalent cations and alcohols (c_6, c_7).

In case the surfactant concentration is below the Critical Micelle Concentration (CMC), the two phases are a water phase containing all the surfactant, water, and electrolytes and a pure excess oil phase. At low salinity, an excess oil phase that is essentially pure oil and a microemulsion phase that contains water plus electrolytes, surfactant, and some solubilized oil exist as shown in Figure 5-8. The tie lines (distribution curves) at low salinity have negative slope. This type of phase environment is called Winsor Type I, or Type II (−). At high salinity, an excess water phase and a microemulsion phase containing most of the surfactant and oil, and some solubilized water exist as illustrated in Figure 5-9. This type of phase environment is called Winsor Type II, or alternatively Type II(+). At intermediate salinity, the mixture separates into three phases. These phases are excess oil and water phases and a microemulsion phase as predicated in Figure 5-10 . This phase environment is called Winsor Type III.

Surfactant phase behavior should be thoroughly modeled with actual reservoir fluids at reservoir conditions to evaluate the performance of surfactant flooding in the presence of solution gas in oil at reservoir temperature and pressure.

In spite of the importance of surfactant phase behavior at high pressure and reservoir temperature with solution gas, only a few studies have been done over the past decades and have been published in literature.

Among these studies, there are contradictions to a significant extent about the effect of solution gas and pressure on the microemulsion phase behavior for different oils. Nelson (1983), Bourrel *et al.* (1987), and Jang *et al.* (2014) have reported a small effect. Several experimental studies report a decrease in the optimum salinity when methane is added to crude oil (Puerto and Reed, 1983; Roshanfekr *et al.,* 2009; Southwick *et al.,* 2012). Sagi *et al.* (2013) also found that adding methane, ethane, and CO_2 caused a decrease in the optimum salinity though there is ambiguity in their observations of the phase transition from type II(-) to type III to Type II(+).

Cottinet *et al.,* (2012) reported a slight increase in optimum salinity for their live oil compared to their dead oil. Pressure also causes a change in microemulsion phase behavior (Kim *et al*., 1985, 1988; Austad *et al.,* 1990; Austad and Strand, 1996; Austad *et al.,*1996; Skauge and Fortland, 1990; Sanderson *et al.,* 2012).

These researchers, as well as Nelson (1978), consistently report that for pure hydrocarbons and crude oils the optimum salinity increases as the pressure increases. This change corresponds to less affinity of the surfactant for the denser oil. However, the shift of the phase behavior with pressure up to several thousand psi is not large compared to the compositional effect of solution gas. These studies provide useful data, but it is still rather difficult to find systematic studies of microemulsion phase behavior using live oil that quantify the individual effects of pressure and solution gas in addition to their net effects.

Some variables such as alcohol type and concentration, and changes in pressure, temperature, and solution gas also cause a phase environment shift from one type of

phase behavior to another type. The effect of solution gas, pressure, and temperature are discussed in sections 5.4 and 5.5 in detail. The surfactant/oil/water phase behavior is thus represented as a function of effective salinity, once the binodal curve and tie lines are described. The oil and gas (water and steam) concentrations used in the calculations are obtained from the solution gas model or steam table model after solving for pressure and before calculating mass balance equations. Since they belong to the solution gas model and they are calculated after mass conservation, they cannot be changed during the explicit chemical phase behavior calculations. This coupling of the phase behaviors (surfactant phase behavior with solution gas and steam table phase behavior) forces the assumptions of negligible changes in oil and in water due to solubilization.

5.4 EFFECT OF TEMPERATURE

Although temperature effect on the surfactant phase behavior is not generalized, an increase in temperature leads to an increase in optimum salinity and a decrease in optimum solubilization of oil.

An increase in temperature leads to shifting the phase equilibrium of surfactant solutions towards the lower phase microemulsion. This means that surfactants normally become more water-soluble and less oil-soluble as temperature increases (Novosad,1982).

Healy and Reed (1976) observed that for constant salinity, increasing the temperature results in a decrease in solubilization of oil and an increase in solubilization of water in the microemulsion phase. Solubilization ratio or solubilization parameter of oil is defined as the ratio of volume of oil in the microemulsion phase to volume of surfactant in that phase, Vo/Vs. A similar definition is used for the solubilization parameter of water as Vw/Vs. Puerto and Reed (1983) presented that the optimum

solubilization parameter decreases with temperature and this causes an increase in optimum salinity.

The Aoudia and Wade (1995) trend of data is the same as suggested by other authors(Austad and Skule (1996)). They also suggest that optimum solubilization ratio decreases with increasing temperature. Dwarakanath and Pope (2000) studied the effect of temperature on phase behavior and found that although optimum salinity increases with temperature, the solubilization ratio versus normalized salinity (salinity divided by optimum salinity) remains the same for a range of temperatures.

5.5 EFFECT OF PRESSURE AND SOLUTION GAS

Surfactant phase behavior should be thoroughly modeled at reservoir conditions to evaluate the performance of surfactant flooding in the presence of solution gas in oil at reservoir temperature and pressure. Despite the importance of surfactant phase behavior at high pressure and reservoir temperature with solution gas, only a few studies have been done over the past decades and published in literature. Although the purpose of this research is not modeling and evaluation of reservoir temperature, pressure and solution gas effect on phase behavior, understanding of phase behavior in the presence of these factors are important to a significant extent.

Among these studies, there are contradictions about the effect of solution gas and pressure on the microemulsion phase behavior for different oils (Nelson ,1983 and Bourrel *et al*.,1987).

Also, several experimental studies report a decrease in the optimum salinity when gas (methane) is added to crude oil (Puerto and Reed, 1983; Roshanfekr *et al*., 2009; Southwick *et al.,* 2012, Sagi *et al.* (2013)). But, Cottin *et al.,* (2012) reported a slight increase in optimum salinity for their live oil compared to their dead oil.

Pressure also causes a change in microemulsion phase behavior (Kimet *et al.,* 1985, 1988; Austadet *et al.,* 1990; Austad and Strand, 1996; Austad *et al*., 1996; Skauge and Fortland, 1990; Sanderson *et al*., 2012).

These studies report that for pure hydrocarbons and crude oils, the optimum salinity increases as the pressure increases. This change corresponds to less affinity of surfactant for the denser oil. However, the shift of the phase behavior by increasing pressure to several thousand psi is not large compared to the compositional effect of solution gas. These studies provide the qualitative understanding of phase behavior in high pressure and solution gas ratio, but it is still rather difficult to find systematic studies of the microemulsion phase behavior using live oil that quantify the individual effects of pressure and solution gas in addition to their clear effects. Therefore, we assume in the modeling of four phase flow at equilibrium condition, solution gas and pressure effect do not impact the surfactant phase behavior due to contradictory in literature.

5.6 EFFECTIVE SALINITY

The effective salinity increases with divalent cations bound to micelles (Glover *et al*., 1979; Hirasaki, 1982; Camilleri *et al.,* 1987) and decreases as the temperature increases for anionic surfactants and increases as the temperature increases for nonionic surfactants as described I the following expression:

$$c_{se} = c_{51}\left(1-\beta_6 f_6^s\right)^{-1}\left(1+\beta_T\left(T-T_{ref}\right)\right)^{-1} \tag{5-12}$$

where c_{51} is the aqueous phase anion concentration; β_6 is a positive constant f_6^s is the fraction of the total divalent cations bound to surfactant micelles as

$$f_6^s = \frac{c_6^s}{c_3^m} \tag{5-13}$$

β_T is the temperature coefficient. The effective salinities at which the three equilibrium phases form or disappear are called lower and upper limits of effective salinity (c_{sel} and c_{seu}).

5.6.1 Binodal Curve Approach

The formulation of the binodal curve using Hand's rule (Hand, 1939; Pope and Nelson, 1978) is assumed to be the same in all phase environments. Hand's rule is based on the empirical observation that equilibrium phase concentration ratios are straight lines on a log-log scale as shown in Figure 5-7. The binodal curve is described by

$$\frac{c_{3l}}{c_{2l}} = A\left(\frac{c_{3l}}{c_{1l}}\right)^B \quad \textit{for} \quad l = 1,2,3 \tag{5-14}$$

For a symmetric bionodal curve B=***-1,*** which is the current formulation used in UTCHEM. All phase concentrations are calculated explicitly in terms of oil concentration.

$$c_{3l} = \frac{1}{2}\left(-Ac_{2l} + \sqrt{\left(A^2c_{2l}^2 + 4Ac_{2l}\left(1-c_{2l}\right)\right)}\right) \textit{ for } l = 1,2 \textit{ or } 3 \tag{5-15}$$

The parameter A is related to the height of binodal curve as follows:

$$A_m = \left(\frac{2c_{3max,m}}{1-c_{3max,m}}\right)^2 \quad \textit{for} \quad m = 0,1 \tag{5-16}$$

where m = 0, 1 and 2 correspond to low, high and optimal salinities. The height of bionodal curve is specified as a linear function of temperature:

$$c_{3,max,m} = H_{BNC,m} + H_{BNT,m}\left(T - T_{ref}\right) \quad for\ m = 0,1,and\ 2 \tag{5-17}$$

where $H_{BNC,m}$ and $H_{BNT,m}$ are input parameters. Am is linearly interpolated as

$$A = \left(A_0 - A_1\right)\left(1 - \frac{c_{se}}{c_{seop}}\right) + A_1 \quad for\ c_{se} \le c_{seop}$$
$$A = \left(A_2 - A_1\right)\left(1 - \frac{c_{se}}{c_{seop}}\right) + A_1 \quad for\ c_{se} \le c_{seop} \tag{5-18}$$

where c_{seop} is the optimum effective salinity and the arithmetic average of c_{sel} and c_{seu}. The heights of the binodal curve at three reference salinities are input to the simulator and are estimated based on phase behavior laboratory experiments.

5.6.2 Tie Lines for Two Phases

For both Type II(-) and Type II(+) phase behavior, there are only two phases below the binodal curve. Tie lines are the lines joining the composition of the equilibrium phases and are given by

$$\frac{c_{3l}}{c_{2l}} = E\left(\frac{c_{3l}}{c_{1l}}\right)^F \quad for \quad l = 1,2,3 \tag{5-19}$$

where $l = 1$ for Type II(+) and $l = 2$ for Type II(-). In the absence of available data for tie lines, F is calculated from F = -1/B. For a symmetric binodal curve (B=-1), F is equal to 1. Since the plait point (p) is on both the binodal curve and the tie line, E can be obtained from

$$E = \frac{c_{1p}}{c_{2p}} = \frac{1 - c_{2p} - c_{3p}}{c_{2p}} \tag{5-20}$$

Applying the binodal curve equation to the plait point and substituting c_{3P} Equation 5.19 into Equation 5.20, we have

$$E = \frac{1 - c_{2p} - \frac{1}{2}\left(-Ac_{2p} + \sqrt{Ac_{2p} + 4Ac_{2p}\left(1 - c_{2p}\right)}\right)}{c_{2p}} \tag{5-21}$$

where c_{2p} is the oil concentration at plait point is an input parameter for Type II(-) and Type II(+) phase environments.

5.6.3 Tie Lines for Type III

The phase composition calculation for the three-phase region of Type **III** is simple because of the assumption that the excess oleic and aqueous phases are pure. The microemulsion phase composition is defined by the coordinates of the invariant point. The coordinates of the invariant point (**M**) are calculated as a function of effective salinity:

$$a = \frac{c_{se} - c_{sel}}{c_{seu} - c_{sel}} \tag{5-22}$$

$$\frac{a - c_{2M}}{c_{3M}} = \cos 60^o \tag{5-23}$$

$$c_{3M} = 2\left(a - c_{2M}\right) \tag{5-24}$$

where invariant point M is on the binodal curve

$$c_{3M} = \frac{1}{2}\left(-Ac_{2M} + \sqrt{\left(A^2 c_{2M}^2 + 4Ac_{2M}\left(1 - c_{2M}\right)\right)}\right) \tag{5-25}$$

and

$$c_{2M} = \frac{1}{2\left(4 - A\right)}\left(2a\left(4 - A\right) + A \pm \sqrt{\left(\left(2a\left(4 - A\right) + A\right)^2 - 16a^2\left(4 - A\right)\right)}\right) \tag{5-26}$$

The invariant point should disappear when c_{se} approaches c_{sel} ($c_{2M} = 0$, $a = 0$) and when c_{se} approaches c_{seu} ($c_{2M} = 1$, $a = 1$). These conditions hold only for the negative sign

in Equation (5-26) The phase composition calculations for lobes II(-) and II(+) are analogous. The plait point must vary from zero to the II(-) value c^*_{2PR} or zero to II(-) value, c^*_{2PR}. Here, we only consider the II(-) lobe. The plait point is calculated by interpolation on effective salinity:

$$c_{2PR} = c^*_{2PR} + \frac{c_{se} - c_{sel}}{c_{seu} - c_{sel}}\left(1 - c^*_{2PR}\right) \tag{5-27}$$

In order to apply Hand's equation, we transform the concentrations as shown in Fig 2.5; the transformed concentrations are

$$c'_{1l} = c_{1l}\sec\theta \tag{5-28}$$

$$c'_{3l} = c_{3l} - c_{2l}\tan\theta \quad \text{for } l = 2 \text{ or } 3 \tag{5-29}$$

$$c'_{2l} = 1 - c'_{1l} - c'_{3l} \tag{5-30}$$

The angle θ can be obtained

$$\tan\theta = \frac{c_{3M}}{c_{1M}}$$
$$\sec\theta = \frac{\sqrt{c^2_{1M} + c^2_{3M}}}{c_{1M}} \tag{5-31}$$

Parameter E of the tie line equation is now calculated in terms of untransformed coordinates of the plait point as

$$E = \frac{c'_{1p}}{c'_{2p}} = \frac{1 - \left(\sec\theta - \tan\theta\right)c_{2PR} - c_{3PR}}{c_{2PR}\sec\theta} \tag{5-32}$$

where c_{3PR} is given by Equation 5.29 and $c_{1PR} = 1 - c_{2PR} - c_{3PR}$.

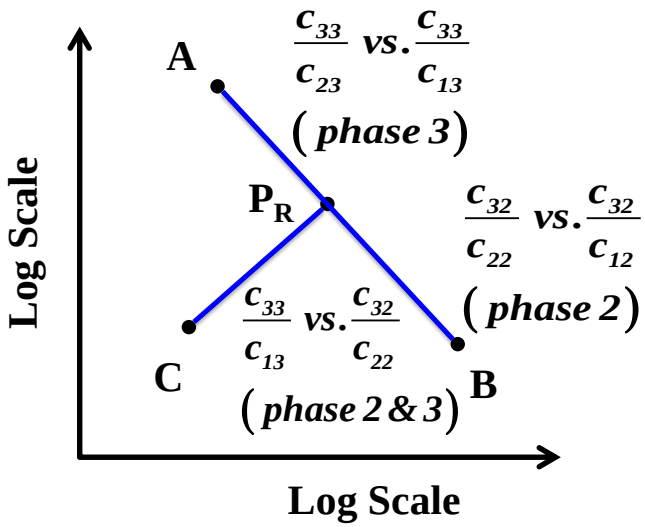

Figure 5-7-Hand's plot corresponded to ternary diagram Type II(-) illustrated in Figure 5-8.

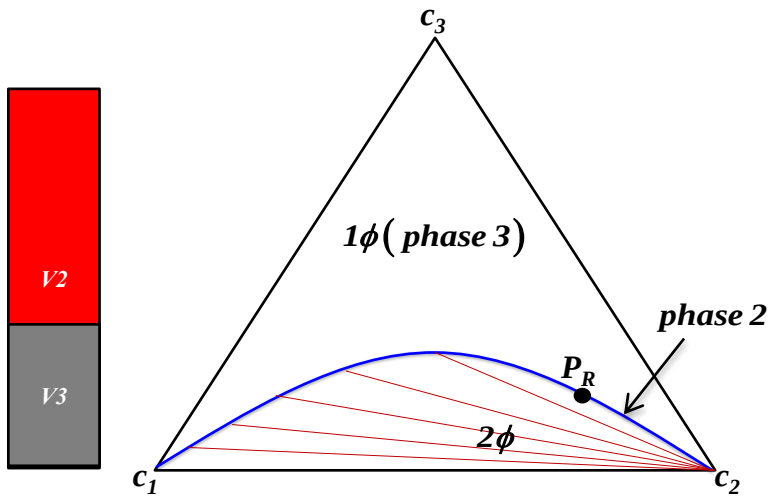

Figure 5-8-Ternary diagram and phase volumes for Type II (-) at low salinity (salinity, C5, is under optimum low salinity), V1 is volume of aqueous phase, V2 is volume of oleic phase and V3 is volume of microemulsion phase

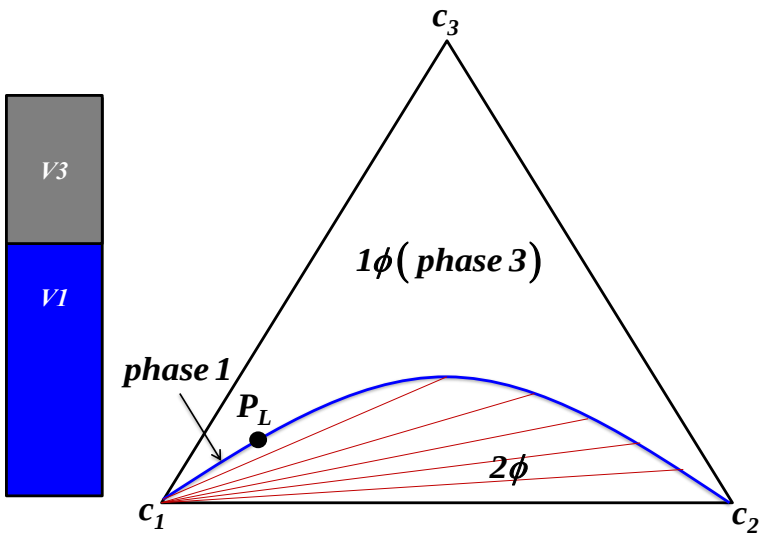

Figure 5-9-Ternary diagram and phase volumes for Type II(+) at high salinity (salinity, C_5, is upper optimum high salinity),V1 is volume of aqueous phase, V2 is volume of oleic phase and V3 is volume of microemulsion phase

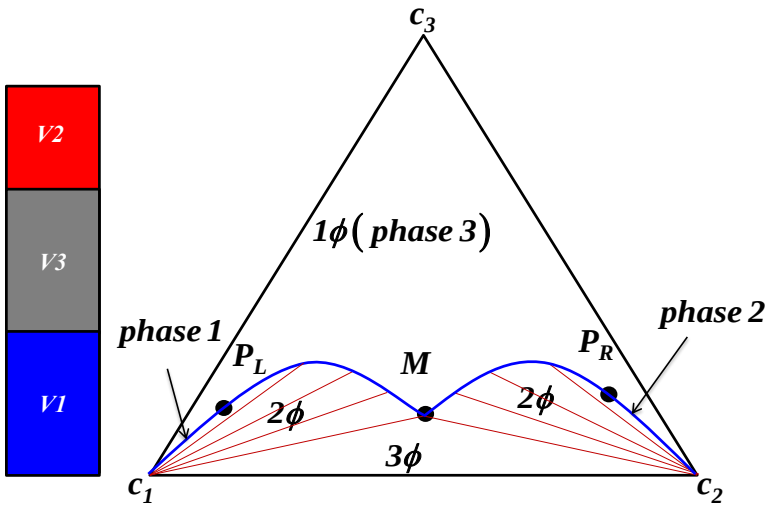

Figure 5-10- Ternary diagram and phase volumes for Type III at the range of optimum salinity (salinity, C_5, is between optimum low and high salinities), V1 is volume of aqueous phase, V2 is volume of oleic phase and V3 is volume of microemulsion phase

5.7 BUBBLE POINT TRACKING IN OIL/GAS PHASE BEHAVIOR

Among the fluid data needed by UTCHEM are the oil and gas formation volume factors B_2 and B_4, the solubility of gas in oil R_{so}, and the oil and gas viscosity, μ_2 and μ_4. These properties are functions of pressure. As mentioned earlier, undersaturated curves are shown by blue lines in Figure 5-2 and saturated curves are depicted by red color lines for a bubble point. The slopes of the straight lines representing the undersaturated curves for the initial bubble point p_{sat}. We consider a constant slope for oil corresponding to each bubble point to calculate fluid data of oil in undersaturated condition.

As the reservoir depletes, the value of each oil property moves along the appropriate curve in the direction of decreasing pressure. When the pressure drops below the bubble point (p_{sat}), free gas concentration forms. In case the free gas concentration exceeds the trapped gas saturation, gas becomes mobile and can be produced or can move in reservoir. Production of the gas changes the local total gas/oil ratio and as a consequence the local saturation pressure changes. In case the reservoir is repressurized by, for instance, waterflooding, the initial bubble point should be change due to solubilization of free gas in oil component. In order to account for this effect, we need to consider the mass balance of gas in a grid block as free and solution gas.

It is assumed that free gas exists in a gridblock containing oil concentration. In order to estimate the pressure at which the free gas component completely dissolves in the oil gridblock, we estimate new gas solubility R_{so}^{new} from the volumes of oil and gas in the gridblock then we use the saturated R_{so} versus p curves to find a new bubble point p_{sat}^{new}. The new solubility is estimated as the sum of the dissolved gas and the free gas in the gridblock divided by oil concentration at standard condition; thus

$$R_{so}^{new} = \frac{\left(R_{so}^{old} c_2^{old} / B_2^{new}\right) + \left(c_8^{old} / B_4^{new}\right)}{c_2^{old} / B_2^{new}} \tag{5-33}$$

In order to consider the effect of solution gas in the flow formulation, we use the following equation to obtain partial mass density of gas in oil component at reservoir condition as

$$\rho_{82}^{new} = \frac{\rho_{8,sc} R_{so}^{new}}{B_2^{new}} \tag{5-34}$$

The saturation pressure corresponding to R_{so}^{new} is the new bubble point pressure p_{sat}^{new}. Undersaturated curves for pressures above p_{sat}^{new} are parallel to the undersaturated curves using the slope from input for oil viscosity and solution gas ratio.

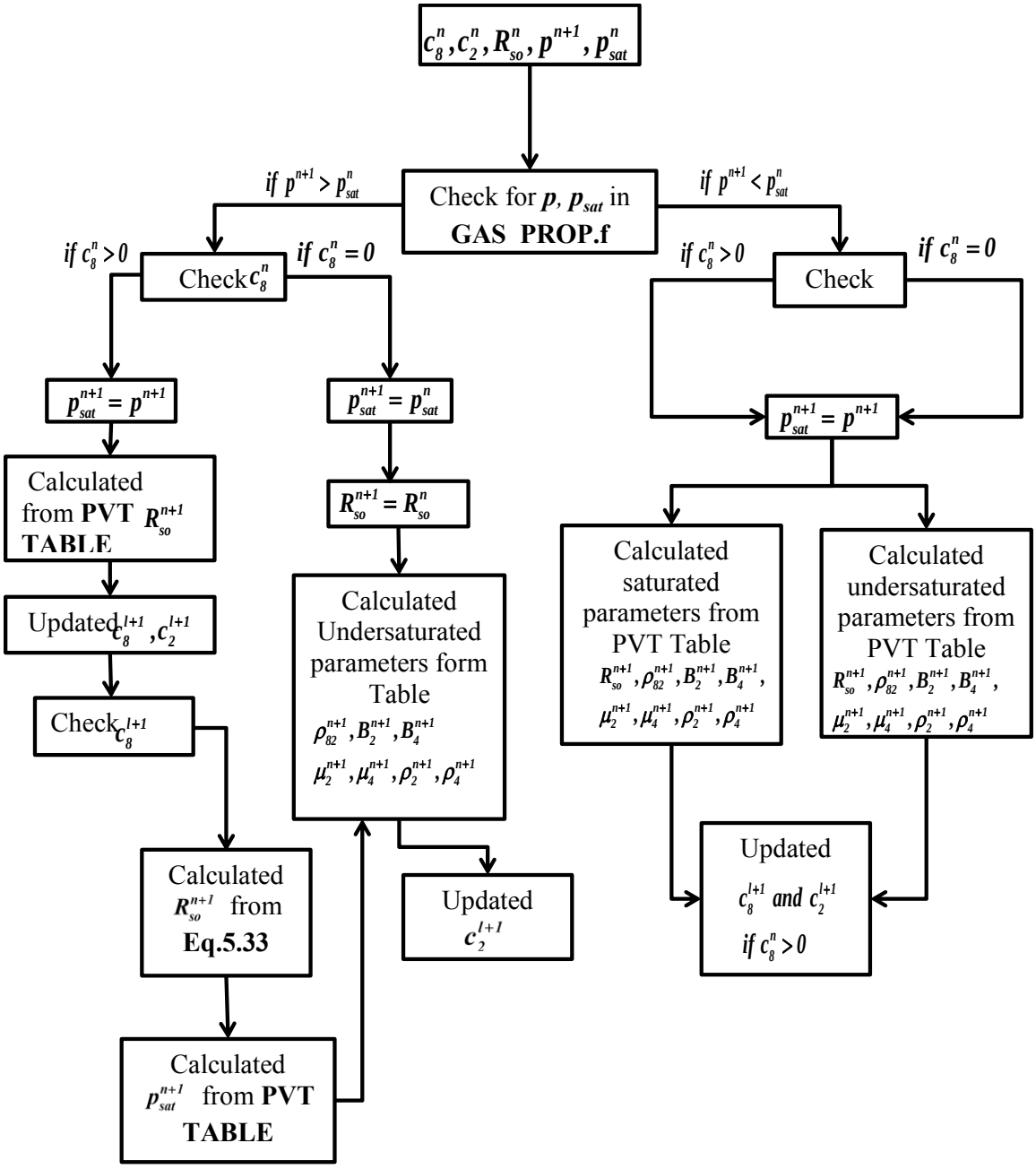

Figure 5-11- The flow chart for calculation of oil/gas phase equilibrium

5.8 PHASE SATURATIONS

Phase saturations in the saturated zone in the presence of surfactant are calculated from the phase concentrations, overall component concentration, and saturation constraints once the phase environment and phase compositions are known. The overall component concentration and saturation constraints are

$$c_h = \sum_{h=1}^{n_c} S_l c_{hl} \quad for \quad l = 1,..,n_p \tag{5-35}$$

$$\sum_{l=1}^{n_p} S_l = 1 \tag{5-36}$$

The phase saturations are computed from the overall component concentration and the saturation constraint by

$$S_l = \sum_{h=1}^{n_c} c_{hl} \quad for \quad l = 1,..,n_p = 3 \tag{5-37}$$

$$S_4 = 1 - \sum_{l=1}^{n_p=3} S_l \tag{5-38}$$

5.9 RELATIVE PERMEABILITY

Multiphase relative permeabilities are modeled using Corey-type functions (Brooks and Corey, 1966; Delshad and Pope, 1989) extension of two-phase flow equation to three-phase flow. In UTCHEM, relative permeability up to four-phase flow is computed using the following model rather than the table look-up method.

$$k_{rl} = k_{rl}^o \; S_{nl}^{e_l} \quad for \quad l = 1,..,4 \tag{5-39}$$

where k_{rl}^o is the endpoint relative permeability phase l, and $S_{nl}^{e_l}$ is the normalized saturation for phase l, and e_l is the exponent of phase l. These parameters are constant for high interfacial tension model. But for low ultra-interfacial tension model

these parameters are function of capillary number. The normalized phase saturation is obtained

$$S_{nl} = \frac{S_l - S_{rl}}{1 - \sum_{1}^{4} S_{rl}} \tag{5-40}$$

Relative permeability experiments with pre equilibrated phases show that oil, water, microemulsion and gas relative permeabilites are function of their phase saturations. This model allows for non-zero residual phase saturation at infinity trapping number, The end point relative permeability, and curvature of the relative permeability, are calculated as function of trapping number as

$$k_{rl}^{o} = k_{rl}^{o,low} + \left(\frac{S_{rl'}^{low} - S_{rl'}}{S_{rl'}^{low} - S_{rl'}^{high}} \right) \left(k_{rl}^{high} - k_{rl}^{low} \right), \; l \neq l' \; ; \; l, l' = oil, water, and \; microemulsion$$
$$k_{rl}^{o} = constant \quad l = gas \tag{5-41}$$

and

$$e_l = e_l^{low} + \left(\frac{S_{rl'}^{low} - S_{rl'}}{S_{rl'}^{low} - S_{rl'}^{high}} \right) \left(e_l^{hight} - e_l^{low} \right) \quad l \neq l' \; ; \; l, l' = oil, water, and \; microemulsion \tag{5-42}$$

The subscript w denotes low capillary number or high interfacial tension (water/oil) values while subscript c depicts high capillary number or low interfacial tension values. The values of the phase indicates l and l' depends of liquid flow as

$$\begin{aligned} &If \; l = 1 \; then \; l' = 3 \\ &If \; l = 2 \; then \; l' = 3 \\ &If \; l = 3 \; S_1 < S_{1r} \; and \; S_2 > S_{2r} \; then \; l' = 2 \\ &If \; l = 3 \; S_1 \geq S_{1r} \; and \; S_2 \leq S_{2r} \; then \; l' = 2 \end{aligned} \tag{5-43}$$

In this four-phase model gas relative permeability is not function of capillary number and other phase saturations but it is only function of its own parameters.

Chapter 6: Verification of Three-Phase Models and Developed Four-Phase Model

In this chapter several test cases are shown to verify the mathematical formulations and derivations in Chapter 3 and the numerical solution methods discussed in Chapter 4 by using the coupled four phase behavior elaborated in Chapter 5. In these test cases, three phase behavior of gas/oil/water results are compared with CMG-IMEX (A commercial blackoil reservoir simulator developed by Computer Modeling Group, 2012.10) results and three phase of microemulsion/oil/water results are validated with original UTCHEM (2011).

A two-phase case and four three-phase cases are simulated and our model results are compared against original model and CMG-IMEX (2012.10) results. Then a four-phase case (microemulsion/oil/gas/water) is modeled to evaluate the performance of our new model.

6.1 WATER INJECTION WITH TWO PHASE FLOW CASE (CASE 1)

After implementation of the four-phase model formulation into UTCHEM simulator, we compare the original formulation (valid for slightly compressible fluid flow) results against our new formulation (functioning for multiphase compressible fluid flow). A simple 1-D case, which is incompressible two phase (oil and water), is setup in UTCHEM to compare four-phase model results against original model results. In order to make consistency, required PVT table in four-phase model is considered as shown in Table 6-1. In this case, water is injected for 100 days into a reservoir. Fluid and reservoir data are explained in Table 6-2. The detail of the input data for this simulation is in Appendix A.

Figure 6-1 and Figure 6-2 demonstrate water (c_1) and oil (c_2) compositions at three different times (25, 50, and 75). Average pressure for both models is plotted in Figure 6-3 and it shows the same results for incompressible two phase flow in Case-1. Since the diffusivity of pressure equation is very high compared to the mass and energy equations and fluids are incompressible, steady state condition is achieved immediately. Water injection and pressure results at different times thoroughly become similar. Oil and water saturation comparisons are depicted in Figure 6-4 through Figure 6-6. Since injector is located at the beginning of the reservoir (the first grid block), water saturation (saturation of injection phase) after a while reach to $1 - S_{or}$. On the other hand, as mentioned earlier in Table 6-2, $S_{or} = 0$, water saturation reaches to 1. But around the production well, which is located at the end of the reservoir, phase saturations in the early time are equal to initial values ($S_{io} = 0.6$ and $S_{iw} = 0.4$), but after water breakthrough time oil saturation is reduced and water saturation increased. All results for original and four-phase models in UTCHEM are similar.

Accordingly, results show good agreement between two models in UTCHEM for an incompressible case.

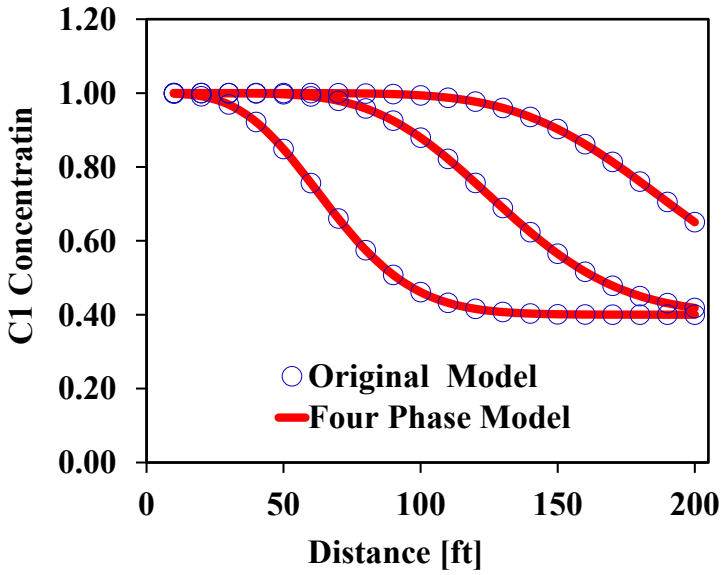

Figure 6-1-Comparison of water concentration (C_1) profiles at the various times (25, 50, and 75) for Case-1.

Table 6-1- Phase behavior oil/gas and PVT table used in CMG-IMEX and UTCHEM four-phase model in Case-1.

Psat (psi)	**Rso** (SCF/STB)	**B1** (RB/STB)	**B4** (RB/SCF)	**vis1** (cp)	**vis4** (cp)
100	0	1.0	0.005	1.0	0.01
800	0	1.0	0.002	1.0	0.01
1200	0	1.0	0.001	1.0	0.01
1600	0	1.0	0.001	1.0	0.01
2000	0	1.0	0.001	1.0	0.01
2400	0	1.0	0.0009	1.0	0.01
2800	0	1.0	0.0008	1.0	0.01
3200	0	1.0	0.0007	1.0	0.01
3600	0	1.0	0.0006	1.0	0.01
4000	0	1.0	0.0005	1.0	0.01
4400	0	1.0	0.0005	1.0	0.01
4800	0	1.0	0.0004	1.0	0.01
5200	0	1.0	0.0004	1.0	0.01
5600	0	1.0	0.0004	1.0	0.01

Table 6-2- Fluid and reservoir input parameters used in Case-1.

Reservoir and Fluid Data	
Reservoir Size	200ftx10ftx10ft
Number of Gridblock	20x1x1
Gridblock Size	10ftx10ftx10ft
Porosity	20%
Permeability	100mD
Basic Rock and Fluid Properties	
Water Density(RC)	0.45 psi/ft
Oil Density(SC)	0.225 psi/ft
Gas Density(SC)	0.0004 psi/ft
Water Compressibility	$1x10^{-6}$ 1/psi
Water Rel. Perm	$S_{rw}=0$, $k^o_{rw}=1.0$, $e_w=1.0$
Oil Rel. Perm	$S_{ro}=0$, $k^o_{ro}=1.0$, $e_o=1.0$
Rock Compressibility	0.0 1/psi
Initial Pressure	2000 psi
Initial Saturations	0.4(water),0.6(oil), 0(gas)
Well	
Number of Wells	1prod. and 1 inj.
Well Constrains	1prod(BHP=2000psi)
	1Inj (Const. Water Rate=$50ft^3$ /day)

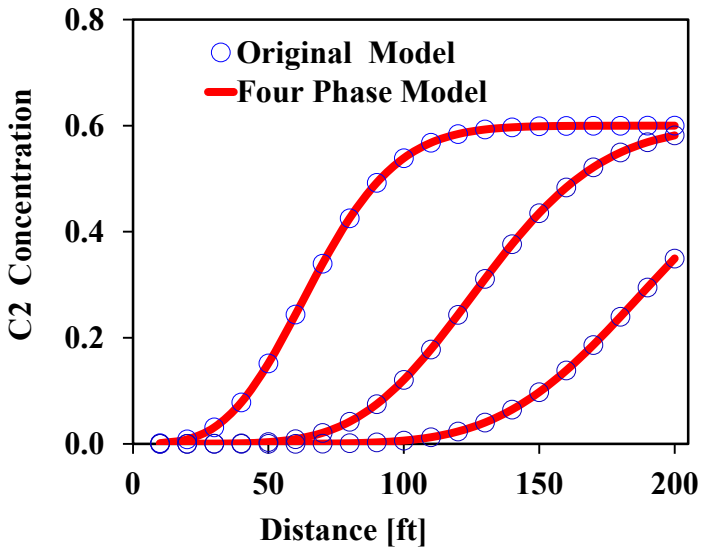

Figure 6-2- Comparison of oil concentration (C_2) profile at the various times (25, 50, and 75) for Case-1.

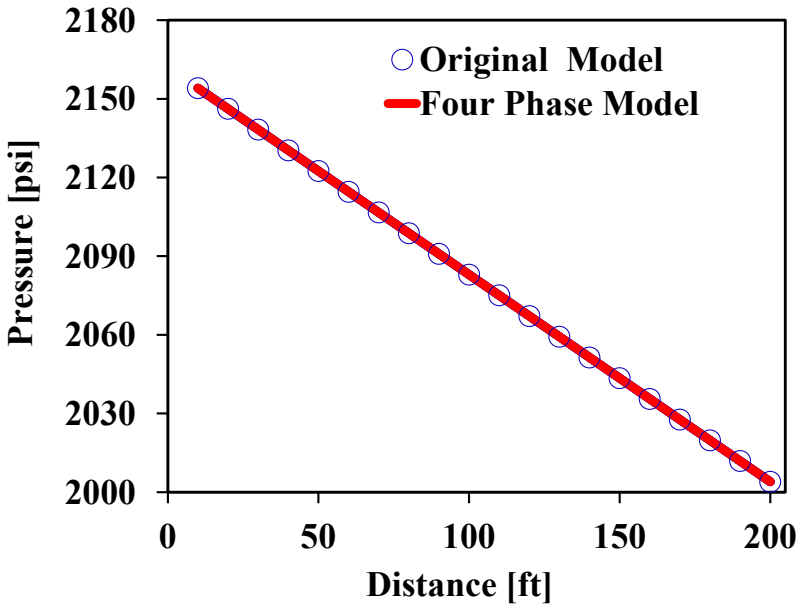

Figure 6-3- Comparison of pressure profile at the various times (25, 50, and 75) for Case-1.

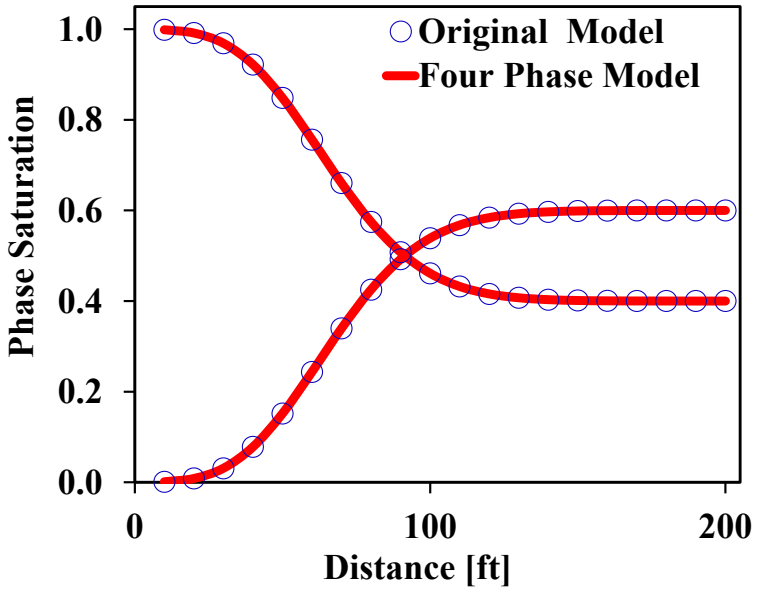

Figure 6-4- Comparison of water and oil saturation profiles after 25 days for Case-1.

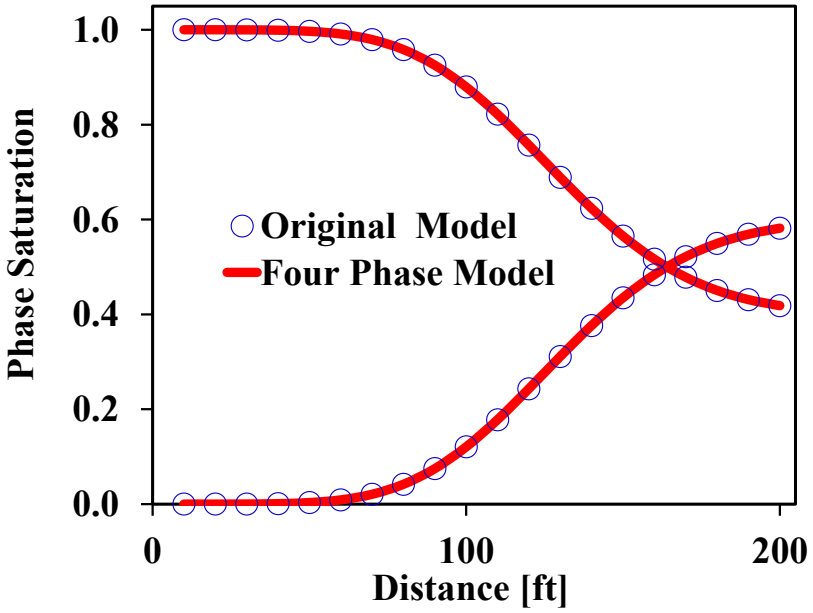

Figure 6-5- Comparison of water and oil saturation profiles after 50 days for Case-1.

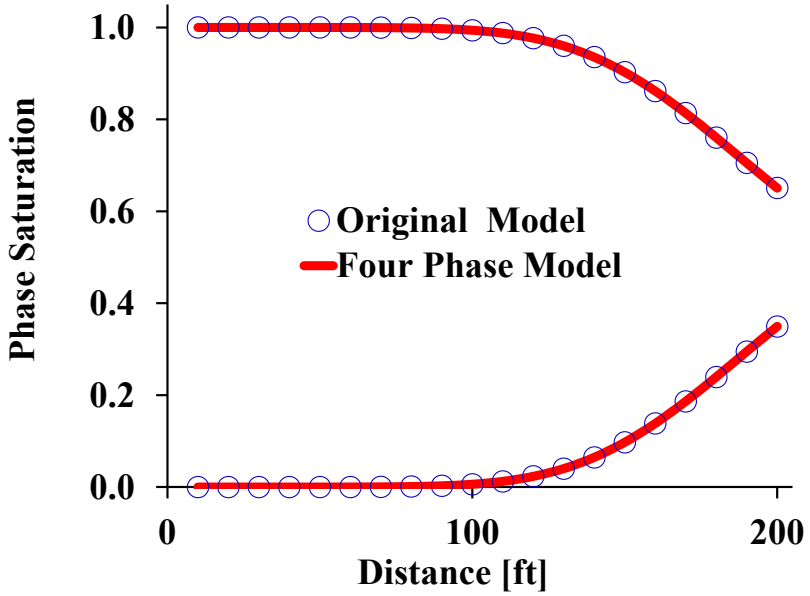

Figure 6-6- Comparison of water and oil saturation profiles after 75 days for Case-1.

6.2 GAS AND WATER INJECTION WITH THREE PHASE FLOW CASE (CASE-2)

In this case, we simulate injection of gas and water with a different schedule. This comparison has been performed between CMG-IMEX and UTCHEM four-phase model. The case is a 1-D problem that starts injecting gas at the beginning for 25 days and then stops injecting gas and water are started to inject after 75 days. Water and gas both together are injected into reservoir as shown Figure 6-7. Phase behavior or PVT table in both simulators is the same as shown in Table 6-3. The input parameters setup for the case is illustrated in Table 6 4. The detail of the input data for this simulation is also presented in Appendix A.

Figure 6-8 through Figure 6-10 show the comparison of production well results between CMG-IMEX and UTCHE four-phase model for production rates of oil, water, gas phases. The initial pressure of reservoir is 3000 psi and production well is specified at the constant bottomhole pressure (2000 psi). Therefore, right after opening the production well, the reservoir pressure suddenly drops and pressure falls below bubble point. Solution gas is released as free gas then production well produces gas around 500 ft^3/day. Then pressure reaches steady state. At steady sate condition, the production well produces gas almost less than injected (100 ft^3/day). Two more transient and steady state conditions are seen in the schedule change of injection rates. UTCHEM four-phase model production rates are thoroughly in good agreement with CMG-IMEX. Also, Figure 6-11 and Figure 6-12 illustrate comparison of oil production and average pressure of reservoir in two simulators. As can be seen, UTCHEM four-phase model results are very similar to that of CMG-IMEX. In order to model and simulate this case, we defined two injection wells in CMG-IMEX to inject at the same time water and gas. But UTCHEM has this capability to inject multiphase and multicomponent at the same time through a well.

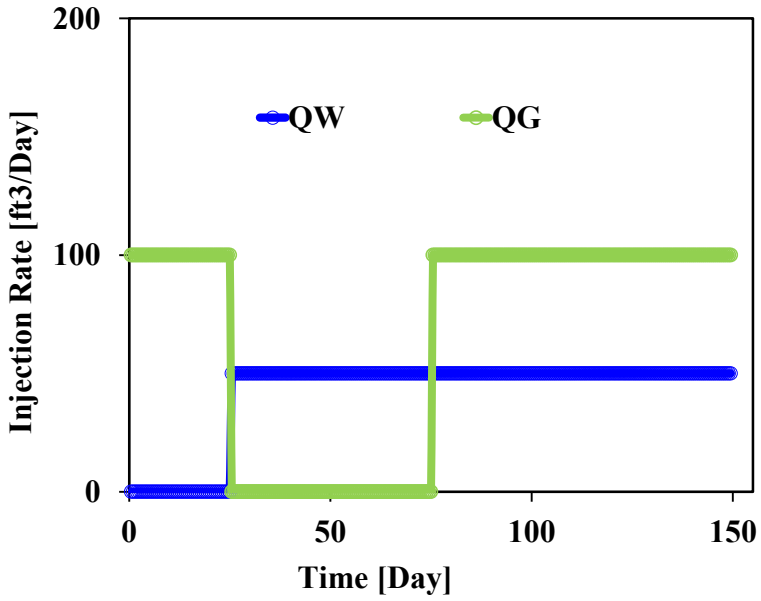

Figure 6-7- Water and gas injection well schedule in Case-2.

Table 6-3-Phase behavior and PVT table used in CMG-IMEX and UTCHEM four-phase model in Case-2.

Psat (psi)	**Rso** (SCF/STB)	**B_1** (RB/STB)	**B_4** (RB/SCF)	**vis_1** (cp)	**vis_4** (cp)
100	165	1.012	0.0059	1.17	0.013
800	335	1.0255	0.00295	1.14	0.0135
1200	500	1.038	0.00196	1.11	0.014
1600	665	1.051	0.00147	1.08	0.0145
2000	828	1.063	0.00118	1.06	0.0150
2400	985	1.075	0.00098	1.03	0.0155
2800	1130	1.087	0.00084	1.00	0.016
3200	1270	1.0985	0.00074	0.98	0.0165
3600	1390	1.11	0.00065	0.95	0.017
4000	1500	1.12	0.00059	0.942	0.0175
4400	1600	1.13	0.00054	0.92	0.018
4800	1676	1.14	0.00049	0.91	0.0185
5200	1750	1.148	0.00045	0.9	0.019
5600	1810	1.155	0.00042	0.89	0.0195

Table 6-4- Fluid and reservoir input parameters used for Case-2.

Reservoir and Fluid Data	**UTCHEM**	**CMG-IMEX**
Reservoir Size	200ftx10ftx10ft	
Number of Gridblock	20x1x1	
Gridblock Size	10ftx10ftx10ft	
Porosity	20%	
Permeability	100mD	
Basic Rock and Fluid Properties		
Water Density(RC)	0.45psi/ft	64.8lbm/ft^3
Oil Density(SC)	0.225psi/ft	32.4lb/ft^3
Gas Density(SC)	0.0004psi/ft	0.0576lbm/ft^3
Water Compressibility	$1x10^{-6}$1/psi	
Water Rel. Perm	S_{rw}=0 , k^o_{rw}=1.0 , e_w=1.0	
Oil Rel. Perm	S_{ro}=0 , k^o_{ro}=1.0 , e_o=1.0	
Gas Rel. Perm	S_{rg}=0 , k^o_{rg}=1.0 , e_g=1.0	
Rock Compressibility	0.0 1/psi	
Initial Pressure	3000 psi	
Initial Saturations	0.4(water),0.6(oil), 0(gas)	
Initial Bubble Point Pressure	3000psi	
Well		
Number of Wells	1prod. and 1 inj.	1prod. and 2 inj.
Well Constrains	1prod(BHP=2000psi) 1Inj (Const. Gas/Water Rate)	1prod(BHP=2000psi) 1Inj (Const.Water Rate) 1Inj (Const.Gas Rate)

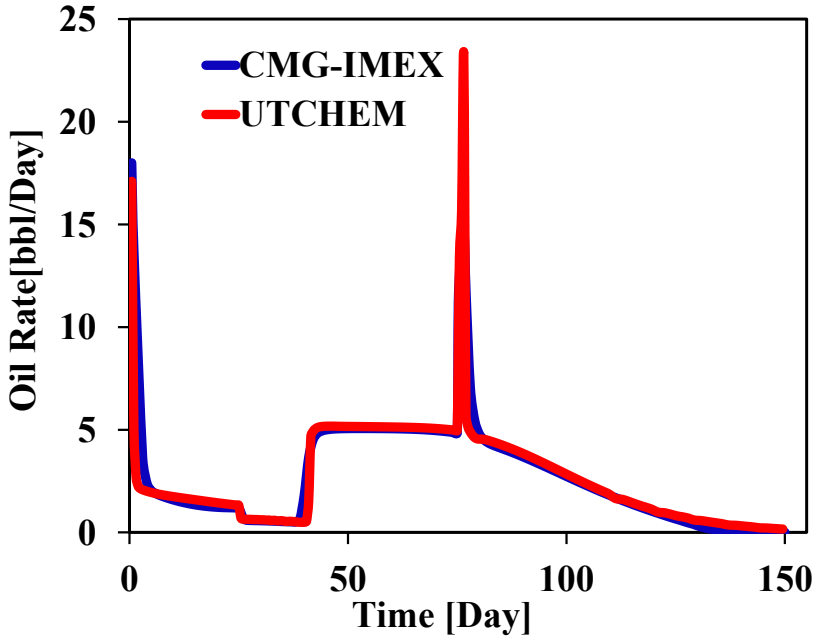

Figure 6-8- Comparison of CMG-IMEX and UTCHEM four-phase model for oil production rate in Case-2.

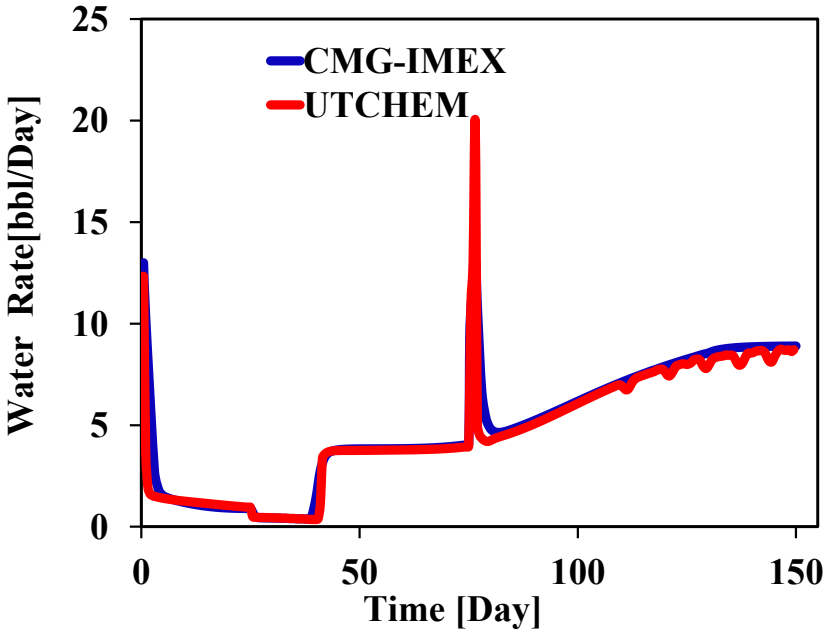

Figure 6-9- Comparison of CMG-IMEX and UTCHEM four-phase model for water production rate in Case-2.

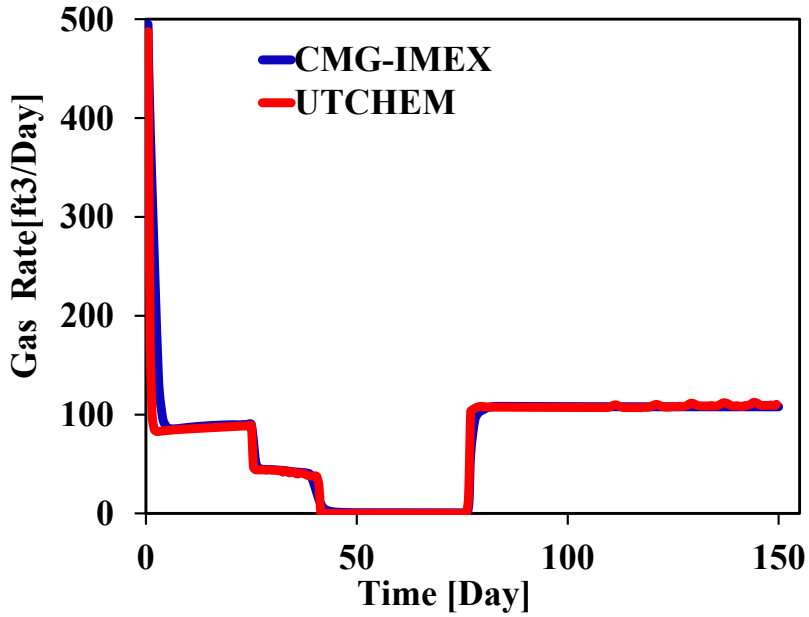

Figure 6-10- Comparison of CMG-IMEX and UTCHEM four-phase model for gas production rate in Case-2

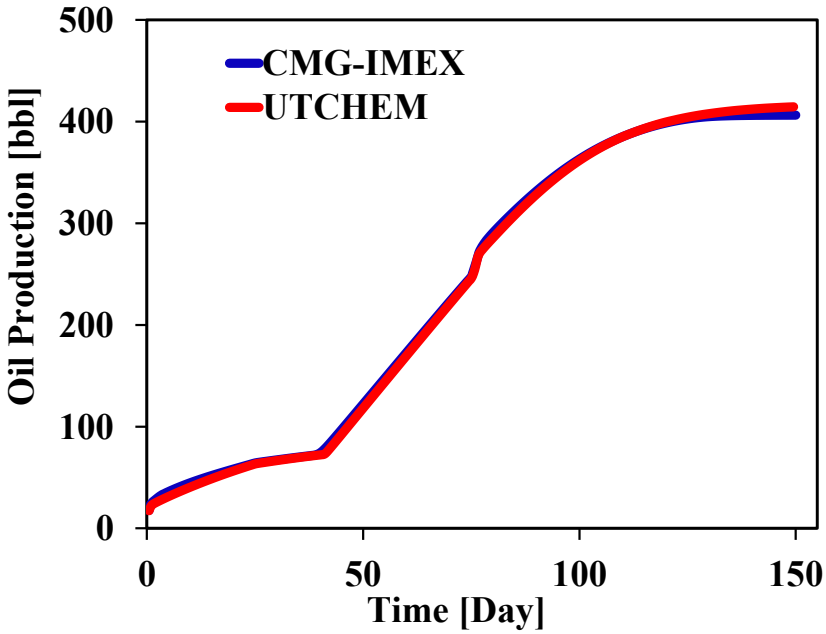

Figure 6-11- Comparison of CMG-IMEX and UTCHEM four-phase model for cumulative oil production rate in Case-2.

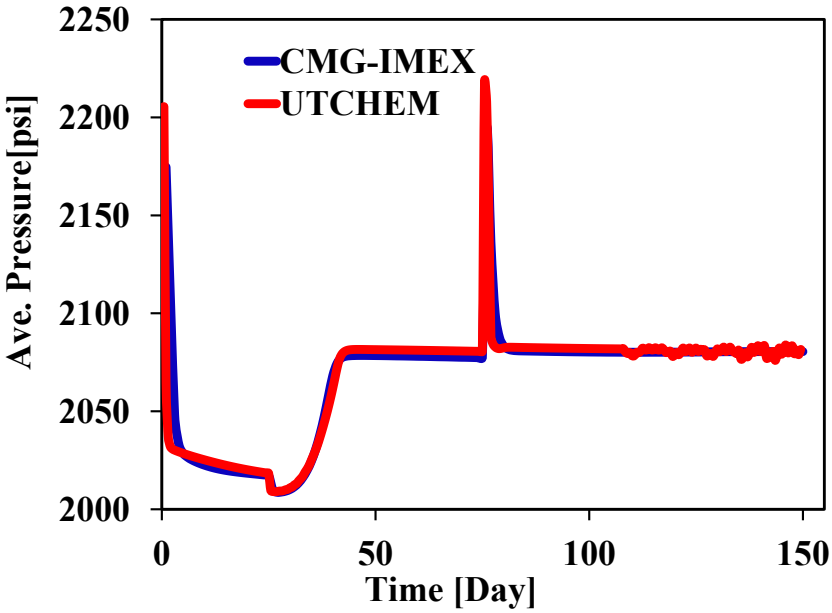

Figure 6-12- Comparison of CMG-IMEX and UTCHEM four-phase model for average pressure in Case-2.

6.3 WATER INJECTION BELOW BUBBLE POINT WITH THREE PHASE FLOW CASE (CASE-3)

We evaluated a problem with injecting constant water rate (50 ft^3/Day) into a reservoir that initially it is above bubble point (3000psi). Production well is open under constant bottomhole pressure (2000psi) and below the initial bubble point pressure of reservoir. In this case, we are interested in comparing the performance of UTCHEM four-phase model results versus CMG-IMEX results. This case is a 3-D problem along with two wells perforated in the diagonal corners of bottom layer (layer 5). Table 6-5 shows the input parameters for phase behavior oil/gas as PVT table consistent with CMG and UTCHEM.

Figure 6-13, Figure 6-14, and Figure 6-15 plot the solution gas ratio, formation volume factor, and viscosity of oil and gas in saturated condition for the case, respectively. Furthermore, Table 6 6 explains the reservoir and fluid parameters used in Case-3 for both simulators. The detail of the input data in this case for both simulators is also in Appendix A.

Since the initial reservoir pressure is around 3000 psi, right after opening the production well, pressure declines and this leads to a decrease in bubble point pressure. A decrease in bubble point pressure causes a decrease in solution gas and free gas forms. Part of free gas is produced through production well. But some of the free gas segregates into top layers and accumulates in the top layer due to low density of gas compared to oil and water densities. This process can be observed among the results as seen in Figure 6-16, Figure 6-17, and Figure 6-18.

As discussed previously, gas is accumulated in the top layer. Moreover, oil saturation increases in the middle layers because of density difference. Water saturation

also increases in the bottom layer due to high density compared to oil and gas; also because of water injection.

Figure 6-22 depicts three phase saturation comparisons for two simulators. In this case, at very early time gas forms while reservoir pressure and bubble point pressure declines from ~ 3000 psi to ~2100 psi. This pressure drop in early time causes to form the free gas. Then gas saturation increases up to 0.05. Afterward gas segregates, because of density difference. Then, gas saturation in the bottom layer gridblocks reduces in later time after day 20.

Figure 6-23 shows the vertical cross-sectional profile for three phase saturations from top to bottom layers in the corner of reservoir intersecting injection well. As can be observed from this plot, all gas segregates from bottom or middle layers to top layer. Therefore, gas saturation reaches to 0.15. Additionally, at the bottom layer where injection well is located, water increase to $1 - S_{or} \simeq 1.0$. But in the middle layer, water is displacing and pushing oil toward the producer.

Figure 6-24 shows the vertical cross-sectional profile for three phase saturations intersecting the production well (production and injection wells are perforated at corners of the reservoir diagonally in bottom layer, layer 5).

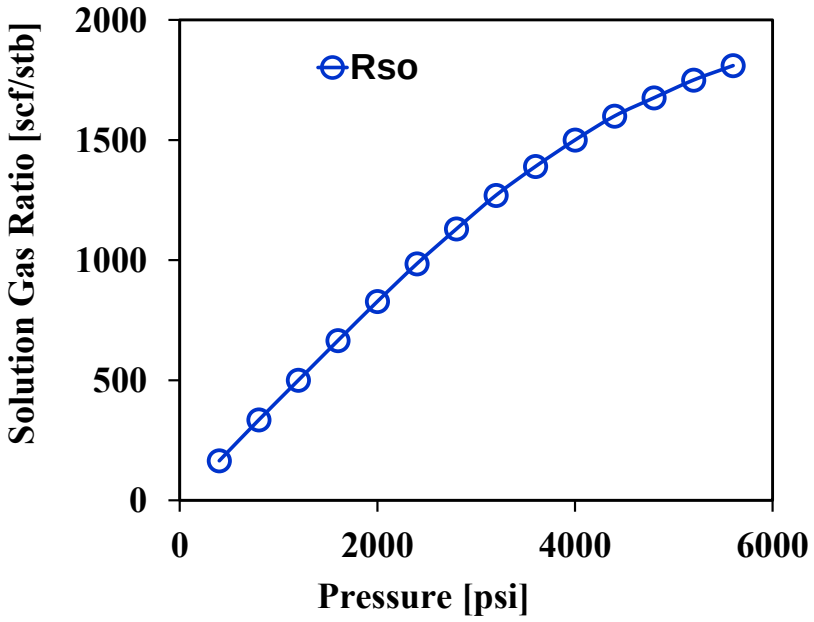

Figure 6-13- Solution gas ratio data at saturated condition used in CMG-IMEX and UTCHEM in Case-3.

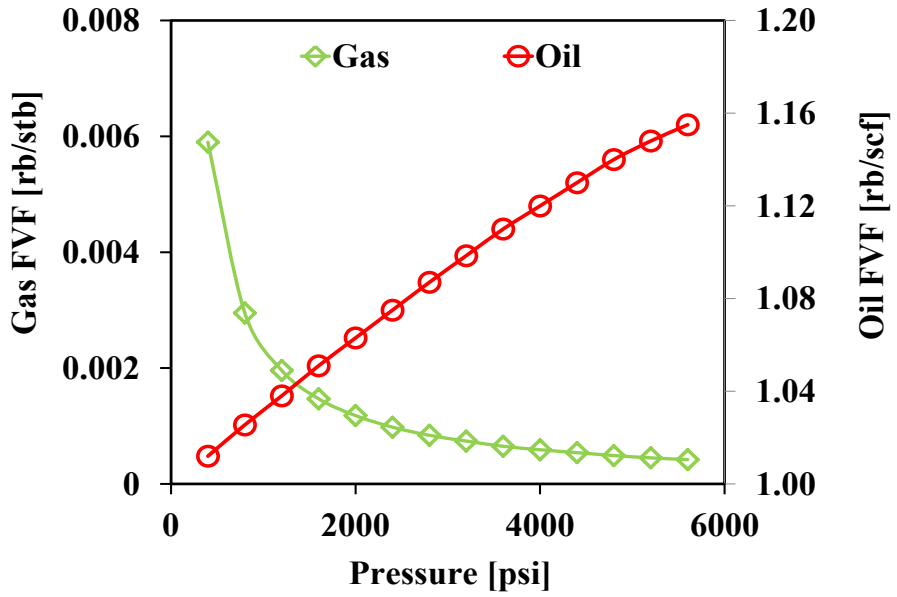

Figure 6-14-Formation volume factor of oil and gas at saturated condition used in CMG-IMEX and UTCHEM in Case-3.

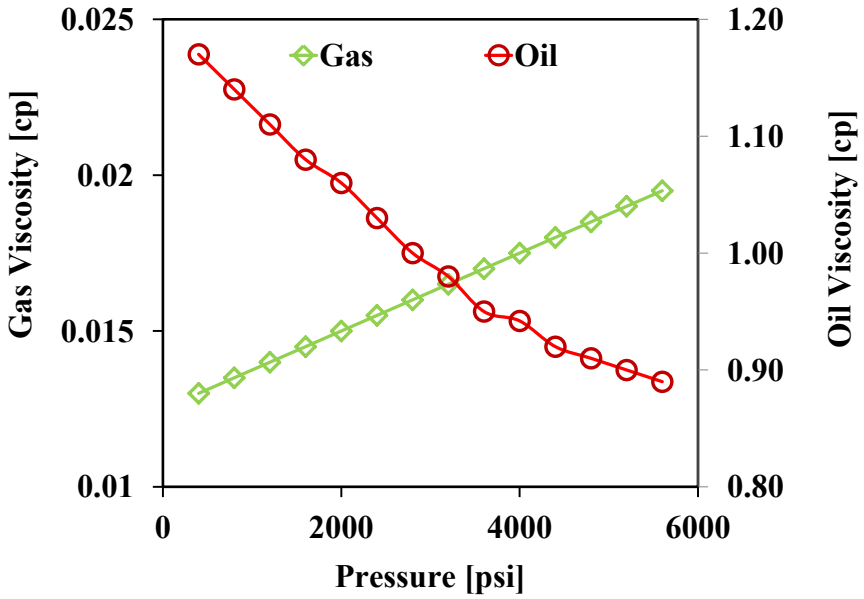

Figure 6-15-Oil and gas viscosity data at saturated condition used in CMG-IMEX and UTCHEM for Case-3.

Table 6-5-Phase behavior and PVT table used in CMG-IMEX and UTCHEM four-phase model in Case-3.

Psat (psi)	**Rso** (SCF/STB)	**B_1** (RB/STB)	**B_4** (RB/SCF)	**vis_1** (cp)	**vis_4** (cp)
100	165	1.012	0.0059	1.17	0.013
800	335	1.0255	0.00295	1.14	0.0135
1200	500	1.038	0.00196	1.11	0.014
1600	665	1.051	0.00147	1.08	0.0145
2000	828	1.063	0.00118	1.06	0.0150
2400	985	1.075	0.00098	1.03	0.0155
2800	1130	1.087	0.00084	1.00	0.016
3200	1270	1.0985	0.00074	0.98	0.0165
3600	1390	1.11	0.00065	0.95	0.017
4000	1500	1.12	0.00059	0.942	0.0175
4400	1600	1.13	0.00054	0.92	0.018
4800	1676	1.14	0.00049	0.91	0.0185
5200	1750	1.148	0.00045	0.9	0.019
5600	1810	1.155	0.00042	0.89	0.0195

Table 6-6- Fluid and reservoir input parameters used in Case-3.

Reservoir and Fluid Data	**UTCHEM**	**CMG-IMEX**
Reservoir Size	50ftx50ftx50ft	
Number of Gridblock	5x5x5	
Gridblock Size	10ftx10ftx10ft	
Porosity	20%	
Permeability	Kx=Ky=50mD, Kz=5md	
Basic Rock and Fluid Properties		
Water Density(RC)	0.45 psi	64.8 lbm/ft^3
Oil Density(SC)	0.225 psi	32.4 lb/ft^3
Gas Density(SC)	0.0004 psi	0.0576 lbm/ft^3
Water Compressibility	$1x10^{-6}$	
Water Rel. Perm	$S_{rw}=0$, $k^o_{rw}=1.0$, $e_w=1.0$	
Oil Rel. Perm	$S_{ro}=0$, $k^o_{ro}=1.0$, $e_o=1.0$	
Gas Rel. Perm	$S_{rg}=0$, $k^o_{rg}=1.0$, $e_g=1.0$	
Rock Compressibility	0.0 1/psi	
Initial Pressure	5500 psi	
Initial Saturations	0.3(water),0.7(oil), 0 (gas)	
Initial Bubble Point Pressure	5500 psi	
Undersaturated Parameters	Oil Vis Slop = 0.0000 cp/psi1 Oil FVF Slop=-0.00023 rb/stb/psi	
Well		
Number of Wells	1prod. and 1 inj.	1prod. and 1 inj.
Well Constrains	1prod(BHP=1000psi) 1Inj (Const. Water Rate) $50ft^3$ /Day	1prod(BHP=4500psi) 1Inj (Const.Water Rate) 8.9 bbl/Day

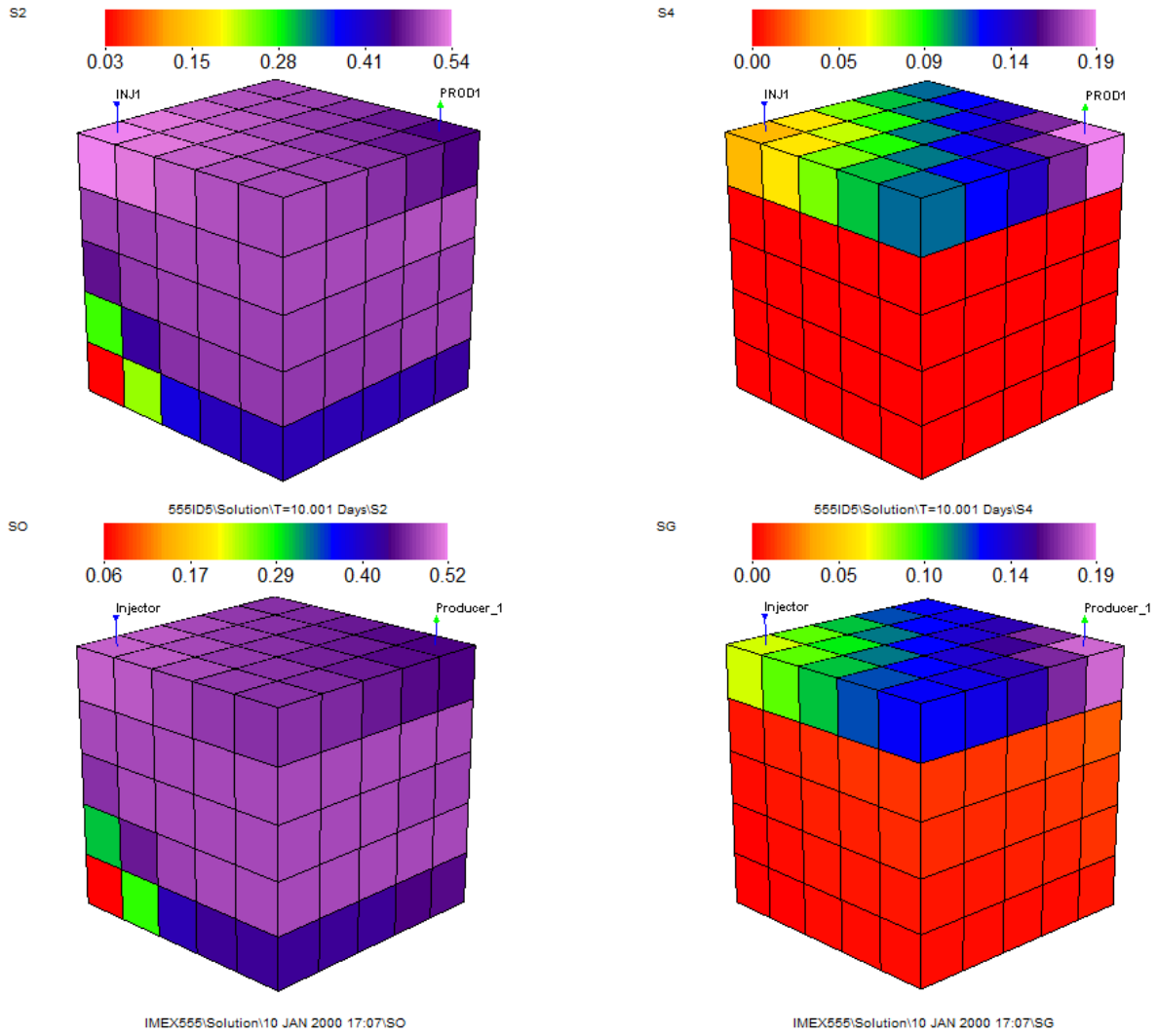

Figure 6-16-Comparison of oil saturation (left) and gas saturation (right) distribution results after 10days between UTCHEM four-phase model (top) and CMG-IMEX (bottom).

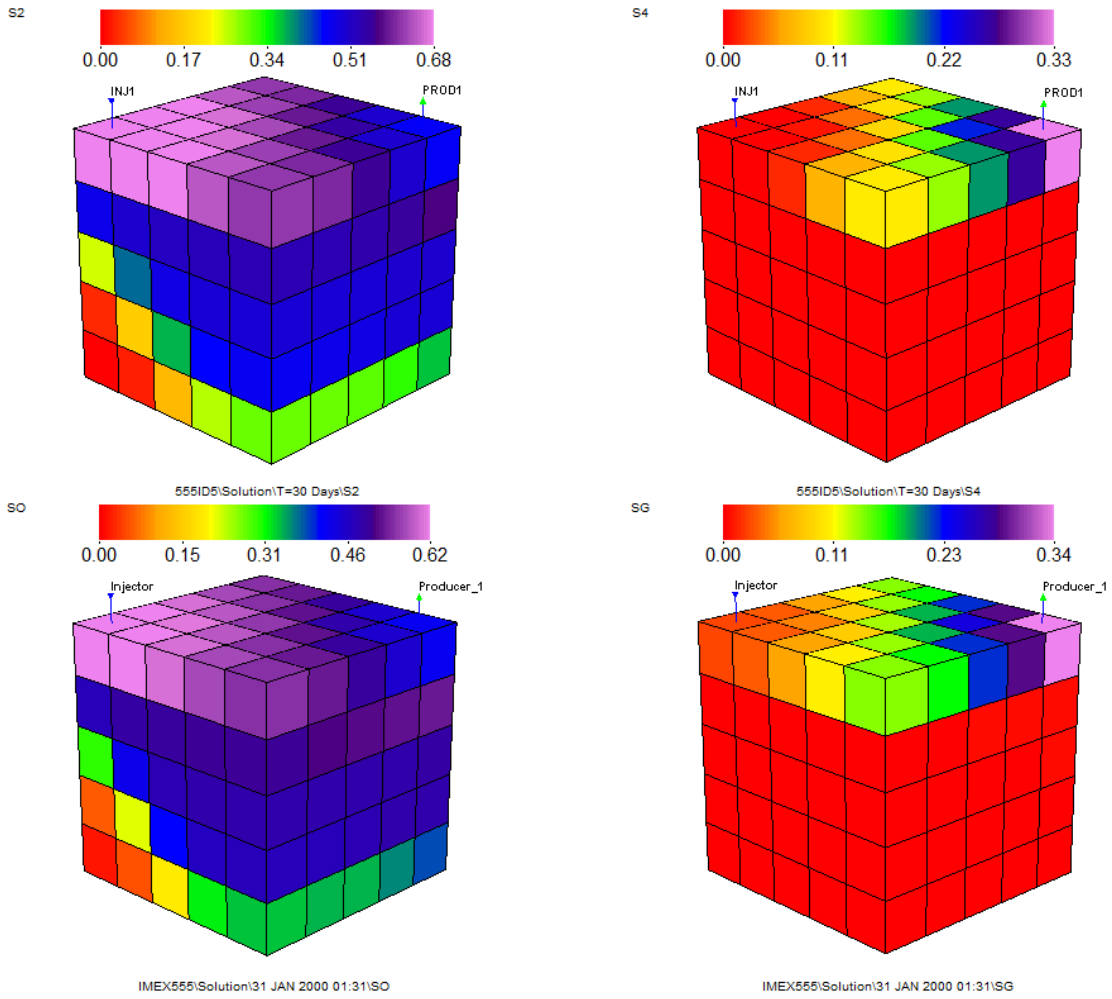

Figure 6-17- Comparison of oil saturation (left) and gas saturation (right) distribution results after 30 days between UTCHEM four-phase model (top) and CMG-IMEX (bottom).

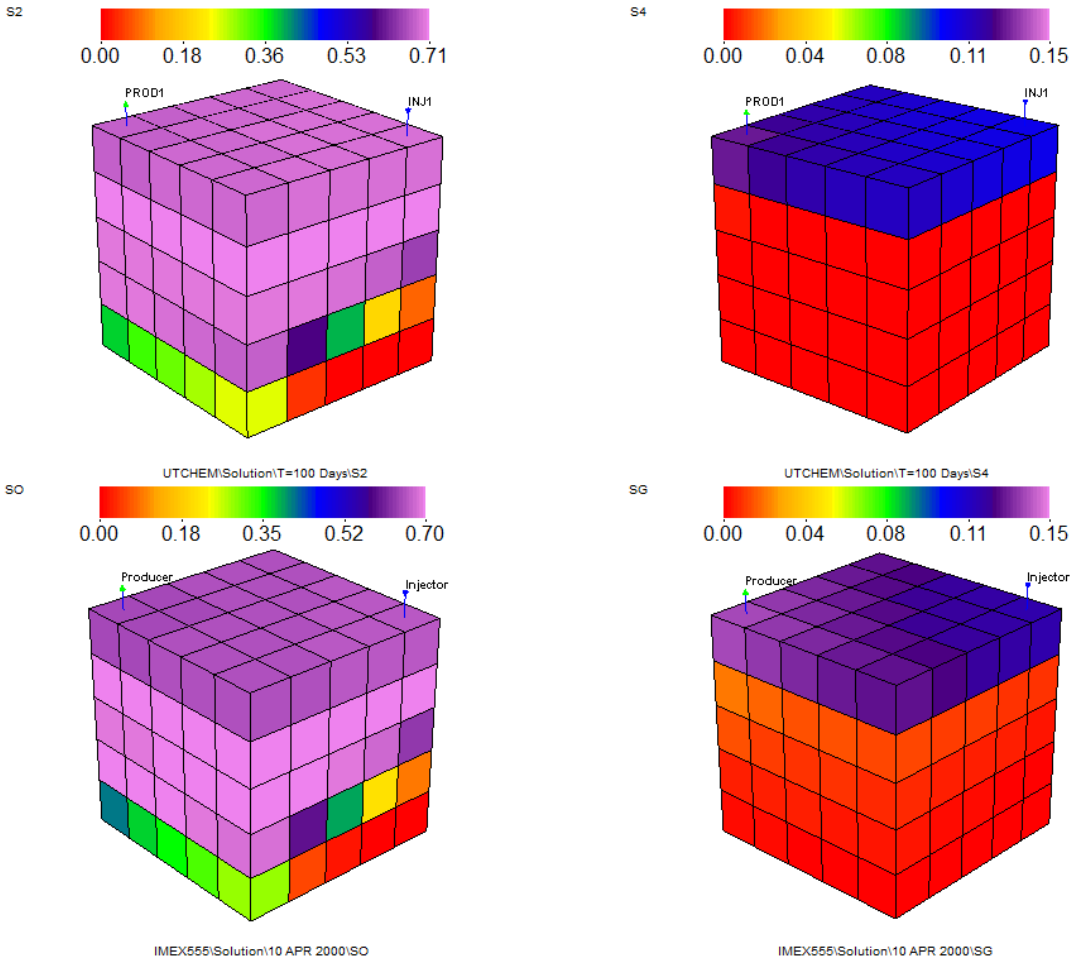

Figure 6-18- Comparison of oil saturation (left) and gas saturation (right) distribution results after 30 days between UTCHEM four-phase model (top) and CMG-IMEX (bottom).

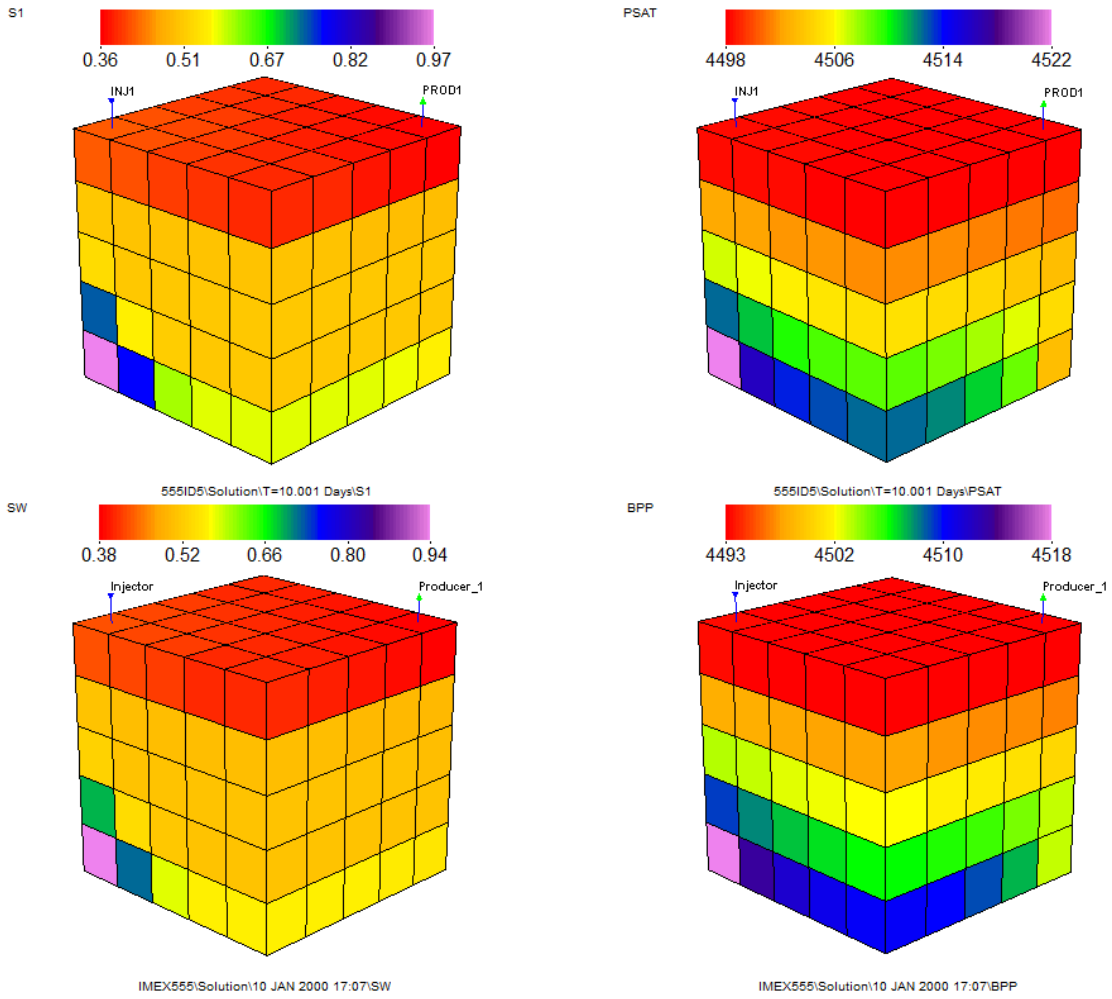

Figure 6-19-Comparison of water saturation (left) and bubble point pressure (right) distribution results after 10 days between UTCHEM four-phase model (top) and CMG-IMEX (bottom).

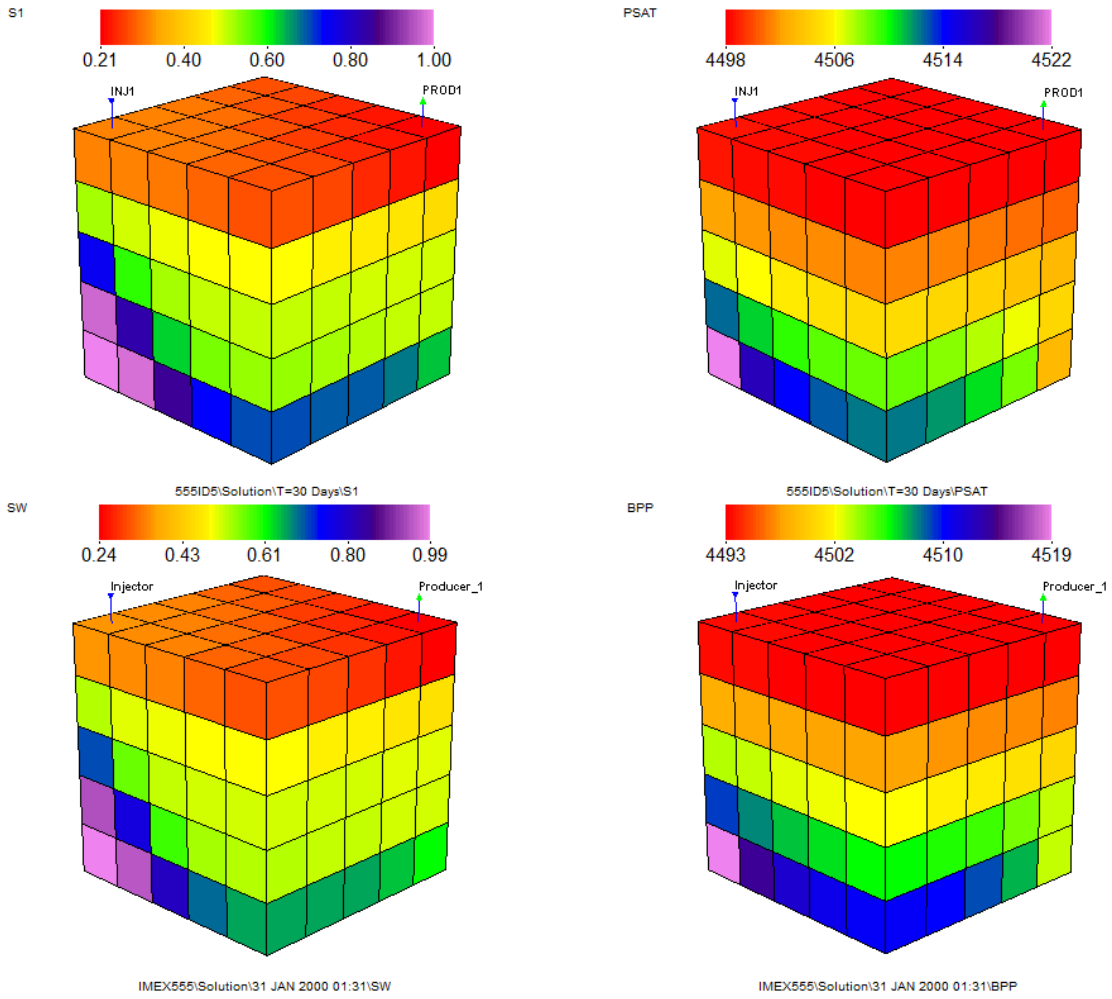

Figure 6-20- Comparison of water saturation (left) and bubble point pressure (right) distribution results after 30 days between UTCHEM four-phase model (top) and CMG-IMEX (bottom).

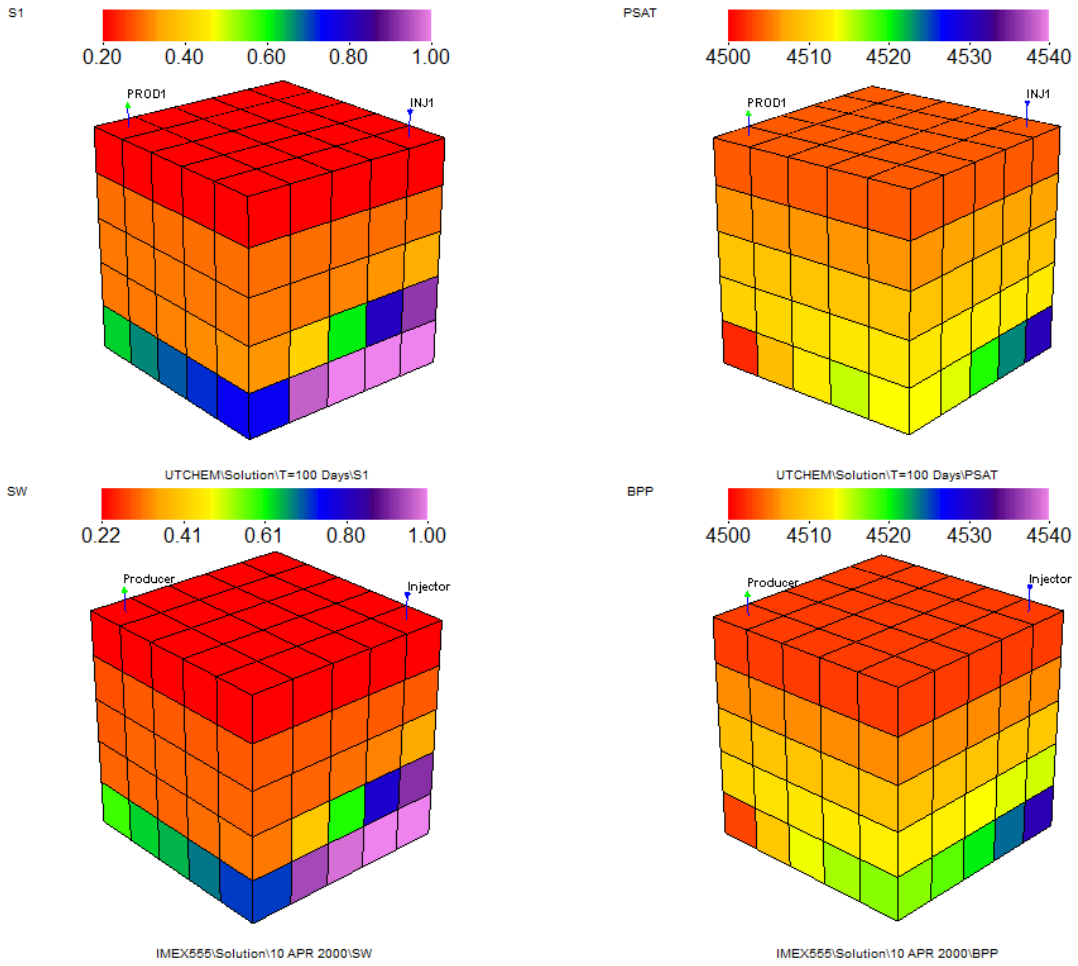

Figure 6-21- Comparison of water saturation (left) and bubble point pressure (right) distribution results after 30 days between UTCHEM four-phase model (top) and CMG-IMEX (bottom).

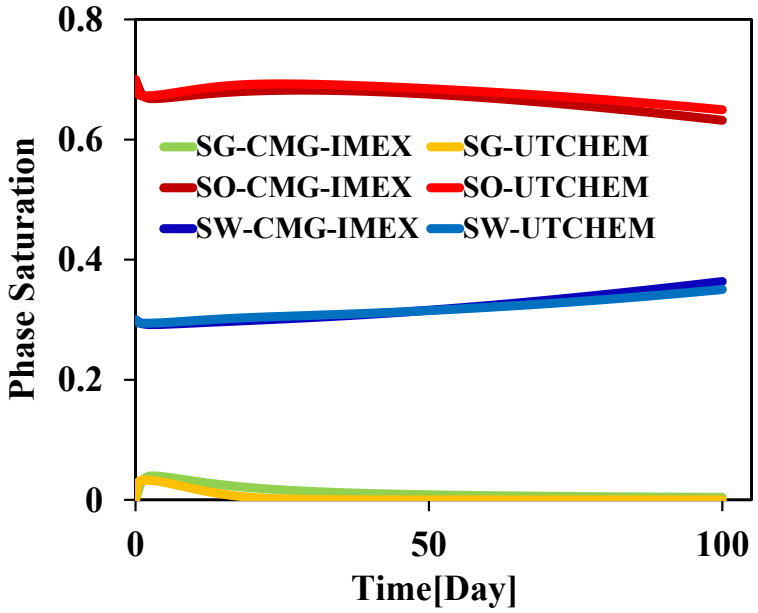

Figure 6-22-Comparison of gas, oil, and water saturation results for a gridblock located in the middle layer (layer 3) above the injector well in Case 3.

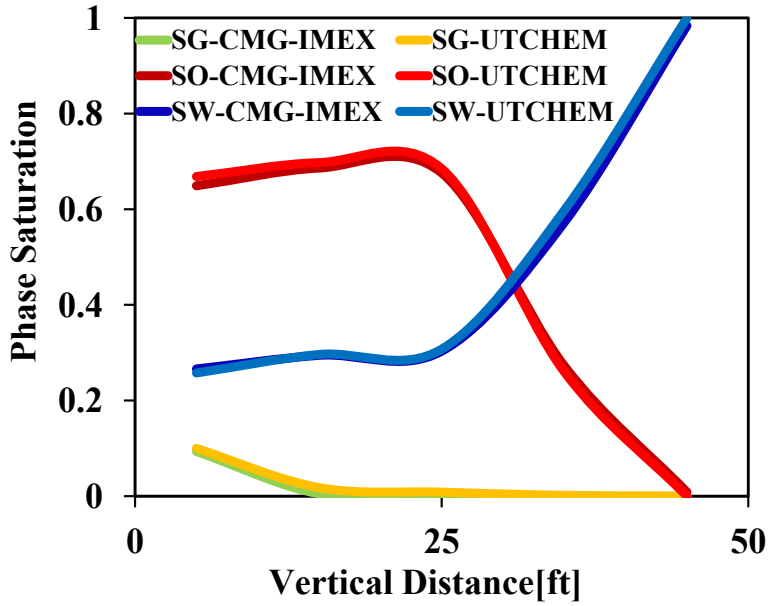

Figure 6-23-Comparison of gas, oil, and water saturation profiles in vertical direction passing through injection well after 30 days in Case-3.

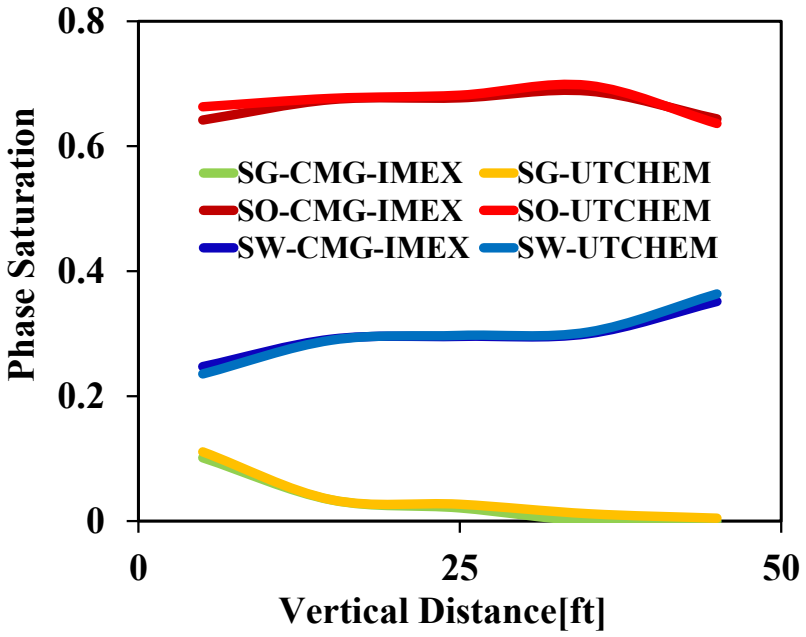

Figure 6-24-Comparison of gas, oil, and water saturation profiles in vertical direction passing through production well after 30 days in Case-3.

6.4 PRODUCTION FROM A FIELD CASE WITH THREE PHASES FLOW CASE (CASE-4)

In this case, we tested a large field case with natural depletion due to initial reservoir pressure and expansion of reservoir fluids. We are interested to compare vaporization process and amount of gas production as well as production of oil and water. In this case, we evaluate the performance of UTCHEM four-phase model versus CMG-IMEX

Four wells are placed on production under constant bottomhole pressure (1000psi), which is below the initial bubble point pressure of reservoir (4000psi). This case is a 3-D problem along with four production wells perforated in the corners of reservoirs from top to bottom layers (layers 1 through 10). Table 6-5 shows the input parameters for phase behavior oil/gas with PVT table consistent with CMG and UTCHEM.

Figure 6-28 shows the comparison of pressure distribution map between two simulators. It is obvious that pressure around the production wells declines. Figure 6-29 illustrates the related gas saturation distribution after 30 days; most gas is segregated to top layers and gas saturation reaches to 0.65. Similar justification as presented in Case-3 is obtainable from results for water and oil saturations showed in Figure 6-30 and Figure 6-31.

Snap shots of a vertical cross-section included two production wells are shown Figure 6-32 through Figure 6-41. These figures show the comparisons of the bubble point pressure, water saturation, oil saturation, and gas saturation in various days, respectively. Furthermore, Figure 6-42 shows the comparison of three phase saturation results for a gridblock located in the layer 1.

Since reservoir pressure declines to below bubble point, gas saturation initially increases from 0 to ~0.08. For instance, bubble point pressure of a gridblock located in

top layer is plotted in Figure 6-43. Therefore, portion of released free gas is segregated to top layer because of density difference; some part of it is produced by production wells. Total field production rates for gas, water, and oil are shown in Figure 6-46 through Figure 6-48.

As average pressure of the reservoir declines from 4000 psi to 1000 psi (see the corresponding plot in Figure 6-49), drawdown pressure is reduced and after 50 days production drops.

Moreover, Figure 6-44 and Figure 6-45 show the compression of water and gas saturation in a vertical profile from top to bottom after 40 days.

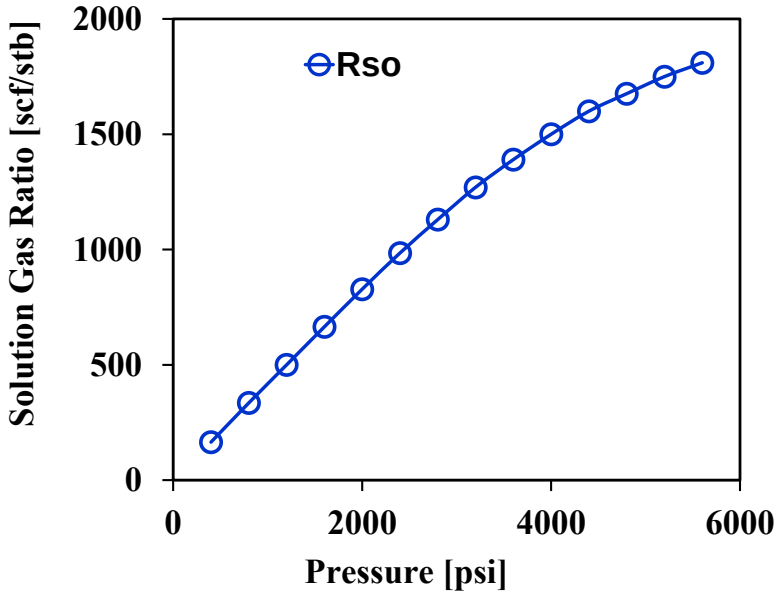

Figure 6-25-Solution gas ratio data at saturated condition used in CMG-IMEX and UTCHEM in Case-4.

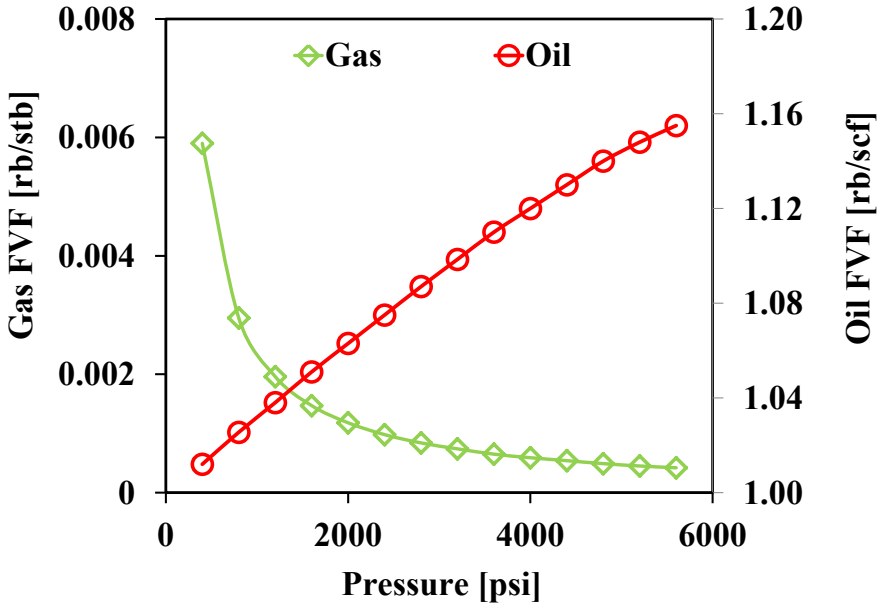

Figure 6-26-Formation volume factor of oil and gas at saturated condition used in CMG-IMEX and UTCHEM in Case-4.

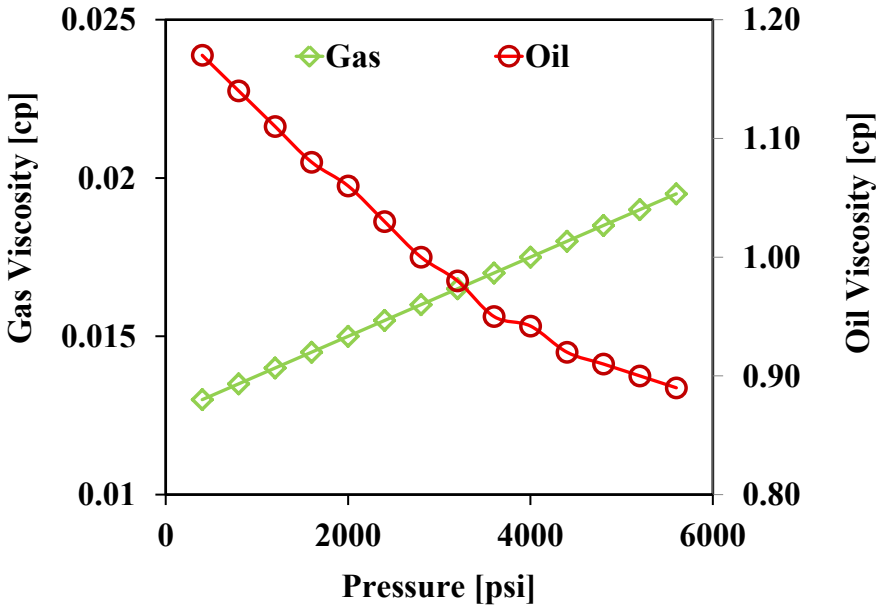

Figure 6-27-Oil and gas viscosity data at saturated condition used in CMG-IMEX and UTCHEM for Case-4

Table 6-7-Phase behavior and PVT table used in CMG-IMEX and UTCHEM four-phase model in Case-4.

Psat (psi)	**Rso** (SCF/STB)	**B1** (RB/STB)	**B4** (RB/SCF)	**vis1** (cp)	**vis4** (cp)
100	165	1.012	0.0059	1.17	0.013
800	335	1.0255	0.00295	1.14	0.0135
1200	500	1.038	0.00196	1.11	0.014
1600	665	1.051	0.00147	1.08	0.0145
2000	828	1.063	0.00118	1.06	0.0150
2400	985	1.075	0.00098	1.03	0.0155
2800	1130	1.087	0.00084	1.00	0.016
3200	1270	1.0985	0.00074	0.98	0.0165
3600	1390	1.11	0.00065	0.95	0.017
4000	1500	1.12	0.00059	0.942	0.0175
4400	1600	1.13	0.00054	0.92	0.018
4800	1676	1.14	0.00049	0.91	0.0185
5200	1750	1.148	0.00045	0.9	0.019
5600	1810	1.155	0.00042	0.89	0.0195

Table 6-8- Fluid and reservoir input parameters used in Case-4.

Reservoir and Fluid Data	**UTCHEM**	**CMG-IMEX**
Reservoir Size	1650ftx1650ftx200ft	
Number of Gridblock	11x11x10	
Gridblock Size	150ftx150ftx20ft	
Porosity	20%	
Permeability	Kx=Ky=100mD, Kz=100md	
Basic Rock and Fluid Properties		
Water Density(RC)	0.45psi/ft	64.8lbm/ft^3
Oil Density(SC)	0.225psi/ft	32.4lb/ft^3
Gas Density(SC)	0.0004psi/ft	0.0576lbm/ft^3
Water Compressibility	$1x10^{-6}$ 1/psi	
Water Rel. Perm	$S_{rw}=0$, $k^o_{rw}=1.0$, $e_w=1.0$	
Oil Rel. Perm	$S_{ro}=0$, $k^o_{ro}=1.0$, $e_o=1.0$	
Gas Rel. Perm	$S_{rg}=0$, $k^o_{rg}=1.0$, $e_g=1.0$	
Rock Compressibility	0.01/psi	
Initial Pressure	4000psi	
Initial Saturations	0.3(water),0.7(oil), 0(gas)	
Initial Bubble Point Pressure	4000psi	
Undersaturated Parameters	Oil Vis Slop = 0.0000cp/psi1 Oil FVF Slop=-0.00023rb/stb/psi	
Well		
Number of Wells	4prod..	4prod.
Well Constrains	4prod(BHP=1000psi)	4prod(BHP=1000psi)

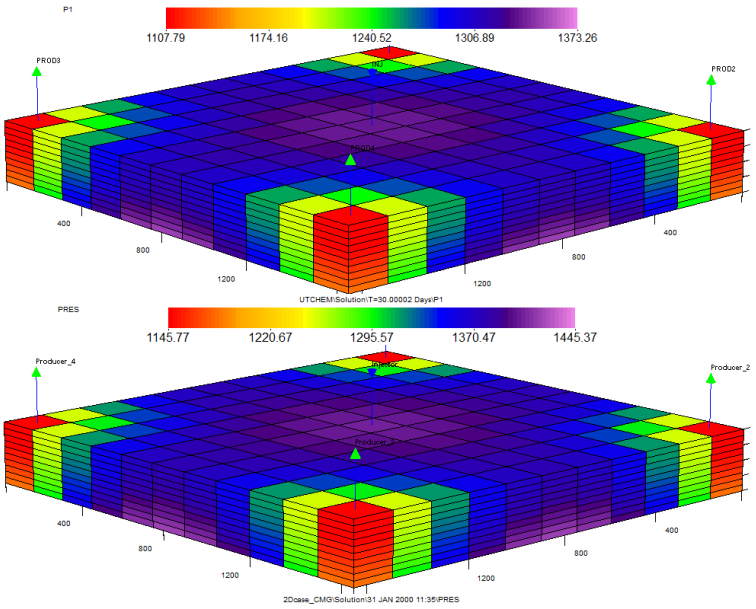

Figure 6-28-Pressure distribution result comparison after 30days between UTCHEM four-phase model in top and CMG-IMEX in bottom in Case-4

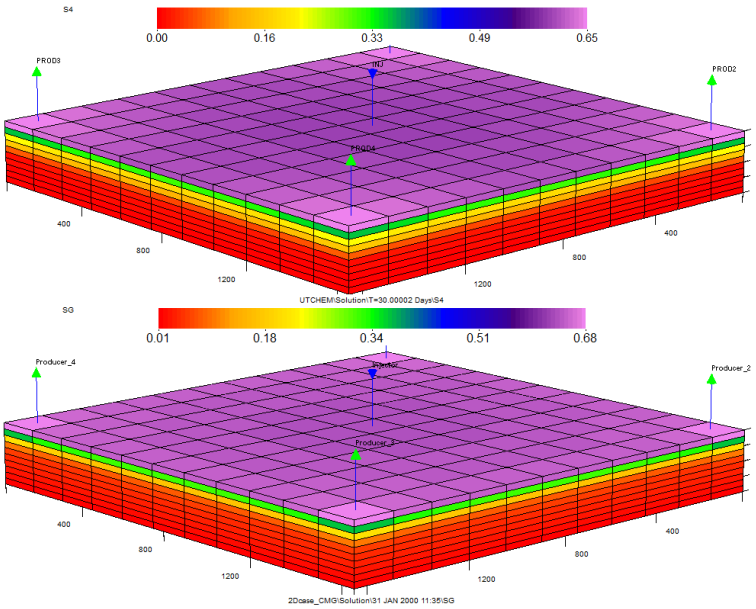

Figure 6-29- Gas saturation distribution result comparison after 30days between UTCHEM four-phase model in top and CMG-IMEX in bottom in Case-4

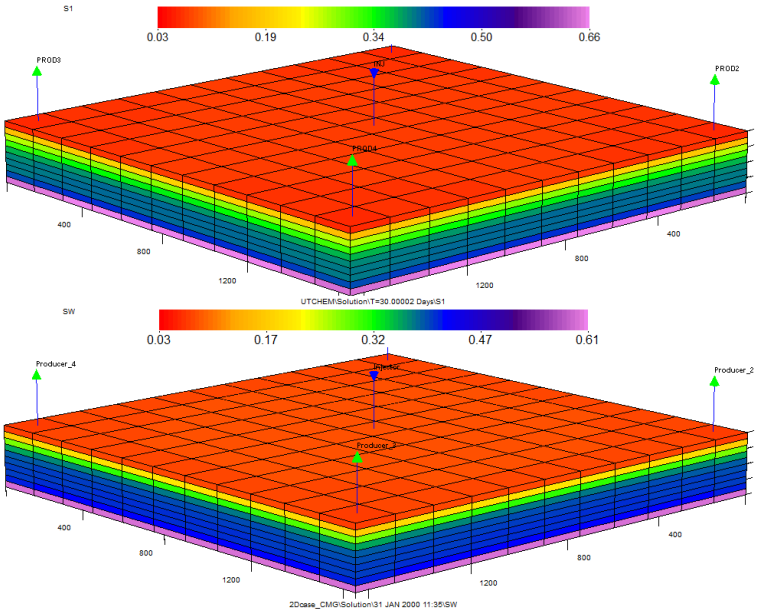

Figure 6-30- Water saturation distribution result comparison after 30days between UTCHEM four-phase model in top and CMG-IMEX in bottom in Case-4

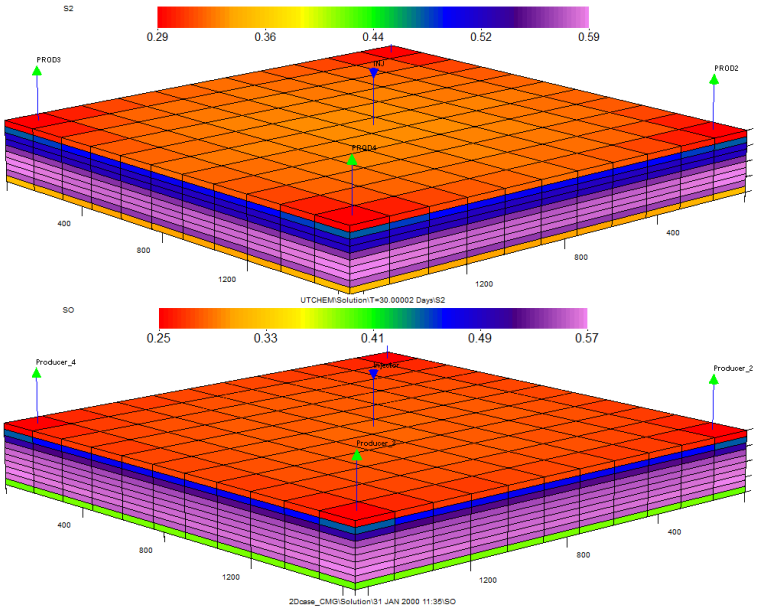

Figure 6-31- Oil saturation distribution result comparison after 30days between UTCHEM four-phase model in top and CMG-IMEX in bottom in Case-4

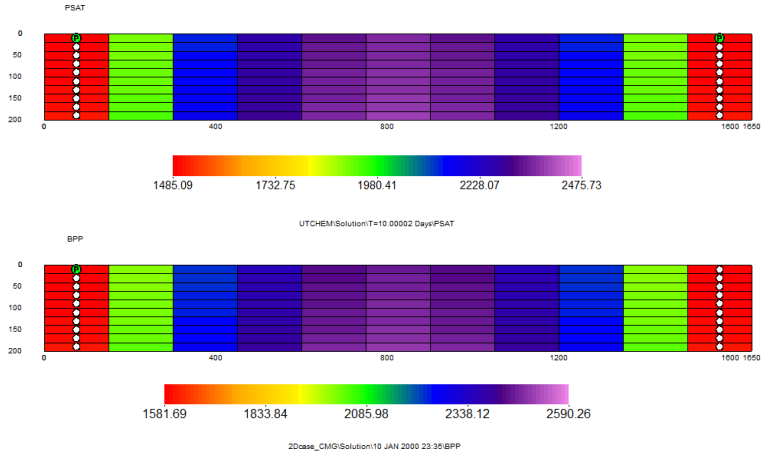

Figure 6-32-A cross section of bubble point pressure distribution that compares results of UTCHEM four-phase model and CMG-IMEX after 10 days in Case-4.

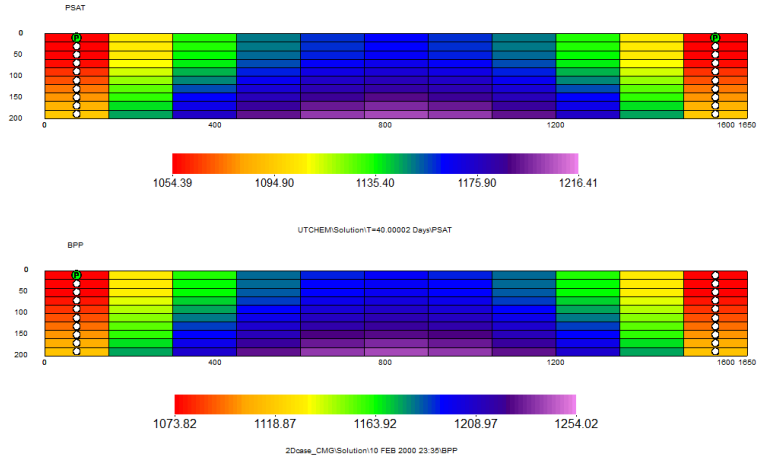

Figure 6-33- A cross section of bubble point pressure distribution that compares results of UTCHEM four-phase model and CMG-IMEX after 40 days in Case-4.

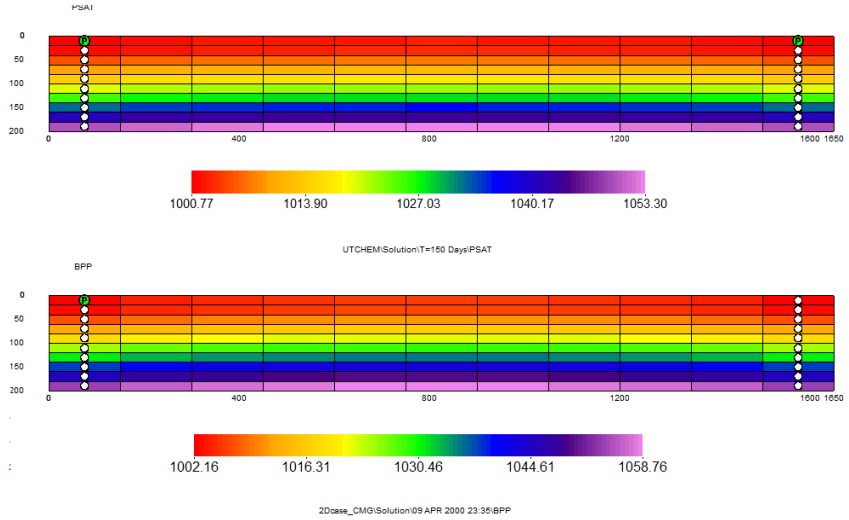

Figure 6-34- A cross section of bubble point pressure distribution that compares results of UTCHEM four-phase model and CMG-IMEX after 150 days in Case-4.

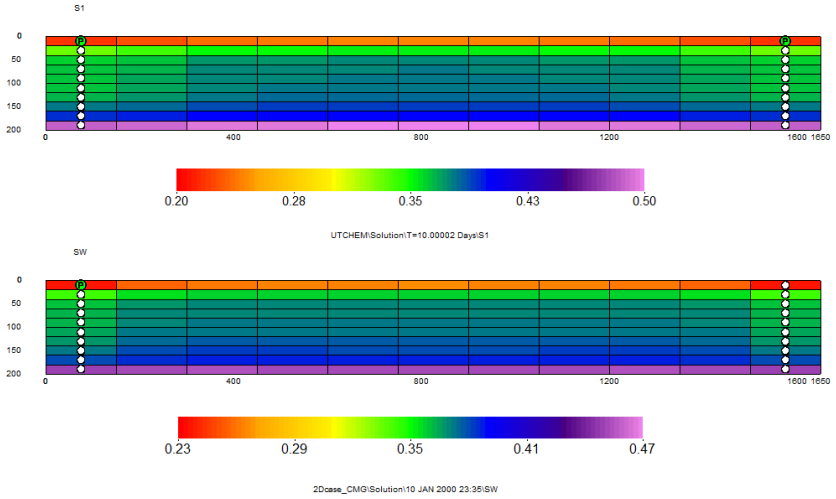

Figure 6-35- A cross section of water saturation distribution that compares results of UTCHEM four-phase model and CMG-IMEX after 10 days in Case-4.

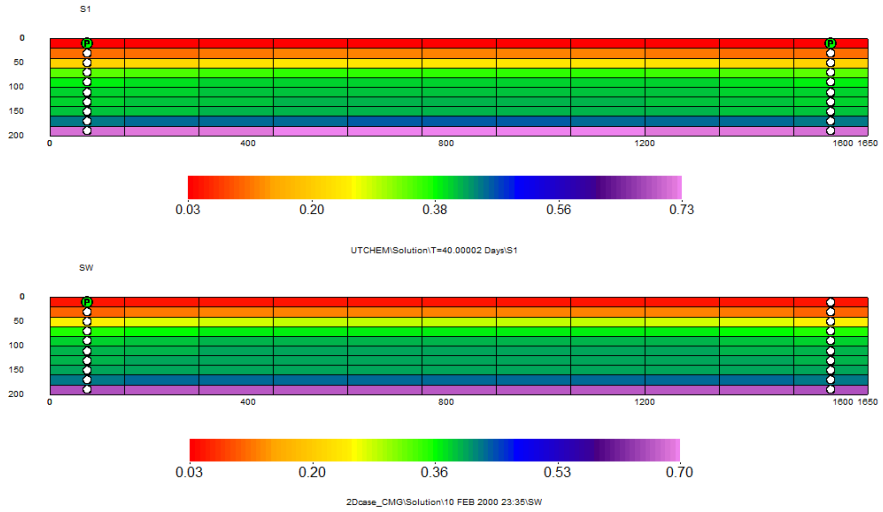

Figure 6-36- A cross section of water saturation distribution that compares results of UTCHEM four-phase model and CMG-IMEX after 40 days in Case-4.

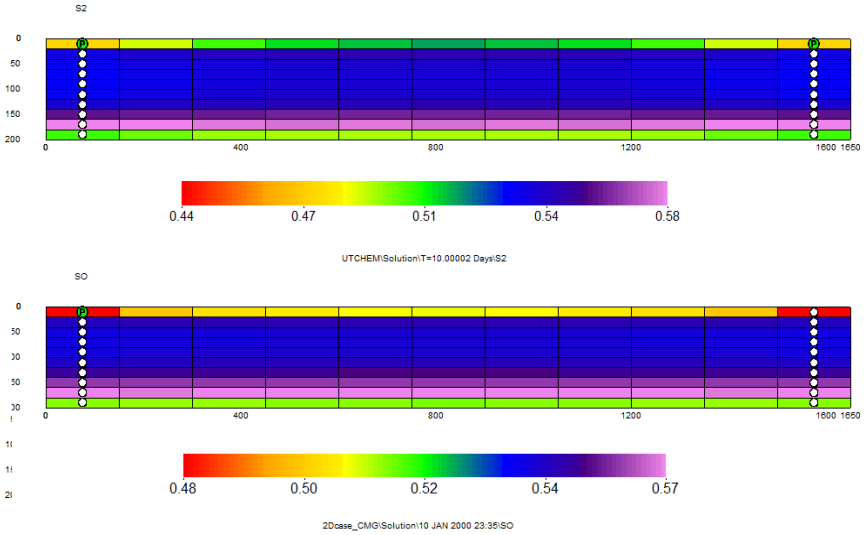

Figure 6-37- A cross section of oil saturation distribution that compares results of UTCHEM four-phase model and CMG-IMEX after 10 days in Case-4.

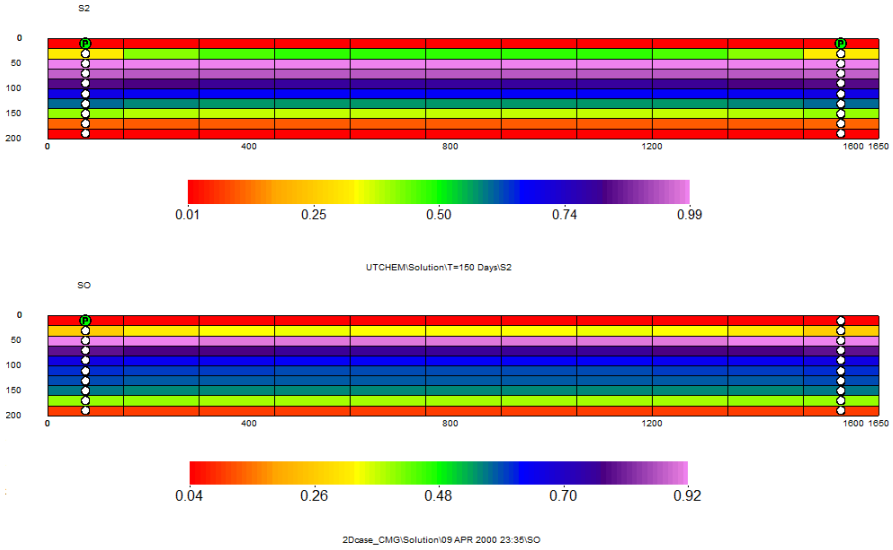

Figure 6-38- A cross section of oil saturation distribution that compares results of UTCHEM four-phase model and CMG-IMEX after 150 days in Case-4.

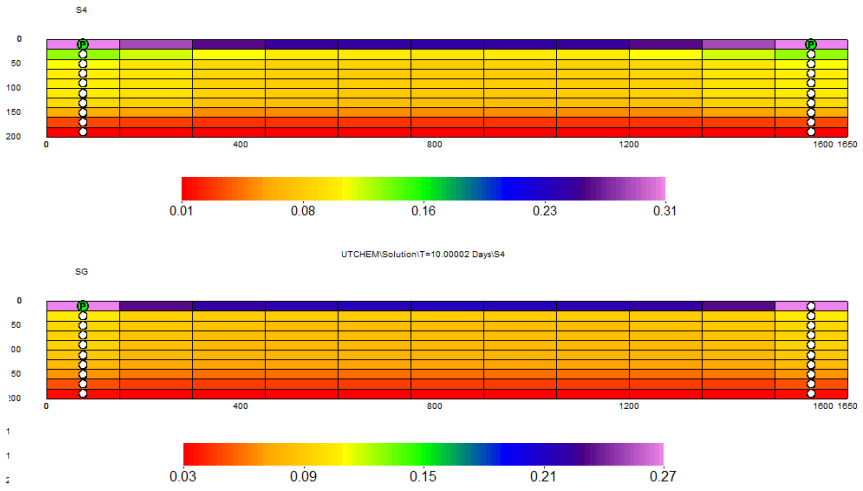

Figure 6-39- A cross section of gas saturation distribution that compares results of UTCHEM four-phase model and CMG-IMEX after 10 days in Case-4.

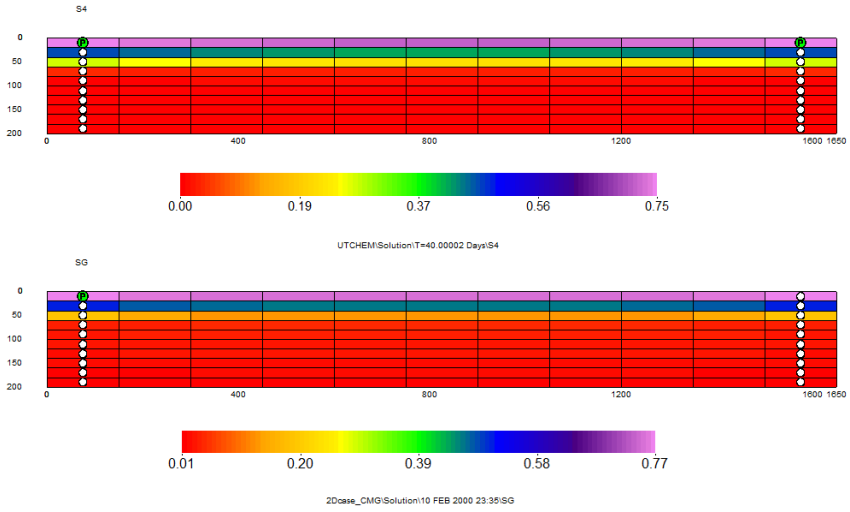

Figure 6-40- A cross section of gas saturation distribution that compares results of UTCHEM four-phase model and CMG-IMEX after 40 days in Case-4.

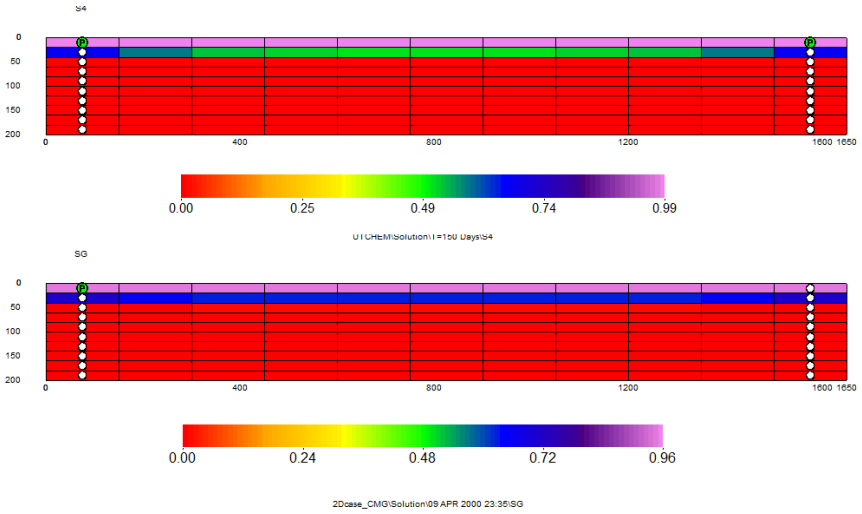

Figure 6-41- A cross section of gas saturation distribution that compares results of UTCHEM four-phase model and CMG-IMEX after 150 days in Case-4.

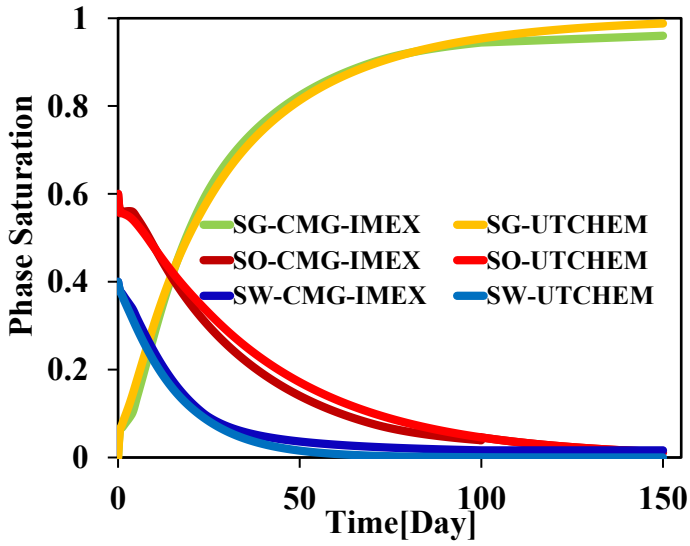

Figure 6-42- Comparison of gas, oil, and water saturation results for a gridblock located in the top layer (layer 1) in Case 4.

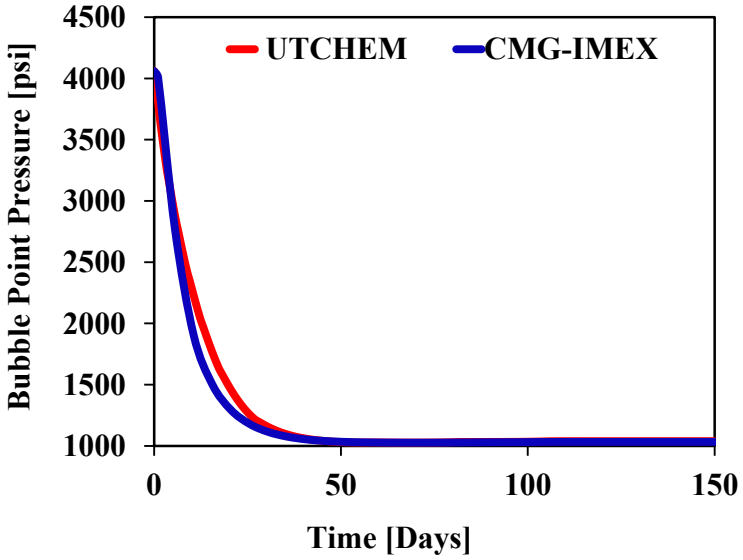

Figure 6-43-Comparison of bubble point pressure results for a gridblock located in the top layer (layer 1) in Case 4.

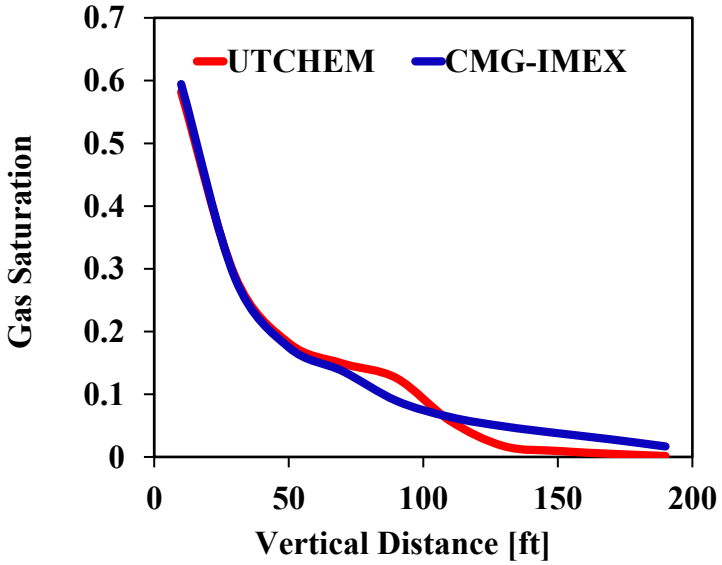

Figure 6-44- Comparison of gas saturation profiles in vertical direction crossed a production well after 40 days in Case-4.

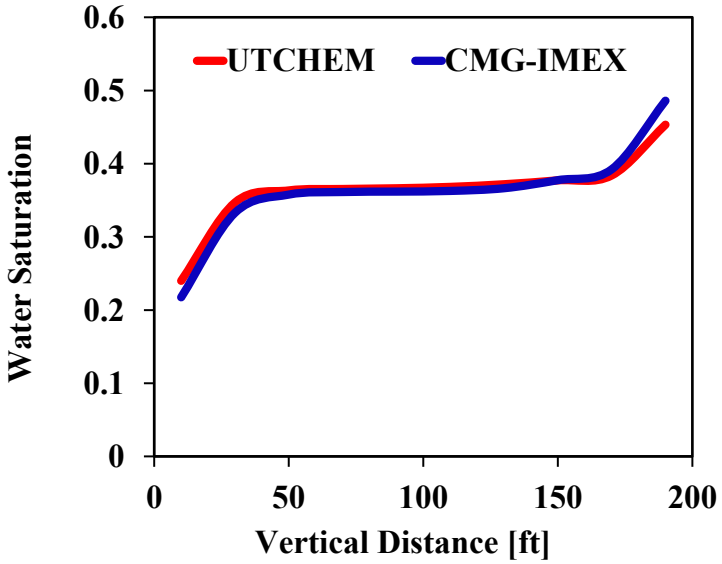

Figure 6-45- Comparison of water saturation profiles in vertical direction located in the middle of reservoir well after 40 days in Case-4.

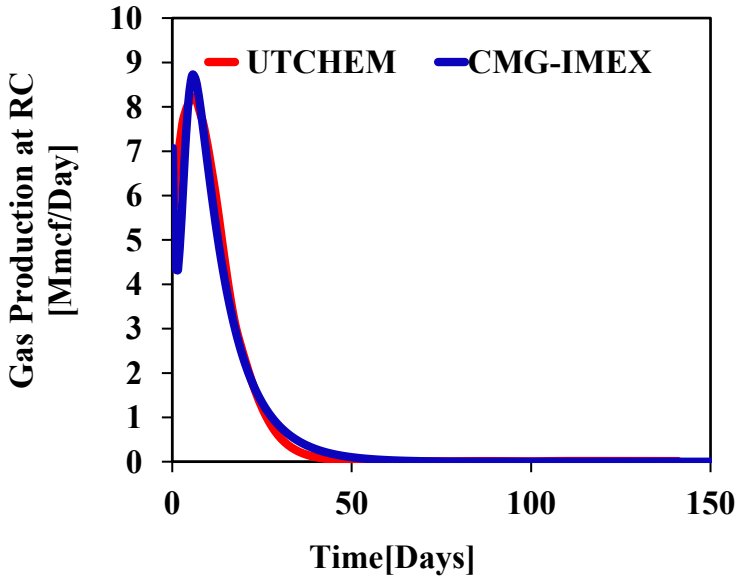

Figure 6-46- Comparison of Field production rate results for gas phase in Case-4.

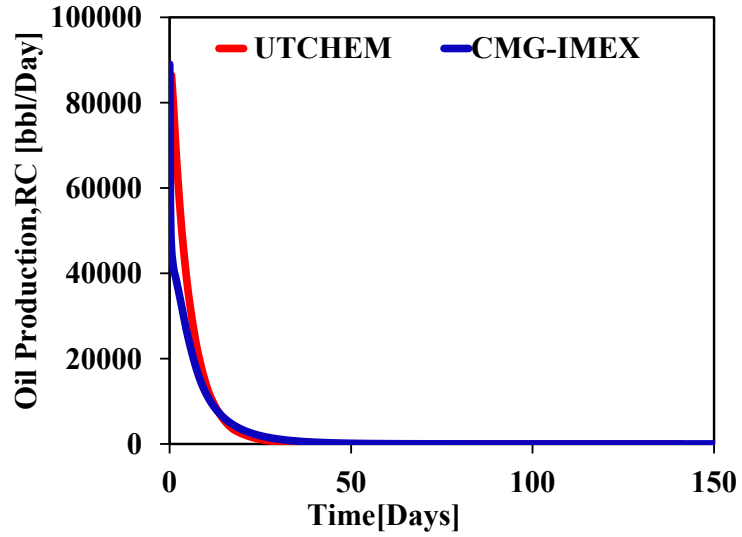

Figure 6-47- Comparison of Field production rate results for oil phase in Case-4.

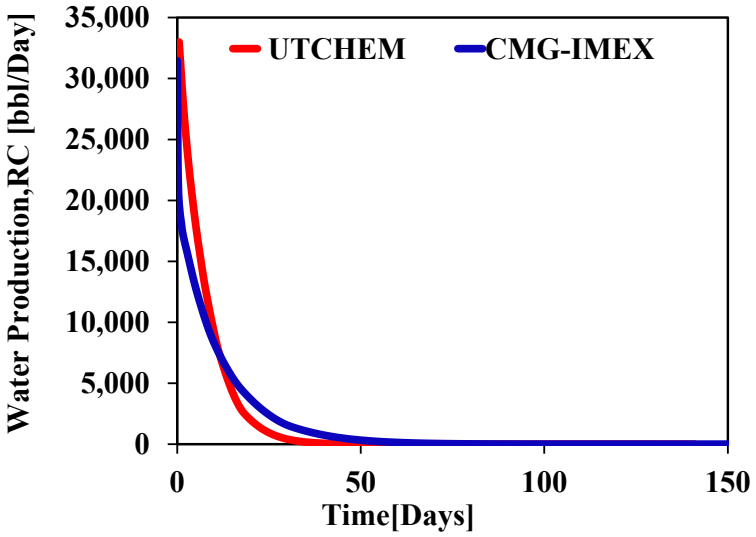

Figure 6-48- Comparison of Field production rate results for water phase in Case-4.

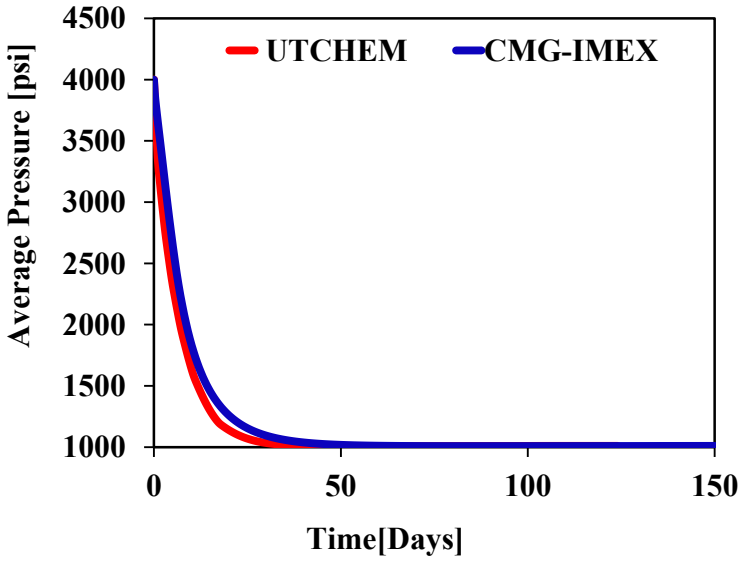

Figure 6-49-Comparison of average pressure of field for gas phase in Case-4.

6.5 SURFACTANT INJECTION WITH THREE PHASE FLOW CASE (CASE-5)

In this case, we tested a 1-D problem similar to Case-1 but surfactant is injected into reservoir under different salinity levels. We are interested to evaluate the surfactant phase behavior results in four-phase model versus the original model. Existing phases in this case are microemulsion/oil/water. This case is also considered as incompressible, similar to Case-1 but as mentioned there are three phases (oil, water, and microemulsion). In order to make the phase behavior between original formulation and four-phase formulation consistent, PVT table is set for the oil formation volume factor to be 1.0 and for solution gas to be zero ($\boldsymbol{R_{so} = 0}$) in different pressures (see Table 6-9). This means oil density stays constant during pressure change and incompressibility of oil is satisfied in four-phase model.

Water is injected (0.99 volume fraction of $50ft^3$/Day) along with surfactant (0.01 volume fraction of $50ft^3$/Day) and anion (0.5 meq/ml) for 100 days into a reservoir. Fluid and reservoir data are explained further in Table 6-10. The detail of the input data for this simulation is in Appendix E.

Figure 6-50 through Figure 6-53 show the comparison of water ($\mathbf{C_1}$), oil ($\mathbf{C_2}$), surfactant ($\mathbf{C_3}$), anion ($\mathbf{C_5}$) concentration profiles at three different times (25, 50, and 75). Results show a slight difference in concentration of components. These differences are due to pressure solution method in transmissibility calculations. In transmissibility calculation for viscosity and density at the boundary of a gridblock in four-phase model, a midpoint weighting is used.

The original model calculates viscosity by upstream weighting. Since viscosity of microemulsion is calculated in the phase tracking section, a change in surfactant concentration leads to a change in microemulsion viscosity (see Equation 5.10). These changes occur mostly in the front of surfactant concentration and microemulsion

saturation. They result in slightly pressure difference as shown in Figure 6-54 for results of two compared models. But the difference is negligible and not crucial in calculations and comparison of results between the two models.

Figure 6-55 through Figure 6-57 show the comparison of oil, water, and microemulsion saturations at three different times (25, 50, and 75) for both four-phase and original models in UTCHEM. Results show a reasonable agreement between the two models. Since surfactant is injected along with water in effective salinity range, microemulsion is generated and the oil and water phases are displaced by microemulsion phase.

Figure 6-59 shows the comparison of oil production rates in both simulators in an excellent agreement. But results of microemulsion and water production rates in both simulators are slightly different after the breakthrough of microemulsion phase. This slight difference is due to pressure solution and surfactant phase tracing as previously discussed.

Although the comparison of results illustrates that the four-phase model is reasonably robust and has less material balance error compared to original formulation, an agreement between production rates in both models are satisfactory. Since oil flow rate is in excellent agreement, the cumulative oil comparison between original model and four-phase model is close enough as illustrated in Figure 6-61.

Average phase saturation comparisons are also evaluated, as plotted in Figure 6-62 through Figure 6-64. Average oil saturation results are in good agreement, similar to production oil rate results and oil saturation profile results at different times.

But average water and microemulsion saturations are fluctuating to some extent as a result of phase tracking and surfactant concentration differences between four-phase model and original models in UTCHEM (as discussed earlier in concentrations part).

Surfactant injections, production, retained surfactant, and adsorbed surfactant are also plotted in Figure 6-65 and Figure 6-66 to evaluate comparisons of both models in UTCHEM.

Incidentally, the input file of this case is presented in Appendix E. In order to run this case for both original and four-phase model, IGMAS flag in input file should be set for IGMAS =1 along with PVT file for four-phase and IGMAS =0 for original UTCHEM.

Table 6-9-Phase behavior and PVT table used in UTCHEM four-phase model in Case-5

Psat (psi)	**Rso** (SCF/STB)	**B1** (RB/STB)	**B4** (RB/SCF)	**vis1** (cp)	**vis4** (cp)
100	0	1.0	0.005	1.0	0.01
800	0	1.0	0.002	1.0	0.01
1200	0	1.0	0.001	1.0	0.01
1600	0	1.0	0.001	1.0	0.01
2000	0	1.0	0.001	1.0	0.01
2400	0	1.0	0.0009	1.0	0.01
2800	0	1.0	0.0008	1.0	0.01
3200	0	1.0	0.0007	1.0	0.01
3600	0	1.0	0.0006	1.0	0.01
4000	0	1.0	0.0005	1.0	0.01
4400	0	1.0	0.0005	1.0	0.01
4800	0	1.0	0.0004	1.0	0.01
5200	0	1.0	0.0004	1.0	0.01
5600	0	1.0	0.0004	1.0	0.01

Table 6-10- Fluid and reservoir input parameters used in UTCHEM four-phase model and original UTCHEM for Case-5

Reservoir and Fluid Data	
Reservoir Size	200ftx10ftx10ft
Number of Gridblock	20x1x1
Gridblock Size	10ftx10ftx10ft
Porosity	20%
Permeability	100mD
Basic Rock and Fluid Properties	
Water Density(RC)	0.45psi/ft
Oil Density(SC)	0.225psi/ft
Gas Density(SC)	0.0004psi
Water Compressibility	$1x10^{-6}$1/psi
Water Rel. Perm	S_{rw}=0 , k^o_{rw}=1.0 , e_w=1.0
Oil Rel. Perm	S_{ro}=0 , k^o_{ro}=1.0 , e_o=1.0
Me Rel. Perm	S_{rme}=0 , k^o_{rme}=1.0 , e_{me}=1.0
Rock Compressibility	0.0 1/psi
Initial Pressure	2000 psi
Initial Saturations	0.4(water),0.6(oil), 0(gas)
Well	
Number of Wells	1prod. and 1 inj.
Well Constrains	1prod(BHP=2000psi)
	1Inj (Const. Water Rate=50 ft^3/Day)
	(c_1=0.99vol/vol,c_3=0.01vol/vol,c_5=0.6meq/ml)

Table 6-11- Chemical fluid and chemical phase behavior parameters used in UTCHEM four-phase model and original UTCHEM for Case-5

Chemical Fluid Properties	
Surfactant Density	0.433psi
Microemulsion Viscosity Parameters	A_{P1}=0 wt%$^{-1}$, A_{P2}=0 wt%$^{-1}$, A_{P3}=1 wt%$^{-1}$, A_{P4}=0 wt%$^{-1}$, A_{P5}=1.7 wt%$^{-1}$,
Phase Behavior	
CMC	10^{-5} vol/vol
Optimal Salinity	0.44meq/ml
Lower Optimal Salinity	0.33meq/ml
Upper Optimal Salinity	0.53meq/ml
Height of Binodal Curve	H_0= 0.05,H_1= 0.03 H_2= 0.05
IFT Parameters	$Log\sigma_{go}$ =1.477dyne/cm, $Log\sigma_{gw}$ = 1.477dyne/cm
Adsorptions	
Surfactant adsorption Parameters	A_{D1}=1.5, A_{D2}=0.5 ml/meq, B_{D3}=1000vol/vol

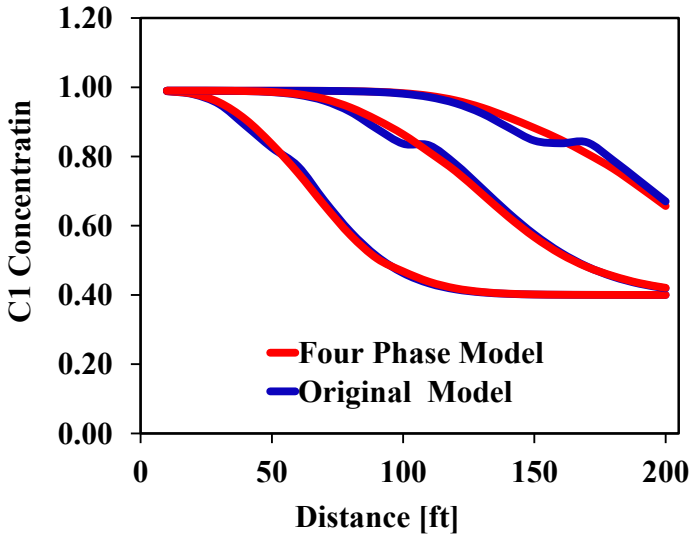

Figure 6-50-Comparison of water concentration profiles in the various days (after 25, 50, and 75 days) in Case-5.

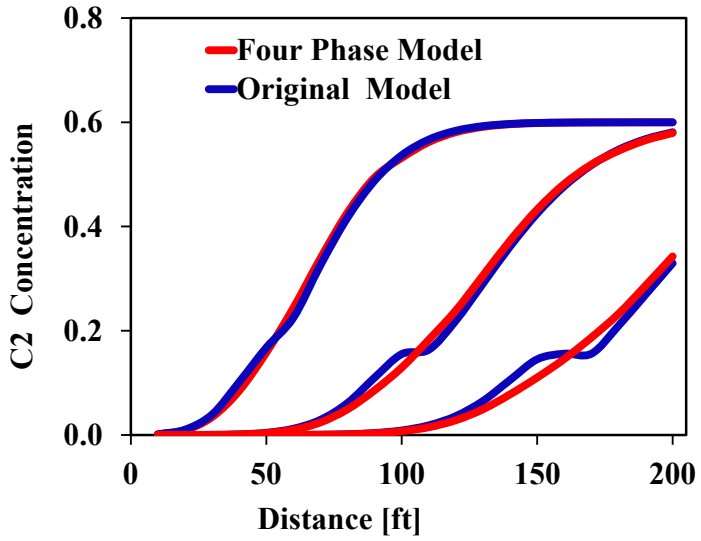

Figure 6-51- Comparison of oil concentration (C_2) profiles in the various days (after 25, 50, and 75 days) in Case-5.

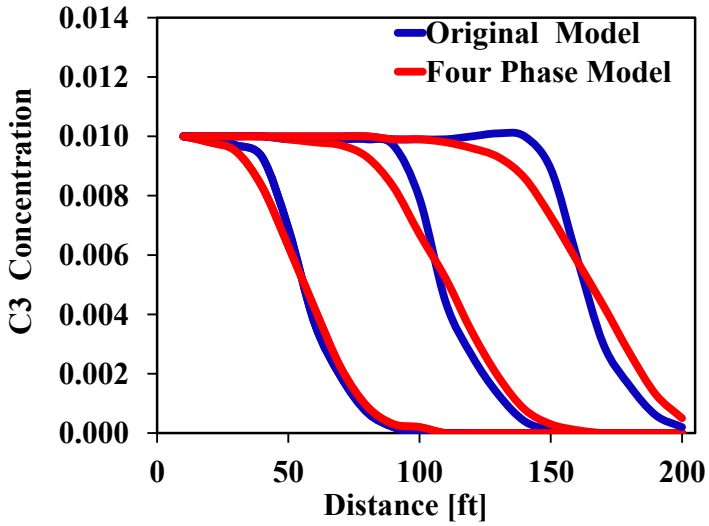

Figure 6-52- Comparison of surfactant concentration profiles in the various days (after 25, 50, and 75 days) in Case-5.

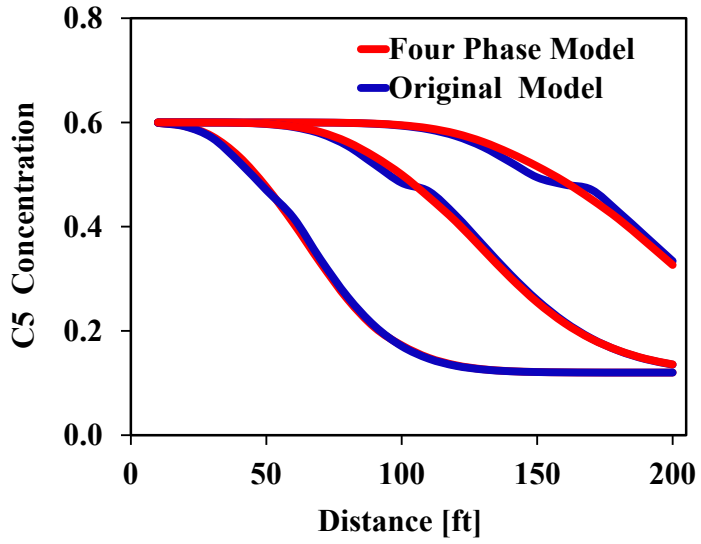

Figure 6-53- Comparison of anion ($\mathbf{C_5}$) concentration profiles in the various days (after 25, 50, and 75 days) in Case-5.

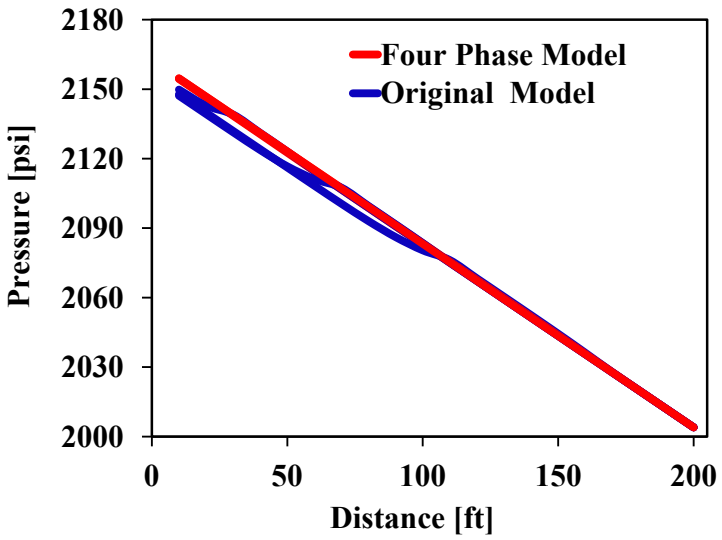

Figure 6-54- Comparison of pressure profiles in the various days (after 25, 50, and 75 days) in Case-5.

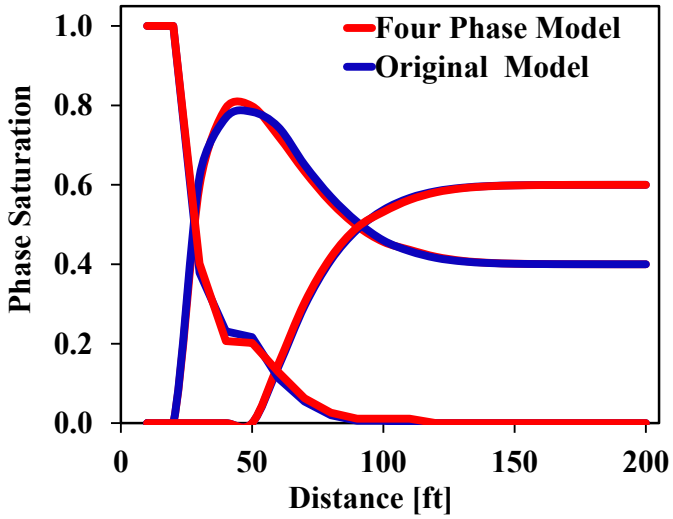

Figure 6-55- Comparison of oil, water, and microemulsion saturation profiles after 25 days in Case-5.

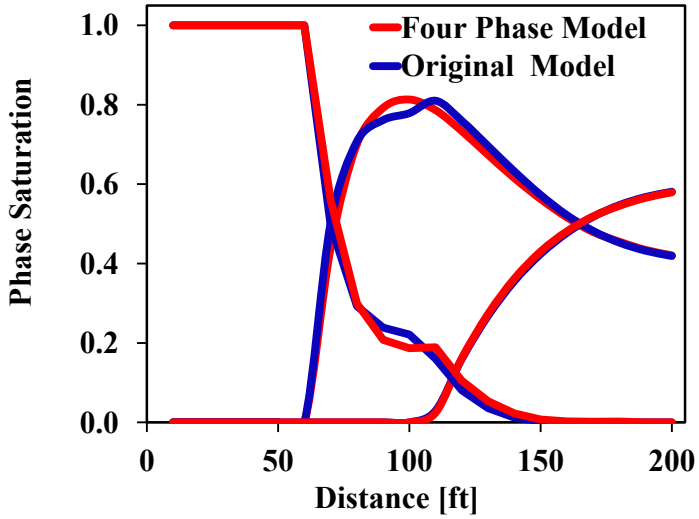

Figure 6-56- Comparison of oil, water, and microemulsion saturation profiles after 50 days in Case-5.

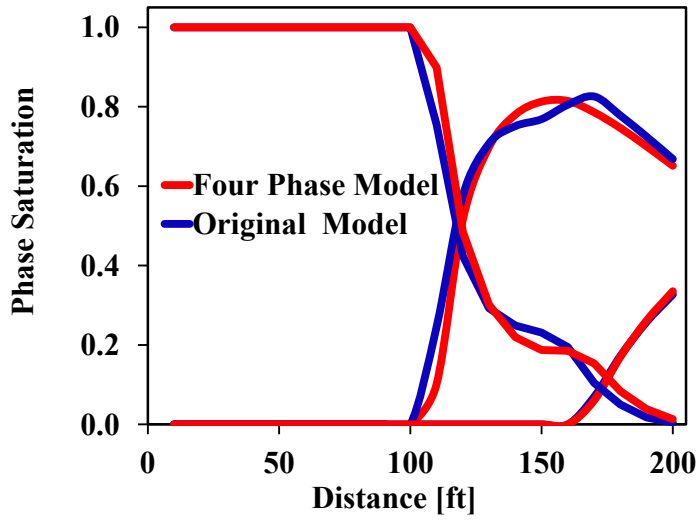

Figure 6-57- Comparison of oil, water, and microemulsion saturation profiles after 75 days in Case-5.

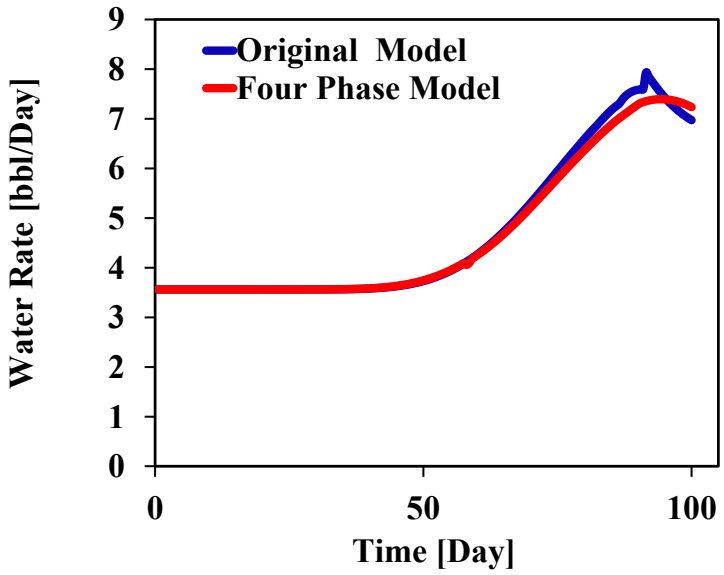

Figure 6-58 -Comparison of water production results for Case-5.

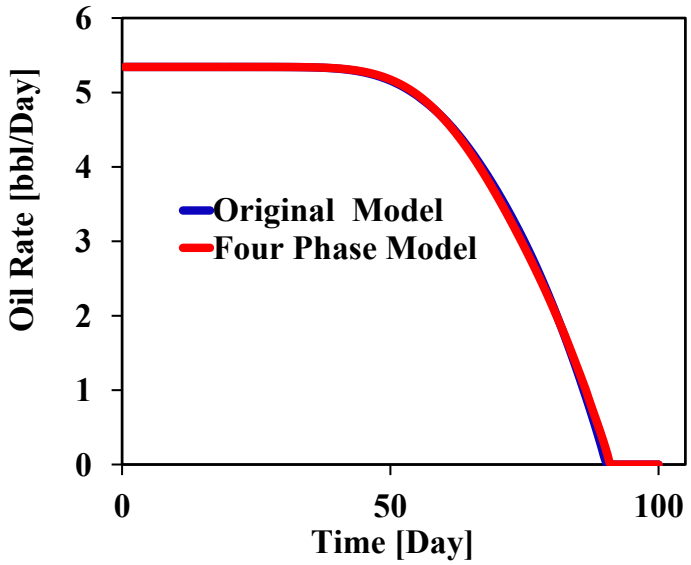

Figure 6-59- Comparison of oil production results for Case-5.

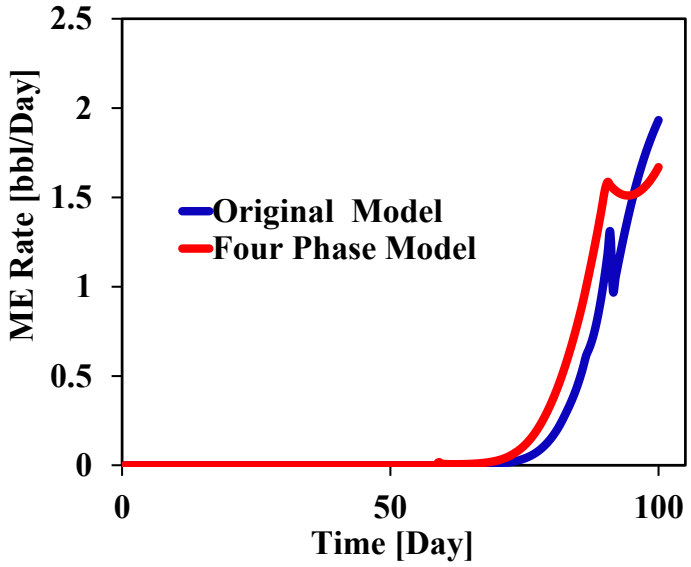

Figure 6-60- Comparison of microemulsion production results for Case-5.

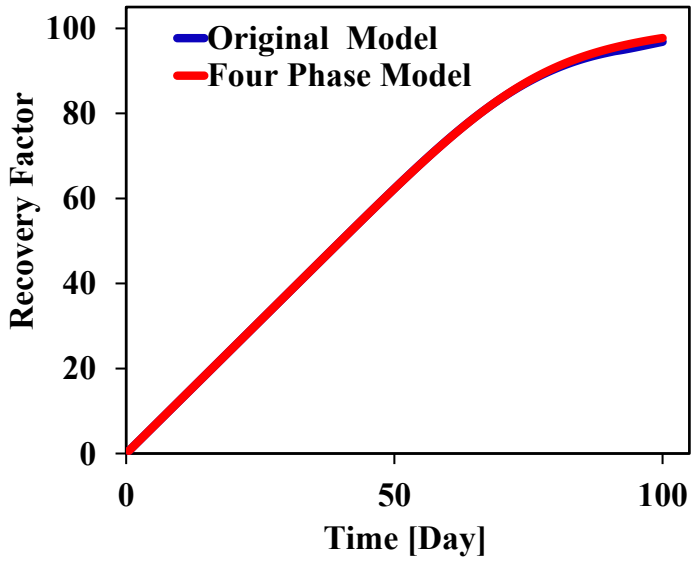

Figure 6-61-Comparison of oil recovers factor results for Case-5.

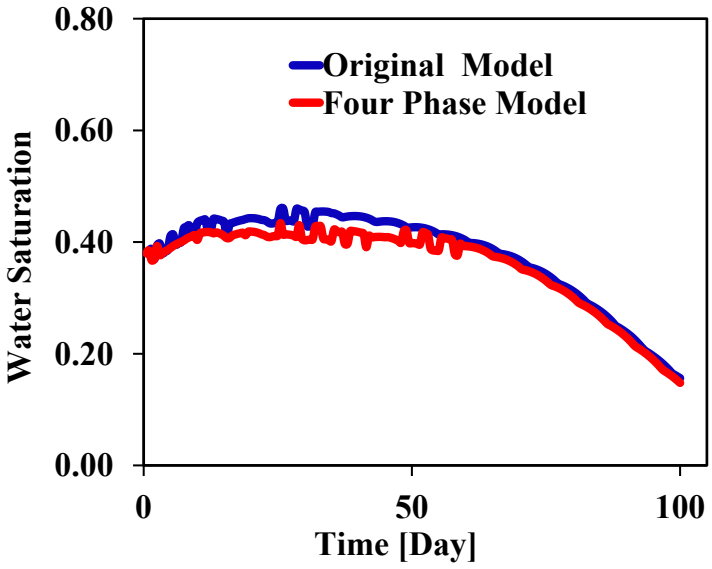

Figure 6-62-Comparison of average water saturation in Case-5.

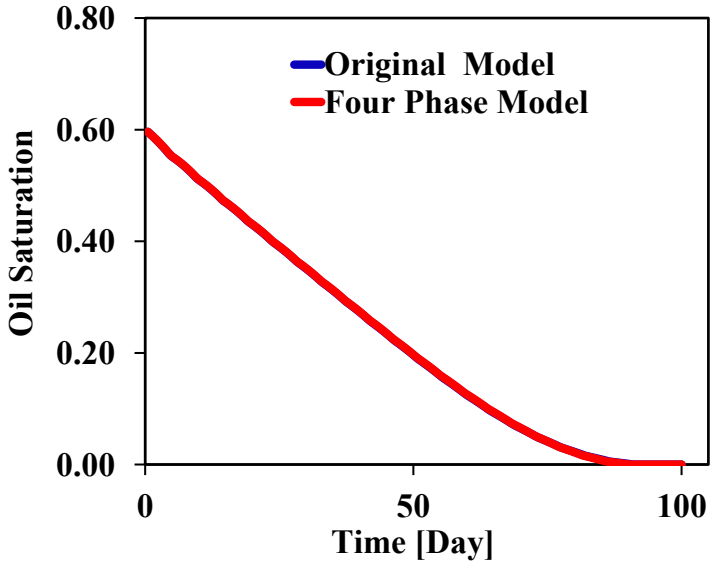

Figure 6-63- Comparison of average oil saturation in Case-5.

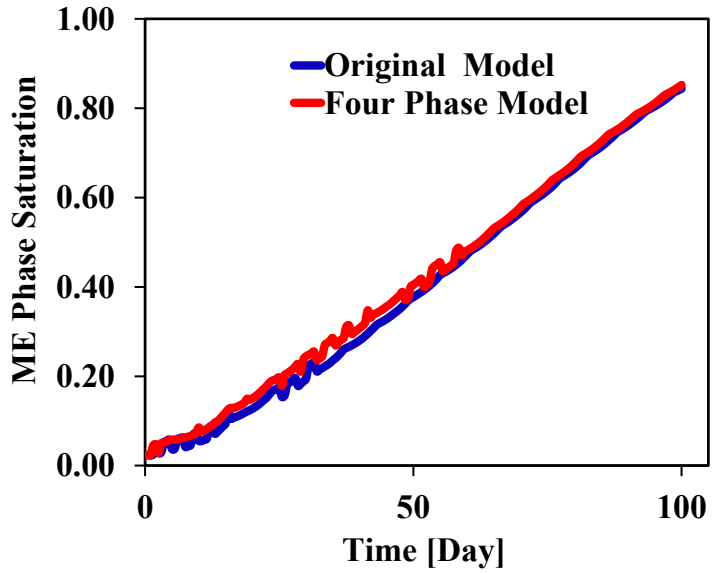

Figure 6-64- Comparison of average microemulsion saturation in Case-5.

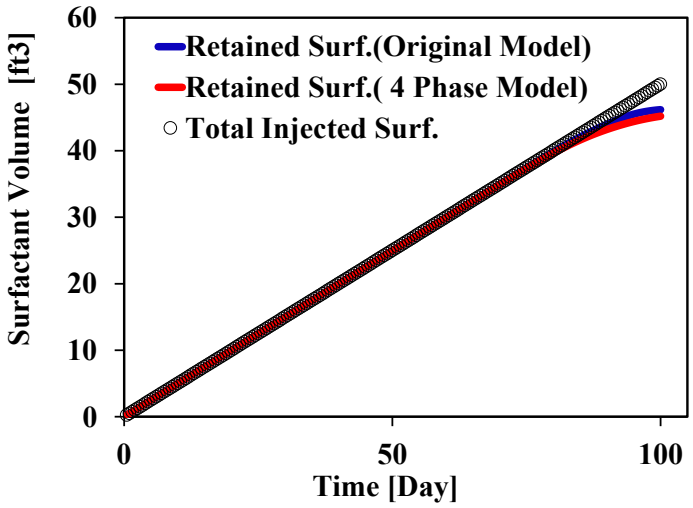

Figure 6-65- Comparison of injected, produced, and retained surfactant in Case-5.

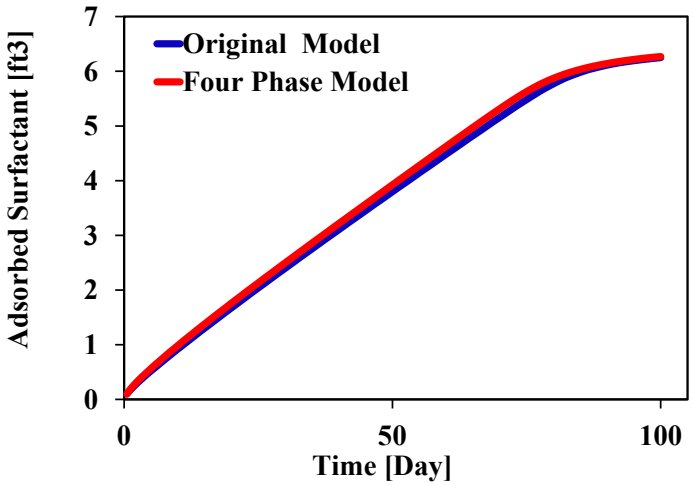

Figure 6-66-Comparison of adsorbed surfactant in Case-5.

6.6 SURFACTANT AND GAS INJECTION WITH FOUR PHASE FLOW CASE (CASE-6)

In Case -1 through Case-5 of this chapter, we validated our new model results of three –phase (gas/oil/water and microemulsion/oil/water) by comparing with CMG-IMEX results and UTCHEM original model results emphasizing on phase behavior and multiphase fluid flow.

This case is a four-phase model (oil/water/gas/microemulsion) which is combination of Case-2 and Case-5. In this case, we are interested to evaluate the surfactant phase behavior in the presence of gas phase. We used input files of Case-5 and Case-2 with the same PVT table used in Cases-2 as shown in Table 6-12.

At the beginning, gas is injected under constant rate 100 ft^3/Day for 25 days. Then gas injection is stopped and water is injected (0.99 volume fraction of 50ft^3/Day) along with surfactant (0.01 volume fraction of 50ft^3/Day) and anion (0.5 meq/ml) for 50 more days into the reservoir. On day 75, gas and water with surfactant are injected for another 75 days. The details of injection well schedule are depicted in Table 6-13 and plotted in

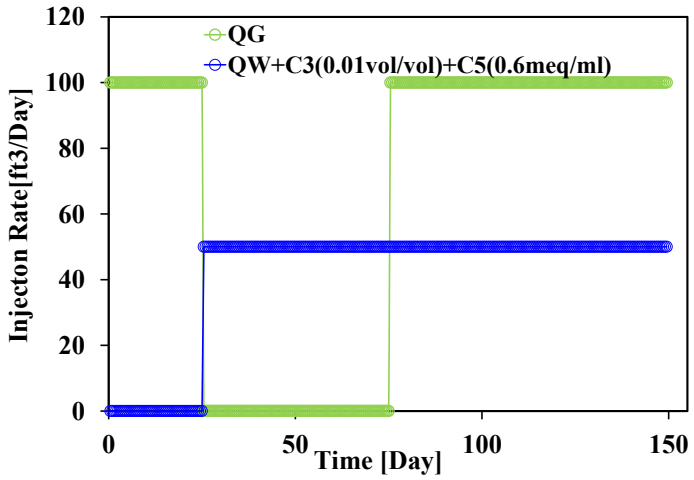

Figure 6-70-Water and gas injection well schedule in Case-6.

Surfactant phase behavior calculation parameters are listed in Table 6-14. The detail of the input data for this simulation is in Appendix E.

Figure 6-71 shows the variation of water concentration profile with time at days 25, 50, 75, 100, and 125. Since gas is injected initially, water concentration decreases before day 25 around injectors and after starting water injection the concentration of water increases until day 75. Water concentration decreases slightly right after gas injection on day 75 as can be observed on days 100 and 125.

Figure 6-72 plots the variation of oil concentration profiles with time. During gas injection period before day 25, oil displacement by gas injection is poor as can be seen on the blue line. Once water injection with surfactant has started on day 25, mobility ratio becomes favorable to some extent and this improves the displacement of oil to achieve more recovery. This improvement can be observed in concentration profiles on days after water injection (50, 70, 100, and 125).

Surfactant is injected continuously from day 25 for 125 days into reservoir under constant rate (0.01 volume fraction of 50 ft^3/Day). This concentration is accumulated slightly in the front. After breakthrough of surfactant, which occurs on day 100, the surfactant accumulation in front decreases to injected amount (0.01vol/vol). The accumulation of surfactant is due to high diffusivity of surfactant in the mass concentration equation compared to oil and water mass equations. Diffusivity of mass equation can simply be controlled by density of component and viscosity in input file.

Figure 6-74 shows the variation of anion concentration with time. The unit of the concentration is considered milliequivalent per milliliter (meq/ml) dissolved in water. Therefore, its variation is a function of water concentration and a change in water concentration causes the same change in the anion concentration.

Figure 6-75 illustrates the variation of gas concentration with time. Once gas is injected at early time, before 25 days, gas concentration, as the blue line shows, is in range 0.5 to 0.1. Same rate of gas (100 ft^3/Day) is started reinjecting with water and

surfactant on day 75 until 150 days. In this time period, since gas is compressible and mobile compared to other components, the volume concentration of gas reduces compared to the first period (first 25 days) of pure gas injection thus its concentration becomes less than 0.04 due to high pressure Figure 6-76 and Figure 6-80 show the results of oil, water, microemulsion, and gas saturation profiles on various days (25, 50, 75, 100, and 125). At early time, after opening the producer we inject gas under constant rate; the gas saturation increases around the injector and reduces around the producer. Displacement process, because of unfavorable mobility ration, is small. Once water and surfactant are injected along with water on day 25, in the effective salinity range, microemulsion is generated then oil and water phases are displaced by microemulsion phase. Gas reinjection is started on day 75 along with water and surfactant injection and four-phases (microemulsion/oil/water/gas) coexist. The injection of gas benefits better displacement by increasing the viscosity.

Figure 6-81 through Figure 6-85 plot the phase behavior calculation profiles for surfactant/oil/water at different times (25, 50, 75, 100, and 125). Microemulsion phase forms in the presence of surfactant, since effective salinity is between optimum upper and lower salinities. In fact, salinity and surfactant are required to generate microemulsion in Hand's rule phase behavior calculations. These requirements cause the existing oil in the oleic phase to be solubilized in microemulsion phase by reducing interfacial tension between oil and water. Blue color line represents water concentrations in microemulsion, while red color line represents oil concentration in the microemulsion. Black color line is assigned to surfactant concentration in microemulsion.

As previously discussed, in this case initially the reservoir pressure is 4000 psi and right after opening the production and injection wells, pressure declines, and gas is released by oil. In addition, gas injection starts.

Figure 6-86 shows a cross plot of average pressure alongside water/surfactant and gas injection rates. Relatively, Figure 6-87 and Figure 6-88 depict production phase rates and production component rates with time.

Gas rate is initially considerable due to gas formation and vaporization phenomena in production well; afterwards it sharply drops at early time and gradually increases to 100 ft^3/day. Gas production before reaching 100 ft^3/Day is reduced because gas injection stopped on day 25. Rapidly gas production reduces until eventually no free gas is produced because free gas is dissolved in oil, corresponding to an increase in pressure. By re-injecting gas on day 75, gas production grows and reaches a steady state condition. Gas injection benefits to increase the viscosity of oil; then it improves the oil recovery properly even though is not a considerable recovery mechanism. On the other hand, surfactant solubilizes oil by reducing interfacial tension (IFT) between oil and water and generates microemulsion phase in the effective salinity range. Although Figure 6-87 shows oil phase production is over at around day 110, oil component is still being produced in microemulsion phase until day 150, as can be seen in Figure 6-88.

Figure 6-89 shows free gas concentration beside solution gas in standard condition in production well. As can be observed, solution gas decreases corresponding to an increase in free gas. The reason: a decrease in pressure leads to a decrease in bubble point pressure (shown in Figure 6-90). This causes to lower solution gas and free gas forms. But after stopping gas injection and starting water/surfactant injection, all existing free gas is dissolved in oil and increases the solution gas and bubble point pressure. This increase in solution gas and bubble point pressure is significant and crucial right after re-injecting gas along water and surfactant injection. In this period, since free gas is being injected and there is enough free gas, only solution gas and bubble point increase; then, by stabilizing the pressure and reaching steady state, they drop to fixed

values. Figure 6-91 shows microemulsion phase behavior calculation in the production well and its compositions with time.

As can be seen, when microemulsion reaches the breakthrough at the production well, the solubilized oil is produced along with surfactant and water components. Concentrations of water, oil, and surfactant in microemulsion are plotted to recognize the compositions of this phase in the production well with time. Considerable amount of oil is solubilized in microemulsion phase at the beginning of breakthrough; it then increases to reach a peak and subsequently sharply reduces in last 25 days.

Average phase saturations are plotted in Figure 6-92. Saturations reasonably confirm the coupled phase behavior calculations for surfactant/oil/water and gas/oil as discussed previously in this case. There is insignificant fluctuating due to phase tracking that occurs between water and microemulsion in the presence of surfactant at different salinities when microemulsion phase forms.

Table 6-12-Phase behavior and PVT table used in UTCHEM four-phase model in Case-6.

Psat (psi)	**Rso** (SCF/STB)	**B1** (RB/STB)	**B4** (RB/SCF)	**vis1** (cp)	**vis4** (cp)
100	165	1.012	0.0059	1.17	0.013
800	335	1.0255	0.00295	1.14	0.0135
1200	500	1.038	0.00196	1.11	0.014
1600	665	1.051	0.00147	1.08	0.0145
2000	828	1.063	0.00118	1.06	0.0150
2400	985	1.075	0.00098	1.03	0.0155
2800	1130	1.087	0.00084	1.00	0.016
3200	1270	1.0985	0.00074	0.98	0.0165
3600	1390	1.11	0.00065	0.95	0.017
4000	1500	1.12	0.00059	0.942	0.0175
4400	1600	1.13	0.00054	0.92	0.018
4800	1676	1.14	0.00049	0.91	0.0185
5200	1750	1.148	0.00045	0.9	0.019
5600	1810	1.155	0.00042	0.89	0.0195

Table 6-13-Fluid and reservoir input parameters used in UTCHEM four-phase model and original UTCHEM for Case-6.

Reservoir and Fluid Data	
Reservoir Size	200ftx10ftx10ft
Number of Gridblock	20x1x1
Gridblock Size	10ftx10ftx10ft
Porosity	20%
Permeability	100mD
Basic Rock and Fluid Properties	
Water Density(RC)	0.45psi/ft
Oil Density(SC)	0.225psi/ft
Gas Density(SC)	0.0004psi/ft
Water Compressibility	$1x10^{-6}$1/psi
Water Rel. Perm	$S_{rw}=0$, $k^o_{rw}=1.0$, $e_w=1.0$
Oil Rel. Perm	$S_{ro}=0$, $k^o_{ro}=1.0$, $e_o=1.0$
Me Rel. Perm	$S_{rme}=0$, $k^o_{rme}=1.0$, $e_{me}=1.0$
Gas Rel. Perm	$S_{rg}=0$, $k^o_{rg}=1.0$, $e_g=1.0$
Rock Compressibility	0.0 1/psi
Initial Pressure	2000psi
Initial Saturations	0.4(water),0.6(oil), 0(gas)
Well	
Number of Wells	1prod. and 1 inj.
Well Constrains	1prod(BHP=2000psi) 1Inj (Const. Gas and Water Rate=50 ft^3/Day) Water Rate=50ft^3 (c_1=0.99vol/vol,c_3=0.01vol/vol, c_5=0.6meq/ml) Gas Rate=100ft^3/Day

Table 6-14-Chemical fluid and chemical phase behavior parameters used in UTCHEM four-phase model and original UTCHEM for Case-6.

Chemical Fluid Properties	
Surfactant Density	0.433psi
Microemulsion Viscosity Parameters	A_{P1}=0 wt%$^{-1}$, A_{P2}=0 wt%$^{-1}$, A_{P3}=1 wt%$^{-1}$, A_{P4}=0 wt%$^{-1}$, A_{P5}=1.7 wt%$^{-1}$,
Phase Behavior	
CMC	10^{-5} vol/vol
Optimal Salinity	0.44meq/ml
Lower Optimal Salinity	0.33meq/ml
Upper Optimal Salinity	0.53meq/ml
Height of Binodal Curve	H_0= 0.05,H_1= 0.03 H_2= 0.05
IFT Parameters	$Log\sigma_{go}$ =1.477dyne/cm, $Log\sigma_{gw}$ = 1.477dyne/cm
Adsorptions	
Surfactant adsorption Parameters	A_{D1}=1.5, A_{D2}=0.5 ml/meq, B_{D3}=1000vol/vol

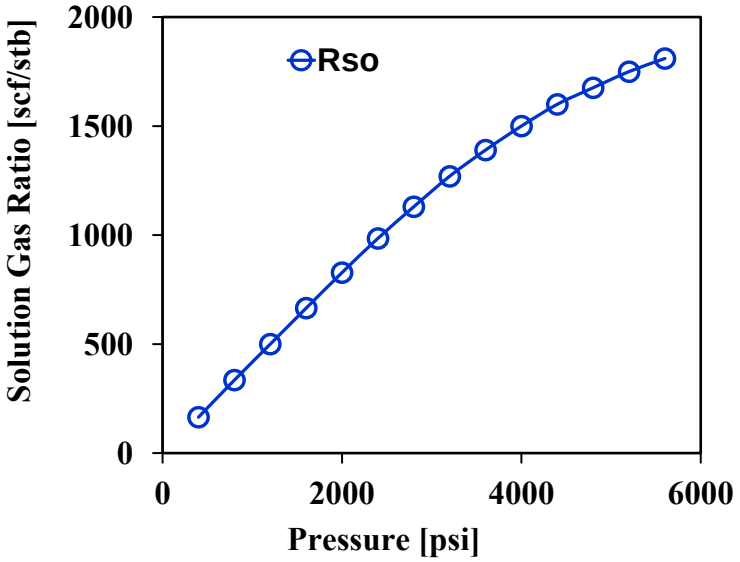

Figure 6-67-Solution gas ratio data at saturated condition used in CMG-IMEX and UTCHEM in Case-6.

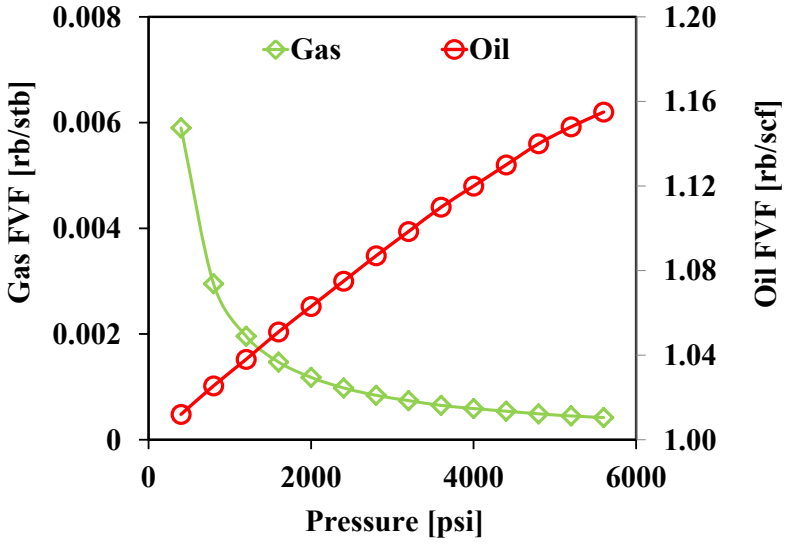

Figure 6-68-Formation volume factor of oil and gas at saturated condition used in CMG-IMEX and UTCHEM in Case-6.

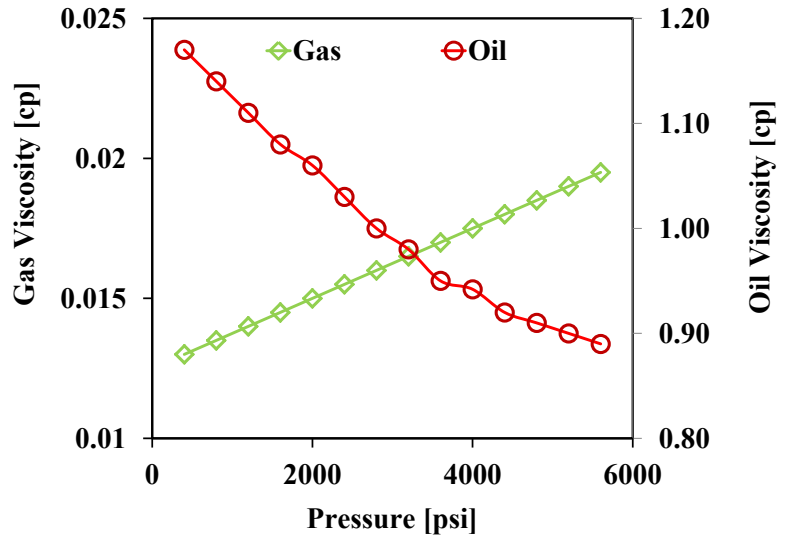

Figure 6-69-Oil and gas viscosity data at saturated condition used in CMG-IMEX and UTCHEM for Case-6.

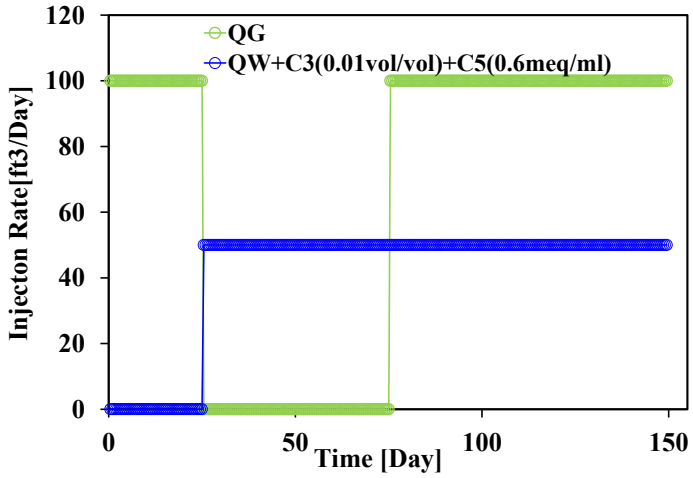

Figure 6-70- Water and gas injection well schedule in Case-6.

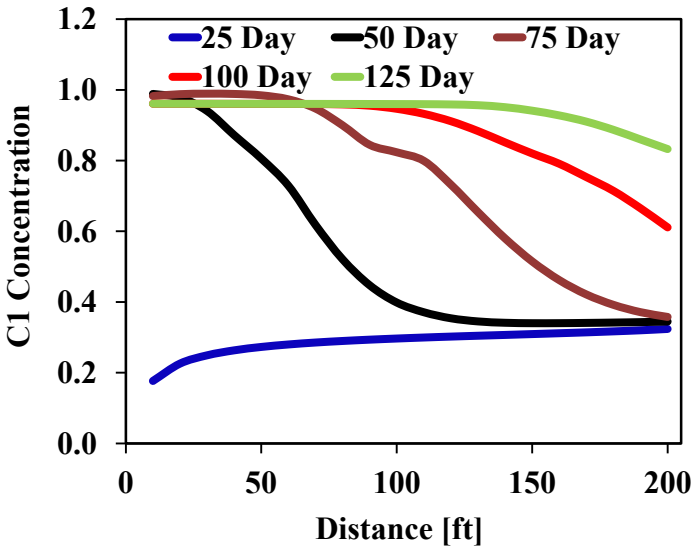

Figure 6-71-water concentration ($\mathbf{c}_1$) profile at the various times for Case-6.

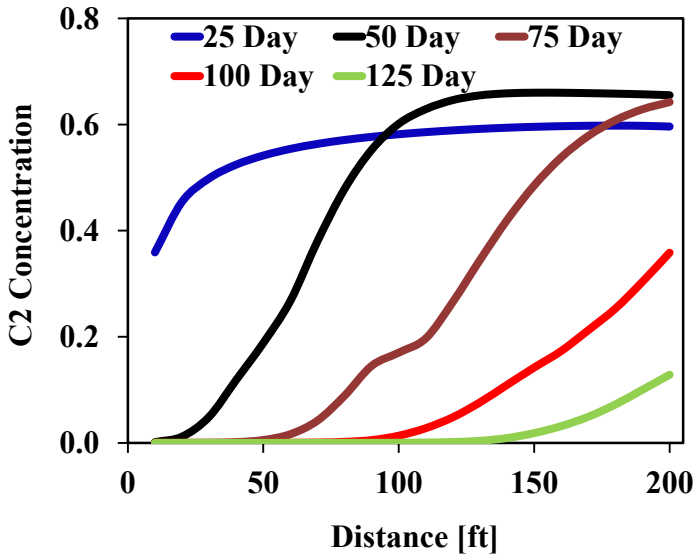

Figure 6-72- Oil concentration ($\mathbf{c}_2$) profile at the various times for Case-6.

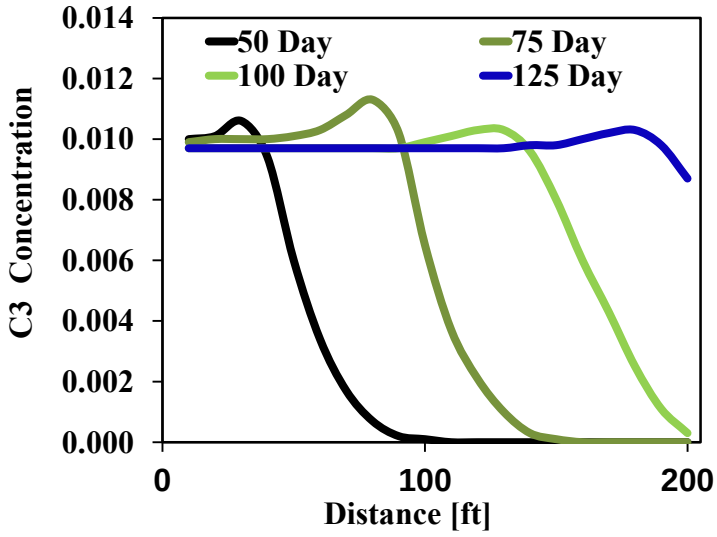

Figure 6-73-Surfactant concentration ($\mathbf{c}_3$) profile at the various times for Case-6.

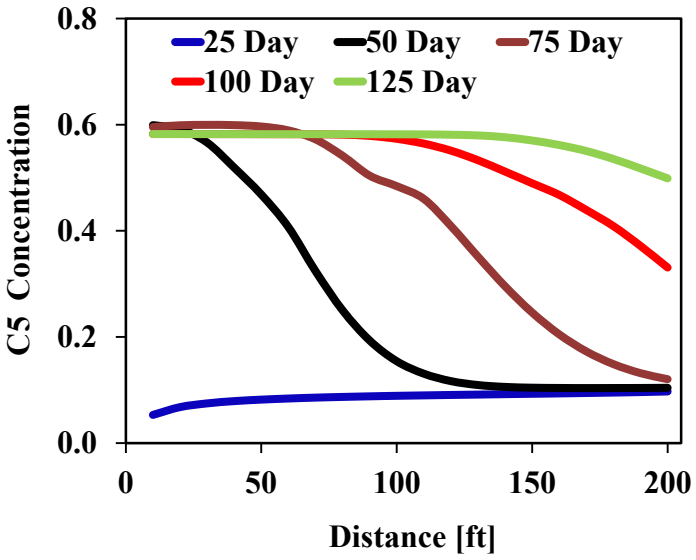

Figure 6-74- Anion concentration ($\mathbf{c}_5$) profile at the various times for Case-6.

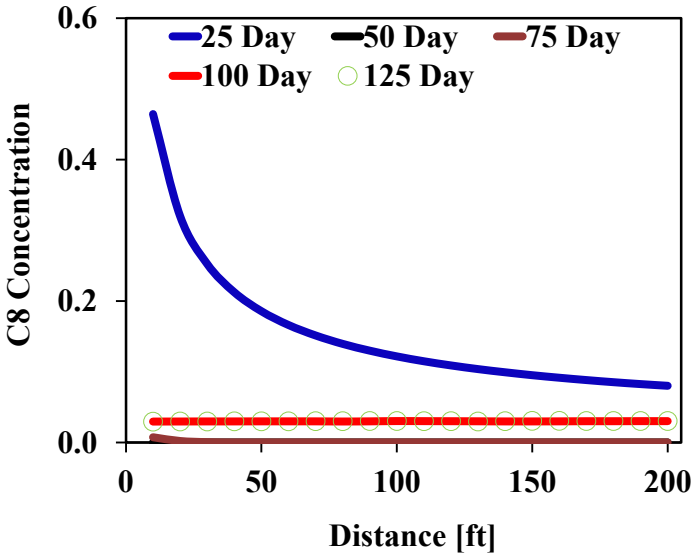

Figure 6-75-Gas concentration ($\mathbf{c}_8$) profile at the various times for Case-6.

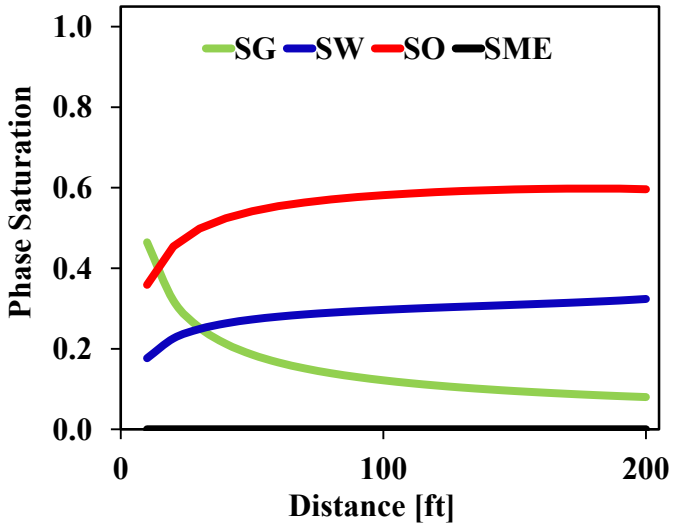

Figure 6-76- Gas, water, oil, and microemulsion saturation results after 25 days for Case-6.

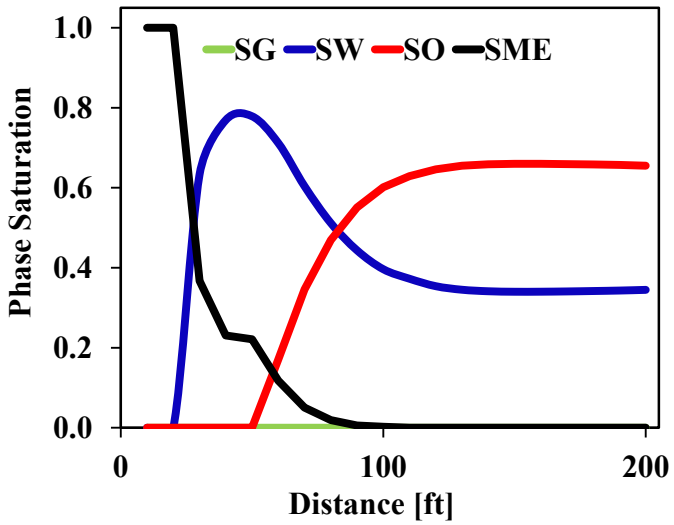

Figure 6-77- Gas, water, oil, and microemulsion saturation results after 50 days for Case-6.

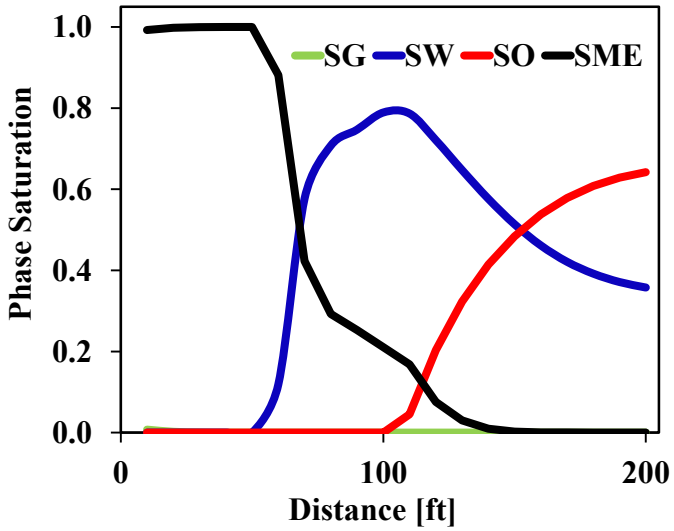

Figure 6-78- Gas, water, oil, and microemulsion saturation results after 75 days for Case-6.

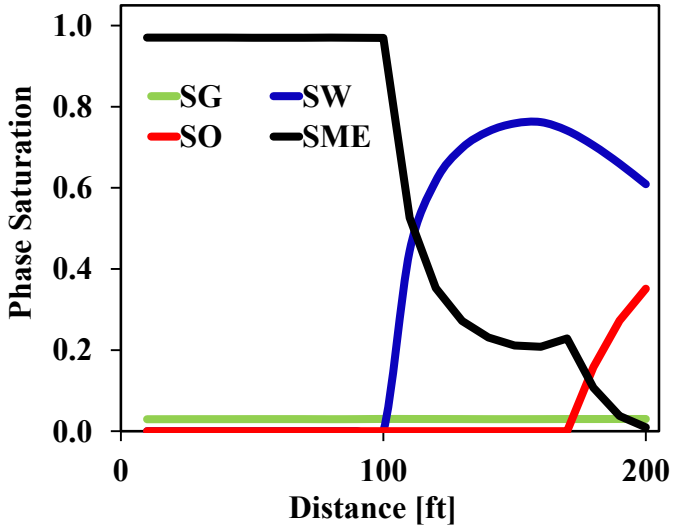

Figure 6-79- Gas, water, oil, and microemulsion saturation results after 100 days for Case-6.

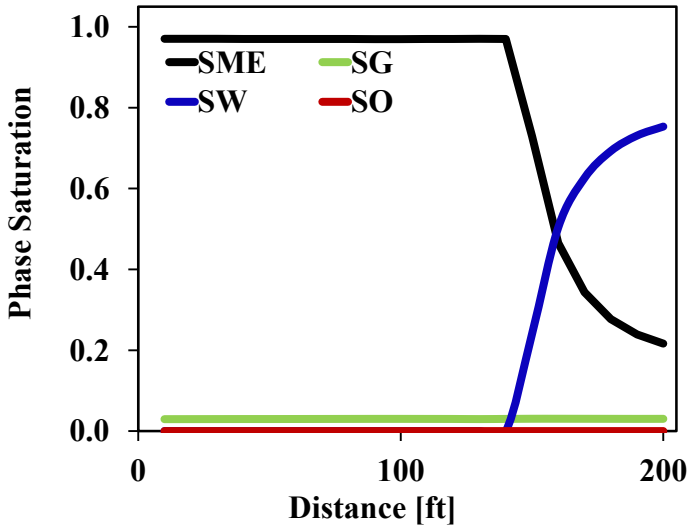

Figure 6-80- Gas, water, oil, and microemulsion saturation results after 125 days for Case-6.

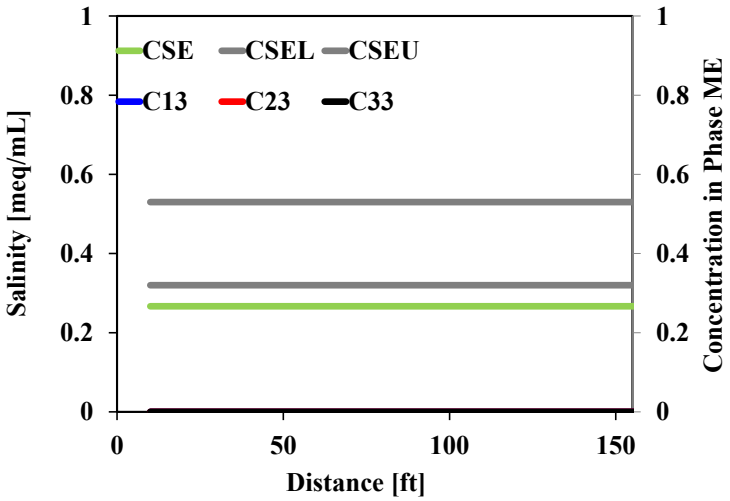

Figure 6-81- Surfactant/oil/water phase behavior window and oil, water, and surfactant concentrations in microemulsion phase (***l=3***) after 25 days for Case-6.

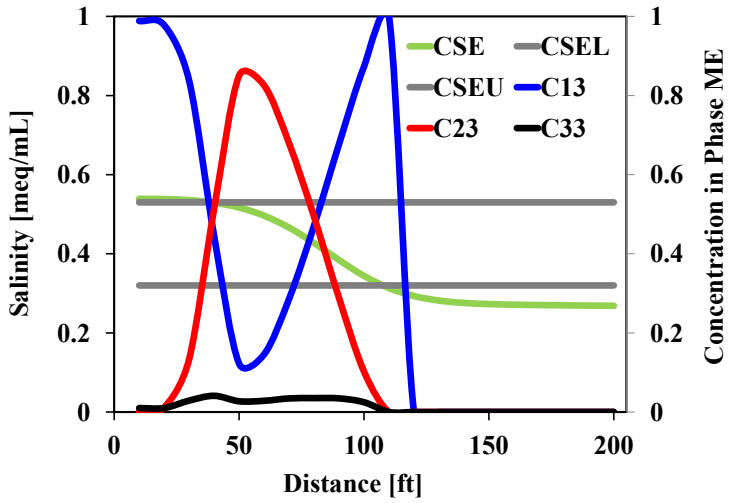

Figure 6-82- Surfactant/oil/water phase behavior window and oil, water, and surfactant concentrations in microemulsion phase (***l=3***) after 50 days for Case-6.

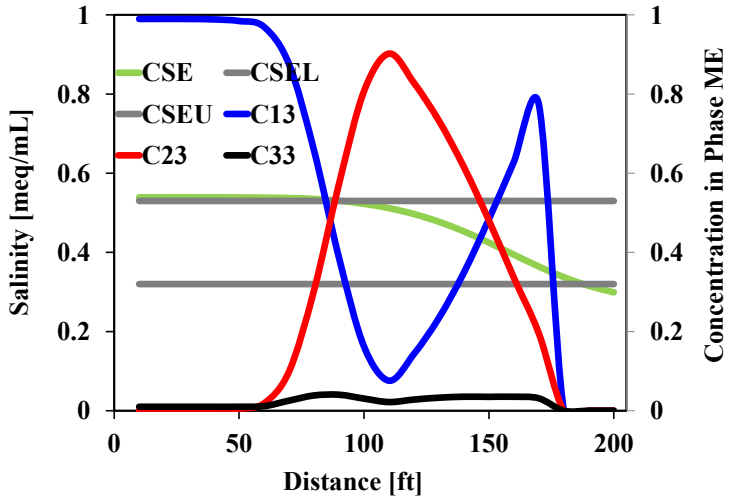

Figure 6-83- Surfactant/oil/water phase behavior window and oil, water, and surfactant concentrations in microemulsion phase (***l=3***) after 75 days for Case-6.

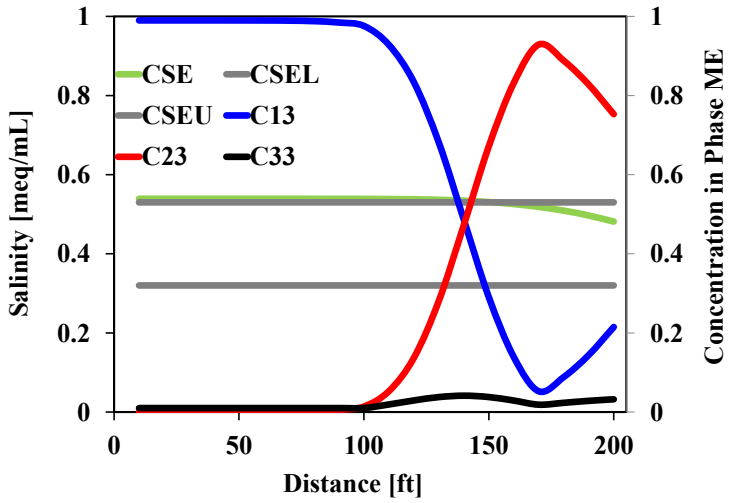

Figure 6-84- Surfactant/oil/water phase behavior window and oil, water, and surfactant concentrations in microemulsion phase (***l=3***) after 100 days for Case-6.

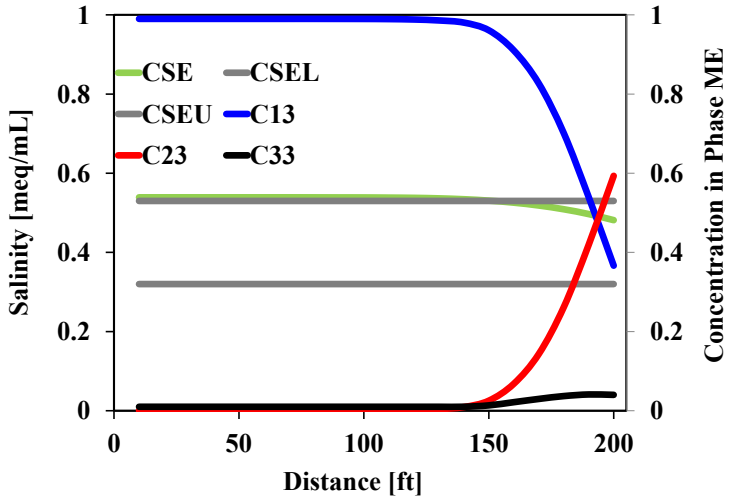

Figure 6-85- Surfactant phase behavior window and oil, water, and surfactant concentrations in microemulsion phase (***l=3***) after 125 days for Case-6.

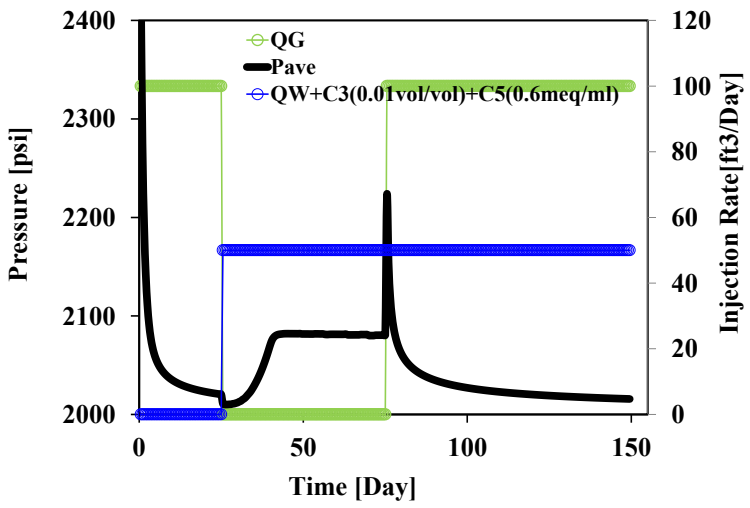

Figure 6-86-Average pressure in the presence of gas and water injection rates in the different time for Case-6.

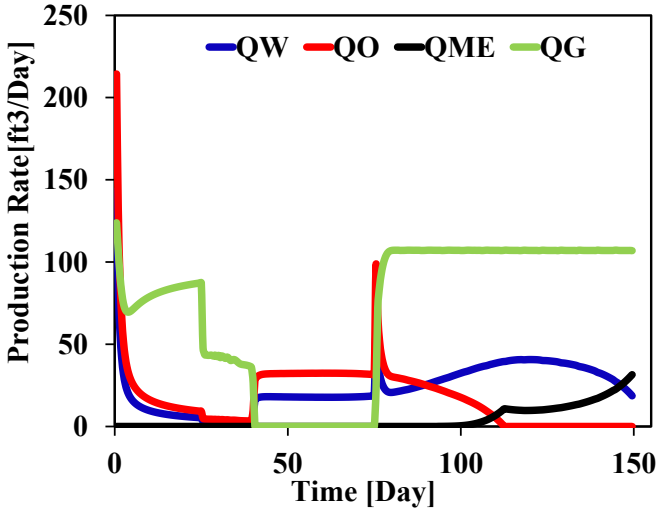

Figure 6-87-Water, oil, microemulsion, and gas production rates in Case-6.

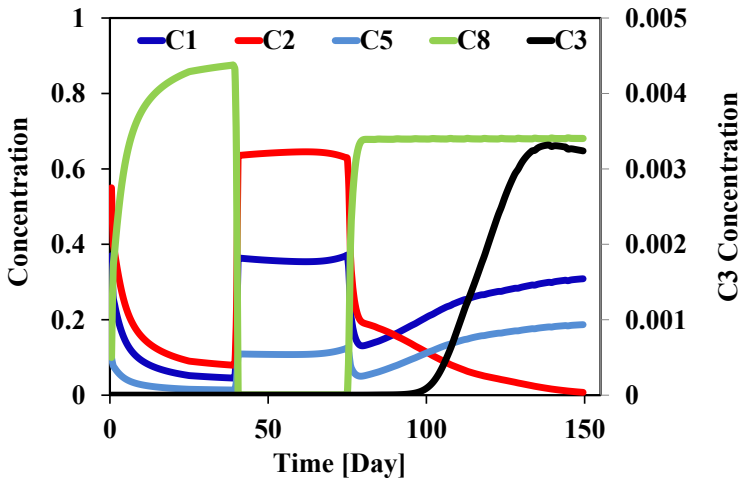

Figure 6-88-Water, oil, anion, gas, and surfactant concentrations in production well ($\mathbf{c_{w1}, c_{w2}, c_{w5}, c_{w8}, and\, c_{w3}}$) for Case-6.

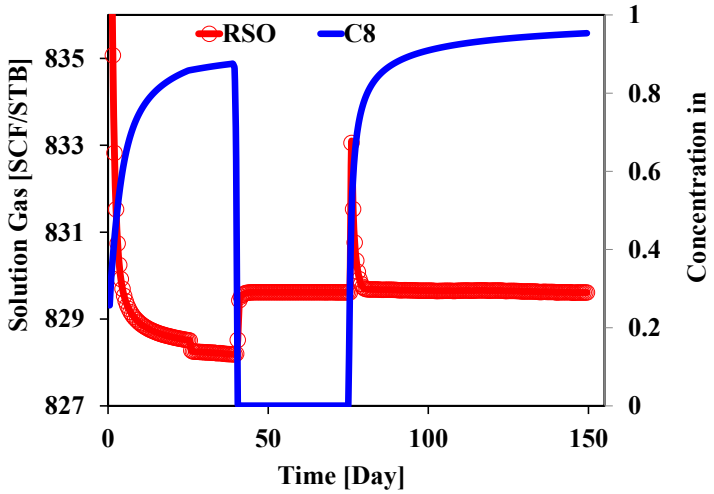

Figure 6-89- Gas concentration and solution gas in production well ($\mathbf{c_{w8}}$, $\mathbf{R_{wso}}$) for Case-6.

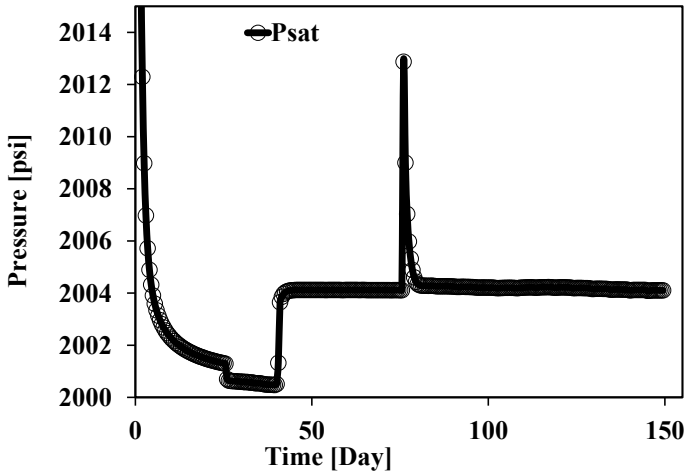

Figure 6-90-Bubble point pressure in the production well for case-6.

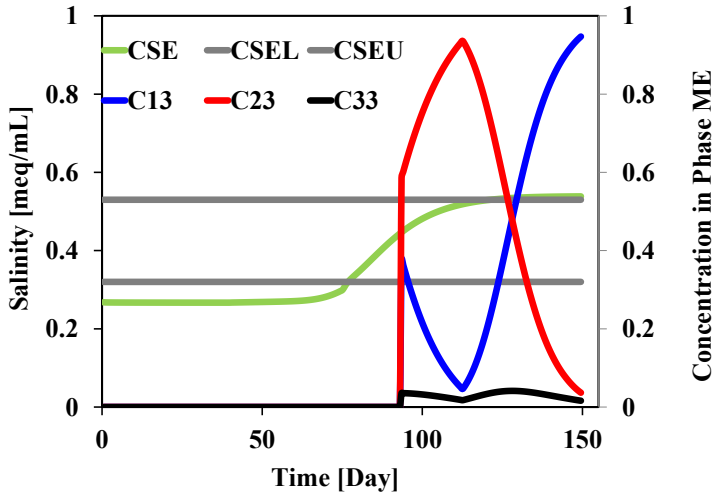

Figure 6-91-Surfactant/oil/water phase behavior and concentration of surfactant, water, and oil in microemulsion (l=3) for production well in Case-6.

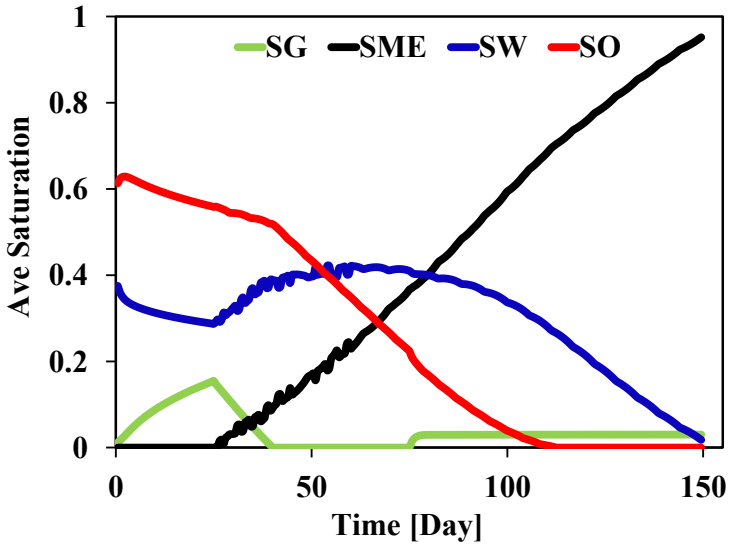

Figure 6-92-Average saturation of gas, microemulsion, water, and oil phases in Case-6.

Chapter 7: Thermal Model

The Development of thermal simulators started in the early 1970's. Thermal computational modeling is challenging due to many complex features including high degree of non-linearity. Better physical understanding of the mechanisms involved in thermal simulation and the advancement of implicit computational technique helped thermal simulators to gain maturity. These improvements and successful applications have given the petroleum research area the confidence to develop reliable simulators. In this section, a comprehensive literature review discusses previous and recent numerical thermal simulators and distinguishes the difference of this work from other works.

The first three-phase, two-dimensional Cartesian model for steam injection was presented by Shutler in 1970s. He proposed a numerical three-phase black oil model to solve pressure and saturations implicitly using Newtonian-Raphson iteration method. The energy balance equation was solved separately by direct method. Interphase mass transfer between water and gas phases was considered, but the oil phase was assumed to be nonvolatile, and the hydrocarbon gas was insoluble in the liquid phases.

An implicit-pressure, explicit-saturation (IMPES) method was used by Abdalla and Coats (1971) to simulate steam drive. They developed a two-dimensional, three-phase (oil/water/steam) model. They neglected the hydrocarbon gas phase. Temperature was calculated from saturated steam pressure. This model was extended to three dimensions by Coats *et al*., (1974). The mass and energy balance equations were solved simultaneously. Water and steam equations were combined to avoid iteration on the mass transfer condensation term. No distillation of the oil was assumed. A new stabilized IMPES method was described by Vinsome (1974). He simulated steam drive and steam

soak process by means of a three-phase (oil/water/steam) model. This model neglected the steam distillation.

Weinstein *et al*., (1974) developed a model that describes three-phase (oil/water/gas) flow in one dimension and considers for inter-phase mass transfer.

Coats (1976) introduced the first algorithm to account for distillation and compositional modeling, which was an extension of Coats et al., (1974). Ferrer and Farouq Ali (1977) presented a two-dimensional compositional model to simulate steam injection. Their model was similar to the Coats (1976) model, but the difference was in the computation of the heat of vaporization. Coats (1978) developed a three-dimensional, highly implicit formulation for the steam flooding process.

Crookston *et al*., (1979) described a linearized implicit combustion model. The model was three dimensional but could not fully handle the well-bore reservoir coupling implicitly. Abou-Kassem (1981) presented a two-dimensional, fully-implicit compositional model for steam flooding. He used the sequential implicit method to solve the governing system of equations.

Ishimoto *et al*., (1987) proposed the first thermal simulator using equation of state (EOS) in a one dimensional fully implicit compositional steam flood model. Rubin and Buchanan (1985) described a general purpose, fully implicit, four-phase, multi-component, multidimensional steam and combustion simulator. They also proposed a fully implicit well model using an iterative method for solving large thermal problems. Chein *et al*., (1989) presented a general purpose thermal compositional simulator using both K-values and the equation of state to calculate the fluid properties in equilibrium condition.

Brantferger (1991) developed a simulator, which had major differences compared to previous formulations. He used an equation of state to calculate thermodynamic

properties of each phase. In this model, he considered water as a non-ideal component and used enthalpy as a primary variable. Mifflin *et al*., (1991) introduced a fully coupled, fully implicit reservoir simulator. Their formulation was implemented in a framework that already supports an IMPES and a sequential semi-implicit formulation.

Chan and Sarioglu (1992) presented a procedure for incorporating fracture models in a thermal reservoir simulator.

An implicit-pressure, explicit-concentration (IMPES) method was described to model for application of surfactant flooding purposes by Delshad *et al*. (1995). Energy balance equation was solved explicitly for temperature.

Cicek and Eretkin (1996) developed and tested a 3-D field scale steam injection simulator. The three-dimensional multi-phase mass and energy flow equations are based on compositional balances. A fully implicit numerical solution method is implemented in the solution of the nonlinear system of equations. Cicek (2005) extended the numerical simulator for steam displacement to model the naturally fractured reservoirs using fully implicit compositional formulation. He investigated the effects of capillary and gravitational forces in the matrix/fracture exchange term.

Naccache (1997) presented a 3D thermal reservoir simulator that models the injection of steam into heavy oil. Pressure, component molar densities, and bulk internal energy density were chosen as primary variables to be solved from volume-balance, component, and energy-conservation equations.

Godderij *et al.*, (1999) introduced a 3D steam drive simulator. They used an interface model, where the single phase steam zone was separated from the two phase liquid region by a steam condensation front. Nilsson *et al*., (2005) developed and implemented an adaptive reservoir simulator to model black-oil steam injection.

This work describes a multicomponent multiphase simulator to simulate the steam injection processes in the presence of foam and surfactant flooding.

7.1 GOVERNING ENERGY AND STEAM EQUATIONS

The conservation of energy in porous media is derived from the first law of thermodynamics. This equation can be simplified by neglecting energy flux due to radiation and reactions and excluding kinetic and potential energies. Therefore a statement of the energy balance or the first law of thermodynamics is suitable for this purpose. We have used this statement as the follow

$$\left\{\begin{matrix}\textit{Accumulation rate}\\ \textit{of energy in V}\end{matrix}\right\}=\left\{\begin{matrix}\textit{Net rate of energy}\\ \textit{transported of}\\ \textit{energy into V}\end{matrix}\right\}+\left\{\begin{matrix}\textit{Energy production}\\ \textit{rate of energy in V}\end{matrix}\right\}$$

where V is an arbitrary volume. This can be written as

$$\int_V \frac{\partial}{\partial t}\left(\rho U+\frac{1}{2}\sum_{\ell=1}^{np}\rho_\ell\,|\vec{u}_\ell|^2-\rho g D_z\right)dV+\int_V \nabla.\vec{E}dV-\dot{W}=0 \qquad (7\text{-}1)$$

where U is an overall internal energy (total energy/total mass), and ρ is the overall density and the term $\frac{1}{2}\sum_{\ell=1}^{np}\rho_\ell\,|\vec{u}_\ell|^2$ represents total kinetic energy per unit bulk volume and $\rho g D_z$ is total potential energy per unit bulk volume with reference to the depth below some horizontal plane; where $\vec{E}$ represents energy flux and $\dot{W}$ is work done and external heating source term in the system. The form of the first law of thermodynamics for open systems expressed in the above equation requires the $\dot{W}$ term to be composed of work components only, in the absence of external heating sources.

External heating sources can often be handled through boundary conditions. We consider only the rate of work done against a pressure field, although other types of work could be included. In this derivation, there is no compression or expansion work done on volume V since it is assumed to be constant.

$$\dot{W} = -\int_V \sum_{\ell=1}^{n_p} \nabla.\left(p_\ell \vec{u}_\ell\right) dV \tag{7-2}$$

This term is the work done by the force exerted by the pressure in phase ℓ . The energy flux term is made up of convective contributions from the flowing phases (internal, kinetic, and potential energy), conduction, and radiation as expressed as

$$\vec{E} = \sum_{l=1}^{n_p} \rho_\ell \vec{u}_\ell \left[U_\ell + \frac{1}{2} |\vec{v}_\ell|^2 + - g D_z \right] - \lambda_{eff} \nabla T + \vec{q}_r \tag{7-3}$$

For brevity, we neglect radiation in the following discussion, although this transport mechanism can be important in estimating heat losses from wells and in certain EOR processes and remediation that involve electromagnetic sources

$$\frac{\partial}{\partial t}\left(\rho U + \frac{1}{2} \sum_{\ell=1}^{n_p} \rho_\ell |\vec{u}_\ell|^2 - \rho g D_z \right) + \nabla.\left(\sum_{\ell=1}^{n_p} \rho_\ell \vec{u}_\ell \left(U_\ell + \frac{1}{2} |\vec{v}_\ell|^2 + - g D_z \right) \right)$$
$$-\nabla.\left(\lambda_{eff} \nabla T\right) + \sum_{\ell=1}^{n_p} \nabla.\left(p_\ell \vec{u}_\ell\right) = q \tag{7-4}$$

The first sum in the energy flux and that in the pressure-volume work expression may be combined to give

$$\frac{\partial}{\partial t}\left(\rho U+\frac{1}{2}\sum_{\ell=1}^{n_p}\rho_\ell|\vec{u}_\ell|^2-\rho g D_z\right)+\nabla.\left(\sum_{\ell=1}^{n_p}\rho_\ell\vec{u}_\ell\left(H_\ell+\frac{1}{2}|\vec{v}_\ell|^2+-gD_z\right)\right) \qquad (7\text{-}5)$$
$$-\nabla.\left(\lambda_{eff}\nabla T\right)=q$$

where $H_\ell=U_\ell+p_\ell/\rho_\ell$ is defined as the enthalpy of phase ℓ per unit mass of ℓ. Neglecting the kinetic and potential energy in accumulation and transport of net rate of energy, then above expression can be written as

$$\frac{\partial}{\partial t}(\rho U)+\vec{\nabla}.\left(\sum_{\ell=1}^{n_p}\rho_\ell\vec{u}_\ell H_\ell\right)-\vec{\nabla}.\left(\lambda_{eff}\nabla T\right)=0 \qquad (7\text{-}6)$$

where $\rho U=(1-\phi)\rho_r U_r+\phi\sum_{\ell=1}^{n_p}\rho_\ell S_\ell U_\ell$ and by plugging this equation into the energy balance equation can be written as

$$\frac{\partial}{\partial t}\left((1-\phi)\rho_r U_r+\phi\sum_{\ell=1}^{n_p}\rho_\ell S_\ell U_\ell\right)+\vec{\nabla}.\left(\sum_{\ell=1}^{n_p}\rho_\ell\vec{u}_\ell H_\ell\right)-\vec{\nabla}.\left(\lambda_{eff}\nabla T\right)=q \qquad (7\text{-}7)$$

Since $H_r=U_r$ and $H_\ell=U_\ell+\frac{p_\ell}{\rho_\ell}$, the above expression can be written as

$$(1-\phi)\rho_r\frac{\partial H_r}{\partial t}+\phi\sum_{\ell=1}^{n_p}\frac{\partial}{\partial t}\left(\rho_\ell S_\ell H_\ell-S_\ell p_\ell\right)+\vec{\nabla}.\left(\sum_{l=1}^{n_p}\rho_\ell\vec{u}_\ell H_\ell\right)-\vec{\nabla}.\left(\lambda_{eff}\nabla T\right)=q \qquad (7\text{-}8)$$

If we assume the pressure work is negligible, $-\phi\sum_{\ell=1}^{n_p}\frac{\partial}{\partial t}\left(S_\ell p_\ell\right)=0$ and the above equation can be written as

$$(1-\phi)\rho_r\frac{\partial H_r}{\partial t}+\phi\sum_{\ell=1}^{n_p}\rho_\ell S_\ell\frac{\partial H_\ell}{\partial t}+\phi\sum_{\ell=1}^{n_p}H_\ell\frac{\partial}{\partial t}\left(\rho_\ell S_\ell\right)+ \qquad (7\text{-}9)$$
$$\sum_{l=1}^{n_p}H_\ell\vec{\nabla}.\left(\rho_\ell\vec{u}_\ell\right)+\sum_{\ell=1}^{n_p}\rho_\ell\vec{u}_\ell.\vec{\nabla}H_\ell-\vec{\nabla}.\left(\lambda_{eff}\nabla T\right)=q$$

If we assume only mass transfer can occur between water and steam, the mass equations for all phases can be written as

$$\frac{\partial}{\partial t}\left(\phi\rho_\ell S_\ell\right)+\vec{\nabla}.\left(\rho_\ell\vec{u}_\ell\right)=0 \quad \ell \neq \textit{water and steam} \tag{7-10}$$

$$\frac{\partial}{\partial t}\left(\phi\rho_w S_w+\phi\rho_s S_s\right)+\vec{\nabla}.\left(\rho_w\vec{u}_w+\rho_s\vec{u}_s\right)=0 \tag{7-11}$$

or

$$\frac{\partial}{\partial t}\left(\phi\rho_w S_w\right)+\vec{\nabla}.\left(\rho_w\vec{u}_w\right)=-\frac{\partial}{\partial t}\left(\phi\rho_s S_s\right)-\vec{\nabla}.\left(\rho_s\vec{u}_s\right)$$

Thereby, energy fluxes in the reservoir occur by conduction and convection; thus the energy equation with considering all possible source terms can be written as

$$\frac{\partial}{\partial t}\left[\left(1-\phi\right)\rho_r U_r+\phi\sum_{\ell=1}^{n_p}\rho_\ell S_\ell U_\ell\right]+\vec{\nabla}\cdot\left(\sum_{\ell=1}^{n_p}\rho_\ell H_\ell\vec{u}_\ell\right)-\vec{\nabla}.\left(\lambda_{eff}\vec{\nabla}T\right) \tag{7-12}$$
$$=\mp q_H \pm q_L + q_{ele} \mp q_{instu}$$

where U_r and U_ℓ are internal energy of rock and fluid phase l per unit mass, respectively, H_ℓ is enthalpy of phase per unit mass, u_ℓ is Darcy's velocity of fluid phase ℓ , ρ_r and ρ_ℓ are rock and mass density of phase ℓ , respectively. ϕ is porosity and S_ℓ is saturation of fluid phase ℓ . In Equation (1), n_p is the number of existing phases and λ_{eff} is an effective thermal conductivity. q_H is the enthalpy rate of source or sink term per bulk volume. A positive sign is assigned to q_H for a hot injection well and a negative sign is considered for a production well. q_L is the heat loss to overburden and underburden rocks. In the case of cold fluid injection where reservoir becomes colder than initial reservoir temperature, a positive sign is assigned to q_L . But in the case of hot

fluid injection which increases reservoir temperature compared to initial temperature, a negative sign for q_L is considered. q_{ele} is the electrical Joule heating as source term, which is always positive. q_{instu} is in-situ thermal generator source that can be placed in the bottomhole of a well. A positive sign in front of q_{instu} is assigned for a heat source and a negative sign for a cold source. The following assumptions are made for simplification (Lake 1989):

- Neglect pressure-volume work ($H = U$) for all fluid phases.
- Neglect the dependency of enthalpies on pressure.
- Heat capacity is considered independent of temperature.
- Consider an effective thermal conductivity of all saturated fluids and rock as arithmetic weighted average as expressed in Equation (3).
- Heat-loss to overburden and underburden, q_L , is computed using Vinsome and Westerveld(1980) analytical method.

We assume that the mass transfer between water and steam phases occurs at the boiling point (saturated condition). The following equation must conserve energy during condensation and vaporization as

$$(1-\phi)\rho_r \frac{\partial H_r}{\partial t} + \phi \sum_{\ell=1}^{n_p} \rho_\ell S_\ell \frac{\partial H_\ell}{\partial t} + (\bar{H}_s - \bar{H}_w) \frac{\partial (\rho_s S_s)}{\partial t} + \left(\sum_{\ell=1}^{n_p} \rho_\ell u_\ell \vec{\nabla} H_\ell \right) + (\bar{H}_s - \bar{H}_w) \vec{\nabla} . (\rho_s \vec{u}_s) - \vec{\nabla} . \left(\lambda_{eff} \vec{\nabla} T \right) = \mp q_H \pm q_L + q_{ele} \mp q_{instu} \quad (7\text{-}13)$$

where $\bar{H}_s$ and $\bar{H}_w$ are steam and water enthalpy per unit mass; $\rho_s, \vec{u}_s$ and, S_s are density of steam phase, Darcy velocity of steam phase, and saturation of steam phase, respectively .Effective thermal conductivity is defined as

$$\lambda_{eff} = (1-\phi)\lambda_r + \phi\sum_{\ell=1}^{n_p} s_\ell \lambda_\ell \tag{7-14}$$

where λ_r is thermal conductivity of rock and λ_ℓ is thermal conductivity of phase ℓ. In addition, it is more convenient to substitute enthalpy with temperature functions based on the above assumptions. Using enthalpy definition of rock and fluid phases corresponding to reference temperature and enthalpy, (enthalpy reference of a reservoir is considered the initial temperature of reservoir in this work) it can be written as

$$\Delta H = \zeta_p \left(T - T_{ini}\right) \tag{7-15}$$

where ζ_p could be heat capacity of rock or fluid phases. Finally, the following energy equation, which is used to implement in UTCHEM to solve for temperature, becomes:

$$\left((1-\phi)\rho_r\zeta_{pr} + \phi\sum_{\ell=1}^{n_p}\rho_\ell S_\ell \zeta_{p\ell}\right)\frac{\partial T}{\partial t} + \left(\sum_{\ell=1}^{n_p}\rho_\ell \vec{u}_\ell \zeta_{p\ell}\vec{\nabla}T - \vec{\nabla}.\left(\lambda_{eff}\vec{\nabla}T\right)\right) + (\bar{H}_s - \bar{H}_w)\left(\frac{\partial(\rho_s S_s)}{\partial t} + \vec{\nabla}.(\rho_s \vec{u}_s)\right) = \mp q_H \pm q_L + q_{ele} \mp q_{instu} \tag{7-16}$$

This equation consists of accumulation, convection, and conduction terms, respectively. The difference between steam and water enthalpy per unit mass $\left(\bar{H}_s - \bar{H}_w\right)$ is called latent heat of water vaporization. This term is a multiplier for mass equation of

gas phase in Equation (7-16). This equation can conserve energy in the presence of vaporization and condensation of water during mass transfer between water and steam. In order to solve this equation numerically, we consider only the latent heat term explicitly and other terms are solved implicitly (Delshad *et al.,* 1996; Lashgari *et al.,* 2014a). Since the UTCHEM simulator is an implicit in pressure and explicit in concentrations (IMPEC) simulator, at first pressure is solved at the new time level; then, the mass balance equations are solved. Water and steam properties are updated based on pressure at the new time level (n+1), concentrations, and temperature at the old time level (n), as demonstrated by the flowchart in Figure 8-2.

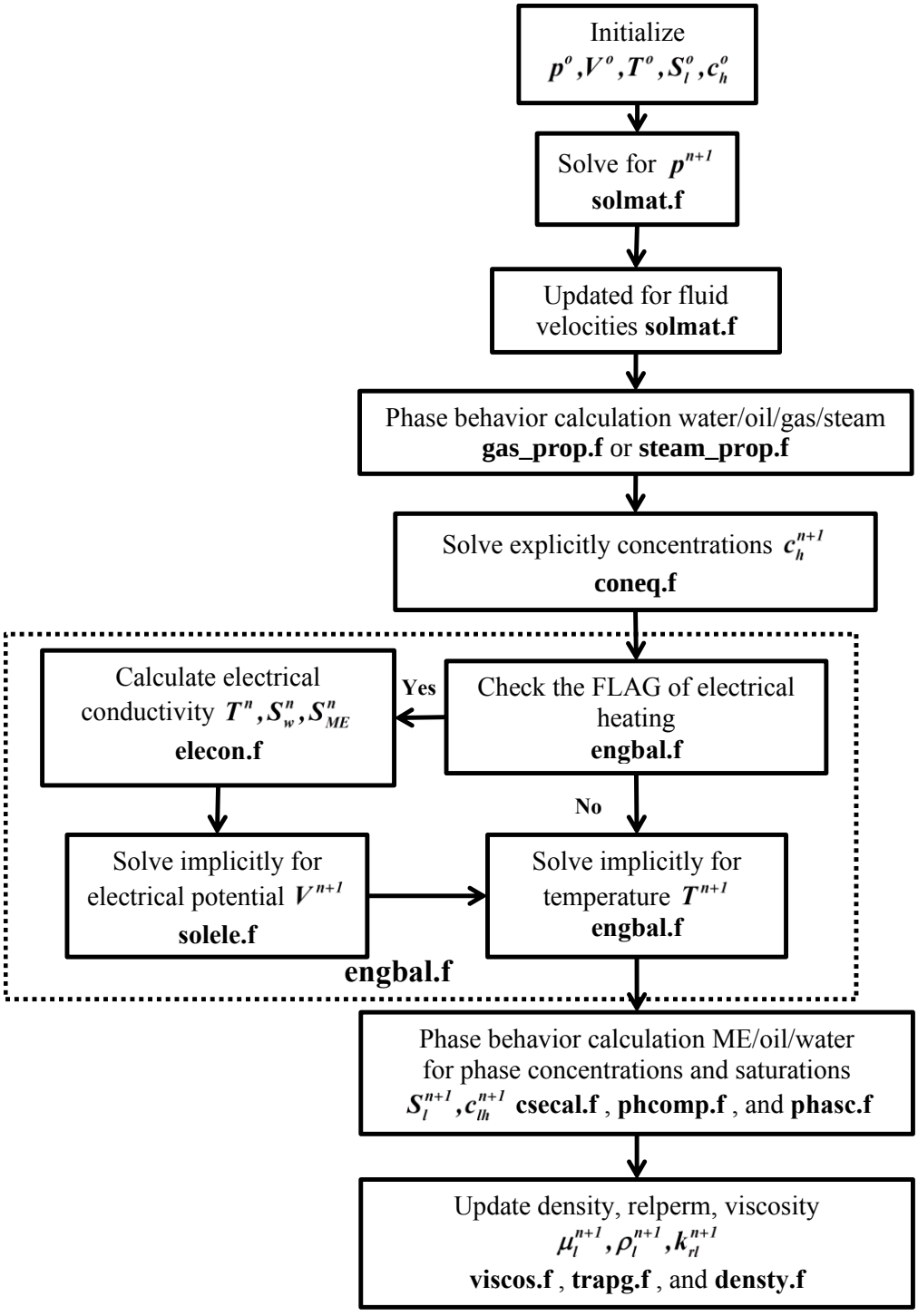

Figure 7-1-Solution-procedure flow chart for thermal model in the UTCHEM simulator.

In order to calculate phase behavior of steam and water, total enthalpy in equilibrium is obtained from energy balance equation and then steam quality is defined and written as

$$\alpha = \frac{H_{tot} - \bar{H}_w}{\bar{H}_s - \bar{H}_w} \tag{7-17}$$

These specific enthalpies, $\bar{H}_w$ and $\bar{H}_s$ of water and steam per unit mass that are calculated directly in phase behavior calculation from steam table as well as phase densities ρ_w and ρ_s , which are function of pressure and temperature, are calculated from steam table in the steam/water phase behavior calculation. c_w and c_s are the volumetric concentrations of water and steam components, respectively. H_{tot} is total enthalpy of water and steam calculated as

$$H_{tot} = \frac{\rho_s c_s \zeta_{ps}(T - T_{ini}) + \rho_w c_w \zeta_{pw}(T - T_{ini})}{\rho_s c_s + \rho_w c_w} \tag{7-18}$$

where ζ_{pw} and ζ_{ps} are heat capacity of water and steam phases, and ρ_s and ρ_w are mass density of water and steam, respectively. Based on a simple definition of mass transfer between water and steam, mass quality of steam can be also defined as

$$\alpha = \frac{(\rho_s c_s)}{(\rho_s c_s + \rho_w c_w)} \tag{7-19}$$

Equations (7-17) and (7-19) express the same content but a difference in calculation. One is obtained from the energy balance equation and the second is

computed from the mass balance equation. Therefore, mass quality can be calculated first; then, since mass must be conserved in Equation (7-17), volume concentration of gas can be solved; then, use the mass balance equation to solve for water (Lashgari *et al.,* 2014b).

7.2 NUMERICAL FORMULATION

The energy balance equation formulation is a nonlinear partial differential equation as derived and discussed earlier in Section 1.1. We consider solving it in this section numerically. The finite-difference form of the energy balance equation is obtained by a first-order approximation to the time derivative term and by a second-order, centered approximation to the spatial derivatives of the heat fluxes. Then an implicit scheme is applied and the energy balance equation is linearized for calculation of temperature using direct method to solve for linear system of equations. Therefore, the discretized form of Equation (7-16) in Cartesian coordinate system is

$$\frac{M_{ijk}^{n+1}-M_{ijk}^{n}}{\Delta t}+\left(\frac{J_{i+1/2\,jk}^{n+1}-J_{i-1/2\,jk}^{n+1}}{\Delta x_{ijk}}+\frac{J_{ij+1/2k}^{n+1}-J_{ij-1/2k}^{n+1}}{\Delta y_{ijk}}+\frac{J_{ijk+1/2}^{n+1}-J_{ijk-1/2}^{n+1}}{\Delta z_{ijk}}\right)+$$
$$\left(\bar{H}_{s,ijk}^{n}-\bar{H}_{w,ijk}^{n}\right)\left(\frac{(\rho_s S_s)_{ijk}^{n+1}-(\rho_s S_s)_{ijk}^{n}}{\Delta t}+\frac{(\rho_s u_s)_{i+1/2\,jk}^{n+1}-(\rho_s u_s)_{i-1/2\,jk}^{n+1}}{\Delta x_{ijk}}+\right.$$
$$\left.\frac{(\rho_s u_s)_{ij+1/2k}^{n+1}-(\rho_s u_s)_{ij-1/2k}^{n+1}}{\Delta y_{ijk}}+\frac{(\rho_s u_s)_{ijk+1/2}^{n+1}-(\rho_s u_s)_{ijk-1/2}^{n+1}}{\Delta z_{ijk}}\right)= \tag{7-20}$$
$$\mp\frac{q_{H,ijk}^{n+1}}{V_{b,ijk}}\pm\frac{q_{L,ijk}^{n+1}}{V_{b,ijk}}+\frac{q_{ele,ijk}^{n+1}}{V_{b,ijk}}\mp\frac{q_{instu,ijk}^{n+1}}{V_{b,ijk}}$$

where $n+1$ and n count new time level and present time level, respectively. S_s, ρ_s and u_s are steam density and Darcy velocity of steam phase, respectively. $\bar{H}_s$ and

$\bar{H}_w$ are specific steam and water enthalpies per unit mass that are read at each time level from steam table. $V_{b,ijk}$ is the bulk volume of a grid block (ijk). q_H is the enthalpy rate of source or sink term per bulk volume. A positive sign is assigned to q_H for a hot injection well and negative sign is considered for a production well. q_L is the heat loss to overburden and underburden rocks. In the case of cold fluid injection where the reservoir becomes colder than initial reservoir temperature, a positive sign is assigned to q_L . But in the case of hot fluid injection that increase the reservoir temperature compared to initial temperature, a negative sign for q_L is considered. q_{ele} is the electrical Joule heating as source term, which is always positive. q_{instu} is an in-situ thermal generator source that can be placed at the bottomhole of a well. A positive sign in front of q_{instu} is assigned for a heat source and negative for a cold source discussed in well M is defined as

$$M = \left((1-\phi)\rho_r \zeta_{pr} + \phi \sum_{\ell=1}^{n_p} \rho_\ell S_\ell \zeta_{p\ell} \right) T \tag{7-21}$$

where ρ_r and ρ_ℓ are rock and mass density of phase ℓ , respectively. ϕ is porosity and S_ℓ is saturation of fluid phase ℓ . n_p is the number of existing phases. J is heat flux defined as

$$J = J_{conv} + J_{cond} = \sum_{\ell=1}^{n_p} \rho_\ell \vec{u}_\ell \zeta_{p\ell} . \vec{\nabla} T - \vec{\nabla} . \left(\lambda_{eff} \vec{\nabla} T \right) \tag{7-22}$$

The boundary conditions are of no flow and no thermal conduction across the boundaries in x and y directions as

$$\begin{aligned} J_{x,\frac{1}{2}jk} &= J_{x,N_x+\frac{1}{2}jk} = 0 \\ J_{y,i\frac{1}{2}k} &= J_{y,jN_y+\frac{1}{2}k} = 0 \end{aligned} \tag{7-23}$$

In z direction, there is heat flux across boundaries into overburden and underburned layers as expressed by

$$J_{z,ij\frac{1}{2}} = \lambda_{OB} \left.\frac{\partial T}{\partial t}\right|_{z=0}$$
$$J_{z,ijN_z+\frac{1}{2}} = \lambda_{UB} \left.\frac{\partial T}{\partial t}\right|_{z=h} \qquad (7\text{-}24)$$

In order to calculate this heat flux that is defined as heat loss, we use Vinsome and Westerveld's model that will be discussed later in this Chapter.

7.2.1 Accumulation Term

As mentioned earlier, a first-order finite difference approximation for the accumulation term is considered. This term is linearized by evaluating all fluid properties at the previous time level as

$$\frac{M_{ijk}^{n+1} - M_{ijk}^{n}}{\Delta t} = \left(\left(1-\phi_{ijk}^{n}\right) \rho_{r,ijk}^{n} \zeta_{pr,ijk}^{n} + \phi_{ijk}^{n} \sum_{\ell=1}^{n_p} \rho_{\ell,ijk}^{n} S_{\ell,ijk}^{n} \zeta_{p\ell,ijk}^{n} \right) \frac{T_{ijk}^{n+1} - T_{ijk}^{n}}{\Delta t} \qquad (7\text{-}25)$$

7.2.2 Convection Term

Convection term of heat flux in x direction at the boundaries ($i+1/2jk$) and ($i-1/2jk$) is calculated

$$J_{conv,i+1/2\,jk}^{n+1} = \sum_{\ell=1}^{n_p} \zeta_{p\ell,i+1/2\,jk} \rho_{\ell,i+1/2\,jk}^{n} T_{i+1/2\,jk}^{n+1} u_{\ell x,i+1/2\,jk}^{n+1}$$
$$J_{conv,i-1/2\,jk}^{n+1} = \sum_{\ell=1}^{n_p} \zeta_{p\ell,i-1/2\,jk} \rho_{\ell,i-1/2\,jk}^{n} T_{i-1/2\,jk}^{n+1} u_{\ell x,i-1/2\,jk}^{n+1} \qquad (7\text{-}26)$$

These equations are evaluated at boundaries by using a single point upstream weighting method that is discussed in Chapter 3 and 4. Darcy velocity defines upstream weight of heat content at these boundaries as

$$\begin{cases} \zeta_{p\ell,i+1/2\,jk}\rho^{n}_{\ell,i+1/2\,jk}T^{n+1}_{i+1/2\,jk}u^{n+1}_{\ell x,i+1/2\,jk} = \zeta_{p\ell,ijk}\rho^{n}_{\ell,ijk}T^{n+1}_{ijk}u^{n+1}_{\ell x,ijk} & \text{if } u^{n+1}_{\ell x,i+1\,jk} < u^{n+1}_{\ell x,ijk} \\ \zeta_{p\ell,i+1/2\,jk}\rho^{n}_{\ell,i+1/2\,jk}T^{n+1}_{i+1/2\,jk}u^{n+1}_{\ell x,i+1/2\,jk} = \zeta_{p\ell,i+1\,jk}\rho^{n}_{\ell,i+1\,jk}T^{n+1}_{i+1\,jk}u^{n+1}_{\ell x,i+1\,jk} & \text{if } u^{n+1}_{\ell x,i+1\,jk} > u^{n+1}_{\ell x,ijk} \\ \zeta_{p\ell,i-1/2\,jk}\rho^{n}_{\ell,i-1/2\,jk}T^{n+1}_{i-1/2\,jk}u^{n+1}_{\ell x,i-1/2\,jk} = \zeta_{p\ell,ijk}\rho^{n}_{\ell,ijk}T^{n+1}_{ijk}u^{n+1}_{\ell x,ijk} & \text{if } u^{n+1}_{\ell x,i-1\,jk} < u^{n+1}_{\ell x,ijk} \\ \zeta_{p\ell,i-1/2\,jk}\rho^{n}_{\ell,i-1/2\,jk}T^{n+1}_{i-1/2\,jk}u^{n+1}_{\ell x,i-1/2\,jk} = \zeta_{p\ell,i-1\,jk}\rho^{n}_{\ell,i-1\,jk}T^{n+1}_{i-1\,jk}u_{\ell x,i-1\,jk} & \text{if } u^{n+1}_{\ell x,i-1\,jk} > u^{n+1}_{\ell x,ijk} \end{cases} \quad (7\text{-}27)$$

Convection term in y direction at the boundaries ($ij+1/2k$) and ($ij-1/2k$) are discretized

$$\begin{aligned} J^{n+1}_{conv,ij+1/2k} &= \sum_{\ell=1}^{n_p}\zeta_{p\ell,ij+1/2k}\rho^{n}_{\ell,ij+1/2k}T^{n+1}_{ij+1/2k}u^{n+1}_{\ell y,ij+1/2k} \\ J^{n+1}_{conv,ij-1/2k} &= \sum_{\ell=1}^{n_p}\zeta_{p\ell,ij-1/2k}\rho^{n}_{\ell,ij-1/2k}T^{n+1}_{ij-1/2k}u^{n+1}_{\ell y,ij-1/2k} \end{aligned} \quad (7\text{-}28)$$

Darcy velocity defines upstream weight of heat content in y direction at corresponding boundaries as

$$\begin{cases} \zeta_{p\ell,ij+1/2k}\rho^{n}_{\ell,ij+1/2k}T^{n+1}_{ij+1/2k}u^{n+1}_{\ell y,ij+1/2k} = \zeta_{p\ell,ijk}\rho^{n}_{\ell,ijk}T^{n+1}_{ijk}u^{n+1}_{\ell y,ijk} & \text{if } u^{n+1}_{\ell y,ij+1k} < u^{n+1}_{\ell y,ijk} \\ \zeta_{p\ell,ij+1/2k}\rho^{n}_{\ell,ij+1/2k}T^{n+1}_{ij+1/2k}u^{n+1}_{\ell y,ij+1/2k} = \zeta_{p\ell,ij+1k}\rho^{n}_{\ell,ij+1k}T^{n+1}_{ij+1k}u^{n+1}_{\ell y,ij+1k} & \text{if } u^{n+1}_{\ell y,ij+1k} > u^{n+1}_{\ell y,ijk} \\ \zeta_{p\ell,ij-1/2k}\rho^{n}_{\ell,ij-1/2k}T^{n+1}_{ij-1/2k}u^{n+1}_{\ell y,ij-1/2k} = \zeta_{p\ell,ijk}\rho^{n}_{\ell,ijk}T^{n+1}_{ijk}u^{n+1}_{\ell y,ijk} & \text{if } u^{n+1}_{\ell y,ij-1k} < u^{n+1}_{\ell y,ijk} \\ \zeta_{p\ell,ij-1/2k}\rho^{n}_{\ell,ij-1/2k}T^{n+1}_{ij-1/2k}u^{n+1}_{\ell y,ij-1/2k} = \zeta_{p\ell,ij-1k}\rho^{n}_{\ell,ij-1k}T^{n+1}_{ij-1k}u^{n+1}_{\ell y,ij-1k} & \text{if } u^{n+1}_{\ell y,ij-1k} > u^{n+1}_{\ell y,ijk} \end{cases} \quad (7\text{-}29)$$

Convection term in y direction at the boundaries ($ijk+1/2$) and ($ijk-1/2$) are discretized

$$\begin{aligned} J^{n+1}_{conv,ijk+1/2} &= \sum_{\ell=1}^{n_p}\zeta_{p\ell,ijk+1/2}\rho^{n}_{\ell,ijk+1/2}T^{n+1}_{ijk+1/2}u_{\ell y,ijk+1/2} \\ J^{n+1}_{conv,ijk-1/2} &= \sum_{\ell=1}^{n_p}\zeta_{p\ell,ijk-1/2}\rho^{n}_{\ell,ijk-1/2}T^{n+1}_{ijk-1/2}u_{\ell y,ijk-1/2} \end{aligned} \quad (7\text{-}30)$$

Darcy velocity defines upstream weight of heat content in y direction at corresponding boundaries as

$$\begin{cases} \zeta_{p\ell,ijk+1/2}\rho^{n}_{\ell,ijk+1/2}T^{n+1}_{ijk+1/2}u^{n+1}_{\ell z,ijk+1/2} = \zeta_{p\ell,ijk}\rho^{n}_{\ell,ijk}T^{n+1}_{ijk}u^{n+1}_{\ell z,ijk} & \text{if } u^{n+1}_{\ell z,ijk+1} < u^{n+1}_{\ell z,ijk} \\ \zeta_{p\ell,ijk+1/2}\rho^{n}_{\ell,ijk+1/2}T^{n+1}_{ijk+1/2}u^{n+1}_{\ell z,ijk+1/2} = \zeta_{p\ell,ijk+1}\rho^{n}_{\ell,ijk+1}T^{n+1}_{ijk+1}u^{n+1}_{\ell z,ijk+1} & \text{if } u^{n+1}_{\ell z,ijk+1} > u^{n+1}_{\ell z,ijk} \\ \zeta_{p\ell,ijk-1/2}\rho^{n}_{\ell,ijk-1/2}T^{n+1}_{ijk-1/2}u^{n+1}_{\ell z,ijk-1/2} = \zeta_{p\ell,ijk}\rho^{n}_{\ell,ijk}T^{n+1}_{ijk}u^{n+1}_{\ell z,ijk} & \text{if } u^{n+1}_{\ell z,ijk-1} < u^{n+1}_{\ell z,ijk} \\ \zeta_{p\ell,ijk-1/2}\rho^{n}_{\ell,ijk-1/2}T^{n+1}_{ijk-1/2}u^{n+1}_{\ell z,ijk-1/2} = \zeta_{p\ell,ijk-1}\rho^{n}_{\ell,ijk-1}T^{n+1}_{ij-1k}u^{n+1}_{\ell z,ijk-1} & \text{if } u^{n+1}_{\ell z,ijk-1} > u^{n+1}_{\ell z,ijk} \end{cases} \quad (7\text{-}31)$$

7.2.3 Conduction Term

Conduction or diffusion term of heat flux in x direction at the boundaries ($i+1/2jk$) and ($i-1/2jk$) are calculated

$$\begin{aligned} J^{n+1}_{cond,i+1/2\,jk} &= -2\lambda^{n}_{eff,i+1/2\,jk}\frac{T^{n+1}_{i+1\,jk}-T^{n+1}_{ijk}}{\Delta x_{i+1\,jk}+\Delta x_{ijk}} \\ J^{n+1}_{cond,i-1/2\,jk} &= -2\lambda^{n}_{eff,i-1/2\,jk}\frac{T^{n+1}_{i-1\,jk}-T^{n+1}_{ijk}}{\Delta x_{i-1\,jk}+\Delta x_{ijk}} \end{aligned} \quad (7\text{-}32)$$

These equations are evaluated at boundaries by using a second-order centered approximation discussed in Chapter 3 and 4 as well. Effective thermal conductivities are evaluated by using an average weighting at boundaries ($i+1/2jk$) and ($i-1/2jk$) in z direction as

$$\begin{aligned} \lambda^{n+1}_{eff,i+1/2\,jk} &= 0.5\left(\lambda^{n+1}_{eff,i+1\,jk}+\lambda^{n+1}_{eff,ijk}\right) \\ \lambda^{n+1}_{eff,i-1/2\,jk} &= 0.5\left(\lambda^{n+1}_{eff,i-1\,jk}+\lambda^{n+1}_{eff,ijk}\right) \end{aligned} \quad (7\text{-}33)$$

Conduction or diffusion term of heat flux in x direction at the boundaries ($ij+1/2k$) and ($ij-1/2k$) are calculated

$$J^{n+1}_{cond,ij+1/2k} = -2\lambda^{n}_{eff,ij+1/2k}\frac{T^{n+1}_{ij+1k} - T^{n+1}_{ijk}}{\Delta y_{i+1jk} + \Delta y_{ijk}}$$
$$J^{n+1}_{cond,ij-1/2k} = -2\lambda^{n}_{eff,ij-1/2k}\frac{T^{n+1}_{ij-1k} - T^{n+1}_{ijk}}{\Delta y_{ij-1k} + \Delta y_{ijk}} \quad (7\text{-}34)$$

Effective thermal conductivities that are evaluated at boundaries ($ij+1/2k$) and ($ij-1/2k$) in y direction are calculated as

$$\lambda^{n+1}_{eff,ij+1/2k} = 0.5\left(\lambda^{n+1}_{eff,ij+1k} + \lambda^{n+1}_{eff,ijk}\right)$$
$$\lambda^{n+1}_{eff,ij-1/2k} = 0.5\left(\lambda^{n+1}_{eff,ij-1k} + \lambda^{n+1}_{eff,ijk}\right) \quad (7\text{-}35)$$

Conduction or diffusion term of heat flux in z direction at the boundaries ($ijk+1/2$) and ($ijk-1/2$) is computed

$$J^{n+1}_{cond,ijk+1/2} = -2\lambda^{n}_{eff,ijk+1/2}\frac{T^{n+1}_{ijk+1} - T^{n+1}_{ijk}}{\Delta z_{i+1jk} + \Delta z_{ijk}}$$
$$J^{n+1}_{cond,ijk-1/2} = -2\lambda^{n}_{eff,ijk-1/2}\frac{T^{n+1}_{ijk-1} - T^{n+1}_{ijk}}{\Delta z_{ijk-1} + \Delta z_{ijk}} \quad (7\text{-}36)$$

Effective thermal conductivities that are evaluated by using average weighting at boundaries ($ijk+1/2$) and ($ijk-1/2$) in z direction are obtained as

$$\lambda^{n+1}_{eff,ij+1/2k} = 0.5\left(\lambda^{n+1}_{eff,ij+1k} + \lambda^{n+1}_{eff,ijk}\right)$$
$$\lambda^{n+1}_{eff,ij-1/2k} = 0.5\left(\lambda^{n+1}_{eff,ij-1k} + \lambda^{n+1}_{eff,ijk}\right) \quad (7\text{-}37)$$

7.3 HEAT LOSS TERM

Vinsome and Westerveld (1980) developed a semi-analytical approach to compute amount of heat loss in case of heat or cold injection into a reservoir layer that is surrounded between impermeable overburden or underburden layers. Their approach

simplifies the heat conduction problem, while providing satisfactory accuracy. Vinsome and Westerveld considered that heat conduction perpendicular to the conductive boundary is more important than parallel to the boundary. Heat conduction tends to wipe out sharp temperature differences; they suggested that the temperature profile in the conductive domain may be approximated by means of a simple trial function that contains a few adjustable parameters. We implemented the same model but we consider that the temperature of overburden and underburden are not changed during heat loss from reservoir layer. The temperature of overburden and underburden are set at the initial temperature of reservoir layer ($T_{OB} = T^{0}_{ij1}$ and $T_{UB} = T^{0}_{ijN_z}$).

The amount of heat flux into overburden can be written as

$$J^{n+1}_{z,ij\frac{1}{2}} = -\lambda_{OB}\left(\frac{T_{OB} - T^{n+1}_{ij1}}{d_{ij1}} - p^{n+1}_{ij1}\right) \tag{7-38}$$

where T_{OB} is temperature of overburden, which is constant, λ_{OB} is thermal conductivity of overburden layer corresponding to grid block ($ij1$) and d^{n}_{ij1} is the overburden thermal diffusivity defined as

$$d_{ij1} = \frac{1}{2}\sqrt{\kappa(t - t_{ch})} \quad where \;\; \kappa = \frac{\lambda_{OB}}{\rho_{OB}\zeta_{pOB}} \tag{7-39}$$

where t is the simulation time at the new time level and t_{ch} indicates the time the temperature of the reservoir is different from that of the overburden rock. κ is the rock thermal diffusivity of overburden. λ_{OB} , ρ_{OB}, ζ_{pOB} are thermal conductivity, rock density, and heat capacity for overburden layer. p^{n+1}_{ij1} is also defined as

$$p_{ij1}^{n+1} = \frac{\frac{\kappa\Delta t\left(T_{ij1}^{n+1} - T_{OB}\right)}{d_{ij1}} + I_{ij1}^{n} - \frac{d_{ij1}^{3}\left(T_{ij1}^{n+1} - T_{ij1}^{n}\right)}{\kappa\Delta t}}{3d_{ij1}^{2}} \tag{7-40}$$

where

$$I_{ij1}^{n} = \left(T_{ij1}^{n} - T_{OB}\right)d_{ij1} + P_{ij1}^{n}d_{ij1}^{2} + 2q_{ij1}^{n+1}d_{ij1}^{3} \tag{7-41}$$

and

$$q_{ij1}^{n+1} = \frac{P_{ij1}^{n}}{d_{ij1}} - \frac{\left(T_{ij1}^{n+1} - T_{OB}\right)}{2d_{ij1}^{2}} + \frac{\left(T_{ij1}^{n+1} - T_{ij1}^{n}\right)}{2\kappa\Delta t} \tag{7-42}$$

Substituting P_{ij1}^{n+1} and q_{ij1}^{n+1} and I_{ij1}^{n} in the overburden heat flux equation, we have

$$\begin{aligned} J_{z,ij\frac{1}{2}}^{n+1} = \lambda_{OB}\Bigg(& \frac{T_{ij1}^{n+1} - T_{OB}}{d_{ij1}} - \frac{\kappa\Delta t}{d_{ij1}\left(3d_{ij1}^{2} + \kappa\Delta t\right)}T_{ij1}^{n+1} + \\ & \frac{\kappa\Delta t}{d_{ij1}\left(3d_{ij1}^{2} + \kappa\Delta t\right)}T_{OB} - \frac{I_{ij1}^{n}}{3d_{ij1}^{2} + \kappa\Delta t} + \\ & \frac{d_{ij1}^{3}}{\kappa\Delta t\left(3d_{ij1}^{2} + \kappa\Delta t\right)}T_{ij1}^{n+1} - \frac{d_{ij1}^{3}}{\kappa\Delta t\left(3d_{ij1}^{2} + \kappa\Delta t\right)}T_{ij1}^{n}\Bigg) \end{aligned} \tag{7-43}$$

The heat flux into the overburden can be written in implicit and explicit parts. Implicit part containing all terms that correspond to the temperature at n+1 time level ($\tau_{ij1}T_{ij1}^{n+1}$) and explicit part containing all terms that correspond to temperature at n time level ($j_{z,ij1}^{n}$) are defined as

$$J_{z,ij\frac{1}{2}}^{n+1} = j_{z,ij1}^{n} + \tau_{ij1}T_{ij1}^{n+1} \tag{7-44}$$

where

$$\tau_{ij1} = \lambda_{OB}\left(\frac{1}{d_{ij1}} - \frac{\kappa\Delta t}{d_{ij1}\left(3d_{ij1}^2 + \kappa\Delta t\right)} + \frac{d_{ij1}^3}{\kappa\Delta t\left(3d_{ij1}^2 + \kappa\Delta t\right)}\right) \tag{7-45}$$

and

$$j_{z,ij1}^n = \lambda_{OB}\left(\left(\frac{1}{d_{ij1}} - \frac{\kappa\Delta t}{d_{ij1}\left(3d_{ij1}^2 + \kappa\Delta t\right)}\right)T_{OB} - \frac{I_{ij1}^n}{3d_{ij1}^2 + \kappa\Delta t} - \frac{d_{ij1}^3}{\kappa\Delta t\left(3d_{ij1}^2 + \kappa\Delta t\right)}T_{ij1}^n\right) \tag{7-46}$$

Accordingly, the total heat loss that is implemented into the UTCHEM simulator for overburden layer is from the following expression

$$\begin{aligned} q_{L,ij1}^{n+1} = \lambda_{OB}\Bigg(&\frac{T_{ij1}^{n+1} - T_{OB}}{d_{ij1}} - \frac{\kappa\Delta t}{d_{ij1}\left(3d_{ij1}^2 + \kappa\Delta t\right)}T_{ij1}^{n+1} + \frac{\kappa\Delta t}{d_{ij1}\left(3d_{ij1}^2 + \kappa\Delta t\right)}T_{OB} \\ &- \frac{I_{ij1}^n}{3d_{ij1}^2 + \kappa\Delta t} + \frac{d_{ij1}^3}{\kappa\Delta t\left(3d_{ij1}^2 + \kappa\Delta t\right)}T_{ij1}^{n+1} - \frac{d_{ij1}^3}{\kappa\Delta t\left(3d_{ij1}^2 + \kappa\Delta t\right)}T_{ij1}^n\Bigg)\Delta x_{ij1}\Delta y_{ij1} \end{aligned} \tag{7-47}$$

Similar formulations are discretized and implemented for underburden layer. The amount of heat flux into underburden located at the bottom of reservoir layer is

$$J_{z,ijNz+1/2}^{n+1} = -\lambda_{OB}\left(\frac{T_{UB} - T_{ijNz}^{n+1}}{d_{ijNz}} - p_{ijNz}^{n+1}\right) \tag{7-48}$$

where T_{UB} is temperature of underburden with a constant value, λ_{UB} is thermal conductivity of underburden layer corresponding to grid block ($ijNz$) and d_{ijNz}^n is the underburden thermal diffusivity defined as

$$d_{ijNz} = \frac{1}{2}\sqrt{\kappa(t - t_{ch})} \quad where \;\; \kappa = \frac{\lambda_{UB}}{\rho_{UB}\zeta_{pUB}} \tag{7-49}$$

where t is the simulation time and t_{ch} indicates the time that the temperature of the reservoir is different from that of the overburden rock. κ is the rock thermal

diffusivity of overburden. λ_{UB} , ρ_{UB}, ζ_{pUB} are thermal conductivity, rock density, and heat capacity for overburden layer. p_{ij1}^{n+1} is also defined as

$$p_{ijNz}^{n+1} = \frac{\frac{\kappa\Delta t\left(T_{ij1}^{n+1} - T_{UB}\right)}{d_{ij1}} + I_{ij1}^{n} - \frac{d_{ij1}^{3}\left(T_{ijNz}^{n+1} - T_{ijNz}^{n}\right)}{\kappa\Delta t}}{3d_{ijNz}^{2}} \tag{7-50}$$

where

$$I_{ijNz}^{n} = \left(T_{ijNz}^{n} - T_{UB}\right)d_{ijNz} + P_{ijNz}^{n}d_{ijNz}^{2} + 2q_{ijNz}^{n+1}d_{ijNz}^{3} \tag{7-51}$$

and

$$q_{ijNz}^{n+1} = \frac{P_{ijNz}^{n}}{d_{ijNz}} - \frac{\left(T_{ijNz}^{n+1} - T_{UB}\right)}{2d_{ijNz}^{2}} + \frac{\left(T_{ijNz}^{n+1} - T_{ijNz}^{n}\right)}{2\kappa\Delta t} \tag{7-52}$$

Substituting P_{ijNz}^{n+1} and q_{ijNz}^{n+1} and I_{ijNz}^{n} in the underburden heat flux equation, we have

$$\begin{aligned} J_{z,ijNz+\frac{1}{2}}^{n+1} = \lambda_{UB}\Bigg(& \frac{T_{ij1}^{n+1} - T_{UB}}{d_{ijNz}} - \frac{\kappa\Delta t}{d_{ijNz}\left(3d_{ijNz}^{2} + \kappa\Delta t\right)}T_{ijNz}^{n+1} + \\ & \frac{\kappa\Delta t}{d_{ijNz}\left(3d_{ijNz}^{2} + \kappa\Delta t\right)}T_{UB} - \frac{I_{ijNz}^{n}}{3d_{ijNz}^{2} + \kappa\Delta t} + \\ & \frac{d_{ijNz}^{3}}{\kappa\Delta t\left(3d_{ijNz}^{2} + \kappa\Delta t\right)}T_{ijNz}^{n+1} - \frac{d_{ijNz}^{3}}{\kappa\Delta t\left(3d_{ijNz}^{2} + \kappa\Delta t\right)}T_{ijNz}^{n}\Bigg) \end{aligned} \tag{7-53}$$

This heat flux also can be written in implicit and explicit parts: the implicit part containing all terms that correspond to the temperature at n+1 time level ($\tau_{ijNz}T_{ijNz}^{n+1}$) and

the explicit part containing all terms that correspond to the temperature at n time level ($j^{n}_{z,ijNz}$) as in

$$J^{n+1}_{z,ijNz+\frac{1}{2}} = j^{n}_{z,ijNz} + \tau_{ijNz} T^{n+1}_{ijNz} \tag{7-54}$$

where

$$\tau_{ijNz} = \lambda_{UB}\left(\frac{1}{d_{ijNz}} - \frac{\kappa\Delta t}{d_{ijNz}\left(3d^{2}_{ijNz} + \kappa\Delta t\right)} + \frac{d^{3}_{ijNz}}{\kappa\Delta t\left(3d^{2}_{ijNz} + \kappa\Delta t\right)}\right) \tag{7-55}$$

and

$$j^{n}_{z,ijNz} = \lambda_{UB}\left(\left(\frac{1}{d_{ijNz}} - \frac{\kappa\Delta t}{d_{ijNz}\left(3d^{2}_{ijNz} + \kappa\Delta t\right)}\right)T_{UB} - \frac{I^{n}_{ijNz}}{3d^{2}_{ijNz} + \kappa\Delta t} - \frac{d^{3}_{ijNz}}{\kappa\Delta t\left(3d^{2}_{ijNz} + \kappa\Delta t\right)} T^{n}_{ijNz}\right) \tag{7-56}$$

Hence, the total heat loss for the underburned layer is expressed as

$$q^{n+1}_{L,ijNz} = \lambda_{UB}\left(\frac{T^{n+1}_{ijNz} - T_{UB}}{d_{ijNz}} - \frac{\kappa\Delta t}{d_{ijNz}\left(3d^{2}_{ijNz} + \kappa\Delta t\right)} T^{n+1}_{ijNz} + \frac{\kappa\Delta t}{d_{ijNz}\left(3d^{2}_{ijNz} + \kappa\Delta t\right)} T_{UB} - \frac{I^{n}_{ijNz}}{3d^{2}_{ijNz} + \kappa\Delta t} + \frac{d^{3}_{ijNz}}{\kappa\Delta t\left(3d^{2}_{ijNz} + \kappa\Delta t\right)} T^{n+1}_{ijNz} - \frac{d^{3}_{ijNz}}{\kappa\Delta t\left(3d^{2}_{ijNz} + \kappa\Delta t\right)} T^{n}_{ijNz}\right)\Delta x_{ijNz}\Delta y_{ijNz} \tag{7-57}$$

7.4 WELL TERMS

The energy source term per bulk volume through an injection well is calculated from the following equation and then added to the energy balance equation

$$q^{n+1}_{H,inj} = \sum_{\ell=1}^{n_p} q_{\ell}\zeta_{p\ell}\rho^{n}_{\ell}\left(T_{inj} - T_{ini}\right) + q_{w}\rho^{n}_{w}\alpha_{Sc}\left(\bar{H}_{s} - \bar{H}_{w}\right)_{Sc} \tag{7-58}$$

where $q_{H,inj}^{n+1}$ is the injected enthalpy rate at time level $n+1$ and q_ℓ is the injection flow rate of phase ℓ; T_{inj} and T_{ini} are injector temperature and initial reservoir temperature, respectively. α is the steam mass quality at surface condition. $\bar{H}_s - \bar{H}_w$ is the latent heat per unit mass at surface condition as well. q_w is the equivalent cold water rate injected into the reservoir. Similarly, the energy sink term per bulk volume produced through a well is obtained from

$$q_{H,prod}^{n+1} = -\sum_{\ell=1}^{n_p} q_\ell \zeta_{p\ell} \rho_\ell^n \left(T_{prd}^{n+1} - T_{ini}\right) - \rho_s^n q_s^{n+1} \left(\bar{H}_s - \bar{H}_w\right)_{Rc} \tag{7-59}$$

where $q_{H,prod}^{n+1}$ is the produced enthalpy rate at time level $n+1$ and , q_ℓ is the production flow rate of phase ℓ, T_{prd}^{n+1} is producer temperature that is assumed to equal to gridblock temperature $T_{prd}^{n+1} = T_{ijk}^{n+1}$. For producer wells the latent heat per unit mass, $\bar{H}_s - \bar{H}_w$, is considered at reservoir condition as well. q_s is the produced steam rate. ρ_s^n is the steam density at reservoir condition.

7.5 CASE STUDIES OF THE THERMAL MODEL

In this section, ` several cases are presented and tested to verify the mathematical thermal model and its numerical solution. Test cases are first run with the UTCHEM simulator and then their results are compared with CMG-STARS results (STARS, 2012.10) for hot water injection and steam injection. CMG-STARS is the undisputed industry standard in thermal reservoir simulation and advanced recovery processes. This simulator is used to simulate changes to the reservoir, based upon fluid behavior, steam, and electrical heating.

7.5.1 One Dimensional Hot Water Injection Case

The first test case is a 1-D two phase (oil and water) case with 10 grid blocks. We compare the results of the UTCHEM simulator with the CMG-STARS simulator results (STARS, 2012.10). CMG-STARS is the undisputed industry standard in thermal reservoir simulation and advanced recovery processes. This simulator is used to simulate changes to the reservoir based upon fluid behavior, steam, and electrical heating.

This case is set up for the UTCHEM and the CMG-STARS simulator to inject hot water with temperature 210 ^{o}F under a constant rate 100ft^{3}/Day. In this case, hot water is injected for 500 days into the reservoir with initial temperature 90 ^{o}F. Fluid and reservoir data are summarized in Table 7-1. The details of the input data of both simulators are presented in Appendix A.

In this case, relative permeability of water and oil are considered to vary linearly with no residual saturation. Figure 7-2 shows the comparison of pressure profiles after 50 days. Since diffusivity of pressure equation is high enough, pressure change can be observed only at very early time; right after injection, pressure reaches a steady state condition. Therefore, pressure does not change with respect to time during 800 days of simulation. In both simulators, thermal conductivities of oil and water are 38 (Btu/lb.Day.^{o}F) and 32 (Btu/lb.Day. ^{o}F), but the heat capacity of water in CMG-STARS is calculated from steam table. Therefore, we read an average value of heat capacity from CMG-STARS output file and used in UTCHEM as constant values for oil 0.5 (Btu/lb.^{o}F) and water 1 (Btu/lb.^{o}F) phases.

Figure 7-3 and Figure 7-4 depict water saturation and temperature profiles at different times (100, 50, 100, 200, and 500). Hot water injection leads to an increase in water saturation as well as temperature. The matched temperature between the CMG-

STARS and the UTCHEM results shows that the energy balance solutions are correct in two different simulators.

Figure 7 5 and Figure 7 6 illustrate the daily production rate of oil and water for both simulators. After 100 days, water breakthrough has occurred; this leads to an increase in water production rate. Figure 7-7 show the cumulative oil recovery over 500 days. The results are in food agreement.

Table 7-1-Reservoir model and fluid flow properties used for one dimensional hot water injection.

Reservoir Model	
Reservoir size	200ftx20ftx20ft
Number of gridblock	10x1x1
Gridblock size	20ftx20ftx20ft
Porosity and Permeability	0.2 and 100 mD
λ and ζ_p for water	38 (Btu/lb.Day. ^{o}F) and 1.0 (Btu/lb. ^{o}F)
λ and ζ_p for oil	32 (Btu/lb.Day. ^{o}F) and 0.5 (Btu/lb. ^{o}F)
λ density, and ζ_p for rock	28 (Btu/lb.Day.^{o}F), 165 (lb/cu.ft), 0.25 (Btu/lb. ^{o}F)
Initial temperature	90.0 ^{o}F
Initial Pressure	2000 psi(top layer)
Initial Saturations	0.3(reservoir layers
Water Rel. Perm	S_{rw}=0 , k^o_{rw}=1.0 , e_w=1.0
Oil Rel. Perm	S_{ro}=0 , k^o_{ro}=1.0 , e_o=1.0
Well	
Number of Wells	1 Prod and1 Inj
Well Constrains	1prod (BHP=1900psi) 1Inj (Water Rate=100ft^3/Day)
Water Injected Temperature	210 ^{o}F

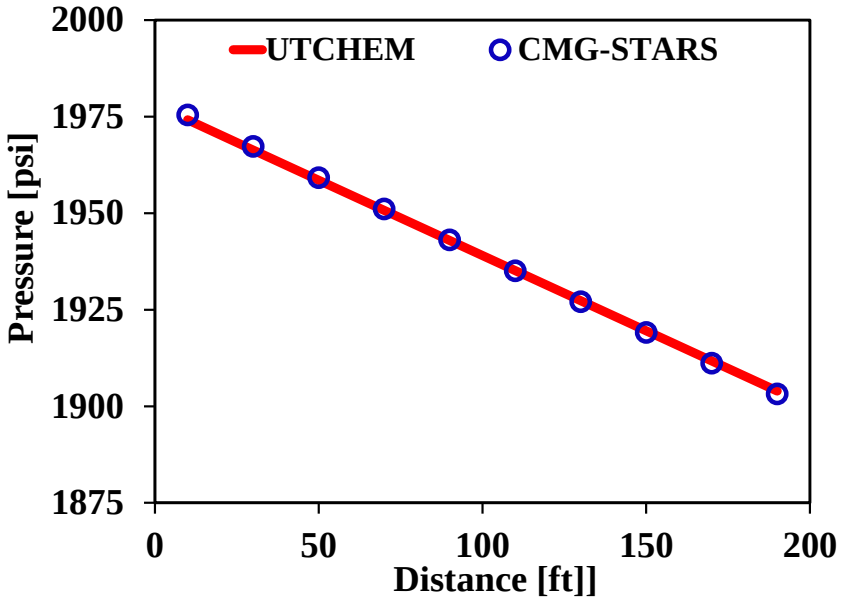

Figure 7-2- Comparison of pressure profile on day 50 for one dimensional hot water injection case.

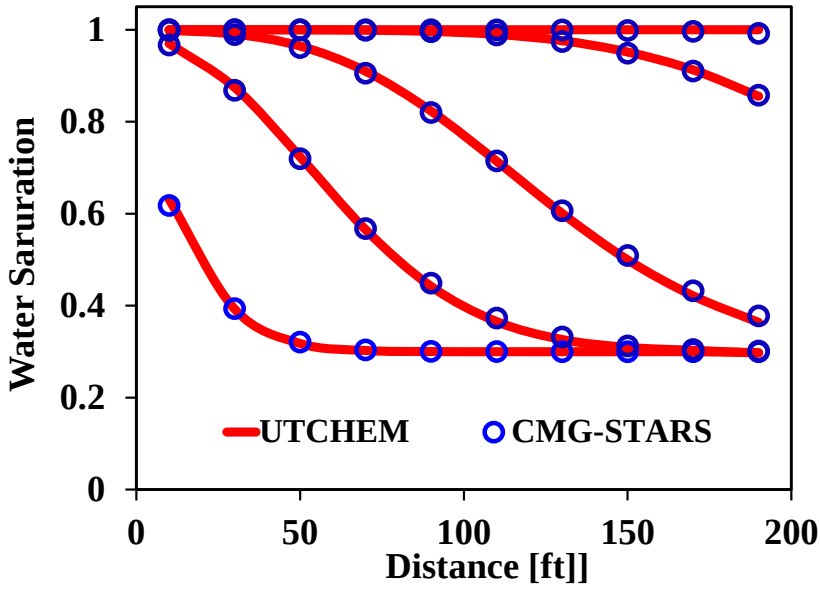

Figure 7-3- Comparison of water saturation profile in the various days (10, 50, 100, 200, and 500) for one dimensional hot water injection.

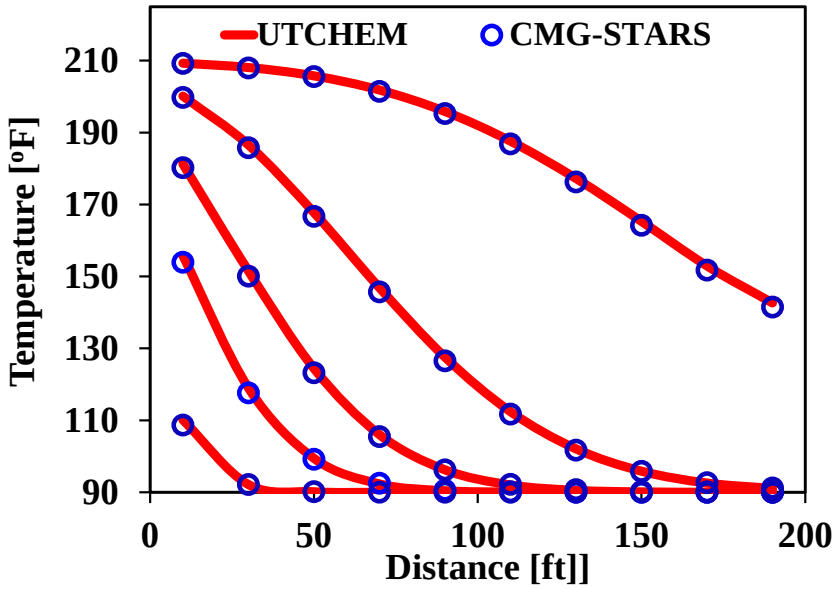

Figure 7-4- Comparison of temperature profile in the various days (10, 50, 100, 200, and 500) for one dimensional hot water injection.

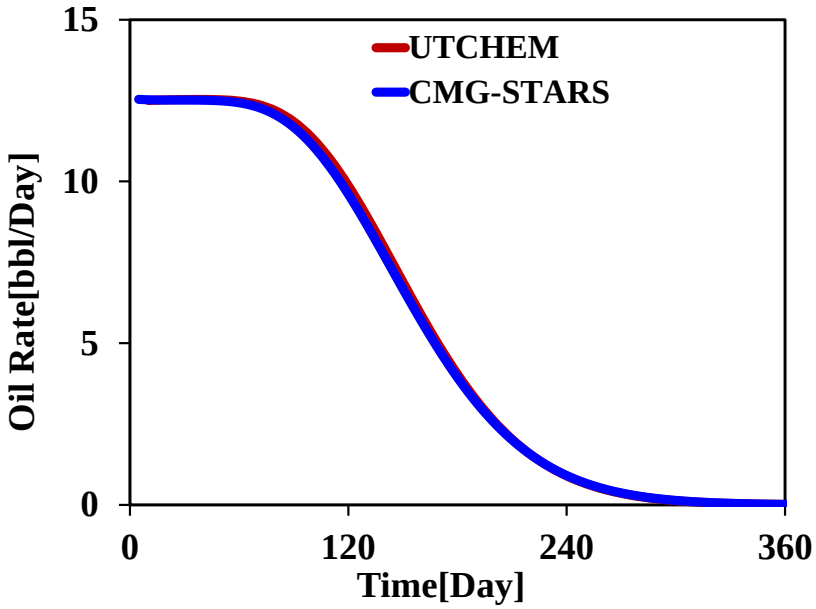

Figure 7-5- Comparison of oil production rate between CMG-STARS and UTCHEM for one dimensional hot water injection.

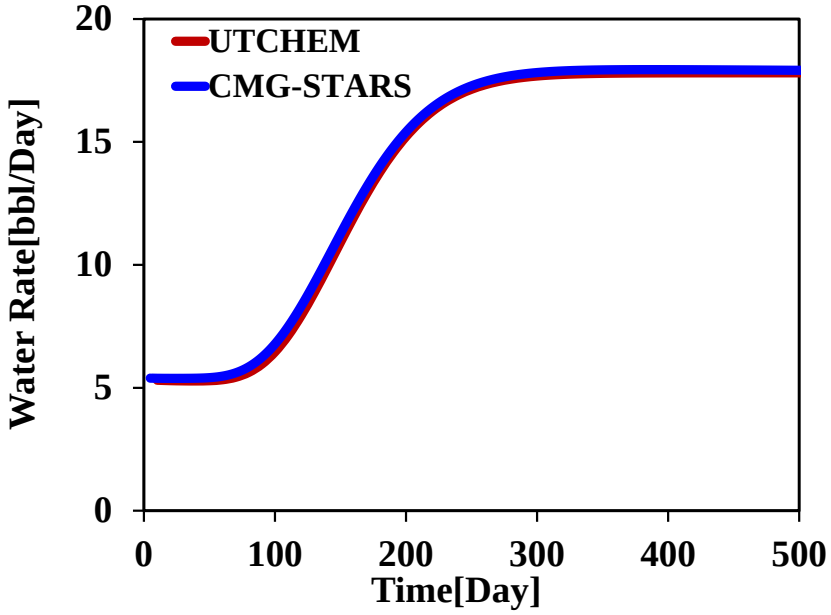

Figure 7-6- Comparison of water production rate between CMG-STARS and UTCHEM for one dimensional hot water injection.

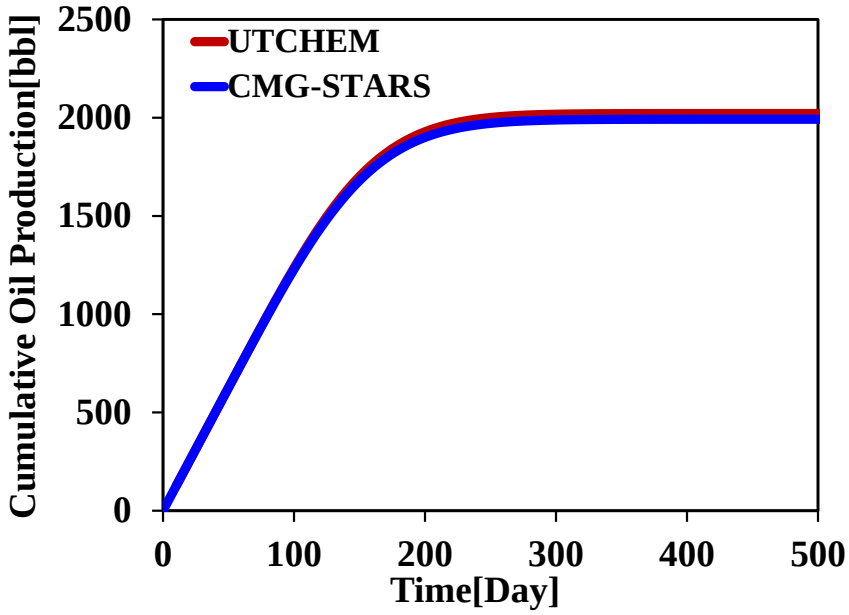

Figure 7-7- Comparison of cumulative oil production between CMG-STARS and UTCHEM) for one dimensional hot water injection.

7.5.2 Three Dimensional Hot Water Injection Case

The second test case is hot water injection into a three-dimensional model with initial temperature 90 ^{o}F. In this case study, a quarter five-spot model including five layers is considered; hot water is injected with 300 ^{o}F. Fluid flow properties such as density, viscosity, and relative permeability values of oil and water phases are consistent in both simulators. Rock density and heat capacity of rock as well as thermal conductivity are the same in the both simulators. Since water and oil heat capacities in CMG-STARS are calculated inside the code using different correlation for oil and steam table for water, we read these values from the output of CMG-STARS and then took an average of them to use for the constant values for water and oil in UTCHEM simulator. All reservoir model parameters and thermal and flow properties that are used in both simulators are summarized in Table 7-2.

Results are plotted and compared for both simulators. Figure 7-8 through Figure 7-15 show the comparison of water saturation and pressure with corresponding temperature and oil saturation at different times. These plots demonstrate that the results are in a good agreement. Figure 7-16 through Figure 7-18 depict a profile of temperature, water saturation, and oil saturation that intersects injection well in x or y direction after 800 days.

Table 7-2-Reservoir model and fluid flow properties used for three dimensional hot water injection case.

Reservoir Model	
Reservoir size	200ftx200ftx50ft
Number of gridblock	20x20x5
Gridblock size	20ftx20ftx20ft
Porosity	0.2
Permeability (x, y, z)	100 mD,100mD, and 10mD
λ and ζ_p for water	38 (Btu/lb.Day.^{o}F) and 1.0 (Btu/lb.^{o}F)
λ and ζ_p for oil	32 (Btu/lb.Day.^{o}F) and 0.5 (Btu/lb.^{o}F)
λ , density, and ζ_p for rock	28 (Btu/lb.Day.^{o}F), 165 (lb/cu.ft), 0.25 (Btu/lb.^{o}F)
Initial temperature	90.0 ^{o}F
Initial Pressure	2000 psi(top layer)
Initial Saturations	0.3(reservoir layers
Water Rel. Perm	S_{rw}=0 , k^o_{rw}=1.0 , e_w=1.0
Oil Rel. Perm	S_{ro}=0 , k^o_{ro}=1.0 , e_o=1.0
Well	
Number of Wells	1 Prod and1 Inj
Well Constrains	1prod (BHP=1900psi) 1Inj(WaterRate=100ft^3/Day)
Water Injected Temperature	300 ^{o}F

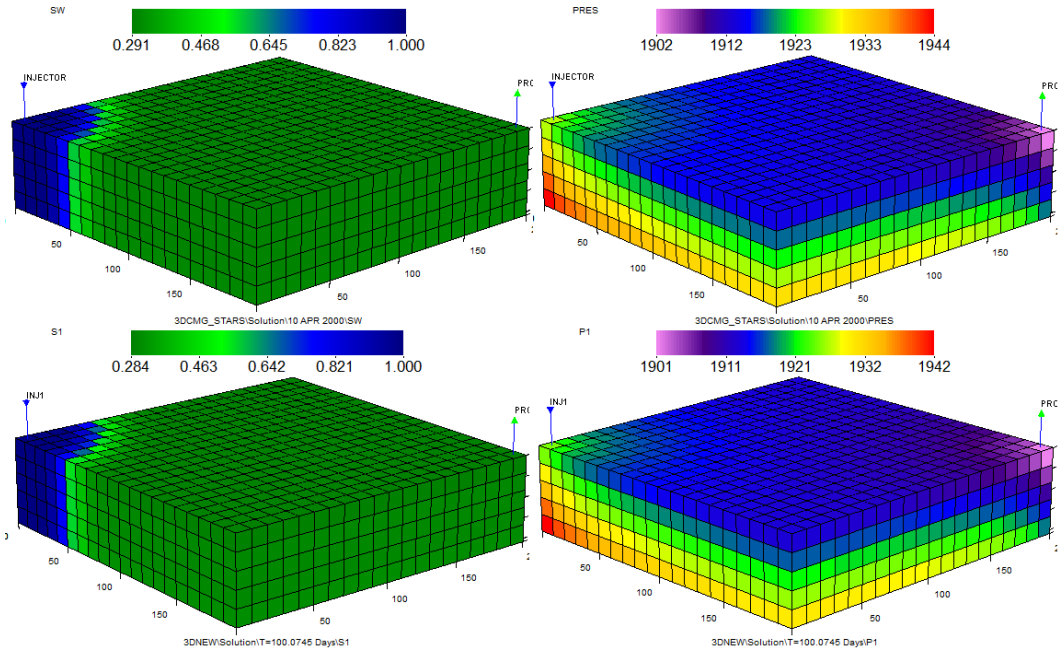

Figure 7-8-Comparison of water saturation (left) and pressure (right) distribution results after 100 days between CMG-STARS (top) and UTCHEM (bottom).

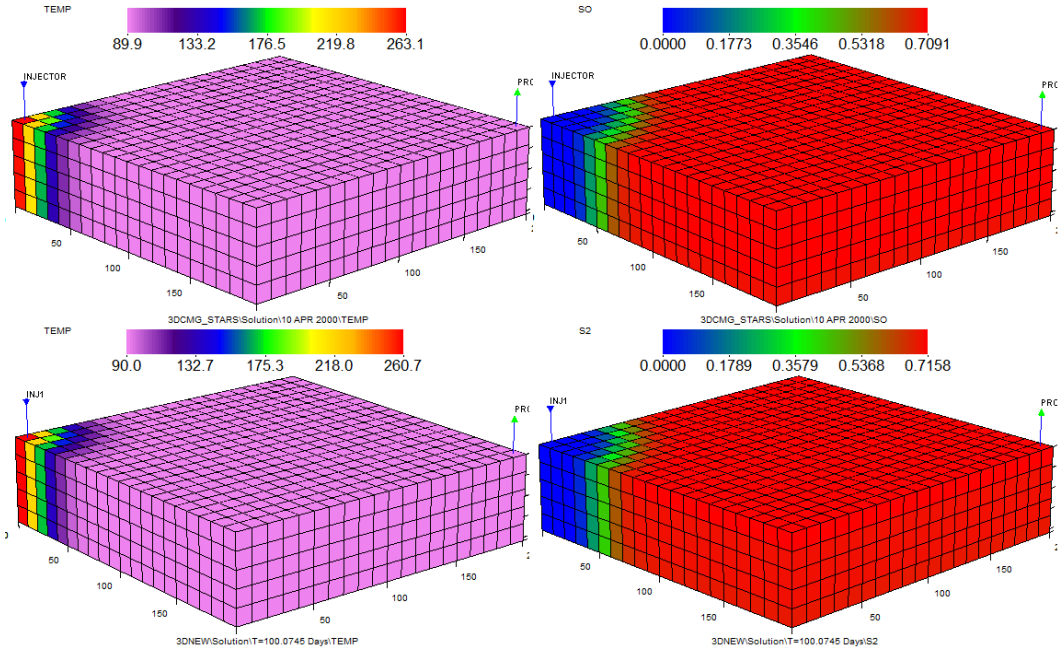

Figure 7-9-Comparison of temperature (left) and oil saturation (right) distribution results after 100 days between CMG-STARS (top) and UTCHEM (bottom).

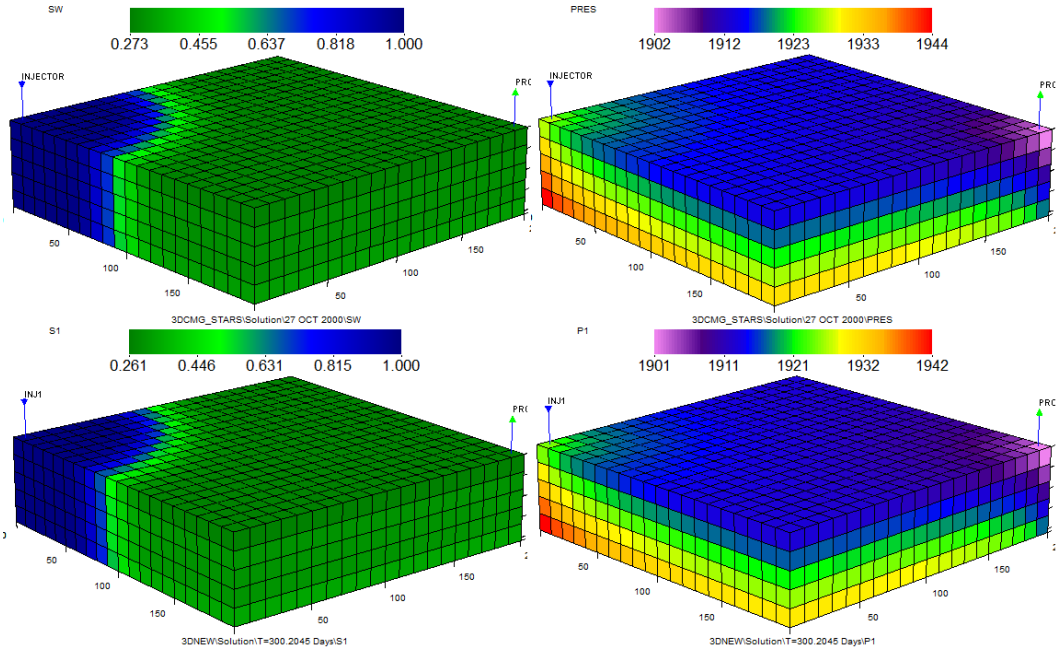

Figure 7-10-Comparison of water saturation (left) and pressure (right) distribution results after 300 days between CMG-STARS (top) and UTCHEM (bottom).

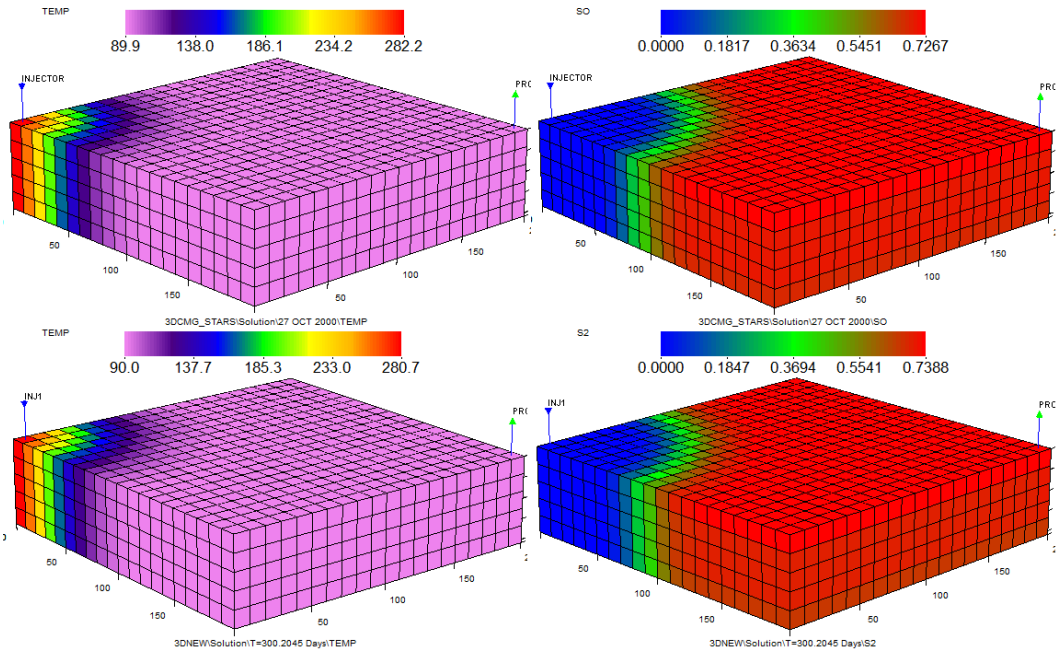

Figure 7-11-Comparison of temperature (left) and oil saturation (right) distribution results after 300 days between CMG-STARS (top) and UTCHEM (bottom).

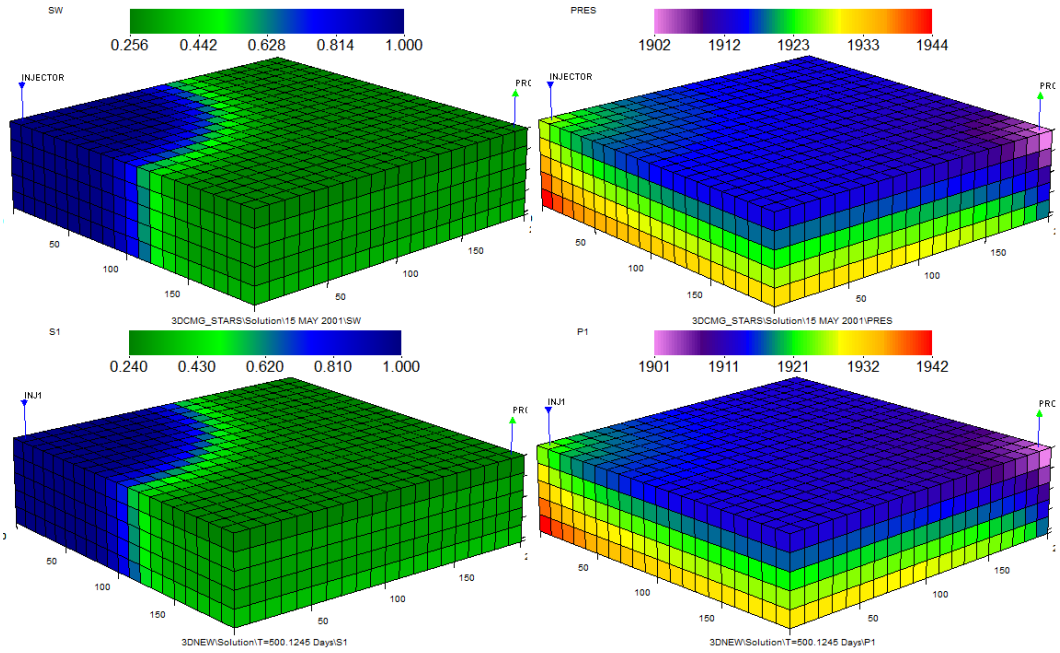

Figure 7-12-Comparison of water saturation (left) and pressure (right) distribution results after 500 days between CMG-STARS (top) and UTCHEM (bottom).

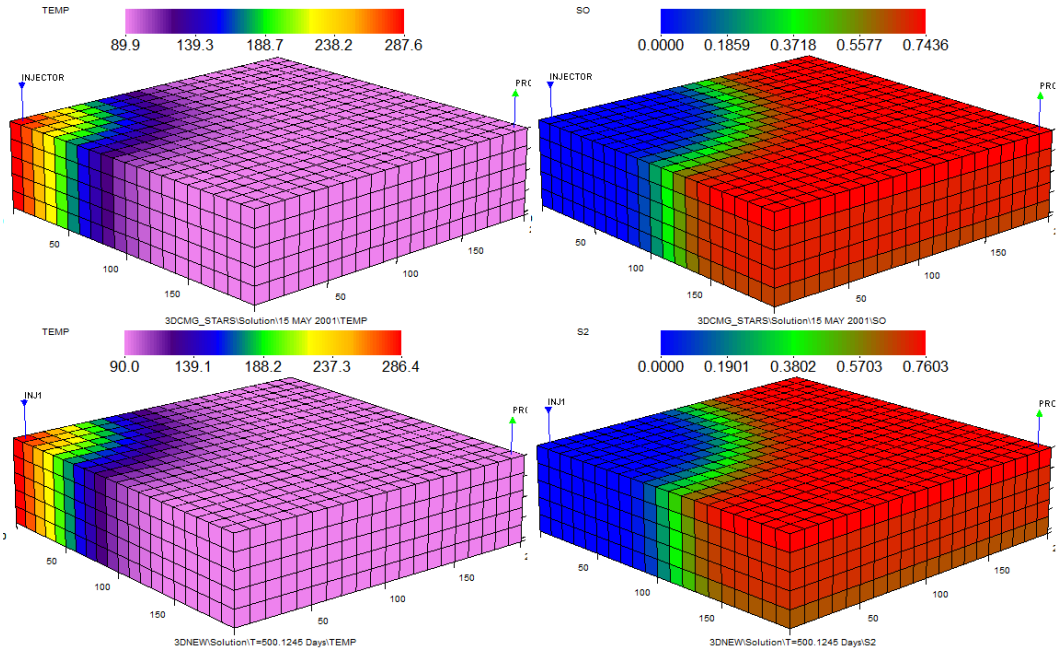

Figure 7-13-Comparison of temperature (left) and oil saturation (right) distribution results after 500 days between CMG-STARS (top) and UTCHEM (bottom).

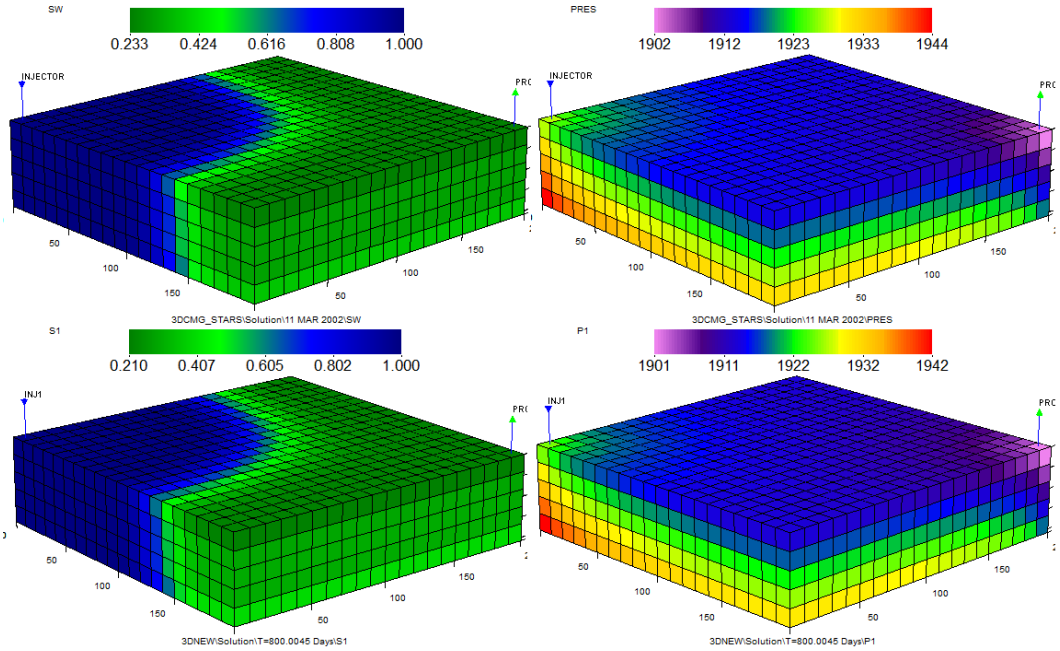

Figure 7-14-Comparison of water saturation (left) and pressure (right) distribution results after 800 days between CMG-STARS (top) and UTCHEM (bottom).

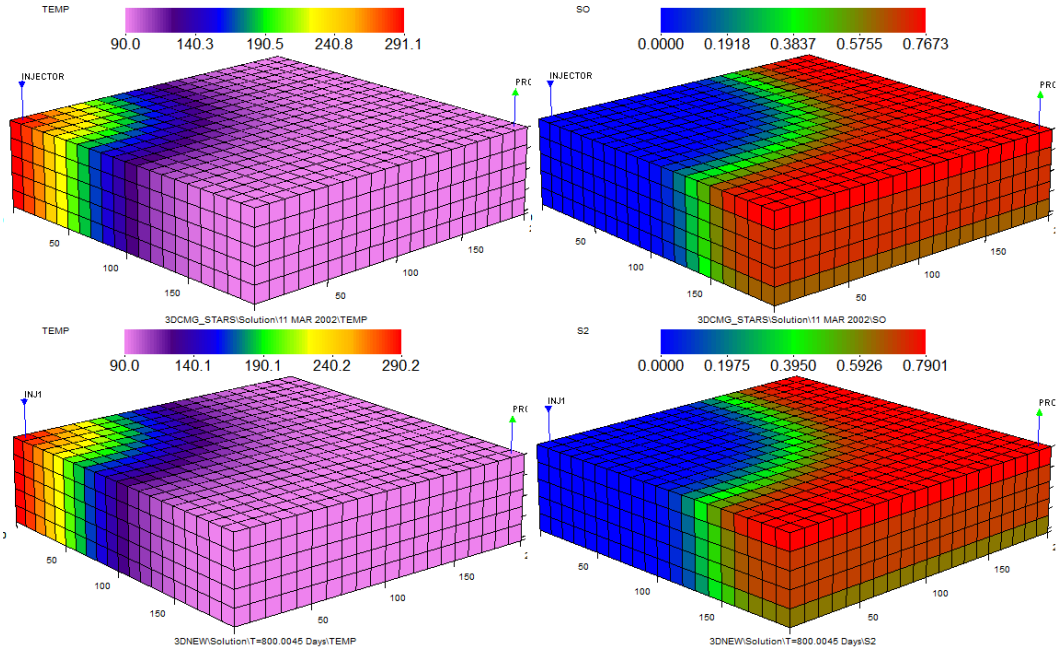

Figure 7-15-Comparison of temperature (left) and oil saturation (right) distribution results after 800 days between CMG-STARS (top) and UTCHEM (bottom).

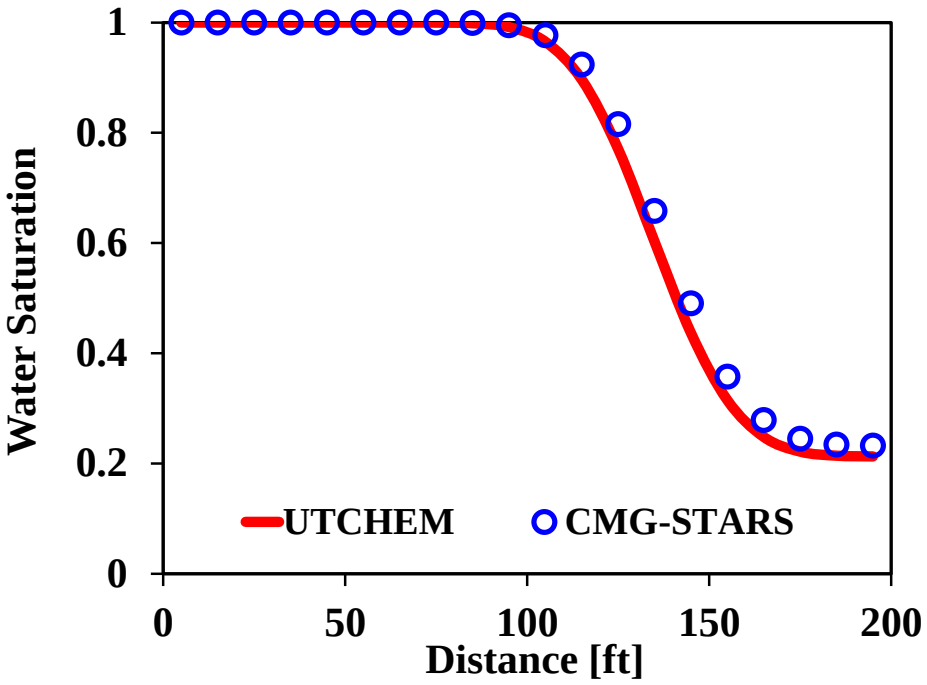

Figure 7-16-Comparison of water saturation profile in x or y direction passing through the injection well at top layer after 800 days.

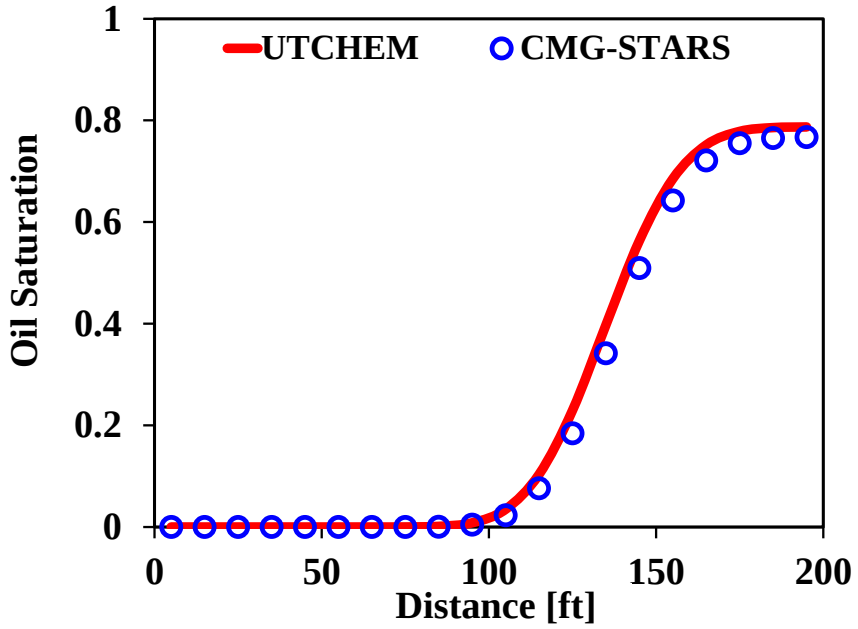

Figure 7-17- Comparison of oil saturation profile in x or y direction passing through the injection well at top layer after 800 days.

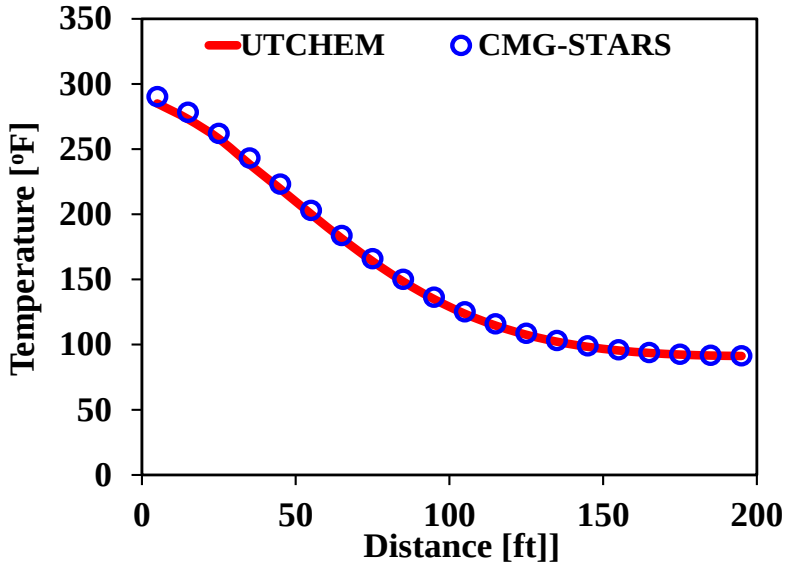

Figure 7-18- Comparison of temperature profile in x or y direction passing through the injection well at top layer after 800 days.

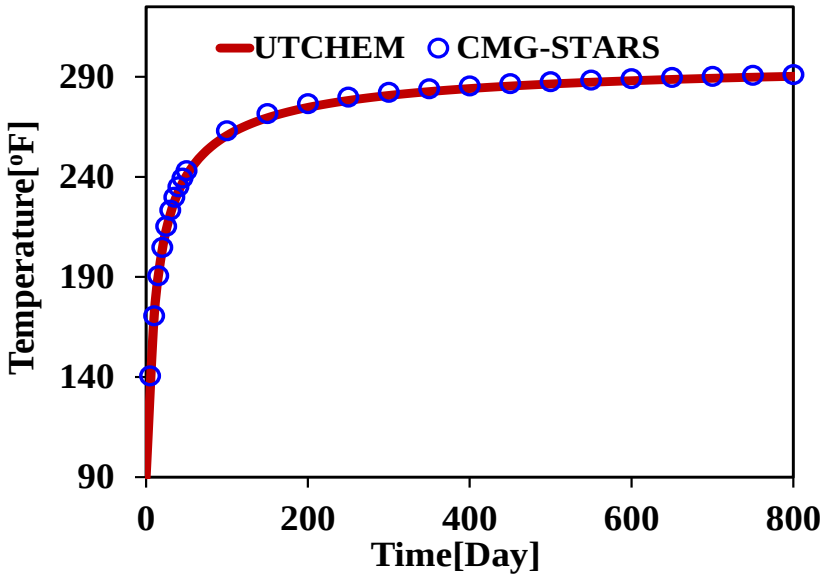

Figure 7-19- Comparison of gridblock temperature of injection well located at top layer between CMG-STARS and UTCHEM results for three dimensional hot water injection case.

7.5.3 One Dimensional Steam Injection Case

In this case, we simulate steam injection into a reservoir model to compare the performance of our model against CMG-STARS. The case is a 1-D problem that starts injecting steam with equivalent cold water 100 ft^3/day and steam mass quality 50 prcent. The injection water temperature is 378 ^oF, but the initial temperature of reservoir is 90 ^oF. Equivalent water is injected into a reservoir model that input parameters are in Table 6 4.

Figure 7-20 shows the comparison of steam saturation between CMG-STARS and UTCHEM four-phase model at different times (after 10, 60, and 80 days). There is small difference in saturation of steam between two simulators. Also, Figure 7-21 shows the comparison of temperature between CMG-STARS and UTCHEM four-phase model at different times (after 10, 60, and 80 days). Same difference can be observed in temperature as well. This plot shows that saturated temperature or boiling temperature at pressure 200 to 215 psi is 376 to 378 ^oF.

Table 7-3-Reservoir model and fluid flow properties used in one dimensional steam injection case.

Parameter	**Values in CMG-STARS and UTCHEM**
Number of gridblocks	50×1×1
Gridblock size	5×10×5 ft^3
Initial temperature	90°F
Initial pressure	200 psi (Top layer)
Number of wells	2
Initial water saturation	0.45
Temp inj.	378°F with 50% Steam quality
BHP producer	200psi
Water injection rate	100 ft^3/Day
Perm X and Por	2000 mD, and 0.2
λ and ζ_p for water	38(Btu/lb.Day.°F) and 1.0(Btu/lb.°F)
λ and ζ_p for steam	34(Btu/lb.Day.°F) and 0.65(Btu/lb.°F)
λ ,and ζ_p for oil	32(Btu/lb.Day.°F) and 0.5(Btu/lb.°F)
λ , density, and ζ_p for rock	28(Btu/lb.Day.°F),165 (lb/ft^3) and 0.5(Btu/lb.°F)

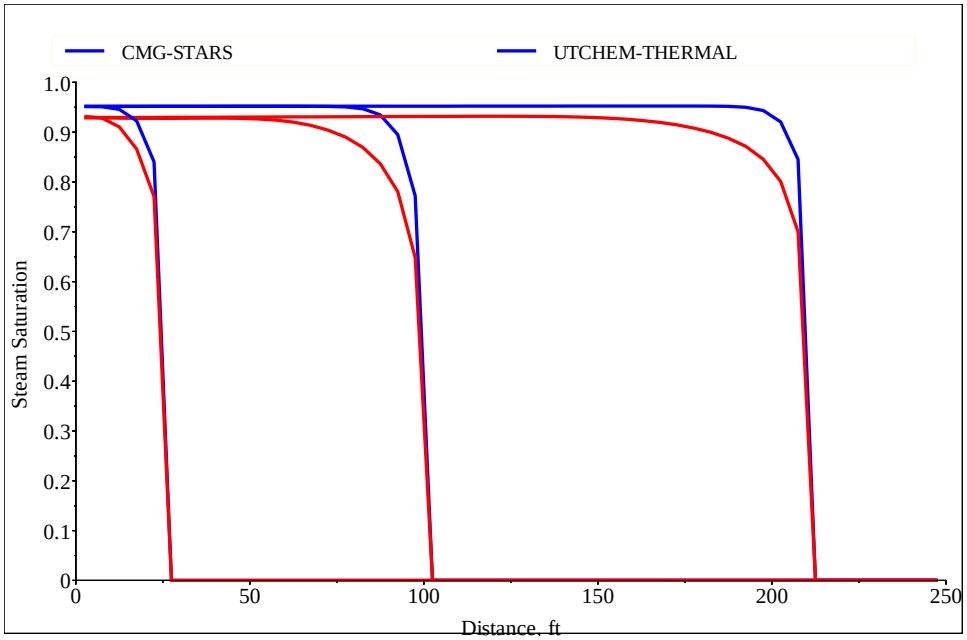

Figure 7-20- Comaprison of steam saturation between CMG-STARS and UTCHEM in different times (after 10days, 60days, and 80days) for 1D steam injection case.

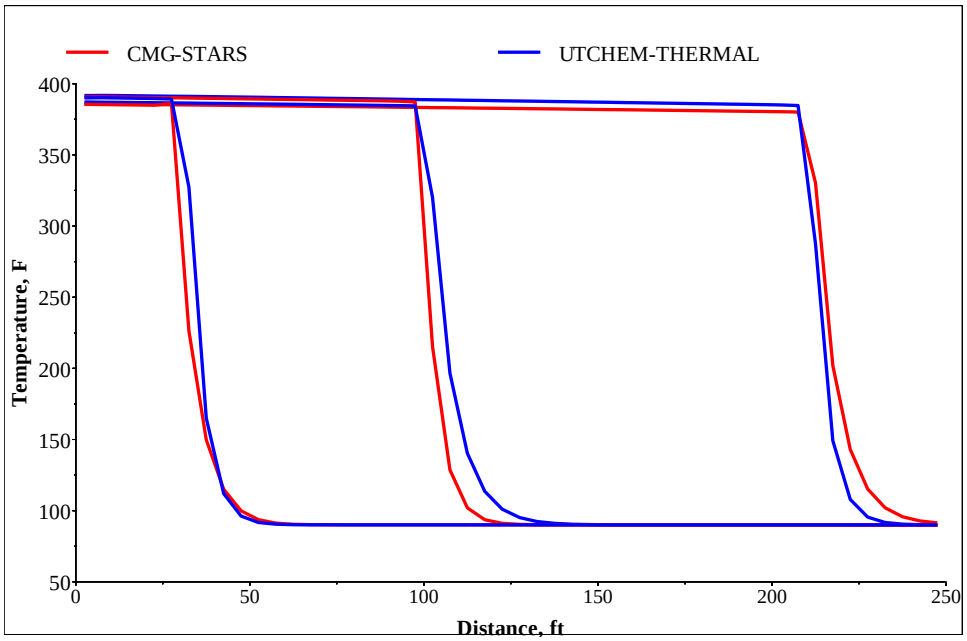

Figure 7-21-Comparison of temperature profiles between CMG-STRS and UTCHEM at different times (after 10days, 60days, and 80days) for 1D steam injection case.

.

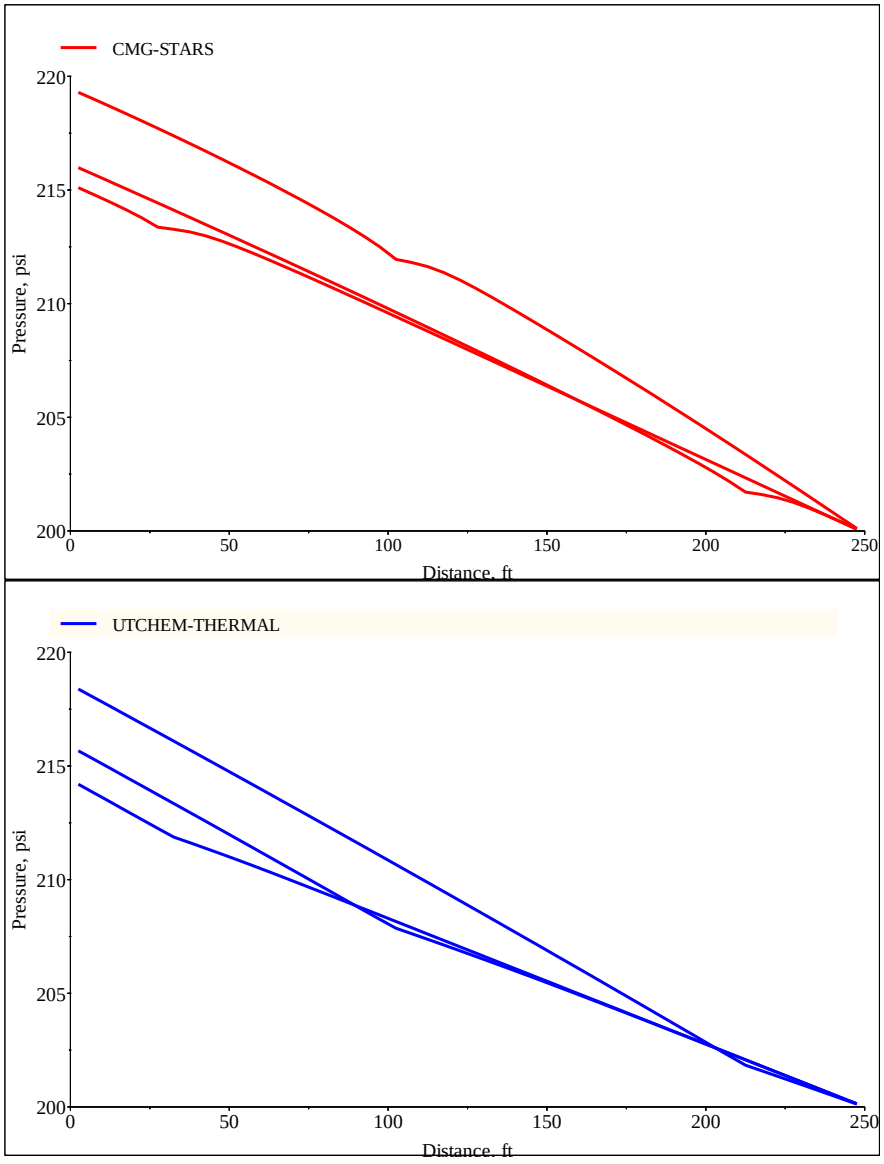

Figure 7-22-Comparison of pressure profiles between CMG-STARS (top) and UTCHEM (bottom) at different times (10, 60, and 80 days) for 1D steam injection case.

7.5.4 Two Dimensional Vertical Steam Injection Case (SAGD)

The last test case of thermal model is a two-dimensional vertical model with initial temperature 90 ^{o}F. In this case study, a Steam Assisted Gravity Drainage model (SAGD) including two horizontal wells is considered. Steam is injected with equivalent cold water 150 ft^3/day and steam mass quality 70 percent into the reservoir. Fluid flow properties such as density and viscosity values of steam and water phases are calculated from steam table directly at both simulators. Rock density and heat capacity of rock as well as thermal conductivity are the same in the both simulators. Since water and oil heat capacities in CMG-STARS are calculated inside the code using different correlation for oil and steam table for water, we read these values from the output of CMG-STARS and then we take an average of them to use for the constant values for water and oil in UTCHEM simulator. All reservoir model parameters and thermal and flow properties that are used in both simulators are summarized in Table 7-4.

In this case steam is injected through horizontal well for 2400 days. Steam condensates then latent heat energy is delivered to sourrending oil and formation. Oil viscosity reduces from 4000 cp to corresponded oil viscosity. Then heated oil and condensated water move toward producer to be produced through the bottom well. Figure 7-23 and Figure 7-24 show the comparison of temperature distribution map between both simulators after 500days, 1000 days, 1320days, and 2400days. Similar comparison has been illustrated in Figure 7-25 and Figure 7-26 for steam saturation between CMG-STARS and UTCHEM in the same days. Results of both simulators are quit reasonably close. The comparison of water production rate and heated oil production rate between both simulators are plotted in Figure 7-27and Figure 7-28.

Table 7-4- Reservoir model and fluid flow properties used in two dimensional steam vertical injection case.

Parameter	**Values in CMG-STARS and UTCHEM**
Number of gridblocks	30×1×50
Gridblock size	10×30×5 ft^3
Initial temperature	90°F
Initial pressure	100 psi (Top layer)
Number of wells	2 Horizontal
Initial water saturation	0.3
Oil viscosity	4000cp (90°F)
Temp inj.	450°F Steam quality (70%)
BHP producer	100psi
Water injection rate	150 ft^3/Day
Perm X, Z and Por	1000 mD,100mD, and 0.2
λ and ζ_p for water	38(Btu/lb.Day.°F) and 1.0(Btu/lb.°F)
λ and ζ_p for steam	34(Btu/lb.Day.°F) and 0.65(Btu/lb.°F)
λ ,and ζ_p for oil	32(Btu/lb.Day.°F) and 0.5(Btu/lb.°F)
λ , density, and ζ_p for rock	28(Btu/lb.Day.°F),165 (lb/ft^3) and 0.5(Btu/lb.°F)

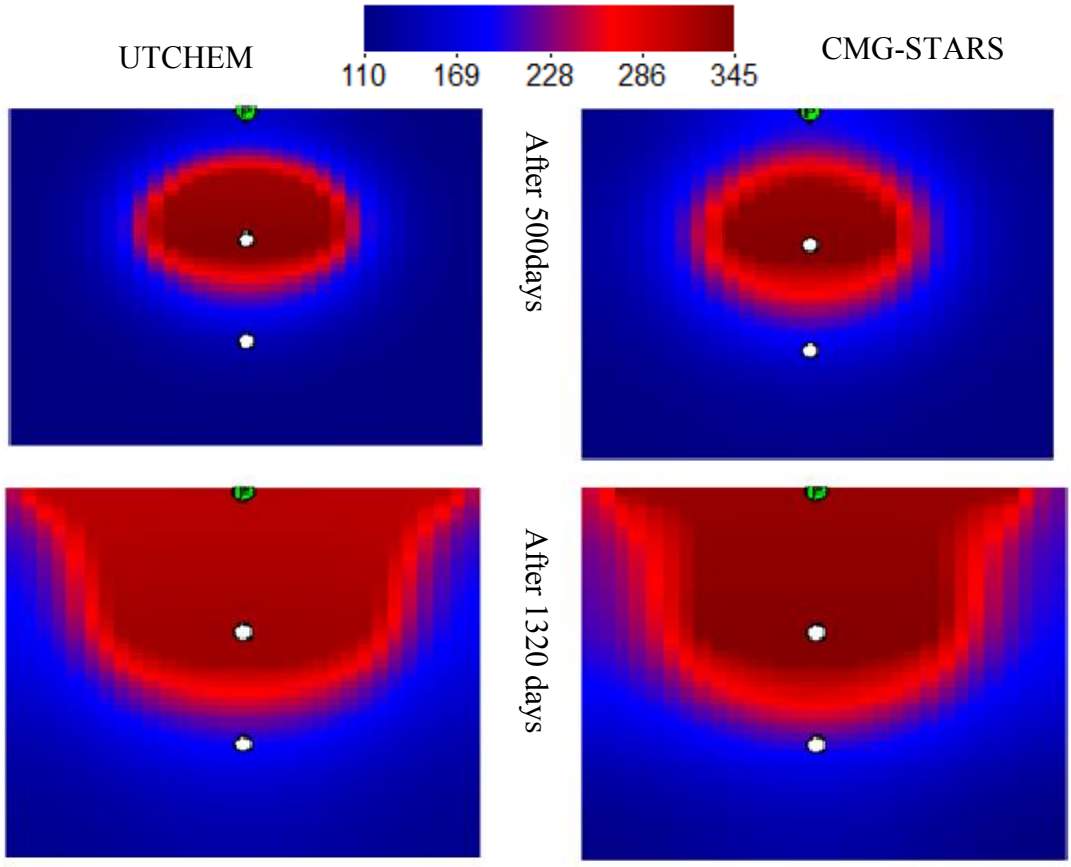

Figure 7-23-Comparisonon of temperature distribution between CMG-STARS and UTCHEM at different times (500 and 1320) for the two dimensional vertical case.

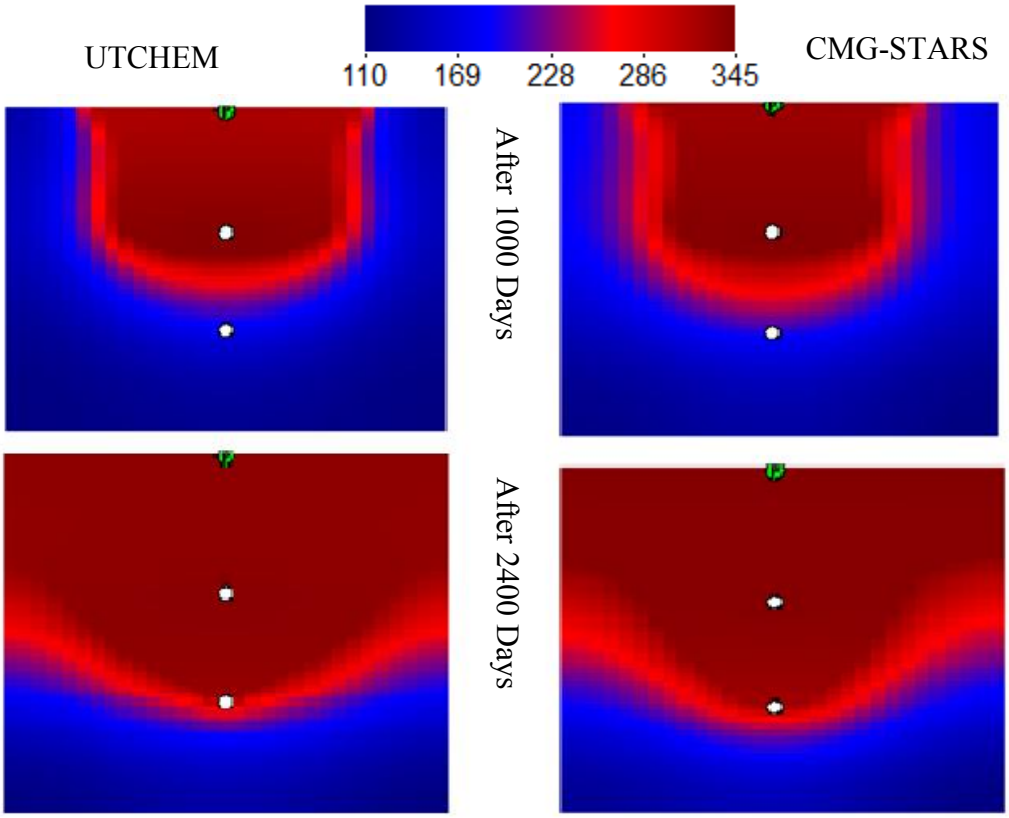

Figure 7-24-Comparisonon of temperature distribution between CMG-STARS and UTCHEM at different times (1000 and 2400) for the two dimensional vertical case.

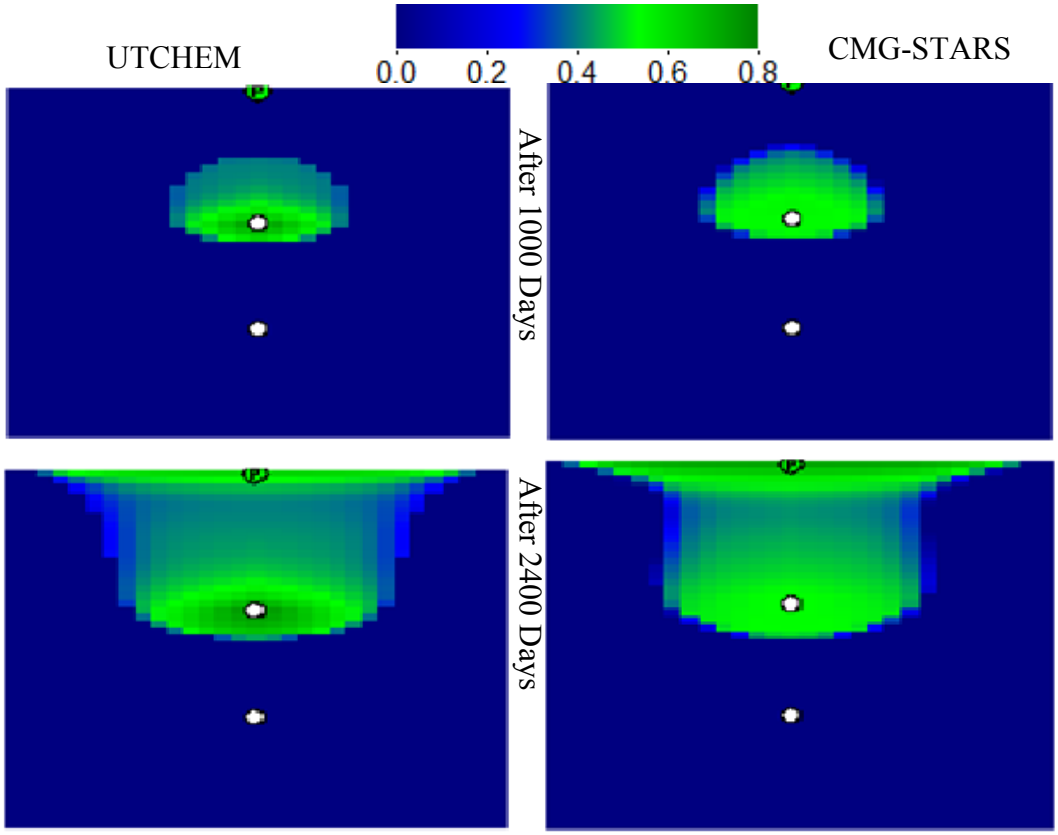

Figure **7-25**-Comparisonon of steam saturation distribution between CMG-STARS and UTCHEM at different times (500 and 1320) for the two dimensional vertical case.

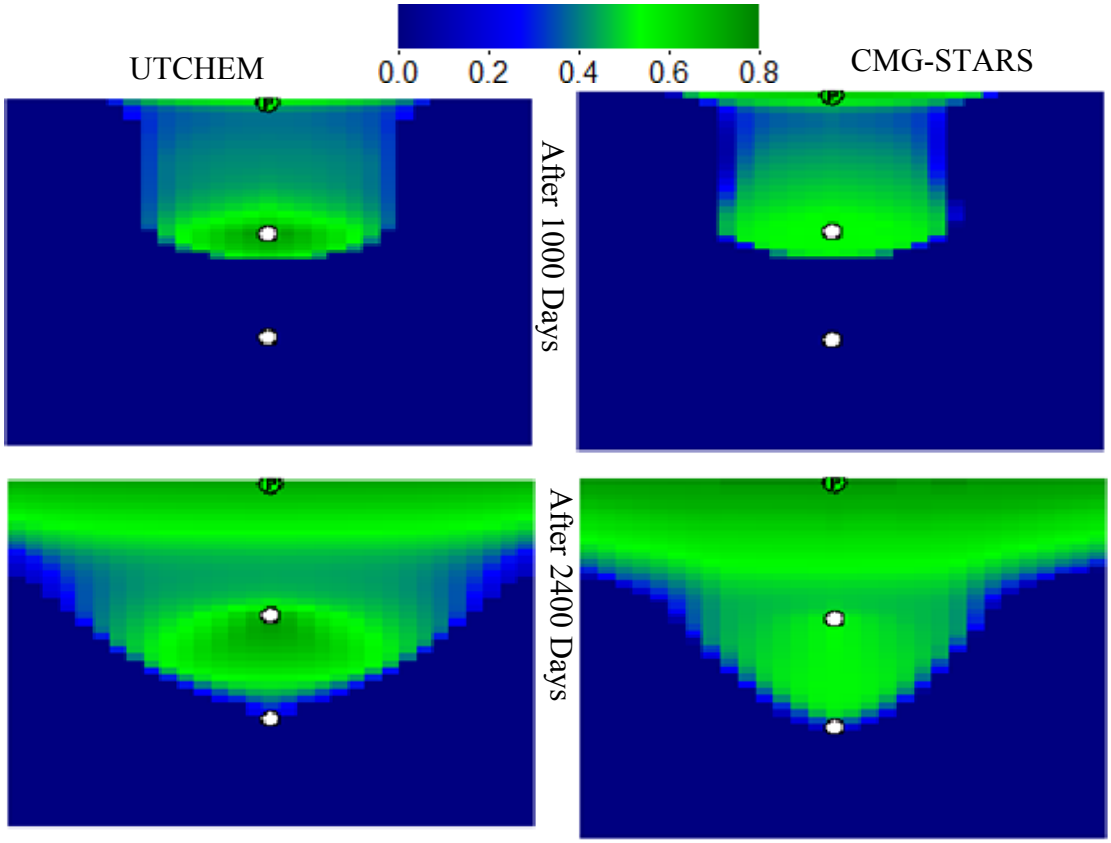

Figure 7-26-Comparisonon of steam saturation distribution between CMG-STARS and UTCHEM at different times (500 and 1320) for the two dimensional vertical case.

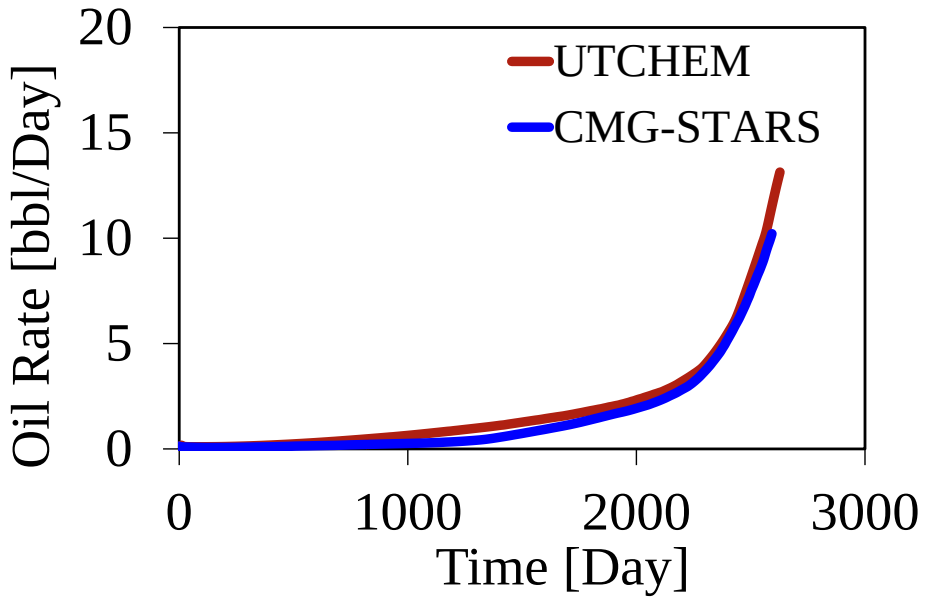

Figure 7-27-Comparison of oil production rate between CMG-STARS and UTCHEM in 2D vertical steam injection case.

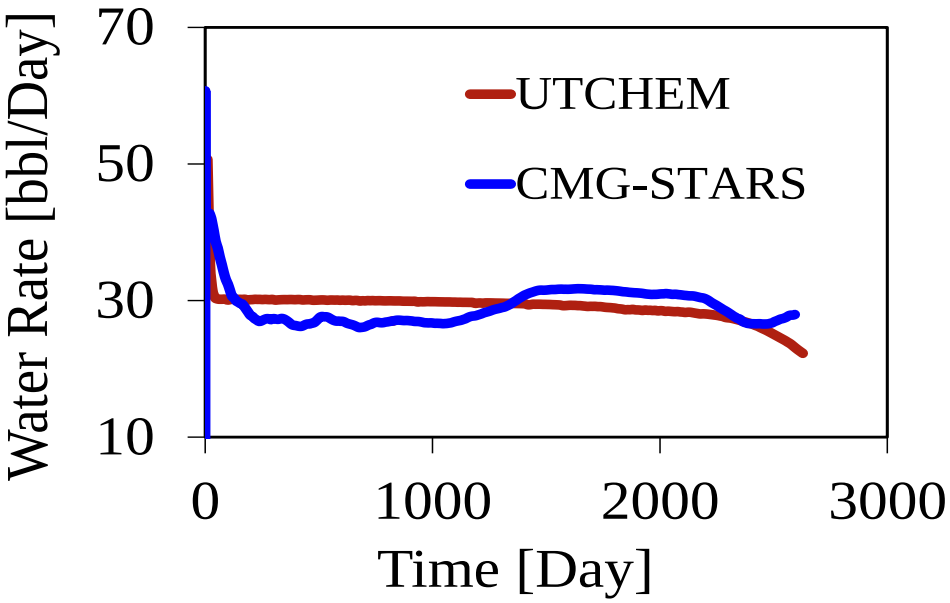

Figure 7-28- Comparison of water production rate between CMG-STARS and UTCHEM in 2D vertical steam injection case.

Chapter 8: Electrical Heating

In the electrical joule-heating process, the reservoirs are heated in-situ by dissipation of electrical energy to reduce the viscosity of oil. In principle, electrical current passes through the reservoir fluids due mostly to the electrical conductivity of saturated fluids, such as saline water. The flow of electrical current through the reservoir leads the heat in the reservoir and thereby drastically reduces the oil viscosity.

In this process, electrical current can flow between electrical potential sources (electrodes) in wells; then, electrical energy is dissipated to generate the heat. Therefore, the regions around the electrodes in the wells are extremely heated. Because the wells act as line sources for the electrical potential, greater heating takes place near the wellbore causing possible vaporization of water in that region. Since steam has very low electrical conductivity, it can reduce the efficiency of this process significantly. In this process, electrical conductivity plays a very important role. In order to increase efficiency of this type of heating process, the presence of optimum saline water saturation is an essential factor.

In order to model the electrical joule-heating in the presence of multiphase fluid flow, we use three Maxwell classical electromagnetism equations. These equations are simplified and assumed for low frequency to obtain the conservation of electrical current equation and Ohm's law. The conservation of electrical current and the Ohm's law are implemented using a finite difference method in a four phase chemical flooding reservoir simulator (UTCHEM). The Joule heating rate due to dissipation of electrical energy is calculated and added to the energy equation as a source term.

The formulation and implementation of electrical heating are validated against a reference analytical solution and a reservoir simulator. A typical reservoir model is built

and constant electrical potential with alternating current (AC) is applied to the model to study the efficiency of the electrical heating process properly. The efficiency of this process is evaluated in the presence of water saturated fractures and evaporation effect. Results illustrate that water saturation in the presence of fracture and electrical conductivity of saturated rock has an important effect on the Joule heating process.

The importance of the fractures saturated by saline water and operation of such processes below the boiling point are key findings in this dissertation to obtain high recovery in comparison to other thermal recovery methods.

8.1 INTRODUCTION

Steam injection is not always the best process for heavy oil production. This can be true for a shallow reservoir due to heat lost across the reservoir or a deep reservoir due to high heat lost along the wellbore (Bogdanov *et al.,* 2011). In order to overcome the above problems, electrical low frequency joule heating of a reservoir was presented by Amba *et al.,* (1964). This method has been proposed to improve recovery of highly viscous oil and heavy oil with API less than 20. In this process, viscous oil is heated by electrical energy to reduce the viscosity of oil. Therefore, the electric joule heating can mainly be beneficial and effective in cases where steam injection cannot be functional in deep reservoirs, low injectivity and productivity, high heat losses area, and existence of thief zones (McGee and Vermeulen, 2007a).

In this process, the electrical current passes through the reservoir fluids, where the reservoir rock and fluids are used as electrical resistance elements (Hiebert *et al.,* 1986c). In principle, the electrical current passes through the reservoir fluids due to fluid electrical conductivity, such as saline water as shown schematically in Fig.1. The flow of electrical current through the reservoir dissipates to heat form and leads to heating the

reservoir and thereby drastically reducing the oil viscosity. This type of flow can be caused by electrical potential that is applied through electrodes placed in bottomhole of production and injection wells in the presence of saline water. Therefore, electrical current flows between electrical potential sources (electrodes in wells) through the reservoir and then it is dissipated and heat is generated. But conductivity and continuity of initial water in porous media is a necessity for electrical current flow and its dissipation.

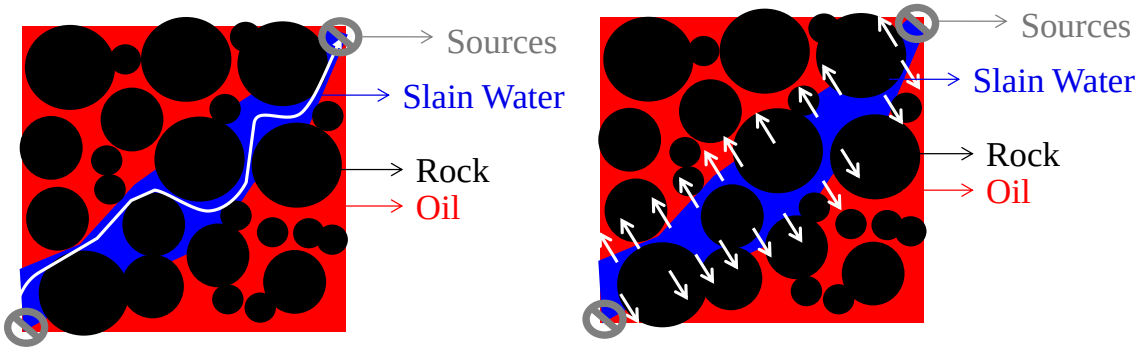

Figure 8-1-A schematic of Joule heating process in a saturated reservoir (left) dissipated electrical energy and generated Joule heating in saline water then (right) heat diffuses from water phase to surrounded oil

A number of studies have been performed in the last decades to develop laboratory experiments, pilot tests, and the modeling of electrical joule heating process. El-Feky (1977) and Harvey *et al*., (1979) studied the feasibility of heating process for heavy oil reservoirs. A set of laboratory experiments was performed to evaluate the efficiency of this process for recovery of oil in a five-spot pattern. They investigated the effect of salinity during waterflooding with and without the electrical heating. Todd and Howell (1978) implemented the electrical joule heating formulation for the radial coordinate to evaluate the electrical potential distribution, the temperature distribution, the heat flow, and the single phase flow produced by thermal expansion of reservoir

fluids. They studied the effects of resistivity, wellbore size, well temperature, and well spacing. They demonstrated that it is possible to maintain the same total energy dissipated into the reservoir for three different levels of initial electrical conductivity by adjusting the electrical potential. It was found that increasing the effective electrode radius and spacing may lead to more rapid heating. Hiebert *et al.,* (1986a) performed the electrical heating formulation in a fluid flow simulator to investigate the pre-heating process for a steam flooding purpose. He showed that electrical pre-heating can establish a fluid connectivity region between injector and producer wells. He also showed that the electric pre-heating period consists of applying a constant power of 1500 KW to the five-spot pattern for one year. The following period consisted of no heating with closed wells for two weeks, and then a steam-drive phase consisting of a sequence of steam and hot water injections over few years. Killough and Gonzales (1986) developed a fully implicit, 3D multi-component reservoir simulator capable of treating the impact of the variation of bulk reservoir electrical conductivity on temperature, water saturation, and salt content. They validated their simulator using laboratory experiences of El-Feky (1977) and with analytical models. Pizarro and Trevisan (1990) performed an interesting analysis of a pilot test in a real field. In this study, the field data was matched with numerical simulations performed with a simulator implemented by them.

McGee and Vermeulen (2007a) presented a numerical simulation study on a reservoir model that is representative of the Athabasca oil sands. They took advantage of a distributed voltage control between the electrode array and the water injection at the end of the electrodes. Water injection prevents boiling of water phase and facilitates heat distribution by flow convection mechanisms. This study was done in three main stages: the first one is a 30-day pre-heating period, followed by a 180 days heating production stage, ending with a 150 days period of production (without any electrical heating in

order to take advantage of the residual heat from previous steps). The oil production peak was observed at the beginning of the second stage. The authors concluded that the recovery factor was comparable with a successful SAGD project.

Bogdanov *et al.* (2010) studied the influence of salt concentration in recirculated water during electrical heating. They displayed that avoiding vaporization around the electrodes (wells), recirculation of saline water can increase the efficiency of heating process around 35%. In order to improve heat distribution in the reservoir during the low frequency electrical heating, water can be recycled around the electrode (McGee 2008b).

These studies in the literature have mostly reported application of the process rather than comprehensive formulation and modeling of different physics. They have not described the effect of fracture and evaporation on the effectiveness of the heating process, even though these are important factors from the operational point of view. In general, simulation of such a process is a challenging multi-physics problem that involves solving Maxwell's equations in addition to the physics of fluid flow under non-isothermal conditions. For our purposes, we have restricted its application to the low frequency regime. This allows us reducing the electromagnetic problem to solving Ohm's law and to the equation of electric current conservation. These equations are implemented using a finite difference four phase flow reservoir simulator (UTCHEM). The joule heating rate due to electrical current is calculated and added as an energy source to the energy balance equation.

In this work, we formulate and implement numerically the electrical resistance heating formulation in a four phase reservoir simulator (UTCHEM) to model vaporization phenomena around the wellbore. Then we study the influence of this phenomenon on the effectiveness of the process. Meanwhile, we evaluate the efficiency of this process in the presence of fracture saturated with saline water phase.

8.2 GOVERNING ENERGY EQUATION

We used the same expression that derived in Chapter 7 for energy balance equation. Since energy fluxes in the reservoir occur by conduction and convection; thus the energy equation with considering all possible source terms can be written as

$$\frac{\partial}{\partial t}\left[(1-\phi)\rho_r U_r + \phi\sum_{\ell=1}^{n_p}\rho_\ell S_\ell U_\ell\right] + \vec{\nabla}\cdot\left(\sum_{\ell=1}^{n_p}\rho_\ell H_\ell \vec{u}_\ell\right) - \vec{\nabla}.\left(\lambda_{eff}\vec{\nabla}T\right) \quad (8\text{-}1)$$
$$= \mp q_H \pm q_L + q_{ele} \mp q_{instu}$$

where U_r and U_ℓ are internal energy of rock and fluid phase l per unit mass, respectively, H_ℓ is enthalpy of phase per unit mass, u_ℓ is Darcy's velocity of fluid phase ℓ , ρ_r and ρ_ℓ are rock and mass density of phase ℓ , respectively. ϕ is porosity and S_ℓ is saturation of fluid phase ℓ . In Equation (1), n_p is the number of existing phases and λ_{eff} is an effective thermal conductivity. q_H is the enthalpy rate of source or sink term per bulk volume. A positive sign is assigned to q_H for a hot injection well and a negative sign is considered for a production well. q_L is the heat loss to overburden and underburden rocks. In the case of cold fluid injection where reservoir becomes colder than initial reservoir temperature, a positive sign is assigned to q_L . But in the case of hot fluid injection which increases reservoir temperature compared to initial temperature, a negative sign for q_L is considered. q_{ele} is the electrical Joule heating as source term, which is always positive. q_{instu} is in-situ thermal generator source that can be placed in the bottomhole of a well. A positive sign in front of q_{instu} is assigned for a heat source and a negative sign for a cold source. The following assumptions are made for simplification (Lake 1989):

- Neglect pressure-volume work ($H = U$) for all fluid phases.
- Neglect the dependency of enthalpies on pressure.

- Heat capacity is considered independent of temperature.
- Consider an effective thermal conductivity of all saturated fluids and rock as arithmetic weighted average as expressed in Equation (3).
- Heat-loss to overburden and underburden, q_L , is computed using Vinsome and Westerveld(1980) analytical method.

We assume that the mass transfer between water and steam phases occurs at the boiling point (saturated condition). The following equation must conserve energy during condensation and vaporization as

$$(1-\phi)\rho_r \frac{\partial H_r}{\partial t} + \phi \sum_{\ell=1}^{n_p} \rho_\ell S_\ell \frac{\partial H_\ell}{\partial t} + (\bar{H}_s - \bar{H}_w)\frac{\partial(\rho_s S_s)}{\partial t} + \left(\sum_{\ell=1}^{n_p} \rho_\ell u_\ell \vec{\nabla} H_\ell\right) + (\bar{H}_s - \bar{H}_w)\vec{\nabla}.(\rho_s \vec{u}_s) - \vec{\nabla}.\left(\lambda_{eff}\vec{\nabla}T\right) = \mp q_H \pm q_L + q_{ele} \mp q_{instu} \quad (8\text{-}2)$$

where $\bar{H}_s$ and $\bar{H}_w$ are steam and water enthalpy per unit mass; $\rho_s, \vec{u}_s$ and, S_s are density of steam phase, Darcy velocity of steam phase, and saturation of steam phase, respectively .Effective thermal conductivity is defined as

$$\lambda_{eff} = (1-\phi)\lambda_r + \phi \sum_{\ell=1}^{n_p} s_\ell \lambda_\ell \quad (8\text{-}3)$$

where λ_r is thermal conductivity of rock and λ_ℓ is thermal conductivity of phase ℓ . In addition, it is more convenient to substitute enthalpy with temperature functions based on the above assumptions. Using enthalpy definition of rock and fluid phases corresponding to reference temperature and enthalpy, (enthalpy reference of a reservoir is considered the initial temperature of reservoir in this work) it can be written as

$$\Delta H = \zeta_p \left(T - T_{ini} \right) \tag{8-4}$$

where ζ_p could be heat capacity of rock or fluid phases. Finally, the following energy equation, which is used to implement in UTCHEM to solve for temperature, becomes:

$$\left((1-\phi)\rho_r \zeta_{pr} + \phi \sum_{\ell=1}^{n_p} \rho_\ell S_\ell \zeta_{p\ell} \right) \frac{\partial T}{\partial t} + \left(\sum_{\ell=1}^{n_p} \rho_\ell \vec{u}_\ell \zeta_{p\ell} \vec{\nabla} T - \vec{\nabla} . \left(\lambda_{eff} \vec{\nabla} T \right) \right) + (\bar{H}_s - \bar{H}_w) \left(\frac{\partial (\rho_s S_s)}{\partial t} + \vec{\nabla} . (\rho_s \vec{u}_s) \right) = \mp q_H \pm q_L + q_{ele} \mp q_{instu} \tag{8-5}$$

This equation consists of accumulation, convection, and conduction terms, respectively. The difference between steam and water enthalpy per unit mass $\left(\bar{H}_s - \bar{H}_w \right)$ is called latent heat of water vaporization. This term is a multiplier for mass equation of gas phase in Equation (8-5). This equation can conserve energy in the presence of vaporization and condensation of water during mass transfer between water and steam. In order to solve this equation numerically, we consider only the latent heat term explicitly and other terms are solved implicitly (Delshad *et al.,* 1996; Lashgari *et al.,* 2014a). Since the UTCHEM simulator is an implicit in pressure and explicit in concentrations (IMPEC) simulator, at first pressure is solved at the new time level; then, the mass balance equations are solved. Water and steam properties are updated based on pressure at the new time level (n+1), concentrations, and temperature at the old time level (n), as demonstrated by the flowchart in Figure 8-2.

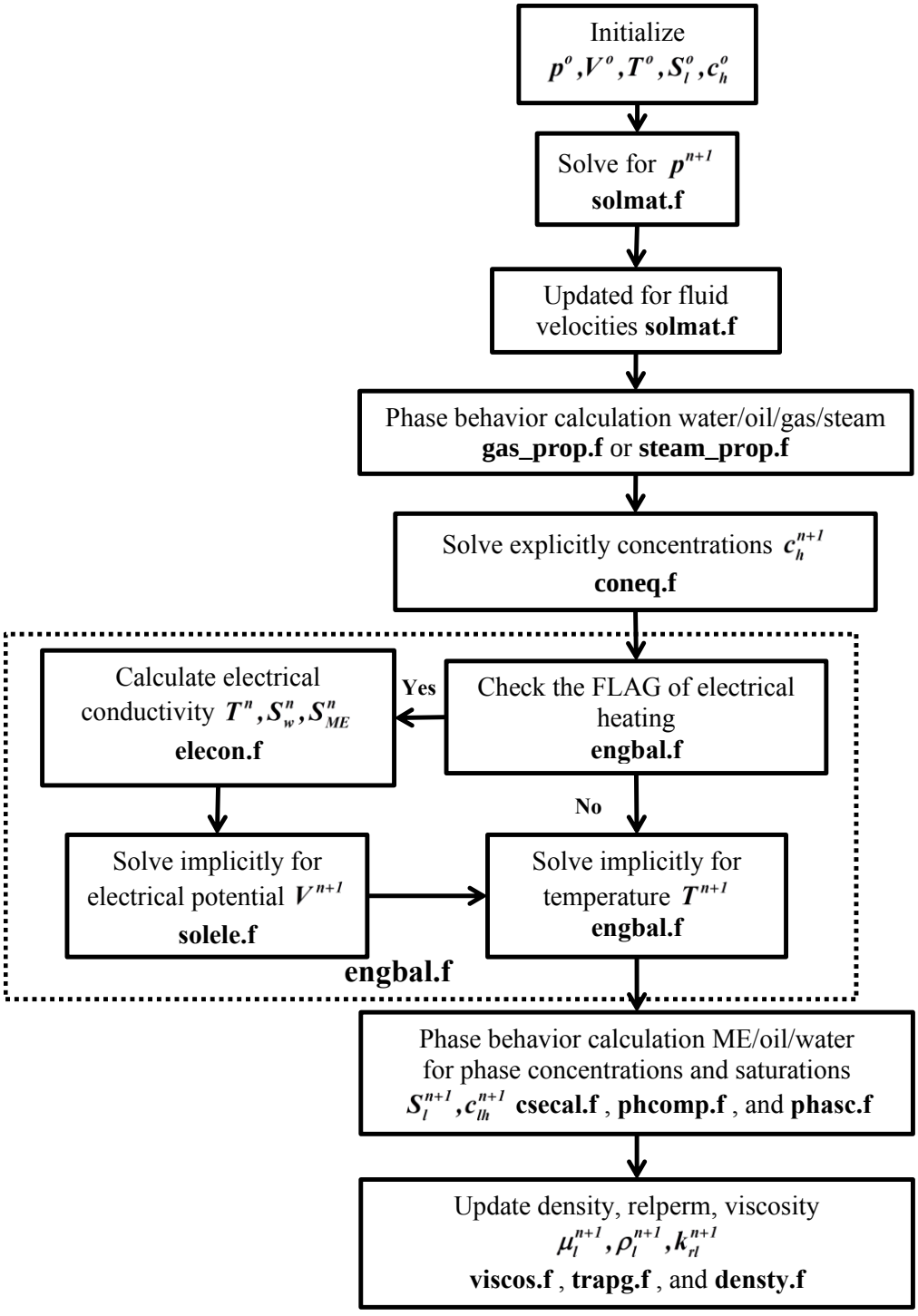

Figure 8-2-Solution-procedure flow chart for electrical Joule heating in the UTCHEM simulator.

In order to calculate phase behavior of steam and water, total enthalpy in equilibrium is obtained from energy balance equation and then steam quality is defined and written as

$$\alpha = \frac{H_{tot} - \bar{H}_w}{\bar{H}_s - \bar{H}_w} \tag{8-6}$$

These specific enthalpies, $\bar{H}_w$ and $\bar{H}_s$ of water and steam per unit mass as well as phase densities ρ_w and ρ_s , which are function of pressure and temperature, are calculated from steam table in the steam/water phase behavior calculation. c_w and c_s are the volumetric concentrations of water and steam components, respectively. H_{tot} is total enthalpy of water and steam calculated as

$$H_{tot} = \frac{\rho_s c_s \zeta_{ps}(T - T_{ini}) + \rho_w c_w \zeta_{pw}(T - T_{ini})}{\rho_s c_s + \rho_w c_w} \tag{8-7}$$

where ζ_{pw} and ζ_{ps} are heat capacity of water and steam phases, and ρ_s and ρ_w are mass density of water and steam, respectively. Based on a simple definition of mass transfer between water and steam, mass quality of steam can be also defined as

$$\alpha = \frac{(\rho_s c_s)}{(\rho_s c_s + \rho_s c_s)} \tag{8-8}$$

Equations (8-6) and (8-8) express the same content but a difference in calculation. One is obtained from the energy balance equation and the second is computed from the mass balance equation. Therefore, mass quality can be calculated first; then, since mass must be conserved in Equation (8-6), volume concentration of gas can be solved; then, use the mass balance equation to solve for water (Lashgari *et al.,* 2014b).

8.3 MATHEMATICAL MODEL

The three principle classical electromagnetism Maxwell's equations with appropriate initial and boundary conditions and material properties can be solved with the following assumption and approximations (Hiebert *et al.,* 1986a).

Anisotropy of electrical conductivity. The electrical conductivity may be anisotropic in reality, but in this formulation, we consider isotropic electrical conductivity. In some cases, the reservoir formation consists of different layers with large differences in electrical conductivity. Considering several isotropic conductivities for different rock-type for each layer is our approach to deal with the anisotropic problem.

The quasi-static approximation. The electrical conductivity, electrical permittivity, and magnetic permeability are not functions of the electric or magnetic field strengths. This assumption can be achieved by approximating the quasi-static regime for the three principle electromagnetic equations.

Low frequency assumption. Low frequency sinusoidal excitations are applied as electrical potential or electrical current into the formation as source term. Therefore, the conduction electrical current is the dominant term compared to the displacement electrical current inside the formation. Furthermore, the frequency is low enough to ignore the time varying magnetic fields that can generate the displacement electrical current.

Furthermore, the potential frequency should be low enough to ignore the displacement current; otherwise, local magnetic fields generate the displacement currents against the conduction currents. Hence, the electrical conduction current and the heating distribution are altered. For hydrocarbon reservoirs, this assumption is well-justified below a potential frequency of 1 MegaHz, and it is strongly valid in the range of 60 Hz. In this range of frequency, neglect of the displacement currents is an appropriate

assumption in the quesi-static regime. Accordingly, the time-dependence of electrical current density in Equation (8-9) can be neglected. However, the Maxwell equation that conserves electrical current is expressed as

$$\nabla.\rho\pm=\frac{\partial\rho}{\partial t} \tag{8-9}$$

where ρ is the electrical charge or the electrical current density; for quasi-static and low frequency assumptions, the time dependence of electrical current density is negligible. We use $\rho=\sigma\nabla\psi$, Ohm's law; then substitute this into Equation (8-9). Since ψ is the electrical potential (i.e. voltage), it can be a phasor with a real part and an imaginary part. The electric potential ψ is equal to $\psi_R+j\psi_I$ where ψ_R and ψ_I vary in the real domain and imaginary domain ($j^2=-1$). The electrical source term is expressed as J and it can be a phasor as well. Hence, it can be decomposed as J_R+jJ_I . The electrical conductivity σ is a diagonal tensor, with no imaginary components. But based on the first assumption, we consider an isotropic parameter in this work. Therefore, electrical conductivity changes as a scalar value.

Since the differential operator is real, Equation (8-9) is decomposed in real and imaginary domains and can be rewritten as

$$\nabla.\left(\sigma\nabla\psi\right)\pm J_R=0 \tag{8-10}$$

$$\nabla.\left(\sigma\nabla\psi\right)\pm J_I=0 \tag{8-11}$$

In the case of a three dimensional Cartesian grid, the equation for real and imaginary components are

$$\frac{\partial}{\partial x}\left(\sigma_x \frac{\partial \psi_R}{\partial x}\right)+\frac{\partial}{\partial y}\left(\sigma_y \frac{\partial \psi_R}{\partial y}\right)+\frac{\partial}{\partial z}\left(\sigma_z \frac{\partial \psi_R}{\partial z}\right)\pm J_R = 0 \tag{8-12}$$

$$\frac{\partial}{\partial x}\left(\sigma_x \frac{\partial \psi_I}{\partial x}\right)+\frac{\partial}{\partial y}\left(\sigma_y \frac{\partial \psi_I}{\partial y}\right)+\frac{\partial}{\partial z}\left(\sigma_z \frac{\partial \psi_I}{\partial z}\right)\pm J_I = 0 \tag{8-13}$$

Electrical conductivity σ depends on temperature, salinity, and the amount of water, but in this model we do not consider the effect of salinity. Thus, σ and ψ may vary slowly with time. This dependence couples the current equations, hence the electrical potential, to the fluid and reservoir properties. I case all source terms are zero the result for electrical potential is zero everywhere, in which case the conservation of electrical current does not need to be solved. This applies to non-alternating as well as single-phase alternating cases (Hiebert *et al.,* 1986b). Electrical energy due to formation resistivity is dissipated in water phase as thermal energy. The heating rate is calculated from Joule's law as

$$q_{ele} = \sigma_x\left(\frac{\partial \psi_R}{\partial x}\right)^2+\sigma_y\left(\frac{\partial \psi_R}{\partial y}\right)^2+\sigma_z\left(\frac{\partial \psi_R}{\partial z}\right)^2+ \sigma_x\left(\frac{\partial \psi_I}{\partial x}\right)^2+\sigma_y\left(\frac{\partial \psi_I}{\partial y}\right)^2+\sigma_z\left(\frac{\partial \psi_I}{\partial z}\right)^2 \tag{8-14}$$

This heating rate couples the fluid and reservoir conditions to the electrical potential as shown in the energy equation. Essentially, this rate should be added to energy equation at each point of the reservoir as source of energy to heat the reservoir. Electrical conductivity as mentioned earlier plays an important role during the generation of Joule heat. In order to calculate saturated electrical conductivity of reservoir, electrical conductivity of water phase is obtained from Archie's law; rock, oil, and steam are considered non-conductive

$$\sigma_w\left(T,\phi,S_w\right)=\sigma_w\left(T\right)\frac{\phi^m S_w^n}{a} \text{ Archie's law n=2,m=1.37, a=0.88} \quad (8\text{-}15)$$

$$\sigma_o\left(T,\phi,S_o\right)\approx 0 \quad (8\text{-}16)$$

$$\sigma_{steam}\approx 0 \;\; and \;\; \sigma_{rock}\approx 0 \quad (8\text{-}17)$$

Although, n, m and **a** are considered constant in this work, important factors, such as wettability, pore size distribution, and geological properties, affect these parameters and lead to a change in electrical conductivity. Therefore, a change in electrical conductivity can cause a change in the efficiency of electrical heating process. Wettability is an important factor affecting the saturation exponent in Equation (8-15). In water- wet rocks, the exponent is typically around 2.0. However, in oil-wet rocks, the exponent can increase to rather high values as the water saturation decreases (Peters 2012). This can also be varied in sandstone and carbonate rocks. Porosity exponent and denominator a are influenced by geology, such as cementation and compactions in different rock types. However, the saturated electrical conductivity is calculated as

$$\sigma_{sat}\left(T,\phi,S_w\right)=\sigma_w\left(T,\phi,S_w\right) \quad (8\text{-}18)$$

As discussed in the section concerning assumptions, we consider electrical conductivity to be isotropic, $\sigma_x=\sigma_y=\sigma_z$. Instead of using electrical conductivity, we use electrical resistivity that can be computed from Equation (8-19). Electrical resistivity (R) is a function of geometrical shape as electrical current passes through length $d\ell$ with area A, as shown schematically in Figure 8-3.

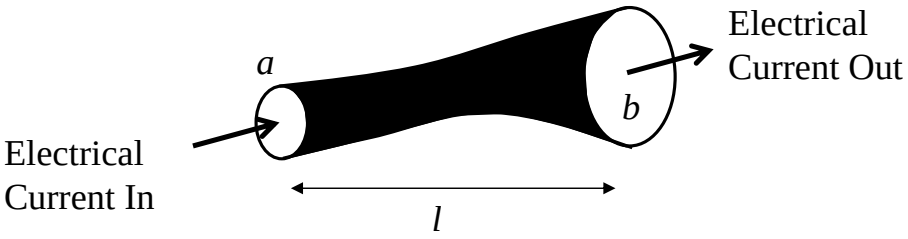

Figure 8-3-A schematic of electrical current through a control volume

Electrical resistivity may not be the same in all three directions (x, y, and z) because of the shape, the length, the width, and the height of gridblock; thus, it can be obtained from

$$\boldsymbol{R} = \int \frac{\boldsymbol{d\ell}}{\boldsymbol{\sigma A}} \tag{8-19}$$

Considering a constant surface area with isotropic electrical conductivity, Equation (8-19) is expressed as

$$\boldsymbol{R} = \frac{\boldsymbol{\ell}}{\boldsymbol{\sigma A}} \tag{8-20}$$

where ℓ is length of control volume and A is a constant surface open to electrical current flow.

8.4 NUMERICAL MODEL

In this section, mathematical model equations are substituted and discretized to numerically solve for electrical potential or voltage. Figure 8-4 shows a schematic of the center of gridblock with resistivity in x and y directions.

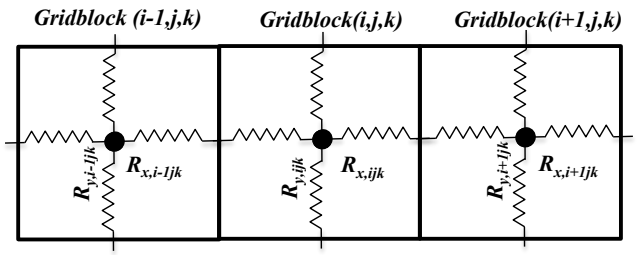

Figure 8-4-A schematic of a gridblock (ijk) with two neighbor gridblocks in x direction that considered electrical resistance elements in x and y directions.

Ohm's law is substituted into the conservation of electrical current and then conservations of current in Equations (8-10) and (8-11) are discretized for a gridblock ***(ijk)*** as

$$\frac{V_{ijk-1}-V_{ijk}}{R_{zijk-1}+R_{zijk}}+\frac{V_{ij-1k}-V_{ijk}}{Ry_{ij-1k}+R_{y,ijk}}+\frac{V_{i-1jk}-V_{ijk}}{R_{x,i-1,j,k}+R_{x,ijk}}- \\ \frac{V_{ijk}-V_{i+1jk}}{R_{x,ijk}+R_{xi+1jk}}-\frac{V_{i,j,k}-V_{ij+1k}}{R_{yijk}+R_{y,ij+1k}}-\frac{V_{ijk}-V_{ijk+1}}{R_{z,ijk}+R_{z,jk+1}}_{i}=BV_{ijk} \tag{8-21}$$

where V_{ijk} is the electrical potential or the voltage of a gridblock (ijk) and the right hand side, BV_{ijk}, consists of a source term for real or imaginary parts expressed as

$$BV_{ijk}=\begin{cases} I_{ijk}^{well} & For\ constant\ \ electrical\ current \\ \left(\frac{1}{R_{x,ijk}}+\frac{1}{R_{y,ijk}}+\frac{1}{R_{z,ijk}}\right)V_{ijk}^{well} & For\ constant\ \ electrical\ \ potential \end{cases} \tag{8-22}$$

where I_{ijk}^{well} is electrical current of electrodes applied under constant current to a reservoir. The detail is discussed in the boundary condition section. In order to solve the above equation, it is rearranged as

$$\frac{1}{R_{z,ijk-1}+R_{z,ijk}}V_{ijk-1}+\frac{1}{R_{y,ij-1k}+R_{y,ijk}}V_{ij-1k}+\frac{1}{R_{x,i-1jk}+R_{x,ijk}}V_{i-1jk}+$$
$$\left(-\frac{1}{R_{z,ijk-1}+R_{z,ijk}}-\frac{1}{R_{y,ij-1k}+R_{y,ijk}}-\frac{1}{R_{x,i-1jk}+R_{x,ijk}}\right.$$
$$\left.-\frac{1}{R_{xijk}+R_{x,i+1jk}}-\frac{1}{Ry_{ijk}+R_{y,ij+1k}}-\frac{1}{R_{z,ijk}+R_{z,ijk+1}}\right)V_{ijk}+ \qquad (8\text{-}23)$$
$$\frac{1}{R_{x,ijk}+R_{x,i+1jk}}V_{i+1jk}+\frac{1}{R_{y,ijk}+R_{y,ij+1k}}V_{ij+1k}+\frac{1}{R_{z,ijk}+R_{z,ijk+1}}V_{ijk+1}$$
$$=BV_{ijk}$$

Afterward, the above equation is converted to a system of linear equations for entire gridblocks as

$$\begin{bmatrix} AC_{111} & AE_{211} & \cdots & AS_{121} & 0 & \cdots & AB_{211} & 0 & \cdots & 0 \\ AW_{111} & & & & & & & & 0 & \vdots \\ \vdots & & & & & & & & & 0 \\ AN_{111} & & & & & & & & & AB_{NxNyNz} \\ 0 & & & & & & & & & \vdots \\ \vdots & & & & & & & & & 0 \\ AT_{111} & & & & & & & & & AS_{NxNyNz} \\ 0 & & & & & & & & & \vdots \\ \vdots & 0 & & & & & & & & AE_{NxNyNz} \\ 0 & \cdots & 0 & AT_{NxNyNz-1} & & & AN_{NxNy-1Nz} & & AW_{Nx-1NyNz} & AC_{NxNyNz} \end{bmatrix} \begin{bmatrix} V_{111} \\ V_{211} \\ \vdots \\ V_{Nx11} \\ \vdots \\ \vdots \\ V_{NxNy-1Nz} \\ \vdots \\ V_{Nx-1NyNz} \\ V_{NxNyNz} \end{bmatrix} = \begin{bmatrix} BV_{111} \\ BV_{211} \\ \vdots \\ BV_{Nx11} \\ \vdots \\ \vdots \\ BV_{NxNy-1Nz} \\ \vdots \\ BV_{Nx-1NyNz} \\ BV_{NxNyNz} \end{bmatrix} \qquad (8\text{-}24)$$

where AC is main diagonal coefficient for gridblock (ijk), at the same row, AW is coefficient of neighbor gridblock (i-1jk), AN is coefficient of neighbor gridblock (ij -1k), AT is coefficient of neighbor gridblock (ijk-1), AE is coefficient of neighbor gridblock (i+1jk), AS is coefficient of neighbor gridblock (ij+1k), and AB is coefficient of neighbor gridblock (ijk+1). This matrix can be written for a gridblock (ijk) as

$$AT_{ijk}\,V^{n+1}_{ijk-1} + AN_{ijk}\,V^{n+1}_{ij-1k} + AW_{ijk}\,V^{n+1}_{i-1jk} + AB_{ijk}\,V^{n+1}_{ijk+1} + AS_{ijk}\,V^{n+1}_{ij+1k} + AE_{ijk}\,V^{n+1}_{i+1jk} + AC_{ijk}V^{n+1}_{ijk} = BV^{n}_{ijk} \tag{8-25}$$

All coefficients are calculated at the old time level for each gridblock. Therefore, the system of algebraic equations is solved for the electrical potential or the voltage at the new time level (n+1). This system of linear equations is expressed in a form using matrix and vector notation as follows:

$$\bar{\bar{A}}^{n}\vec{V}^{n+1} = \vec{b}^{n+1} \tag{8-26}$$

where $\bar{\bar{A}}$ is a real coefficient matrix with seven diagonal with dimension(NxNyNz , NxNyNz) and $\vec{V}^{n+1}$ is unknown vectors, but it is complex. $\vec{b}^{n+1}$ is the right hand side known vector which includes source terms at the present time and it is a complex vector. Both vectors have the dimension (NxNyNz). Since vectors are in the complex domain, to solve the complex system of linear equations, we transfer these linear equations to a real domain and solve for imaginary and real parts as the follow:

$$\begin{bmatrix} \bar{\bar{A}}^{n} & 0 \\ 0 & \bar{\bar{A}}^{n} \end{bmatrix}\begin{bmatrix} Re\left(\vec{V}^{n+1}\right) \\ Im\left(\vec{V}^{n+1}\right) \end{bmatrix} = \begin{bmatrix} Re\left(\vec{b}^{n+1}\right) \\ Im\left(\vec{b}^{n+1}\right) \end{bmatrix} \tag{8-27}$$

where Re is an operator that selects the real part of vectors $\vec{V}$ and $\vec{b}$. Besides Im is an operator that choses imaginary part of vectors $\vec{V}$ and $\vec{b}$. The solution methods using the different solver with different algorithms are not discussed in this work.

When voltage is solved, we use Joule's law to calculate the heat rate. Thus, Joule's law is discretized for a gridblock (ijk) as in

$$q_{ele,ijk} = \begin{pmatrix} I^2_{i\to i+1\,jk}\, R_{x,i\to i+1\,jk} + I^2_{i\to i-1\,jk}\, R_{x,i\to i-1\,jk} + \\ I^2_{ij\to j+1k}\, R_{z,ij\to j+1k} + I^2_{ij\to j-1k}\, R_{y,ij\to j-1k} + \\ I^2_{ijk\to k+1}\, R_{y,ijk\to k+1} + I^2_{ijk\to k-1}\, R_{z,ijk\to k-1} \end{pmatrix} \tag{8-28}$$

where for instance, $I_{i\to i+1\,jk}$ is the electrical current that flows from gridblock i to i+1 and this current can be impaired by resistivity of corresponding gridblocks in the x direction. Therefore $R_{x,i\to i+1\,jk}$ is defined as

$$R_{x,i\to i+1\,jk} = \frac{R_{x,ijk} + R_{x,i+1\,jk}}{2} \tag{8-29}$$

Similar definition is considered for electrical current at the boundary of gridblocks and calculation is performed for electrical resistivity that dissipated the electrical energy to generate heat between neighbor gridblocks. We use Equation (8-22) and discretize resistivity in x, y, and z directions (Rx, Ry, and Rz) for gridlock (ijk) as

$$R_{x,ijk} = \frac{\Delta x_{ijk}}{\sigma_{sat,ijk}\Delta y_{ijk}\Delta z_{ijk}} \tag{8-30}$$

$$R_{y,ijk} = \frac{\Delta y_{ijk}}{\sigma_{sat,ijk}\Delta x_{ijk}\Delta z_{ijk}} \tag{8-31}$$

$$R_{z,ijk} = \frac{\Delta z_{ijk}}{\sigma_{sat,ijk}\Delta y_{ijk}\Delta x_{ijk}} \tag{8-32}$$

8.5 BOUNDARY CONDITIONS

This section describes the numerical form of inner and outer boundary conditions as boundary. For the outer boundary condition, we consider a close outer boundary similar to fluid flow outer boundary. This means that electrical current at outer boundary is zero, since boundaries are closed. But in the case of inner boundary (electrical sources

or electrodes), two types of constraints are considered in this formulation. The first constraint is constant current which is applied to electrodes and the second constraint is the constant electrical potential or constant voltage. For the first constraint, the constant current is considered directly in the right hand side $\boldsymbol{BV_{ijk} = I_{ijk}^{well}}$.

In the second constraint, that is constant voltage, we need to evaluate the source or the electrode effect as in the following equation

$$\boldsymbol{I_{ijk}^{well} = \left(\frac{1}{R_{x,ijk}} + \frac{1}{R_{y,ijk}} + \frac{1}{R_{z,ijk}} \right) V_{ijk}^{n+1} - \left(\frac{1}{R_{x,ijk}} + \frac{1}{R_{y,ijk}} + \frac{1}{R_{z,ijk}} \right) V_{ijk}^{well}} \tag{8-33}$$

Then, the resistivity term of unknown voltage in the above equation is added to the main diagonal coefficient (AC) of a well gridblock (ijk). The rest of terms in Equation (8-33) are added to the right hand side of the well gridblock (ijk) as expressed in Equation (8-24).

8.6 SOLUTION PROCEDURE

In this study, we coupled the solution of the electrical potential (i.e. voltage) with fluid flow solution. The simulator first initializes electrical potential similar to other fluid flow properties. Then pressure and concentrations are calculated. The electrical conductivity is updated for the new time level before temperature solution and saturation calculations. Subsequently, electrical potential is solved and the electrical current flow and the dissipated electrical energy are calculated from the electrical potential distribution. Electrical heating is the source term for the energy equation in temperature calculation. All finite difference equations are solved for pressure implicitly, for concentration explicitly, for electrical potential implicitly, and a sequential implicit scheme is used for calculation of temperature as shown in Figure 8-2.

8.7 NUMERICAL SIMULATION RESULTS

8.7.1 Validation of Test Cases

In this section, two test cases are considered to validate and verify the mathematical formulation, numerical approach, and results against a simple available analytical solution and a Computer Modeling Group (CMG-STARS) simulator.

8.7.1.1 Comparison of analytical solution and simulation results.

A simple 1-D case is setup for UTCHEM to model voltage and heat rate in a reservoir with two wells or electrodes. The reservoir dimension is 200ft×10ft×20ft in x, y, and z directions, respectively. Twenty gridblocks are considered in the UTCHEM simulator to compare results with analytical solution results.

Constant voltage (220 vol) with electrical phases 0o and 180o is applied to the reservoir through electrodes located in the bottomhole of the wells. A constant electrical resistivity is considered for the entire reservoir (100Ω). Figure 8-5a shows the results of the voltage profile comparison between the analytical and the UTCHEM simulator results. Voltage has a constant slop due to constant electrical resistivity. Hence, electrical current that is calculated from Ohm's law is constant as well. Therefore, dissipated electrical energy is uniform since resistivity is constant (4Wat-ft) as shown Figure 8-5b. This figure also shows the comparison of electrical heat rate between analytical and simulation results.

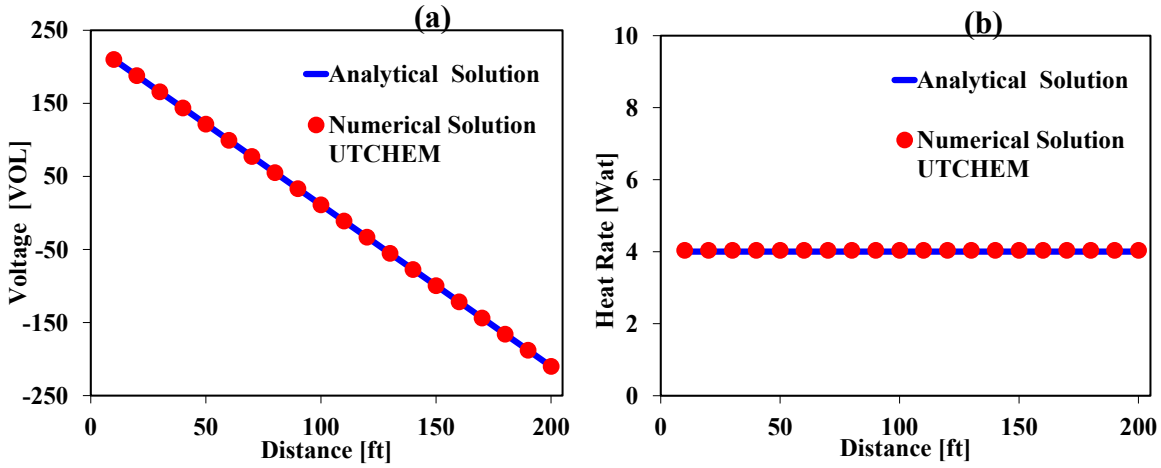

Figure 8-5- Comparison of voltage and electrical heat rate profile results in constant electrical resistivity.

8.7.1.2 Comparison of numerical simulation results.

A 2-D case is used to compare the UTCHEM and the CMG-STARS results. In this case, a vertical section of a heavy oil reservoir sealed by cap rocks in top and bottom with three horizontal wells (two wells are located in top and a well in bottom) is considered. A three electrical phase configuration for the electrical heating is used in this case. Three electrodes are placed in the bottomhole of the wells at the vertices of an equilateral triangle with electrical potentials at 220vol, but differing in phase by 120° (0°, 120°, 240°). Electrical potential 220vol is applied with electrical phases (0°, 120°, 240°) to heat the reservoir. Initial oil viscosity of reservoir is 4700cp (at 60°F); the oil viscosity against temperature is plotted in Figure 8-6. Electrical conductivity model in UTCHEM is calculated from Equation (8-22), but it is slightly different from the electrical conductivity model in CMG-STARS. The reservoir model parameters and fluid properties are summarized in Table 8-1 and thermal and electrical properties of reservoir are given in Table 8-2. Two-phase flow (oil and water) is considered in the case; it was run by UTCHEM and CMG-STARS.

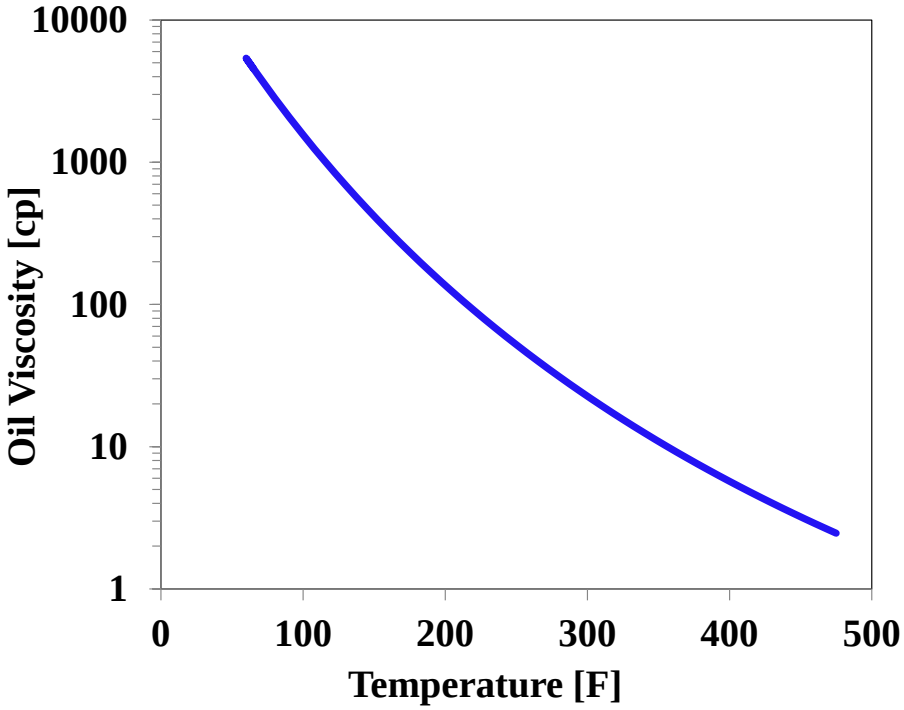

Figure 8-6-The effect of temperature on oil viscosity for all cases.

Table 8-1-Reservoir model and fluid flow properties used in all cases.

Reservoir Model	
Reservoir Size	39ftx10ftx37ft
Number of Gridblock	77x1x73
Gridblock Size	0.5ftx10ftx0.5ft
Porosity	0.3(reservoir layers), 0.01(seal layers)
Permeability in X and Z	1000 mD, 100mD (reservoir layers) 0.01 mD, 0.01mD (seal layers)
Thickness	8.75ft (top seal layer) 19.5ft (reservoir) 8.75ft (bottom seal layer)
Basic Rock and Fluid Properties	
Water Compressibility	$1x10^{-6}$
Water Rel. Perm	rsat=0 , endpt.=1.0 exp=1.0
Oil Rel. Perm	rsat=0 , endpt.=1.0 exp=1.0
Gas Rel. Perm	rsat=0 , endpt.=1.0 exp=1.0
Rock Compressibility	0.0
Initial Pressure	250 psi(top layer)
Initial Saturations	0.3(reservoir layers), 0.01(seal layers)
Well	
Number of Wells	2prod.(top wells) and 1 inj.(bottom well)
Well Constrains	2prod (BHP=100psi) 1Inj (Const. Water Rate= 10 ft^3/day)
Applied electrical potential	220 vol (0, 120, 240 degree)

Table 8-2-Thermal and electrical properties for all cases.

Thermal Properties	
λ and ζ_p for water	38 (Btu/ft.Day.F) and 1.0(Btu/lb.F)
λ and ζ_p for steam	38 (Btu/ft.Day.F) and 0.65(Btu/lb.F)
λ and ζ_p for oil	32 (Btu/ft.Day.F) and 0.5(Btu/lb.F)
λ density, and ζ_p for rock	28 (Btu/ft.Day.F),165 (lb/cu.ft),0.25 (Btu/lb.F)
Electrical Properties	
Electrical conductivity at **80 (^{o}F)**	water 2 (sem/m), oil 0.01((sem/m), steam 0.0 (sem/m)
Electrical conductivity at **150 (^{o}F)**	water 6 (sem/m), oil 0.05((sem/m), steam 0.0 (sem/m)
Electrical conductivity at **600 (^{o}F)**	water 7.5 (sem/m), oil 0.09((sem/m), steam 0.0 (sem/m)

The reservoir is electrically heated for 50 days and voltage magnitude, electrical phase distribution, imaginary and real component of voltage are plotted in Figure 8-7. Results show a good agreement between the two simulators. Real and imaginary parts of voltage are plotted for both simulators. Electrical phases also satisfy inner boundary conditions in the well locations, which both simulator results are in good agreement. Figure 8-8 shows the electrical conductivity of the entire field on day 50. As can be seen, the top and bottom layers (cap rocks) due to low porosity have low electrical conductivity. However, the reservoir layer, because of high porosity and water saturation, becomes high conductive. Since an increase in temperature leads to an increase in the electrical conductivity, reservoir conductivity is being increased within 50 days as shown in. Therefore, the hottest gridblocks are at the well locations as shown in Figure 8-9. Temperature around the wellbore increases up to 500^{o}F in both simulators and this causes a significant reduction in oil viscosity from 4700cp to 1cp.

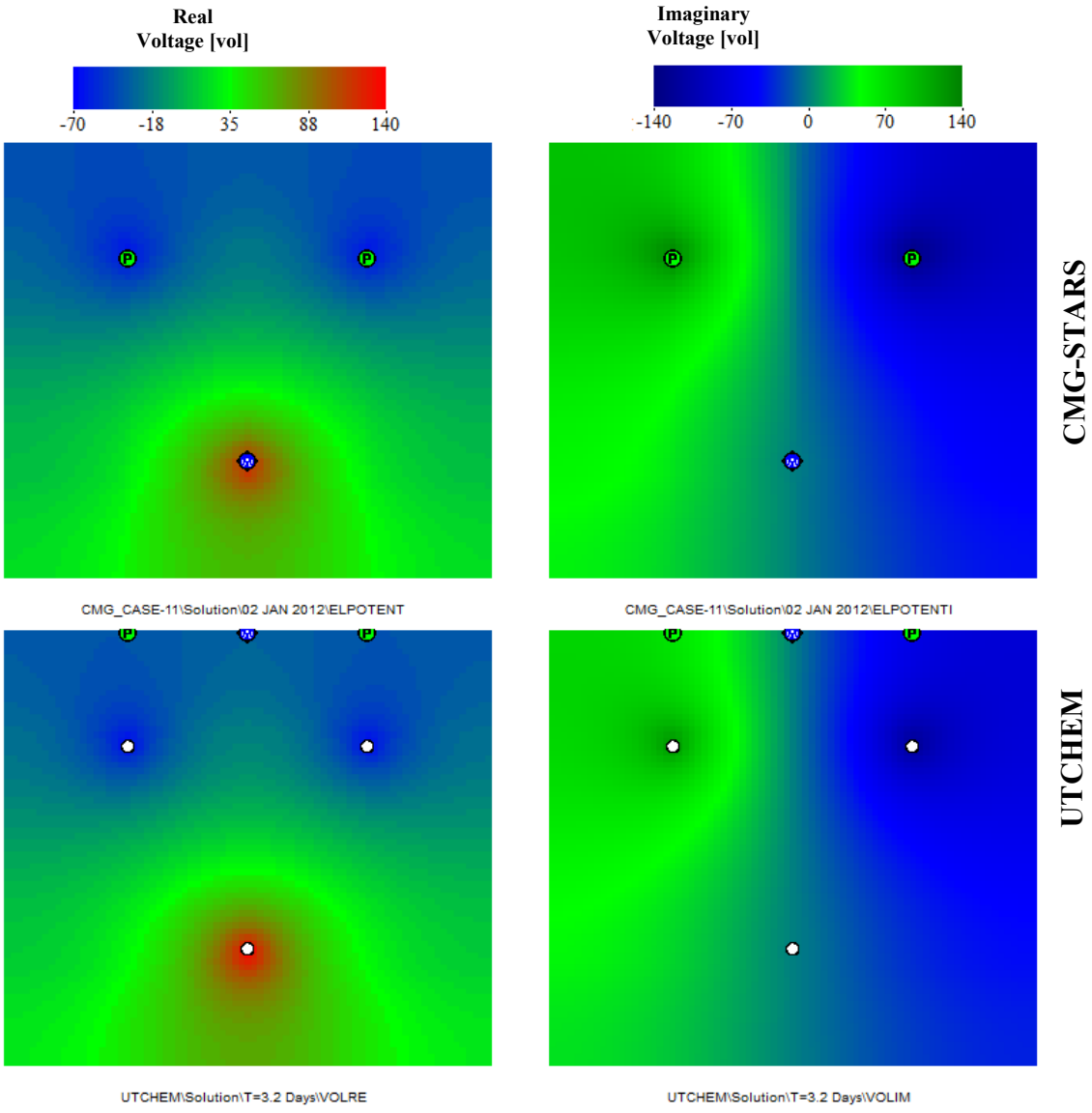

Figure 8-7-Comparison of real voltage and imaginary voltage results between CMG-STARS and UTCHEM after 50days.

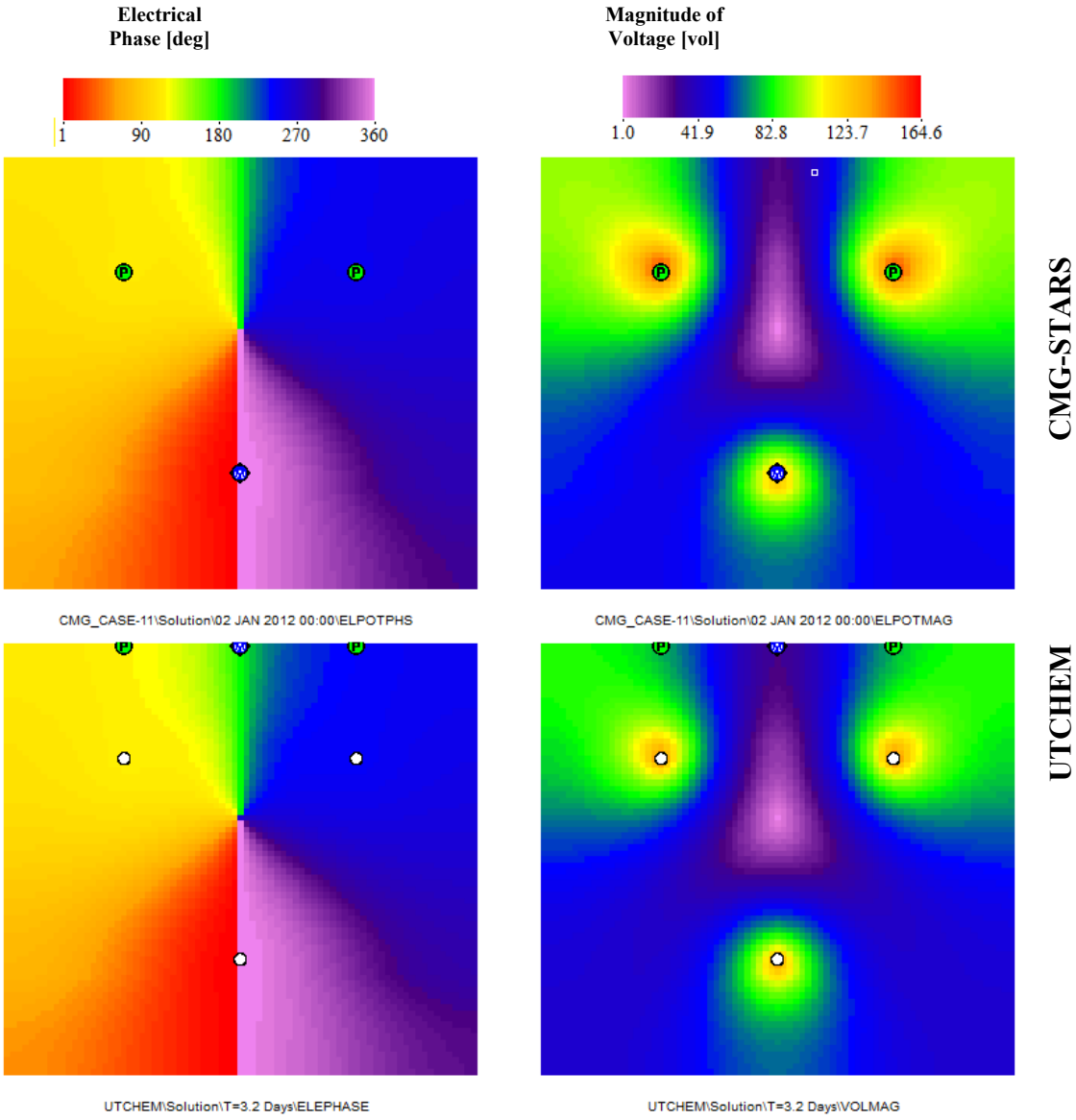

Figure 8-8-Comparison of electrical phase and magnitude of voltage, distribution results between CMG-STARS and UTCHEM after 50days.

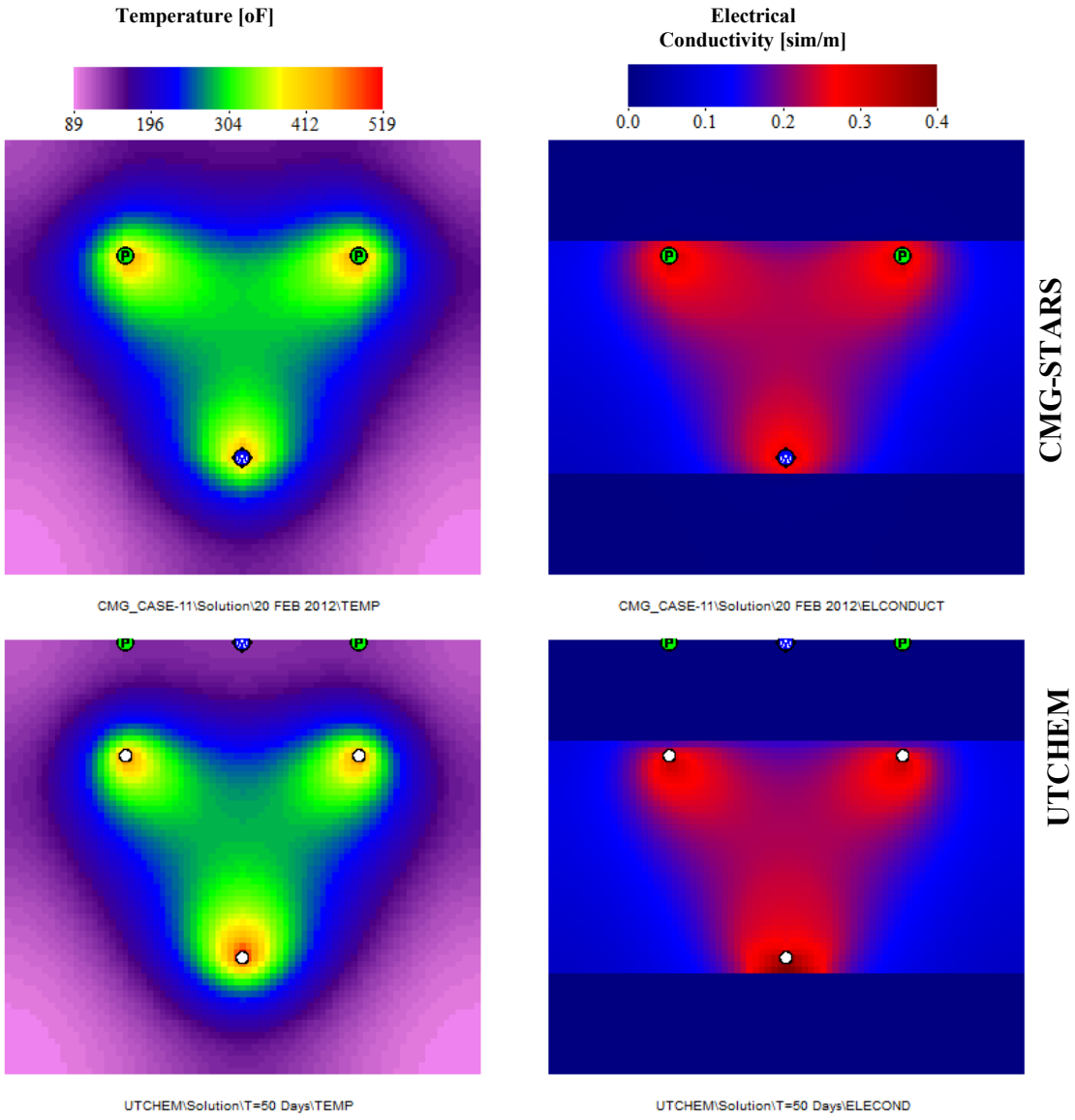

Figure 8-9-Comparison of temperature and electrical conductivity distribution results between CMG-STARS and UTCHEM after 50days.

Figure 8-10 and Figure 8-10 show the comparison of electrical phase and magnitude of voltage profiles that are intersecting and passing through the top wells after 50 days. As can been observed in the well gridblocks magnitude of voltage is reach to 164vol with electrical phases (120^{o} and 240^{o}). Imaginary and real voltages corresponding

to the same crossed profile after 50 days are plotted in Figure 8-10 and Figure 8-10, respectively.

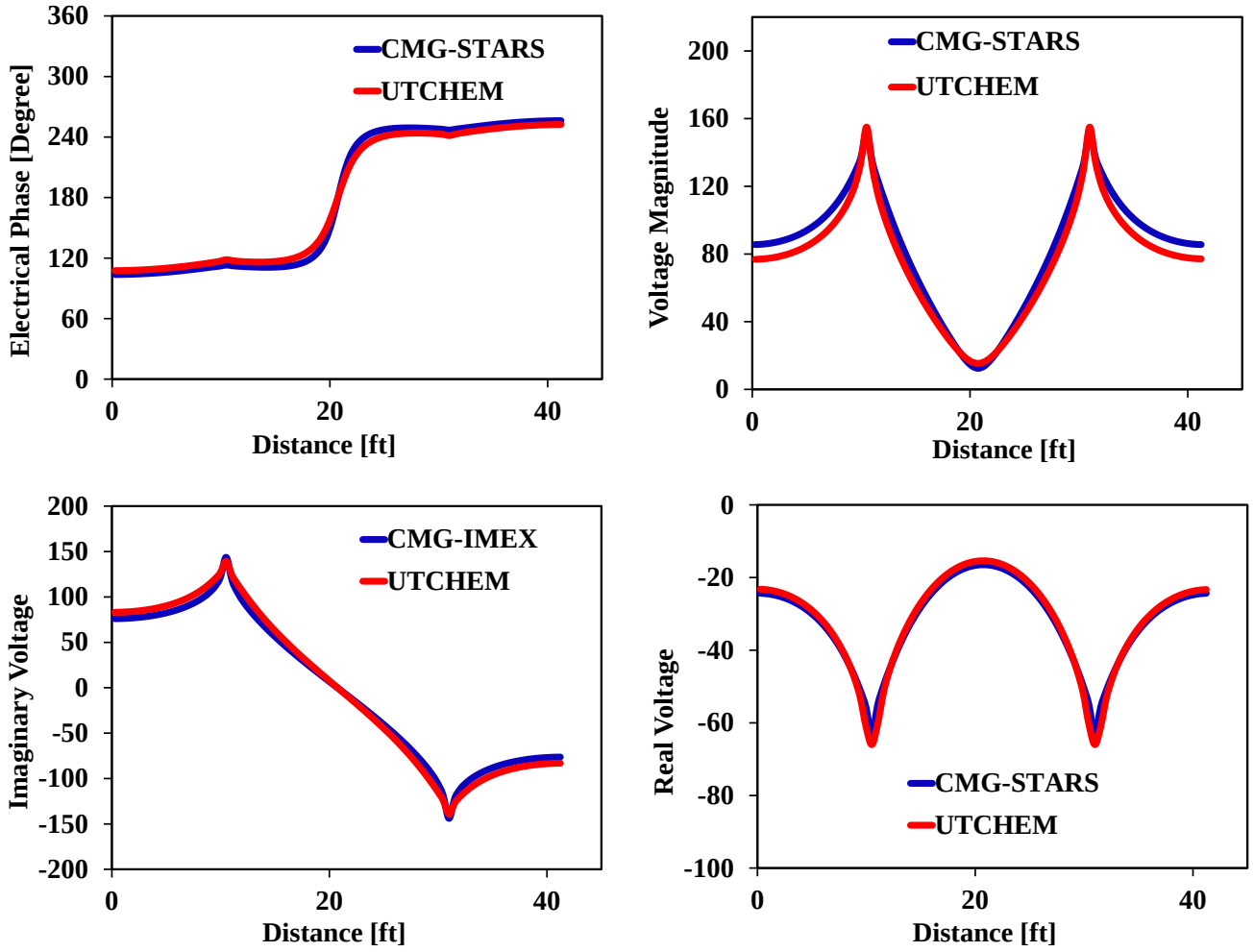

Figure 8-10- Comparison of electrical phase, magnitude of voltage, real voltage, and imaginary voltage profiles passing through two top wells after 50 days.

The comparison of results between numerical simulations and analytical solution shows a good agreement in the modeling of electrical heating process. The formulation has been implemented and the electrical heating model has been coupled to a four-phase chemical flooding simulator in order to evaluate the performance of a thermal-surfactant

or thermal-alkaline injection processes as well (Lashgari *et al.,* 2014a). In addition, the evaporation phenomenon in electrical Joule heating around the electrodes can be modeled in this simulator to evaluate the efficiency of the process. These capabilities that have been developed in UTCHEM enable us to investigate the influence of water saturated fractures. Therefore, we consider the same vertical cross-section of the seal type reservoir used in the validation section to investigate the effect of evaporation and fractures in electrical heating process. As discussed in the validation section, the reservoir model parameters and the fluid properties are the same as the validation case properties listed in Table 8-1 and Table 8-2. In this case, we heat the reservoir electrically for 50 days and then two top horizontal wells are placed on production for 300 days and the bottom well is placed to inject water in evaporation and fracture cases to maintain the reservoir pressure.

8.7.2 Hot and Cold Water Injection Effect during Electrical Heating in UTCHEM

In this part, we investigate the effect of hot and cold water injections on oil recovery from a heavy oil reservoir model while applying electrical heating. Table 8-3 shows the reservoir model parameters with an initial reservoir temperature of 90 ^{o}F and an oil viscosity of 5000 cp.

Table 8-3- Reservoir model parameters.

Number of gridblocks	30×1×40
Gridblock size	5×2.5×1.25 ft^3
Initial temperature	90 ^oF
Initial pressure	2000 psia
Number of wells	2
Flooding	Water Flooding
Initial viscosity of oil	5000 cp at 90 ^oF (40000 cp at 65 ^oF)
Voltage in Producer (VOL)	110 vol, 0 Deg
Voltage in Injection(VOL)	110,vol 180 Deg
Specific gravity of oil	1 (12 ^{o}API)
Viscosity thermal coefficient of oil	15000
Viscosity thermal coefficient of water	1500
Water injection rate	100 ft^3/Day
Perm X,Y,Z and Porosity	1000 mD, 1000 mD,100 mD and 0.2

We first apply electrical heating for 50 days on four cases INJ250, INJ150, INJ90, and INJ50, and then water injection starts for 150 more days under temperatures of 250 oF, 150 oF, 90 oF, and 50 oF, respectively. The fifth case (AL90) includes electrical heating for 200 days along with starting water injection for the last 150 days at temperature 90 oF. The sixth case (NOELE) is an isothermal case with only water injection at similar rate of injections as in the previous cases (100 ft3/Day). Table 8-3 reveals the input parameters for the six cases andTable 8 4 describes the flooding strategy. Electrodes for electrical heating purposes are located only between numerical layers 20 and 21 (2.5 ft electrical heating height)

Table 8-4-Description of the six cases with different heating and flooding strategy.

INJ250	Heat the reservoir electrically first for 50 days, then stop electrical heating and inject water for 150 more days under temperature 250 ^{o}F
INJ150	Heat the reservoir electrically first for 50 days then stop electrical heating and inject water for 150 more days under temperature 150 ^{o}F
INJ90	Heat the reservoir electrically first for 50 days then stop electrical heating and inject water for 150 more days more under temperature 90 ^{o}F
INJC50	Heat the reservoir electrically first for 50 days then stop electrical heating and inject water for 150 more days under temperature 50 ^{o}F
AL90	Heat the reservoir electrically entire for 200 days but inject water starts after 50 days under temperature 90 ^{o}F
NOELE	Isothermal scenario, no electrical heating and just inject water from day 50

Figure 8-11 shows case INJ250 results after applying electrical heating and injecting hot water of 250 ^{o}F, where the increase at reservoir temperature can significantly reduce the high viscosity of oil. Oil recovery for this case is around 35 percent in comparison to 25 percent in case AL90, where the reservoir is heated electrically for the entire 200 days, but water injection starts after 50 days under the temperature of 90 ^{o}F. The results show that the worst scenario is the isothermal case with almost 4 percent recovery.

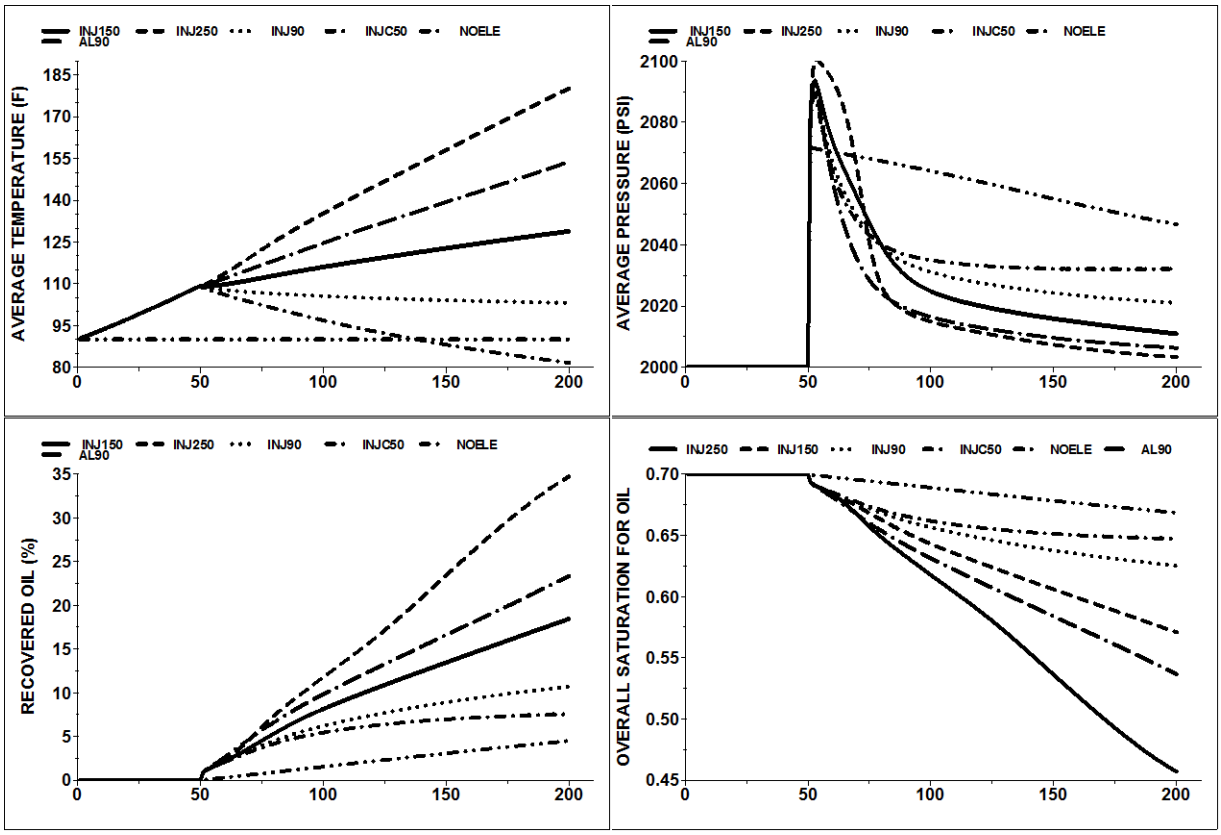

Figure 8-11- Comparison of the six scenarios based on average reservoir temperature, average reservoir pressure, average oil saturation, and oil recovery.

The results of reservoir temperature and oil viscosity of the six cases at the middle point of reservoir thickness (25ft) between producer and injector wells are shown in Figure 8-12.

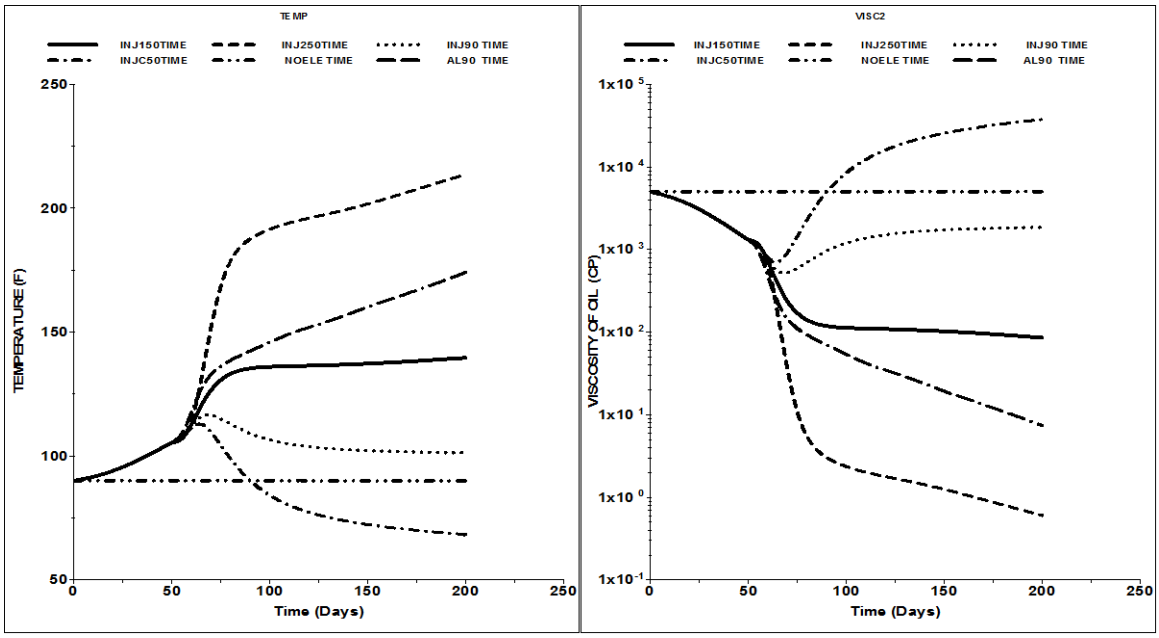

Figure 8-12- Comparison of the six cases at the middle point of reservoir thickness (25ft) between producer and injector wells in terms of temperature and oil viscosity.

8.7.3 Effect of Water Saturation During Electrical heating

The conducting path for electrical current is through the continuous water phase. Electrical energy is converted to heat along these pathways and the heat is transferred to oil by conduction. Therefore, to increase the amount of heat, water saturation plays the main role because of high electrical conductivity in comparison to rock and oil phase. In case SWINJ90, the reservoir is heated electrically for first 50 days and then electrical heating is stopped and water is injected for 150 more days under temperature 90 ^{o}F. Another case, which is NSWINJ90, doesn't have saturated layer. It has uniform water saturation (0.2) initially. Reservoir is heated electrically for 50 days and then electrical heating is stopped and water is injected for 150 more days under a temperature of 90 ^{o}F. The only difference between these two cases is the existence of high-water saturation layers in SWINJ90. The reservoir model parameters are the same as the previous cases.

Figure 8-13 illustrates the effect of high water saturated layers that make up significant heat due to high electrical conductivity of water. This generated heat lowers the oil viscosity considerably; water saturation is placed in the middle layer 20 and 21. Figure 8-13 at the top left illustrates these two layers' location where are highly saturated by slain water. This could be a good representative model of channelizing or fingering due water flooding.

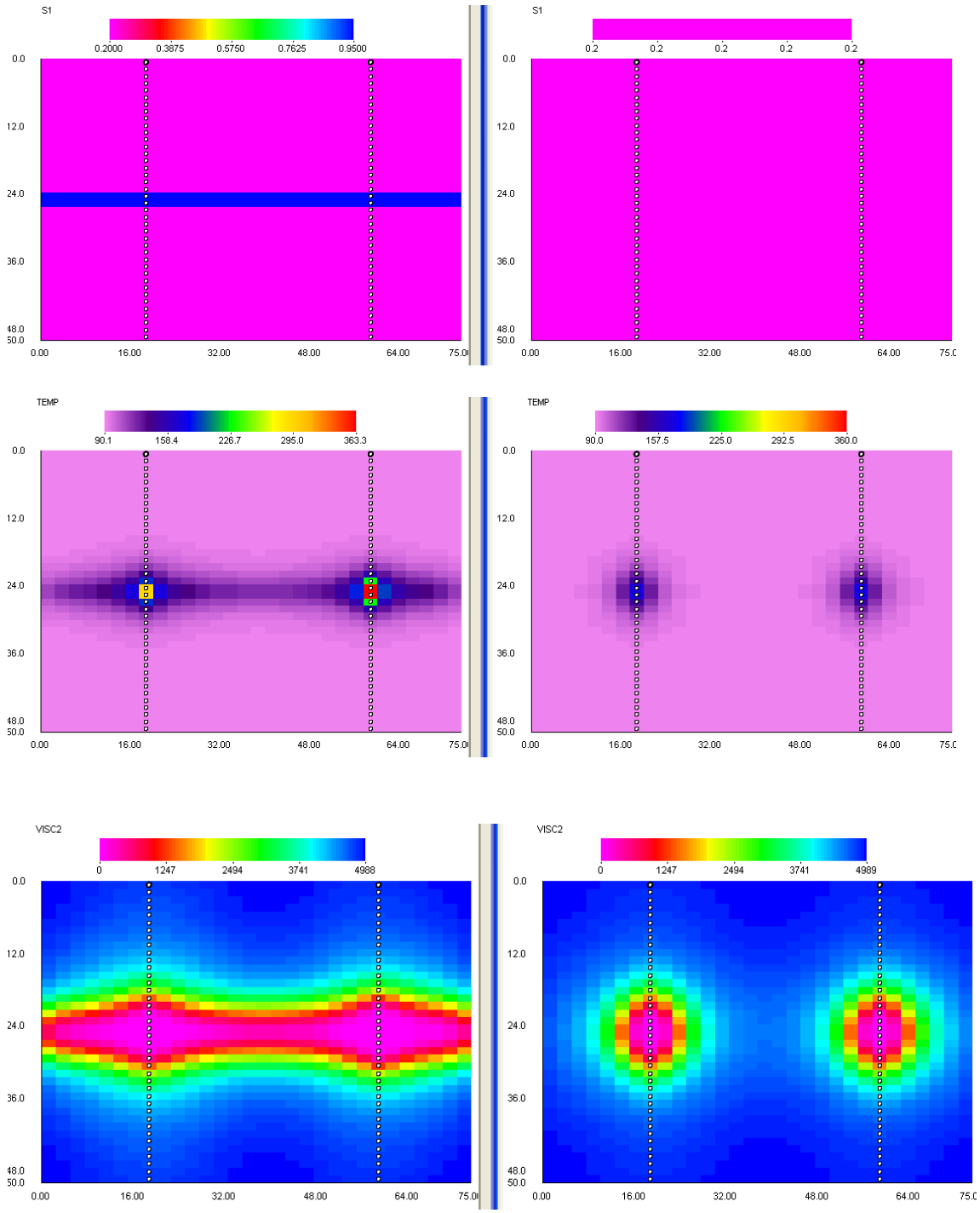

Figure 8-13- Effect of high water saturated layers that make more heat electrically to reduce oil viscosity significantly due to high electrical conductivity of water.

Figure 8-14 shows results of two cases with different water saturations in the same grid block mentioned for Figure 8-12 at the middle point of reservoir thickness (25ft) between producer and injector wells. In this figure, bottom plots are the comparisons of average temperature and oil recoveries.

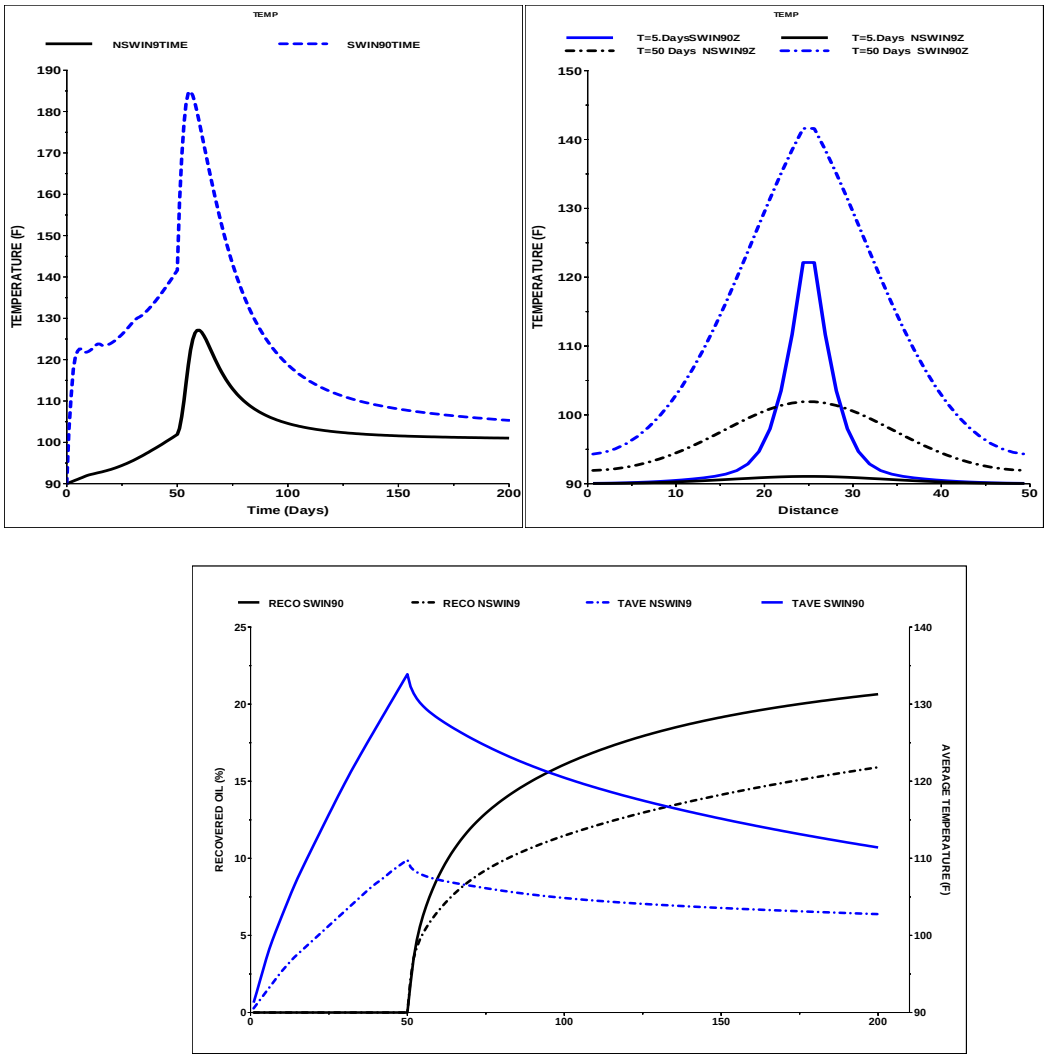

Figure 8-14- Top plots are comparison of two different water saturation cases at the middle point of reservoir thickness (25ft) between producer and injector wells; and bottom plots are of average reservoir temperature and oil recovery.

8.7.4 The Effect of Water Evaporation

In order to model evaporation and condensation of water when temperature around a well reaches the boiling point, a similar case as used in the validation section is considered here, but with three phases (oil, water, and steam). The electrical conductivity of saline water is relatively high compared to rock and hydrocarbon phases and this leads to an increase in the electrical current density in water phase. Therefore, most of the generation of heat takes place in the water phase. Then, water heats the surrounding oil, and the rock formation causes temperature to increase and reach the boiling point (saturated condition). The formation of water evaporation occurs around the electrodes because of high temperature spots generation. This is one of the crucial problems in the electrical heating process. Steam forms; since steam is roughly non-conductible, it disconnects the conductive paths near the electrodes when temperature declines sharply until steam condenses and again electrical conductivity increases in the presence of condensed water. Subsequently, heat rate is generated again and temperature increases until it reaches the boiling point as shown in Figure 8-15 causing a significant reduction in the efficiency. Temperature, steam saturation, total electrical conductivity, electrical current in x direction, and magnitude of the heat rate in the gridblock of the bottom well are shown in Figure 8-15. These fluctuations in temperature, heat rate, electrical conductivity, electrical current, and voltage are caused by steam formation and contain contributions from numerical fluctuation as well. In such cases, temperature cannot exceed the boiling (saturated) temperature at corresponding pressure and this drastically alters the heat rate and reduces the total dissipated electrical energy injection into the reservoir.

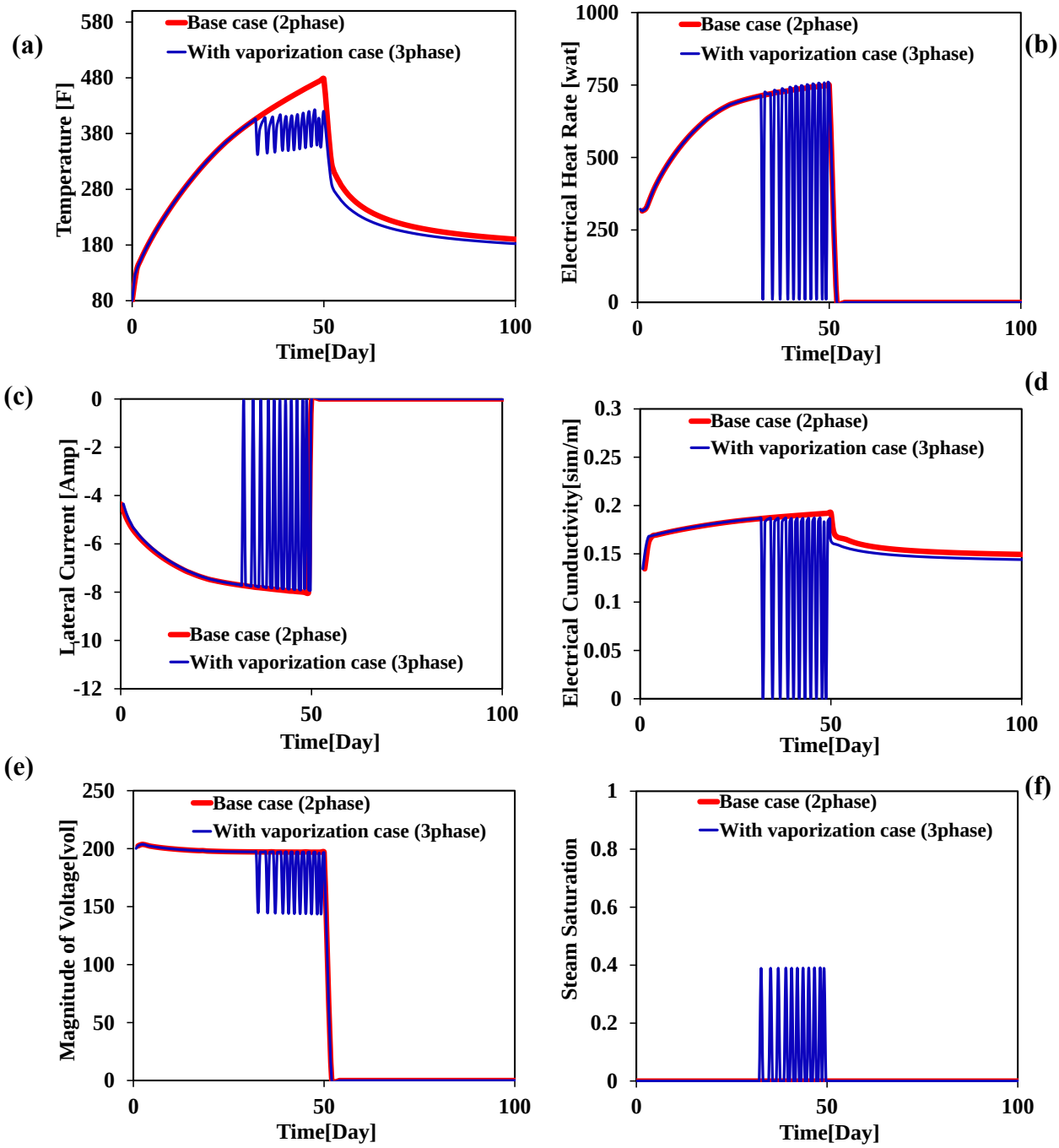

Figure 8-15-Temperature (a), magnitude of heat(b), electrical current in X direction(c), saturated electrical conductivity(d), magnitude of voltage (e), and generated steam saturation(f) in the bottom well gridblock for cases with and without vaporization phenomenon.

Of course, there is doubt that whether these fluctuations are actually observed in the field or they are attributed to the numerical oscillation due to phase-change in an IMPEC formulation. To investigate this problem numerically, several test cases were performed by varying the grid-block size and time-step to understand the discretization and numerical error in the computations. Simulation parameters of these test cases are summarized in Table 8-5. We consider three different grid-block sizes with twice larger (Δx=1.0ft, Δy=10ft, Δz=1.0ft) and twice smaller (Δx=0.25ft, Δy=10ft, Δz=0.25ft) than the base case grid-block size (Δx=0.5ft, Δy=10ft, Δz=0.5ft). Then all cases were run with the same schedule and the same time-step (0.5 day).

Results are displayed in Figure 8-16a. The temperatures of the bottom well grid-block are plotted for all three cases. As can be seen, temperature for the larger-grid-block case reaches the boiling point later than the small-grid-block cases. This means that larger-grid-block needs more energy for increasing the temperature by one degree. The frequency of temperature variations for all cases is similar since test cases have been run with the same constant time-step (Δt=0.5day). The amplitudes of temperature variations in the larger-grid-block case are smaller, because more energy is needed for increasing temperature. In the small grid-block cases, temperature increases faster and reaches the boiling point earlier. Therefore, the difference in the grid-block size affects the amplitude of fluctuations and is not related to numerical instability in such cases.

Other test cases also have been run with the different time-steps (Δt=0.1day, Δt=0.5day, Δt=1.0day). The results in Figure 8-16b show that smaller time-step leads to lowering the amplitude of temperature variations but the frequency of variation is increased.

Table 8-5- Comparison of simulation parameters for test cases.

Case Description	Gridblock size	Number of gridblock	Time step	Simulation time for 50 days electrical heating
Base case	0.5ft×10ft×0.5ft	5621 (77×1×73)	0.5 day	863 seconds
Base case	0.5ft×10ft×0.5ft	5621 (77×1×73)	0.1 day	4342seconds
Base case	0.5ft×10ft×0.5ft	5621(77×1×73)	1 day	466 seconds
Large-gridblock case	1.0ft×10ft×1.0ft	1443 (39×1×37)	0.5 day	232 seconds
Small-gridblock case	0.25ft×10ft×0.25ft	22785 (155×1×147)	0.5 day	3784 seconds

It is obvious that in the saturated condition, temperature around the electrode cannot exceed the boiling temperature at constant pressure and the dissipated electrical energy is consumed in the phase change between water and steam by increasing the mass quality of steam as shown in Figure 8-17. Therefore, energy balance is conserved as well, as energy balance error shows the same order of magnitude at saturated (~8. $3x10^{-4}$) and undersaturated (~$1.041x10^{-4}$) conditions.

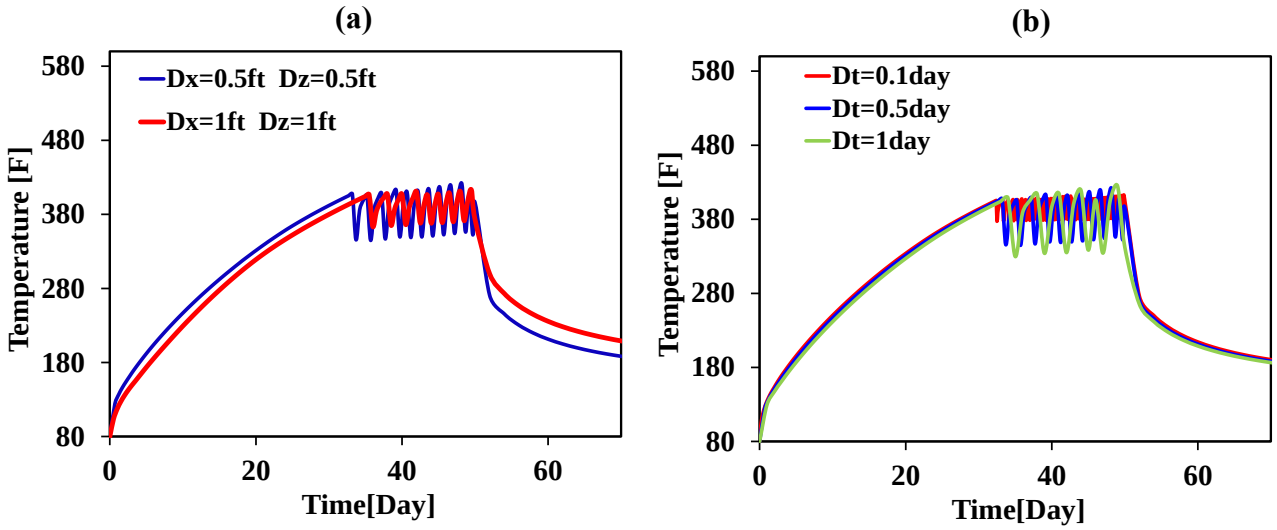

Figure 8-16-Effect of different gridblock size and timestep in boilling point or saturated condition in the bottom well gridblock.

Accordingly, the variation of boiling point around the well can occur in reality, as numerical simulation shows. However, the major uncertainty is the contribution of numerical error.

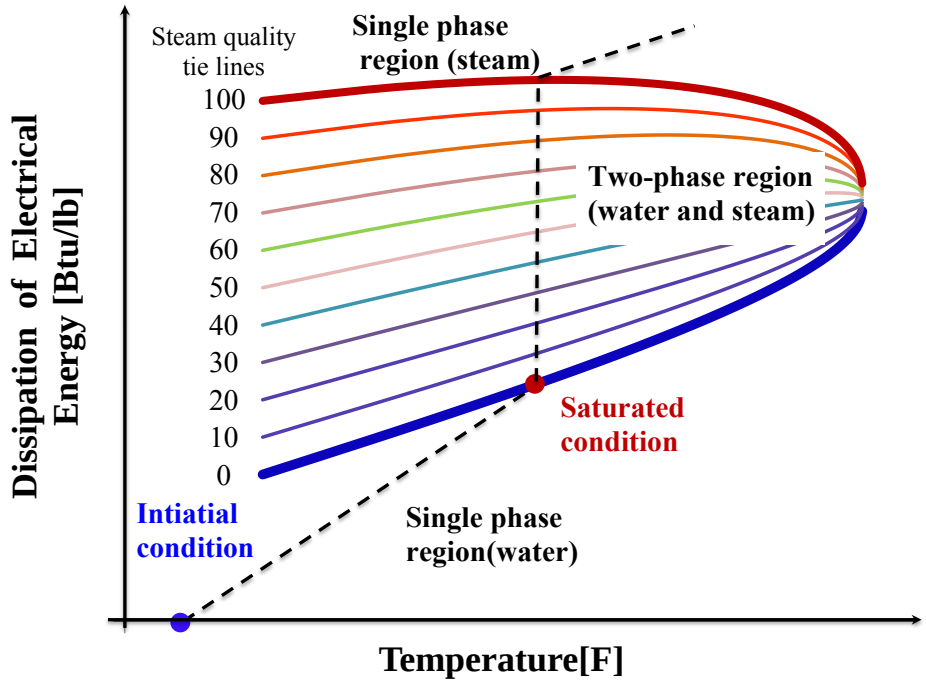

Figure 8-17-A schematic of the dissipation of electrical energy and temperature change in the presence of single-phase and two-phase.

As simulation results demonstrate, the fluctuation can be controlled by using small time-steps. It is obvious that evaporation phenomenon does not allow temperature to exceed the boiling temperature at corresponding pressure. In addition, steam formation creates discontinuity in electrical current by increasing electrical resistivity or reducing electrical conductivity. Accordingly, vaporization leads to a decrease in the efficiency of electrical heating.

There is a difference between electrical energy and dissipation of electrical energy. Electrical energy is electrical power that is applied to reservoir through the electrodes in the wells. The dissipation of electrical energy is strongly a function of electrical conductivity or resistivity and is generated in the reservoir because of electrical current and electrical conductivity of reservoir (Joule's law). Therefore, the amount of dissipation of electrical energy must be in balance with the amount of heat in the reservoir. The energy balance is always conserved in such cases, since energy balance error is small enough. This effect can be seen in the total oil recoveries in base case and in the case with vaporization as shown in Figure 8-18. Vaporization of water decreases the recovery factor from 35% to around 17%. Therefore, the process should be designed to keep the temperature below the boiling point or saline water should be injected during the heating process to avoid evaporation.

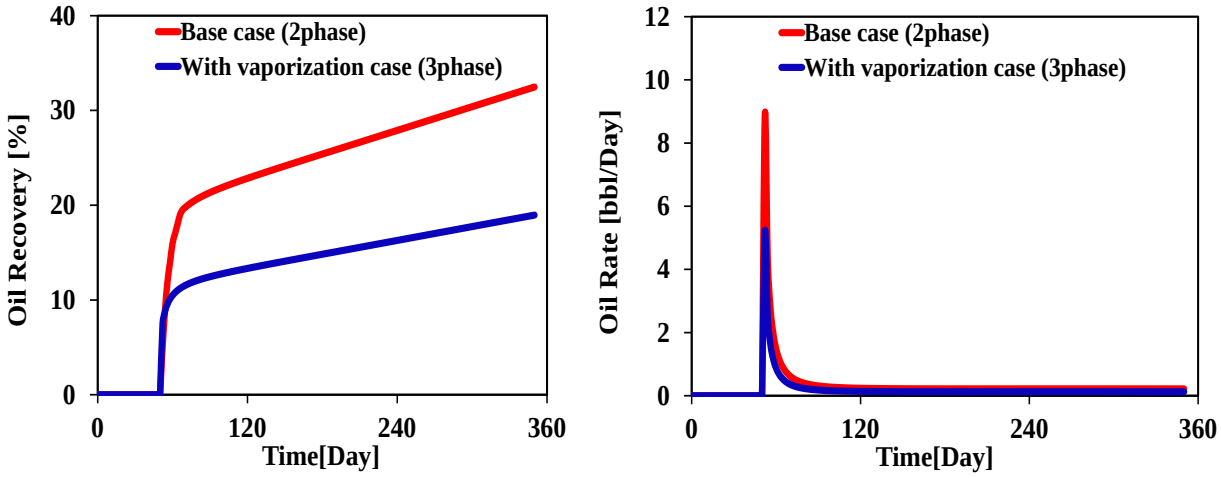

Figure 8-18-The oil recovery and oil rate for with and without vaporization cases.

8.7.5 The Effect of Saturated Fracture by Saline Water.

We consider a set of fractures to create conductive paths for electrical current that flows through the continuous water phase. Reservoir model and fluid properties are similar to the base case in validation and evaporation sections as given in Table 8-1 and also thermal and electrical properties are given in Table 8-2. In order to model the fractures, since the size of grid-blocks are small enough, a high water saturation (Sw=1.0) and permeability (k_{xf}=3000md, k_{zf}=1000md) are assigned to the fracture grid-blocks. These fractures are intersected by the well grid-blocks. The fractures, which are saturated with 100% saline water, are electrically conductible compared to matrix conductivity. Figure 8-19 displays the water saturation distributions in the fracture case and in the base case. Electrical energy is dissipated to heat along these pathways in the fractures and the heat is transferred to oil by heat conduction.

Figure 8-20 compares the generated heat rate for the case with fractures and the base case at different times (i.e. 5, 20, 35, and 50 days). These figures show that the water saturated fractures play an important role with high electrical conductivity. Therefore, high electrical conductivity leads to more dissipation of electrical energy at the same electrical power. As it can be seen in these figures, initially (days 5 and 20) electrical heat rate is high; then the generated heat rate is reduced after a while (35 and 50day). The reason for this reduction in heat rate is an increase in temperature that leads to a decrease in oil viscosity. Thus, oil can easily move into the fractures because of density difference between water and oil phases and finally reduce the electrical conductivity of fractures as displayed in Figure 8-20 after 35 days and 50 days.

However, the temperature in the fractures increases substantially compared to the base case as shown in Figure 8-21. Accordingly, the presence of the water saturated fractures has an extreme impact on the efficiency of electrical heating process.

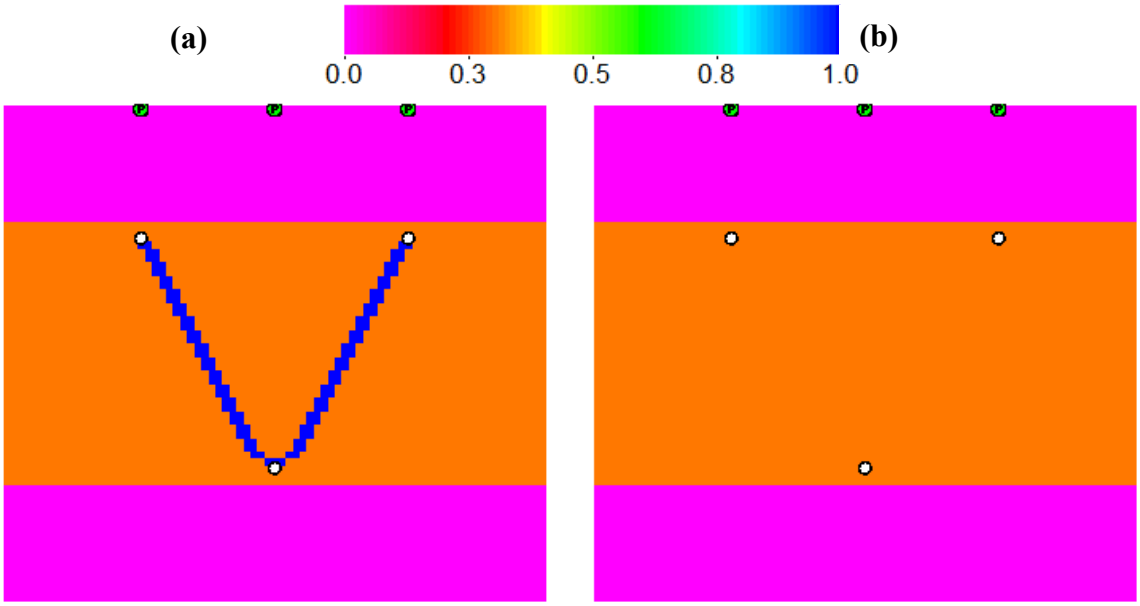

Figure 8-19- Water saturation distribution with overburden and underburden seal layers in (a) fracture case and (b) base case.

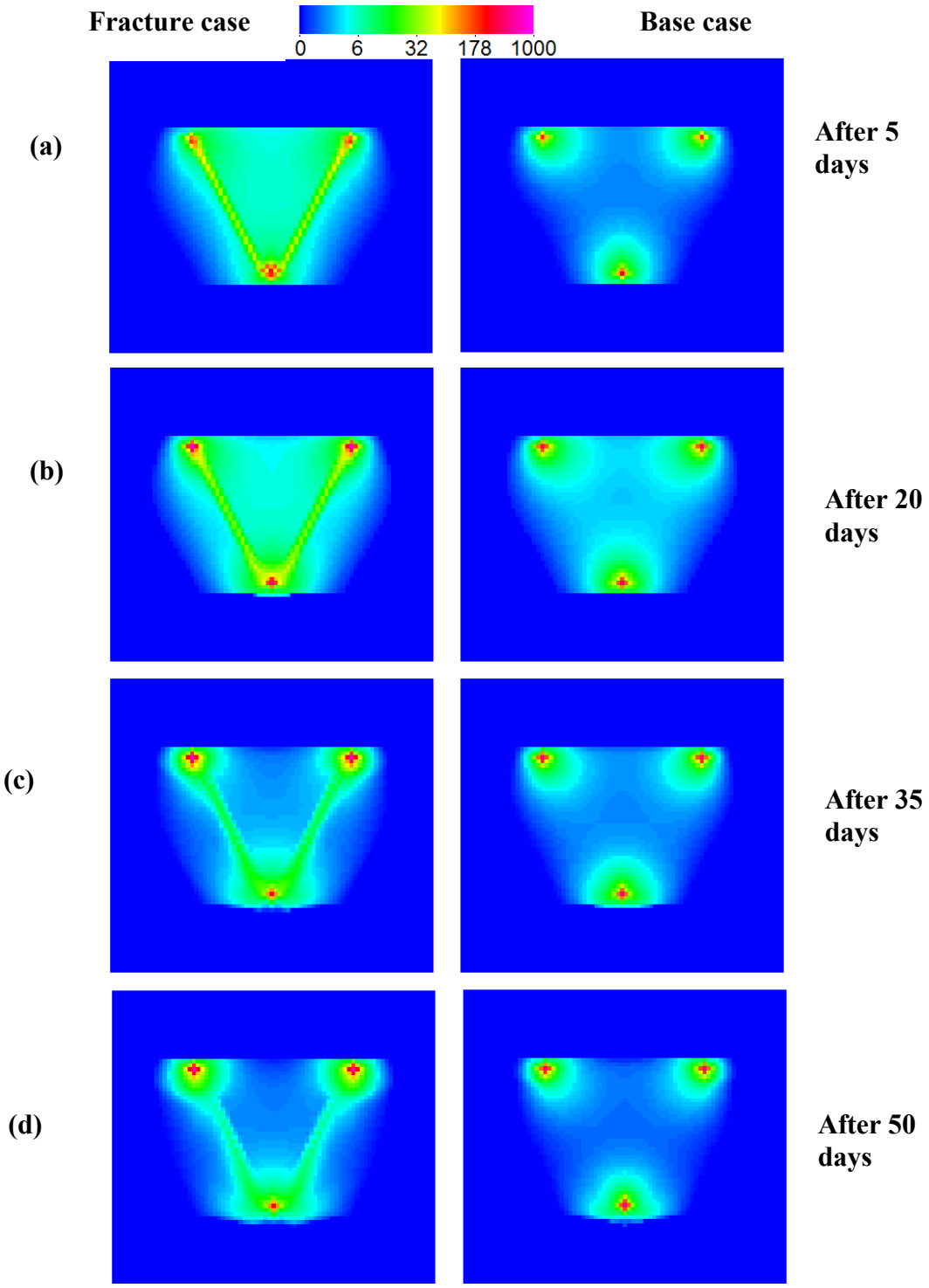

Figure 8-20-Magnitude of heat rate(wat) distribution (a) after 5 days, (b) after 20 days, (c) after 35 days, and (d) after 50 days in the fracture case and base case.

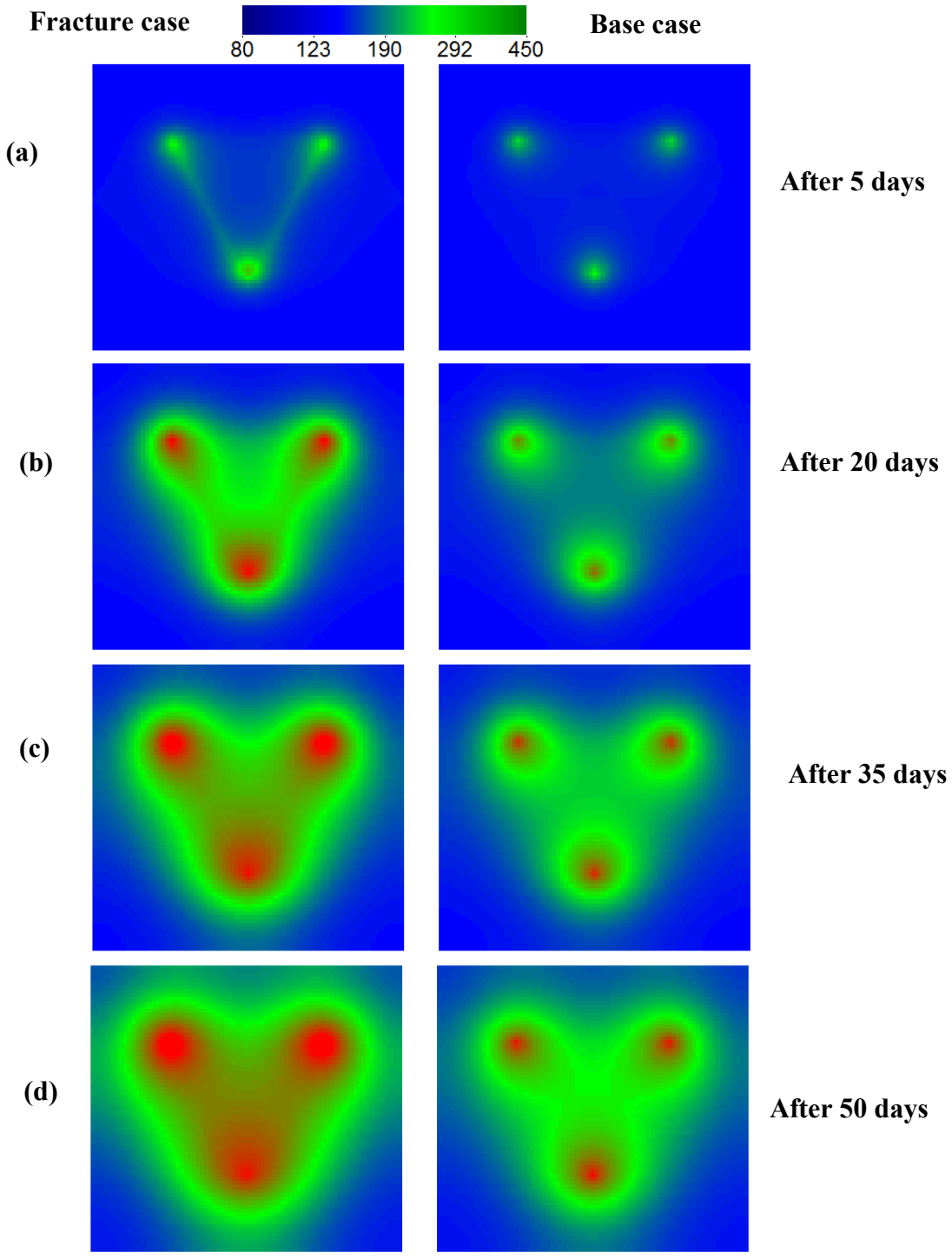

Figure 8-21-Temperature (°F) distribution (a) after 5 days, (b) after 20 days, (c) after 35 days, and (d) after 50 days in the fracture case and base case.

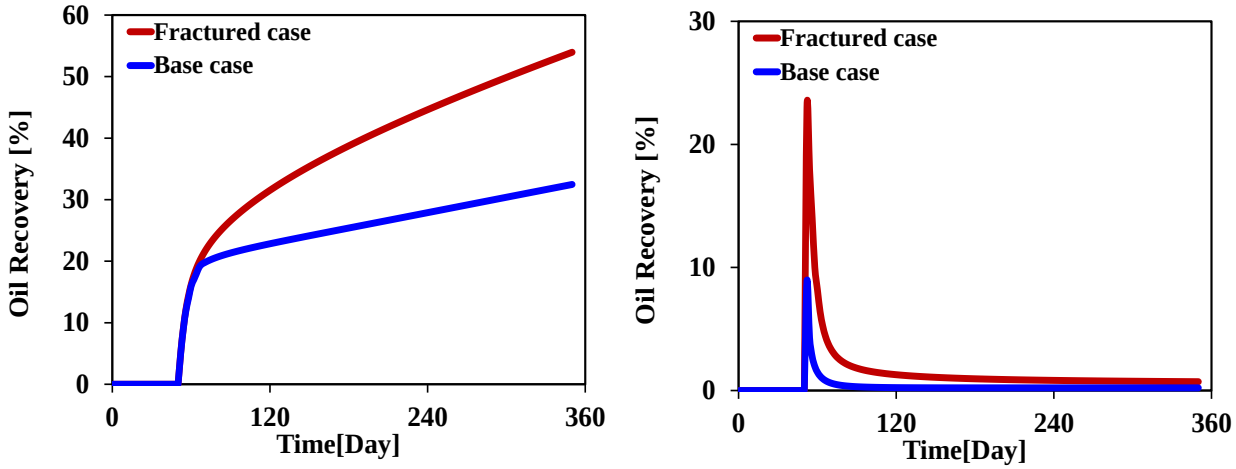

Figure 8-22-The effect of a fracture saturated with water on oil recovery.

Figure 8-22 shows the comparison of oil recovery between the fracture case and the base case. The recovery factor increases from 35% of the base case to about 55% in the presence of fractures. High oil recovery in the case with fractures is due to high temperature in the reservoir caused by high conductivity and subsequently by greater dissipated electrical energy.

8.8 SUMMARY AND CONCLUSION

We formulated and implemented the energy equation and the electrical Joule heating into the UTCHEM simulator to model vaporization of water near the wells during electrical heating. We also evaluated the effect of water saturated fractures during electrical heating. The main conclusions are the following:

Dissipation of electrical energy is a strong function of electrical conductivity. More dissipated electrical energy rate needs a high electrical conductivity.

Vaporization of water decreases the dissipation of electrical energy and this restricts the generation of heat. Consequently, vaporization of water has significant impact on the efficiency of the electrical Joule heating process.

The high water saturated fractures and electrical conductivity of water phase have an important effect on the Joule heating process. The presence of fractures can significantly increase the effectiveness of the process.

Due to the increase in electrical conductivity, the dissipation of electrical energy increases in the form of heat and hence it increases the reservoir temperature and reduces the oil viscosity.

Chapter 9: Steam-Surfactant-Foam Modeling in Heavy Oil Reservoirs

Steam foam is a hybrid and a novel method of thermal and chemical flooding to improve the sweep efficiency of steam for producing heavy crude oils. Steam injection is a mature process to substantially reduce the oil viscosity in heavy oil reservoirs and thus increase its mobility. Steam flooding is an unstable displacement, since the gravity of steam causes poor vertical sweep efficiency due to the gravity override in thick high permeability pay zones and poor areal sweep efficiency in high permeability channels with high connectivity. On the other hand, foam reduces the mobility of steam by stabilizing the liquid lamellae that cause some or all of the steam to exist as a discontinuous phase. Therefore, foam plugs large pores to divert the flow into the low permeability zones and controls gravity override. Foam increases the pressure gradient slightly in the steam-swept regions and leads to heating oil more efficiently when steam diverts into the cold unswept regions. Furthermore, surfactant mobilizes the high viscous oil by emulsification and reduction of interfacial tension. The synergy of steam, surfactant, and foam has the potential to greatly improve the recovery of heavy oil reservoirs.

Based on a literature survey, steam foam injection has been conducted in both laboratory core floods and few field pilots. On the other hand, existing numerical simulators have not been able to capture the mechanisms involved in such a process. In this chapter, we present the development and the implementation of a new robust steam formulation in a four phase chemical flooding reservoir simulator (UTCHEM) to model and understand the contribution of each mechanism, such as viscosity reduction, emulsification, and foam for mobility control. Results illustrate that the steam-foam process controls the mobility of steam to avoid incomplete vertical sweep due to gravity

segregation. Formation of the emulsion phase by condensing steam along with the presence of water leads to an increase in the emulsion viscosity and thereby decreases water production. The presence of surfactant and emulsification of oil either as water in oil or as oil in water emulsions can also influence the displacement and the propagation of viscous oil.

The mechanistic understanding of steam foam process and improvement of the heat transfer compared to conventional steam flooding is a key finding in this research to optimize the technology that unlocks heavy oil reservoirs with favorable economics.

9.1 INTRODUCTION

Conventional cyclic steam stimulation (CSS), referred to as Huff 'n' Puff, is a thermal recovery method which involves periodic injection of steam with the purpose of heating the reservoir near the wellbore. In this process, one well is operated as both injector and producer with repeated cycles of steam injection, soak, and production to enhance the oil production rate. Steam is injected into the well for a period of time to heat the oil to a temperature at which it flows. When enough amount of steam has been injected, the well is shut in and the steam is left to soak for a few days. During this time, steam is condensed and delivers energy to reservoir. The reservoir is heated and oil viscosity decreases. This stage is called soaking stage. Then, well is placed on production and it is operated. After a while, the reservoir temperature around the well decreases and it results in to reduce oil flow rate. Afterward, another cycle is repeated until the production reaches an economically determined level. Typical CCS process is well suited for the thick formation with poor geological connectivity (Prats 1985, and Thomas 2008). Application of CCS targets to produce the formation of oil saturation by several driving mechanisms: viscosity reduction, changes in wettability and thermal and solution gas

expansion (Prats, 1978) which depend on reservoir rock and fluid properties. The efficiency of this process can be affected by gravity segregation of steam or presence of a high permeability or thief zone.

Heavy oil has low mobility, because of high viscosity and very low relative permeability. As a result, the mobility ratio is unfavorable. Surfactant flooding can improve recovery in two ways: first, the oil-water interfacial tension is lowered, resulting in lower residual oil saturation despite an inefficient displacement; second, the low IFT supports the formation of an emulsion phase and this makes the effective mobility ratio less unfavorable. Surfactant flooding is used to improve the mobility and reduce the oil viscosity in conventional oil reservoirs. (Pope and Nelson, 1978; Pope *et al.,* 1978; Delshad *et al.,* 1996). The main mechanism for recovery is lowering oil-water interfacial tension in conventional oil reservoirs to reduce the capillary forces and the concept of capillary desaturation, but in heavy oil, emulsification is the main mechanism. However, the formations of water in oil (W-O) emulsion phase and oil in water (O-W) emulsion phase have been reported as possible recovery mechanisms for heavy oils during surfactant flooding (Bryan and Kantzas, 2007; Liu *et al.,* 2007; Dong *et al.,* 2009)

On the other hand, steam injection that is unstable by gravity can have a poor vertical sweep efficiency due to gravity override in a thick high permeability layer and poor areal sweep efficiency in high permeability channels with high conductivity. One combination thermal and surfactant recovery process is the steam foam process proposed by Needham (1968). He described a process to plug a high permeability zone to divert steam into a low permeability zone and control gravity override due to gravity segregation. Therefore, the application of steam foam was developed to control mobility and thus improve the sweep efficiency (Hirasaki, 1989; Patzek, 1996). The pressure gradient in the steam swept region is increased due to reduction of mobility of steam

foam. This leads to displacing the heated oil better and to divert steam to the cold regions. (Hirasaki, 1989; Patzek and Myhill, 1989). Surfactants lower the steam mobility by stabilizing the liquid lamellae that cause some or all of the steam to exist as a discontinuous phase. The propagation of the surfactant is retarded by its adsorption on rock surfaces.

Although there are only few pilot field projects of steam foam, the majority of these projects only consider viscosity reduction and mobility control mechanisms and not the oil solubilization in water and emulsification. This is the main reason that numerical modeling of the surfactant flooding in the presence of steam for heavy oil recovery is far from satisfactory in the current reservoir simulators. Therefore, there is a need for mechanistic steam surfactant and foam flooding reservoir simulator to provide an effective way to evaluate steam, surfactant, and foam injection for enhanced heavy oil recovery and aid in making decisions in the early stage of field developments.

In this chapter, we present a four phase reservoir simulator to study the contribution of steam foam flooding to capture all possible mechanisms of foam mobility control, oil viscosity reduction, and emulsification. We consider a CCS case along with different injection scenarios such as steam drive, steam-surfactant injection, and steam-surfactant-foam injection.

9.2 GOVERNING MECHANISMS

Viscosity reduction, emulsification, and foam mobility control are three primary mechanisms that impact the performance of steam foam flooding. In this section, we discuss in detail the contribution of each mechanism during steam, surfactant, and foam injection.

9.2.1 Viscosity Reduction

Heavy oil is difficult to flow in the reservoir at the original pressure and temperature. Upon heating, the viscosity of the oil is significantly reduced whereby oil production is improved (Nasr and Ayodele, 2005). The heaviest oils at the relatively high temperature around 200 ^{o}C (400 ^{o}F) have the viscosity about 1cp (Farough Ali, 2003). The following exponential function is implemented in UTCHEM to compute oil viscosity as a function of temperature (T):

$$\mu_{oil} = \mu_{oil,ref}\, exp\left[b_{oil}\left(\frac{1}{T} - \frac{1}{T_{ref}} \right) \right] \tag{9-1}$$

where $\mu_{oil,ref}$ is the viscosity at a reference temperature (T_{ref}) and b_{oil} is a constant reduction factor. Figure 9-2 shows the viscosity reduction respect to temperature in this study, which is calculated using b_{oil} of 5000 ^{o}F and a reference of viscosity 5000 cp at temperature 65 ^{o}F.

9.2.2 Emulsification

In heavy oil reservoirs, oil trapping during water flooding and low mobility of oil is due to its high viscosity and instability or hydrodynamic fingering resulting from a highly unfavorable or adverse mobility ratio between displaced and displacing fluids (Wang and Dong, 2009). Surfactant flooding can improve recovery of heavy oils in two ways: first, the oil-water interfacial tension is lowered; second, the low IFT supports the solubilization of oil in water by the formation of an emulsion phase. Water in oil (W-O) and oil in water (O-W) are two possible emulsion types during surfactant flooding. Figure 9-1a schematic of phase distribution in a typical steam surfactant flooding.

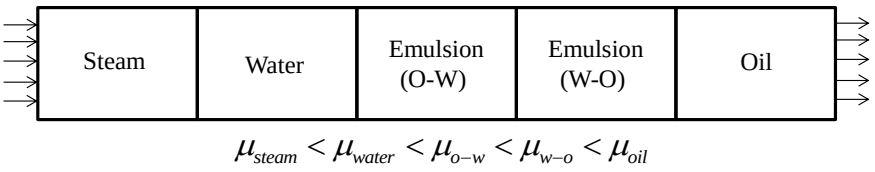

Figure 9-1-A schematic of four phase fluid distribution in steam surfactant flooding

The W-O emulsion phase almost has the same viscosity as the oil and forms behind the oil bank. The O-W emulsion phase often forms behind the W-O emulsion phase and has a lower viscosity compared to the W-O emulsion phase. The gradual reduction of phase viscosity from the oil to steam improves the sweep efficiency significantly. However, the oil droplets in O-W emulsion can plug rock pores and increase the resistance to water phase flow in water channels or finger and divert the injected water to upswept regions (Bryan and Kantzas, 2007; Liu *et al*., 2007; Dong *et al*., 2009). In this study we only consider the oil in water emulsion. Temperature dependency of surfactant phase behavior is discussed in Chapter 5.

9.2.3 Mobility Control using Foam

Mobility control is an essential factor to the effectiveness of EOR processes. The gas or steam EOR processes often suffer from poor sweep efficiency due to high mobility gravity segregation as the result of low density steam. Steam override leads to heat loss to overburden rock and reduces the steam performance.

The use of foam for mobility control in steam applications is one such novel technique that has the potential to improve oil recovery. Foam reduces the mobility of steam and improves its volumetric sweep efficiency. Therefore, steam contacts more oil in the reservoir and its performance increases significantly. We use the foam model

developed by Rossen *et al*. (1994) based on the limiting capillary pressure p_c^* as the controlling mechanism as follows:

$$k_{rg}^{f} = \begin{cases} k_{rg} \quad ; S_w < S_w^* - \varepsilon \text{ or } C_S < C_S^* \text{ or } S_o \geq S_o^* \\ \dfrac{k_{rg}}{(1+((R-1)(S_w - S_w^* + \varepsilon))/2\varepsilon)} \quad ; \\ S_w^* - \varepsilon \leq S_w \leq S_w^* + \varepsilon \ \& \ C_S \geq C_S^* \ \& \ S_o < S_o^* \\ k_{rg}{}^{f} = \dfrac{k_{rg}}{R} \quad ; S_w > S_w^* + \varepsilon \ \& \ C_S \geq C_S^* \ \& \ S_o < S_o^* \end{cases} \tag{9-2}$$

where C_S is the surfactant concentration in the aqueous phase, C_S^* is threshold surfactant concentration, S_w^* is the water saturation at which foam collapses, S_o^* is the maximum oil saturation at which foam remains stable, $k_{rg}{}^{f}$ is effective gas relative permeability modified for foam, k_{rg} is the gas relative permeability in the absence of foam, ε determines the range of water saturation for high quality regime and finally R is the foam model parameter. The foam parameter R is modified according to gas flow rate to allow for shear thinning behavior of foam in low-quality regime as follows

$$R = R_{ref}\left(\frac{u_g}{u_{g,ref}}\right)^{\sigma-1} \tag{9-3}$$

where u_g is volumetric gas flux, R_{ref} is the value of R at reference gas volumetric flux, and σ is the power-law exponent. For Newtonian-foam behavior, $\sigma = 1$ and for shear thinning behavior $\sigma < 1$.

9.3 NUMERICAL SIMULATION STUDY

Although there is very little experience from pilot tests (modeling and observed data) in steam foam flooding, reservoir simulation approach provides an effective way to evaluate steam, surfactant, and foam injection for enhanced heavy oil recovery and to make decisions in the early stage of field developments. In this simulation study, steam formulation and a foam model were implemented in UTCHEM to study the contribution of the mentioned mechanisms during steam, surfactant, and foam injection. In this implementation, distillation and condensation of hydrocarbon are neglected and mass transfer only occurs between water and steam phases.

A CSS numerical model with a single well for injection and production is set up. Reservoir model and fluid properties have been summarized in Table 9-1. Oil viscosity against temperature is plotted in Figure 9-2. We perform a series of simulations to study the effects of oil viscosity reduction, emulsification, and steam mobility control on oil recovery in three separate case studies.

Table 9-1- Input reservoir parameters and well schedules

Parameters	**Values in UTCHEM**
Number of grid blocks	61x1x30
Grid block size	5x10x2.5 ft^3
Initial reservoir temperature	100 ^oF
Initial reservoir pressure	100 psia (top layer)
insitu oil viscosity	5000cp (65^oF)
Number of wells	1 vertical
Initial water saturation	0.3
Injection temperature and steam quality	450^oF and 70%
Boundary condition	Open boundary
BHP of producer	75psi
Injection rate (CWE)	150 ft^3/Day
X,Z permeability and porosity	2000 mD, 500mD and 0.3
λ and C_p for water	38(Btu/ft.Day.F) and 1.0(Btu/lb.F)
λ and C_p for steam	38(Btu/ft.Day.F) and 0.65(Btu/lb.F)
λ and C_p for oil	32 (Btu/ft.Day.F) and 0.5 (Btu/lb.F)
λ and C_p for emulsion	38 (Btu/ft.Day.F) and 1.0 (Btu/lb.F)
λ, density, and C_p for rock	28 (Btu/ft.Day.F),165 (lb/cu.ft),0.25 (Btu/lb.F)

Table 9-2-Cyclic steam injection, soaking and production paramteres

Parameters	Values
CWE injection rate	150 ft^3/day (26.7 bbl/day)
Steam quality	70%
Number of cycles	2
Injection time	30 days
Soaking time	15 days
Production time	205 days

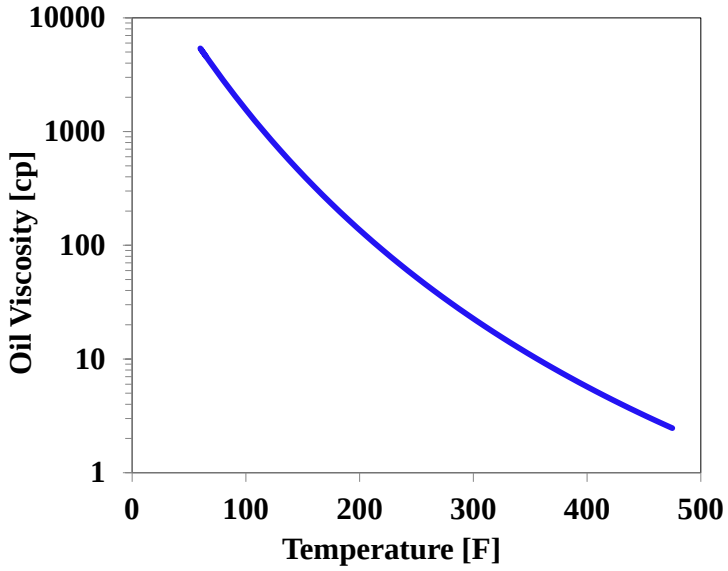

Figure 9-2-The effect of temperature on oil viscosity for all cases.

Case-1. Steam Injection Only (Base Case). The process is performed in two cycles. Steam with 70% quality and the rate 150 ft^3/day cold water equivalent volumes (CWE) is injected for 30 days. Afterward, the well is shut in for 15 days to provide

enough time for steam to deliver heat to the oil. Subsequently, the well is placed on the production for 205 days or when the water oil ratio becomes around 99%. Then, cycle is repeated.

In this case, viscosity reduction is the only production mechanism. Figure 9-3 shows the steam saturation at various times. Figure 9-3**a** shows the steam saturation after 30 days at the end of steam injection in the first cycle. It shows that steam heats oil and overrides the upper layers of the reservoir due to the lower density of steam compared to oil and water. The gravity override leads to loss of steam energy to overburden rocks. However, we do not consider the heat loss in this simulation study although the energy balance equation has the heat-loss option. Figure 9-3**b** demonstrates steam saturation after 45 days as the end of soaking time, indicating that gas segregation continues during soaking time, since upper layers are fairly heated at this time. Once again Figure 9-3**c** and Figure 9-3**d** show gas saturation after 280 days (the end of the second cycle of steam injection) and 295 days (the end of the second soak period), respectively. Gravity override is more severe in the second cycle where the upper layers are already at high temperature. This effect can be clearly observed in Figure 9-4 and Figure 9-5 with corresponding temperature and viscosity distributions similar to Figure 9-3.

Case-2. Steam-Surfactant Injection. The case description is the same as Case-1, but steam is injected along with 0.01vol/vol surfactant. Surfactant does not partition in the steam phase and always remains in the emulsion phase. Unlike conventional oil, ultra-low interfacial tension is not always the dominant mechanism for heavy oils. The dominant mechanism can be emulsification where surfactant solubilizes oil in water phase to form an emulsion phase. Steam saturation, temperature, and oil viscosity in this case are almost the same as Case-1 as shown in Figure 9-3 through Figure 9-5.

Case-3. Steam-Surfactant-Foam Injection. In this case, we inject 0.01vol/vol surfactant along with 0.01 vol/vol and co-surfactant as a foaming agent. Foam forms during steam injection and prevents steam overrides to the upper layers thereby improving its volumetric sweep efficiency. Figure 9-7a shows the steam saturation after 30 days of steam-surfactant-foam injection in the first cycle. The low steam saturation is indicated compared to Case-1 and Case-2, where the steam cannot segregate to the upper layers in the presence of foam and it condenses around the well to deliver its energy to the surrounding oil. The steam condensation continues during the soaking time, and its saturation decreases as shown in Figure 9-7b. Figure 9-7c and Figure 9-7d show steam saturation after steam injection and soaking time in the second cycle respectively, where the steam completely condenses after soaking period and delivers all its latent heat to the reservoir fluids and rocks. Figure 9-8 and Figure 9-9 show the corresponding temperature and viscosity distributions**.** These figures show that foam lowers the mobility of steam to provide enough time for heat conduction to effectively transfer the energy to near well regions. The reservoir pressure increases slightly in the presence of the foam, but not sufficient to decrease the injectivity. Figure 9-6 shows pressure distributions in the absence and in the presence of foam after 30 days of injection in the first cycle in Case-1 and Case-3. Since steam is such a condensable gas, pressure around the wellbore cannot be increased to reduce injectivity of well.

Daily oil production rate is plotted in Figure 9-10 for all simulation cases**.** This plot shows that when the well is open to production, oil rate is initially low, because oil is already pushed away from the well during steam injection. As a result of drawdown pressure, oil bank reaches to the highest value after a short period of production. Emulsion production rates in Case-2 and Case-3 are produced at a high rate initially along with solubilized oil when wells are placed on production as shown in Figure 9-11.

Figure 9-12 shows the comparison of the oil recovery for all three cases. In Case-2, the oil solubilization in water (emulsion phase) increases the oil recovery compared to the base Case-1. The higher oil recovery in Case-3 is attributed to both the oil solubilization and the better volumetric sweep of steam.

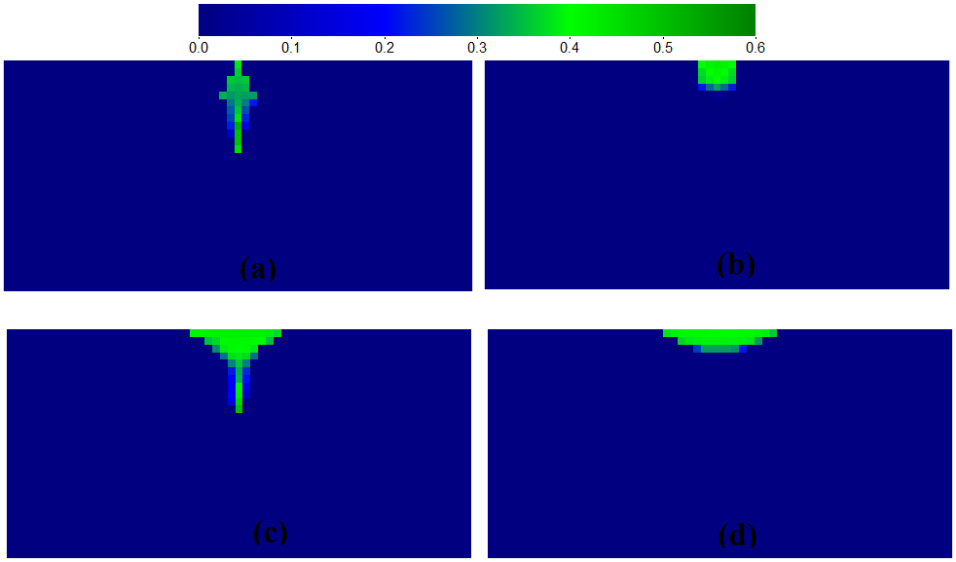

Figure 9-3-Steam saturation for Case-1 and Case-2 (a) after steam injection in the first cycle (b) after soaking in the first cycle (c) after steam injection in the second cycle (b) after soaking in the second cycle

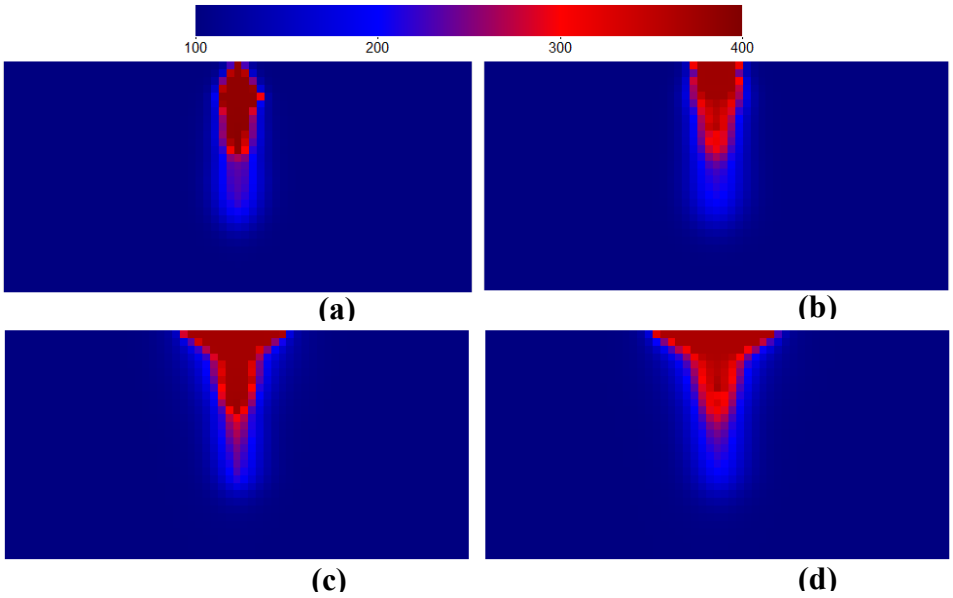

Figure 9-4-Temperature for Case-1 and Case-2 (a) after steam injection in the first cycle (b) after soaking in the first cycle (c) after steam injection in the second cycle (b) after soaking in the second cycle

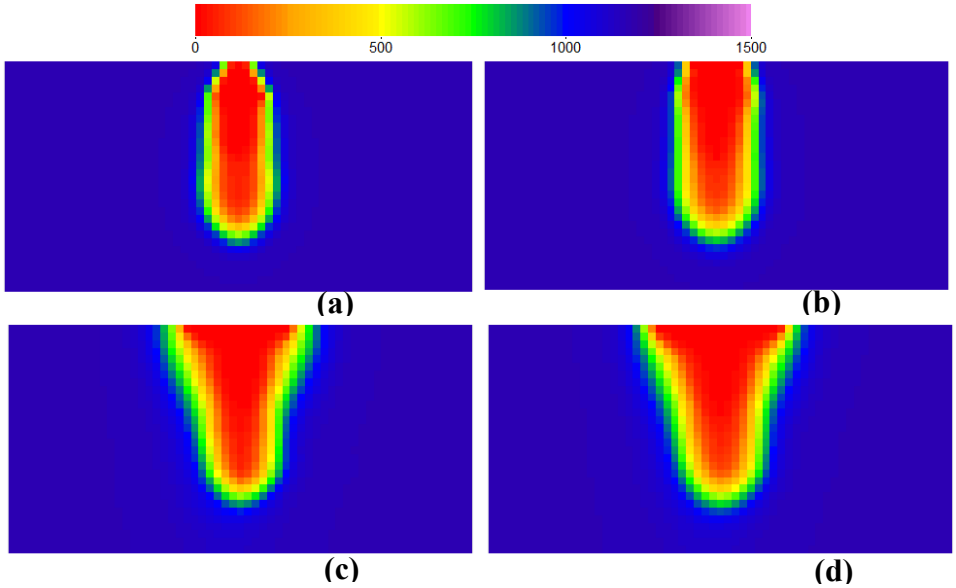

Figure 9-5-Oil viscosity for Case-1 and Case-2 (a) after steam injection in the first cycle (b) after soaking in the first cycle (c) after steam injection in the second cycle (b) after soaking in the second cycle

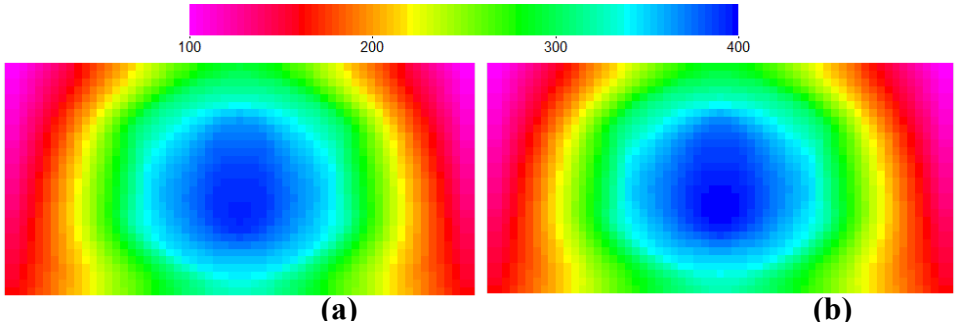

Figure 9-6-Pressure map (a) Case-1 (b) Case-3

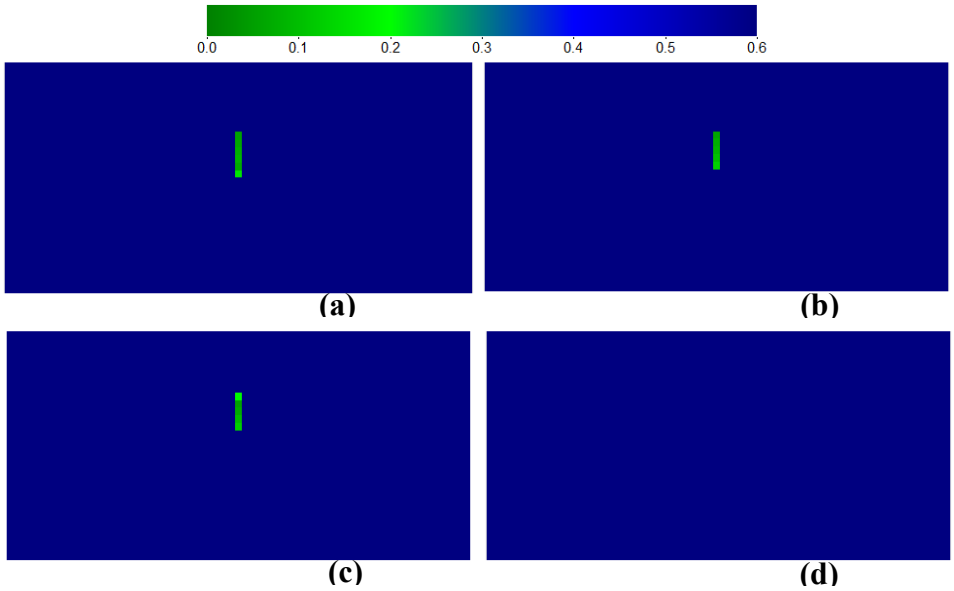

Figure 9-7- Steam saturation for Case-3 (a) after steam injection in the first cycle (b) after soaking in the first cycle (c) after steam injection in the second cycle (b) after soaking in the second cycle

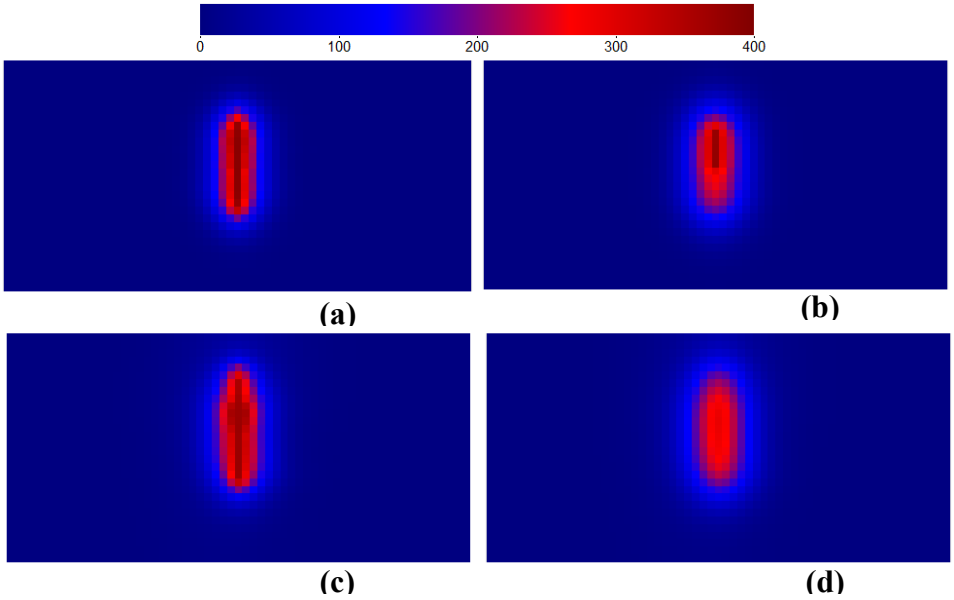

Figure 9-8- Temperature(°F) for case-3 (a) after steam injection in the first cycle (b) after soaking in the first cycle (c) after steam injection in the second cycle (b) after soaking in the second cycle

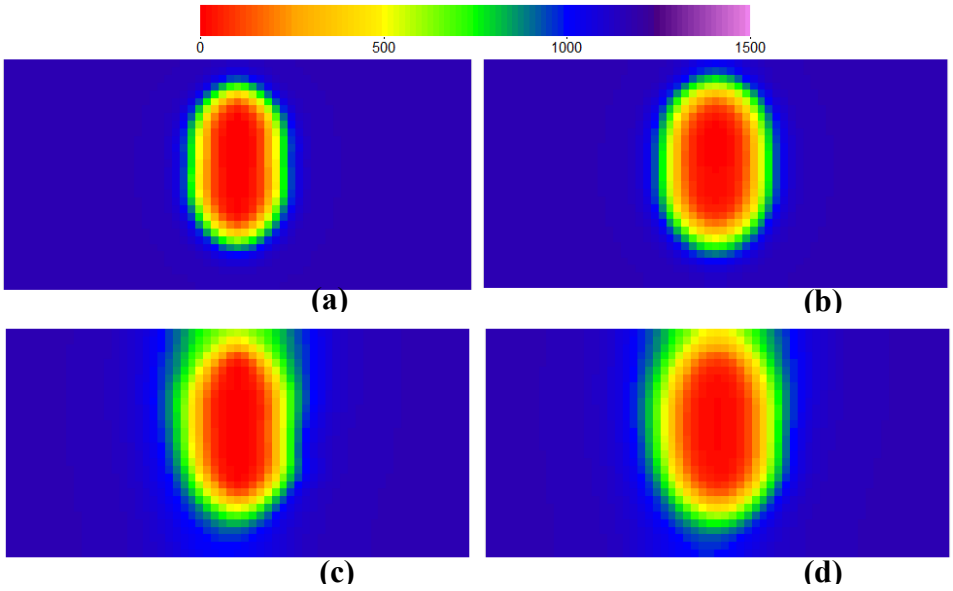

Figure 9-9-Oil viscosity(cp) for case-3 (a) after steam injection in the first cycle (b) after soaking in the first cycle (c) after steam injection in the second cycle (b) after soaking in the second cycle

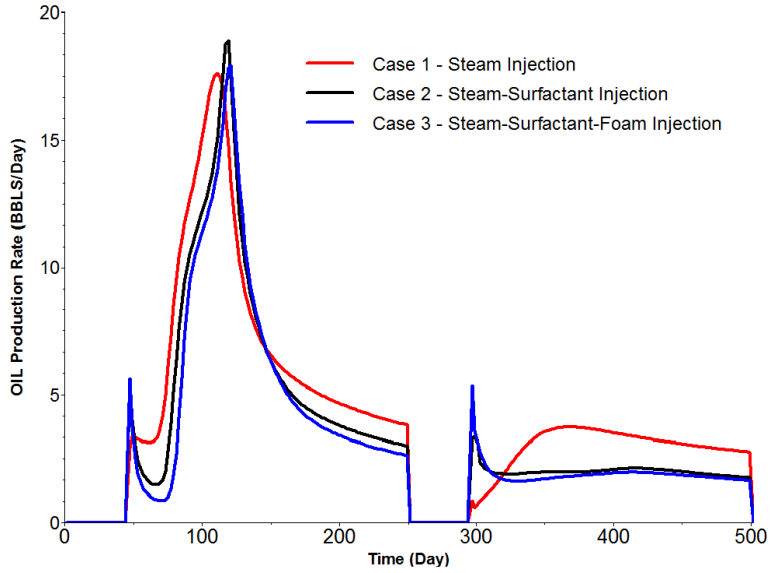

Figure 9-10- Daily oil production rate of all simulations.

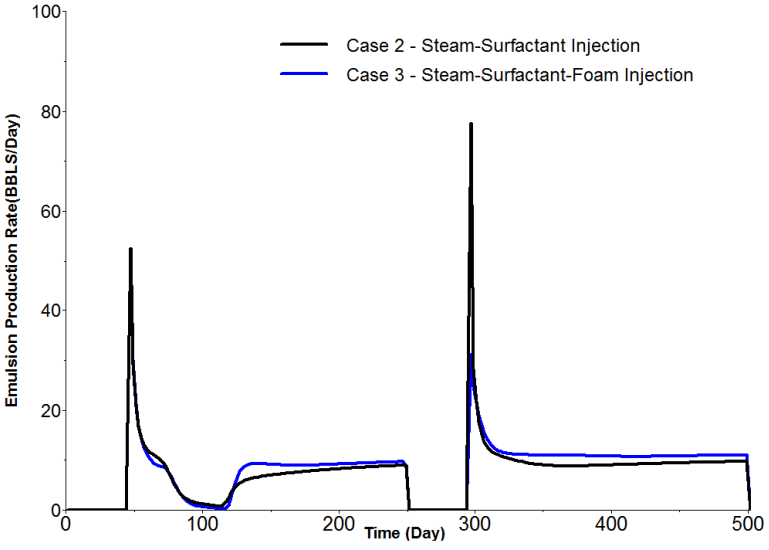

Figure 9-11- Daily emulsion production rate of Case 2 and Case 3.

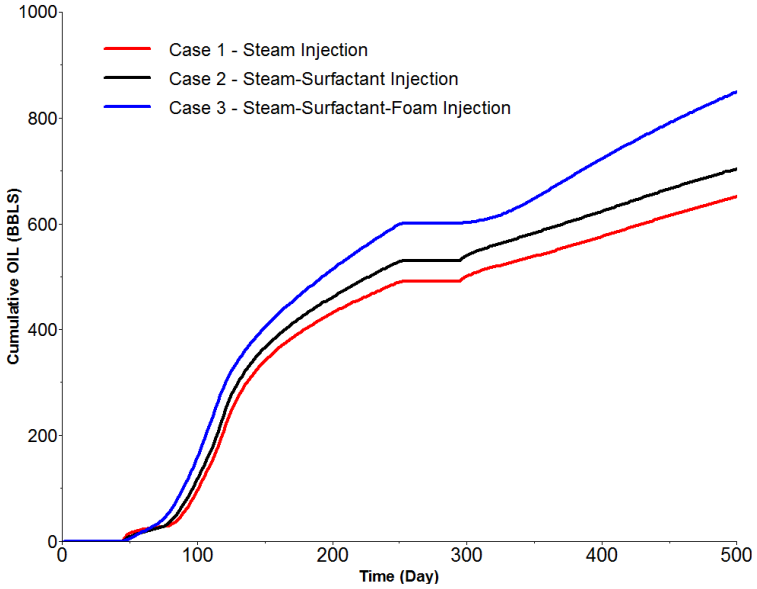

Figure 9-12-Comparison of cumulative oil recovery for three case studies

Table 9-3summarizes the cumulative oil production from emulsion and oil phases for all simulation cases with respect to cumulative steam injection. This table shows that the cumulative oil production in Case-2 is increased by 11% compared to the base case, which was mostly in the first cycle. The cumulative oil recovery for Case-3 was increased by 39% in comparison to the base case. Major increase in the oil recovery for Case-3 occurred in the second cycle.

Table 9-3-Comparison of cumulative steam ratio in different cases.

	Cum. Oil Production (BBLS)	**Cum. Water Injection* (BBLS)**	**Ratio**
Case-1	631	1602	2.5
Case-2	697	1602	2.3
Case-3	875	1602	1.8

*** Cold Water Equivalent (CWE)**

9.4 SUMMARY AND CONCLUSION

We extended the energy balance equation to model steam and fully coupled it with surfactant and foam modules to model all possible mechanisms in steam-surfactant-foam injection. Afterward, a series of cyclic steam injection simulations was performed to evaluate the efficiency of oil viscosity reduction, emulsification, and foam mobility control on heavy oil production. The main conclusions are:

Although the ultra-low IFT is not a dominant mechanism in the heavy oil reservoirs to reduce residual saturation, our results indicate that the oil in water emulsification increases the oil recovery by 11% compared to conventional steam injection.

Foam controls the mobility of steam to prevent gravity segregation and override. Steam foam improves oil recovery significantly and economically avoids injecting additional thermal energy.

Foam improves the volumetric sweep efficiency and heats the reservoir laterally around the wellbore. The total recovery was increased by 39% in comparison to the conventional steam injection.

Steam override was severe in the second cycle and mobility control using foam injection was crucial in order to enhance the oil recovery.

Chapter 10:Summary, Conclusions and Recommendations

In this chapter, we summarize the tasks performed in this research and conclude the insights of this dissertation and then several recommendations are discussed for future extension of this work.

10.1 SUMMARY

In this research the following tasks were performed

- A four-phase flow model was developed for oil/water/microemulsion/gas or steam at reservoir condition compatible with original UTCHEM formulation and its framework.
- Developed the four-phase flow formulation and considered compressible fluid flow as a real mixture using blackoil model concept.
- A new pressure equation was derived to consider the volume balance in the presence of four phases at equilibrium.
- Pressure equation was discretized and then implemented into the UTCHEM simulator using an implicit method.
- Conservation of mass equations for a wide range of components (water, oil, surfactant, polymer, anion, cation, alcohol, and gas) existing in the original UTCHEM simulator were derived and then this set of partial differential equations was linearized, discretized, and finally implemented into the UTCHEM simulator.
- Mass transfer between the phases oil/gas and water/steam were considered using black oil model concept or steam table.
- A partial mass density of gas component in oil phase was presented at this work in the fluid flow formulation to convert the solution gas ratio from standard condition to reservoir condition.

- Production and injection rates were calculated at reservoir condition, consistent with the original formulation of UTCHEM.
- Fluid properties for saturated and undersaturated conditions were calculated from given table, consistent with commercial simulators and PVT packages.
- Surfactant phase behavior was successfully incorporated in the new fluid flow formulation.
- Coupled four-phase behavior between gas/oil or water/steam and microemulsion/water/oil were successfully incorporated into the UTCHEM simulator.
- Our four-phase flow model was successfully compared with three-phase flow models existing in commercial reservoir simulators and in the original UTCHEM.
- The conservation of energy equation is derived from the first law of thermodynamics for a four-phase fluid flow model. This energy balance equation considers latent heat effect in solving for temperature due to phase change between water and steam.
- The energy balance equation was implemented and incorporated into the UTCHEM simulator using sequential implicit scheme.
- An analytical heat-loss model (Vinsome and Westerveld model) to overburden and underburden was incorporated in energy balance equation and then implemented into UTCEM.
- New thermal model was successfully compared with the existing thermal model in CMG-STARS.
- Electrical Joule heating model was developed for constant voltage and constant electrical current constraints. This model was incorporated into the UTCHEM simulator with four-phase flow model in order to be coupled with chemical flooding options.

- New thermal model was successfully compared with the existing thermal model in CMG-STARS.
- Developed electrical Joule heating model was successfully tested against CMG-STARS for different case studies. Coupled electrical heating and surfactant/alkali injection was performed in UTCHEM as a promising recovery process for heavy oil production.
- All models that have been developed in this research study were implemented in the Cartesian coordinates.
- The effects of fracture saturated with saline water and vaporization of water near wellbore during electrical heating were investigated in this study.
- For modeling of a hybrid process, we discussed the cyclic steam injection case with different foam and surfactant injections to show the effect of different mechanisms. This application of a thermal-chemical process was modeled to compare the different mechanisms including oil solubilization in microemulsion phase, mobility control, and oil viscosity reduction due to steam injection.
- Our simulation results reveal that our models can accurately and successfully model the hybrid thermal chemical processes in comparison to existing models and simulators.

10.2 CONCLUSION

We conclude the following from this research:

- The four phase model was tested and successfully compared to three phase models for the different cases. In this four-phase model, the transport of four phases can simultaneously occur; and all four of them can be in thermodynamic equilibrium.

This equilibrium is obtained for oil/gas (using blackoil model) or steam/water (using steam table) as well as oil/water/microemulsion (using Hand's rule).

- The thermal chemical model was tested in one, two, and three dimensional cases and the results were successfully compared with existing reservoir simulators results.
- We observed that establishment of a large pressure drop between reservoir pressure and the bottomhole pressure of a production well causes an increase in the material balance error. In order to overcome to this problem, a small time step is required.
- The energy balance equation that has been developed for thermal model in this research is more robust compared to the enthalpy base energy equation. This energy equation can be modified for multi components rather than multiphase and then used for compositional simulators. In enthalpy base energy equation, calculation of enthalpy references for phase compositions and components causes a large mess. Although, we made different simplifications and assumptions in this energy balance equation, results showed this form of energy balance equation is a fair approximation of the exact solution.
- We investigated the effect of vaporization of water near the wells during electrical heating on the efficiency of this process. We also evaluated the effect of water saturated fractures during the electrical heating. Results reveal that dissipation of electrical energy is a strong function of electrical conductivity. More dissipated electrical energy rate needs a high electrical conductivity. Vaporization of water decreases the dissipation of electrical energy and this restricts the generation of heat. Consequently, vaporization of water has significant impact on the efficiency of the electrical Joule heating process. The high water saturated fractures and electrical conductivity of water phase have an important effect on the Joule heating process. The presence of fractures can significantly increase the effectiveness of the process.

Due to the increase in electrical conductivity, the dissipation of electrical energy increases in the form of the heat and hence increases the reservoir temperature and reduces the oil viscosity.

- We applied the developed models to a cyclic steam injection case along with surfactant and foam injection to model all possible mechanisms in steam-surfactant-foam injection to evaluate the efficiency of this hybrid method including the oil viscosity reduction, emulsification, and foam mobility control on heavy oil production. The results indicate that the ultra-low IFT is not a dominant mechanism in the heavy oil reservoirs to reduce residual saturation. Also, results show that the oil in water emulsification increases the oil recovery compared to conventional steam injection. Foam controls the mobility of steam to prevent gravity segregation and override. Steam foam improves oil recovery significantly and economically avoids injecting additional thermal energy. Foam improves the volumetric sweep efficiency and heats the reservoir laterally around the wellbore.
- Since original UTCHEM includes several existing mechanism, coupling of these mechanisms with the four-phase flow model helps to capture the most of the underlying mechanisms for evaluating hybrid a thermal-chemical or chemical-gas case study.

10.3 RECOMMENDATIONS FOR FUTURE WORK

Thermal and chemical EOR methods are quit complicated processes. Therefore, more research in this area is strongly recommended to develop a deeper conceptual understanding and to capture more physical mechanisms for field operations. During this research study, we developed a robust numerical four-phase compressible model along with thermal model into UTCHEM simulator to study the physical processes of different

mechanisms to improve recovery for heavy oil reservoirs as well as conventional reservoirs. Recommendations for further study are listed as following:

- Governing equations that have been developed for pressure and concentrations in this research can be used for a fully implicit solution scheme to speed up a numerical reservoir simulator and increase the robustness of the flow and thermal models.
- Since mass transfer was considered between oil and gas using blackoil model in this research, a similar concept can be applied to model the mass transfer between water and gas phases.
- The extension and the incorporation of a fracture model into this four-phase, thermal chemical model can increase the capability and the accuracy a reservoir study case.
- Since electrical Joules heating and steam flooding can be coupled with the surfactant module, we recommend several test or field cases to be selected from literature along with experimental or observed field data to model and simulate all included mechanisms, such as mobility control, IFT reduction, Emulsification (W/O or O/W) as Type I or Type II, wettability alteration due to temperature, and viscosity reduction due to temperature.
- Hot gas injection with chemical and/or foam injection can be easily tested to capture the different mechanisms.
- The effect of solution gas and high pressure on surfactant phase behavior can be observed from the literature study and then incorporated into phase behavior in the UTCHEM simulator.
- We recommend further work on tuning and optimization of linear solvers used in this code.

- Although, modeling of hybrid processes such as electrical heating with chemical injection, pre-electrical heating and steam injection with solvent, steam foam, steam-surfactant, steam-solvent is complicated, this four-phase flow model can properly simulate such these processes. A set of experimental or field observed data are required to study and show the performance of this reservoir simulator.
- We recommend further parallelization of the code to speed up in the case of the gas or steam flooding where a small time step is needed.
- Further research is recommended on the effect of temperature on alkaline phase behavior in the presence of the chemical reactions as well as solution gas and pressure for light oil.
- We also recommend to incorporate a comprehensive and accurate four phase relative permeability model and other petrophysical and fluid flow parameter models (e.g. IFT, viscosity, and adsorption).

Glossary

Fluid Flow Properties

A_{D1}, A_{D2} =surfactant adsorption parameters

A_{P1}, A_{P1}, A_{P1} = microemulsion viscosity parameters

A_{P4}, A_{P5} = microemulsion viscosity parameters

B_{D3} = surfactant adsorption parameters

B_2, B_4 = formation volume factor oil and gas, [L^3/L^3]

b = formation volume factor oil and gas, [T]

c_{sel}, c_{seu} = lower and upper effective salinity limit, respectively, [eq/L^3]

c_{se}, c_{seop} = effective and optimum effective salinity, respectively, [eq/L^3]

$\hat{c}_h$ = adsorbed concentration of component h, [L^3/L^3]

$\tilde{c}_h$ = overall concentration of component h in the mobile and stationary phases, [L^3/L^3]

c_h = volume concentration of component h, [L^3/L^3]

c_{hl} = volume concentration of component h in phase l, [L^3/L^3]

c_{1p}, c_{2p}, c_{3p} = water, oil, surfactant concentrations at plait points, [L^3/L^3]

$\bar{\bar{D}}_{hl}$ = molecular diffusion and dispersion coefficient tensor of component h in phase l, [$L^2\ t^{-1}$]

e_l = exponent of relative permeability of phase l

e_l^{low}, e_l^{high} = exponent of relative permeability of low and high interfacial cases for phase l

H_0, H_1, H_2 = height of binodal curve for microemulsion phase behavior

$\bar{\bar{K}}$ = permeability, [L^2]

k_{rl} = relative permeability of phase l

k_{rl}^{o} = endpoint relative permeability of phase l

$k_{rl}^{o,low}, k_{rl}^{o,high}$ = endpoint of relative permeability of low and high interfacial cases for phase l

N_p =number of phases

Nc =number of components

M =mass, [M]

p_{cl} = capillary pressure between water and phase l, [ML^{-1} t^{-2}]

p_l = pressure of phase l, [ML^{-1} t^{-2}]

p_{sat} = bubble point pressure, [ML^{-1} t^{-2}]

u_l = Darcy velocity for phase l, [Lt^{-1}]

t = time, [t]

T = temperature, [T]

T_{ref} = reference temperature, [T]

q_h = source and sink for component h per bulk volume, [L^3 t^{-1}/L^3]

R_{so} = amount of dissolved gas in oil [L^3/L^3]

S_l = fluid saturation of phase l, [L^3/L^3]

S_{rl} = residual saturation of phase l, [L^3/L^3]

S_{nl} = normalized saturation of phase l, [L^3/L^3]

$S_{rl}^{o,low}, S_{rl}^{o,high}$ = residual saturation of phase l at high and low capillary number, respectively, [L^3/L^3]

ρ_l = mass density of phase l, [ML^{-3}]

ρ_h = mass density of component h, [ML^{-3}]

σ = interfacial tension between two phases, [Mt^2]

ς_h, ς_r = compressibility of component h and rock, [$M^{-1}L$ t^2]

λ_{rl} = mobility ratio of phase l, [M-1L t]

ϕ = porosity, [L^3/L^3]

μ_l = viscosity of phase *l*, [$ML^{-1}\ t^{-1}$]

$\alpha_1,...,\alpha_5$ = microemulsion phase viscosity parameters

τ = tortuosity factor [L/L]

Thermal and Electrical Properties

Q = energy,[$Q=M\ L^2t^{-2}$]

M =mass, [M]

H = enthalpy [QM^{-1}]

U = internal energy [QM^{-1}]

$\bar{H}$ = specific enthalpy of phases [QM^{-1}]

q_H = enthalpy source or sink term rate [$QL^{-3}t^{-1}$]

q_L = heat loss rate to overburden and underburden rocks [$QL^{-3}t^{-1}$]

q_{ele} = electrical joule heating source term and [$QL^{-3}t^{-1}$]

q_{instu} = insitu thermal conduction source rate [$QL^{-3}t^{-1}$]

λ = thermal conductivity of phases [$Qt^{-1}L^{-1}T^{-1}$]

c_w = volume concentration of steam component [L3/L3]

c_s = volume concentration of water component [L3/L3]

ζ_{pw} = heat capacity of water, [$QM^{-1}T^{-1}$]

ζ_{ps} = heat capacity of aqueous, [$QM^{-1}T^{-1}$]

α = steam mass quality [M/M]

μ = viscosity, [$ML^{-1}\ t^{-1}$]

T = temperature [T]

P = pressure [$ML^{-1}\ t^{-2}$]

u = Darcy velocity for each phase [Lt^{-1}]]

ρ = current density [amp/L^3]

σ = electrical conductivity [sim/L]

ψ = the electric potential [vol]

V = discretized form of electric potential or Voltage [vol]

J = the electric source [amp/L3]

R = electrical resistivity [ohm]

I = discretized form of electrical current [amp]

Subscripts:

h = component number, where 1 = water; 2 = oil; 3 = surfactant; 4 = polymer;5 = anion; 6 = cation; 7 = alcohol; 8 = gas

l = phase number, where 1 = water (aqueous); 2 = oil (oleic); 3 = microemulsion; 4 = gas

Appendix A: Sample Input Data

A.1 WATER INJECTION WITH TWO PHASE EXISTING CASE (CASE-1)

The following is the input data file for UTCHEM simulator. We used this case in Chapter 6 for two-phase flow comparison between original model and four-phase model. In order to run this case for both original and four-phase model, IGMAS flag in input file should be set IGMAS=1 along with PVT file for four-phase and IGMAS =0 for original. This case is similar to Case-5 and only difference is in well injection schedule. Difference part is presented below

```
HEAD
:
:
:
INPUT
:
:
:
:
CC*********************************************************************
CC                                                                    *
CC   WELL DATA                                                        *
CC                                                                    *
CC*********************************************************************
:
:
:
:
CC  ID,INJ. RATE AND INJ. COMP. FOR RATE CONS. WELLS FOR EACH PHASE (L=1,3)
*----  ID     QI(M,L)     C(M,KC,L)
     1     50.   1.0     0.0    0.0    0.0    0.0   0.0  0.0 0.0  0.0
     1     0.0   0.0     0.0    0.0    0.0    0.0   0.0  0.0 0.0  0.0
     1     0.0   0.0     0.0    0.0    0.0    0.0   0.0  0.0 0.0  0.0
     1     0.0   0.0     0.0    0.0    0.0    0.0   0.0  0.0 0.0  0.0
:
:
:
PVT
:
:
```

A.2 GAS AND WATER INJECTION WITH THREE PHASE EXISTING CASE (CASE-2)

The following are the input data files for UTCHEM and CMG-IMEX simulators. We used this case in Chapter 6 for three-phase flow validation and comparison between

UTCHEM four-phase model and CMG-IMEX. The input file of this case is similar to Case-6 and only difference is in well injection schedule. Difference part is presented for UTCHEM.

CMG-IMEX

```
**************************************************************************
** CMG IMEX:    GAS AND WATER INJECTION                                  **
**************************************************************************
**************************************************************************
**                                                                       **
** FILE:  1D COMPARISON FOR GAS INJECTION                                **
**                                                                       **
** MODEL:  20X1X1            GAS AND WATER INJECTION          FIELD UNIT  **
**                                                                       **
**************************************************************************

RESULTS SIMULATOR IMEX

**************************************************************************
** I/O CONTROL SECTION                                                  **
**************************************************************************
*TITLE1
'GAS  AND WATER INJECTION'
*TITLE2
'GAS IS RECYCLED WITH ADDITIONAL MAKEUP GAS.'
*INUNIT *FIELD
*WPRN   *WELL   10
*WPRN   *GRID   *TIME
*WPRN   *ITER   *BRIEF
*OUTPRN *WELL   *BRIEF
*OUTPRN *RES    *NONE
*OUTPRN *TABLES *NONE
*OUTPRN *GRID   *SO *SG *PRES
*WSRF   *GRID   *TIME
*WSRF   *WELL   1
*OUTSRF *GRID   *SO *SG *PRES
**************************************************************************
** RESERVOIR DESCRIPTION SECTION                                        **
**************************************************************************
*GRID *CART 20   1    1
*DI *CON 10
*DJ *CON 10
*DK *CON  10
*DEPTH 1 1 1 100
*POR *CON 0.2
*CPOR   3.0E-9
*PRPOR 14.7
*PERMI *CON    100.0
*PERMJ *CON    100.0
*PERMK *KVAR   100
**************************************************************************
** COMPONENT PROPERTIES SECTION                                         **
**************************************************************************
*MODEL *BLACKOIL              ** THREE PHASE - THREE EQUATION
*PVT
**    P       RS       BO         EG      VISO     VISG
   400.000   165.000   1.01200   169.490   1.17000 0.0130000
   800.000   335.000   1.02550   338.980   1.14000 0.0135000
  1200.000   500.000   1.03800   510.200   1.11000 0.0140000
  1600.000   665.000   1.05100   680.270   1.08000 0.0145000
  2000.000   828.000   1.06300   847.460   1.06000 0.0150000
  2400.000   985.000   1.07500  1020.400   1.03000 0.0155000
  2800.000  1130.000   1.08700  1190.500   1.00000 0.0160000
  3200.000  1270.000   1.09850  1351.400 0.9800000 0.0165000
  3600.000  1390.000   1.11000  1538.500 0.9500000 0.0170000
  4000.000  1500.000   1.12000  1694.900 0.9400002 0.0175000
  4400.000  1600.000   1.13000  1851.900 0.9200000 0.0180000
  4800.000  1676.000   1.14000  2040.800 0.9100000 0.0185000
```

```
  5200.000  1750.000   1.14800  2222.200 0.9000000 0.0190000
  5600.000  1810.000   1.15500  2381.000 0.8900000 0.0195000

*DENSITY *OIL    32.4
*DENSITY *GAS     0.0576
*DENSITY *WATER  64.8
*CO             1.0E-5       ** OIL COMPRESSIBILITY
*CVO             0.0          ** VISCOSITY DEPENDENCE ON OIL COMPRESSIBILITY
*BWI             1.010       ** WATER FORMATION VOLUME FACTOR
*CW              3.0E-8       ** WATER COMPRESSIBILITY
*REFPW           14.7         ** REFERENCE PRESSURE
*VWI             0.96         ** WATER VISCOSITY AT REFERENCE PRESSURE
*CVW             0.0          ** PRESSURE DEPENDENCE ON WATER COMPRESSIBILITY
*TRES     100
*ROCKFLUID
********************************************************************************
** ROCK-FLUID PROPERTY SECTION                                                 **
********************************************************************************
*RPT 1
*SWT
** SW        KRW   KROW
0     0    1
1     1    0
*SLT
**  SL     KRG        KROG
 0    1    0
 1     0   1
*INITIAL
********************************************************************************
** INITIAL CONDITIONS SECTION                                                  **
********************************************************************************
*USER_INPUT
*PB   *MATRIX   *CON    4000
*PRES *CON  3000
*SW   *CON   0.4
*SO   *CON   0.6
*GASZONE   *OIL
*NUMERICAL
********************************************************************************
** NUMERICAL CONTROL SECTION                                                   **
********************************************************************************
*DTMAX      5        ** MAXIMUM TIME STEP SIZE
*MAXSTEPS      5000          ** MAXIMUM NUMBER OF TIME STEPS
*NORM *PRESS   20000.0        ** NORMAL MAXIMUM CHANGES PER TIME STEP
*NORM *SATUR     0.20
*RUN
********************************************************************************
** WELL AND RECURRENT DATA SECTION                                           **
********************************************************************************
*DATE 2000   01   01
*DTWELL 1.0
*WELL 1  'INJ 1'
*INJECTOR  *UNWEIGHT  1
*INCOMP *GAS
*OPERATE  *MAX  *BHG  100
**           RAD    GEOFAC  WFRAC   SKIN
*GEOMETRY *K  0.25    0.34    1.0    0.0
*PERF *GEO 1
** IF     JF     KF     WI
   1      1      1      1
*WELL 2  'PRODUCER'
*PRODUCER  2
*OPERATE *MIN  *BHP  2000.0
** WELL GEOMETRY FOR THE PRODUCER.
**           RAD    GEOFAC  WFRAC   SKIN
*GEOMETRY *K  0.25    0.34    1.0    0.0
*PERF *GEO 2
** IF     JF     KF     FF
   20     1      1     1.0
     *WELL 3  'INJ 2'
     *INJECTOR  *UNWEIGHT 3
     *INCOMP *WATER
     *OPERATE  *MAX  *BHW  8.904
     **           RAD    GEOFAC  WFRAC   SKIN
     *GEOMETRY *K  0.25    0.34    1.0    0.0
     *PERF *GEO 3
     ** IF     JF     KF     WI
```

```
     1      1      1      1
SHUTIN 3
   *TIME     1
   *TIME     25
SHUTIN 1
OPEN 3
   *TIME     26
   *TIME     75
OPEN 1
OPEN 3
   *TIME     76
   *TIME     150
*STOP
```

HEAD

:
:
:

INPUT

```
CC*************************************************************************
CC                                                                        *
CC    WELL DATA                                                           *
CC                                                                        *
CC*************************************************************************
CC
CC
CC FLAG FOR SPECIFIED BOUNDARY AND ZONE IS MODELED
*---- IBOUND     IZONE
      0      0
CC
CC TOTAL NUMBER OF WELLS, WELL RADIUS FLAG, FLAG FOR TIME OR COURANT NO.
*---- NWELL   IRO    ITIME    NWREL
      2      2      0        2
CC
CC WELL ID,LOCATIONS,AND FLAG FOR SPECIFYING WELL TYPE, WELL RADIUS, SKIN
*---- IDW    IW    JW    IFLAG    RW     SWELL   IDIR   IFIRST   ILAST   IPRF
     1     1     1      1    0.5      0      3      1     1    0
CC
CC WELL NAME
*----  WELNAM
INJ1
CC
CC ICHEK , MAX. AND MIN. ALLOWABLE BOTTOMHOLE PRESSURE AND RATE
*---- ICHEK     PWFMIN     PWFMAX    QTMIN    QTMAX
      0          0         10000      0        20000
CC
CC WELL ID,LOCATIONS,AND FLAG FOR SPECIFYING WELL TYPE, WELL RADIUS, SKIN
*---- IDW    IW    JW    IFLAG    RW     SWELL   IDIR   IFIRST   ILAST   IPRF
     2     20     1     2     1      0      3         1   1       0
CC
CC WELL NAME
*----  WELNAM
PROD1
CC
CC ICHEK , MAX. AND MIN. ALLOWABLE BOTTOMHOLE PRESSURE AND RATE
*---- ICHEK     PWFMIN     PWFMAX    QTMIN    QTMAX
      0          0         1000      -0       -20000
CC
CC  ID,INJ. RATE AND INJ. COMP. FOR RATE CONS. WELLS FOR EACH PHASE (L=1,3)
*----  ID     QI(M,L)     C(M,KC,L)
     1      0.   0.0   0.0     0.0   0.0    0.0  0.0  0.0  0.0  0.0
     1      0.0    0.0     0.0    0.0    0.0    0.0  0.0  0.0  0.0   0.0
     1      0.0    0.0     0.0    0.0    0.0    0.0  0.0  0.0  0.0   0.0
     1      100.0    0.0     0.0    0.0    0.0    0.0  0.0  0.0 1  0.0
CC
CC
*--- ID, INJ. TEMP (F)
    1    90.
CC
CC
*----  ID    PWF
    2      2000
CC
CC CUM. INJ. TIME , AND INTERVALS (PV OR DAY) FOR WRITING TO OUTPUT FILES
*---- TINJ     CUMPR1     CUMHI1     WRHPV     WRPRF      RSTC
```

```
     25      5*0.5
CC
CC THE INI. TIME STEP,CONC. TOLERANCE,MAX.,MIN. TIME STEPS
*----  DT     DELC(I)              CNMAX             CNMIN
  0.0001       9*0.005          0.005               0.00001
CC
CC FLAG FOR INDICATING BOUNDARY CHANGE
*---- IBMOD
       0
CC
CC IRO, ITIME, NEW FLAGS FOR ALL THE WELLS ( WATER INJ.)
*---- IRO   ITIME  IFLAG
     2       0   1   2
CC
CC NUMBER OF WELLS CHANGES IN LOCATION OR SKIN OR PWF
*----NWEL1
    0
CC
CC NUMBER OF WELLS WITH RATE CHANGES, ID
*----NWEL1   ID
    2       1    2
CC
CC  ID,INJ. RATE AND INJ. COMP. FOR RATE CONS. WELLS FOR EACH PHASE (L=1,3)
*----  ID     QI(M,L)     C(M,KC,L)
      1      50.  1   0.0     0.00   0.0    0.0  0.0  0.0  0.0  0.0
      1      0.0    0.0     0.0    0.0    0.0    0.0  0.0  0.0  0.0   0.0
      1      0.0    0.0     0.0    0.0    0.0    0.0  0.0  0.0  0.0   0.0
      1      0.0    0.0     0.0    0.0    0.0    0.0  0.0  0.0  0.0   0.0
CC
CC
*--- ID, INJ. TEMP (F)
    1    90.
CC
CC
*----  ID    PWF
    2      2000
CC
CC CUM. INJ. TIME , AND INTERVALS (PV OR DAY) FOR WRITING TO OUTPUT FILES
*---- TINJ     CUMPR1     CUMHI1     WRHPV     WRPRF      RSTC
     75      5*0.5
CC
CC THE INI. TIME STEP,CONC. TOLERANCE,MAX.,MIN. TIME STEPS
*----  DT     DELC(I)              CNMAX             CNMIN
  0.0001       9*0.005          0.005               0.00001
CC
CC FLAG FOR INDICATING BOUNDARY CHANGE
*---- IBMOD
       0
CC
CC IRO, ITIME, NEW FLAGS FOR ALL THE WELLS ( WATER INJ.)
*---- IRO   ITIME  IFLAG
     2       0   1   2
CC
CC NUMBER OF WELLS CHANGES IN LOCATION OR SKIN OR PWF
*----NWEL1
    0
CC
CC NUMBER OF WELLS WITH RATE CHANGES, ID
*----NWEL1   ID
    2       1    2
CC
CC  ID,INJ. RATE AND INJ. COMP. FOR RATE CONS. WELLS FOR EACH PHASE (L=1,3)
*----  ID     QI(M,L)     C(M,KC,L)
      1      50.   1.0    0.0     0.00    0.0    0.0  0.0  0.0  0.0  0.0
      1      0.0    0.0     0.0    0.0    0.0    0.0  0.0  0.0  0.0   0.0
      1      0.0    0.0     0.0    0.0    0.0    0.0  0.0  0.0  0.0   0.0
      1      100    0.0     0.0    0.0    0.0    0.0  0.0  0.0  1.0   0.0
CC
CC
*--- ID, INJ. TEMP (F)
    1    90
CC
CC
*----  ID    PWF
    2      2000
CC
CC CUM. INJ. TIME , AND INTERVALS (PV OR DAY) FOR WRITING TO OUTPUT FILES
```

```
*---- TINJ     CUMPR1     CUMHI1     WRHPV     WRPRF      RSTC
     150      5*0.5
CC
CC THE INI. TIME STEP,CONC. TOLERANCE,MAX.,MIN. TIME STEPS
*----  DT     DELC(I)              CNMAX             CNMIN
   0.0001      9*0.005         0.005               0.00001
```

PVT

:

:

A.3 WATER INJECTION BELOW BUBBLE POINT WITH THREE PHASE EXISTING CASE (CASE-3)

The following are the input data files for UTCHEM and CMG-IMEX simulators. We used this case in Chapter 6 for three-phase flow validation and comparison between UTCHEM four-phase model and CMG-IMEX.

```
**********************************************************************
** CMG IMEX:    VAPORIZATION                                          **
**********************************************************************
**********************************************************************
**                                                                   **
** FILE:  3D COMPARISON FOR GAS PRODUCTION                           **
**                                                                   **
** MODEL:  5X5X5        PRODUCTION TO VAPORRIZE GAS          FIELD UNIT     **
**                                                                    **
**********************************************************************
** 2014-07-17, 6:49:00 PM, HL7675
RESULTS SIMULATOR IMEX 201210
 *TITLE1
 'UTCHEM VALIDATION'
 *TITLE2
 'PRODUCTION TO VAPORRIZE GAS'
 *TITLE3
 'COATS, THOMAS AND PIERSON, 1995.'
 *INUNIT    *FIELD
 *WPRN      *WELL 1
 *WPRN      *GRID *TIME
 *OUTPRN    *GRID *ALL
 *OUTPRN    *WELL *ALL
  *OUTSRF *RES *ALL
  *OUTSRF *GRID  *ALL
 *WSRF      *GRID 5
 *WSRF      *WELL 1
  **********************************************************************
 ** RESERVOIR DESCRIPTION SECTION
 **********************************************************************
 *GRID *CART    5   5   5
 *KDIR *DOWN
 *DI *CON  10.0
 *DJ *CON  10.0
 *DK *CON  10.0
 *DEPTH 1    1   1   0
 *POR  *CON     0.2
 *PRPOR 200.0
 *CPOR  0
 *PERMI *CON 50
 PERMJ EQUALSI
  PERMK *CON 5
 **********************************************************************
 ** COMPONENT PROPERTIES SECTION
 **********************************************************************
 *MODEL *BLACKOIL              ** THREE PHASE - THREE EQUATION
 *PVT
 **    P       RS       BO        EG      VISO     VISG
    400.000   165.000   1.01200   169.490   1.17000 0.0130000
    800.000   335.000   1.02550   338.980   1.14000 0.0135000
   1200.000   500.000   1.03800   510.200   1.11000 0.0140000
   1600.000   665.000   1.05100   680.270   1.08000 0.0145000
   2000.000   828.000   1.06300   847.460   1.06000 0.0150000
   2400.000   985.000   1.07500  1020.400   1.03000 0.0155000
   2800.000  1130.000   1.08700  1190.500   1.00000 0.0160000
   3200.000  1270.000   1.09850  1351.400 0.9800000 0.0165000
   3600.000  1390.000   1.11000  1538.500 0.9500000 0.0170000
   4000.000  1500.000   1.12000  1694.900 0.9400002 0.0175000
   4400.000  1600.000   1.13000  1851.900 0.9200000 0.0180000
   4800.000  1676.000   1.14000  2040.800 0.9100000 0.0185000
   5200.000  1750.000   1.14800  2222.200 0.9000000 0.0190000
   5600.000  1810.000   1.15500  2381.000 0.8900000 0.0195000
```

```
  *DENSITY *OIL    32.4
  *DENSITY *GAS     0.0576
  *DENSITY *WATER  64.8
  *CO              1.0E-5       ** OIL COMPRESSIBILITY
  *CVO              0.0         ** VISCOSITY DEPENDENCE ON OIL COMPRESSIBILITY
  *BWI             1.00       ** WATER FORMATION VOLUME FACTOR
  *CW              3.0E-7       ** WATER COMPRESSIBILITY
  *REFPW            14.7        ** REFERENCE PRESSURE
  *VWI             0.96        ** WATER VISCOSITY AT REFERENCE PRESSURE
  *CVW              0.0         ** PRESSURE DEPENDENCE ON WATER COMPRESSIBILITY
  *TRES     100
  ************************************************************************
  **ROCK-FLUID PROPERTY SECTION                                          **
  ************************************************************************
  *ROCKFLUID
RPT 1
** WATER-OIL RELATIVE PERMEABILITY TABLE.
**   SW    KRW    KROW    PCOW
SWT
      0     0.0      1.0
       1.00      1.0      0.0
** LIQUID-GAS RELATIVE PERMEABILITY TABLE.
**   SL   KRW  KEO
*SGT
 0.0     0.0      1.0
 1.0     1.0      0.0
*KROIL *STONE1
************************************************************************
** INITIAL CONDITIONS SECTION                                          **
************************************************************************
*INITIAL
*USER_INPUT
*PRES *KVAR  5500  5505  5510  5515  5520
*PB   *CON  5500
*SO   *CON    0.7
*SW   *CON   0.3
************************************************************************
** NUMERICAL CONTROL SECTION                                          **
************************************************************************
*NUMERICAL
*DTMAX       1
*MAXSTEPS    1000             ** MAXIMUM NUMBER OF TIME STEPS
*NORM *PRESS  650.
*AIM *THRESH  .25 .25
************************************************************************
** WELL DATA SECTION                                                  **
************************************************************************
*RUN
*DATE 2000 01 01
*DTWELL  1
*WELL 1 'PRODUCER'
*PRODUCER  1
*OPERATE  MIN  BHP  4500
*GEOMETRY  K  0.5  0.34  1.  0.
*PERF  GEO   1
 5   5   5   1.
*WELL 2  'INJECTOR'
*INJECTOR  *UNWEIGHT 2
*INCOMP  WATER
*OPERATE  MAX  BHW  8.90
*GEOMETRY  K  0.5  0.34  1.  0.
*PERF  GEO  2
 1   1   5   1.
*AIMWELL *WELLN
*TIME         1
*TIME         100
 *STOP
```

HEAD

```
CASE3
NX     NY    NZ       N     NWELL
5   5    5      9    5
NTW       NTA
0         0
NO        NPHAS
0         4
NSUB      MSUB
```

```
0       0
NTABL NPHEL
3     2
```

INPUT

```
CC*********************************************************************
CC                                                                     *
CC    BRIEF DESCRIPTION OF DATA SET: UTCHEM FOUR PHASE THERMAL 2014    *
CC                                                                     *
CC*********************************************************************
CC                                                                     *
CC  WATER  FLOODING GAS PRODUCTION     THRE PHASE GAS/OIL/WATER        *
CC                                                                     *
CC  LENGTH (FT) : 10                PROCESS : WATER FLOODING           *
CC  THICKNESS (FT) : 10               INJ. PRESSURE (PSI) :            *
CC  WIDTH (FT) : 10                 COORDINATES : CARTESIAN            *
CC  POROSITY :                                                         *
CC  GRID BLOCKS : 5X5X5                                                *
CC  DATE :   AUGUST 2014                                               *
CC  CREATED BY : HAMID REZA LASHGARI                                   *
CC*********************************************************************
CC
CC
CC*********************************************************************
CC                                                                     *
CC    RESERVOIR DESCRIPTION                                            *
CC                                                                     *
CC*********************************************************************
CC
CC
*---- RUNNO
CASE3
CC
CC
*----HEADER
CASE3
WATER INJECTION BELOW BUBBLE POINT
************************************************************
CC
CC SIMULATION FLAGS
*---- IMODE IMES IDISPC ICWM ICAP IREACT IBIO ICOORD ITREAC ITC  IGAS  IENG IHEATW IELECHV IELECHI  ISTEAM   IGMAS
      1          4          0          0       0       0    0    1     0       0       1       1       0       0       0       0       1
CC
CC NUMBER OF GRID BLOCKS AND FLAG SPECIFIES CONSTANT OR VARIABLE GRID SIZE
*---- NX    NY    NZ  IDXYZ  IUNIT
    5    5 5    0      0
CC
CC  CONSTANT GRID BLOCK SIZE IN X, Y, AND Z
*---- DX        DY        DZ
     10        10        10
CC
CC TOTAL NO. OF COMPONENTS, NO. OF TRACERS, NO. OF GEL COMPONENTS
*----N   NO NTW NTA NGC  NG  NOTH
    9    0 0   0 0    0    0
CC
CC
*---- SPNAME(I),I=1,N
WATER
OIL
SURFACTANT
POLYMER
ANION
CATION
ALCOHOL
GAS
TRACER
CC
CC FLAG INDICATING IF THE COMPONENT IS INCLUDED IN CALCULATIONS OR NOT
*----ICF(KC) FOR KC=1,N
    1  1  1  0  1  0  0  1  0
CC
CC*********************************************************************
CC                                                *
CC    OUTPUT OPTIONS                                        *
CC                                                *
CC*********************************************************************
CC
```

```
CC
CC FLAG TO WRITE TO UNIT 3,FLAG FOR PV OR DAYS TO PRINT OR TO STOP THE RUN
*---- ICUMTM  ISTOP  IOUTGMS      IS3G
      0      0       2        2
CC
CC FLAG INDICATING IF THE PROFILE OF KCTH COMPONENT SHOULD BE WRITTEN
*---- IPRFLG(KC),KC=1,N
      1  1  1 1   1  0  0  1  0
CC
CC FLAG FOR PRES.,SAT.,TOTAL CONC.,TRACER CONC.,CAP.,GEL, ALKALINE PROFILES
*---- IPPRES IPSAT IPCTOT IPBIO IPCAP IPGEL IPALK IPTEMP IPOBS
      1      1      1      0     0     0     1     1      0
CC
CC FLAG FOR WRITING SEVERAL PROPERTIES TO UNIT 4 (PROF)
*---- ICKL IVIS IPER ICNM ICSE IHYSTP IFOAMP INONEQ
     1    1    1    1    1    1    0    0   0
CC
CC FLAG FOR WRITING SEVERAL PROPERTIES TO PROF
*---- IADS IVEL IRKF IPHSE
     1    1    1    1
CC
CC*********************************************************************
CC                                                                     *
CC    RESERVOIR PROPERTIES                                             *
CC                                                                     *
CC*********************************************************************
CC
CC
CC MAX. SIMULATION TIME ( DAYS)
*---- TMAX
    100
CC
CC ROCK COMPRESSIBILITY (1/PSI), STAND. PRESSURE(PSIA)
*---- COMPR               PSTAND
      0                 200
CC
CC FLAGS INDICATION CONSTANT OR VARIABLE POROSITY, X,Y,AND Z PERMEABILITY
*----IPOR1 IPERMX IPERMY IPERMZ  IMOD  ITRNZ   INTG
     0      0     3      3      0     0       0
CC
CC CONSTANT POROSITY FOR WHOLE RESERVOIR
*---- PORC1
      0.2
CC
CC CONSTANT X-PERMEABILITY (MILIDARCY) FOR LAYER K = 1,NZ
*----PERMX
    50
CC
CC Y DIRECTION PERMEABILITY IS DEPENDENT ON X DIRECTION PERMEABILITY
*---- CONSTANT PERMEABILITY MULTIPLIER FOR Y DIRECTION PERMEABILITY
       1
CC
CC Z DIRECTION PERMEABILITY IS DEPENDENT ON X DIRECTION PERMEABILITY
*---- CONSTANT PERMEABILITY MULTIPLIER FOR Z DIRECTION PERMEABILITY
      0.1
CC
CC FLAG FOR CONSTANT OR VARIABLE DEPTH, PRESSURE, WATER SATURATION,INITIAL AQUEOUS PHASE COMPOSITIONS
*----IDEPTH  IPRESS  ISWI  ICWI
     0       0      0     -1
CC
CC CONSTANT DEPTH (FT)
*---- D111
      0
CC
CC INITIAL PRESSURE (PSIA)
*----PINIT   DEPTH
   5500.  0.0
CC
CC CONSTANT INITIAL WATER SATURATION (RESIDUAL OIL)
*---- SWI
    0.3
CC
CC FLAG INDICATING TYPE OF INITIAL GAS SATURATION
*---ISGI
   0
CC
CC CONSTANT INITIAL GAS SATURATION FOR WHOLE RESERVOIR
```

```
*---- SGI
     0.0
CC
CC BRINE SALINITY AND DIVALENT CATION CONCENTRATION (MEQ/ML)
*---- C50       C60
      0.3    0.00
CC
CC*********************************************************************
CC                                                  *
CC    PHYSICAL PROPERTY DATA                                *
CC                                                  *
CC*********************************************************************
CC
CC
CC OIL CONC. AT PLAIT POINT FOR TYPE II(+)AND TYPE II(-), CMC
*---- C2PLC  C2PRC   EPSME   IHAND
      0      1     0.00001     0
CC
CC 3.4.2 FLAG INDICATING TYPE OF PHASE BEHAVIOR PARAMETERS
*---- IFGHBN=0 FOR INPUT HEIGHT OF BINODAL CURVE; =1 FOR INPUT SOL. RATIO
       0
CC SLOPE AND INTERCEPT OF BINODAL CURVE AT ZERO, OPT., AND 2XOPT SALINITY
CC FOR ALCOHOL 1
*---- HBNS70   HBNC70   HBNS71   HBNC71   HBNS72   HBNC72
      0    0.05       0     0.03     0     0.05
CC
CC SLOPE OF BINODAL WITH TEMP., SLOPE OF SALINITY WITH TEMP. (1/F)
*---- HBNT0     HBNT1     HBNT2     CSET(0.00415)
     0.00017  0.00017  0.00017   0.00415
CC SLOPE AND INTERCEPT OF BINODAL CURVE AT ZERO, OPT., AND 2XOPT SALINITY
CC FOR ALCOHOL 2
*---- HBNS80  HBNC80  HBNS81  HBNC81  HBNS82  HBNC82
      0       0       0       0       0       0
CC
CC LOWER AND UPPER EFFECTIVE SALINITY FOR ALCOHOL 1 AND ALCOHOL 2
*---- CSEL7   CSEU7   CSEL8   CSEU8
      0.33    0.53     0       0
CC
CC THE CSE SLOPE PARAMETER FOR CALCIUM AND ALCOHOL 1 AND ALCOHOL 2
*---- BETA6    BETA7    BETA8
       0.       0       0
CC
CC FLAG FOR ALCOHOL PART. MODEL AND PARTITION COEFFICIENTS
*---- IALC   OPSK7O   OPSK7S   OPSK8O   OPSK8S
       1      0        0        0        0
CC
CC NO. OF ITERATIONS, AND TOLERANCE
*---- NALMAX     EPSALC
       20        0.0001
CC 3.4.10 ALCOHOL 1 PARTITIONING PARAMETERS IF IALC=1
CC   AQ-OLEIC   AQ-OLEIC  SURF-OLEIC
*---- AKWC7     AKWS7    AKM7     AK7      PT7
      4.671    1.79      48     35.31    0.222
CC
CC ALCOHOL 2 PARTITIONING PARAMETERS IF IALC=1
*---- AKWC8     AKWS8    AKM8    AK8     PT8
       0         0        0      0       0
CC
CC 3.4.22 IFT MODEL FLAG
*----  IFT=0 FOR HEALY&REED; =1 FOR CHUN HUH CORREL.
       1
CC 3.4.24 INTERFACIAL TENSION PARAMETERS
CC    TYP=.1-.35   TYP=5-20
*---- CHUH     AHUH
     0.35       10
CC
CC LOG10 OF OIL/WATER INTERFACIAL TENSION
*---- XIFTW
      1.3
CC
CC ORGANIC MASS TRANSFER FLAG
*---- IMASS ICOR
                0    0
CC
CC
*--- IWALT  IWALF
       0       0
```

```
CC
CC CAPILLARY DESATURATION PARAMETERS FOR PHASE 1, 2, AND 3
*---- ITRAP      T11      T22      T33
      0         300    1000    300
CC
CC  RELATIVE PERM  AND PC MODEL
*----IPERM      IRTYPE
     0          0
CC
CC FLAG FOR CONSTANT OR VARIABLE REL. PERM. PARAMETERS
*---- ISRW    IPRW    IEW
      0      0       0
CC
CC CONSTANT RES. SATURATION OF PHASES 1,2,AND 3 AT LOW CAPILLARY NO.
*---- S1RWC    S2RWC     S3RWC
      0.0      0.0      0.0
CC
CC CONSTANT ENDPOINT REL. PERM. OF PHASES 1,2,AND 3 AT LOW CAPILLARY NO.
*---- P1RWC     P2RWC    P3RWC
      1        1       1
CC
CC CONSTANT REL. PERM. EXPONENT OF PHASES 1,2,AND 3 AT LOW CAPILLARY NO.
*---- E1WC     E2WC     E3WC
      1        1        1
CC
CC WATER AND OIL VISCOSITY , RESERVOIR TEMPERATURE
*---- VIS1    VIS2   TSTAND
      1       1      60
CC
CC GAS VISCOSITY AT REF. TEMPERATURE AND PRESSURE,SLOPE OF GAS VISCOSITY
*---- VIS4      VSLOPG
      0.02   0
CC
CC VISCOSITY-TEMP PARAMETERS
*----BVI(1)  BVI(2)
    0    0
CC
CC VISCOSITY-TEMP PARAMETERS
*----BVI(4)
    0
CC
CC CONSTANT RESIDUAL OIL/GAS SATURATION FOR ENTIRE RESERVOIR
*---- S2RWC4
      0.0  0.0
CC
CC CONSTANT RESIDUAL OIL/GAS SATURATION FOR ENTIRE RESERVOIR
*----  S4RWC
      1
CC
CC CONSTANT GAS ENDPOINT RELATIVE PERMEABILITY FOR ENTIRE RESERVOIR
*--- P4RWC
      1
CC
CC LOG OF INTERFACIAL TENSION BETWEEN GAS AND OIL (AND WATER)
*----  XIFTG   XIFTGW
      1.477    1.477
CC
CC COMPOSITIONAL PHASE VISCOSITY PARAMETERS
*----   ALPHAV1   ALPHAV2   ALPHAV3   ALPHAV4  ALPHAV5
        0         0       1         0         1.7
CC
CC PARAMETERS TO CALCULATE POLYMER VISCOSITY AT ZERO SHEAR RATE
*---- AP1      AP2      AP3
      10.21     17.77     626.14
CC
CC PARAMETER TO COMPUTE CSEP,MIN. CSEP, AND SLOPE OF LOG VIS. VS. LOG CSEP
*---- BETAP    CSE1     SSLOPE
      20      0.01     -0.6
CC
CC PARAMETER FOR SHEAR RATE DEPENDENCE OF POLYMER VISCOSITY
*---- GAMMAC   GAMHF   POWN       IPMOD   ISHEAR  RWEFF GAMHF2
      4       56.1      1.643               0       0      0.25   0
CC
CC CC FLAG FOR POLYMER PARTITIONING, PERM. REDUCTION PARAMETERS
*---- IPOLYM    EPHI3    EPHI4    BRK     CRK                      RKCUT
      1         1       1      1000    0.0186                            10
CC
```

```
CC SPECIFIC WEIGHT FOR COMPONENTS 1,2,3,7,8 ,COEFFIENT OF OIL AND GRAVITY FLAG
*---- DEN1    DEN2    DEN23    DEN3   DEN7   DEN8   IDEN
    0.45    0.225   0.26    0.433    0.39   0.005    2
CC
CC FLAG FOR CHOICE OF UNITS ( 0:BOTTOMHOLE CONDITION , 1: STOCK TANK)
*----- ISTB
      0
CC
CC COMPRESSIBILITY FOR VOL. OCCUPYING COMPONENTS 1,2,3,7,AND 8
*---- COMPC(1)  COMPC(2)  COMPC(3)  COMPC(7)  COMPC(8)
       0.0000001       0.0000001        0.000001     0    0.000001
CC
CC CONSTANT OR VARIABLE PC PARAM., WATER-WET OR OIL-WET PC CURVE FLAG
*---- ICPC   IEPC   IOW
     0      0     0
CC
CC CAPILLARY PRESSURE PARAMETER, CPC0
*---- CPC0
     0
CC
CC CAPILLARY PRESSURE PARAMETER, EPC0
*---- EPC0
     2
CC
CC MOLECULAR DIFFUSION COEF. KCTH COMPONENT IN PHASE 1
*---- D(KC,1),KC=1,N
      0       0       0       0       0       0       0       0       0       0       0       0       0
CC
CC MOLECULAR DIFFUSION COEF. KCTH COMPONENT IN PHASE 2
*---- D(KC,2),KC=1,N
      0       0       0       0       0       0       0       0       0       0       0       0       0
CC
CC MOLECULAR DIFFUSION COEF. KCTH COMPONENT IN PHASE 3
*---- D(KC,3),KC=1,N
      0       0       0       0       0       0       0       0       0       0       0       0       0
CC
CC MOLECULAR DIFFUSION COEF. KCTH COMPONENT IN PHASE 4
*---- D(KC,3),KC=1,N
      0       0       0       0       0       0       0       0       0       0       0       0       0
CC
CC LONGITUDINAL AND TRANSVERSE DISPERSIVITY OF PHASE 1
*---- ALPHAL(1)     ALPHAT(1)
      0.0           0.000
CC
CC LONGITUDINAL AND TRANSVERSE DISPERSIVITY OF PHASE 2
*---- ALPHAL(2)     ALPHAT(2)
      0.0           0.000
CC
CC LONGITUDINAL AND TRANSVERSE DISPERSIVITY OF PHASE 3
*---- ALPHAL(3)     ALPHAT(3)
      0.0           0.000
CC
CC LONGITUDINAL AND TRANSVERSE DISPERSIVITY OF PHASE 4
*---- ALPHAL(3)     ALPHAT(3)
      0.0           0.000
CC
CC FLAG TO SPECIFY ORGANIC ADSORPTION CALCULATION
*---- IADSO
      0
CC
CC SURFACTANT AND POLYMER ADSORPTION PARAMETERS
*---- AD31    AD32   B3D    AD41   AD42   B4D   IADK  IADS1   FADS    REFK
    1.5      0.5    1000    9.5     0     100     0     0      0       0
CC
CC PARAMETERS FOR CATION EXCHANGE OF CLAY AND SURFACTANT
*---- QV      XKC     XKS     EQW
    0.00    0.      0.      450
CC
CC INITIAL TEMPERATURE
*--- TEMPI (F)
   90
CC
CC ROCK DENSITY,CONDUCTIVITY,HEAT CAPACITY
*---- DENS   CTCR  CTCL(1:NPHASE) CVSPR   CVSPL(1:NPHASE)
    165.43   100   100    100   100  100   0.242    1   0.5   1    1
CC
CC THERMAL EXPANTION OF COMPONENTS AND ROCK
```

```
*--- THEXP(1:N), THEXPR
   0.001   0.001  0.0  0.0  0.0  0.0 0.0 0.0 0.01  0.0001
CC
CC HEATLOSS FLAG, ANALYTICAL SOLUTION ANALYTICAL SHOULD BE CHECKED
*---- IHLOS  IANAL
      0     0
CC
CC*****************************************************************
CC                                                 *
CC    WELL DATA                                        *
CC                                                 *
CC*****************************************************************
CC
CC
CC FLAG FOR SPECIFIED BOUNDARY AND ZONE IS MODELED
*---- IBOUND     IZONE
      0      0
CC
CC TOTAL NUMBER OF WELLS, WELL RADIUS FLAG, FLAG FOR TIME OR COURANT NO.
*---- NWELL   IRO    ITIME    NWREL
      2      2       0        2
CC
CC WELL ID,LOCATIONS,AND FLAG FOR SPECIFYING WELL TYPE, WELL RADIUS, SKIN
*---- IDW    IW    JW    IFLAG    RW     SWELL   IDIR   IFIRST   ILAST   IPRF
      1     1     1       1    0.5       0       3      5     5    0
CC
CC WELL NAME
*----  WELNAM
INJ1
CC
CC ICHEK , MAX. AND MIN. ALLOWABLE BOTTOMHOLE PRESSURE AND RATE
*---- ICHEK     PWFMIN     PWFMAX    QTMIN    QTMAX
      0          0         10000      0        20000
CC
CC WELL ID,LOCATIONS,AND FLAG FOR SPECIFYING WELL TYPE, WELL RADIUS, SKIN
*---- IDW    IW    JW    IFLAG    RW     SWELL   IDIR   IFIRST   ILAST   IPRF
      2     5     5     2     1       0       3         5   5      0
CC
CC WELL NAME
*----  WELNAM
PROD1
CC
CC ICHEK , MAX. AND MIN. ALLOWABLE BOTTOMHOLE PRESSURE AND RATE
*---- ICHEK     PWFMIN     PWFMAX    QTMIN    QTMAX
      0          0         1000      -0       -20000
CC
CC  ID,INJ. RATE AND INJ. COMP. FOR RATE CONS. WELLS FOR EACH PHASE (L=1,3)
*----  ID     QI(M,L)     C(M,KC,L)
      1      50    1.0     0.0    0.00   0.0    0.0   0.0 0.0 0.0 0.0
      1      0.0   0.0     0.0    0.0    0.0     0.0   0.0 0.0 0.0 0.0
      1      0.0   0.0     0.0    0.0    0.0     0.0   0.0 0.0 0.0 0.0
      1      0.0   0.0     0.0    0.0    0.0     0.0   0.0 0.0 0.0 0.0
CC
CC
*--- ID, INJ. TEMP (F)
    1    90.
CC
CC
*----  ID    PWF
    2      4500
CC
CC CUM. INJ. TIME , AND INTERVALS (PV OR DAY) FOR WRITING TO OUTPUT FILES
*---- TINJ     CUMPR1     CUMHI1     WRHPV     WRPRF      RSTC
      100      5*0.5
CC
CC THE INI. TIME STEP,CONC. TOLERANCE,MAX.,MIN. TIME STEPS
*----  DT     DELC(I)             CNMAX             CNMIN
   0.000001       9*0.005          0.005               0.00001
```

PVT

```
CC NUMBER OF DATA SET FOR CASE 3
CC
14
CC SARURATED          SOLUTION GAS    OIL FVF         GAS FVF              OIL_VISCOSITY       GAS_VISCOSITY
CC PRESSURE(PSI)       RS(SCF/STB)    BO(RB/STB)     BG(RB/SCF)                (CP)              (CP)
```

```
100          165          1.012                    0.005900053          1.17         0.013
800          335          1.0255                   0.002950027          1.14         0.0135
1200         500          1.038                    0.001960016          1.11         0.014
1600         665          1.051                    0.001470005          1.08         0.0145
2000         828          1.063                    0.001179997          1.06         0.015
2400         985          1.075                    0.000980008          1.03         0.0155
2800         1130         1.087                    0.000839983          1         0.016
3200         1270         1.0985                   0.000739973          0.98         0.0165
3600         1390         1.11                     0.000649984          0.95         0.017
4000         1500         1.12                     0.000590005          0.942        0.0175
4400         1600         1.13                     0.000539986          0.92         0.018
4800         1676         1.14                     0.000490004          0.91         0.0185
5200         1750         1.148                    0.000450005          0.9          0.019
5600         1810         1.155                    0.000419992          0.89         0.0195
CC  SURFACE GAS DENISTY     SURFACE OIL DENISITY    BUBBLE POINT PRESSURE
CC     PSI                    PSI              PSI
       0.0004                 0.225            5500
CC UNDERSATURATED PROPERTY SLOP FOR OIL FORMATION VOLUME FACTOR (DEL_BO/DEL_P) AND OIL VISCOSITY (DEL_VIS/DEL_P)
CC     VIOSLOP        BOSLOP
  0.00001      -0.00023
```

A.4 PRODUCTION FROM A FIELD CASE WITH THREE PHASES EXISTING (CASE-4)

The following are the input data files for UTCHEM and CMG-IMEX simulators. We used this case in Chapter 6 for three-phase flow validation and comparison between UTCHEM four-phase model and CMG-IMEX.

```
**********************************************************************************
** CMG IMEX:    NATURAL DEPLETION                          **
**********************************************************************************
**********************************************************************************************
**                                                        **
** FILE:  3D COMPARISON FOR GAS PRODUCTION                                  **
**                                                        **
** MODEL:  11X11X10       PRODUCTION TO VAPORRIZE GAS              FIELD UNIT **
**                                                        **
**********************************************************************************************
** 2014-07-17, 6:49:00 PM, HL7675
RESULTS SIMULATOR IMEX 201210
*TITLE1
'UTCHEM VALIDATION'
*TITLE2
'PRODUCTION TO VAPORRIZE GAS'
*TITLE3
'NATURAL DEPLETION'
*INUNIT    *FIELD
*WPRN      *WELL 1
*WPRN      *GRID *TIME
*OUTPRN    *GRID *ALL
*OUTPRN    *WELL *ALL
 *OUTSRF *RES *ALL
 *OUTSRF *GRID  *ALL
*WSRF      *GRID 5
*WSRF      *WELL 1
**********************************************************************************
** RESERVOIR DESCRIPTION SECTION
**********************************************************************************
*GRID *CART    11    11   10   ** THIS IS AN X-Z CROSS SECTIONAL PROBLEM
*KDIR *DOWN
*DI *CON  150.0
*DJ *CON 150.0
*DK *CON    20
*DEPTH 1    1   1   0
*POR  *CON     0.2
*PRPOR 200.0
*CPOR  0
*PERMI *CON 100
PERMJ EQUALSI
 PERMK EQUALSI
PINCHOUTARRAY CON          1
**********************************************************************************
** COMPONENT PROPERTIES SECTION
**********************************************************************************
*MODEL *BLACKOIL
*PVT
**    P        RS       BO         EG      VISO     VISG
   400.000   165.000   1.01200   169.490    1.17000 0.0130000
   800.000   335.000   1.02550   338.980    1.14000 0.0135000
  1200.000   500.000   1.03800   510.200    1.11000 0.0140000
  1600.000   665.000   1.05100   680.270    1.08000 0.0145000
  2000.000   828.000   1.06300   847.460    1.06000 0.0150000
  2400.000   985.000   1.07500 1020.400    1.03000 0.0155000
  2800.000 1130.000   1.08700 1190.500    1.00000 0.0160000
  3200.000 1270.000   1.09850 1351.400 0.9800000 0.0165000
  3600.000 1390.000   1.11000 1538.500 0.9500000 0.0170000
  4000.000 1500.000   1.12000 1694.900 0.9400002 0.0175000
  4400.000  1600.000   1.13000  1851.900 0.9200000 0.0180000
```

```
    4800.000  1676.000   1.14000  2040.800 0.9100000 0.0185000
    5200.000  1750.000   1.14800  2222.200 0.9000000 0.0190000
    5600.000  1810.000   1.15500  2381.000 0.8900000 0.0195000
   *DENSITY *OIL    32.4
   *DENSITY *GAS     0.0576
   *DENSITY *WATER  64.8
   *CO              1.0E-5       ** OIL COMPRESSIBILITY
   *CVO              0.0         ** VISCOSITY DEPENDENCE ON OIL COMPRESSIBILITY
   *BWI              1.00        ** WATER FORMATION VOLUME FACTOR
   *CW               3.0E-7       ** WATER COMPRESSIBILITY
   *REFPW            14.7        ** REFERENCE PRESSURE
   *VWI             0.96         ** WATER VISCOSITY AT REFERENCE PRESSURE
   *CVW              0.0         ** PRESSURE DEPENDENCE ON WATER COMPRESSIBILITY
   *TRES     100
   ***************************************************************************
   **ROCK-FLUID PROPERTY SECTION
   ***************************************************************************
   *ROCKFLUID
RPT 1
** WATER-OIL RELATIVE PERMEABILITY TABLE.
**   SW    KRW    KROW    PCOW
      SWT
       0     0.0      1.0
        1.00      1.0      0.0
** LIQUID-GAS RELATIVE PERMEABILITY TABLE.
**   SL     KRG    KROG     PCOG
    SGT
         0      0.0      1.0
       1    1       0.0
   *KROIL *STONE1
   ***************************************************************************
   ** INITIAL CONDITIONS SECTION
   ***************************************************************************
*INITIAL
*USER_INPUT
*PRES *KVAR   4000  4009  4018  4027  4036  4046  4055 4064     4073  4081
*PB   *CON 4000.0
*SO   *CON    0.6
*SW   *CON    0.4
   ***************************************************************************
   ** NUMERICAL CONTROL SECTION
   ***************************************************************************
   *NUMERICAL
   *DTMAX        1
   *MAXSTEPS    1000
   *NORM *PRESS  650.
   *AIM *THRESH  .25 .25
   ***************************************************************************
   ** WELL DATA SECTION
   ***************************************************************************
   *RUN
   *DATE 2000 01 01
   *DTWELL   0.1
    *DTMAX   0.1
**    *WELL 1 'PRODUCER 1' *VERT  1  1
**$
WELL  'PRODUCER 1'  VERT  1  1
PRODUCER 'PRODUCER 1'
OPERATE  MIN  BHP  1000.  CONT REPEAT
**    *WELL 2 'PRODUCER 2' *VERT  11 1
**$
WELL  'PRODUCER 2'  VERT  11  1
PRODUCER 'PRODUCER 2'
OPERATE  MIN  BHP  1000.  CONT REPEAT
**    *WELL 3 'PRODUCER 3' *VERT  11 11
**$
WELL  'PRODUCER 3'  VERT  11  11
PRODUCER 'PRODUCER 3'
OPERATE  MIN  BHP  1000.  CONT REPEAT
**    *WELL 4 'PRODUCER 4' *VERT  1  11
**$
WELL  'PRODUCER 4'  VERT  1  11
PRODUCER 'PRODUCER 4'
OPERATE  MIN  BHP  1000.  CONT REPEAT
**    *WELL 5 'INJECTOR '  *VERT   6  6
**$
WELL  'INJECTOR'  VERT  6  6
```

```
INJECTOR MOBWEIGHT 'INJECTOR'
INCOMP  WATER
OPERATE  MAX  STW  2000.  CONT
**           RAD     GEOFAC   WFRAC  SKIN
** KF      FF
**$         RAD  GEOFAC  WFRAC  SKIN
GEOMETRY  K  0.5  0.34  1.  0.
PERF  GEO  'PRODUCER 1'
**$ UBA     FF  STATUS  CONNECTION
   1 1 1:10   1.  OPEN    FLOW-TO  'SURFACE'  REFLAYER
**           RAD     GEOFAC   WFRAC  SKIN
** KF      FF
**$         RAD  GEOFAC  WFRAC  SKIN
    GEOMETRY  K  0.5  0.34  1.  0.
    PERF  GEO  'PRODUCER 2'
**$ UBA     FF  STATUS  CONNECTION
    11 1 1:10   1.  OPEN    FLOW-TO  'SURFACE'  REFLAYER
**           RAD     GEOFAC   WFRAC  SKIN
** KF      FF
**$         RAD  GEOFAC  WFRAC  SKIN
    GEOMETRY  K  0.5  0.34  1.  0.
    PERF  GEO  'PRODUCER 3'
**$ UBA      FF  STATUS  CONNECTION
   11 11 1:10   1.  OPEN    FLOW-TO  'SURFACE'  REFLAYER
**           RAD     GEOFAC   WFRAC  SKIN
** KF      FF
**$         RAD  GEOFAC  WFRAC  SKIN
GEOMETRY  K  0.5  0.34  1.  0.
PERF  GEO  'PRODUCER 4'
**$ UBA     FF  STATUS  CONNECTION
    1 11 1:10   1.  OPEN    FLOW-TO  'SURFACE'  REFLAYER
**      RAD     GEOFAC   WFRAC  SKIN
** KF      FF
**$         RAD  GEOFAC  WFRAC  SKIN
    GEOMETRY  K  0.5  0.34  1.  0.
   PERF  GEO  'INJECTOR'
**$ UBA     FF  STATUS  CONNECTION
   6 6   1:10  10.  OPEN    FLOW-FROM  'SURFACE'  REFLAYER
SHUTIN 'INJECTOR'
*AIMWELL *WELLN
*TIME         150
  *STOP
```

HEAD

```
CASE4
NX     NY    NZ       N     NWELL
11    11    10      9    5
NTW       NTA
0         0
NO        NPHAS
0         4
NSUB      MSUB
0         0
NTABL NPHEL
3     2
```

INPUT

```
CC*************************************************************************
CC                                                                       *
CC   BRIEF DESCRIPTION OF DATA SET: UTCHEM FOUR PHASE THERMAL 2014  *
CC                                                                       *
CC*************************************************************************
CC                                                                       *
CC  NATURAL DEPLETION                                              *
CC                                                                       *
CC  LENGTH (FT) : 150                 PROCESS : NATURAL DEPLETION *
CC  THICKNESS (FT) :20                INJ. PRESSURE (PSI) :         *
CC  WIDTH (FT) : 150.                 COORDINATES : CARTESIAN       *
CC  POROSITY :                                                    *
CC  GRID BLOCKS : 11X11X10                                          *
CC  DATE :   FEB 2012                                            *
CC                                                                       *
CC*************************************************************************
CC
CC*************************************************************************
```

```
CC                                                  *
CC    RESERVOIR DESCRIPTION                                 *
CC                                                  *
CC*********************************************************************
CC
CC
*---- RUNNO
CASE4
CC
CC
*----HEADER
CASE4
NATURAL DEPLETION PRODUCATION
************************************************************
CC
CC SIMULATION FLAGS
*---- IMODE IMES IDISPC ICWM ICAP IREACT IBIO ICOORD ITREAC ITC  IGAS  IENG IHEATW IELECHV IELECHI  ISTEAM   IGMAS
      1    3     0     0    0     0     0     1     0     0    1     1    0       0        0        0    1
CC
CC NUMBER OF GRID BLOCKS AND FLAG SPECIFIES CONSTANT OR VARIABLE GRID SIZE
*---- NX    NY    NZ  IDXYZ  IUNIT
    11   11  10    0      0
CC
CC  CONSTANT GRID BLOCK SIZE IN X, Y, AND Z
*---- DX         DY         DZ
     150        150        20
CC
CC TOTAL NO. OF COMPONENTS, NO. OF TRACERS, NO. OF GEL COMPONENTS
*----N   NO NTW NTA NGC  NG  NOTH
    9    0 0   0 0    0    0
CC
CC
*---- SPNAME(I),I=1,N
WATER
OIL
SURFACTANT
POLYMER
ANION
CATION
ALCOHOL
GAS
TRACER
CC
CC FLAG INDICATING IF THE COMPONENT IS INCLUDED IN CALCULATIONS OR NOT
*----ICF(KC) FOR KC=1,N
    1  1  0  0  0  0  0  0  1  0
CC
CC*********************************************************************
CC                                                  *
CC    OUTPUT OPTIONS                                        *
CC                                                  *
CC*********************************************************************
CC
CC
CC FLAG TO WRITE TO UNIT 3,FLAG FOR PV OR DAYS TO PRINT OR TO STOP THE RUN
*---- ICUMTM  ISTOP  IOUTGMS      IS3G
      0      0       2        2
CC
CC FLAG INDICATING IF THE PROFILE OF KCTH COMPONENT SHOULD BE WRITTEN
*---- IPRFLG(KC),KC=1,N
      1  1  1  1    1  0  0  1  0
CC
CC FLAG FOR PRES.,SAT.,TOTAL CONC.,TRACER CONC.,CAP.,GEL, ALKALINE PROFILES
*---- IPPRES IPSAT IPCTOT IPBIO IPCAP IPGEL IPALK IPTEMP IPOBS
      1      1      1      0     0     0     1     1      0
CC
CC FLAG FOR WRITING SEVERAL PROPERTIES TO UNIT 4 (PROF)
*---- ICKL IVIS IPER ICNM ICSE IHYSTP IFOAMP INONEQ
     1    1    1    1    1    1    0    0  0
CC
CC FLAG FOR WRITING SEVERAL PROPERTIES TO PROF
*---- IADS IVEL IRKF IPHSE
     1    1    1    1
CC
CC*********************************************************************
CC                                                  *
CC    RESERVOIR PROPERTIES                                  *
```

```
CC                                                  *
CC*********************************************************************
CC
CC
CC MAX. SIMULATION TIME ( DAYS)
*---- TMAX
    500
CC
CC ROCK COMPRESSIBILITY (1/PSI), STAND. PRESSURE(PSIA)
*---- COMPR               PSTAND
      0                 200
CC
CC FLAGS INDICATION CONSTANT OR VARIABLE POROSITY, X,Y,AND Z PERMEABILITY
*----IPOR1 IPERMX IPERMY IPERMZ  IMOD  ITRNZ   INTG
     0     0    3     3     0    0      0
CC
CC CONSTANT POROSITY FOR WHOLE RESERVOIR
*---- PORC1
     0.2
CC
CC CONSTANT X-PERMEABILITY (MILIDARCY) FOR LAYER K = 1,NZ
*----PERMX
    100
CC
CC Y DIRECTION PERMEABILITY IS DEPENDENT ON X DIRECTION PERMEABILITY
*---- CONSTANT PERMEABILITY MULTIPLIER FOR Y DIRECTION PERMEABILITY
      1
CC
CC Z DIRECTION PERMEABILITY IS DEPENDENT ON X DIRECTION PERMEABILITY
*---- CONSTANT PERMEABILITY MULTIPLIER FOR Z DIRECTION PERMEABILITY
     1
CC
CC FLAG FOR CONSTANT OR VARIABLE DEPTH, PRESSURE, WATER SATURATION,INITIAL AQUEOUS PHASE COMPOSITIONS
*----IDEPTH  IPRESS  ISWI  ICWI
     0       0      0     -1
CC
CC CONSTANT DEPTH (FT)
*---- D111
     0
CC
CC INITIAL PRESSURE (PSIA)
*----PINIT   DEPTH
    4000.  0.0
CC
CC CONSTANT INITIAL WATER SATURATION (RESIDUAL OIL)
*---- SWI
    0.4
CC
CC FLAG INDICATING TYPE OF INITIAL GAS SATURATION
*---ISGI
   0
CC
CC CONSTANT INITIAL GAS SATURATION FOR WHOLE RESERVOIR
*---- SGI
     0.0
CC
CC BRINE SALINITY AND DIVALENT CATION CONCENTRATION (MEQ/ML)
*---- C50       C60
     0.3    0.00
CC
CC*********************************************************************
CC                                                  *
CC    PHYSICAL PROPERTY DATA                                *
CC                                                  *
CC*********************************************************************
CC
CC
CC OIL CONC. AT PLAIT POINT FOR TYPE II(+)AND TYPE II(-), CMC
*---- C2PLC  C2PRC   EPSME   IHAND
      0     1     0.00001     0
CC
CC 3.4.2 FLAG INDICATING TYPE OF PHASE BEHAVIOR PARAMETERS
*---- IFGHBN=0 FOR INPUT HEIGHT OF BINODAL CURVE; =1 FOR INPUT SOL. RATIO
      0
CC SLOPE AND INTERCEPT OF BINODAL CURVE AT ZERO, OPT., AND 2XOPT SALINITY
CC FOR ALCOHOL 1
*---- HBNS70   HBNC70   HBNS71   HBNC71   HBNS72   HBNC72
```

```
      0    0.05       0     0.03     0     0.05
CC
CC SLOPE OF BINODAL WITH TEMP., SLOPE OF SALINITY WITH TEMP. (1/F)
*---- HBNT0     HBNT1    HBNT2    CSET(0.00415)
     0.00017  0.00017  0.00017   0.00415
CC SLOPE AND INTERCEPT OF BINODAL CURVE AT ZERO, OPT., AND 2XOPT SALINITY
CC FOR ALCOHOL 2
*---- HBNS80  HBNC80  HBNS81  HBNC81  HBNS82  HBNC82
      0       0       0       0       0       0
CC
CC LOWER AND UPPER EFFECTIVE SALINITY FOR ALCOHOL 1 AND ALCOHOL 2
*---- CSEL7   CSEU7   CSEL8   CSEU8
      0.32    0.53     0       0
CC
CC THE CSE SLOPE PARAMETER FOR CALCIUM AND ALCOHOL 1 AND ALCOHOL 2
*---- BETA6    BETA7    BETA8
      0.       0       0
CC
CC FLAG FOR ALCOHOL PART. MODEL AND PARTITION COEFFICIENTS
*---- IALC   OPSK7O   OPSK7S   OPSK8O   OPSK8S
      1      0        0        0        0
CC
CC NO. OF ITERATIONS, AND TOLERANCE
*---- NALMAX     EPSALC
       20       0.0001
CC 3.4.10 ALCOHOL 1 PARTITIONING PARAMETERS IF IALC=1
CC   AQ-OLEIC   AQ-OLEIC  SURF-OLEIC
*---- AKWC7     AKWS7    AKM7     AK7      PT7
      4.671    1.79      48     35.31    0.222
CC
CC ALCOHOL 2 PARTITIONING PARAMETERS IF IALC=1
*---- AKWC8     AKWS8    AKM8    AK8     PT8
      0         0        0      0       0
CC
CC 3.4.22 IFT MODEL FLAG
*----  IFT=0 FOR HEALY&REED; =1 FOR CHUN HUH CORREL.
       1
CC 3.4.24 INTERFACIAL TENSION PARAMETERS
CC    TYP=.1-.35   TYP=5-20
*---- CHUH     AHUH
     0.35       10
CC
CC LOG10 OF OIL/WATER INTERFACIAL TENSION
*---- XIFTW
      1.3
CC
CC ORGANIC MASS TRANSFER FLAG
*---- IMASS ICOR
                0    0
CC
CC
*--- IWALT  IWALF
      0       0
CC
CC CAPILLARY DESATURATION PARAMETERS FOR PHASE 1, 2, AND 3
*---- ITRAP      T11      T22      T33
      0        300    1000    300
CC
CC  RELATIVE PERM  AND PC MODEL
*----IPERM      IRTYPE
     0          0
CC
CC FLAG FOR CONSTANT OR VARIABLE REL. PERM. PARAMETERS
*---- ISRW    IPRW    IEW
      0      0       0
CC
CC CONSTANT RES. SATURATION OF PHASES 1,2,AND 3 AT LOW CAPILLARY NO.
*---- S1RWC    S2RWC     S3RWC
      0.0      0.0       0.0
CC
CC CONSTANT ENDPOINT REL. PERM. OF PHASES 1,2,AND 3 AT LOW CAPILLARY NO.
*---- P1RWC     P2RWC    P3RWC
      1        1       1
CC
CC CONSTANT REL. PERM. EXPONENT OF PHASES 1,2,AND 3 AT LOW CAPILLARY NO.
*---- E1WC     E2WC     E3WC
      1        1        1
```

```
CC
CC WATER AND OIL VISCOSITY , RESERVOIR TEMPERATURE
*---- VIS1    VIS2   TSTAND
     1      1     60
CC
CC GAS VISCOSITY AT REF. TEMPERATURE AND PRESSURE,SLOPE OF GAS VISCOSITY
*---- VIS4      VSLOPG
     0.02   0
CC
CC VISCOSITY-TEMP PARAMETERS
*----BVI(1)  BVI(2)
    0       0
CC
CC VISCOSITY-TEMP PARAMETERS
*----BVI(4)
    0
CC
CC CONSTANT RESIDUAL OIL/GAS SATURATION FOR ENTIRE RESERVOIR
*---- S2RWC4
     0.0  0.0
CC
CC CONSTANT RESIDUAL OIL/GAS SATURATION FOR ENTIRE RESERVOIR
*----  S4RWC
     1
CC
CC CONSTANT GAS ENDPOINT RELATIVE PERMEABILITY FOR ENTIRE RESERVOIR
*--- P4RWC
     1
CC
CC LOG OF INTERFACIAL TENSION BETWEEN GAS AND OIL (AND WATER)
*----  XIFTG   XIFTGW
     1.477    1.477
CC
CC COMPOSITIONAL PHASE VISCOSITY PARAMETERS
*----   ALPHAV1   ALPHAV2   ALPHAV3   ALPHAV4  ALPHAV5
        0         0       1         0         1.7
CC
CC PARAMETERS TO CALCULATE POLYMER VISCOSITY AT ZERO SHEAR RATE
*---- AP1       AP2      AP3
     10.21      17.77     626.14
CC
CC PARAMETER TO COMPUTE CSEP,MIN. CSEP, AND SLOPE OF LOG VIS. VS. LOG CSEP
*---- BETAP     CSE1      SSLOPE
     20       0.01      -0.6
CC
CC PARAMETER FOR SHEAR RATE DEPENDENCE OF POLYMER VISCOSITY
*---- GAMMAC   GAMHF   POWN       IPMOD   ISHEAR  RWEFF GAMHF2
     4       56.1      1.643               0       0      0.25   0
CC
CC CC FLAG FOR POLYMER PARTITIONING, PERM. REDUCTION PARAMETERS
*---- IPOLYM     EPHI3     EPHI4     BRK      CRK                       RKCUT
      1         1       1       1000    0.0186                          10
CC
CC SPECIFIC WEIGHT FOR COMPONENTS 1,2,3,7,8 ,COEFFIENT OF OIL AND GRAVITY FLAG
*---- DEN1      DEN2     DEN23      DEN3     DEN7     DEN8     IDEN
    0.45      0.225    0.26      0.433      0.39     0.005      2
CC
CC FLAG FOR CHOICE OF UNITS ( 0:BOTTOMHOLE CONDITION , 1: STOCK TANK)
*----- ISTB
      0
CC
CC COMPRESSIBILITY FOR VOL. OCCUPYING COMPONENTS 1,2,3,7,AND 8
*---- COMPC(1)  COMPC(2)  COMPC(3)  COMPC(7)  COMPC(8)
       0.0000001       0.0000001         0.000001      0    0.000001
CC
CC CONSTANT OR VARIABLE PC PARAM., WATER-WET OR OIL-WET PC CURVE FLAG
*---- ICPC     IEPC   IOW
     0       0      0
CC
CC CAPILLARY PRESSURE PARAMETER, CPC0
*---- CPC0
     0
CC
CC CAPILLARY PRESSURE PARAMETER, EPC0
*---- EPC0
     2
CC
```

```
CC MOLECULAR DIFFUSION COEF. KCTH COMPONENT IN PHASE 1
*---- D(KC,1),KC=1,N
      0       0       0       0       0       0       0       0       0       0       0       0       0
CC
CC MOLECULAR DIFFUSION COEF. KCTH COMPONENT IN PHASE 2
*---- D(KC,2),KC=1,N
      0       0       0       0       0       0       0       0       0       0       0       0       0
CC
CC MOLECULAR DIFFUSION COEF. KCTH COMPONENT IN PHASE 3
*---- D(KC,3),KC=1,N
      0       0       0       0       0       0       0       0       0       0       0       0       0
CC
CC MOLECULAR DIFFUSION COEF. KCTH COMPONENT IN PHASE 4
*---- D(KC,3),KC=1,N
      0       0       0       0       0       0       0       0       0       0       0       0       0
CC
CC LONGITUDINAL AND TRANSVERSE DISPERSIVITY OF PHASE 1
*---- ALPHAL(1)     ALPHAT(1)
       0.0           0.000
CC
CC LONGITUDINAL AND TRANSVERSE DISPERSIVITY OF PHASE 2
*---- ALPHAL(2)     ALPHAT(2)
       0.0           0.000
CC
CC LONGITUDINAL AND TRANSVERSE DISPERSIVITY OF PHASE 3
*---- ALPHAL(3)     ALPHAT(3)
       0.0           0.000
CC
CC LONGITUDINAL AND TRANSVERSE DISPERSIVITY OF PHASE 4
*---- ALPHAL(3)     ALPHAT(3)
       0.0           0.000
CC
CC FLAG TO SPECIFY ORGANIC ADSORPTION CALCULATION
*---- IADSO
      0
CC
CC SURFACTANT AND POLYMER ADSORPTION PARAMETERS
*---- AD31    AD32   B3D    AD41   AD42   B4D   IADK  IADS1   FADS   REFK
     1.5      0.5    1000    9.5     0     100     0     0      0      0
CC
CC PARAMETERS FOR CATION EXCHANGE OF CLAY AND SURFACTANT
*---- QV      XKC     XKS     EQW
     0.00    0.      0.      450
CC
CC INITIAL TEMPERATURE
*--- TEMPI (F)
    90
CC
CC ROCK DENSITY,CONDUCTIVITY,HEAT CAPACITY
*---- DENS   CTCR  CTCL(1:NPHASE) CVSPR   CVSPL(1:NPHASE)
     165.43   100   100    100   100  100   0.242    1   0.5   1    1
CC
CC THERMAL EXPANTION OF COMPONENTS AND ROCK
*--- THEXP(1:N), THEXPR
   0.001   0.001  0.0  0.0  0.0  0.0 0.0 0.0 0.01  0.0001
CC
CC HEATLOSS FLAG, ANALYTICAL SOLUTION ANALYTICAL SHOULD BE CHECKED
*---- IHLOS  IANAL
      0     0
CC
CC*********************************************************************
CC                                                  *
CC    WELL DATA                                          *
CC                                                  *
CC*********************************************************************
CC
CC
CC FLAG FOR SPECIFIED BOUNDARY AND ZONE IS MODELED
*---- IBOUND     IZONE
      0      0
CC
CC TOTAL NUMBER OF WELLS, WELL RADIUS FLAG, FLAG FOR TIME OR COURANT NO.
*---- NWELL   IRO    ITIME    NWREL
      5      2       0       5
CC
CC WELL ID,LOCATIONS,AND FLAG FOR SPECIFYING WELL TYPE, WELL RADIUS, SKIN
*---- IDW    IW    JW    IFLAG    RW     SWELL   IDIR   IFIRST   ILAST   IPRF
```

```
     1    6     6      1     1      0      3     1    10      0
CC
CC WELL NAME
*----  WELNAM
INJ
CC
CC ICHEK , MAX. AND MIN. ALLOWABLE BOTTOMHOLE PRESSURE AND RATE
*---- ICHEK     PWFMIN     PWFMAX    QTMIN    QTMAX
      0          0         10000      0        20000
CC
CC WELL ID,LOCATIONS,AND FLAG FOR SPECIFYING WELL TYPE, WELL RADIUS, SKIN
*---- IDW    IW    JW    IFLAG    RW     SWELL   IDIR   IFIRST   ILAST   IPRF
     2    1    1     2     1       0      3      1    10      0
CC
CC WELL NAME
*----  WELNAM
PROD1
CC
CC ICHEK , MAX. AND MIN. ALLOWABLE BOTTOMHOLE PRESSURE AND RATE
*---- ICHEK     PWFMIN     PWFMAX    QTMIN    QTMAX
      0          0         1000      -0       -20000
CC
CC WELL ID,LOCATIONS,AND FLAG FOR SPECIFYING WELL TYPE, WELL RADIUS, SKIN
*---- IDW    IW    JW    IFLAG    RW     SWELL   IDIR   IFIRST   ILAST   IPRF
     3    11    1     2     1       0      3      1   10      0
CC
CC WELL NAME
*----  WELNAM
PROD2
CC
CC ICHEK , MAX. AND MIN. ALLOWABLE BOTTOMHOLE PRESSURE AND RATE
*---- ICHEK     PWFMIN     PWFMAX    QTMIN    QTMAX
      0          0         1000      -0       -20000
CC
CC WELL ID,LOCATIONS,AND FLAG FOR SPECIFYING WELL TYPE, WELL RADIUS, SKIN
*---- IDW    IW    JW    IFLAG    RW     SWELL   IDIR   IFIRST   ILAST   IPRF
     4    1    11     2     1       0      3      1   10      0
CC
CC WELL NAME
*----  WELNAM
PROD3
CC
CC ICHEK , MAX. AND MIN. ALLOWABLE BOTTOMHOLE PRESSURE AND RATE
*---- ICHEK     PWFMIN     PWFMAX    QTMIN    QTMAX
      0          0         1000      -0       -20000
CC
CC WELL ID,LOCATIONS,AND FLAG FOR SPECIFYING WELL TYPE, WELL RADIUS, SKIN
*---- IDW    IW    JW    IFLAG    RW     SWELL   IDIR   IFIRST   ILAST   IPRF
     5    11    11     2     1       0      3     1    10       0
CC
CC WELL NAME
*----  WELNAM
PROD4
CC
CC ICHEK , MAX. AND MIN. ALLOWABLE BOTTOMHOLE PRESSURE AND RATE
*---- ICHEK     PWFMIN     PWFMAX    QTMIN    QTMAX
      0          0         1000      -0       -20000
CC
CC  ID,INJ. RATE AND INJ. COMP. FOR RATE CONS. WELLS FOR EACH PHASE (L=1,3)
*----  ID     QI(M,L)     C(M,KC,L)
     1      0.0          0.00     0.0   0.01    0.0   0.0    0.0   0.0   0.0   0.0
     1      0.0          0.0     0.0    0.0    0.0    0.0    0.0   0.0   0.0   0.0
     1      0.0          0.0     0.0    0.0    0.0    0.0    0.0   0.0   0.0   0.0
     1      0.0          0.0     0.0    0.0    0.0    0.0     0.0   0.0   0.0   0.0
CC
CC
*--- ID, INJ. TEMP (F)   STEAM QUALITY
    1   90.         0.0
CC
CC ID, BOTTOM HOLE PRESSURE FOR PRESSURE CONSTRAINT WELL (IFLAG=2 OR 3)
*----  ID    PWF
    2      1000
CC
CC ID, BOTTOM HOLE PRESSURE FOR PRESSURE CONSTRAINT WELL (IFLAG=2 OR 3)
*----  ID    PWF
    3      1000
CC
```

```
CC ID, BOTTOM HOLE PRESSURE FOR PRESSURE CONSTRAINT WELL (IFLAG=2 OR 3)
*----  ID    PWF
    4       1000
CC
CC ID, BOTTOM HOLE PRESSURE FOR PRESSURE CONSTRAINT WELL (IFLAG=2 OR 3)
*----  ID    PWF
    5       1000
CC
CC CUM. INJ. TIME , AND INTERVALS (PV OR DAY) FOR WRITING TO OUTPUT FILES
*---- TINJ     CUMPR1     CUMHI1     WRHPV     WRPRF      RSTC
      150     5*0.5
CC
CC THE INI. TIME STEP,CONC. TOLERANCE,MAX.,MIN. TIME STEPS
*----  DT     DELC(I)              CNMAX             CNMIN
  0.00001     8*0.01    0.01      0.01                0.00001
```

PVT

```
CC NUMBER OF DATA SET FOR CASE4
CC
14
CC SARURATED          SOLUTION GAS    OIL FVF         GAS FVF              OIL_VISCOSITY       GAS_VISCOSITY
CC PRESSURE(PSI)       RS(SCF/STB)    BO(RB/STB)     BG(RB/SCF)                 (CP)             (CP)
100             0              1              0.005900053          1              0.013
800             0              1              0.002950027          1              0.0135
1200            0              1              0.001960016          1              0.014
1600            0              1              0.001470005          1              0.0145
2000            0              1              0.001179997          1              0.015
2400            0              1              0.000980008          1              0.0155
2800            0              1              0.000839983          1              0.016
3200            0              1              0.000739973          1              0.0165
3600            0              1              0.000649984          1              0.017
4000            0              1              0.000590005          1              0.0175
4400            0              1              0.000539986          1              0.018
4800            0              1              0.000490004          1              0.0185
5200            0              1              0.000450005          1              0.019
5600            0              1              0.000419992          1              0.0195
CC  SURFACE GAS DENISTY     SURFACE OIL DENISITY    BUBBLE POINT PRESSURE
CC     PSI                    PSI              PSI
       0.0004                 0.225            4000
CC UNDERSATURATED PROPERTY SLOP FOR OIL FORMATION VOLUME FACTOR(DEL_BO/DEL_P) AND OIL VISCOSITY(DEL_VIS/DEL_P)
CC     VIOSLOP        BOSLOP
  0.00001      -0.00023
```

A.5 SURFACTANT INJECTION WITH THREE PHASE EXISTING CASE(CASE-5)

The following is the input data file for UTCHEM simulator. We used this case in Chapter 6 for three-phase flow model. In order to run this case for both original and four-phase model, IGMAS flag in input file, should be set IGMAS=1 along with PVT file for four-phase and IGMAS =0 for original UTCHEM.

HEAD

```
CASE5
NX     NY    NZ       N     NWELL
20    1    1      9    2
NTW       NTA
0         0
NO        NPHAS
0         4
NSUB      MSUB
0         0
NTABL NPHEL
3         2
```

INPUT

```
CC*********************************************************************
CC                                                                    *
CC    BRIEF DESCRIPTION OF DATA SET:UTCHEM FOUR PHASE THERMAL 2014  *
CC                                                                    *
CC*********************************************************************
CC                                          *
CC  SURFACTANT  FLOODING    THRE PHASE ME/OIL/WATER                          *
CC                                          *
CC  LENGTH (FT) : 200              PROCESS : SURF FLOODING       *
CC  THICKNESS (FT) : 10              INJ. PRESSURE (PSI) :        *
CC  WIDTH (FT) : 10                COORDINATES : CARTESIAN       *
CC  POROSITY :                                 *
CC  GRID BLOCKS : 20X1X1                         *
CC  DATE :   AUGUST 2014                         *
CC  CREATED BY : HAMID REZA LASHGARI                                      *
CC*********************************************************************
CC
CC*********************************************************************
CC                                          *
CC    RESERVOIR DESCRIPTION                          *
CC                                          *
CC*********************************************************************
CC
CC
*---- RUNNO
CASE6
CC
CC
*----HEADER
CASE6
1D S FLODDING            COMPARISON OF OF ORIGINAL AND FOUR-PHASE MODEL
*************************************************************
CC
CC SIMULATION FLAGS
*---- IMODE IMES IDISPC ICWM ICAP IREACT IBIO ICOORD ITREAC ITC  IGAS  IENG IHEATW IELECHV IELECHI  ISTEAM   IGMAS
       1         3     0        0     0      0       0      1         0       0     1       1      0         0         0         0         1
CC
CC NUMBER OF GRID BLOCKS AND FLAG SPECIFIES CONSTANT OR VARIABLE GRID SIZE
*---- NX    NY    NZ  IDXYZ  IUNIT
    20    1 1    0      0
CC
CC  CONSTANT GRID BLOCK SIZE IN X, Y, AND Z
*---- DX        DY         DZ
     10       10         10
CC
CC TOTAL NO. OF COMPONENTS, NO. OF TRACERS, NO. OF GEL COMPONENTS
```

```
*----N   NO NTW NTA NGC  NG  NOTH
    9   0 0  0 0   0   0
CC
CC
*---- SPNAME(I),I=1,N
WATER
OIL
SURFACTANT
POLYMER
ANION
CATION
ALCOHOL
GAS
TRACER
CC
CC FLAG INDICATING IF THE COMPONENT IS INCLUDED IN CALCULATIONS OR NOT
*----ICF(KC) FOR KC=1,N
   1  1  1  0  1  0  0  1  0
CC
CC*************************************************************************
CC                                                  *
CC    OUTPUT OPTIONS                                        *
CC                                                  *
CC*************************************************************************
CC
CC
CC FLAG TO WRITE TO UNIT 3,FLAG FOR PV OR DAYS TO PRINT OR TO STOP THE RUN
*---- ICUMTM  ISTOP  IOUTGMS      IS3G
      0      0       2       2
CC
CC FLAG INDICATING IF THE PROFILE OF KCTH COMPONENT SHOULD BE WRITTEN
*---- IPRFLG(KC),KC=1,N
      1  1  1 1   1  0  0  1  0
CC
CC FLAG FOR PRES.,SAT.,TOTAL CONC.,TRACER CONC.,CAP.,GEL, ALKALINE PROFILES
*---- IPPRES IPSAT IPCTOT IPBIO IPCAP IPGEL IPALK IPTEMP IPOBS
      1     1     1     0    0    0    1    1     0
CC
CC FLAG FOR WRITING SEVERAL PROPERTIES TO UNIT 4 (PROF)
*---- ICKL IVIS IPER ICNM ICSE IHYSTP IFOAMP INONEQ
     1   1   1   1   1   1   0   0  0
CC
CC FLAG FOR WRITING SEVERAL PROPERTIES TO PROF
*---- IADS IVEL IRKF IPHSE
     1   1   1   1
CC
CC*************************************************************************
CC                                                  *
CC    RESERVOIR PROPERTIES                                  *
CC                                                  *
CC*************************************************************************
CC
CC
CC MAX. SIMULATION TIME ( DAYS)
*---- TMAX
   100
CC
CC ROCK COMPRESSIBILITY (1/PSI), STAND. PRESSURE(PSIA)
*---- COMPR               PSTAND
      0                200
CC
CC FLAGS INDICATION CONSTANT OR VARIABLE POROSITY, X,Y,AND Z PERMEABILITY
*----IPOR1 IPERMX IPERMY IPERMZ  IMOD  ITRNZ   INTG
     0     0    3     3     0    0      0
CC
CC CONSTANT POROSITY FOR WHOLE RESERVOIR
*---- PORC1
     0.2
CC
CC CONSTANT X-PERMEABILITY (MILIDARCY) FOR LAYER K = 1,NZ
*----PERMX
   100
CC
CC Y DIRECTION PERMEABILITY IS DEPENDENT ON X DIRECTION PERMEABILITY
*---- CONSTANT PERMEABILITY MULTIPLIER FOR Y DIRECTION PERMEABILITY
      1
CC
```

```
CC Z DIRECTION PERMEABILITY IS DEPENDENT ON X DIRECTION PERMEABILITY
*---- CONSTANT PERMEABILITY MULTIPLIER FOR Z DIRECTION PERMEABILITY
     1
CC
CC FLAG FOR CONSTANT OR VARIABLE DEPTH, PRESSURE, WATER SATURATION,INITIAL AQUEOUS PHASE COMPOSITIONS
*----IDEPTH  IPRESS  ISWI  ICWI
     0      0     0     -1
CC
CC CONSTANT DEPTH (FT)
*---- D111
     0
CC
CC INITIAL PRESSURE (PSIA)
*----PINIT   DEPTH
    3000.  0.0
CC
CC CONSTANT INITIAL WATER SATURATION (RESIDUAL OIL)
*---- SWI
    0.4
CC
CC FLAG INDICATING TYPE OF INITIAL GAS SATURATION
*---ISGI
   0
CC
CC CONSTANT INITIAL GAS SATURATION FOR WHOLE RESERVOIR
*---- SGI
     0.0
CC
CC BRINE SALINITY AND DIVALENT CATION CONCENTRATION (MEQ/ML)
*---- C50       C60
     0.3    0.00
CC
CC*********************************************************************
CC                                          *
CC    PHYSICAL PROPERTY DATA                          *
CC                                          *
CC*********************************************************************
CC
CC
CC OIL CONC. AT PLAIT POINT FOR TYPE II(+)AND TYPE II(-), CMC
*---- C2PLC  C2PRC   EPSME   IHAND
      0     1     0.00001     0
CC
CC 3.4.2 FLAG INDICATING TYPE OF PHASE BEHAVIOR PARAMETERS
*---- IFGHBN=0 FOR INPUT HEIGHT OF BINODAL CURVE; =1 FOR INPUT SOL. RATIO
      0
CC SLOPE AND INTERCEPT OF BINODAL CURVE AT ZERO, OPT., AND 2XOPT SALINITY
CC FOR ALCOHOL 1
*---- HBNS70   HBNC70   HBNS71   HBNC71   HBNS72   HBNC72
      0    0.05      0     0.03     0     0.05
CC
CC SLOPE OF BINODAL WITH TEMP., SLOPE OF SALINITY WITH TEMP. (1/F)
*---- HBNT0     HBNT1    HBNT2    CSET(0.00415)
     0.00017  0.00017  0.00017   0.00415
CC SLOPE AND INTERCEPT OF BINODAL CURVE AT ZERO, OPT., AND 2XOPT SALINITY
CC FOR ALCOHOL 2
*---- HBNS80  HBNC80  HBNS81  HBNC81  HBNS82  HBNC82
      0       0       0       0       0       0
CC
CC LOWER AND UPPER EFFECTIVE SALINITY FOR ALCOHOL 1 AND ALCOHOL 2
*---- CSEL7   CSEU7   CSEL8   CSEU8
     0.32    0.53     0       0
CC
CC THE CSE SLOPE PARAMETER FOR CALCIUM AND ALCOHOL 1 AND ALCOHOL 2
*---- BETA6    BETA7    BETA8
      0.       0       0
CC
CC FLAG FOR ALCOHOL PART. MODEL AND PARTITION COEFFICIENTS
*---- IALC   OPSK7O   OPSK7S   OPSK8O   OPSK8S
      1      0        0        0        0
CC
CC NO. OF ITERATIONS, AND TOLERANCE
*---- NALMAX      EPSALC
      20       0.0001
CC 3.4.10 ALCOHOL 1 PARTITIONING PARAMETERS IF IALC=1
CC   AQ-OLEIC   AQ-OLEIC  SURF-OLEIC
*---- AKWC7     AKWS7    AKM7     AK7      PT7
```

```
      4.671    1.79      48     35.31    0.222
CC
CC ALCOHOL 2 PARTITIONING PARAMETERS IF IALC=1
*---- AKWC8     AKWS8    AKM8    AK8     PT8
       0         0        0      0       0
CC
CC 3.4.22 IFT MODEL FLAG
*----  IFT=0 FOR HEALY&REED; =1 FOR CHUN HUH CORREL.
       1
CC 3.4.24 INTERFACIAL TENSION PARAMETERS
CC    TYP=.1-.35   TYP=5-20
*---- CHUH     AHUH
     0.35       10
CC
CC LOG10 OF OIL/WATER INTERFACIAL TENSION
*---- XIFTW
      1.3
CC
CC ORGANIC MASS TRANSFER FLAG
*---- IMASS ICOR
                 0    0
CC
CC
*--- IWALT  IWALF
       0       0
CC
CC CAPILLARY DESATURATION PARAMETERS FOR PHASE 1, 2, AND 3
*---- ITRAP      T11      T22      T33
       0        300     1000     300
CC
CC  RELATIVE PERM  AND PC MODEL
*----IPERM      IRTYPE
     0          0
CC
CC FLAG FOR CONSTANT OR VARIABLE REL. PERM. PARAMETERS
*---- ISRW    IPRW    IEW
       0      0       0
CC
CC CONSTANT RES. SATURATION OF PHASES 1,2,AND 3 AT LOW CAPILLARY NO.
*---- S1RWC    S2RWC     S3RWC
      0.0      0.0       0.0
CC
CC CONSTANT ENDPOINT REL. PERM. OF PHASES 1,2,AND 3 AT LOW CAPILLARY NO.
*---- P1RWC     P2RWC    P3RWC
      1        1       1
CC
CC CONSTANT REL. PERM. EXPONENT OF PHASES 1,2,AND 3 AT LOW CAPILLARY NO.
*---- E1WC     E2WC     E3WC
      1        1        1
CC
CC WATER AND OIL VISCOSITY , RESERVOIR TEMPERATURE
*---- VIS1     VIS2   TSTAND
      1       1      60
CC
CC GAS VISCOSITY AT REF. TEMPERATURE AND PRESSURE,SLOPE OF GAS VISCOSITY
*---- VIS4       VSLOPG
      0.02   0
CC
CC VISCOSITY-TEMP PARAMETERS
*----BVI(1)  BVI(2)
    0       0
CC
CC VISCOSITY-TEMP PARAMETERS
*----BVI(4)
    0
CC
CC CONSTANT RESIDUAL OIL/GAS SATURATION FOR ENTIRE RESERVOIR
*---- S2RWC4
      0.0  0.0
CC
CC CONSTANT RESIDUAL OIL/GAS SATURATION FOR ENTIRE RESERVOIR
*----  S4RWC
      1
CC
CC CONSTANT GAS ENDPOINT RELATIVE PERMEABILITY FOR ENTIRE RESERVOIR
*--- P4RWC
      1
```

```
CC
CC LOG OF INTERFACIAL TENSION BETWEEN GAS AND OIL (AND WATER)
*----  XIFTG   XIFTGW
     1.477    1.477
CC
CC COMPOSITIONAL PHASE VISCOSITY PARAMETERS
*----   ALPHAV1   ALPHAV2   ALPHAV3   ALPHAV4  ALPHAV5
        0         0       1         0         1.7
CC
CC PARAMETERS TO CALCULATE POLYMER VISCOSITY AT ZERO SHEAR RATE
*---- AP1      AP2      AP3
     10.21      17.77     626.14
CC
CC PARAMETER TO COMPUTE CSEP,MIN. CSEP, AND SLOPE OF LOG VIS. VS. LOG CSEP
*---- BETAP    CSE1     SSLOPE
     20      0.01     -0.6
CC
CC PARAMETER FOR SHEAR RATE DEPENDENCE OF POLYMER VISCOSITY
*---- GAMMAC   GAMHF    POWN       IPMOD   ISHEAR  RWEFF GAMHF2
     4       56.1      1.643               0       0      0.25   0
CC
CC CC FLAG FOR POLYMER PARTITIONING, PERM. REDUCTION PARAMETERS
*---- IPOLYM    EPHI3    EPHI4    BRK     CRK                       RKCUT
      1         1       1       1000    0.0186                            10
CC
CC SPECIFIC WEIGHT FOR COMPONENTS 1,2,3,7,8 ,COEFFIENT OF OIL AND GRAVITY FLAG
*---- DEN1     DEN2    DEN23     DEN3    DEN7    DEN8    IDEN
    0.45     0.225    0.26     0.433     0.39    0.005      2
CC
CC FLAG FOR CHOICE OF UNITS ( 0:BOTTOMHOLE CONDITION , 1: STOCK TANK)
*------ ISTB
       0
CC
CC COMPRESSIBILITY FOR VOL. OCCUPYING COMPONENTS 1,2,3,7,AND 8
*---- COMPC(1)  COMPC(2)  COMPC(3)  COMPC(7)  COMPC(8)
       0.0000001       0.0000001         0.000001      0    0.000001
CC
CC CONSTANT OR VARIABLE PC PARAM., WATER-WET OR OIL-WET PC CURVE FLAG
*---- ICPC    IEPC   IOW
     0       0      0
CC
CC CAPILLARY PRESSURE PARAMETER, CPC0
*---- CPC0
     0
CC
CC CAPILLARY PRESSURE PARAMETER, EPC0
*---- EPC0
     2
CC
CC MOLECULAR DIFFUSION COEF. KCTH COMPONENT IN PHASE 1
*---- D(KC,1),KC=1,N
       0       0       0       0       0       0       0       0       0       0       0       0       0
CC
CC MOLECULAR DIFFUSION COEF. KCTH COMPONENT IN PHASE 2
*---- D(KC,2),KC=1,N
       0       0       0       0       0       0       0       0       0       0       0       0       0
CC
CC MOLECULAR DIFFUSION COEF. KCTH COMPONENT IN PHASE 3
*---- D(KC,3),KC=1,N
       0       0       0       0       0       0       0       0       0       0       0       0       0
CC
CC MOLECULAR DIFFUSION COEF. KCTH COMPONENT IN PHASE 4
*---- D(KC,3),KC=1,N
       0       0       0       0       0       0       0       0       0       0       0       0       0
CC
CC LONGITUDINAL AND TRANSVERSE DISPERSIVITY OF PHASE 1
*---- ALPHAL(1)     ALPHAT(1)
       0.0           0.000
CC
CC LONGITUDINAL AND TRANSVERSE DISPERSIVITY OF PHASE 2
*---- ALPHAL(2)     ALPHAT(2)
       0.0           0.000
CC
CC LONGITUDINAL AND TRANSVERSE DISPERSIVITY OF PHASE 3
*---- ALPHAL(3)     ALPHAT(3)
       0.0           0.000
CC
```

```
CC LONGITUDINAL AND TRANSVERSE DISPERSIVITY OF PHASE 4
*---- ALPHAL(3)     ALPHAT(3)
       0.0           0.000
CC
CC FLAG TO SPECIFY ORGANIC ADSORPTION CALCULATION
*---- IADSO
      0
CC
CC SURFACTANT AND POLYMER ADSORPTION PARAMETERS
*---- AD31    AD32   B3D    AD41   AD42   B4D   IADK  IADS1   FADS   REFK
     1.5      0.5    1000    9.5     0     100     0     0      0      0
CC
CC PARAMETERS FOR CATION EXCHANGE OF CLAY AND SURFACTANT
*---- QV      XKC     XKS     EQW
     0.00    0.      0.      450
CC
CC INITIAL TEMPERATURE
*--- TEMPI (F)
    90
CC
CC ROCK DENSITY,CONDUCTIVITY,HEAT CAPACITY
*---- DENS   CTCR  CTCL(1:NPHASE) CVSPR   CVSPL(1:NPHASE)
     165.43   100   100    100   100  100   0.242    1   0.5   1    1
CC
CC THERMAL EXPANTION OF COMPONENTS AND ROCK
*--- THEXP(1:N), THEXPR
   0.001   0.001  0.0  0.0  0.0  0.0 0.0 0.0 0.01  0.0001
CC
CC HEATLOSS FLAG, ANALYTICAL SOLUTION ANALYTICAL SHOULD BE CHECKED
*---- IHLOS  IANAL
      0     0
CC
CC*********************************************************************
CC                                                 *
CC    WELL DATA                                          *
CC                                                 *
CC*********************************************************************
CC
CC
CC FLAG FOR SPECIFIED BOUNDARY AND ZONE IS MODELED
*---- IBOUND     IZONE
      0      0
CC
CC TOTAL NUMBER OF WELLS, WELL RADIUS FLAG, FLAG FOR TIME OR COURANT NO.
*---- NWELL   IRO    ITIME    NWREL
      2      2       0        2
CC
CC WELL ID,LOCATIONS,AND FLAG FOR SPECIFYING WELL TYPE, WELL RADIUS, SKIN
*---- IDW    IW    JW    IFLAG    RW     SWELL   IDIR   IFIRST   ILAST   IPRF
      1     1     1       1     0.5       0       3      1     1    0
CC
CC WELL NAME
*----  WELNAM
INJ1
CC
CC ICHEK , MAX. AND MIN. ALLOWABLE BOTTOMHOLE PRESSURE AND RATE
*---- ICHEK     PWFMIN     PWFMAX    QTMIN    QTMAX
      0          0         10000      0       20000
CC
CC WELL ID,LOCATIONS,AND FLAG FOR SPECIFYING WELL TYPE, WELL RADIUS, SKIN
*---- IDW    IW    JW    IFLAG    RW     SWELL   IDIR   IFIRST   ILAST   IPRF
      2     20     1     2     1       0       3         1   1       0
CC
CC WELL NAME
*----  WELNAM
PROD1
CC
CC ICHEK , MAX. AND MIN. ALLOWABLE BOTTOMHOLE PRESSURE AND RATE
*---- ICHEK     PWFMIN     PWFMAX    QTMIN    QTMAX
      0          0         1000      -0       -20000
CC
CC  ID,INJ. RATE AND INJ. COMP. FOR RATE CONS. WELLS FOR EACH PHASE (L=1,3)
*----  ID     QI(M,L)     C(M,KC,L)
      1      50.0  0.99  0.0   0.01   0.0    0.6  0.0  0.0  0.0   0.0
      1      0.0   0.0   0.0    0.0   0.0    0.0 0.0  0.0  0.0   0.0
      1      0.0   0.0   0.0    0.0   0.0    0.0 0.0  0.0  0.0   0.0
      1      0.0   0.0   0.0    0.0   0.0    0.0 0.0  0.0  0.0   0.0
```

```
CC
CC
*--- ID, INJ. TEMP (F)
    1    90.
CC
CC
*----  ID    PWF
    2     2000
CC
CC CUM. INJ. TIME , AND INTERVALS (PV OR DAY) FOR WRITING TO OUTPUT FILES
*---- TINJ     CUMPR1     CUMHI1     WRHPV     WRPRF      RSTC
     100      5*0.5
CC
CC THE INI. TIME STEP,CONC. TOLERANCE,MAX.,MIN. TIME STEPS
*----  DT     DELC(I)             CNMAX            CNMIN
  0.0001       9*0.005         0.005              0.00001
```

PVT

```
CC NUMBER OF DATA SET FOR CASE5
CC
14
CC SARURATED          SOLUTION GAS    OIL FVF         GAS FVF              OIL_VISCOSITY       GAS_VISCOSITY
CC PRESSURE(PSI)       RS(SCF/STB)    BO(RB/STB)     BG(RB/SCF)                 (CP)              (CP)
100            0              1              0.005900053              1              0.013
800            0              1              0.002950027              1              0.0135
1200           0              1              0.001960016              1              0.014
1600           0              1              0.001470005              1              0.0145
2000           0              1              0.001179997              1              0.015
2400           0              1              0.000980008              1              0.0155
2800           0              1              0.000839983              1              0.016
3200           0              1              0.000739973              1              0.0165
3600           0              1              0.000649984              1              0.017
4000           0              1              0.000590005              1              0.0175
4400           0              1              0.000539986              1              0.018
4800           0              1              0.000490004              1              0.0185
5200           0              1              0.000450005              1              0.019
5600           0              1              0.000419992              1              0.0195
CC  SURFACE GAS DENISTY     SURFACE OIL DENISITY    BUBBLE POINT PRESSURE
CC     PSI                      PSI               PSI
       0.0004                 0.225              4000
CC UNDERSATURATED PROPERTY SLOP FOR OIL FORMATION VOLUME FACTOR(DEL_BO/DEL_P) AND OIL VISCOSITY(DEL_VIS/DEL_P)
CC     VIOSLOP        BOSLOP
  0.00001      -0.00023
```

A.6 SURFACTANT AND GAS INJECTION WITH FOUR PHASE EXISTING CASE (CASE-6)

The following is the input data file for UTCHEM simulator. We used this case in Chapter 6 for four-phase flow model.

HEAD

```
CASE6
NX     NY    NZ       N     NWELL
20    1    1      9    2
NTW       NTA
0         0
NO        NPHAS
0         4
NSUB      MSUB
0         0
NTABL NPHEL
3         2
```

INPUT

```
CC*********************************************************************
CC                                                  *
CC    BRIEF DESCRIPTION OF DATA SET:UTCHEM FOUR PHASE THERMAL 2014  *
CC                                                  *
CC*********************************************************************
CC                                                  *
CC  SURFACTANT  FLOODING  FOUR PHASE ME/GAS/OIL/WATER                              *
CC                                                  *
CC  LENGTH (FT) : 200              PROCESS : SURF FLOODING       *
CC  THICKNESS (FT) : 10              INJ. PRESSURE (PSI) :        *
CC  WIDTH (FT) : 10                COORDINATES : CARTESIAN        *
CC  POROSITY :                                      *
CC  GRID BLOCKS : 20X1X1                                 *
CC  DATE :    AUGUST 2014                                *
CC  CREATED BY : HAMID REZA LASHGARI                                          *
CC*********************************************************************
CC
CC*********************************************************************
CC                                                  *
CC    RESERVOIR DESCRIPTION                                 *
CC                                                  *
CC*********************************************************************
CC
CC
*---- RUNNO
CASE6
CC
CC
*----HEADER
CASE6
1D S FLODDING
************************************************************
CC
CC SIMULATION FLAGS
*---- IMODE IMES IDISPC ICWM ICAP IREACT IBIO ICOORD ITREAC ITC  IGAS  IENG IHEATW IELECHV IELECHI  ISTEAM   IGMAS
       1          3     0         0     0      0       0       1          0       0      1       1      0          0          0          0          1
CC
CC NUMBER OF GRID BLOCKS AND FLAG SPECIFIES CONSTANT OR VARIABLE GRID SIZE
*---- NX    NY    NZ  IDXYZ  IUNIT
    20    1  1    0      0
CC
CC  CONSTANT GRID BLOCK SIZE IN X, Y, AND Z
*---- DX        DY         DZ
     10        10         10
CC
CC TOTAL NO. OF COMPONENTS, NO. OF TRACERS, NO. OF GEL COMPONENTS
*----N   NO NTW NTA NGC  NG  NOTH
    9    0 0   0  0    0    0
```

```
CC
CC
*---- SPNAME(I),I=1,N
WATER
OIL
SURFACTANT
POLYMER
ANION
CATION
ALCOHOL
GAS
TRACER
CC
CC FLAG INDICATING IF THE COMPONENT IS INCLUDED IN CALCULATIONS OR NOT
*----ICF(KC) FOR KC=1,N
   1  1  1  0  1  0  0  1  0
CC
CC*********************************************************************
CC                                                  *
CC    OUTPUT OPTIONS                                          *
CC                                                  *
CC*********************************************************************
CC
CC
CC FLAG TO WRITE TO UNIT 3,FLAG FOR PV OR DAYS TO PRINT OR TO STOP THE RUN
*---- ICUMTM  ISTOP  IOUTGMS      IS3G
      0      0       2        2
CC
CC FLAG INDICATING IF THE PROFILE OF KCTH COMPONENT SHOULD BE WRITTEN
*---- IPRFLG(KC),KC=1,N
      1  1  1 1   1  0  0  1  0
CC
CC FLAG FOR PRES.,SAT.,TOTAL CONC.,TRACER CONC.,CAP.,GEL, ALKALINE PROFILES
*---- IPPRES IPSAT IPCTOT IPBIO IPCAP IPGEL IPALK IPTEMP IPOBS
      1      1      1      0     0     0     1     1      0
CC
CC FLAG FOR WRITING SEVERAL PROPERTIES TO UNIT 4 (PROF)
*---- ICKL IVIS IPER ICNM ICSE IHYSTP IFOAMP INONEQ
      1    1    1    1    1    1    0    0   0
CC
CC FLAG FOR WRITING SEVERAL PROPERTIES TO PROF
*---- IADS IVEL IRKF IPHSE
      1    1    1    1
CC
CC*********************************************************************
CC                                                  *
CC    RESERVOIR PROPERTIES                                      *
CC                                                  *
CC*********************************************************************
CC
CC
CC MAX. SIMULATION TIME ( DAYS)
*---- TMAX
    150
CC
CC ROCK COMPRESSIBILITY (1/PSI), STAND. PRESSURE(PSIA)
*---- COMPR               PSTAND
      0                200
CC
CC FLAGS INDICATION CONSTANT OR VARIABLE POROSITY, X,Y,AND Z PERMEABILITY
*----IPOR1 IPERMX IPERMY IPERMZ  IMOD  ITRNZ   INTG
      0      0     3      3      0     0       0
CC
CC CONSTANT POROSITY FOR WHOLE RESERVOIR
*---- PORC1
      0.2
CC
CC CONSTANT X-PERMEABILITY (MILIDARCY) FOR LAYER K = 1,NZ
*----PERMX
    100
CC
CC Y DIRECTION PERMEABILITY IS DEPENDENT ON X DIRECTION PERMEABILITY
*---- CONSTANT PERMEABILITY MULTIPLIER FOR Y DIRECTION PERMEABILITY
      1
CC
CC Z DIRECTION PERMEABILITY IS DEPENDENT ON X DIRECTION PERMEABILITY
*---- CONSTANT PERMEABILITY MULTIPLIER FOR Z DIRECTION PERMEABILITY
```

```
      1
CC
CC FLAG FOR CONSTANT OR VARIABLE DEPTH, PRESSURE, WATER SATURATION,INITIAL AQUEOUS PHASE COMPOSITIONS
*----IDEPTH  IPRESS  ISWI  ICWI
      0      0      0     -1
CC
CC CONSTANT DEPTH (FT)
*---- D111
      0
CC
CC INITIAL PRESSURE (PSIA)
*----PINIT   DEPTH
    3000.  0.0
CC
CC CONSTANT INITIAL WATER SATURATION (RESIDUAL OIL)
*---- SWI
    0.4
CC
CC FLAG INDICATING TYPE OF INITIAL GAS SATURATION
*---ISGI
   0
CC
CC CONSTANT INITIAL GAS SATURATION FOR WHOLE RESERVOIR
*---- SGI
     0.0
CC
CC BRINE SALINITY AND DIVALENT CATION CONCENTRATION (MEQ/ML)
*---- C50       C60
      0.3    0.00
CC
CC*********************************************************************
CC                                          *
CC    PHYSICAL PROPERTY DATA                                *
CC                                          *
CC*********************************************************************
CC
CC
CC OIL CONC. AT PLAIT POINT FOR TYPE II(+)AND TYPE II(-), CMC
*---- C2PLC  C2PRC   EPSME   IHAND
      0     1     0.00001     0
CC
CC 3.4.2 FLAG INDICATING TYPE OF PHASE BEHAVIOR PARAMETERS
*---- IFGHBN=0 FOR INPUT HEIGHT OF BINODAL CURVE; =1 FOR INPUT SOL. RATIO
      0
CC SLOPE AND INTERCEPT OF BINODAL CURVE AT ZERO, OPT., AND 2XOPT SALINITY
CC FOR ALCOHOL 1
*---- HBNS70   HBNC70   HBNS71   HBNC71   HBNS72   HBNC72
      0    0.05      0     0.03     0     0.05
CC
CC SLOPE OF BINODAL WITH TEMP., SLOPE OF SALINITY WITH TEMP. (1/F)
*---- HBNT0     HBNT1    HBNT2    CSET(0.00415)
     0.00017  0.00017  0.00017   0.00415
CC SLOPE AND INTERCEPT OF BINODAL CURVE AT ZERO, OPT., AND 2XOPT SALINITY
CC FOR ALCOHOL 2
*---- HBNS80  HBNC80  HBNS81  HBNC81  HBNS82  HBNC82
      0       0       0       0       0       0
CC
CC LOWER AND UPPER EFFECTIVE SALINITY FOR ALCOHOL 1 AND ALCOHOL 2
*---- CSEL7   CSEU7   CSEL8   CSEU8
      0.32    0.53     0       0
CC
CC THE CSE SLOPE PARAMETER FOR CALCIUM AND ALCOHOL 1 AND ALCOHOL 2
*---- BETA6    BETA7    BETA8
      0.       0       0
CC
CC FLAG FOR ALCOHOL PART. MODEL AND PARTITION COEFFICIENTS
*---- IALC   OPSK7O   OPSK7S   OPSK8O   OPSK8S
      1      0        0        0        0
CC
CC NO. OF ITERATIONS, AND TOLERANCE
*---- NALMAX      EPSALC
       20        0.0001
CC 3.4.10 ALCOHOL 1 PARTITIONING PARAMETERS IF IALC=1
CC   AQ-OLEIC   AQ-OLEIC  SURF-OLEIC
*---- AKWC7     AKWS7    AKM7     AK7      PT7
      4.671    1.79      48     35.31    0.222
CC
```

```
CC ALCOHOL 2 PARTITIONING PARAMETERS IF IALC=1
*---- AKWC8     AKWS8    AKM8    AK8     PT8
      0         0        0       0       0
CC
CC 3.4.22 IFT MODEL FLAG
*----  IFT=0 FOR HEALY&REED; =1 FOR CHUN HUH CORREL.
       1
CC 3.4.24 INTERFACIAL TENSION PARAMETERS
CC    TYP=.1-.35   TYP=5-20
*---- CHUH     AHUH
     0.35       10
CC
CC LOG10 OF OIL/WATER INTERFACIAL TENSION
*---- XIFTW
      1.3
CC
CC ORGANIC MASS TRANSFER FLAG
*---- IMASS ICOR
                0    0
CC
CC
*--- IWALT  IWALF
      0       0
CC
CC CAPILLARY DESATURATION PARAMETERS FOR PHASE 1, 2, AND 3
*---- ITRAP      T11      T22      T33
      0        300    1000    300
CC
CC  RELATIVE PERM  AND PC MODEL
*----IPERM      IRTYPE
     0          0
CC
CC FLAG FOR CONSTANT OR VARIABLE REL. PERM. PARAMETERS
*---- ISRW    IPRW    IEW
      0      0       0
CC
CC CONSTANT RES. SATURATION OF PHASES 1,2,AND 3 AT LOW CAPILLARY NO.
*---- S1RWC    S2RWC     S3RWC
      0.0      0.0       0.0
CC
CC CONSTANT ENDPOINT REL. PERM. OF PHASES 1,2,AND 3 AT LOW CAPILLARY NO.
*---- P1RWC     P2RWC    P3RWC
      1        1       1
CC
CC CONSTANT REL. PERM. EXPONENT OF PHASES 1,2,AND 3 AT LOW CAPILLARY NO.
*---- E1WC     E2WC     E3WC
      1        1        1
CC
CC WATER AND OIL VISCOSITY , RESERVOIR TEMPERATURE
*---- VIS1     VIS2   TSTAND
      1       1      60
CC
CC GAS VISCOSITY AT REF. TEMPERATURE AND PRESSURE,SLOPE OF GAS VISCOSITY
*---- VIS4       VSLOPG
      0.02   0
CC
CC VISCOSITY-TEMP PARAMETERS
*----BVI(1)  BVI(2)
    0       0
CC
CC VISCOSITY-TEMP PARAMETERS
*----BVI(4)
    0
CC
CC CONSTANT RESIDUAL OIL/GAS SATURATION FOR ENTIRE RESERVOIR
*---- S2RWC4
      0.0  0.0
CC
CC CONSTANT RESIDUAL OIL/GAS SATURATION FOR ENTIRE RESERVOIR
*----  S4RWC
      1
CC
CC CONSTANT GAS ENDPOINT RELATIVE PERMEABILITY FOR ENTIRE RESERVOIR
*--- P4RWC
      1
CC
CC LOG OF INTERFACIAL TENSION BETWEEN GAS AND OIL (AND WATER)
```

```
*---- XIFTG   XIFTGW
     1.477    1.477
CC
CC COMPOSITIONAL PHASE VISCOSITY PARAMETERS
*----  ALPHAV1   ALPHAV2   ALPHAV3   ALPHAV4  ALPHAV5
       0         0       1         0         1.7
CC
CC PARAMETERS TO CALCULATE POLYMER VISCOSITY AT ZERO SHEAR RATE
*---- AP1      AP2      AP3
     10.21     17.77     626.14
CC
CC PARAMETER TO COMPUTE CSEP,MIN. CSEP, AND SLOPE OF LOG VIS. VS. LOG CSEP
*---- BETAP    CSE1     SSLOPE
     20       0.01     -0.6
CC
CC PARAMETER FOR SHEAR RATE DEPENDENCE OF POLYMER VISCOSITY
*---- GAMMAC   GAMHF   POWN       IPMOD   ISHEAR  RWEFF GAMHF2
     4        56.1     1.643               0       0       0.25   0
CC
CC CC FLAG FOR POLYMER PARTITIONING, PERM. REDUCTION PARAMETERS
*---- IPOLYM    EPHI3    EPHI4    BRK     CRK                       RKCUT
      1         1        1       1000    0.0186                    10
CC
CC SPECIFIC WEIGHT FOR COMPONENTS 1,2,3,7,8 ,COEFFIENT OF OIL AND GRAVITY FLAG
*---- DEN1     DEN2    DEN23     DEN3    DEN7    DEN8    IDEN
    0.45     0.225    0.26     0.433     0.39    0.005     2
CC
CC FLAG FOR CHOICE OF UNITS ( 0:BOTTOMHOLE CONDITION , 1: STOCK TANK)
*------ ISTB
       0
CC
CC COMPRESSIBILITY FOR VOL. OCCUPYING COMPONENTS 1,2,3,7,AND 8
*---- COMPC(1)  COMPC(2)  COMPC(3)  COMPC(7)  COMPC(8)
       0.0000001       0.0000001         0.000001      0    0.000001
CC
CC CONSTANT OR VARIABLE PC PARAM., WATER-WET OR OIL-WET PC CURVE FLAG
*---- ICPC    IEPC   IOW
     0       0      0
CC
CC CAPILLARY PRESSURE PARAMETER, CPC0
*---- CPC0
     0
CC
CC CAPILLARY PRESSURE PARAMETER, EPC0
*---- EPC0
     2
CC
CC MOLECULAR DIFFUSION COEF. KCTH COMPONENT IN PHASE 1
*---- D(KC,1),KC=1,N
       0       0       0       0       0       0       0       0       0       0       0       0       0
CC
CC MOLECULAR DIFFUSION COEF. KCTH COMPONENT IN PHASE 2
*---- D(KC,2),KC=1,N
       0       0       0       0       0       0       0       0       0       0       0       0       0
CC
CC MOLECULAR DIFFUSION COEF. KCTH COMPONENT IN PHASE 3
*---- D(KC,3),KC=1,N
       0       0       0       0       0       0       0       0       0       0       0       0       0
CC
CC MOLECULAR DIFFUSION COEF. KCTH COMPONENT IN PHASE 4
*---- D(KC,3),KC=1,N
       0       0       0       0       0       0       0       0       0       0       0       0       0
CC
CC LONGITUDINAL AND TRANSVERSE DISPERSIVITY OF PHASE 1
*---- ALPHAL(1)     ALPHAT(1)
       0.0           0.000
CC
CC LONGITUDINAL AND TRANSVERSE DISPERSIVITY OF PHASE 2
*---- ALPHAL(2)     ALPHAT(2)
       0.0           0.000
CC
CC LONGITUDINAL AND TRANSVERSE DISPERSIVITY OF PHASE 3
*---- ALPHAL(3)     ALPHAT(3)
       0.0           0.000
CC
CC LONGITUDINAL AND TRANSVERSE DISPERSIVITY OF PHASE 4
*---- ALPHAL(3)     ALPHAT(3)
```

```
       0.0          0.000
CC
CC FLAG TO SPECIFY ORGANIC ADSORPTION CALCULATION
*---- IADSO
      0
CC
CC SURFACTANT AND POLYMER ADSORPTION PARAMETERS
*---- AD31    AD32   B3D    AD41   AD42   B4D   IADK  IADS1   FADS   REFK
     1.5      0.5    1000    9.5     0     100    0     0      0      0
CC
CC PARAMETERS FOR CATION EXCHANGE OF CLAY AND SURFACTANT
*---- QV      XKC     XKS     EQW
     0.00    0.     0.      450
CC
CC INITIAL TEMPERATURE
*--- TEMPI (F)
    90
CC
CC ROCK DENSITY,CONDUCTIVITY,HEAT CAPACITY
*---- DENS   CTCR  CTCL(1:NPHASE) CVSPR   CVSPL(1:NPHASE)
     165.43   100   100    100   100  100   0.242    1   0.5   1    1
CC
CC THERMAL EXPANTION OF COMPONENTS AND ROCK
*--- THEXP(1:N), THEXPR
   0.001   0.001  0.0  0.0  0.0  0.0 0.0 0.0 0.01  0.0001
CC
CC HEATLOSS FLAG, ANALYTICAL SOLUTION ANALYTICAL SHOULD BE CHECKED
*---- IHLOS  IANAL
      0     0
CC
CC*********************************************************************
CC                                                  *
CC    WELL DATA                                           *
CC                                                  *
CC*********************************************************************
CC
CC
CC FLAG FOR SPECIFIED BOUNDARY AND ZONE IS MODELED
*---- IBOUND     IZONE
      0      0
CC
CC TOTAL NUMBER OF WELLS, WELL RADIUS FLAG, FLAG FOR TIME OR COURANT NO.
*---- NWELL   IRO    ITIME    NWREL
      2      2       0        2
CC
CC WELL ID,LOCATIONS,AND FLAG FOR SPECIFYING WELL TYPE, WELL RADIUS, SKIN
*---- IDW    IW    JW    IFLAG    RW     SWELL   IDIR   IFIRST   ILAST   IPRF
     1     1     1       1    0.5       0       3      1     1    0
CC
CC WELL NAME
*----  WELNAM
INJ1
CC
CC ICHEK , MAX. AND MIN. ALLOWABLE BOTTOMHOLE PRESSURE AND RATE
*---- ICHEK     PWFMIN     PWFMAX    QTMIN    QTMAX
      0          0         10000      0        20000
CC
CC WELL ID,LOCATIONS,AND FLAG FOR SPECIFYING WELL TYPE, WELL RADIUS, SKIN
*---- IDW    IW    JW    IFLAG    RW     SWELL   IDIR   IFIRST   ILAST   IPRF
     2     20     1     2     1       0       3          1   1       0
CC
CC WELL NAME
*----  WELNAM
PROD1
CC
CC ICHEK , MAX. AND MIN. ALLOWABLE BOTTOMHOLE PRESSURE AND RATE
*---- ICHEK     PWFMIN     PWFMAX    QTMIN    QTMAX
      0          0         1000      -0       -20000
CC
CC  ID,INJ. RATE AND INJ. COMP. FOR RATE CONS. WELLS FOR EACH PHASE (L=1,3)
*----  ID     QI(M,L)     C(M,KC,L)
      1      0.0   0.0   0.0    0.0   0.0    0.0  0.0  0.0  0.0   0.0
      1      0.0   0.0   0.0    0.0   0.0    0.0  0.0  0.0  0.0   0.0
      1      0.0   0.0   0.0    0.0   0.0    0.0  0.0  0.0  0.0   0.0
      1      100   0.0   0.0    0.0   0.0    0.0  0.0  0.0  1.0   0.0
CC
CC
```

```
*--- ID, INJ. TEMP (F)
    1    90.
CC
CC
*----  ID    PWF
    2      2000
CC
CC CUM. INJ. TIME , AND INTERVALS (PV OR DAY) FOR WRITING TO OUTPUT FILES
*---- TINJ     CUMPR1     CUMHI1     WRHPV     WRPRF      RSTC
     25      5*0.5
CC
CC THE INI. TIME STEP,CONC. TOLERANCE,MAX.,MIN. TIME STEPS
*----  DT     DELC(I)             CNMAX             CNMIN
  0.0001       9*0.005          0.005              0.00001
CC
CC FLAG FOR INDICATING BOUNDARY CHANGE
*---- IBMOD
       0
CC
CC IRO, ITIME, NEW FLAGS FOR ALL THE WELLS ( WATER INJ.)
*---- IRO   ITIME  IFLAG
     2       0   1   2
CC
CC NUMBER OF WELLS CHANGES IN LOCATION OR SKIN OR PWF
*----NWEL1
    0
CC
CC NUMBER OF WELLS WITH RATE CHANGES, ID
*----NWEL1   ID
    2       1    2
CC
CC  ID,INJ. RATE AND INJ. COMP. FOR RATE CONS. WELLS FOR EACH PHASE (L=1,3)
*----  ID     QI(M,L)     C(M,KC,L)
      1      50.    0.99    0.0    0.01   0.0    0.6  0.0  0.0  0.0   0.0
      1      0.0    0.0     0.0    0.0    0.0    0.0  0.0  0.0  0.0   0.0
      1      0.0    0.0     0.0    0.0    0.0    0.0  0.0  0.0  0.0   0.0
      1      0.0    0.0     0.0    0.0    0.0    0.0  0.0  0.0  0.0   0.0
CC
CC
*--- ID, INJ. TEMP (F)
    1    90.
CC
CC
*----  ID    PWF
    2      2000
CC
CC CUM. INJ. TIME , AND INTERVALS (PV OR DAY) FOR WRITING TO OUTPUT FILES
*---- TINJ     CUMPR1     CUMHI1     WRHPV     WRPRF      RSTC
     75      5*0.5
CC
CC THE INI. TIME STEP,CONC. TOLERANCE,MAX.,MIN. TIME STEPS
*----  DT     DELC(I)             CNMAX             CNMIN
  0.0001       9*0.005          0.005              0.00001
CC
CC FLAG FOR INDICATING BOUNDARY CHANGE
*---- IBMOD
       0
CC
CC IRO, ITIME, NEW FLAGS FOR ALL THE WELLS ( WATER INJ.)
*---- IRO   ITIME  IFLAG
     2       0   1   2
CC
CC NUMBER OF WELLS CHANGES IN LOCATION OR SKIN OR PWF
*----NWEL1
    0
CC
CC NUMBER OF WELLS WITH RATE CHANGES, ID
*----NWEL1   ID
    2       1    2
CC
CC  ID,INJ. RATE AND INJ. COMP. FOR RATE CONS. WELLS FOR EACH PHASE (L=1,3)
*----  ID     QI(M,L)     C(M,KC,L)
      1    50.   0.99   0.0   0.01  0.0  0.6  0.0  0.0  0.0   0.0
      1    0.0    0.0   0.0   0.0   0.0  0.0  0.0  0.0  0.0   0.0
      1    0.0    0.0   0.0   0.0   0.0  0.0  0.0  0.0  0.0   0.0
      1    100    0.0   0.0   0.0   0.0  0.0  0.0  0.0  1.0   0.0
CC
```

```
CC
*--- ID, INJ. TEMP (F)
    1    90
CC
CC
*----  ID    PWF
    2     2000
CC
CC CUM. INJ. TIME , AND INTERVALS (PV OR DAY) FOR WRITING TO OUTPUT FILES
*---- TINJ     CUMPR1     CUMHI1     WRHPV     WRPRF      RSTC
    150      5*0.5
CC
CC THE INI. TIME STEP,CONC. TOLERANCE,MAX.,MIN. TIME STEPS
*----  DT     DELC(I)              CNMAX             CNMIN
  0.0001       9*0.005         0.005              0.00001
```

PVT

```
CC NUMBER OF DATA SET FOR CASE6
CC
14
CC SARURATED          SOLUTION GAS    OIL FVF         GAS FVF               OIL_VISCOSITY       GAS_VISCOSITY
CC PRESSURE(PSI)       RS(SCF/STB)    BO(RB/STB)      BG(RB/SCF)                 (CP)             (CP)
100                    165                    1.012        0.005900053            1.17          0.013
800                    335                    1.0255       0.002950027            1.14          0.0135
1200                   500                    1.038        0.001960016            1.11          0.014
1600                   665                    1.051        0.001470005            1.08          0.0145
2000                   828                    1.063        0.001179997            1.06          0.015
2400                   985                    1.075        0.000980008            1.03          0.0155
2800                   1130                   1.087        0.000839983            1             0.016
3200                   1270                   1.0985       0.000739973            0.98          0.0165
3600                   1390                   1.11         0.000649984            0.95          0.017
4000                   1500                   1.12         0.000590005            0.942         0.0175
4400                   1600                   1.13         0.000539986            0.92          0.018
4800                   1676                   1.14         0.000490004            0.91          0.0185
5200                   1750                   1.148        0.000450005            0.9           0.019
5600                   1810                   1.155        0.000419992            0.89          0.0195
CC  SURFACE GAS DENISTY     SURFACE OIL DENISITY    BUBBLE POINT PRESSURE
CC     PSI                      PSI              PSI
       0.0004                0.225             4000
CC UNDERSATURATED PROPERTY SLOP FOR OIL FORMATION VOLUME FACTOR(DEL_BO/DEL_P) AND OIL VISCOSITY(DEL_VIS/DEL_P)
CC     VIOSLOP        BOSLOP
  0.00001      -0.00023
```

A.7 THREE DIMENSIONAL HOT WATER INJECTION CASE

The following are the input data files for UTCHEM and CMG-STARS simulators. We used this case in Chapter 7 for thermal model validation and comparison between both simulators.

CMG-STARS INPUT

```
** ************************************************************************
** CMG-STARS                                    **
** ************************************************************************
** ************************************************************************************************                                    **
** **
** MODEL: 3D MODEL HOT WATER INJECTION                    **                          **
** **
** **
** ************************************************************************************
** ==============  INPUT/OUTPUT CONTROL  ======================
RESULTS SIMULATOR STARS 200900


*INTERRUPT *STOP

*TITLE1 'HOTWATER '
*TITLE2 ' HOT WATER FLOOD'
*TITLE3 ' HOT WATER FLOOD '

*INUNIT  *FIELD   ** OUTPUT SAME AS INPUT

*OUTPRN *GRID ALL
*OUTPRN *WELL *ALL


*OUTSRF *GRID  ALL

**$ ************************************************************************
**$ DEFINITION OF FUNDAMENTAL CARTESIAN GRID
**$ ************************************************************************
GRID CART 20 20 5
KDIR DOWN


DI CON  10
DJ CON  10
DK CON 10

NULL CON          1
POR CON 0.2
PERMI CON 100
PERMJ EQUALSI
PERMK CON 10

*END-GRID
ROCKTYPE 1

*CPOR 5E-9
*PRPOR 75
*ROCKCP 40
*THCONR 28
*THCONW 38
*THCONO 32
*THCONG 32


** ==============  FLUID DEFINITIONS  ======================
```

```
*MODEL 2 2 2   ** COMPONENTS ARE WATER AND DEAD OIL.  MOST WATER
           ** PROPERTIES ARE DEFAULTED (=0).  DEAD OIL K VALUES
           ** ARE ZERO, AND NO GAS PROPERTIES ARE NEEDED.

*COMPNAME       'WATER'    'OIL'
**              -----    -------
    *CMM         18.02      600
    *PCRIT       3206.2      0       ** THESE FOUR PROPERTIES
    *TCRIT       705.4       0       ** ARE FOR THE GAS PHASE.
    *AVG         1.13E-5     0       ** THE DEAD OIL COMPONENT DOES
    *BVG         1.075       0       ** NOT APPEAR IN THE GAS PHASE.

    *MOLDEN      0        0.10113
    *CP          0        5.E-6
    *CT1         0        3.8E-4

    *CPL1        0        300

*VISCTABLE

**      TEMP
    60       1      1
    90       1      1
   200       1      1
   300       1      1
   400       1      1
   500       1      1
   600       1      1

*PRSR 14.7
*TEMR 60
*PSURF 14.7
*TSURF 60


** ==============  ROCK-FLUID PROPERTIES  ======================


*ROCKFLUID

*SWT   **  WATER-OIL RELATIVE PERMEABILITIES

**   SW         KRW        KROW
** ------     -------     -------
     0.0        0.0        1.0
     1.0        1.0        0.0

*SLT   **  LIQUID-GAS RELATIVE PERMEABILITIES

**   SL       KRG      KROG      PCOG
** ------    -------  -------   -------
     0.0        1.0        0.0
     1.0        0.0        1.0


** ==============  INITIAL CONDITIONS  ======================


*INITIAL

** AUTOMATIC STATIC VERTICAL EQUILIBRIUM
*VERTICAL *DEPTH_AVE
*REFPRES 2000
*REFBLOCK 1 1 1

*TEMP *CON 90
*PRES *CON 200
*SW *CON 0.3
*SO *CON 0.7


** ==============  NUMERICAL CONTROL  ======================
```

```
*NUMERICAL   ** ALL THESE CAN BE DEFAULTED.  THE DEFINITIONS
** HERE MATCH THE PREVIOUS DATA.
NORM PRESS 500
SATUR 0.2
TEMP 50
*DTMAX 1

*RUN
**  ==============  RECURRENT DATA  ======================

** PROJECT STARTS ON JULY 27, 2011

*TIME        0
DTWELL 0.01
WELL  'INJECTOR'  VERT  1  1  FRAC  1.
INJECTOR MOBWEIGHT 'INJECTOR'
INCOMP  WATER  1.  0.
*TINJW 300
*OPERATE  MAX  STW  35.62  CONT
**$         RAD  GEOFAC  WFRAC  SKIN
GEOMETRY  K  0.28  0.235  1.  0.
PERF  GEO  'INJECTOR'
**$ UBA    FF  STATUS  CONNECTION
   1 1 1:5  1.  OPEN    FLOW-FROM  'SURFACE'  REFLAYER



WELL  'PRODUCER'  VERT  10  1  FRAC  1.
*PRODUCER 'PRODUCER'
*OPERATE  *BHP 1900
**OPERATE *MAX *STEAM  .5    ** STEAM CWE IN BBL/DAY
**$ UBA    FF  STATUS  CONNECTION
**$         RAD  GEOFAC  WFRAC  SKIN
GEOMETRY  K  0.28  0.235  1.  0.
PERF  GEO  'PRODUCER'
**$ UBA     FF  STATUS  CONNECTION
   20  20  1:5  1.  OPEN    FLOW-TO  'SURFACE'  REFLAYER

*TIME        5
*TIME        10

*TIME        750

*TIME        800

*STOP
```

UTCHEM INPUT

```
CC*************************************************************************
CC                                                                       *
CC    BRIEF DESCRIPTION OF DATA SET : UTCHEM (VERSION 2013_1)      *
CC                                                                       *
CC*************************************************************************
CC                                                                       *
CC  HOT WATER   FLOODING                              *
CC                                                                       *
CC  LENGTH (FT) :                 PROCESS : HOT WATER FLOODING       *
CC  THICKNESS (FT) :               INJ. PRESSURE (PSI) :          *
CC  WIDTH (FT) : .               COORDINATES : CARTESIAN        *
CC  POROSITY :                                          *
CC  GRID BLOCKS :                                     *
CC  DATE :   FEB 2014                                            *
CC                                                                       *
CC*************************************************************************
CC
CC*************************************************************************
CC                                                                       *
CC    RESERVOIR DESCRIPTION                           *
CC                                                                       *
CC*************************************************************************
CC
CC
```

```
*---- RUNNO
ELECH
CC
CC
*----HEADER
ELECH
HOT WATER FLOODING
************************************************************
CC
CC SIMULATION FLAGS
*---- IMODE IMES IDISPC ICWM ICAP IREACT IBIO ICOORD ITREAC ITC  IGAS  IENG IHEATW IELECHV IELECHI  ISTEAM  IGMAS
      1    3     0     0    0     0     0     1     0     0    0     1     1      1    1    0    0    1
CC
CC NUMBER OF GRID BLOCKS AND FLAG SPECIFIES CONSTANT OR VARIABLE GRID SIZE
*---- NX    NY    NZ  IDXYZ  IUNIT
     20  20    5     0      0
CC
CC  CONSTANT GRID BLOCK SIZE IN X, Y, AND Z
*---- DX         DY          DZ
    10         10          10
CC
CC TOTAL NO. OF COMPONENTS, NO. OF TRACERS, NO. OF GEL COMPONENTS
*----N   no NTw nta ngc  ng  noth
   5    0 0   0 0    0    0
CC
CC
*---- SPNAME(I),I=1,N
WATER
OIL
SURFACTANT
POLYMER
ANION
CC
CC FLAG INDICATING IF THE COMPONENT IS INCLUDED IN CALCULATIONS OR NOT
*----ICF(KC) FOR KC=1,N
   1  1  1  1  1
CC
CC*********************************************************************
CC                                                   *
CC    OUTPUT OPTIONS                                          *
CC                                                   *
CC*********************************************************************
CC
CC
CC FLAG TO WRITE TO UNIT 3,FLAG FOR PV OR DAYS TO PRINT OR TO STOP THE RUN
*---- ICUMTM  ISTOP  IOUTGMS      IS3G
      0      0       2        2
CC
CC FLAG INDICATING IF THE PROFILE OF KCTH COMPONENT SHOULD BE WRITTEN
*---- IPRFLG(KC),KC=1,N
      1  1  1 1 1
CC
CC FLAG FOR PRES.,SAT.,TOTAL CONC.,TRACER CONC.,CAP.,GEL, ALKALINE PROFILES
*---- IPPRES IPSAT IPCTOT IPBIO IPCAP IPGEL IPALK IPTEMP IPOBS
      1      1      1      0     0     0     1     1      0
CC
CC FLAG FOR WRITING SEVERAL PROPERTIES TO UNIT 4 (Prof)
*---- ICKL IVIS IPER ICNM ICSE IHYSTP IFOAMP INONEQ
     1    1    1    1    1    1    0    0  0
CC
CC FLAG FOR WRITING SEVERAL PROPERTIES TO PROF
*---- IADS IVEL IRKF IPHSE
     1    1    1    1
CC
CC*********************************************************************
CC                                                   *
CC    RESERVOIR PROPERTIES                                        *
CC                                                   *
CC*********************************************************************
CC
CC
CC MAX. SIMULATION TIME ( DAYS)
*---- TMAX
    805
CC
CC ROCK COMPRESSIBILITY (1/PSI), STAND. PRESSURE(PSIA)
*---- COMPR               PSTAND
```

```
      0                0
CC
CC FLAGS INDICATION CONSTANT OR VARIABLE POROSITY, X,Y,AND Z PERMEABILITY
*----IPOR1 IPERMX IPERMY IPERMZ  IMOD  ITRNZ   INTG
     0     0    3     3     0    0      0
CC
CC CONSTANT POROSITY FOR WHOLE RESERVOIR
*---- PORC1
     0.2
CC
CC CONSTANT X-PERMEABILITY (MILIDARCY) FOR LAYER K = 1,NZ
*----PERMX
    100
CC
CC Y DIRECTION PERMEABILITY IS DEPENDENT ON X DIRECTION PERMEABILITY
*---- CONSTANT PERMEABILITY MULTIPLIER FOR Y DIRECTION PERMEABILITY
      1
CC
CC Z DIRECTION PERMEABILITY IS DEPENDENT ON X DIRECTION PERMEABILITY
*---- CONSTANT PERMEABILITY MULTIPLIER FOR Z DIRECTION PERMEABILITY
      0.1
CC
CC FLAG FOR CONSTANT OR VARIABLE DEPTH, PRESSURE, WATER SATURATION,INITIAL AQUEOUS PHASE cOMPOSITIONS
*----IDEPTH  IPRESS  ISWI  ICWI
     0      0     0    -1
CC
CC CONSTANT DEPTH (FT)
*---- D111
     0
CC
CC INITIAL PRESSURE (PSIA)
*----PINIT   DEPTH
    2000  0.0
CC
CC CONSTANT INITIAL WATER SATURATION (residual oil)
*---- SWI
     0.3
CC
CC BRINE SALINITY AND DIVALENT CATION CONCENTRATION (MEQ/ML)
*---- C50       C60
     0.3    0.00
CC
CC*********************************************************************
CC                                          *
CC    PHYSICAL PROPERTY DATA                          *
CC                                          *
CC*********************************************************************
CC
CC
CC OIL CONC. AT PLAIT POINT FOR TYPE II(+)AND TYPE II(-), CMC
*---- c2plc  c2prc   epsme   ihand
      0     1     0.00001     0
CC
CC 3.4.2 flag indicating type of phase behavior parameters
*---- ifghbn=0 for input height of binodal curve; =1 for input sol. ratio
      0
CC SLOPE AND INTERCEPT OF BINODAL CURVE AT ZERO, OPT., AND 2XOPT SALINITY
CC FOR ALCOHOL 1
*---- hbns70   hbnc70   hbns71   hbnc71   hbns72   hbnc72
      0    0.05       0     0.03     0     0.05
CC
CC SLOPE OF BINODAL WITH TEMP., SLOPE OF SALINITY WITH TEMP. (1/F)
*---- HBNT0     HBNT1    HBNT2    CSET(0.00415)
     0.00017  0.00017  0.00017   0.00415
CC SLOPE AND INTERCEPT OF BINODAL CURVE AT ZERO, OPT., AND 2XOPT SALINITY
CC FOR ALCOHOL 2
*---- hbns80  hbnc80  hbns81  hbnc81  hbns82  hbnc82
      0       0       0       0       0       0
CC
CC LOWER AND UPPER EFFECTIVE SALINITY FOR ALCOHOL 1 AND ALCOHOL 2
*---- csel7   cseu7   csel8   cseu8
     0.33    0.53     0       0
CC
CC THE CSE SLOPE PARAMETER FOR CALCIUM AND ALCOHOL 1 AND ALCOHOL 2
*---- beta6    beta7    beta8
      0.       0       0
CC
```

```
CC FLAG FOR ALCOHOL PART. MODEL AND PARTITION COEFFICIENTS
*---- ialc   opsk7o   opsk7s   opsk8o   opsk8s
       1      0        0        0        0
CC
CC NO. OF ITERATIONS, AND TOLERANCE
*---- nalmax     epsalc
       20       0.0001
CC 3.4.10 ALCOHOL 1 PARTITIONING PARAMETERS IF IALC=1
CC   aq-oleic   aq-oleic  surf-oleic
*---- akwc7     akws7    akm7     ak7      pt7
      4.671    1.79      48     35.31    0.222
CC
CC ALCOHOL 2 PARTITIONING PARAMETERS IF IALC=1
*---- akwc8     akws8    akm8    ak8     pt8
       0         0        0      0       0
CC
CC 3.4.22 ift model flag
*----  ift=0 for Healy&Reed; =1 for Chun Huh correl.
       1
CC 3.4.24 INTERFACIAL TENSION PARAMETERS
CC    typ=.1-.35   typ=5-20
*---- chuh      ahuh
     0.35       10
CC
CC LOG10 OF OIL/WATER INTERFACIAL TENSION
*---- xiftw
      1.3
CC
CC ORGANIC MASS TRANSFER FLAG
*---- imass icor
                 0    0
cc
cc
*--- iwalt  iwalf
       0       0
CC
CC CAPILLARY DESATURATION PARAMETERS FOR PHASE 1, 2, AND 3
*---- itrap       t11       t22       t33
       0         300     1000     300
CC
CC  RELATIVE PERM  and pc model
*----IPERM      IRTYPE
     0          0
CC
CC FLAG FOR CONSTANT OR VARIABLE REL. PERM. PARAMETERS
*---- isrw    iprw    iew
       0      0       0
CC
CC CONSTANT RES. SATURATION OF PHASES 1,2,AND 3 AT LOW CAPILLARY NO.
*---- s1rwc    s2rwc     s3rwc
      0.0      0.0      0.0
CC
CC CONSTANT ENDPOINT REL. PERM. OF PHASES 1,2,AND 3 AT LOW CAPILLARY NO.
*---- p1rwc     p2rwc    p3rwc
      1        1       1
CC
CC CONSTANT REL. PERM. EXPONENT OF PHASES 1,2,AND 3 AT LOW CAPILLARY NO.
*---- e1wc     e2wc     e3wc
      1        1        1.0
CC
CC WATER AND OIL VISCOSITY , RESERVOIR TEMPERATURE
*---- VIS1    VIS2   TSTAND
      1       1      60
CC
CC VISCOSITY-TEMP PARAMETERS
*----BVI(1)  BVI(2)
    0    0
CC
CC COMPOSITIONAL PHASE VISCOSITY PARAMETERS
*----   ALPHAV1   ALPHAV2   ALPHAV3   ALPHAV4  ALPHAV5
         0         0         0         0         1.7
CC
CC PARAMETERS TO CALCULATE POLYMER VISCOSITY AT ZERO SHEAR RATE
*---- AP1       AP2       AP3
      10.21      17.77     626.14
CC
CC PARAMETER TO COMPUTE CSEP,MIN. CSEP, AND SLOPE OF LOG VIS. VS. LOG CSEP
```

```
*---- BETAP    CSE1     SSLOPE
      20      0.01     -0.6
CC
CC PARAMETER FOR SHEAR RATE DEPENDENCE OF POLYMER VISCOSITY
*---- GAMMAC   GAMHF   POWN       IPMOD   ishear  rweff GAMHF2
      4       56.1     1.643               0       0      0.25   0
CC
CC CC FLAG FOR POLYMER PARTITIONING, PERM. REDUCTION PARAMETERS
*---- IPOLYM    EPHI3    EPHI4    BRK     CRK                      RKCUT
       1         1        1       1000    0.0186                   10
CC
CC SPECIFIC WEIGHT FOR COMPONENTS 1,2,3,7,8 ,Coeffient of oil and GRAVITY FLAG
*---- DEN1     DEN2    DEN23     DEN3    DEN7    DEN8    IDEN
     0.433     0.415     0.26     0.433     0.39    0       2
CC
CC FLAG FOR CHOICE OF UNITS ( 0:BOTTOMHOLE CONDITION , 1: STOCK TANK)
*----- ISTB
       0
CC
CC COMPRESSIBILITY FOR VOL. OCCUPYING COMPONENTS 1,2,3,7,AND 8
*---- COMPC(1)  COMPC(2)  COMPC(3)  COMPC(7)  COMPC(8)
       0.000001         0.00001          0          0          0
CC
CC CONSTANT OR VARIABLE PC PARAM., WATER-WET OR OIL-WET PC CURVE FLAG
*---- ICPC    IEPC   IOW
      0       0      0
CC
CC CAPILLARY PRESSURE PARAMETER, CPC0
*---- CPC0
      0
CC
CC CAPILLARY PRESSURE PARAMETER, EPC0
*---- EPC0
      2
CC
CC MOLECULAR DIFFUSION COEF. KCTH COMPONENT IN PHASE 1
*---- D(KC,1),KC=1,N
       0       0       0       0       0       0       0       0       0       0       0       0       0
CC
CC MOLECULAR DIFFUSION COEF. KCTH COMPONENT IN PHASE 2
*---- D(KC,2),KC=1,N
       0       0       0       0       0       0       0       0       0       0       0       0       0
CC
CC MOLECULAR DIFFUSION COEF. KCTH COMPONENT IN PHASE 3
*---- D(KC,3),KC=1,N
       0       0       0       0       0       0       0       0       0       0       0       0       0
CC
CC LONGITUDINAL AND TRANSVERSE DISPERSIVITY OF PHASE 1
*---- ALPHAL(1)     ALPHAT(1)
       0.0           0.000
CC
CC LONGITUDINAL AND TRANSVERSE DISPERSIVITY OF PHASE 2
*---- ALPHAL(2)     ALPHAT(2)
       0.0           0.000
CC
CC LONGITUDINAL AND TRANSVERSE DISPERSIVITY OF PHASE 3
*---- ALPHAL(3)     ALPHAT(3)
       0.0           0.000
CC
CC flag to specify organic adsorption calculation
*---- iadso
       0
CC
CC SURFACTANT AND POLYMER ADSORPTION PARAMETERS
*---- AD31    AD32   B3D    AD41   AD42   B4D   IADK  IADS1   FADS   REFK
     1.5      0.5    1000    9.5     0     100     0     0      0      0
CC
CC PARAMETERS FOR CATION EXCHANGE OF CLAY AND SURFACTANT
*---- QV      XKC     XKS     EQW
     0.00    0.      0.      450
CC
CC INITIAL TEMPERATURE
*--- TEMPI (F)
    90
CC
CC INITIAL VOLTAGE
*--- VOLTAGEI
```

```
    0.0
CC
CC TABLE OF TEMPERATURS(1:NTABL)(F or C)
*--- TEM_TABL
   90  150  200
CC
CC TABLE OF ELECTRICAL CONDUCTIVITIES FOR WATER (1:NTABL)
*--- CONDW
    0.10   0.10   0.10
CC
CC TABLE OF ELECTRICAL CONDUCTIVITIES FOR OIL (1:NTABL)
*--- CONDO
    0.01  0.01  0.01
CC
CC TABLE OF ELECTRICAL CONDUCTIVITIES FOR ROCK (1:NTABL)
*--- CONDR
    0.1   0.1   0.1
CC
CC ROCK DENSITY,CONDUCTIVITY,HEAT CAPACITY
*---- DENS   CTCR  CTCL(1:NPHASE) CVSPR   CVSPL(1:NPHASE)
     165.43  28  38   32  32   0.242   1  0.5  0.6
CC
CC HEATLOSS FLAG, ANALYTICAL SOLUTION Analytical should be checked
*---- IHLOS  IANAL
      0    0
CC
CC*********************************************************************
CC                                                  *
CC    WELL DATA                                           *
CC                                                  *
CC*********************************************************************
CC
CC
CC FLAG FOR SPECIFIED BOUNDARY AND ZONE IS MODELED
*---- IBOUND     IZONE
      0      0
CC
CC TOTAL NUMBER OF WELLS, WELL RADIUS FLAG, FLAG FOR TIME OR COURANT NO.
*---- NWELL   IRO    ITIME    NWREL
      2      2       0        2
CC
CC WELL ID,LOCATIONS,AND FLAG FOR SPECIFYING WELL TYPE, WELL RADIUS, SKIN
*---- IDW    IW    JW    IFLAG    RW     SWELL   IDIR   IFIRST   ILAST   IPRF
     1     1     1       1      1       0       3      1      5   0
CC
CC WELL NAME
*----  WELNAM
INJ1
CC
CC ICHEK , MAX. AND MIN. ALLOWABLE BOTTOMHOLE PRESSURE AND RATE
*---- ICHEK     PWFMIN     PWFMAX    QTMIN    QTMAX
      0          0         10000      0        20000
CC
CC WELL ID,LOCATIONS,AND FLAG FOR SPECIFYING WELL TYPE, WELL RADIUS, SKIN
*---- IDW    IW    JW    IFLAG    RW     SWELL   IDIR   IFIRST   ILAST   IPRF
     2     20    20       2      1       0       3      1   5       0
CC
CC WELL NAME
*----  WELNAM
PROD1
CC
CC ICHEK , MAX. AND MIN. ALLOWABLE BOTTOMHOLE PRESSURE AND RATE
*---- ICHEK     PWFMIN     PWFMAX    QTMIN    QTMAX
      0          0         1000      -0       -20000
CC
CC  ID,INJ. RATE AND INJ. COMP. FOR RATE CONS. WELLS FOR EACH PHASE (L=1,3)
*----  ID     QI(M,L)     C(M,KC,L)
      1     200       1.0      0.0      0.0       0.0    0.0
      1      0.0       0.0      0.0      0.0       0.0    0.0
      1      0.0       0.0      0.0      0.0       0.0    0.0
CC
CC
*--- ID, INJ. TEMP (F)   STEAM QUALITY
    1   300      0.0
CC
CC HEATENERGY  WELL FLAG(OFF=0 or ON=1)
*--- ID   IBOUNDQ
```

```
    1    0
CC
CC VOLTAGE WELL FLAG(OFF=0 or ON=1)
*--- ID   IBOUNDV
    1    0
CC
CC ELE CURR  WELL FLAG(OFF=0 or ON=1)
*--- ID   IBOUNDI
    1    0
CC
CC ID, BOTTOM HOLE PRESSURE FOR PRESSURE CONSTRAINT WELL (IFLAG=2 OR 3)
*---- ID    PWF
   2      1900
CC
CC HEATENERGY  WELL FLAG(OFF=0 or ON=1)
*--- ID   IBOUNDQ
    2    0
CC
CC VOLTAGE WELL FLAG(OFF=0 or ON=1)
*--- ID   IBOUNDV
    2    0
CC
CC ELE CURR  WELL FLAG(OFF=0 or ON=1)
*--- ID   IBOUNDI
   2    0
CC
CC CUM. INJ. TIME , AND INTERVALS (PV OR DAY) FOR WRITING TO OUTPUT FILES
*---- TINJ     CUMPR1     CUMHI1     WRHPV     WRPRF      RSTC
      805      10          10        10        10         10
CC
CC THE INI. TIME STEP,CONC. TOLERANCE,MAX.,MIN. time steps
*----  DT     DELC(I)             CNMAX            CNMIN
  .001        5*0.01          0.21              0.0001
```

A.8 TWO DIMENSIONAL VERTICAL STEAM INJECTION CASE (SAGD)

The following are the input data files for UTCHEM and CMG-STARS simulators. We used this case in Chapter 7 for thermal model validation and comparison between both simulators.

CMG-STARS INPUT

```
** ***************************************************************************************
** **
** FILE :  SD1.DAT                                          **
** **
** MODEL:  COMPARISON CASE WITH UTCHEM       **
**                        **
** VERTICAL SECTION XZ                                  **
** **
** **
** USAGE: COMPARE TO UTCHEM SOLUTION              **
** ***************************************************************************************
** ==============  INPUT/OUTPUT CONTROL  ======================
** 2014-07-27, 9:54:57 PM, HAMID

RESULTS SIMULATOR STARS 200900


*INTERRUPT *STOP

*TITLE1 'WAS STARS TEST BED NO. 7'
*TITLE2 ' MODIFIED FOR LINEAR SD BY EDR'
*TITLE3 ' STEAM FLOOD WITH DEAD OIL'

*INUNIT  *FIELD   ** OUTPUT SAME AS INPUT

*OUTPRN *GRID *ALL
*OUTPRN *WELL *ALL
*WRST 300
*WPRN *GRID 300
*WPRN *ITER 300
OUTSRF GRID ALL
OUTSRF SPECIAL MATBAL  WELL 'OIL'
           OBHLOSS
           OBHLOSSRATE
           BLOCKVAR SG 1,1,1
           BLOCKVAR TEMP 1,1,1
           BLOCKVAR SO 1,1,1
           BLOCKVAR PRES 1,1,1
           BLOCKVAR QUALBLK 1,1,1
           BLOCKVAR STEAMQUAL 1,1,1
           TFRONT 140 9:1,1,1
           TFRONT 300 9:1,1,1
           TFRONT 350 9:1,1,1
           TFRONT 400 9:1,1,1
           WELLENERGY  'INJECTOR' RATE
           WELLENERGY  'INJECTOR' CUM
           WELLENERGY  'PRODUCER' RATE
           WELLENERGY  'PRODUCER' CUM
           PRODSTEAMR  'PRODUCER'
           STMQUAL 'INJECTOR'
           OSR 'PRODUCER' 'INJECTOR' INST
           OSR 'PRODUCER' 'INJECTOR' CUM
           PHWELL 'INJECTOR' PRES DOWNHOLE
           PHWELL 'INJECTOR' TEMP DOWNHOLE

OUTSRF WELL LAYER ALL
**WPRN SECTOR 1
**WSRF SECTOR 1
**$  DISTANCE UNITS: FT
```

```
RESULTS XOFFSET          0.0000
RESULTS YOFFSET          0.0000
RESULTS ROTATION          0.0000  **$  (DEGREES)
RESULTS AXES-DIRECTIONS 1.0 -1.0 1.0
**$ *****************************************************************************
**$ DEFINITION OF FUNDAMENTAL CARTESIAN GRID
**$ *****************************************************************************
GRID CART 30 1 50
KDIR DOWN
**NINEPOINT IJ
DI IVAR
  30*10
DJ JVAR
  30
DK KVAR
50*5
**$ PROPERTY: NULL BLOCKS  MAX: 1  MIN: 1
**$  0 = NULL BLOCK, 1 = ACTIVE BLOCK
NULL CON            1
POR CON 0.3
PERMI CON 1000
PERMJ EQUALSI
PERMK EQUALSI / 10
**$ PROPERTY: PINCHOUT ARRAY  MAX: 1  MIN: 1
**$  0 = PINCHED BLOCK, 1 = ACTIVE BLOCK
**PINCHOUTARRAY CON            1

*END-GRID
ROCKTYPE 1

*CPOR 5E-4
*PRPOR 75
*ROCKCP 33.71
*THCONR 100
*THCONW 100
*THCONO 100
*THCONG 100
*HLOSSPROP  *OVERBUR 0 0  *UNDERBUR 0 0



** ==============  FLUID DEFINITIONS  ======================


*MODEL 2 2 2   ** COMPONENTS ARE WATER AND DEAD OIL.  MOST WATER
           ** PROPERTIES ARE DEFAULTED (=0).  DEAD OIL K VALUES
           ** ARE ZERO, AND NO GAS PROPERTIES ARE NEEDED.

*COMPNAME       'WATER'     'OIL'
**              -----     -------
    *CMM        18.02      600
    *PCRIT      3206.2      0       ** THESE FOUR PROPERTIES
    *TCRIT      705.4       0       ** ARE FOR THE GAS PHASE.
    *AVG        1.13E-5     0       ** THE DEAD OIL COMPONENT DOES
    *BVG        1.075       0       ** NOT APPEAR IN THE GAS PHASE.

    *MOLDEN     0        0.10113
    *CP         0        5.E-6
    *CT1        0        3.8E-4

    *CPL1       0        300

*VISCTABLE

**      TEMP
        60     0      5000
       110     0      1093
       350     0      8
       400     0      7


*PRSR 14.7
*TEMR 60
*PSURF 14.7
*TSURF 60
```

```
** ============== ROCK-FLUID PROPERTIES ======================


*ROCKFLUID
RPT 1 WATWET

*SWT   **  WATER-OIL RELATIVE PERMEABILITIES
**   SW       KRW       KROW
**  ----    --------   -------        ** SG = 0 BY DEFAULT
0.0000       0.0000       0.9000
0.0500       0.0009       0.8040
0.1000       0.0040       0.7138
0.1500       0.0093       0.6295
0.2000       0.0170       0.5509
0.2500       0.0272       0.4779
0.3000       0.0399       0.4106
0.3500       0.0551       0.3489
0.4000       0.0730       0.2925
0.4500       0.0935       0.2416
0.5000       0.1166       0.1959
0.5500       0.1425       0.1553
0.6000       0.1710       0.1199
0.6500       0.2023       0.0894
0.7000       0.2364       0.0637
0.7500       0.2733       0.0426
0.8000       0.3129       0.0261
0.8500       0.3554       0.0139
0.9000       0.4008       0.0057
0.9500       0.4489       0.0012
1.0000       0.5000       0.0000


*SLT   **  LIQUID-GAS RELATIVE PERMEABILITIES

**   SL       KRG        KROG
**  ----    -------    -------
0.000        0.800        0.000
0.100        0.634        0.008
0.250        0.425        0.054
0.300        0.365        0.080
0.350        0.310        0.110
0.400        0.260        0.146
0.450        0.215        0.187
0.500        0.174        0.233
0.550        0.138        0.285
0.600        0.107        0.342
0.650        0.079        0.405
0.700        0.057        0.473
0.750        0.038        0.547
0.800        0.023        0.626
0.850        0.012        0.711
0.900        0.005        0.802
0.950        0.001        0.898
1.000        0.000        0.9


** ============== INITIAL CONDITIONS ======================


*INITIAL

** AUTOMATIC STATIC VERTICAL EQUILIBRIUM
**VERTICAL *DEPTH_AVE
**REFPRES 75
**REFBLOCK 1 1 1

*TEMP *CON 110
*PRES *CON 147
*SW *CON 0.4
*SO *CON 0.6


** ============== NUMERICAL CONTROL ======================


*NUMERICAL   ** ALL THESE CAN BE DEFAULTED.  THE DEFINITIONS
```

```
** HERE MATCH THE PREVIOUS DATA.
NORM PRESS 250
SATUR 0.5
TEMP 200


*RUN


** ============== RECURRENT DATA ======================


** PROJECT STARTS ON JULY 27, 2011
*TIME 0
DTWELL 0.01

WELL  'INJECTOR'  VERT  15  1  FRAC  1.
WELL  'PRODUCER'  VERT  15  1  FRAC  1.
INJECTOR MOBWEIGHT 'INJECTOR'
INCOMP  WATER  1.  0.
*TINJW 450
QUAL 0.7
OPERATE  MAX  STW  17.9  CONT
**OPERATE  MAX  BHP  1000.  CONT
**$          RAD  GEOFAC  WFRAC  SKIN
GEOMETRY  K  0.28  0.235  1.  0.
PERF  GEO  'INJECTOR'
**$ UBA     FF  STATUS  CONNECTION
   15 1 20  1.  OPEN    FLOW-FROM  'SURFACE'  REFLAYER

*PRODUCER 'PRODUCER'
*OPERATE  *BHP 100

**$          RAD  GEOFAC  WFRAC  SKIN
GEOMETRY  K  0.28  0.235  1.  0.
PERF  GEO  'PRODUCER'
**$ UBA     FF  STATUS  CONNECTION
   15 1 35  1.  OPEN    FLOW-TO  'SURFACE'  REFLAYER

*TIME        1
*TIME        10
*TIME        19
*TIME        2611
*TIME        2845
*TIME        2854
*TIME        2863
*TIME        2872
*TIME        2881
*TIME        2890
*TIME        2899
*TIME        2908
*TIME        2917
*TIME        2926
*TIME        2935
*TIME        2944
*TIME        2953
*TIME        2962
*TIME        2971
*TIME        2980
*TIME        2989
*TIME        2998
*TIME        3000
*STOP
```

UTCHEM INPUT

```
CC*****************************************************************
CC                                                               *
CC    BRIEF DESCRIPTION OF DATA SET : UTCHEM (VERSION 2011_1)      *
CC                                                               *
CC*****************************************************************
CC                                                               *
CC  STEAM FLOODING IN VERTICAL SECTION                 *
CC                                                               *
CC  LENGTH (FT) :                 PROCESS : SAGD        *
CC  THICKNESS (FT) :               INJ. PRESSURE (PSI) :          *
```

```
CC  WIDTH (FT) : .              COORDINATES : CARTESIAN         *
CC  POROSITY :                                          *
CC  GRID BLOCKS :                                       *
CC  DATE :   FEB 2014                                           *
CC                                                      *
CC*****************************************************************
CC
CC*****************************************************************
CC                                                      *
CC    RESERVOIR DESCRIPTION                                 *
CC                                                      *
CC*****************************************************************
CC
CC
*---- RUNNO
ELECH
CC
CC
*----HEADER
ELECH
SAGD OR STEAM FLODDING
**********************************************************
CC
CC SIMULATION FLAGS
*---- IMODE IMES IDISPC ICWM ICAP IREACT IBIO ICOORD ITREAC ITC  IGAS  IENG IHEATW IELECHV IELECHI  ISTEAM
      1   3    0    0   0    0    0    1     0    0   1    1    0      0   0 1
CC
CC NUMBER OF GRID BLOCKS AND FLAG SPECIFIES CONSTANT OR VARIABLE GRID SIZE
*---- NX    NY    NZ  IDXYZ  IUNIT
     31     1    50     0      0
CC
CC  CONSTANT GRID BLOCK SIZE IN X, Y, AND Z
*---- DX        DY         DZ
     10      30         5
CC
CC TOTAL NO. OF COMPONENTS, NO. OF TRACERS, NO. OF GEL COMPONENTS
*----N   NO NTW NTA NGC  NG  NOTH
    9   0 0   0 0    0    0
CC
CC
*---- SPNAME(I),I=1,N
WATER
OIL
SURFACTANT
POLYMER
ANION
CATION
ALCOHOL
GAS
TRACER
CC
CC FLAG INDICATING IF THE COMPONENT IS INCLUDED IN CALCULATIONS OR NOT
*----ICF(KC) FOR KC=1,N
   1  1  1  0  0  0  0  1  0
CC
CC*****************************************************************
CC                                                      *
CC    OUTPUT OPTIONS                                        *
CC                                                      *
CC*****************************************************************
CC
CC
CC FLAG TO WRITE TO UNIT 3,FLAG FOR PV OR DAYS TO PRINT OR TO STOP THE RUN
*---- ICUMTM  ISTOP  IOUTGMS      IS3G
      0      0       2        2
CC
CC FLAG INDICATING IF THE PROFILE OF KCTH COMPONENT SHOULD BE WRITTEN
*---- IPRFLG(KC),KC=1,N
      1  1  1 1   0  0  0  1  0
CC
CC FLAG FOR PRES.,SAT.,TOTAL CONC.,TRACER CONC.,CAP.,GEL, ALKALINE PROFILES
*---- IPPRES IPSAT IPCTOT IPBIO IPCAP IPGEL IPALK IPTEMP IPOBS
      1      1      1      0     0     0     1     1      0
CC
CC FLAG FOR WRITING SEVERAL PROPERTIES TO UNIT 4 (PROF)
*---- ICKL IVIS IPER ICNM ICSE IHYSTP IFOAMP INONEQ
     1    1    1    1    1    1    0    0   0
```

```
CC
CC FLAG FOR WRITING SEVERAL PROPERTIES TO PROF
*---- IADS IVEL IRKF IPHSE
      1    1    1    1
CC
CC*********************************************************************
CC                                                  *
CC    RESERVOIR PROPERTIES                                  *
CC                                                  *
CC*********************************************************************
CC
CC
CC MAX. SIMULATION TIME ( DAYS)
*---- TMAX
    3000
CC
CC ROCK COMPRESSIBILITY (1/PSI), STAND. PRESSURE(PSIA)
*---- COMPR               PSTAND
      0                 200
CC
CC FLAGS INDICATION CONSTANT OR VARIABLE POROSITY, X,Y,AND Z PERMEABILITY
*----IPOR1 IPERMX IPERMY IPERMZ  IMOD  ITRNZ   INTG
      0      0     3      3      0     0       0
CC
CC CONSTANT POROSITY FOR WHOLE RESERVOIR
*---- PORC1
      0.32
CC
CC CONSTANT X-PERMEABILITY (MILIDARCY) FOR LAYER K = 1,NZ
*----PERMX
    1000
CC
CC Y DIRECTION PERMEABILITY IS DEPENDENT ON X DIRECTION PERMEABILITY
*---- CONSTANT PERMEABILITY MULTIPLIER FOR Y DIRECTION PERMEABILITY
       1
CC
CC Z DIRECTION PERMEABILITY IS DEPENDENT ON X DIRECTION PERMEABILITY
*---- CONSTANT PERMEABILITY MULTIPLIER FOR Z DIRECTION PERMEABILITY
       0.1
CC
CC FLAG FOR CONSTANT OR VARIABLE DEPTH, PRESSURE, WATER SATURATION,INITIAL AQUEOUS PHASE COMPOSITIONS
*----IDEPTH  IPRESS  ISWI  ICWI
      0       0      0     -1
CC
CC CONSTANT DEPTH (FT)
*---- D111
      0
CC
CC INITIAL PRESSURE (PSIA)
*----PINIT   DEPTH
    100.  0.0
CC
CC CONSTANT INITIAL WATER SATURATION (RESIDUAL OIL)
*---- SWI
    0.4
CC
CC FLAG INDICATING TYPE OF INITIAL GAS SATURATION
*---ISGI
   0
CC
CC CONSTANT INITIAL GAS SATURATION FOR WHOLE RESERVOIR
*---- SGI
     0.0
CC
CC BRINE SALINITY AND DIVALENT CATION CONCENTRATION (MEQ/ML)
*---- C50       C60
      0.3    0.00
CC
CC*********************************************************************
CC                                                  *
CC    PHYSICAL PROPERTY DATA                                *
CC                                                  *
CC*********************************************************************
CC
CC
CC OIL CONC. AT PLAIT POINT FOR TYPE II(+)AND TYPE II(-), CMC
*---- C2PLC  C2PRC   EPSME   IHAND
```

```
      0     1     0.00001     0
CC
CC 3.4.2 FLAG INDICATING TYPE OF PHASE BEHAVIOR PARAMETERS
*---- IFGHBN=0 FOR INPUT HEIGHT OF BINODAL CURVE; =1 FOR INPUT SOL. RATIO
      0
CC SLOPE AND INTERCEPT OF BINODAL CURVE AT ZERO, OPT., AND 2XOPT SALINITY
CC FOR ALCOHOL 1
*---- HBNS70   HBNC70   HBNS71   HBNC71   HBNS72   HBNC72
      0    0.05       0     0.03     0     0.05
CC
CC SLOPE OF BINODAL WITH TEMP., SLOPE OF SALINITY WITH TEMP. (1/F)
*---- HBNT0     HBNT1    HBNT2    CSET(0.00415)
     0.00017  0.00017  0.00017   0.00415
CC SLOPE AND INTERCEPT OF BINODAL CURVE AT ZERO, OPT., AND 2XOPT SALINITY
CC FOR ALCOHOL 2
*---- HBNS80  HBNC80  HBNS81  HBNC81  HBNS82  HBNC82
      0       0       0       0       0       0
CC
CC LOWER AND UPPER EFFECTIVE SALINITY FOR ALCOHOL 1 AND ALCOHOL 2
*---- CSEL7   CSEU7   CSEL8   CSEU8
      0.33    0.53     0       0
CC
CC THE CSE SLOPE PARAMETER FOR CALCIUM AND ALCOHOL 1 AND ALCOHOL 2
*---- BETA6    BETA7    BETA8
       0.       0        0
CC
CC FLAG FOR ALCOHOL PART. MODEL AND PARTITION COEFFICIENTS
*---- IALC   OPSK7O   OPSK7S   OPSK8O   OPSK8S
       1      0        0        0        0
CC
CC NO. OF ITERATIONS, AND TOLERANCE
*---- NALMAX      EPSALC
       20        0.0001
CC 3.4.10 ALCOHOL 1 PARTITIONING PARAMETERS IF IALC=1
CC   AQ-OLEIC   AQ-OLEIC  SURF-OLEIC
*---- AKWC7     AKWS7    AKM7     AK7      PT7
      4.671    1.79      48     35.31    0.222
CC
CC ALCOHOL 2 PARTITIONING PARAMETERS IF IALC=1
*---- AKWC8     AKWS8    AKM8    AK8     PT8
       0         0        0      0       0
CC
CC 3.4.22 IFT MODEL FLAG
*----  IFT=0 FOR HEALY&REED; =1 FOR CHUN HUH CORREL.
       1
CC 3.4.24 INTERFACIAL TENSION PARAMETERS
CC    TYP=.1-.35   TYP=5-20
*---- CHUH     AHUH
     0.35        10
CC
CC LOG10 OF OIL/WATER INTERFACIAL TENSION
*---- XIFTW
      1.3
CC
CC ORGANIC MASS TRANSFER FLAG
*---- IMASS ICOR
                0    0
CC
CC
*--- IWALT  IWALF
       0       0
CC
CC CAPILLARY DESATURATION PARAMETERS FOR PHASE 1, 2, AND 3
*---- ITRAP      T11      T22      T33
       0        300    1000    300
CC
CC  RELATIVE PERM  AND PC MODEL
*----IPERM      IRTYPE
     0          0
CC
CC FLAG FOR CONSTANT OR VARIABLE REL. PERM. PARAMETERS
*---- ISRW    IPRW    IEW
       0      0       0
CC
CC CONSTANT RES. SATURATION OF PHASES 1,2,AND 3 AT LOW CAPILLARY NO.
*---- S1RWC    S2RWC     S3RWC
      0.1      0.20      0.0
```

```
CC
CC CONSTANT ENDPOINT REL. PERM. OF PHASES 1,2,AND 3 AT LOW CAPILLARY NO.
*---- P1RWC     P2RWC    P3RWC
     0.5      0.90      1
CC
CC CONSTANT REL. PERM. EXPONENT OF PHASES 1,2,AND 3 AT LOW CAPILLARY NO.
*---- E1WC     E2WC     E3WC
     2.1       2.2       1.0
CC
CC WATER AND OIL VISCOSITY , RESERVOIR TEMPERATURE
*---- VIS1     VIS2   TSTAND
    0.75      5000     60
CC
CC GAS VISCOSITY AT REF. TEMPERATURE AND PRESSURE,SLOPE OF GAS VISCOSITY
*---- VIS4      VSLOPG
     0.02   0
CC
CC VISCOSITY-TEMP PARAMETERS
*----BVI(1)  BVI(2)
   1    5000
CC
CC VISCOSITY-TEMP PARAMETERS
*----BVI(4)
   0
CC
CC CONSTANT RES. SAT. FOR OIL TO GAS AND GAS PHASE (FRACTION)
*---- S2RWC4
     0.18   0.0
CC
CC CONSTANT GAS ENDPOINT REL. PERM. (FRACTION
*----  S4RWC
     0.8
CC
CC CONSTANT REL. PERM. EXPONENT FOR GAS PHASE
*--- P4RWC
     1.2
CC
CC LOG OF INTERFACIAL TENSION BETWEEN GAS AND OIL (AND WATER)
*----  XIFTG   XIFTGW
     1.477    1.477
CC
CC COMPOSITIONAL PHASE VISCOSITY PARAMETERS
*----   ALPHAV1   ALPHAV2   ALPHAV3   ALPHAV4  ALPHAV5
        0         0         0         0         1.7
CC
CC PARAMETERS TO CALCULATE POLYMER VISCOSITY AT ZERO SHEAR RATE
*---- AP1       AP2      AP3
     10.21      17.77     626.14
CC
CC PARAMETER TO COMPUTE CSEP,MIN. CSEP, AND SLOPE OF LOG VIS. VS. LOG CSEP
*---- BETAP     CSE1      SSLOPE
     20       0.01      -0.6
CC
CC PARAMETER FOR SHEAR RATE DEPENDENCE OF POLYMER VISCOSITY
*---- GAMMAC   GAMHF   POWN       IPMOD   ISHEAR  RWEFF GAMHF2
     4       56.1      1.643               0       0      0.25   0
CC
CC CC FLAG FOR POLYMER PARTITIONING, PERM. REDUCTION PARAMETERS
*---- IPOLYM    EPHI3     EPHI4     BRK      CRK                       RKCUT
      1         1       1       1000    0.0186                          10
CC
CC SPECIFIC WEIGHT FOR COMPONENTS 1,2,3,7,8 ,COEFFIENT OF OIL AND GRAVITY FLAG
*---- DEN1      DEN2     DEN23     DEN3     DEN7     DEN8     IDEN
    0.43      0.375     0.36      0.40      0.39     0.005        2
CC
CC FLAG FOR CHOICE OF UNITS ( 0:BOTTOMHOLE CONDITION , 1: STOCK TANK)
*------ ISTB
      0
CC
CC COMPRESSIBILITY FOR VOL. OCCUPYING COMPONENTS 1,2,3,7,AND 8
*---- COMPC(1)  COMPC(2)  COMPC(3)  COMPC(7)  COMPC(8)
       0.000         0.0001          0       0    0.000
CC
CC CONSTANT OR VARIABLE PC PARAM., WATER-WET OR OIL-WET PC CURVE FLAG
*---- ICPC     IEPC    IOW
     0       0      0
CC
```

```
CC CAPILLARY PRESSURE PARAMETER, CPC0
*---- CPC0
     0
CC
CC CAPILLARY PRESSURE PARAMETER, EPC0
*---- EPC0
     2
CC
CC MOLECULAR DIFFUSION COEF. KCTH COMPONENT IN PHASE 1
*---- D(KC,1),KC=1,N
      0      0      0      0      0      0      0      0      0      0      0      0      0
CC
CC MOLECULAR DIFFUSION COEF. KCTH COMPONENT IN PHASE 2
*---- D(KC,2),KC=1,N
      0      0      0      0      0      0      0      0      0      0      0      0      0
CC
CC MOLECULAR DIFFUSION COEF. KCTH COMPONENT IN PHASE 3
*---- D(KC,3),KC=1,N
      0      0      0      0      0      0      0      0      0      0      0      0      0
CC
CC MOLECULAR DIFFUSION COEF. KCTH COMPONENT IN PHASE 4
*---- D(KC,3),KC=1,N
      0      0      0      0      0      0      0      0      0      0      0      0      0
CC
CC LONGITUDINAL AND TRANSVERSE DISPERSIVITY OF PHASE 1
*---- ALPHAL(1)     ALPHAT(1)
      0.0          0.000
CC
CC LONGITUDINAL AND TRANSVERSE DISPERSIVITY OF PHASE 2
*---- ALPHAL(2)     ALPHAT(2)
      0.0          0.000
CC
CC LONGITUDINAL AND TRANSVERSE DISPERSIVITY OF PHASE 3
*---- ALPHAL(3)     ALPHAT(3)
      0.0          0.000
CC
CC LONGITUDINAL AND TRANSVERSE DISPERSIVITY OF PHASE 4
*---- ALPHAL(3)     ALPHAT(3)
      0.0          0.000
CC
CC FLAG TO SPECIFY ORGANIC ADSORPTION CALCULATION
*---- IADSO
     0
CC
CC SURFACTANT AND POLYMER ADSORPTION PARAMETERS
*---- AD31    AD32   B3D    AD41   AD42   B4D   IADK  IADS1   FADS   REFK
    1.5      0.5    1000    9.5     0     100     0     0      0      0
CC
CC PARAMETERS FOR CATION EXCHANGE OF CLAY AND SURFACTANT
*---- QV      XKC     XKS     EQW
    0.00    0.     0.      450
CC
CC INITIAL TEMPERATURE
*--- TEMPI (F)
   110
CC
CC ROCK DENSITY,CONDUCTIVITY,HEAT CAPACITY
*---- DENS   CTCR  CTCL(1:NPHASE) CVSPR   CVSPL(1:NPHASE)
    165.43  25  25   25  25 25  0.21   1.07   0.5  0.5  0.6
CC
CC THERMAL EXPANTION OF COMPONENTS AND ROCK
*--- THEXP(1:N), THEXPR
  0.000   0.00  0.0  0.0  0.0  0.0 0.0 0.0 0.00  0.0000
CC
CC HEATLOSS FLAG, ANALYTICAL SOLUTION ANALYTICAL SHOULD BE CHECKED
*---- IHLOS  IANAL
     0     0
CC
CC*****************************************************************
CC                                                 *
CC    WELL DATA                                          *
CC                                                 *
CC*****************************************************************
CC
CC
CC FLAG FOR SPECIFIED BOUNDARY AND ZONE IS MODELED
*---- IBOUND     IZONE
```

```
      0      0
CC
CC TOTAL NUMBER OF WELLS, WELL RADIUS FLAG, FLAG FOR TIME OR COURANT NO.
*---- NWELL   IRO    ITIME    NWREL
      2      2       0        2
CC
CC WELL ID,LOCATIONS,AND FLAG FOR SPECIFYING WELL TYPE, WELL RADIUS, SKIN
*---- IDW    IW    JW    IFLAG    RW     SWELL   IDIR   IFIRST   ILAST   IPRF
     1     16     1       1      1       0       3      20     20     0
CC
CC WELL NAME
*----  WELNAM
INJ1
CC
CC ICHEK , MAX. AND MIN. ALLOWABLE BOTTOMHOLE PRESSURE AND RATE
*---- ICHEK     PWFMIN     PWFMAX    QTMIN    QTMAX
      0          0         10000      0        20000
CC
CC WELL ID,LOCATIONS,AND FLAG FOR SPECIFYING WELL TYPE, WELL RADIUS, SKIN
*---- IDW    IW    JW    IFLAG    RW     SWELL   IDIR   IFIRST   ILAST   IPRF
     2     16    1       2      1       0       3      35    35       0
CC
CC WELL NAME
*----  WELNAM
PROD1
CC
CC ICHEK , MAX. AND MIN. ALLOWABLE BOTTOMHOLE PRESSURE AND RATE
*---- ICHEK     PWFMIN     PWFMAX    QTMIN    QTMAX
      0          0         1000      -0        -20000
CC
CC  ID,INJ. RATE AND INJ. COMP. FOR RATE CONS. WELLS FOR EACH PHASE (L=1,3)
*----  ID     QI(M,L)     C(M,KC,L)
     1      100.0   1.0   0.0    0.0    0.0    0.0  0.0  0.0 0.0  0.0
     1      0.0   0.0   0.0    0.0    0.0    0.0  0.0  0.0 0.0  0.0
     1      0.0   0.0   0.0    0.0    0.0    0.0  0.0  0.0 0.0  0.0
     1      0.0   0   0.0    0.0    0.0    0.0  0.0  0.0 0.0  0.0
CC
CC
*--- ID, INJ. TEMP (F), STEAM QUALITY
    1  450.   0.65
CC
CC ID, BOTTOM HOLE PRESSURE FOR PRESSURE CONSTRAINT WELL (IFLAG=2 OR 3)
*----  ID    PWF
    2      100
CC
CC CUM. INJ. TIME , AND INTERVALS (PV OR DAY) FOR WRITING TO OUTPUT FILES
*---- TINJ     CUMPR1     CUMHI1     WRHPV     WRPRF      RSTC
      3000      10          10       10     10       10
CC
CC THE INI. TIME STEP,CONC. TOLERANCE,MAX.,MIN. TIME STEPS
*----  DT     DELC(I)              CNMAX             CNMIN
  0.01     9*0.01         0.1               0.0001
```

A.9 ELECTRICAL HEATING WITH FRACTURE CASE

The following are the input data files for UTCHEM simulator. We used this case in Chapter 8 for investigation of saturated fracture case in electrical heating process.

```
CC*************************************************************************
CC                                                                       *
CC    BRIEF DESCRIPTION OF DATA SET : UTCHEM (VERSION 2013_1)      *
CC                                                                       *
CC*************************************************************************
CC                                                                       *
CC  ELECTRICAL HEATING                                  *
CC                                                                       *
CC  LENGTH (FT) :                  PROCESS : ELECTRICAL HEATING *
CC  THICKNESS (FT) :                INJ. PRESSURE (PSI) :          *
CC  WIDTH (FT) :.                COORDINATES : CARTESIAN         *
CC  POROSITY :                                                  *
CC  GRID BLOCKS : *
CC  DATE :   FEB 2012                                                *
CC                                                                       *
CC*************************************************************************
CC
CC*************************************************************************
CC                                                                       *
CC    RESERVOIR DESCRIPTION                                 *
CC                                                                       *
CC*************************************************************************
CC
CC
*---- RUNNO
ELECH
CC
CC
*----HEADER
ELECH
2D WATER FLODDING  USING ELECTRICAL HEATING WITH UTCHEM2012_9
************************************************************
CC
CC SIMULATION FLAGS
*---- IMODE IMES IDISPC ICWM ICAP IREACT IBIO ICOORD ITREAC ITC  IGAS  IENG IHEATW IELECHV IELECHI ISTEAM
      1    3     0     0   0     0     0     1      0     0    1    1     0       1    0       0
CC
CC NUMBER OF GRID BLOCKS AND FLAG SPECIFIES CONSTANT OR VARIABLE GRID SIZE
*---- NX    NY    NZ  IDXYZ  IUNIT
     77    1    73     0      0
CC
CC  CONSTANT GRID BLOCK SIZE IN X, Y, AND Z
*---- DX        DY         DZ
     0.5389    10        0.5174
CC
CC TOTAL NO. OF COMPONENTS, NO. OF TRACERS, NO. OF GEL COMPONENTS
*----N   NO NTW NTA NGC  NG  NOTH
   9   0 0   0 0    0    0
CC
CC
*---- SPNAME(I),I=1,N
WATER
OIL
SURFACTANT
POLYMER
ANION
CATION
ALCOHOL
GAS
TRACER
CC
CC FLAG INDICATING IF THE COMPONENT IS INCLUDED IN CALCULATIONS OR NOT
```

```
*----ICF(KC) FOR KC=1,N
   1  1  1  0  0  0  0  1  0
CC
CC*********************************************************************
CC                                                  *
CC    OUTPUT OPTIONS                                        *
CC                                                  *
CC*********************************************************************
CC
CC
CC FLAG TO WRITE TO UNIT 3,FLAG FOR PV OR DAYS TO PRINT OR TO STOP THE RUN
*---- ICUMTM  ISTOP  IOUTGMS      IS3G
      0      0       2        1
CC
CC FLAG INDICATING IF THE PROFILE OF KCTH COMPONENT SHOULD BE WRITTEN
*---- IPRFLG(KC),KC=1,N
    1  1  1  0  0  0  0  1  0
CC
CC FLAG FOR PRES.,SAT.,TOTAL CONC.,TRACER CONC.,CAP.,GEL, ALKALINE PROFILES
*---- IPPRES IPSAT IPCTOT IPBIO IPCAP IPGEL IPALK IPTEMP IPOBS
      1      1      1      0     0     0     1     1      0
CC
CC FLAG FOR WRITING SEVERAL PROPERTIES TO UNIT 4 (PROF)
*---- ICKL IVIS IPER ICNM ICSE IHYSTP IFOAMP INONEQ
      1    1    1    1    1    1    0    0   0
CC
CC FLAG FOR WRITING SEVERAL PROPERTIES TO PROF
*---- IADS IVEL IRKF IPHSE
      1    1    1    1
CC
CC*********************************************************************
CC                                                  *
CC    RESERVOIR PROPERTIES                                      *
CC                                                  *
CC*********************************************************************
CC
CC
CC MAX. SIMULATION TIME ( DAYS)
*---- TMAX
     350
CC
CC ROCK COMPRESSIBILITY (1/PSI), STAND. PRESSURE(PSIA)
*---- COMPR               PSTAND
       0                 0
CC
CC FLAGS INDICATION CONSTANT OR VARIABLE POROSITY, X,Y,AND Z PERMEABILITY
*----IPOR1 IPERMX IPERMY IPERMZ  IMOD  ITRNZ   INTG
      2      2     3      3      0     0       0
CC
CC CONSTANT POROSITY FOR WHOLE RESERVOIR
*---- PORC1
    399*0.25  0.25  759*0.25 0.25  945*0.25 0.25  3515*0.25
CC
CC CONSTANT X-PERMEABILITY (MILIDARCY) FOR LAYER K = 1,NZ
*----PERMX
  5621*1000
CC
CC Y DIRECTION PERMEABILITY IS DEPENDENT ON X DIRECTION PERMEABILITY
*---- CONSTANT PERMEABILITY MULTIPLIER FOR Y DIRECTION PERMEABILITY
       1
CC
CC Z DIRECTION PERMEABILITY IS DEPENDENT ON X DIRECTION PERMEABILITY
*---- CONSTANT PERMEABILITY MULTIPLIER FOR Z DIRECTION PERMEABILITY
       0.1
CC
CC FLAG FOR CONSTANT OR VARIABLE DEPTH, PRESSURE, WATER SATURATION,INITIAL AQUEOUS PHASE COMPOSITIONS
*----IDEPTH  IPRESS  ISWI  ICWI
      0       0      2     -1
CC
CC CONSTANT DEPTH (FT)
*---- D111
      0
CC
CC INITIAL PRESSURE (PSIA)
*----PINIT   DEPTH
    250  0.0
CC
```

```
CC CONSTANT INITIAL WATER SATURATION (RESIDUAL OIL)
*---- SWI
1309*0.01               154*0.3
19*0.3                  39*0.3                  19*0.3
38*0.3                  0.3                     38*0.3
20*0.3                  2*1                     33*0.3                  2*1                     20*0.3
20*0.3                  2*1                     33*0.3                  2*1                     20*0.3
21*0.3                  2*1                     31*0.3                  2*1                     21*0.3
21*0.3                  2*1                     31*0.3                  2*1                     21*0.3
22*0.3                  2*1                     29*0.3                  2*1                     22*0.3
22*0.3                  2*1                     29*0.3                  2*1                     22*0.3
23*0.3                  2*1                     27*0.3                  2*1                     23*0.3
23*0.3                  2*1                     27*0.3                  2*1                     23*0.3
24*0.3                  2*1                     25*0.3                  2*1                     24*0.3
24*0.3                  2*1                     25*0.3                  2*1                     24*0.3
25*0.3                  2*1                     23*0.3                  2*1                     25*0.3
25*0.3                  2*1                     23*0.3                  2*1                     25*0.3
26*0.3                  2*1                     21*0.3                  2*1                     26*0.3
26*0.3                  2*1                     21*0.3                  2*1                     26*0.3
27*0.3                  2*1                     19*0.3                  2*1                     27*0.3
27*0.3                  2*1                     19*0.3                  2*1                     27*0.3
28*0.3                  2*1                     17*0.3                  2*1                     28*0.3
28*0.3                  2*1                     17*0.3                  2*1                     28*0.3
29*0.3                  2*1                     15*0.3                  2*1                     29*0.3
29*0.3                  2*1                     15*0.3                  2*1                     29*0.3
30*0.3                  2*1                     13*0.3                  2*1                     30*0.3
30*0.3                  2*1                     13*0.3                  2*1                     30*0.3
31*0.3                  2*1                     11*0.3                  2*1                     31*0.3
31*0.3                  2*1                     11*0.3                  2*1                     31*0.3
32*0.3                  2*1                     9*0.3                   2*1                     32*0.3
32*0.3                  2*1                     9*0.3                   2*1                     32*0.3
33*0.3                  2*1                     7*0.3                   2*1                     33*0.3
33*0.3                  2*1                     7*0.3                   2*1                     33*0.3
34*0.3                  2*1                     5*0.3                   2*1                     34*0.3
34*0.3                  2*1                     5*0.3                   2*1                     34*0.3
35*0.3                  2*1                     3*0.3                   2*1                     35*0.3
38*0.3                  0.3                     38*0.3
38*0.3                  0.3                     38*0.3
154*0.3                 1309*0.01   10000*1
CC
CC FLAG INDICATING TYPE OF INITIAL GAS SATURATION
*---ISGI
   0
CC
CC CONSTANT INITIAL GAS SATURATION FOR WHOLE RESERVOIR
*---- SGI
    0.0
CC
CC BRINE SALINITY AND DIVALENT CATION CONCENTRATION (MEQ/ML)
*---- C50       C60
     0.3    0.00
CC
CC*********************************************************************
CC                                          *
CC    PHYSICAL PROPERTY DATA                          *
CC                                          *
CC*********************************************************************
CC
CC
CC OIL CONC. AT PLAIT POINT FOR TYPE II(+)AND TYPE II(-), CMC
*---- C2PLC  C2PRC   EPSME   IHAND
      0     1     0.00001     0
CC
CC 3.4.2 FLAG INDICATING TYPE OF PHASE BEHAVIOR PARAMETERS
*---- IFGHBN=0 FOR INPUT HEIGHT OF BINODAL CURVE; =1 FOR INPUT SOL. RATIO
      0
CC SLOPE AND INTERCEPT OF BINODAL CURVE AT ZERO, OPT., AND 2XOPT SALINITY
CC FOR ALCOHOL 1
*---- HBNS70   HBNC70   HBNS71   HBNC71   HBNS72   HBNC72
      0    0.05       0     0.03     0     0.05
CC
CC SLOPE OF BINODAL WITH TEMP., SLOPE OF SALINITY WITH TEMP. (1/F)
*---- HBNT0     HBNT1     HBNT2     CSET(0.00415)
     0.00017  0.00017  0.00017   0.00415
CC SLOPE AND INTERCEPT OF BINODAL CURVE AT ZERO, OPT., AND 2XOPT SALINITY
CC FOR ALCOHOL 2
*---- HBNS80  HBNC80  HBNS81  HBNC81  HBNS82  HBNC82
```

```
      0       0       0       0       0       0
CC
CC LOWER AND UPPER EFFECTIVE SALINITY FOR ALCOHOL 1 AND ALCOHOL 2
*---- CSEL7   CSEU7   CSEL8   CSEU8
     0.33    0.53     0       0
CC
CC THE CSE SLOPE PARAMETER FOR CALCIUM AND ALCOHOL 1 AND ALCOHOL 2
*---- BETA6    BETA7    BETA8
      0.       0       0
CC
CC FLAG FOR ALCOHOL PART. MODEL AND PARTITION COEFFICIENTS
*---- IALC   OPSK7O   OPSK7S   OPSK8O   OPSK8S
      1      0        0        0        0
CC
CC NO. OF ITERATIONS, AND TOLERANCE
*---- NALMAX     EPSALC
      20       0.0001
CC 3.4.10 ALCOHOL 1 PARTITIONING PARAMETERS IF IALC=1
CC   AQ-OLEIC   AQ-OLEIC  SURF-OLEIC
*---- AKWC7     AKWS7    AKM7     AK7      PT7
     4.671    1.79      48     35.31    0.222
CC
CC ALCOHOL 2 PARTITIONING PARAMETERS IF IALC=1
*---- AKWC8     AKWS8    AKM8    AK8      PT8
      0         0        0      0        0
CC
CC 3.4.22 IFT MODEL FLAG
*----  IFT=0 FOR HEALY&REED; =1 FOR CHUN HUH CORREL.
      1
CC 3.4.24 INTERFACIAL TENSION PARAMETERS
CC    TYP=.1-.35   TYP=5-20
*---- CHUH     AHUH
    0.35       10
CC
CC LOG10 OF OIL/WATER INTERFACIAL TENSION
*---- XIFTW
     1.3
CC
CC ORGANIC MASS TRANSFER FLAG
*---- IMASS ICOR
                0    0
CC
CC
  *--- IWALT  IWALF
      0       0
CC
CC CAPILLARY DESATURATION PARAMETERS FOR PHASE 1, 2, AND 3
*---- ITRAP      T11      T22      T33
     0        300    1000    300
CC
CC  RELATIVE PERM  AND PC MODEL
*----IPERM      IRTYPE
    0          0
CC
CC FLAG FOR CONSTANT OR VARIABLE REL. PERM. PARAMETERS
*---- ISRW    IPRW    IEW
      0      0       0
CC
CC CONSTANT RES. SATURATION OF PHASES 1,2,AND 3 AT LOW CAPILLARY NO.
*---- S1RWC    S2RWC     S3RWC
     0.2      0.3      0.2
CC
CC CONSTANT ENDPOINT REL. PERM. OF PHASES 1,2,AND 3 AT LOW CAPILLARY NO.
*---- P1RWC     P2RWC    P3RWC
     .2       1      .2
CC
CC CONSTANT REL. PERM. EXPONENT OF PHASES 1,2,AND 3 AT LOW CAPILLARY NO.
*---- E1WC     E2WC     E3WC
     1.5       1.3       1.5
CC
CC WATER AND OIL VISCOSITY , RESERVOIR TEMPERATURE
*---- VIS1    VIS2   TSTAND
    1      5000     65
CC
CC GAS VISCOSITY AT REF. TEMPERATURE AND PRESSURE,SLOPE OF GAS VISCOSITY
*---- VIS4      VSLOPG
     0.02   0
```

```
CC
CC VISCOSITY-TEMP PARAMETERS
*----BVI(1)  BVI(2)
     1500    7500
CC
CC VISCOSITY-TEMP PARAMETERS
*----BVI(4)
    0
CC
CC CONSTANT RESIDUAL OIL/GAS SATURATION FOR ENTIRE RESERVOIR
*---- S2RWC4
      0.25  0.0
CC
CC CONSTANT RESIDUAL OIL/GAS SATURATION FOR ENTIRE RESERVOIR
*----  S4RWC
      1
CC
CC CONSTANT GAS ENDPOINT RELATIVE PERMEABILITY FOR ENTIRE RESERVOIR
*--- P4RWC
      1
CC
CC LOG OF INTERFACIAL TENSION BETWEEN GAS AND OIL (AND WATER)
*----  XIFTG   XIFTGW
      1.477    1.477
CC
CC COMPOSITIONAL PHASE VISCOSITY PARAMETERS
*----   ALPHAV1   ALPHAV2   ALPHAV3   ALPHAV4  ALPHAV5
        0         0         0         0         1.7
CC
CC PARAMETERS TO CALCULATE POLYMER VISCOSITY AT ZERO SHEAR RATE
*---- AP1       AP2       AP3
      10.21      17.77     626.14
CC
CC PARAMETER TO COMPUTE CSEP,MIN. CSEP, AND SLOPE OF LOG VIS. VS. LOG CSEP
*---- BETAP     CSE1      SSLOPE
      20       0.01      -0.6
CC
CC PARAMETER FOR SHEAR RATE DEPENDENCE OF POLYMER VISCOSITY
*---- GAMMAC   GAMHF   POWN       IPMOD   ISHEAR  RWEFF GAMHF2
      4       56.1      1.643               0       0      0.25   0
CC
CC CC FLAG FOR POLYMER PARTITIONING, PERM. REDUCTION PARAMETERS
*---- IPOLYM    EPHI3    EPHI4    BRK      CRK                      RKCUT
       1         1        1       1000    0.0186                   10
CC
CC SPECIFIC WEIGHT FOR COMPONENTS 1,2,3,7,8 ,COEFFIENT OF OIL AND GRAVITY FLAG
*---- DEN1      DEN2     DEN23      DEN3     DEN7     DEN8     IDEN
     0.45    0.40      0.26      0.433      0.39     0.005        2
CC
CC FLAG FOR CHOICE OF UNITS ( 0:BOTTOMHOLE CONDITION , 1: STOCK TANK)
*------ ISTB
       0
CC
CC COMPRESSIBILITY FOR VOL. OCCUPYING COMPONENTS 1,2,3,7,AND 8
*---- COMPC(1)  COMPC(2)  COMPC(3)  COMPC(7)  COMPC(8)
        0.001         0.0001          0       0    0.001
CC
CC CONSTANT OR VARIABLE PC PARAM., WATER-WET OR OIL-WET PC CURVE FLAG
*---- ICPC     IEPC    IOW
      0       0       0
CC
CC CAPILLARY PRESSURE PARAMETER, CPC0
*---- CPC0
      0
CC
CC CAPILLARY PRESSURE PARAMETER, EPC0
*---- EPC0
      2
CC
CC MOLECULAR DIFFUSION COEF. KCTH COMPONENT IN PHASE 1
*---- D(KC,1),KC=1,N
       0       0       0       0       0       0       0       0       0       0       0       0       0
CC
CC MOLECULAR DIFFUSION COEF. KCTH COMPONENT IN PHASE 2
*---- D(KC,2),KC=1,N
       0       0       0       0       0       0       0       0       0       0       0       0       0
CC
```

```
CC MOLECULAR DIFFUSION COEF. KCTH COMPONENT IN PHASE 3
*---- D(KC,3),KC=1,N
      0       0       0       0       0       0       0       0       0       0       0       0       0
CC
CC MOLECULAR DIFFUSION COEF. KCTH COMPONENT IN PHASE 4
*---- D(KC,3),KC=1,N
      0       0       0       0       0       0       0       0       0       0       0       0       0
CC
CC LONGITUDINAL AND TRANSVERSE DISPERSIVITY OF PHASE 1
*---- ALPHAL(1)     ALPHAT(1)
      0.0           0.000
CC
CC LONGITUDINAL AND TRANSVERSE DISPERSIVITY OF PHASE 2
*---- ALPHAL(2)     ALPHAT(2)
      0.0           0.000
CC
CC LONGITUDINAL AND TRANSVERSE DISPERSIVITY OF PHASE 3
*---- ALPHAL(3)     ALPHAT(3)
      0.0           0.000
CC
CC LONGITUDINAL AND TRANSVERSE DISPERSIVITY OF PHASE 4
*---- ALPHAL(3)     ALPHAT(3)
      0.0           0.000
CC
CC FLAG TO SPECIFY ORGANIC ADSORPTION CALCULATION
*---- IADSO
      0
CC
CC SURFACTANT AND POLYMER ADSORPTION PARAMETERS
*---- AD31    AD32   B3D    AD41   AD42   B4D   IADK  IADS1   FADS   REFK
     1.5      0.5    1000    9.5     0     100     0     0      0      0
CC
CC PARAMETERS FOR CATION EXCHANGE OF CLAY AND SURFACTANT
*---- QV      XKC     XKS     EQW
     0.00    0.      0.      450
CC
CC INITIAL TEMPERATURE
*--- TEMPI (F)
    80.0
CC
CC INITIAL VOLTAGE
*--- VOLTAGEI
    0.0
CC
CC TABLE OF TEMPERATURS(1:NTABL)(R)
*--- TEM_TABL
   80 150  600
CC
CC TABLE OF ELECTRICAL CONDUCTIVITIES FOR WATER (1:NTABL)
*--- CONDW
       2    6     7
CC
CC TABLE OF ELECTRICAL CONDUCTIVITIES FOR OIL (1:NTABL)
*--- CONDO
    0.01   0.05   0.09
CC
CC TABLE OF ELECTRICAL CONDUCTIVITIES FOR ROCK (1:NTABL)
*--- CONDR
    0.031  0.032  0.033
CC
CC ROCK DENSITY,CONDUCTIVITY,HEAT CAPACITY
*---- DENS       CRTC  CON(1)   CON(2)  CON(3)      CVSPR   CVSPL(1) CVSPL(2) CVSPL(3)  CVSPL(4)
    165.43     24     28       28      28   28      0.24      1      0.5      0.5       0.6
CC
CC  THERMAL EXPANTION OF COMPONENTS AND ROCK
*---  THEXP(1:N) THEXPR
 0.01   0.01  0.0  0.0  0.0  0.0 0.0 0.0 0.0 0.01  0.001
CC
CC HEATLOSS FLAG, ANALYTICAL SOLUTION ANALYTICAL SHOULD BE CHECKED
*---- IHLOS  IANAL
     1      1
CC
CC  HEAT LOSS
*---TCONO, DENO, CVSPO, TCONU, DENU, CVSPU
    0  145   0.   0  145 0.
CC
CC*********************************************************************
```

```
CC                                                  *
CC    WELL DATA                                          *
CC                                                  *
CC*****************************************************************
CC
CC
CC FLAG FOR SPECIFIED BOUNDARY AND ZONE IS MODELED
*---- IBOUND     IZONE
      0      0
CC
CC TOTAL NUMBER OF WELLS, WELL RADIUS FLAG, FLAG FOR TIME OR COURANT NO.
*---- NWELL   IRO    ITIME    NWREL
      3      2       0        3
CC
CC WELL ID,LOCATIONS,AND FLAG FOR SPECIFYING WELL TYPE, WELL RADIUS, SKIN
*---- IDW    IW    JW    IFLAG    RW     SWELL   IDIR   IFIRST   ILAST   IPRF
     1     39     1       2      1       0       3      54       54      0
CC
CC WELL NAME
*----  WELNAM
PROD3
CC
CC ICHEK , MAX. AND MIN. ALLOWABLE BOTTOMHOLE PRESSURE AND RATE
*---- ICHEK     PWFMIN     PWFMAX    QTMIN    QTMAX
      0          0         20000      0        200
CC
CC WELL ID,LOCATIONS,AND FLAG FOR SPECIFYING WELL TYPE, WELL RADIUS, SKIN
*---- IDW    IW    JW    IFLAG    RW     SWELL   IDIR   IFIRST   ILAST   IPRF
     2     20     1       2      1       0       3      20       20      0
CC
CC WELL NAME
*----  WELNAM
PROD1
CC
CC ICHEK , MAX. AND MIN. ALLOWABLE BOTTOMHOLE PRESSURE AND RATE
*---- ICHEK     PWFMIN     PWFMAX    QTMIN    QTMAX
      0          0         20000      0        200
CC
CC WELL ID,LOCATIONS,AND FLAG FOR SPECIFYING WELL TYPE, WELL RADIUS, SKIN
*---- IDW    IW    JW    IFLAG    RW     SWELL   IDIR   IFIRST   ILAST   IPRF
     3     58     1       2      1       0       3      20       20      0
CC
CC WELL NAME
*----  WELNAM
PROD2
CC
CC ICHEK , MAX. AND MIN. ALLOWABLE BOTTOMHOLE PRESSURE AND RATE
*---- ICHEK     PWFMIN     PWFMAX    QTMIN    QTMAX
      0          0         20000      0        0
CC
CC ID, BOTTOM HOLE PRESSURE FOR PRESSURE CONSTRAINT WELL (IFLAG=2 OR 3)
*----  ID    PWF
    1   -9999
CC
CC VOLTAGE WELL FLAG(OFF=0 OR ON=1)
*--- ID   IBOUNDV
     1    1
CC
CC
*--- ID,  VOLTAGE(VOL) PHASE,  FREQ(HZ)
    1    220    0     60
CC
CC ID, BOTTOM HOLE PRESSURE FOR PRESSURE CONSTRAINT WELL (IFLAG=2 OR 3)
*----  ID    PWF
    2   -9999
CC
CC VOLTAGE WELL FLAG(OFF=0 OR ON=1)
*--- ID   IBOUNDV
     2    1
CC
CC
*--- ID,  VOLTAGE(VOL) PHASE,  FREQ(HZ)
     2  220    120     60
CC
CC ID, BOTTOM HOLE PRESSURE FOR PRESSURE CONSTRAINT WELL (IFLAG=2 OR 3)
*----  ID    PWF
    3   -9999
```

```
CC
CC VOLTAGE WELL FLAG(OFF=0 OR ON=1)
*--- ID   IBOUNDV
     3    1
CC
CC
*--- ID,  VOLTAGE(VOL) PHASE,  FREQ(HZ)
     3   220    240      60
CC
CC CUM. INJ. TIME , AND INTERVALS (PV OR DAY) FOR WRITING TO OUTPUT FILES
*---- TINJ     CUMPR1     CUMHI1     WRHPV     WRPRF      RSTC
      50      0.5     0.5       0.5   0.5    0.5
CC
CC THE INI. TIME STEP,CONC. TOLERANCE,MAX.,MIN. TIME STEPS
*----  DT     DELC(I)             CNMAX            CNMIN
     0.1      9*0.5       0.5             0.001
CCCC
```

A.10 STEAM-FOAM-SURFACTANT CASE

The following are the input data files for UTCHEM simulator. We used this case in Chapter 9 for investigation of steam injection with surfactant and foam on oil recovery from heavy oil reservoirs.

```
 CC*********************************************************************
CC                                                *
CC    BRIEF DESCRIPTION OF DATA SET : UTCHEM (VERSION 2014_1)      *
CC                                                *
CC*********************************************************************
CC                                                *
CC  STEAM SURFACTANT FOAM   FLOODING                          *
CC                                                *
CC  LENGTH (FT) :                PROCESS : S/FOAM FLOODING       *
CC  THICKNESS (FT) :               INJ. PRESSURE (PSI) :          *
CC  WIDTH (FT) : .               COORDINATES : CARTESIAN        *
CC  POROSITY :                                    *
CC  GRID BLOCKS :                                  *
CC  DATE :   FEB 2014                                       *
CC                                                *
CC*********************************************************************
CC
CC*********************************************************************
CC                                                *
CC    RESERVOIR DESCRIPTION                          *
CC                                                *
CC*********************************************************************
CC
CC
*---- RUNNO
STEAM INJECTION
CC
CC
*----HEADER
ELECH
2D STEAM SOUTFACTANT FOAM FLODDING  CASE
************************************************************
CC
CC SIMULATION FLAGS
*---- IMODE IMES IDISPC ICWM ICAP IREACT IBIO ICOORD ITREAC ITC  IGAS  IENG IHEATW IELECHV IELECHI  ISTEAM
      1    3    0     0     0    0     0     1     0     0    2     1     1      0  0    1
CC
CC NUMBER OF GRID BLOCKS AND FLAG SPECIFIES CONSTANT OR VARIABLE GRID SIZE
*---- NX    NY    NZ  IDXYZ  IUNIT
     61     1    30     0      0
CC
CC  CONSTANT GRID BLOCK SIZE IN X, Y, AND Z
*---- DX        DY         DZ
     5         30         5
CC
CC TOTAL NO. OF COMPONENTS, NO. OF TRACERS, NO. OF GEL COMPONENTS
*----N   NO NTW NTA NGC  NG  NOTH
    9    0  0   0  0    0    0
CC
CC
*---- SPNAME(I),I=1,N
WATER
OIL
SURFACTANT
POLYMER
ANION
CATION
ALCOHOL
GAS
TRACER
CC
CC FLAG INDICATING IF THE COMPONENT IS INCLUDED IN CALCULATIONS OR NOT
*----ICF(KC) FOR KC=1,N
    1  1  1  0  1  0  0  1  0
```

```
CC
CC*********************************************************************
CC                                                  *
CC    OUTPUT OPTIONS                                          *
CC                                                  *
CC*********************************************************************
CC
CC
CC FLAG TO WRITE TO UNIT 3,FLAG FOR PV OR DAYS TO PRINT OR TO STOP THE RUN
*---- ICUMTM  ISTOP  IOUTGMS      IS3G
      0      0       2       1
CC
CC FLAG INDICATING IF THE PROFILE OF KCTH COMPONENT SHOULD BE WRITTEN
*---- IPRFLG(KC),KC=1,N
      1  1  1  0  1  0  0  1  0
CC
CC FLAG FOR PRES.,SAT.,TOTAL CONC.,TRACER CONC.,CAP.,GEL, ALKALINE PROFILES
*---- IPPRES IPSAT IPCTOT IPBIO IPCAP IPGEL IPALK IPTEMP IPOBS
      1      1      1      0     0     0     1     1      0
CC
CC FLAG FOR WRITING SEVERAL PROPERTIES TO UNIT 4 (PROF)
*---- ICKL IVIS IPER ICNM ICSE IHYSTP IFOAMP INONEQ
      1    1    1    1    1    1    0    0   0
CC
CC FLAG FOR WRITING SEVERAL PROPERTIES TO PROF
*---- IADS IVEL IRKF IPHSE
      1    1    1    1
CC
CC*********************************************************************
CC                                                  *
CC    RESERVOIR PROPERTIES                                    *
CC                                                  *
CC*********************************************************************
CC
CC
CC MAX. SIMULATION TIME ( DAYS)
*---- TMAX
     1000
CC
CC ROCK COMPRESSIBILITY (1/PSI), STAND. PRESSURE(PSIA)
*---- COMPR               PSTAND
      0.00001             200
CC
CC FLAGS INDICATION CONSTANT OR VARIABLE POROSITY, X,Y,AND Z PERMEABILITY
*----IPOR1 IPERMX IPERMY IPERMZ  IMOD  ITRNZ   INTG
      0      0     3      3      0     0       0
CC
CC CONSTANT POROSITY FOR WHOLE RESERVOIR
*---- PORC1
      0.2
CC
CC CONSTANT X-PERMEABILITY (MILIDARCY) FOR LAYER K = 1,NZ
*----PERMX
     2000
CC
CC Y DIRECTION PERMEABILITY IS DEPENDENT ON X DIRECTION PERMEABILITY
*---- CONSTANT PERMEABILITY MULTIPLIER FOR Y DIRECTION PERMEABILITY
       1
CC
CC Z DIRECTION PERMEABILITY IS DEPENDENT ON X DIRECTION PERMEABILITY
*---- CONSTANT PERMEABILITY MULTIPLIER FOR Z DIRECTION PERMEABILITY
      .3
CC
CC FLAG FOR CONSTANT OR VARIABLE DEPTH, PRESSURE, WATER SATURATION,INITIAL AQUEOUS PHASE COMPOSITIONS
*----IDEPTH  IPRESS  ISWI  ICWI
      0       0      0     -1
CC
CC CONSTANT DEPTH (FT)
*---- D111
      0
CC
CC INITIAL PRESSURE (PSIA)
*----PINIT   DEPTH
    100.     0.0
CC
CC CONSTANT INITIAL WATER SATURATION (RESIDUAL OIL)
*---- SWI
```

```
    0.4
CC
CC FLAG INDICATING TYPE OF INITIAL GAS SATURATION
*---ISGI
    0
CC
CC CONSTANT INITIAL GAS SATURATION FOR WHOLE RESERVOIR
*---- SGI
    0.0
CC
CC BRINE SALINITY AND DIVALENT CATION CONCENTRATION (MEQ/ML)
*---- C50       C60
    0.        0.
CC
CC*****************************************************************
CC                                          *
CC    PHYSICAL PROPERTY DATA                          *
CC                                          *
CC*****************************************************************
CC
CC
CC OIL CONC. AT PLAIT POINT FOR TYPE II(+)AND TYPE II(-), CMC
*---- C2PLC  C2PRC   EPSME   IHAND
      0     1     0.00001      0
CC
CC 3.4.2 FLAG INDICATING TYPE OF PHASE BEHAVIOR PARAMETERS
*---- IFGHBN=0 FOR INPUT HEIGHT OF BINODAL CURVE; =1 FOR INPUT SOL. RATIO
      0
CC SLOPE AND INTERCEPT OF BINODAL CURVE AT ZERO, OPT., AND 2XOPT SALINITY
CC FOR ALCOHOL 1
*---- HBNS70             HBNC70      HBNS71   HBNC71   HBNS72   HBNC72
    0        0.06   0       0.03     0        0.06
CC
CC SLOPE OF BINODAL WITH TEMP., SLOPE OF SALINITY WITH TEMP. (1/F)
*---- HBNT0     HBNT1     HBNT2     CSET(0.00415)
    0.0003    0.0003   0.0003    0.0145
CC SLOPE AND INTERCEPT OF BINODAL CURVE AT ZERO, OPT., AND 2XOPT SALINITY
CC FOR ALCOHOL 2
*---- HBNS80  HBNC80  HBNS81  HBNC81  HBNS82  HBNC82
      0       0       0       0       0       0
CC
CC LOWER AND UPPER EFFECTIVE SALINITY FOR ALCOHOL 1 AND ALCOHOL 2
*---- CSEL7   CSEU7   CSEL8   CSEU8
    0.5     0.75     0       0
CC
CC THE CSE SLOPE PARAMETER FOR CALCIUM AND ALCOHOL 1 AND ALCOHOL 2
*---- BETA6    BETA7    BETA8
      0.       0       0
CC
CC FLAG FOR ALCOHOL PART. MODEL AND PARTITION COEFFICIENTS
*---- IALC   OPSK7O   OPSK7S   OPSK8O   OPSK8S
      1      0        0        0        0
CC
CC NO. OF ITERATIONS, AND TOLERANCE
*---- NALMAX     EPSALC
       20       0.0001
CC 3.4.10 ALCOHOL 1 PARTITIONING PARAMETERS IF IALC=1
CC   AQ-OLEIC   AQ-OLEIC  SURF-OLEIC
*---- AKWC7     AKWS7    AKM7     AK7      PT7
      4.671    1.79      48     35.31    0.222
CC
CC ALCOHOL 2 PARTITIONING PARAMETERS IF IALC=1
*---- AKWC8     AKWS8    AKM8    AK8     PT8
      0         0        0      0       0
CC
CC 3.4.22 IFT MODEL FLAG
*----  IFT=0 FOR HEALY&REED; =1 FOR CHUN HUH CORREL.
       1
CC 3.4.24 INTERFACIAL TENSION PARAMETERS
CC    TYP=.1-.35   TYP=5-20
*---- CHUH     AHUH
    0.35       10
CC
CC LOG10 OF OIL/WATER INTERFACIAL TENSION
*---- XIFTW
      1.3
CC
```

```
CC ORGANIC MASS TRANSFER FLAG
*---- IMASS ICOR
      0       0
CC
CC
*--- IWALT  IWALF
      0       0
CC
CC CAPILLARY DESATURATION PARAMETERS FOR PHASE 1, 2, AND 3
*---- ITRAP      T11      T22      T33
      0        300    1000    300
CC
CC  RELATIVE PERM  AND PC MODEL
*----IPERM      IRTYPE
      0          0
CC
CC FLAG FOR CONSTANT OR VARIABLE REL. PERM. PARAMETERS
*---- ISRW    IPRW    IEW
      0      0       0
CC
CC CONSTANT RES. SATURATION OF PHASES 1,2,AND 3 AT LOW CAPILLARY NO.
*---- S1RWC    S2RWC     S3RWC
     0.3      0.3      0.3
CC
CC CONSTANT ENDPOINT REL. PERM. OF PHASES 1,2,AND 3 AT LOW CAPILLARY NO.
*---- P1RWC     P2RWC    P3RWC
     0.2      0.8     1
CC
CC CONSTANT REL. PERM. EXPONENT OF PHASES 1,2,AND 3 AT LOW CAPILLARY NO.
*---- E1WC     E2WC     E3WC
     3       2         1.
CC
CC WATER AND OIL VISCOSITY , RESERVOIR TEMPERATURE
*---- VIS1     VIS2   TSTAND
    0.75    4000   60
CC
CC GAS VISCOSITY AT REF. TEMPERATURE AND PRESSURE,SLOPE OF GAS VISCOSITY
*---- VIS4      VSLOPG
    0.01      0
CC
CC VISCOSITY-TEMP PARAMETERS
*----BVI(1)  BVI(2)
   1       5000
CC
CC VISCOSITY-TEMP PARAMETERS
*----BVI(4)
   0
CC
CC CONSTANT RES. SAT. FOR OIL TO GAS AND GAS PHASE (FRACTION)
*---- S2RWC4
    0.3     0.0
CC
CC CONSTANT GAS ENDPOINT REL. PERM. (FRACTION
*----  S4RWC
      1
CC
CC CONSTANT REL. PERM. EXPONENT FOR GAS PHASE
*--- P4RWC
     1.3
CC
CC LOG OF INTERFACIAL TENSION BETWEEN GAS AND OIL (AND WATER)
*----  XIFTG   XIFTGW
     1.477    1.477
CC
CC COMPOSITIONAL PHASE VISCOSITY PARAMETERS
*----   ALPHAV1   ALPHAV2   ALPHAV3   ALPHAV4  ALPHAV5
      0        0        0        0        1.7
CC
CC PARAMETERS TO CALCULATE POLYMER VISCOSITY AT ZERO SHEAR RATE
*---- AP1      AP2     AP3
    10.21    10      626.14
CC
CC PARAMETER TO COMPUTE CSEP,MIN. CSEP, AND SLOPE OF LOG VIS. VS. LOG CSEP
*---- BETAP    CSE1     SSLOPE
     20       0.01     -0.6
CC
CC PARAMETER FOR SHEAR RATE DEPENDENCE OF POLYMER VISCOSITY
```

```
*---- GAMMAC   GAMHF   POWN     IPMOD   ISHEAR   RWEFF    GAMHF2
     4        56.1    1.643 0       0        0.25     0
CC
CC CC FLAG FOR POLYMER PARTITIONING, PERM. REDUCTION PARAMETERS
*---- IPOLYM    EPHI3    EPHI4    BRK     CRK       RKCUT
      1         1        1       1000    0.0186     10
CC
CC SPECIFIC WEIGHT FOR COMPONENTS 1,2,3,7,8 ,COEFFIENT OF OIL AND GRAVITY FLAG
*---- DEN1     DEN2    DEN23     DEN3    DEN7    DEN8    IDEN
     0.5     0.4    0.5     0.40     0.39    0.05        2
CC
CC FLAG FOR CHOICE OF UNITS ( 0:BOTTOMHOLE CONDITION , 1: STOCK TANK)
*----- ISTB
       0
CC
CC COMPRESSIBILITY FOR VOL. OCCUPYING COMPONENTS 1,2,3,7,AND 8
*---- COMPC(1)  COMPC(2)  COMPC(3)      COMPC(7)  COMPC(8)
     0.00001   0.00001   0.000001      0         0.001
CC
CC CONSTANT OR VARIABLE PC PARAM., WATER-WET OR OIL-WET PC CURVE FLAG
*---- ICPC    IEPC   IOW
     0       0      0
CC
CC CAPILLARY PRESSURE PARAMETER, CPC0
*---- CPC0
     0
CC
CC CAPILLARY PRESSURE PARAMETER, EPC0
*---- EPC0
     2
CC
CC MOLECULAR DIFFUSION COEF. KCTH COMPONENT IN PHASE 1
*---- D(KC,1),KC=1,N
      0       0       0       0       0       0       0       0       0       0       0       0       0
CC
CC MOLECULAR DIFFUSION COEF. KCTH COMPONENT IN PHASE 2
*---- D(KC,2),KC=1,N
      0       0       0       0       0       0       0       0       0       0       0       0       0
CC
CC MOLECULAR DIFFUSION COEF. KCTH COMPONENT IN PHASE 3
*---- D(KC,3),KC=1,N
      0       0       0       0       0       0       0       0       0       0       0       0       0
CC
CC MOLECULAR DIFFUSION COEF. KCTH COMPONENT IN PHASE 4
*---- D(KC,3),KC=1,N
      0       0       0       0       0       0       0       0       0       0       0       0       0
CC
CC LONGITUDINAL AND TRANSVERSE DISPERSIVITY OF PHASE 1
*---- ALPHAL(1)     ALPHAT(1)
      0.0           0.000
CC
CC LONGITUDINAL AND TRANSVERSE DISPERSIVITY OF PHASE 2
*---- ALPHAL(2)     ALPHAT(2)
      0.0           0.000
CC
CC LONGITUDINAL AND TRANSVERSE DISPERSIVITY OF PHASE 3
*---- ALPHAL(3)     ALPHAT(3)
      0.0           0.000
CC
CC LONGITUDINAL AND TRANSVERSE DISPERSIVITY OF PHASE 4
*---- ALPHAL(3)     ALPHAT(3)
      0.0           0.000
CC
CC FLAG TO SPECIFY ORGANIC ADSORPTION CALCULATION
*---- IADSO
      0
CC
CC SURFACTANT AND POLYMER ADSORPTION PARAMETERS
*---- AD31    AD32   B3D    AD41   AD42   B4D   IADK  IADS1   FADS   REFK
     1.5     0.5    1000    9.5     0     100     0     0      0      0
CC
CC PARAMETERS FOR CATION EXCHANGE OF CLAY AND SURFACTANT
*---- QV      XKC     XKS     EQW
     0.00    0.      0.      450
CC
CC INITIAL TEMPERATURE
*--- TEMPI (F)
```

```
    100
CC
CC ROCK DENSITY,CONDUCTIVITY,HEAT CAPACITY
*---- DENS   CTCR  CTCL(1:NPHASE) CVSPR   CVSPL(1:NPHASE)
     165.43  50  50   50  50 50  0.21   1   0.5  0.5  0.6
CC
CC THERMAL EXPANTION OF COMPONENTS AND ROCK
*--- THEXP(1:N), THEXPR
   0.000   0.00  0.0  0.0  0.0  0.0 0.0 0.0 0.00  0.0000
CC
CC HEATLOSS FLAG, ANALYTICAL SOLUTION ANALYTICAL SHOULD BE CHECKED
*---- IHLOS  IANAL
      0     0
CC
CC
*---- RFMAX              SOSTAR     CSTAR    EPXLO    SHERTN               VELGR
     1000      0.4       0.0001    .02        1          1
CC
CC
*---- SWSATR
     1830*.35
CC
CC*********************************************************************
CC                                                  *
CC    WELL DATA                                           *
CC                                                  *
CC*********************************************************************
CC
CC
CC FLAG FOR SPECIFIED BOUNDARY AND ZONE IS MODELED
*---- IBOUND     IZONE
      0      0
CC
CC TOTAL NUMBER OF WELLS, WELL RADIUS FLAG, FLAG FOR TIME OR COURANT NO.
*---- NWELL   IRO    ITIME    NWREL
      4      2       0        4
CC
CC WELL ID,LOCATIONS,AND FLAG FOR SPECIFYING WELL TYPE, WELL RADIUS, SKIN
*---- IDW    IW    JW    IFLAG    RW     SWELL   IDIR   IFIRST   ILAST   IPRF
      1     31     1       1      1       0       3      10      20      0
CC
CC WELL NAME
*----  WELNAM
INJ1
CC
CC ICHEK , MAX. AND MIN. ALLOWABLE BOTTOMHOLE PRESSURE AND RATE
*---- ICHEK     PWFMIN     PWFMAX    QTMIN    QTMAX
      0          0         10000      0        20000
CC
CC WELL ID,LOCATIONS,AND FLAG FOR SPECIFYING WELL TYPE, WELL RADIUS, SKIN
*---- IDW    IW    JW    IFLAG    RW     SWELL   IDIR   IFIRST   ILAST   IPRF
      2     31     1       2      1       0       3      10       20       0
CC
CC WELL NAME
*----  WELNAM
PROD1
CC
CC ICHEK , MAX. AND MIN. ALLOWABLE BOTTOMHOLE PRESSURE AND RATE
*---- ICHEK     PWFMIN     PWFMAX    QTMIN    QTMAX
  0          0         1000      -0        -20000
CC
CC WELL ID,LOCATIONS,AND FLAG FOR SPECIFYING WELL TYPE, WELL RADIUS, SKIN
*---- IDW    IW    JW    IFLAG    RW     SWELL   IDIR   IFIRST   ILAST   IPRF
      3     1      1       2      1       0       3       1      30      0
CC
CC WELL NAME
*----  WELNAM
BOUND1
CC
CC ICHEK , MAX. AND MIN. ALLOWABLE BOTTOMHOLE PRESSURE AND RATE
*---- ICHEK     PWFMIN     PWFMAX    QTMIN    QTMAX
  0          0         1000      -0        -20000
CC
CC WELL ID,LOCATIONS,AND FLAG FOR SPECIFYING WELL TYPE, WELL RADIUS, SKIN
*---- IDW    IW    JW    IFLAG    RW     SWELL   IDIR   IFIRST   ILAST   IPRF
      4     61     1       2      1       0       3       1       30       0
CC
```

```
CC WELL NAME
*----  WELNAM
BOUND2
CC
CC ICHEK , MAX. AND MIN. ALLOWABLE BOTTOMHOLE PRESSURE AND RATE
*---- ICHEK     PWFMIN     PWFMAX    QTMIN    QTMAX
      0          0         1000      -0       -20000
CC
CC  ID,INJ. RATE AND INJ. COMP. FOR RATE CONS. WELLS FOR EACH PHASE (L=1,3)
*----  ID     QI(M,L)     C(M,KC,L)
      1      200    .99   0.0    0.01   0.0    0.3  0.0  0.0  0.0  0.0  0.0
      1      0.0    0.    0.0    0.0    0.0    0.0  0.0  0.0  0.0  0.0  0.0
      1      0.0    0.    0.0    0.0    0.0    0.0  0.0  0.0  0.0  0.0  0.0
      1      0.0    0     0.0    0.0    0.0    0.0  0.0  0.0  0.0  0.0  0.0
CC
CC
*--- ID, INJ. TEMP (F), STEAM QUALITY
      1    450   0.7
CC
CC
*---- ID,    IBOUNDQ
      1         1
CC
CC
*---- ID,    HEAT RATE
      1         5000
CC
CC ID, BOTTOM HOLE PRESSURE FOR PRESSURE CONSTRAINT WELL (IFLAG=2 OR 3)
*----  ID    PWF
      2      -9999
CC
CC
*---- ID,    IBOUNDQ
      2         0
CC
CC ID, BOTTOM HOLE PRESSURE FOR PRESSURE CONSTRAINT WELL (IFLAG=2 OR 3)
*----  ID    PWF
      3     150
CC
CC
*---- ID,    IBOUNDQ
      3         0
CC
CC ID, BOTTOM HOLE PRESSURE FOR PRESSURE CONSTRAINT WELL (IFLAG=2 OR 3)
*----  ID    PWF
      4     150
CC
CC
*---- ID,    IBOUNDQ
      4         0
CC
CC CUM. INJ. TIME , AND INTERVALS (PV OR DAY) FOR WRITING TO OUTPUT FILES
*---- TINJ      CUMPR1      CUMHI1      WRHPV      WRPRF       RSTC
      70        1           1      1    1       1
CC
CC THE INI. TIME STEP,CONC. TOLERANCE,MAX.,MIN. TIME STEPS
*----  DT         DELC(I)         CNMAX             CNMIN
      0.0001    9*0.01          0.01              0.0001
CCCCCCCCCCCCCCCCCCCCCCCCCCCCCCCCCCCCCC SOAKING CYCLE
1CCCCCCCCCCCCCCCCCCCC
```

```
 *----  ID     QI(M,L)     C(M,KC,L)
      1      0.0    0     0.0    0.00   0.0    0.0  0.0  0.0  0.0  0.0
      1      0.0    0.    0.0    0.0    0.0    0.0  0.0  0.0  0.0  0.0
      1      0.0    0.    0.0    0.0    0.0    0.0  0.0  0.0  0.0  0.0
      1      0.0    0     0.0    0.0    0.0    0.0  0.0  0.0  0.0  0.0
CC
CC
*--- ID, INJ. TEMP (F), STEAM QUALITY
     1    100.   0
CC
CC
*---- ID,    IBOUNDQ
     1        0
CC
CC ID, BOTTOM HOLE PRESSURE FOR PRESSURE CONSTRAINT WELL (IFLAG=2 OR 3)
*----  ID    PWF
     2     -999
CC
CC
*---- ID,    IBOUNDQ
     2        0
CC
CC ID, BOTTOM HOLE PRESSURE FOR PRESSURE CONSTRAINT WELL (IFLAG=2 OR 3)
*----  ID    PWF
     3     -999
CC
CC
*---- ID,    IBOUNDQ
     3        0
CC
CC ID, BOTTOM HOLE PRESSURE FOR PRESSURE CONSTRAINT WELL (IFLAG=2 OR 3)
*----  ID    PWF
     4      -999
CC
CC
*---- ID,    IBOUNDQ
     4        0
CC
CC CUM. INJ. TIME , AND INTERVALS (PV OR DAY) FOR WRITING TO OUTPUT FILES
*---- TINJ     CUMPR1     CUMHI1     WRHPV     WRPRF      RSTC
    100      2         2         2          2         100
CC
CC THE INI. TIME STEP,CONC. TOLERANCE,MAX.,MIN. TIME STEPS
*----  DT     DELC(I)             CNMAX            CNMIN
    0.0001    9*0.01         0.01             0.0001
CCCCCCCCCCCCCCCCCCCCCCCCCCCCCCCCCCCCCCCCCCCCCCCCCCCCCCC PRODUCTION CYCLE 1
CCCCCCCCCCCCCCCCCCCC
```

```
CC
CC ID, BOTTOM HOLE PRESSURE FOR PRESSURE CONSTRAINT WELL (IFLAG=2 OR 3)
*----  ID    PWF
     2     100
CC
CC
*---- ID,    IBOUNDQ
     2         1
CC
CC
*---- ID,    HEAT RATE
     2        5000
CC
CC ID, BOTTOM HOLE PRESSURE FOR PRESSURE CONSTRAINT WELL (IFLAG=2 OR 3)
 *----  ID     QI(M,L)     C(M,KC,L)
      3      1.0          1     0.0    0.00   0.0     0.0  0.0  0.0  0.0  0.0
      3      0.0          0.    0.0    0.0    0.0     0.0  0.0  0.0  0.0  0.0
      3      0.0          0.    0.0    0.0    0.0     0.0  0.0  0.0  0.0  0.0
      3      0.0          0     0.0    0.0    0.0     0.0  0.0  0.0  0.0  0.0
CC
CC ID, BOTTOM HOLE PRESSURE FOR PRESSURE CONSTRAINT WELL (IFLAG=2 OR 3)
*----  ID    PWF
     3     150
CC
CC
*--- ID, INJ. TEMP (F), STEAM QUALITY
     3    100.    0
CC
CC
*---- ID,    IBOUNDQ
     3         0
CC
CC ID, BOTTOM HOLE PRESSURE FOR PRESSURE CONSTRAINT WELL (IFLAG=2 OR 3)
 *----  ID     QI(M,L)     C(M,KC,L)
      4      1.0          1     0.0    0.0    0.0     0.0   0.0   0.0   0.0   0.0
      4      0.0          0.    0.0    0.0    0.0     0.0   0.0   0.0   0.0   0.0
      4      0.0          0.    0.0    0.0    0.0     0.0   0.0   0.0   0.0   0.0
      4      0.0          0     0.0    0.0    0.0     0.0   0.0   0.0   0.0   0.0
CC
CC ID, BOTTOM HOLE PRESSURE FOR PRESSURE CONSTRAINT WELL (IFLAG=2 OR 3)
*----  ID    PWF
     4      150
CC
CC
*--- ID, INJ. TEMP (F), STEAM QUALITY
     4      100.     0
CC
CC
*---- ID,    IBOUNDQ
     4         0
CC
CC CUM. INJ. TIME , AND INTERVALS (PV OR DAY) FOR WRITING TO OUTPUT FILES
*---- TINJ      CUMPR1      CUMHI1      WRHPV      WRPRF       RSTC
     350       2          2          2          2          100
CC
CC THE INI. TIME STEP,CONC. TOLERANCE,MAX.,MIN. TIME STEPS
*----  DT      DELC(I)              CNMAX             CNMIN
    0.0001    9*0.01         0.01              0.0001
CCCCCCCCCCCCCCCCCCCCCCCCCCCCCCCCCCCCCCCCCCCCCCCCCCCCC STEAM INJECTION CYCLE 2
CCCCCCCCCCCCCCCCCCCCCCCCCCCCCCCCCCCCCCCCCCCCCCCCCCCCC
CC FLAG FOR INDICATING BOUNDARY CHANGE
*---- IBMOD
      0
CC
CC IRO, ITIME, NEW FLAGS FOR ALL THE WELLS ( WATER INJ.)
*---- IRO   ITIME  IFLAG
     2      0      1   2  2  2
CC
CC NUMBER OF WELLS CHANGES IN LOCATION OR SKIN OR PWF
*----NWEL1
   0
CC
CC NUMBER OF WELLS WITH RATE CHANGES, ID
*----NWEL1   ID
    4       1    2   3   4
CC
CC  ID,INJ. RATE AND INJ. COMP. FOR RATE CONS. WELLS FOR EACH PHASE (L=1,3)
```

```
*----  ID     QI(M,L)     C(M,KC,L)
     1      200    .99   0.0    0.01   0.0    0.3  0.0  0.0  0.0  0.0
     1      0.0    0.    0.0    0.0    0.0    0.0  0.0  0.0  0.0  0.0
     1      0.0    0.    0.0    0.0    0.0    0.0  0.0  0.0  0.0  0.0
     1      0.0    0     0.0    0.0    0.0    0.0  0.0  0.0  0.0  0.0
CC
CC
*--- ID, INJ. TEMP (F), STEAM QUALITY
    1    450   0.7
CC
CC
*---- ID,    IBOUNDQ
     1        1
CC
CC
*---- ID,    HEAT RATE
     1       5000
CC
CC ID, BOTTOM HOLE PRESSURE FOR PRESSURE CONSTRAINT WELL (IFLAG=2 OR 3)
*----  ID    PWF
     2      -9999
CC
CC
*---- ID,    IBOUNDQ
     2        0
CC
CC ID, BOTTOM HOLE PRESSURE FOR PRESSURE CONSTRAINT WELL (IFLAG=2 OR 3)
*----  ID    PWF
     3     150
CC
CC
*---- ID,    IBOUNDQ
     3        0
CC
CC ID, BOTTOM HOLE PRESSURE FOR PRESSURE CONSTRAINT WELL (IFLAG=2 OR 3)
*----  ID    PWF
     4     150
CC
CC
*---- ID,    IBOUNDQ
     4        0
CC
CC CUM. INJ. TIME , AND INTERVALS (PV OR DAY) FOR WRITING TO OUTPUT FILES
*---- TINJ     CUMPR1      CUMHI1     WRHPV     WRPRF      RSTC
     420        1           1      1    1       1
CC
CC THE INI. TIME STEP,CONC. TOLERANCE,MAX.,MIN. TIME STEPS
*----  DT        DELC(I)        CNMAX            CNMIN
     0.0001    9*0.01         0.01             0.0001
CCCC
```

```
CC
CC
*---- ID,    IBOUNDQ
     1        0
CC
CC ID, BOTTOM HOLE PRESSURE FOR PRESSURE CONSTRAINT WELL (IFLAG=2 OR 3)
*----  ID    PWF
     2     -999
CC
CC
*---- ID,    IBOUNDQ
     2        0
CC
CC ID, BOTTOM HOLE PRESSURE FOR PRESSURE CONSTRAINT WELL (IFLAG=2 OR 3)
*----  ID    PWF
     3     -999
CC
CC
*---- ID,    IBOUNDQ
     3        0
CC
CC ID, BOTTOM HOLE PRESSURE FOR PRESSURE CONSTRAINT WELL (IFLAG=2 OR 3)
*----  ID    PWF
     4     -999
CC
CC
*---- ID,    IBOUNDQ
     4        0
CC
CC CUM. INJ. TIME , AND INTERVALS (PV OR DAY) FOR WRITING TO OUTPUT FILES
*---- TINJ     CUMPR1      CUMHI1     WRHPV     WRPRF      RSTC
    450      2         2          2          2         100
CC
CC THE INI. TIME STEP,CONC. TOLERANCE,MAX.,MIN. TIME STEPS
*----  DT     DELC(I)              CNMAX             CNMIN
   0.0001    9*0.01         0.01              0.0001
CCCC
```

```
CC
*---- ID,    HEAT RATE
     2        5000
CC
CC ID, BOTTOM HOLE PRESSURE FOR PRESSURE CONSTRAINT WELL (IFLAG=2 OR 3)
 *----  ID     QI(M,L)     C(M,KC,L)
      3      1.0          1     0.0    0.00   0.0     0.0  0.0  0.0  0.0  0.0  0.0
      3      0.0          0.    0.0    0.0    0.0     0.0  0.0  0.0  0.0  0.0  0.0
      3      0.0          0.    0.0    0.0    0.0     0.0  0.0  0.0  0.0  0.0  0.0
      3      0.0          0     0.0    0.0    0.0     0.0  0.0  0.0  0.0  0.0  0.0
CC
CC ID, BOTTOM HOLE PRESSURE FOR PRESSURE CONSTRAINT WELL (IFLAG=2 OR 3)
*----  ID    PWF
     3     150
CC
CC
*--- ID, INJ. TEMP (F), STEAM QUALITY
     3    100.    0
CC
CC
*---- ID,    IBOUNDQ
     3         0
CC
CC ID, BOTTOM HOLE PRESSURE FOR PRESSURE CONSTRAINT WELL (IFLAG=2 OR 3)
 *----  ID     QI(M,L)     C(M,KC,L)
      4      1.0          1     0.0    0.0    0.0    0.0   0.0   0.0   0.0   0.0
      4      0.0          0.    0.0    0.0    0.0    0.0   0.0   0.0   0.0   0.0
      4      0.0          0.    0.0    0.0    0.0    0.0   0.0   0.0   0.0   0.0
      4      0.0          0     0.0    0.0    0.0    0.0   0.0   0.0   0.0   0.0
CC
CC ID, BOTTOM HOLE PRESSURE FOR PRESSURE CONSTRAINT WELL (IFLAG=2 OR 3)
*----  ID    PWF
     4      150
CC
CC
*--- ID, INJ. TEMP (F), STEAM QUALITY
     4      100.     0
CC
CC
*---- ID,    IBOUNDQ
     4         0
CC
CC CUM. INJ. TIME , AND INTERVALS (PV OR DAY) FOR WRITING TO OUTPUT FILES
*---- TINJ     CUMPR1     CUMHI1     WRHPV     WRPRF      RSTC
     700      2          2          2          2          100
CC
CC THE INI. TIME STEP,CONC. TOLERANCE,MAX.,MIN. TIME STEPS
*----  DT     DELC(I)              CNMAX             CNMIN
    0.0001    9*0.01          0.01              0.0001
CCCCCCCCCCCCCCCCCCCCCCCCCCCCCCCCCCCCCCCCCCCCCCCC INJECTION STEAM CYCLE 3
CCCCCCCCCCCCCCCCCCCC
```

```
CC
CC
*---- ID,    IBOUNDQ
     1        1
CC
CC
*---- ID,    HEAT RATE
     1        5000
CC
CC ID, BOTTOM HOLE PRESSURE FOR PRESSURE CONSTRAINT WELL (IFLAG=2 OR 3)
*----  ID    PWF
     2      -9999
CC
CC ID, BOTTOM HOLE PRESSURE FOR PRESSURE CONSTRAINT WELL (IFLAG=2 OR 3)
*----  ID    PWF
     3     150
CC
CC
*---- ID,    IBOUNDQ
     3        0
CC
CC ID, BOTTOM HOLE PRESSURE FOR PRESSURE CONSTRAINT WELL (IFLAG=2 OR 3)
*----  ID    PWF
     4     150
CC
CC
*---- ID,    IBOUNDQ
     4        0
CC
CC CUM. INJ. TIME , AND INTERVALS (PV OR DAY) FOR WRITING TO OUTPUT FILES
*---- TINJ     CUMPR1      CUMHI1      WRHPV      WRPRF       RSTC
     770        1           1      1    1       1
CC
CC THE INI. TIME STEP,CONC. TOLERANCE,MAX.,MIN. TIME STEPS
*----  DT        DELC(I)        CNMAX             CNMIN
     0.0001    9*0.01         0.01              0.0001
CCCCCCCCCCCCCCCCCCCCCCCCCCCCCCCCCCCCCCCCCCCCCCCCCCCCCCCCCCC SOAKING CYCLE 3
CCCCCCCCCCCCCCCCCCCCCCCCCCCCCCCCCCCCCCCCCCCCCCCCCCCCCCCCCC
CC FLAG FOR INDICATING BOUNDARY CHANGE
*---- IBMOD
      0
CC
CC IRO, ITIME, NEW FLAGS FOR ALL THE WELLS ( WATER INJ.)
*---- IRO   ITIME  IFLAG
     2      0      1   2  2  2
CC
CC NUMBER OF WELLS CHANGES IN LOCATION OR SKIN OR PWF
*----NWEL1
   0
CC
CC NUMBER OF WELLS WITH RATE CHANGES, ID
*----NWEL1   ID
    4       1    2   3   4
CC
CC ID, BOTTOM HOLE PRESSURE FOR PRESSURE CONSTRAINT WELL (IFLAG=2 OR 3)
 *----  ID     QI(M,L)     C(M,KC,L)
      1      0.0    0     0.0    0.00   0.0    0.0  0.0  0.0  0.0  0.0
      1      0.0    0.    0.0    0.0    0.0    0.0  0.0  0.0  0.0  0.0
      1      0.0    0.    0.0    0.0    0.0    0.0  0.0  0.0  0.0  0.0
      1      0.0    0     0.0    0.0    0.0    0.0  0.0  0.0  0.0  0.0
CC
CC
*--- ID, INJ. TEMP (F), STEAM QUALITY
     1    100.   0
CC
CC
*---- ID,    IBOUNDQ
     1        0
CC
CC ID, BOTTOM HOLE PRESSURE FOR PRESSURE CONSTRAINT WELL (IFLAG=2 OR 3)
*----  ID    PWF
     2     -999
CC
CC
*---- ID,    IBOUNDQ
     2        0
CC
```

```
CC ID, BOTTOM HOLE PRESSURE FOR PRESSURE CONSTRAINT WELL (IFLAG=2 OR 3)
*----  ID    PWF
     3    -999
CC
CC
*---- ID,    IBOUNDQ
     3        0
CC
CC ID, BOTTOM HOLE PRESSURE FOR PRESSURE CONSTRAINT WELL (IFLAG=2 OR 3)
*----  ID    PWF
     4     -999
CC
CC
*---- ID,    IBOUNDQ
     4        0
CC
CC CUM. INJ. TIME , AND INTERVALS (PV OR DAY) FOR WRITING TO OUTPUT FILES
*---- TINJ     CUMPR1     CUMHI1     WRHPV     WRPRF      RSTC
     800      2         2         2         2         100
CC
CC THE INI. TIME STEP,CONC. TOLERANCE,MAX.,MIN. TIME STEPS
*----  DT     DELC(I)             CNMAX            CNMIN
    0.0001    9*0.01        0.01            0.0001
CCCCCCCCCCCCCCCCCCCCCCCCCCCCCCCCCCCCCCCCCCPRODUCTION CUCLE 3
CCCCCCCCCCCCCCCCCCCCCCCCCCCCCCCCCCCCCCCCCCCCCCCCCCCCCCCCCCCCCCCCCCCCCCCCCCCCCCC
CC FLAG FOR INDICATING BOUNDARY CHANGE
*---- IBMOD
      0
CC
CC IRO, ITIME, NEW FLAGS FOR ALL THE WELLS ( WATER INJ.)
*---- IRO   ITIME  IFLAG
     2      0      1   2  3  3
CC
CC NUMBER OF WELLS CHANGES IN LOCATION OR SKIN OR PWF
*----NWEL1
   0
CC
CC NUMBER OF WELLS WITH RATE CHANGES, ID
*----NWEL1   ID
    4       1    2   3   4
CC
CC ID, BOTTOM HOLE PRESSURE FOR PRESSURE CONSTRAINT WELL (IFLAG=2 OR 3)
 *----  ID     QI(M,L)     C(M,KC,L)
      1      0.0    0     0.0    0.00   0.0    0.0  0.0  0.0  0.0  0.0
      1      0.0    0.    0.0    0.0    0.0    0.0  0.0  0.0  0.0  0.0
      1      0.0    0.    0.0    0.0    0.0    0.0  0.0  0.0  0.0  0.0
      1      0.0    0     0.0    0.0    0.0    0.0  0.0  0.0  0.0  0.0
CC
CC
*--- ID, INJ. TEMP (F), STEAM QUALITY
     1    100.    0
CC
CC
*---- ID,    IBOUNDQ
     1        0
CC
CC ID, BOTTOM HOLE PRESSURE FOR PRESSURE CONSTRAINT WELL (IFLAG=2 OR 3)
*----  ID    PWF
     2     100
CC
CC
*---- ID,    IBOUNDQ
     2        1
CC
CC
*---- ID,    HEAT RATE
     2        5000
CC
CC ID, BOTTOM HOLE PRESSURE FOR PRESSURE CONSTRAINT WELL (IFLAG=2 OR 3)
 *----  ID     QI(M,L)     C(M,KC,L)
      3      1.0          1     0.0    0.00   0.0    0.0  0.0  0.0  0.0  0.0
      3      0.0          0.    0.0    0.0    0.0    0.0  0.0  0.0  0.0  0.0
      3      0.0          0.    0.0    0.0    0.0    0.0  0.0  0.0  0.0  0.0
      3      0.0          0     0.0    0.0    0.0    0.0  0.0  0.0  0.0  0.0
CC
CC ID, BOTTOM HOLE PRESSURE FOR PRESSURE CONSTRAINT WELL (IFLAG=2 OR 3)
*----  ID    PWF
```

```
      3     150
CC
CC
*--- ID, INJ. TEMP (F), STEAM QUALITY
      3    100.   0
CC
CC
*---- ID,    IBOUNDQ
      3        0
CC
CC ID, BOTTOM HOLE PRESSURE FOR PRESSURE CONSTRAINT WELL (IFLAG=2 OR 3)
 *----  ID     QI(M,L)     C(M,KC,L)
       4      1.0        1     0.0    0.0    0.0    0.0   0.0   0.0   0.0   0.0
       4      0.0        0.    0.0    0.0    0.0    0.0   0.0   0.0   0.0   0.0
       4      0.0        0.    0.0    0.0    0.0    0.0   0.0   0.0   0.0   0.0
       4      0.0        0     0.0    0.0    0.0    0.0   0.0   0.0   0.0   0.0
CC
CC ID, BOTTOM HOLE PRESSURE FOR PRESSURE CONSTRAINT WELL (IFLAG=2 OR 3)
*----  ID    PWF
      4      150
CC
CC
*--- ID, INJ. TEMP (F), STEAM QUALITY
      4      100.     0
CC
CC
*---- ID,    IBOUNDQ
      4        0
CC
CC CUM. INJ. TIME , AND INTERVALS (PV OR DAY) FOR WRITING TO OUTPUT FILES
*---- TINJ     CUMPR1      CUMHI1     WRHPV     WRPRF      RSTC
    1250      2         2          2         2         100
CC
CC THE INI. TIME STEP,CONC. TOLERANCE,MAX.,MIN. TIME STEPS
*----  DT     DELC(I)              CNMAX             CNMIN
    0.0001    9*0.01         0.01             0.0001
```

Bibliography

Abbas A.A., and Shedid S.A.: "Experimental Investigation of the Feasibility of Steam/Chemical Steam Flooding Processes through Horizontal Wells," Paper SPE 68767 presented at SPE Conference, Jakarta, Indonesia, April 2001.

Abdalla, A., and Coast, K.H.: "A Three-Phase Experimental and Numerical Simulation Study of the Steam Flood Process," Paper SPE 3600 presented at the 46th Annual Fall Meeting of the Society of the Petroleum Engineers of AIME, New Orleans, Louisiana, October 1971.

Abou-Kassem, J., Farouq Ali,S.: "Modelling of Emulsion Flow in Porous Media," Journal of Canadian Petroleum Technology 34, No.6:30-38. 1995. PETSOC-95-06-02

Abou-Kassem, J.H.: "Practical considerations in developing numerical simulators for thermal recovery," Journal of Petroleum Science and Engineering, V.15, pp.281-290. 1981.

Abu-Khamsin, S.A., Bringham, W.E., and Ramey, H.J.Jr.: "Reaction Kinetics of Fuel Formation for In-Situ Combustion," Paper SPE 15736, SPE Reservoir Engineering, V.3, No.4, pp.1308-1316, 1988.

Acs, G., Doleschall, S., and Farkas, E. "General Purpose compositional Model," SPEJ, V.25, No.4, pp.543-553, 1985.

Akin, S, Castanier, L.M., and Brigham, W.E.: "Effect of Temperature on Heavy Oil/Water Relative permeabilities," Paper SPE 54120 presented at SPE International Thermal Operations Symposium, Bakersfield, California, March 1999.

Alvarado, D.A., and S.S. Marsden "Flow of Oil-in-Water Emulsions through Tubes and Porous Media," Society of Petroleum Engineers Journal 19, No.6, December 1979.

Amba, S.A., Chilingar, G.V., and Beeson, C.M.: "Use of Direct Electrical Current for Increasing the Flow Rate of Reservoir Fluids during Petroleum Recovery," Journal of Canadian Petroleum Technology.3, No.01:8 – 14, 1964.

Aoudia, M., and Wade, W. H.: "Optimum microemulsions formulated with propoxylated Guerbet alcohol and propoxylated tridecyl alcohol sodium sulfates," Journal of Dispersion Science and Technology, V.16, No.2, pp. 115-35, 1995.

Austad, T. and Skule, S.: "Chemical Flooding of Oil reservoirs, Effects of Temperature and Pressure on the middle Phase Solubilization Parameters Close to Optimum Flood Conditions," Colloids and Surfaces, A: Physicochemical and Engineering Aspects, V.108, No.2/3, pp. 243-252, 1996.

Babadagli, T.: "Evaluation of EOR Methods for Heavy-oil Recovery in Naturally Fractured Reservoirs," Journal of Petroleum Science and Engineering 37, No. 1–2: 25–37, February 2003.

Baker, R.S., and Bierschenk, J.M.: "In-Situ Thermal Destruction makes Stringent Soil and Sediment Cleanup Goals Attainable," Presented in Proceeding of the Forth Tri-Service Environmental Technology Symposium, San Diego, California, June 2001.

Balay, S., Gropp, W., MnInnes, L.C., and Smith, B.: "PETSc 2.0 User Manual, Argonne National Laboratory," ANL-95/11-Revision 2.0.22, April 1998.

Bang, Vishal.: "Phase Behavior Study of Hydrocarbon-Water-Alcohol Mixture," MS. Thesis, The University of Texas at Austin, 2005.

Beattie, C.I., Boberg, T.C., and McNab, G.S.: "Reservoir Simulation of Cyclic Steam Stimulation in the Cold Lake Oil Sands," SPE Reservoir Engineering 6, no. 2, May 1991.

Beattie, C.I., Boberg, T.C., McNab, G.S.: "Reservoir Simulation of Cyclic Steam Stimulation in the Cold Lake Oil Sands," Journal of SPE Reservoir Engineering, 6 No.2: 200 - 206, 1991. SPE-18752-PA

Bell, C.W., and Titus, C.H.: "Electro-Thermal Process for Production of Offshore Oil through Onshore Wells," U.S. Patent No.3724543, 1973.

Bell, C.W.: "Electrolitically Promoting the Flow of Oil from a Well," U.S. Patent No.2799641, 1957.

Bogdanov, I.I., Torres J.A., Akhlaghi, H.A., and Kamp, A.M.: "The Influence of Salt Concentration in Injected Water on Low Frequency Electrical-Heating Assisted Bitumen Recovery," SPE Journal 16, No.03: 548-558, 2011.

Bowen, G., and Crumpton, P.: "A New Formulation for the Implicit Compositional Simulation of Miscible Gas Injection Processes," Paper SPE 79692 presented at SPE Reservoir Simulation Symposium, Houston, Texas, February 2003.

Branco, C.M., and Rodrigues, F.: "A semi-Implicit Formulation for Compositional Reservoir Simulation," Paper SPE 27053, SPE Advanced Technology Series, 1995, V.4, No.1, pp.171-177.

Brantferger, K. M.: "Development of a Thermodynamically Consistent, Fully Implicit, Compositional, Equation-Of-State, Steamflood Simulator," PhD Dissertation, University of Texas at Austin, May 1991.

Briens, F.J.L., Wu, C.H., Gazdag, J., and Wang, L.H.: "Compositional Reservoir Simulation in Parallel Supercomputing Environments," Paper SPE 21214 presented at the 11th SPE Symposium on Reservoir simulation of the Society of Petroleum Engineers, Anaheim, California, February 1991.

Bryan, J., and Kantzas, A.: "Enhanced Heavy-Oil Recovery by Alkali-Surfactant Flooding," Society of Petroleum Engineers, 2007.

Bryan, J., Kantzas A.: "Enhanced Heavy-Oil Recovery by Alkali-Surfactant Flooding," Paper SPE-110738. Annual Technical Conference and Exhibition, Anaheim, California, November 11-14, 2007.

Buchwalter, J.K., and Miller, C.A.: "A New Simplified Compositional Simulator," Paper SPE 25858 presented at SPE Rocky Mountain Regional/Low Permeability Reservoirs Symposium, Denver, Colorado, April 1993.

Butler, R.: "A New Approach To The Modelling Of Steam-Assisted Gravity Drainage," Journal of Canadian Petroleum Technology,1985.

Butler, R.: "Steam-assisted Gravity Drainage: Concept, Development, Performance And Future," Journal of Canadian Petroleum Technology 33, no. 2, February 1994).

Butler, R.: "A New Approach to the Modelling of Steam-Assisted Gravity Drainage," Journal of Canadian Petroleum Technology, 24, No.03:42-51, 1985.

Butler, R. M., Mcnab, G. S., Lo, H. Y.: "Theoretical Studies on the Gravity Drainage of Heavy Oil During In-situ Steam Heating," The Canadian Journal of Chemical Engineering, 59, No.04: 455–460, 1981. DOI: 10.1002/cjce.5450590407

Butler, R., and Stephens, D.: "The Gravity Drainage of Steam-heated Heavy Oil to Parallel Horizontal Wells," Journal of Canadian Petroleum Technology, 1981.

Butler, R., and Jiang, Q.: "Improved Recovery of Heavy Oil by Vapex with Widely Spaced Horizontal Injectors and Producers," Journal of Canadian Petroleum Technology 39, No. 1, January 2000.

Cao, H., and Aziz, K.: "Performance of IMPSAT and IMPSAT-AIM Models in Compositional Simulations," Paper SPE 77720 presented at the SPE Annual Technical Conference and Exhibition, San Antonio, Texas, October 2002.

Chan, M.Y.S., and Sarioglu, G.: "Numerical Modeling of Cyclically Steamed and Fractured Oil-Sand Reservoirs," Paper SPE 22369 presented at the International Meeting on Petroleum Engineering, Beijing, China, March 1992.

Chang, Y.B.: "Development and Application of an Equation of State Compositional Simulator," Ph.D. Dissertation, the University of Texas at Austin, 1990.

Chein, M.C.H., Lee, S.T., and Chen, W.H.: "A New Fully Implicit Compositional Simulator," SPE 13385, presented at the 8th SPE Symposium on Reservoir Simulation of the Society of Petroleum Engineers, Dallas, TX, 1985.

Chein, M.C.H., Yardumain, H.E., Chung, E.Y., and Todd, W.W.: "The Formulation of a Thermal Simulation Model in a Vectorized, General Purpose Reservoir Simulator," Paper SPE 18418 presented at the Tenth SPE Symposium on Reservoir Simulation, Houston, Texas, February 1989.

Chen, Q., Gerritsen, M., Kovscek, A.: Improving Steam-Assisted Gravity Drainage Using Mobility Control Foams: Foam Assisted-SAGD (FA-SAGD). SPE Paper-129847. Improved Oil Recovery Symposium, Tulsa, Oklahoma, April 24-28, 2010.

Chen, Q., Gerritsen, M., and Kovscek, A.: "Improving Steam-Assisted Gravity Drainage Using Mobility Control Foams: Foam Assisted-SAGD (FA-SAGD)," Society of Petroleum Engineers, 2010.

Chilingar, G.V., Chang, K.S., Davis, J.E., Farhangi, H.J., Adamson, L.G., and Sawabini, S.: "Possible Use of Direct Electrical Current for Augmenting Reservoir Energy during Petroleum Production," The Compass, V.45 (4), pp.272-285, 1968.

Chilingar, G.V., El-Nassir, A., and Stevens, R.G.: "Effect of Electrical Current on Permeability of Sandstone Cores," Journal of Petroleum Technology, V.22 (7), pp. 830-836, 1970.

Chilingar, G.V., Loo, W.W., Khilyux, L.F., and Katz, S.A.: "Electro-bioremediation of Soil Contaminated with Hydrocarbons and Metals," Energy Sources, V.19, pp. 129-146, 1997.

Cicek, O. and Ertekin, T.: "Development and Testing of a new 3D Field Scale Fully Implicit Multi-Phase Compositional Steam Injection Simulator," Paper SPE 35516 presented at European 3D Reservoir Modeling Conference, Norway, April 1996.

Cicek, O.: "Numerical Simulation of Steam Displacement of Oil in Naturally Fractured Reservoirs Using Fully Implicit Compositional Formulation: A Comparative Analysis of the Effects of Capillary and Gravitational Forces in Matrix/Fracture Exchange Term," Paper SPE 97005 presented at SPE Annual Technical Conference and Exhibition, Dallas, Texas, October 2005.

Cieck, O.: "Modeling and Designing Oil Recovery by Steam Injection in Naturally Fractured Reservoirs," Paper SPE 93574 presented at SPE Western Regional Meeting, Irvine, California, 2005.

Cinar, M., Castainer, L.M., and Kovscek, A.: " Improved Analysis of the Kinetics of Crude-Oil In-Situ Combustion," Paper SPE 113948 presented at Western Regional and Pacific Section AAPG Joint Meeting, Bakersfield, California, 2008.

Closmann, P.J., Waxman, M.H., and Deeds, C.T.: "Steady-State Tar/Water Relative Permeabilities in Peace River Cores at Elevated Termprature," Paper SPE 14227 presented at SPE 60th Annual Technical Conference and Exhibition, Las Vegas, Nevada, September 1985.

Coats, K.H., and George, W.D., Chu, C., and Marcum, B.E.: "Three-Dimensional Simulation of Steamflooding," Society of Petroleum Engineers Journal 14, No. 6 December 1974.

Coats, K.H., George, W.D., Chu, C., and Marcum, B.E.: "Three-Dimensional Simulation of Steam Flooding," Trans., AIME, V.257, pp. 573-592, 1974.

Coats, K.H., George, W.D., Chu, C., Marcum, B.E.: "Three-Dimensional Simulation of Steam flooding" Society of Petroleum Engineers Journal, 14, No.6: 573- 592, 1974.

Coats, K.H.: "Simulation of Steam Flooding with Distillation and Solution Gas," SPEJ, V.16 (5), pp. 235-247, 1976.

Coats, K.H.: "A Highly Implicit Steam Flood Model," SPEJ, V.18 (5), pp. 369- 383, 1978.

Collins, D.A., Nghiem, L.X., and Li, Y.-K.: "An Efficient Approach to Adaptive-Implicit Compositional Simulation with an Equation of State," Paper SPE 15133 presented at the 56th Annual California Regional Meting of the Society of Petroleum Engineers,Oakland, CA, 1986.

Corey, A.T.: "The Interrelation between Gas and Oil Relative Permeabilities," Producers Monthly, pp. 38-41, November 1954.

Crookston, R.B., Culham, W.E., and Chen, W.H.: "A Numerical Simulation Model for Thermal Recovery Processes," SPEJ, V.20, No.1, pp. 37-58, 1979.

D'Elia-S, Rafael, and Jose Ferrer, G.: "Emulsion Flooding of Viscous Oil Reservoirs," Society of Petroleum Engineers, 1973.

D'Elia-S, Rafael, Ferrer-G J.: "Emulsion Flooding of Viscous Oil Reservoirs," Paper SPE- 4674. Fall Meeting of the Society of Petroleum Engineers of AIME, Las Vegas, Nevada, 1973.

Das, S. K., and Butler R. M.: "Mechanism of the Vapor Extraction Process for Heavy Oil and Bitumen," Journal of Petroleum Science and Engineering 21, No. 1–2 43–59, September 1998.

Das, S., and Butler, R.: "Effect of Asphaltene Deposition on the Vapex Process: A Preliminary Investigation Using a Hele-Shaw Cell," Journal of Canadian Petroleum Technology 33, No. 6, June 1994.

Delshad, M., Pope, G. A., and Sepehrnoori, K.: "A compositional simulator for modeling surfactant enhanced aquifer remediation, 1 formulation," Journal of Contaminant Hydrology 23 No.4: 303-327, August 1996.

Dong, B., Y.Y, Li, W. Song, Y.: "Lattice Boltzmann Simulation of Viscous Fingering Phenomenon of Immiscible Fluids Displacement in a Channel," Computers & Fluids, 39, No.5: 768–779, May 2010.

Dong, M., Ma, S., and Liu, Q.: "Enhanced Heavy Oil Recovery Through Interfacial Instability: A Study of Chemical Flooding for Brintnell Heavy Oil," Fuel 88, No. 6: 1049–1056, June 2009.

Douglas, J. Jr., Peaceman, D.W., and Rachford, H.H.: "A Method for Calculating Multi-Dimensional Immiscible Displacements," Petroleum Transactions, AIME,V.216, pp. 297-308, 1959.

Dusseault, M.: "Comparing Venezuelan and Canadian Heavy Oil and Tar Sands," Society of Petroleum Engineers, 2001.

Dwarakanath, V., Pope, G. A.: "Surfactant Phase Behavior with Field Degreasing Solvent,"Environmental Science and Technology, V.34 (22), pp. 4842-8, 2000.

Edmondson, T.A.: "Effects of Temperature on Water Flooding," J. Can. Pet.Tech., pp. 263-242, 1965.

El-Feky, S.A.: "Theoretical and Experimental Investigation of Oil Recovery by the Electrothermic Technique," University of Missouri-Rolls, PhD Dissertation, 1977.

Elliot, Lucas J., Pope, Gary A., and John, Russell T.: "In-Situ Thermal Remediation of Contaminant below the Water Table," Paper SPE 81204 presented at SPE/EPA/DOE Exploration and Production Environmental Conference in San Antonio, Texas, March 2003.

Fagin, R.G., and Stewart, C.H.: "A New Approach to the Two-Dimensional Multiphase Reservoir Simulator," Paper SPE 1188 presented at SPE Annual Fall Meeting, Denver, Colorado, October 1965.

Fan, Y., Durlofsky, L., and Tchelepi, H.: "Numerical Simulation of the In-situ Upgrading of Oil Shale," Society of Petroleum Engineers, 2009.

Farough Ali, S.M.: "Steam Injection Theories - A Unified Approach," Paper SPE 10746 presented at SPE California Regional Meeting, San Francisco, California, March 1982.

Farouq Ali, S.M.: "Heavy Oil—evermore Mobile," Journal of Petroleum Science and Engineering 37, No.1–2 5–9, February 2003.

Farouq Ali, S.M.: "Heavy Oil-evermore Mobile," Journal of Petroleum Science and Engineering 37, No.1–2: 5–9, 2003.

Farouq Ali, S.M., and Meldau, R.F.: "Current Steamflood Technology," Journal of Petroleum Technology 31, No. 10, October 1979.

Farouq Ali, S.M.: "Multiphase, Multidimensional Simulation of In-Situ Combustion," Paper SPE 6896 presented at SPE 52nd Annual Technical Conference and Exhibition, Denver, Colorado, October 1977.

Farouq Ali, S.M., Meldau, R.F.. "Current Steam flood Technology. Journal of Petroleum Technology 31, No.10:1332 – 1342. SPE-7183, 1979.

Ferrer, J. and Farouq Ali, S.M.: "A Three-Phase, Two- Dimensional Compositional Thermal Simulator for Steam Injection Process," J. Can. Pet.Tech., pp. 78-90, 1977.

Firoozabadi, A.: "Mechanisms of Solution Gas Drive in Heavy Oil Reservoirs," Journal of Canadian Petroleum Technology 40, No. 3, March 2001.

Fortenberry, R.P. PhD. Dissertation, The University of Texas at Austin.May 2013."Experimental Demonstration and Improvement of Chemical EOR Techniques in Heavy Oils" M.SE. Thesis, The University of Texas at Austin.

Fussell, L.T. and Fussell, D.D.: "An Iterative Technique for Compositional Reservoir Models," SPEJ, V.19 (4), pp.211-220, 1979.

Gill, P.E., and Murray, W.: "Newton-Type Methods for Unconstrained and Linearly Constrained Optimization," Mathematical Programming, V.4, pp.311-350, 1974.

Gill, W. G.: "Electrical Method and Apparatus for Recovery of Oil," U.S. Patent No. 3542066, 1972.

Godderij, R.R., Bruining, J., and Molenaar, J.: "A Fast 3D Interface Simulator for Steamdrives," Paper SPE 59269 SPE Journal, V. 4, No.4, December 1999.

Grabowski, J.W., Vinsome, P.K., Lin, R.C., Behie, A., and Rubin, B.: "A Fully Implicit General Purpose Finite Difference Thermal Model for In-Situ Combustion and Steam," Paper SPE 8396 presented at Annual Meeting of the Society of Petroleum Engineering of AIME, Las Vegas, Nevada, 1979.

Griswold, J. and Kasch, J.E.: "Hydrocarbon-Water Solubilities at Elevated Temperature and Pressure," Ind. Eng. Chem., V.34, No.7, p.804, 1942.

Goudarzi, A., Delshad, M., Sepehrnoori, K.: "A Critical Assessment of Several Reservoir Simulators for Modeling Chemical Enhanced Oil Recovery Processes, Paper SPE 163578, SPE Reservoir Simulation Symposium, Woodlands, Texas, February 18-20, 2013.

Goudarzi, Delshad, M., Mohanty, K.K, and Sepehrnoori, K.: "Surfactant Oil Recovery in Fractured Carbonates: Experiments and Modelling of Different Matrix Dimensions," Under re-review by Journal of Petroleum Science and Engineering, September, 2014.

Hamouda, A.A., Karoussi, O., and Chukwudeme, E.A.: "Relative Permeability as a Function of Temperature, Initial Water Saturation and Flooding Fluid Compositions for Modified Oil-Wet Chalk," Journal of Petroleum Science and Engineering, 2008,V.63, pp.61-72.

Han, C., Delshad, M., Sepehrnoori, K., and Pope, G.A.: "A Fully Implicit, Parallel, Compositional Chemical Flooding Simulator," Paper SPE 97217 presented at SPE Annual Technical Conference and Exhibition, Dallas, Texas, October 2005.

Hansen, K.S., Conley, D.M., Vinegar, H.J., Coles, J.M., Menotti, J.L., and Stegemeier, G.L.: "In-Situ Thermal Desorption of Coal Tar," Proceeding of the Institute of Gas Technology/Gas Research Institute International Symposium on Environmental Biotechnologies and Site Remediation Technologies, Orlando, Forida, December1998.

Harvey, A. H., Arnold M.D. and El-Feky, S.A. "Selective Electric Reservoir Heating," JCPT 18, No.3: 47-57, 1979.

Harvey, A., Arnold M., and El-Feky, S.: "Selective Electric Reservoir Heating," Journal of Canadian Petroleum Technology, 1979.

Healy, R. N., and Reed, R. L.: "Multiphase Microemulsion Systems,"SPEJ , June 1976, p.174.

Hiebert, A.D., Vermeulen, F.E., F.S.C., and Capjack, C.E: "Numerical Simulation Results for the Electrical Heating of Athabasca Oil-Sand Formations" SPE Reservoir Engineering 1, No. 1, January 1986.

Hiebert, A.D., Vermeulen, F.E. and Chute, F.S. 1989c. Application of Numerical Modeling to The Simulation of the Electric-Preheat Steam-Drive (EPSD) Process In Athabasca Oil Sands. Journal of Canadian Petroleum Technology, 28(05): 74-86.

Hilbert, A. D.: "Numerical Simulation of the Electrical Pre-heat and Steam Drive Bitumen Recovery Process for the Athabasca Oil Sands," PhD Dissertation, Department of Electrical Engineering, University of Alberta, 1986.

Hirasaki, G.: "The Steam-Foam Process," Journal of Petroleum Technology 41, No.5: 449 – 456. SPE-19505, 1989.

Iben, I.E.T., Edelstein, W.A, Sheldon, R.B., Shapiro, A.P. Uzgiris, E.E., Scatena, C.R., Blaha, S.R., Silverstein, W.B., Brown, G.R., Stegemeier, G.L., and Vinegar, H.J.: "Thermal Blanket for In-Situ Remediation of Surficial Contamination: A Pilot Test," Environmental Science and Technology, V.30(11), pp. 3144-3154, 1966.

IMEX 2012.10.: "Advanced Black Oil/Gas Reservoir Simulator," By Computer Modelling Group Ltd.

Ishimoto, K., Pope, G.A., and Sepehrnoori, K.: "An Equation of State Steam Simulator," In Situ, V.11 (1), pp.1-37, 1987.

Ishimoto, K.: "One – Dimensional Fully Implicit Compositional Model for Steam Flooding," MS Thesis, University of Texas at Austin, Texas, 1985.

Ito, Y., and Suzuki S.: "Numerical Simulation of the SAGD Process in the Hangingstone Oil Sands Reservoir," Journal of Canadian Petroleum Technology 38, No.9 September 1999.

Ito, Y., Suzuki ,S.: "Numerical Simulation of the SAGD Process in the Hangingstone Oil Sands Reservoir," Journal of Canadian Petroleum Technology 38, No.9: 27-35.PETSOC-99-09-02, 1999.

Jang S. H., Liyanage P. J., Lu J., Kim D. H., Arachchilage G.W.P.P., Britton C., Weerasooriya U., and Pope G. A. "Microemulsion Phase Behavior Measurements Using Live Oils at High Temperature and Pressure" Paper SPE 169169, SPE Improved Oil Recovery Symposium, Tulsa, Oklahoma, April 12-16, 2014.

Jennings H.Y., Johnson, C.E., and McAuliffe, C.D.: "A Caustic Waterflooding Process for Heavy Oils," Journal of Petroleum Technology 26, No. 12, December 1974.

Jha, K.: "A Laboratory Study of Heavy Oil Recovery with Carbon Dioxide," Journal of Canadian Petroleum Technology, 1986.

Johnson. C.E.: "Status of Caustic and Emulsion Methods," Journal of Petroleum Technology 28, No. 1, January 1976.

Johnson. C.E.: Status of Caustic and Emulsion Methods" Journal of Petroleum Technology 28, No.0 1:85-91, 1976. SPE-5561-PA.

Kazemi, H., Vestal, C.R., and Shank, G.D.: "An Efficient Multicomponent Simulator," Paper SPE 6890 presented at 52nd SPE Annual Fall Technical Conference and Exhibition, Denver, Colorado, October 1977.

Kazemi Nia, A.K., Sepehrnoori, K., Delshad, M.: "A Mechanistic Integrated Geochemical and Chemical Flooding Tool for Alkaline/Surfactant/Polymer Floods" Paper SPE 169094. SPE Improved Oil Recovery Symposium, 12-16 April, Tulsa, Oklahoma, USA, 2014.

Kell, G.S.: "Density, Thermal Expansivity and Compressibility of liquid water from 0° to 150° Correlations and Tables for atmospheric Pressure and Saturation," J.Therm Eng. Data, 1975, V.20, pp.97-105.

Killough, J.E. and Gonzalez, J.A.: "A Fully-lmplicit Model for Electrically Enhanced Oil Recovery,"Society of Petroleum Engineers of AIME, Paper SPE15605. Presented at the SPE Annual Technical Conference and Exhibition, New Orleans, Louisiana, USA, October 5-8, 1986.

Killough, J.E., and Kossack, C.A.: “Fifth Comparison Solution Project: Evaluation of Miscible Flood Simulators,” Paper SPE 16000 presented at the 9th SPE Symposium on Reservoir Simulation , San Antonio, Texas, February 1987.

Kristensen, M.R., Gerritsen, M.G., and Thomsen, P.G.: “Coupling Chemical Kinetics and Flashes in Reactive, Thermal and Compositional Reservoir Simulation,” Presented at SPE Reservoir Simulation Symposium, Houston, Texas, February 2007.

Korrani. A.K.N. Dec. 2014. Mechanistic Modeling of Low Salinity Water Injection. PhD. Dissertation, The University of Texas at Austin.

Kumar, J., Fusetti, L., and Corre, B.: “Modeling In-Situ Upgrading of Extraheavy Oils/Tar Sands by Subsurface Pyrolysis,” Society of Petroleum Engineers, 2011.

Lake, L.W.: “Enhanced Oil Recovery,” 166. Englewood Cliffs, New Jersey: Prentice Hall, 1989.

Lashgari, H.R., Lotfollahi, M., Delshad,M., Sepehrnoori,K., and DeRouffignac, E.: “Steam Foam Modeling in Heavy Oil Reservoirs,” Paper SPE-170178. Heavy Oil Conference, Calgary, Alberta Canada, June 10-12, 2014a.

Lashgari, H., El Rabaa W., Chan H., Vaidya, R.: “Estimation of Hydraulic Fracture Contribution on Vertical Well Performance in Medium to High Permeability Reservoirs,” Paper SPE 169554, SPE Western North America Conference, Denver, Colorado, USA, April 15-18, 2014b.

Lashgari, H.R., Delshad, M., Sepehrnoori,K., and DeRouffignac ,E.: “Development of Electrical Joule‘s Heating Simulation for Heavy Oil Reservoirs,” Paper SPE-170173. Heavy Oil Conference, Calgary, Alberta Canada, June 10-12, 2014c.

Lashgari, H.R. Delshad, M., Sepehrnoori, K., DeRouffignac, E.: “Development of Electrical Joule's Heating Simulation for Heavy Oil Reservoirs,” Paper SPE-170173. Heavy Oil Conference, Calgary, Alberta Canada, June 10-12, 2014.

Lauwerier, H.A.: “The Transport of Heat in an Oil Layer by the Injection of Hot Fluid,” Applied Scientific Research, Section A, V.5, pp.145-150, 1955.

Liu, Q., Dong, M., and Ma, S.: “Alkaline/Surfactant Flood Potential in Western Canadian Heavy Oil Reservoirs,” Society of Petroleum Engineers, 2006.

Liu, Q., M. Dong, Ma, S.: “Alkaline/Surfactant Flood Potential in Western Canadian Heavy Oil Reservoirs,” SPE-Paper 99791-MS. SPE/DOE Symposium on Improved Oil Recovery, Tulsa, Oklahoma, USA, April 22-26, 2006.

Liu, Q., M. Dong, Ma, S., and Tu, Y.: “Surfactant Enhanced Alkaline Flooding for Western Canadian Heavy Oil Recovery,” Colloids and Surfaces A: Physicochemical and Engineering Aspects 293, No. 1–3, 63–71, February 1, 2007.

Luo, Sh., and Barrufet, M.A.: "The Effect of Water-in-Oil Solubility on Oil Reservoir in the Steam-Injection Process," Paper SPE 89407 presented at SPE symposium on Improved Oil Recovery, Tulsa, Oklahoma, 2005.

Mai, A., and Kantzas, A.: "Heavy Oil Water flooding: Effects of Flow Rate and Oil Viscosity," Journal of Canadian Petroleum Technology 48, No. 3, March 2009.

Mai, A., J. Bryan, Goodarzi, N., and Kantzas, A.: "Insights Into Non-Thermal Recovery of Heavy Oil," Journal of Canadian Petroleum Technology 48, No. 3, March 2009.

Maini, B.: "Foamy-Oil Flow," Journal of Petroleum Technology 53, No. 10, October 2001.

Maini, B.B, and Batycky, J.P.: "Effect of Temperature on Heavy Oil/Water Relative Permeabilities and Vertically Drilled Core Plugs," J. Pet.Tech., V.37, pp.1500-1510, 1985.

McAuliffe,C.: "Oil-in-Water Emulsions and Their Flow Properties in Porous Media," Journal of Petroleum Technology, 25, No.6: 727 – 733, 1973. SPE-4369.

McGee, B. C.W., Vermeulen, F. E.: "The Mechanisms of Electrical Heating for the Recovery of Bitumen From Oil Sands" JCPT 46, No.1: 28-34, 2007a.

McGee, B.C.W., Vermeulen, F.E., and Yu, L.: "Field Test of Electrical Heating with Horizontal and Vertical Wells," J. of Can. Pet.Tech, V.38, No.3, pp. 46-53,1999.

McGee, B., and Vermeulen, F.: "Electrical Heating with Horizontal Wells, the Heat Transfer Problem," Society of Petroleum Engineers, 1996.

Mcgee, B., Vermeulen, F., and Yu, L.: "Field Test of Electrical Heating with Horizontal and Vertical Wells," Journal of Canadian Petroleum Technology 38, No. 3,March 1999.

McGee, B.C.W.: "Electro-thermal pilot in the Athabasca oil sands: Theory versus performance," World Oil, 229(11): 47-54, 2008b.

Memon, A., Gao, J., Taylor, S., Engel, T., and Jia N.: "A Systematic Workflow Process for Heavy Oil Characterization: Experimental Techniques and Challenges," Society of Petroleum Engineers, 2010.

Mifflin, R.T., Watts, J.W. and Weiser, A.: "A Fully Coupled, Fully Implicit Reservoir Simulator for Thermal and other Complex Reservoir Processes," Paper SPE 21252 presented at SPE Symposium on Reservoir Simulation, California, February 1991.

Miller, M.A., and Ramey, H.J Jr.: "Effects of Temperature on Oil/Water Relative Permeabilities of Unconsolidated and Consolidated Sands," J. Pet.Tech., V.37, pp. 945-953,1985.

Mohanty, K.K., Davis, H.T., and Scriven, L.E.: "Physics of Oil Entrapment in Water-Wet Rock," SPE Reservoir Engineering 2, February 1987.

Mokrys, I., and Butler, R.: The Rise of Interfering Solvent Chambers: Solvent Analog Model of Steam-Assisted Gravity Drainage," Journal of Canadian Petroleum Technology 32, No. 3, March 1993.

Nasr, T., and Ayodele, O.: "Thermal Techniques for the Recovery of Heavy Oil and Bitumen," Society of Petroleum Engineers, 2005.

Nasr, T., Ayodele,O. "Thermal Techniques for the Recovery of Heavy Oil and Bitumen," SPE- 97488. International Improved Oil Recovery Conference in Asia Pacific, Kuala Lumpur, Malaysia, 5-6 December, 2005.

Nghiem, L.X, and Li, Y.K.: "Computation of Multiphase Equilibrium Phenomena with an Equation of State," Fluid Phase Equilibria, , V.17, pp.77-95, 1984.

Nilsson, J., Gerritsen, M. and Younis, R.: "An Adaptive, High-Resolution Simulator for Steam Injection Processes," Paper SPE 93881 presented at SPE Western Regional Meeting, Irvine, California, April 2005.

Noll, L. A.: "The Effect of Temperature, Salinity, and Alcohol on the Critical Micelle Concentration of Surfactants," Paper SPE 21032 presented at the SPE International Symposium on Oil Field Chemistry, Anaheim, California, February 1991.

Novosad, J.: "Surfactant Retention in Berea Sandstone- Effect of Phase Behavior and Temperature," SPE J., pp. 962-70, December 1982.

Patzek, T.W.: "Field Applications of Steam Foam for Mobility Improvement and Profile Control," SPE Reservoir Engineering 11, No.2: 79 – 86, 1996. SPE-29612.

Patzek, T.W., Koinis, M.T.: "Kern River Steam-Foam Pilots," Journal of Petroleum Technology 42, No.4: 496 – 503, 1990. SPE-17380.

Patzek, T.W., Myhill, N.A.: "Simulation of the Bishop Steam Foam Pilot," Paper SPE-18786, California Regional Meeting, Bakersfield, California, April 5-7, 1989.

Peaceman, D.W.: "Interpretation of Well-Block Pressure in Numerical Reservoir Simulation with Nonsquare Grid Blocks and Anisotropic Permeability," SPEJ , , V.23, No.3, pp.531-543, 1983.

Peaceman, D.W.: "Interpretation of Well-Block Pressures in Numerical Reservoir Simulation," SPEJ, V.18, No.3, pp.183-194, 1978.

Peters, Ekwere J.: "Advanced petrophysics: Volume 2: Dispersion, interfacial phenomena/wettability, capillarity/capillary pressure, relative permeability," Vol. 2. Greenleaf Book Group, 2012.

Pettersen, Ø., and T. G. Kristiansen.: "Improved Compaction Modeling in Reservoir Simulation and Coupled Rock Mechanics-Flow Simulation, With Examples From the Valhall Field," SPE Reservoir Evaluation & Engineering 12, April 2009.

Pizarro, J.O.S., and O.V. Trevisan.: "Electrical Heating of Oil Reservoirs: Numerical Simulation and Field Test Results," Journal of Petroleum Technology 42, No. 10, October 1990.

Polikar, M., Ferracuti, F., Decastro, V., Puttagunta, V.R., and Ali, F.S.M.: "Effects of Temperature on Bitumen-Water End Point Relative Permeabilities and Saturations," J. Can. Pet.Tech., V.25, pp. 44-50, 1986.

Pooladi-Darvish, M., and A. Firoozabadi.: "Solution-gas Drive In Heavy Oil Reservoirs." Journal of Canadian Petroleum Technology 38, No. 4, April 1999.

Pope, G.A., L.W. Lake, and F.G. Helfferich.: "Cation Exchange in Chemical Flooding: Part 1-Basic Theory without Dispersion," Society of Petroleum Engineers Journal 18, no. 6, December 1978.

Pope, G.A., Nelson, R.C.: "A Chemical Flooding Compositional Simulator," Society of Petroleum Engineers Journal 18(05): 339 – 354, 1978. SPE-6725-PA

Popov, Y., M. Spasennykh, D. Miklashevskiy, A. Parshin, V. Stenin, M. Chertenkov, S. Novikov, and N. Tarelko.: "Thermal Properties of Formations From Core Analysis: Evolution in Measurement Methods, Equipment, and Experimental Data in Relation to Thermal EOR," Society of Petroleum Engineers, 2010.

Popov, Y., M. Spasennykh, D. Miklashevskiy, A. Parshin, V. Stenin, M. Chertenkov, S. Novikov, and N. Tarelko. 2010.Thermal Properties of Formations From Core Analysis: Evolution in Measurement Methods, Equipment, and Experimental Data in Relation to Thermal EOR. Paper-SPE-137639. Canadian Unconventional Resources and International Petroleum Conference, Calgary, Alberta, Canada, 19-21 October.

Poston, S.W., Israel, S., Hossain, A.K.M.S., Montgomery, E.F.III., and Ramey, H.J Jr.: "The Effect of Temperature on Irreducible Water Saturation and Relative Permeability of Unconsolidated Sands," SPEJ, pp. 171-180, 1970.

Prats,M.: "A Current Appraisal of Thermal Recovery," Journal of Petroleum Technology. 30(08):1129-1136. SPE-7044, 1978.

Puetro, M. C. and Reed, R. L.: "A Three-Parameter Representation of Surfactant Oil Brine Interaction," SPE J ., pp.669-682, August 1983.

Rangel-German, E.R., Schembre, J., Sandberg, C., and Kovscek, A.R.: "Electrical-heating-assisted Recovery for Heavy Oil," Journal of Petroleum Science and Engineering, 45(3–4): 213–231, 2004.

Rao, D.: "Wettability Effects in Thermal Recovery Operations," SPE Reservoir Evaluation & Engineering 2, No. 5, October 1999.

Reis, J.C: "Numerical and Experimental Studies of Produced Oil Composition during Light Oil Steam flooding," presented at the Spring Meeting of the AICHE Symposium on Enhanced Oil Recovery, Orlando, Florida, March 1990.

Rezaveisi, M., Sepehrnoori, K., and Johns, R. T. "Tie-Simplex-Based Phase-Behavior Modeling in an IMPEC Reservoir Simulator" SPE Journal 19(02):327– 339. 2014.

Roshanfekr, M., Johns, R.T., Pope, G.A., Britton, L., Linnemeyer, H., Britton, C.,Vyssotski, A. 2009. Effect of Pressure, Temperature, and Solution Gas from Surfacatnt Polymer Floods. SPE 125095, SPE Annual Technical Conference and Exhibition New Orleans, Louisiana, 4-7 October.

Rossen,W.R., Zeilinger,S.C. Shi, J., Lim, M.T.: "Mechanistic Simulation of Foam Processes in Porous Media," Paper SPE-28940. SPE Annual Technical Conference and Exhibition, New Orleans, Louisiana, September 25-28, 1994.

Rubin, B., and Buchanan, W.L.: "A General Purpose Thermal Model," SPEJ, V.15 (2), pp. 202-214, 1985.

Sarma, H., B. Maini, and K. Jha.: "Evaluation of Emulsified Solvent Flooding For Heavy Oil Recovery," Journal of Canadian Petroleum Technology 37, No. 7, July 1998.

SATRS 2012.10.: "Steam; Thermal and Advanced Processes Reservoir Simulator," By Computer Modelling Group Ltd.

Schembre, J.M., Tang, G. Q. and Kovscek, A.R.: "Effect of Temperature on RelativePermeability for Heavy-Oil Diatomite Reservoirs," Paper SPE 93831 presented at SPE Western Regional Meeting, Irvine, California, 2005.

Schmidt, D.P., Soo, H., Radke, C.J.: "Linear Oil Displacement by the Emulsion Entrapment Process," Society of Petroleum Engineers Journal 24(03): 351 –360, 1984. SPE-11333-PA

Scott, G.R., Collins, H.N., and Flock, D.L.: "Improving Waterflood Recovery of Viscous Crude Oils by Chemical Control." Journal of Canadian Petroleum Technology (1965).

Singh, H. Dec. 2014. Scale-up of Reactive Processes in Heterogeneous Media. PhD. Dissertation. The University of Texas at Austin.

Shahin, G., Moosa, R., Al-Kharusi, B., and Chilek, G.: "The Physics of Steam Injection in Fractured Carbonate Reservoirs: Engineering Development Options That Minimize Risk". Society of Petroleum Engineers, 2006.

Shedid, S. Ali and El Abbas A. A.: "Experimental Study of surfactant Alkaline Steam Flood through Vertical Wells," Paper SPE 62562 presented at SPE/AAPG Western Regional Meeting, Long Beach, California, June 2000.

Sheldon, J.W., Harris, C.D., and Bavly, D.: "A Method for General Reservoir Behavior Simulation on Digital Computers," Paper SPE 1521-G presented at 35th Annual Fall Meeting of the Society of Petroleum Engineers, Denver, Colorado, October 1960.

Shinta, A.A. and Firoozabadi, A.: "Prediction Phase Behavior of Water/Reservoir Crude Systems with the Association Concept," Paper SPE 27872, SPE Reservoir Engineering, May 1997.

Shulter, N.D.: "Numerical Three-Phase Model of the Two-Dimensional Steam Flood Process," SPEJ, V. 10(6), pp.405-417,1970.

Shutler, N.D.: "Numerical Three-Phase Simulation of the Linear Steam Flood Process," Trans., AIME, V. 246, pp.232-246, 1969.

Smith, G.: "Fluid Flow and Sand Production in Heavy-Oil Reservoirs Under Solution-Gas Drive," SPE Production Engineering 3, No. 2, May 1988.

Somerton, W.H., Keese, J.A., and Chu, S.L.: "Thermal Behavior of Unconsolidated Oil Sands," Paper SPE 4506 presented at 48th Annual Fall Meeting of the Society of Petroleum Engineers, Las Vegas, Nevada, 1974.

Spillette, A.G., Hillestad, J.G., and Stone, H.L.: "A High-Stability Sequential Solution Approach to Reservoir Simulation," Paper SPE 4542, presented at the 48th Annual Fall Meeting of the Society of Petroleum Engineering of AIME, Las Vegas, NV, 1973.

Stegemeier, G.L. and Vinegar, H.J.: "Soil Remediation by Surface Heating and Vacuum Extraction," Paper SPE 29771 presented at the SPE/EPA Exploration and Production Environmental Conference, Houston, Texas, March 1995.

Stegemeier, G.L. and Vinegar, H.J.: "Thermal Conduction Heating for In-Situ Thermal Desorption of Soil," Hazardous and Radioactive Waste Treatment Technologies Handbook , CRC Press, Boca Raton, FL., 2001.

Sufi, A.H., Ramey, H.J Jr., and Brigham, W.E.: "Temperature Effects on Relative Permeabilities of Oil-water," Paper SPE 11071 presented at SPE Annual Fall Technical Conference and Exhibition, New Orleans, Louisiana, September 1982.

Taber, J.J., F.D. Martin, and R.S. Seright.: "EOR Screening Criteria Revisited - Part 1: Introduction to Screening Criteria and Enhanced Recovery Field Projects," SPE Reservoir Engineering 12, No. 3, August 1997.

Tang, G. Q., and Firoozabadi, A.: "Effect of GOR, Temperature, and Initial water Saturation on Solution-Gas Drive in Heavy-Oil Reservoirs," Paper SPE 71499 presented at SPE Annual Technical Conference and Exhibition, New Orleans, Louisiana, 2001.

Tang, G. Q., and Kovscek A. R.: "Wettability Alteration of Diatomite Induced by Hot-Fluid Injection" Paper SPE 77461 presented at SPE Annual Technical Conference and Exhibition, San Antonio, Texas, 2002.

Tavassoli, S. 2014. Investigation of the Effects of Buoyancy and Heterogeneity on the Performance of Surfactant Floods. PhD Dissertation. The University of Texas at Austin.

Taghavifar, M., Fortenberry R.P., DeRouffignac E., Sepehrnoori, K., Pope, G.A., "Hybrid Thermal-Chemical Processes (HTCP) for Heavy-Oil and Oil-Sand Recovery" Paper SPE 170161. SPE Heavy Oil Conference-Canada, 10-12 June, Alberta, Canada, 2014

Thele, K.J., Lake, L.W., and Sepehrnoori, K.: "A Comparison of Three Equation-of-State Compositional Simulators," SPE 12245, presented at the 7th SPE Symposium on Reservoir simulation of the Society of Petroleum Engineers, San Francisco, CA, 1983.

Thomas, S., Farouq Ali, S., Scoular, J., and Verkoczy, B.: "Chemical Methods for Heavy Oil Recovery," Journal of Canadian Petroleum Technology 40, No. 3, March 2001.

Tikhomolova, K. P., "Electro-Osmosis," Ellis Horwood Publication, New York, 1993.

Titus, C.H., Wittle, J.K., and Bell, C.W.: "Apparatus for Passing Electrical Current Through an Underground Formation," US Patent No.4495990, 1985.

Todd, J.C., Howell, E.P. 1978. Numerical Simulation of In-situ Electrical Heating to Increase Oil Mobility, Journal of Canadian Petroleum Technology, 17(2): 31-41. JCPT Paper No.78-02-01.

Torabzadey, S.J.: "The Effect of Temperature and Interfacial Tension on Water/Oil Relative Permeabilities of Consolidated Sands," Paper SPE 12689 presented at SPE Enhanced Oil Recovery Symposium, Tulsa, Oklahoma, April 1984.

Tortike, W.S., and Farouq Ali, S.M.: "Saturated-Steam-Property Functional Correlation for Fully Implicit Thermal Reservoir Simulation," SPE Reservoir Eng., V.4 (4),pp. 471-474,1989.

Trangenstein, J.A.: "Analysis of a Model and Sequential Numerical Method for Thermal Reservoir Simulation," presented at the European Conference on the Mathematics of Oil Recovery, University of Cambridge, England, July 1989.

UTCHEM-2011.7.: "Three-Dimensional Chemical Flood Simulator," Prepared by Reservoir Engineering Research Program Center for Petroleum and Geosystems Engineering, The University of Texas at Austin.

Varavei, A., and Sepehrnoori, K.: "An EOS-Based Compositional Thermal Reservoir Simulator," Paper SPE 119154, presented at SPE Reservoir Simulation Symposium, Woodland, Texas, February 2009.

Vinegar, H.J., DeRouffignac, E.P., Menotti, J.L., Coles, J.M., Stegemeier, G.L., Sheldon, R.B., and Edelstein, W.A.: "Remediation of Deep Soil Contaminants Using Thermal Vacuum Wells," Paper SPE 39291, Proceedings of the SPE Annual Technical Conference, San Antonio, Texas, October 1997.

Vinegar, H.J., DeRouffignac, E.P., Rosen, R.L., Stegemeier, G.L., Bonn, M.M., Conley, D.M., Phillips, S.H., Hirsch, J.M., Carl, F.G., Steed, J.R., Arrington, D.H., Brunette, P.T., Mueller, W.M., and Siedhof, T.E.: "In-Situ Thermal Desorption (ISTD) of PCBs," Proceeding of the HazWaste/World Superfund XVIII Conference, Washington, DC, December 1997.

Vinegar, H.J., Stegemeier, G.L., Carl, F.G., Stevenson, J.D., and Dudley, R.J.: "In-Situ Thermal Desorption of Soil Impacted with Chlorinated Solvents," Proceeding of the Annual meetings of the Air and Waste Management Association, Paper No.99-450, 1999.

Vinsome, P.K.W., Westerveld, J.: "A Simple Method For Predicting Cap And Base Rock Heat Losses In Thermal Reservoir Simulators" Journal of Canadian Petroleum Technology, 19(03): 87-90. Paper No.80-03-04, 1980.

Vinsome, P.K.W.: "A Numerical of Hot-Water and Steam Drive by the Finite-Difference Method," Paper SPE 5248 presented at the Annual Meeting of the Society of Petroleum Eng. of AIME, Houston, Texas, 1974.

Voskov, D.V., and Tchelepi, H.A.: "Compositional Parameterization for Multi-Phase Flow in Porous Media," Paper SPE 113492 presented at the SPE/DOE Symposium on Improved Oil Recovery, Tulsa, Oklahoma, April 2008.

W. McGee, B., and Vermeulen, F.: "The Mechanisms of Electrical Heating for the Recovery of Bitumen from Oil Sands," Journal of Canadian Petroleum Technology 46, No. 1, January 2007.

Walters, D.A., Settari, A. and. Kry, P.R.: "Poroelastic Effects of Cyclic Steam Stimulation in the Cold Lake Reservoir," Paper SPE 62590 presented at SPE/AAPG Western Regional Meeting, Long Beach, California, June 2000.

Wang, J., Dong, M.. Simulation of O/W Emulsion Flow in Alkaline/Surfactant Flood for Heavy Oil Recovery. SPE Paper- PETSOC-2009-066. Canadian International Petroleum Conference, Calgary, Alberta, Canada, June 16-18, 2009.

Wang, P., Balay, S., Sepehrnoori, K., Wheeler, J., Abate, J., Smith, B., and Pope, G.A.: "A Fully Implicit Parallel EOS Compositional Simulator for Large Scale Reservoir Simulation," Paper SPE 51885 presented at the 15 th SPE Reservoir Simulation Symposium, Houston, Texas, February 1999.

Watts, J.W.: "A Compositional Formulation of the pressure and Saturation Equations," SPERE , V.16 (3), pp.243-252, May 1986.

Weinstein, H.G., Wheeler, J.A., and Woods, E.G.: "Numerical Model for Thermal Processes," SPEJ, V.17 (2), pp.65-78, 1986.

West, W.J., Garvin, W.W., and Sheldon, J.W.: "Solution of the Equations of Unsteady State Two-Phase Flow in Oil reservoirs," Trans., AIME, 1954, V. 201, p.217.

Willman, B.T., Valleroy, V.V., Runberg, G.W., Cornelius, A.J., Powers L.W.: "Laboratory Studies of Oil Recovery by Steam Injection," Journal of Petroleum Technology, 13, No.7:681-691, 1961. SPE-1537-G-PA

Wittle, J.K., and Bell, C.W.: "Method for Enhancing Oil Production Using Electricity," U.S. Patent application No.2005/0199387 A1, 2005.

Wittle, J.K., Hill, D.G., and Chilingar G.V.: "Direct Current Electrical Enhanced Recovery in Heavy-Oil Reservoirs to Improve Recovery, Reduce Water Cut, and Reduce H_2S Production while Increasing API Gravity," Paper SPE 114012 presented at SPE Western Regional and Pacific Section AAPG Joint Meeting in Bakersfield, California, 2008.

Wong, T.W., Firoozabadi, A., Nutakki, R., and Aziz, K.: "A Comparison of Two Approaches to compositional and Black Oil Simulation," Paper SPE 15999 presented at the 9th SPE Symposium on reservoir Simulation of the Society of Petroleum Engineers, San Antonio, Texas, February 1987.

Workman, P. E.: "Method of Recovering and Increasing the Production of Oil," U.S. Patent No.1784214, 1930.

Wu, G., and A. Kantzas.: "Experimental Study of Gas Solvent Flooding for Lloydminster Heavy Oil Reservoirs," Society of Petroleum Engineers, 2008.

Yoshiaki, Ito, Settari, A. and Jha, K.N.: "Development and Application of Pseudo - Functions for Reservoir Simulation to Represent Shear Failure during the Cyclic Steam Process," Paper SPE 25800 presented at SPE International Thermal Operations Symposium, Bakersfield, California, February 1993.

Young, L.C. and Stephenson, R.E.: "A Generalized Compositional Approach for Reservoir Simulation," SPEJ, V.13, No.6, pp.727-742, October 1983.

Young, L.C.: "Continues Compositional Volume-Balance Equations," Paper SPE 66346 presented at the SPE Reservoir Simulation Symposium, Houston, Texas, February 2001.

Youngren, G.K.: "Development and Application of an In-Situ Combustion Reservoir Simulator," SPEJ, pp. 39-51, February 1980.

Zhang, K., Wu, Y.S., Ding, C., Pruess, K., and Elmroth, E.: "Parallel Computing Techniques for Large-Scale Reservoir Simulation Multi-Component and Multiphase Fluid Flow," Paper SPE 66343 presented at the SPE Reservoir Simulation Symposium, Houston, Texas, February 2001.

Zhang, P., and Austad, T.: “The Relative Effects of Acid Number and Temperature on Chalk Wettability,” Society of Petroleum Engineers, 2005.

Ziegler, V. M.: “Laboratory Investigation of High Temperature Surfactant Flooding,” SPERE , pp.586-5, May 1988.